BIOCHEMISTRY RESEARCH TRENDS SERIES

Biochemistry and Histocytochemistry Research Developments

Stefan Fuchs
Max Auer
Editors

NOVA

BIOCHEMISTRY RESEARCH TRENDS SERIES

BIOCHEMISTRY AND HISTOCYTOCHEMISTRY RESEARCH DEVELOPMENTS

No part of this digital document may be reproduced, stored in a retrieval system or transmitted in any form or by any means. The publisher has taken reasonable care in the preparation of this digital document, but makes no expressed or implied warranty of any kind and assumes no responsibility for any errors or omissions. No liability is assumed for incidental or consequential damages in connection with or arising out of information contained herein. This digital document is sold with the clear understanding that the publisher is not engaged in rendering legal, medical or any other professional services.

BIOCHEMISTRY RESEARCH TRENDS SERIES

Glycolysis: Regulation, Processes and Diseases
Paul N. Lithaw (Editor)
2009. ISBN: 978-1-60741-103-1

HDL and LDL Cholesterol: Physiology and Clinical Significance
Irwin S. Pagano and Nathan B. Strait (Editors)
2009. ISBN: 978-1-60741-767-5

HDL and LDL Cholesterol: Physiology and Clinical Significance
Irwin S. Pagano and Nathan B. Strait (Editors)
2009. ISBN: 978-1-60876-728-1 (Online Book)

Biochemistry and Histocytochemistry Research Developments
Stefan Fuchs and Max Auer (Editors)
2010. ISBN: 978-1-60876-283-5

BIOCHEMISTRY RESEARCH TRENDS SERIES

BIOCHEMISTRY AND HISTOCYTOCHEMISTRY RESEARCH DEVELOPMENTS

STEFAN FUCHS
AND
MAX AUER
EDITORS

Nova Science Publishers, Inc.
New York

Copyright © 2010 by Nova Science Publishers, Inc.

All rights reserved. No part of this book may be reproduced, stored in a retrieval system or transmitted in any form or by any means: electronic, electrostatic, magnetic, tape, mechanical photocopying, recording or otherwise without the written permission of the Publisher.

For permission to use material from this book please contact us:
Telephone 631-231-7269; Fax 631-231-8175
Web Site: http://www.novapublishers.com

NOTICE TO THE READER

The Publisher has taken reasonable care in the preparation of this book, but makes no expressed or implied warranty of any kind and assumes no responsibility for any errors or omissions. No liability is assumed for incidental or consequential damages in connection with or arising out of information contained in this book. The Publisher shall not be liable for any special, consequential, or exemplary damages resulting, in whole or in part, from the readers' use of, or reliance upon, this material.

Independent verification should be sought for any data, advice or recommendations contained in this book. In addition, no responsibility is assumed by the publisher for any injury and/or damage to persons or property arising from any methods, products, instructions, ideas or otherwise contained in this publication.

This publication is designed to provide accurate and authoritative information with regard to the subject matter covered herein. It is sold with the clear understanding that the Publisher is not engaged in rendering legal or any other professional services. If legal or any other expert assistance is required, the services of a competent person should be sought. FROM A DECLARATION OF PARTICIPANTS JOINTLY ADOPTED BY A COMMITTEE OF THE AMERICAN BAR ASSOCIATION AND A COMMITTEE OF PUBLISHERS.

LIBRARY OF CONGRESS CATALOGING-IN-PUBLICATION DATA

Biochemistry and histocytochemistry research developments / editors, Stefan Fuchs and Max Auer.
p. ; cm.
Includes bibliographical references and index.
ISBN 978-1-61668-932-2 (E-Book)
1. Histochemistry. 2. Immunohistochemistry. 3. Noradrenaline. I. Fuchs, Stefan, 1960- II. Auer, Max, 1962-
[DNLM: 1. Immunohistochemistry. QW 504.5 B615 2009]
QR183.6.B56 2009
572--dc22 2009037446

Published by Nova Science Publishers, Inc. † New York

CONTENTS

Preface		**vii**
Chapter 1	Function of Norepinephrine in Neuroinflammation and Chronic Neurodegenerative Diseases *Johannes C.M. Schlachetzki, Antonio C. Pinheiro de Oliveira, and Bernd L. Fiebich*	**1**
Chapter 2	The Role of Noradrenaline on Interpersonal Functioning *Wai S. Tse and Alyson J. Bond*	**25**
Chapter 3	The Neurotransmitter Norepinephrine and its Role in Affective Disorders *Eliyahu Dremencov*	**45**
Chapter 4	The Role of Sympathetic Nerve Activity in Renal Injury *Kazuko Masuo, Gavin W. Lambert and Murray D. Esler*	**65**
Chapter 5	Quantitative Immunohistology - Problems and Solutions *Anthony S.Y. Leong and Trishe Y.M. Leong*	**81**
Chapter 6	Immunohistochemical Basis for Orthodontic Treatment *Toshiyuki Kawakam, Keisuke Nakano, Takako Shimizu, Takehiro Watanabe, Rina Muraoka, Akihiro Kimura and Hiromasa Hasegawa*	**117**
Chapter 7	Pathological Research on Molecular-Targeted Therapy and Advanced Immunohistochemical Approaches *Yutaka Hatanaka, Yuki Imaoka, Kaoru Hashizume, and Robert Y Osamura*	**143**
Chapter 8	Pre-Embedding Scarce Biological Specimens for Light and Electron Microscopy *Philippe Taupin*	**153**
Chapter 9	Role of Surrogate Light Chain Expressing B Cells in the Formation of Self-Reactive Antibodies *Pieter Fokko van Loo, Laurens P. Kil and Rudi W. Hendriks*	**159**

Chapter 10 Unique Enzymes of Aspergillus Fungi Used in Japanese Bioindustries **181**
Eiji Ichishima

Chapter 11 Extracellular Proteases of Entomopathogenic Fungi **273**
Lóránt Hatvani, László Kredics, Sándor Kocsubé, László Manczinger, Csaba Vágvölgyi, Zsuzsanna Antal

Chapter 12 Glycoside Hydrolases from Hyperthermophiles: Structure, Function and Exploitation in Oligosaccharide Synthesis **299**
Beatrice Cobucci-Ponzano, Mosè Rossi and Marco Moracci

Chapter 13 Studies on the Thermal Stability of the Therapeutic Enzyme L-Asparaginase from Erwinia Carotovora **323**
Katerina Lappa, Georgia A. Kotzia and Nikolaos E. Labrou

Expert Commentary

A Novel Method for Generation of Monoclonal Antibodies **335**
Masahiro Tomita

Index **337**

PREFACE

Biochemistry is the organic chemistry of compounds and processes occurring in organisms. Histocytochemistry is the study of intracellular distribution of chemical, reaction sites, enzymes, etc. by means of staining reactions, radioactive isotope uptake, selective metal distribution in electron microscopy, or other methods. This book focuses on the role of norepinephrine in neuroinflammation, discusses the contribution of norepinephrine to Alzheimer's (AD) and Parkinson's Disease (PD) and provides an overview of potential therapeutical options targeting this neurotransmitter. Using methodologies such as questionnaires and laboratory tasks, experimental results showing specific effects related to noradrenaline in both clinical and experimental studies are described. This book also provides the current findings on the relationships between sympathetic nerve activity, B-adrenoceptor polymorphisms, and renal function. Recent methodologies that are useful for advanced immunohistochemistry (IHC) analysis in pathological research into therapeutic agents is also analyzed. Other chapters in this book discuss the unresolved areas of plasma cell research, an analysis of a new technology based on B-Cell targeting and its advantages over conventional methods for selective generation of novel monoclonal antibodies, as well as a review of the regulation of proteases and their role during the biocontrol process. Recent advances in the isolation and characterization of glycosidases from hyperthermophilic microorganisms and the methods used for their application in oligosaccharide synthesis are explored as well.

Chapter 1 - Neuroinflammation emerges as a driving force in chronic neurodegenerative processes like Alzheimer’s (AD) or Parkinson’s disease (PD). Neuroinflammatory mediators such as cytokines, reactive oxygen species and molecules of the arachidonic acid pathway are generated and released by microglia, astrocytes and neurons upon stimulation and activation. In general, enhanced release of these substances has been considered to be detrimental.

Different neurotransmitters participate in the regulation of the production of these inflammatory mediators. The adrenergic system seems to play an important role in neuroinflammation and neurodegeneration. For example, norepinephrine has been considered to be immunosuppressive and adrenergic agonists attenuate the release of potentially toxic molecules. In AD and PD, degeneration of the locus coeruleus, an assembly of aminergic nuclei and major source for norepinephrine, is part of the disease process. In both diseases, a reduction in norepinephrine levels accelerates disease progression and pathology as well as worsening of clinical symptoms. Therefore, an increase in the content of norepinephrine may therefore be beneficial in reducing inflammatory damage in the brain.

This review focuses on the role of norepinephrine in neuroinflammation, discusses the contribution of norepinephrine to AD and PD and provides an overview of potential therapeutical options targeting this neurotransmitter.

Chapter 2 - The aim of this chapter is to examine the role of noradrenaline in interpersonal functioning. Healthy interpersonal functioning is important for the development of relationships in both work and personal situations. Many psychiatric disorders including depression are associated with poor interpersonal functioning and less social activity but improvement in interpersonal functioning can be independent of symptom resolution. Noradrenaline may be involved in the adaptive function of human social behaviours.

Concepts relevant to interpersonal behaviours leading to interpersonal rejection and the relationship between social skills and depression will be briefly reviewed. Then the methodology involved in this type of research will be described. This will involve both techniques developed to measure interpersonal functioning, from questionnaires to laboratory tasks, and psychotropic drugs which have been used to study noradrenergic function.

Using these methodologies, experimental results showing specific effects related to noradrenaline in both clinical and experimental studies will be described. Reboxetine has been shown to be associated with increased cooperative behaviour and other socially adaptive behaviours.

It is concluded that noradrenaline modulates cooperation and other socially adaptive behaviours and this action may promote friendship formation and facilitate social support.

Chapter 3 - There are number of lines of evidence that the neurotransmitter norepinephrine (NE) might be very important in pathophysiology of anxiety and mood disorders. Firstly, NE projections innervate the limbic system, suggesting the involvement of NE in the regulation of emotions and cognition. Secondly, NE interacts with serotonin (5-HT) and dopamine (DA) systems, which also play very important roles in the regulation of mood. Thirdly, it has been shown that various agents for increasing NE availability, such as NE reuptake inhibitors, are also effective antidepressant drugs. And fourthly, the depletion of NE can result in the relapse of depression after successful treatment with antidepressant drugs. All these pieces of evidence suggest that the stimulation of NE transmission can be beneficial in the treatment of affective disorders. However, different psychiatric medications have distant effects on NE transmission. The current chapter analyses the effect of psychiatric medications on NE system and proposes how the treatment outcome might be improved.

Chapter 4 - Renal injury, chronic renal disease and end-stage renal disease are often associated with obesity, hypertension, and diabetes mellitus. Heightened sympathetic nerve activity is observed in patients with renal injury, renovascular hypertension, chronic renal disease and end-stage renal disease (ESRD). Further, heightened sympathetic nerve activity as observed in plasma norepinephrine concentrations predicts survival and the incidence of cardiovascular events in patients with end-stage renal disease, and future renal injury in normotensive healthy subjects with a normal range of renal function. Hypertension, obesity and diabetes are currently among the World Health Organization’s top 10 global health risks. Hypertension and diabetes mellitus, which occur often with obesity, together account for approximately 70% of end-stage renal diseases in the United States and Japan. Obesity also leads to increases in the incidence of cardiovascular diseases including renal injury. Many clinical and epidemiological studies have also documented that heightened sympathetic nerve activity plays an important role in obesity and hypertension. Thus, one could speculate that heightened sympathetic nerve activity might be an important mechanism of the onset and

maintenance of renal injury, and that obesity and hypertension might emphasize the relationship between heightened sympathetic nerve activity and renal injury.

Human obesity and hypertension have strong genetic as well as environmental determinants. Several observations show associations of β2- and β3-adrenoceptor polymorphisms with hypertension and obesity, although these findings have not been confirmed. In addition, relationships between adrenoceptor polymorphisms, plasma norepinephrine levels, and renal function have not been fully studied. Understanding the contribution of plasma norepinephrine and β-adrenoceptor polymorphisms with the onset and maintenance of renal injury might aid in the prevention of renal injury, chronic renal disease and end-stage renal disease in obesity and hypertension. It may theoretically help rational, pharmacological treatments for renal injury in obesity and hypertension.

The purpose of this review is to provide the current findings on the relationships between sympathetic nerve activity, β-adrenoceptor polymorphisms and renal function. Also, to further understand the precise roles of sympathetic nerve activity in renal injury in the context of obesity and hypertension, which may lead to the prevention and treatment of renal injury in these patients.

Chapter 5 - As immunohistochemistry enters its fourth decade as a diagnostic tool this analytical procedure continues to experience poor reproducibility, albeit in specific situations. The problem becomes more important with the mounting pressure to employ the assay in a quantitative manner for the assessment of therapeutic and prognostic markers in a number of neoplasms. Qualitative applications of immunohistochemistry are well established and continue to increase with the range of sensitive antibodies and detection systems available, however, numerous variables that influence the immunoexpression of proteins in formalin-fixed tissue continue to exist in the pre-analytical and analytical phases of the test procedure. Many pre-analytical variables are currently beyond the control of the laboratory. Tissue fixation is critical but the exposure to fixative prior to accessioning by the laboratory is not controlled. Antigen retrieval, another pivotal procedure in immunohistology, continues to be employed in an empirical manner with the actual mechanism of action remaining elusive. There is great variation in reagents, method, and duration of tissue processing and immunostaining procedure, and detection system employed is not standardized between laboratories. While many of these variables are offset by the application of antigen retrieval, which enables the detection of a wide variety of antigens in fixed tissue, the method itself is not standardized. This myriad of variables makes it inappropriate to provide meaningful comparisons of results obtained in different laboratories and even in the same laboratory as in current practice each specimen experiences different pre-analytical variables. Importantly, it calls into question the use of immunohistochemistry as a quantitative assay. Furthermore, variables in interpretation exist and cutoff thresholds for positivity differ. Failure to recognize false positive and false-negative stains leads to further errors of quatitative measurement. Many of the problems relating to the technology and interpretation of immunostaining originate from failure to recognize that this procedure is different from other histological stains and involves many more steps that cannot be monitored until the end result is attained. While several remedial measures can be suggested to address some of these problems, accurate and reproducible quantitative assessment of immunostains presently remains elusive as important variables that impact on antigen preservation in the paraffin-embedded biopsy cannot be standardized.

Chapter 6 - It is important to establish the biological basis of immunohistochemical characteristics of mandibular bone and cartilage, as well as periodontal tissue reaction to mechanical stress for orthodontic treatment.

The mandible is composed of mandibular bone and cartilage. This cartilage is classified as secondary, together with condylar, coronoid and angular cartilages. The mandibular bone formation pattern attracts many researchers because it suggests large possibilities for orthodontic treatment. Mandibular condylar cartilage has bone characteristics which are more significant than cartilaginous characteristics. In general, Runx2 is a transcription factor necessary for osteoblast differentiation and bone formation. Therefore, we focused on Runx2 and investigated the distribution of Runx2 in developing mouse mandibular condylar cartilage, with Jagged-Notch signaling, using immunohistochemistry (IHC) and in situ hybridization (ISH) techniques. These IHC and ISH results suggest that Runx2 plays an essential role for mandibular condylar cartilage development, especially that Runx2 is essential for the onset of secondary cartilage differentiation.

In addition, to establish an immunohistochemical basis for orthodontic treatment, we examined early changes of Runx2 and Msx2 immunohistochemical expressions by immunohistochemistry in mouse periodontal ligament exposed to mechanical stress. At 20 minutes, 1 hour, 3 hours, 9 hours and 24 hours, relevant parts of the mouse tissues were histopathologically evaluated, and they were examined for Runx2, Msx2 and alkaline phosphatase (ALP) expressions. Strong expressions of Runx2 and Msx2 were seen in periodontal fibroblasts of the tension side at 20 minutes after mechanical stress. Expressions of Runx2 and Msx2 became stronger in parallel with time, and at 24 hours after mechanical stress, the periodontal fibroblasts, cementoblasts, and osteoblasts showed strong expression. Moreover, ALP has also demonstrated similar strong expression. All these results strongly suggested that Runx2 promoted differentiation of osteoblasts at an early stage and Msx2 worked as an activator of Runx2 function. Furthermore, because Heat Shock Proteins (HSPs) serve as molecular chaperones to maintain homeostasis in tissues, we examined the immunohistochemical profile change of one such protein, HSP70, in periodontal ligament cells after receiving mechanical stress during orthodontic treatment in the course of up to 24 hours. We thought that the mechanical stress for orthodontic treatment might cause dynamic histological change occurred within a short time and might also cause expression of HSP70 in periodontal ligament tissue.

Chapter 7 - With the development of highly specific antibodies and improvements in detection systems, immunohistochemistry has become a common analytical technique, and detection techniques such as the avidin/biotin- and polymer-based methods are widely used in pathological research and diagnosis. Meanwhile, the development of molecular-targeted agents that make attacks against proteins and their sites via kinase activity has led to increasing demand for a next generation IHC approach. Here, we outline recent methodologies that are useful for advanced IHC analysis in pathological research into therapeutic agents.

Chapter 8 - Processing biological specimens for light microscopy (LM) and electron microscopy (EM) requires a critical amount of samples. We report a pre-embedding technique for processing scarce biological specimens for LM and EM. The technique is based on immobilizing the samples in bovine serum albumin (BSA) and bis-acrylamide (BA), cross-linked and polymerized. The preparation is compatible with a broad range of histological and electron microscopy protocols and procedures. It presents several advantages

over other pre-embedding techniques; it is rapid, simple, and permits efficient and reproducible analysis of scarce biological specimens by LM and EM. The technique may be particularly useful for processing specimens, like biopsies, cystic and amniotic-fluid cells.

Chapter 9 - Autoimmune diseases, such as rheumatoid arthritis (RA) and systemic lupus erythematosus (SLE) are facilitated by B cells that have lost self-tolerance. B cells contribute to autoimmune diseases by production of autoantibodies, by presenting autoantigens or by secreting proinflammatory cytokines. For that reason, it is important to understand the origin of autoreactive B cells and their role in the pathogenesis of autoimmune disease. Many autoreactive B cell receptors (BCR) are normally generated during B cell development, but in healthy individuals most of the B cells carrying an autoreactive BCR are silenced by deletion, receptor editing, inclusion or anergy. Interestingly, in humans a unique self-reactive $VpreB^{+}LC^{+}$ B cell subset was identified, which comprises 0.5-1% of circulating B cells and co-expresses conventional immunoglobulin light chain (Ig LC) and the non-rearranging surrogate light chain (SLC), which was previously thought to be exclusively expressed during early B cell development. These $VpreB^{+}LC^{+}$ B cells are present in healthy individuals and accumulate in the joints of some patients with RA. They manifest an unusual Ig heavy chain (HC) and LC repertoire, which displays evidence for receptor editing and is associated with autoimmunity. To elucidate the role of these autoreactive $VpreB^{+}LC^{+}$ B cells in the development of autoimmunity, we have recently generated a novel SLC-transgenic mouse model in which all B cells coexpress SLC components. Here we review the characteristics of the unique subset of $VpreB^{+}LC^{+}$ B cells identified in human and discuss our findings in the SLC-transgenic mouse model in the context of the involvement of $VpreB^{+}LC^{+}$ B cells in the etiology of autoimmune disease.

Chapter 10 – The most widely used organisms are fungi, and several enzymes and organic acids are synthesized by species of *Aspergillus*. Over than the past 1,000 years the use of hydrolytic enzymes from fungi has become more prevalent in Japanese fermentation industries. The molds *Aspergillus oryzae*, *A. sojae*, *A. awamori*, and *A. saitoi* are of great practical importance in the fermentation industries, enzyme technologies, food industries, and civilization in Japan. In the eastern world rice is used instead of malt or mashed grapes for fermentation. Here a mold, usually *A. oryzae*, initiates the fermentation process by hydrolyzing rice starch to fermentable sugars. Later on the sugar is converted to change by spontaneous fermentation by either yeast or bacteria leading to products such as ‘Sake’, Japanese rice wine. Other examples of the traditional use of fungi in food production are in the making of soy sauce and miso paste. In the fermented vegetable protein, soy sauce, the cooked soybeans are mixed with equal amounts of roasted wheat and then inoculated with a pure cultured ‘Koji’ starter or ‘seed mold’.

Another important field for the early industrial application of fungi was the production of enzymes, and enzymes are now being used in a wide variety of processes. The invention and production of ‘Takadiastase’ for *A. oryzae* by Takamine J. in 1894 became an enzyme industry from the late nineteen century. After Takadiastase was discovered it was produced in appreciable amounts during the Second World War, initially with *A. oryzae*, *A. sojae*, *A. awamori*, and *A. niger*. *Aspergillus saitoi*, which is a food microorganism, a black *Aspergillus* used in ‘Shochu’, a traditional Japanese spirit, was described taxonomically by Sakaguchi *et al*.. An acid stable proteolytic enzyme ‘Molsin’ from *A. saitoi* produced on an industrial scale by us used in the preparation of a human digestant (Fujisawa Pharmaceutical Co., Osaka).

The genome of *Aspergillus oryzae* has been sequenced in 2005. The ability to secrete large amounts of proteins and the development of a transformation system have facilitated the use of *A. oryzae* in modern biotechnology. In 2006, the Brewing Society of Japan gave its seal of approval to the decision: '*Aspergillus oryzae* and related food *Aspergilli* are the national microorganisms of Japan'.

In this chapter, catalytic and molecular properties of unique and characteristic enzymes obtained from *Aspergillus* fungi used in Japanese bioindustries are described.

Chapter 11 - During the infection of entomopathogenic fungi, extracellular hydrolytic enzymes are important for the degradation of the insect cuticle, facilitating penetration and providing nutrients for further growth. A common feature between different insect pathogenic fungi is the involvement of extracellular proteolytic enzymes in these processes.

Regarding proteases, the most extensively studied entomopathogenic fungal genera are *Metarhizium* and *Beauveria*. The majority of the protease enzymes described from these genera belong to the family of serine proteases, however, the expression of metalloproteases and aminopeptidases under biocontrol-related conditions was also demonstrated. Detailed knowledge on protease genes and enzymes involved in fungal biological control will assist further strain improvement enabling the overexpression of genes encoding effective proteases.

The aim of this chapter is to summarize the information available about the extracellular proteases of entomopathogenic fungi, focusing on *Metarhizium* and *Beauveria* species. A large number of protease enzymes have been purified, cloned and characterized from these beneficial organisms. These results will be reviewed and data about the regulation of proteases as well as their role during the biocontrol process will be discussed.

Chapter 12 - Hyperthermophilic microorganisms thrives at temperatures higher than 80°C and proteins and enzymes extracted from these sources are optimally stable and active in the presence of temperatures close to the boiling point of water and of other denaturants, i.e. chaotropic agents, pH, organic solvents, detergents, etc. Therefore, hyperstable enzymes are considered attractive alternatives in biocatalysis and in chemo-enzymatic synthesis. In addition, the molecular bases of the extreme stability to heat and to the ability to work optimally at high temperatures are not completely understood and intrigued biochemists, enzymologists, and biophysics in the last twenty years. In particular, hyperstable glycosidases, enzymes catalysing the hydrolysis of *O*- and *N*-glycosidic bonds, have been studied in detail as they are simple model systems promoting single-substrate reactions, and, more importantly, can be exploited for the enzymatic synthesis of oligosaccharides. The importance of these molecules increased enormously in recent years for their potential application in biomedicine. Hyperstable glycosidases, working in transglycosylation mode, can be excellent alternatives to the classical chemical methods helping in the control of regio- and stereoselectivity as conventional enzymes, but also resisting to the organics used in chemical synthesis. We will review here recent advances in the isolation and characterization of glycosidases from hyperthermophilic microorganisms and the methods used for their application in oligosaccharide synthesis.

Chapter 13 - L-Asparaginase (E.C.3.5.1.1, L-ASNase) catalyzes the hydrolysis of L-Asn, producing L-Asp and ammonia. This enzyme is an anti-neoplastic agent; it is used extensively in the chemotherapy of acute lymphoblastic leukemia (ALL). L-asparaginase from *Erwinia carotovora* (*Eca*L-ASNase) was cloned and expressed in *E. coli*. The enzyme was purified to homogeneity by a two-step procedure comprising cation-exchange chromatography and

affinity chromatography on immobilized L-asparagine. The purified enzyme was subjected to thermal inactivation studies. Thermodynamic parameters (E_a, $\Delta H^{\neq}$ and $\Delta S^{\neq}$) for the thermal inactivation process of the enzyme were determined. It was concluded that the low thermal stability of the enzyme is of entropic origin and is most likely due to structural determinants that cause a higher degree of local disorders at specific locations.

In: Biochemistry and Histocytochemistry…
Editors: S. Fuchs, M. Auer, pp. 1-24
ISBN: 978-1-60876-283-5
© 2010 Nova Science Publishers, Inc.

Chapter 1

FUNCTION OF NOREPINEPHRINE IN NEUROINFLAMMATION AND CHRONIC NEURODEGENERATIVE DISEASES

Johannes C.M. Schlachetzki, Antonio C. Pinheiro de Oliveira, and Bernd L. Fiebich
Department of Psychiatry and Psychotherapy
University of Freiburg Medical School[1] ,Germany

ABSTRACT

Neuroinflammation emerges as a driving force in chronic neurodegenerative processes like Alzheimer's (AD) or Parkinson's disease (PD). Neuroinflammatory mediators such as cytokines, reactive oxygen species and molecules of the arachidonic acid pathway are generated and released by microglia, astrocytes and neurons upon stimulation and activation. In general, enhanced release of these substances has been considered to be detrimental.

Different neurotransmitters participate in the regulation of the production of these inflammatory mediators. The adrenergic system seems to play an important role in neuroinflammation and neurodegeneration. For example, norepinephrine has been considered to be immunosuppressive and adrenergic agonists attenuate the release of potentially toxic molecules. In AD and PD, degeneration of the locus coeruleus, an assembly of aminergic nuclei and major source for norepinephrine, is part of the disease process. In both diseases, a reduction in norepinephrine levels accelerates disease progression and pathology as well as worsening of clinical symptoms. Therefore, an increase in the content of norepinephrine may therefore be beneficial in reducing inflammatory damage in the brain.

This review focuses on the role of norepinephrine in neuroinflammation, discusses the contribution of norepinephrine to AD and PD and provides an overview of potential therapeutical options targeting this neurotransmitter.

1 Address: Hauptstr. 5 79104 Freiburg i. Br. Germany.

1. INTRODUCTION

The brain and the immune system are accepted as the two major body's adaptive systems (Elenkov et al., 2000). The brain can modulate immune functions and the immune system also sends messages to the brain. The communication between these two systems is done mainly by the hypothalamic-pituitary-adrenal axis and the autonomic nervous system (ANS). The sympathetic nervous system (SNS), which is part of the ANS, innervates the lymphoid organs (Elenkov et al., 2000) (Flierl et al., 2007). Catecholamines, like dopamine, serotonin, epinephrine and norepinephrine, are the end products of the SNS.

Norepinephrine (NE) is a classical neurotransmitter of the central nervous system (CNS). NE is a catecholamine belonging to the group of biogenic amines. Like other biogenic amines, NE is produced in distinct neuronal populations within the CNS, from which axons project widely throughout the CNS. Therefore, alterations in NE levels and/or adrenergic receptor levels lead to ample changes in brain homeostasis. Classically, the NE system has been studied for its involvement in human behaviour and psychiatric diseases. Recent studies have even further widened possible functions of NE. NE has gained widespread attention because it seems to modulate neuroinflammation and thereby contributes to disease pathogenesis. The scope of this review is to give insights into *in vitro* and *in vivo* findings contributing to the role NE in the CNS.

2. THE LOCUS COERULEUS

NE is mainly synthesized in the neurons of the locus coeruleus (LC), but also in the lateral tegmental field. In this review, we focus on the LC because of its implication in neurodegenerative diseases and cognition (Friedman et al., 1999).

Neurons of the LC constitute the largest and most important aggregation of NE cells within the brain. LC is latin for "blue place" and was named so because of its high neuronal content of melanin, formed by polymerization of norepinephrine. The LC is located below the floor of the fourth ventricle in the rostrolateral part of the pons (Figure 1). Neurons of the LC project through the medial forebrain bundle to the cerebral cortex including the frontal and entorhinal cortices, the limbic system (amygdala, hippiocampus, cingulate gyrus, fornix, hypothalamus, and thalamus) and to the cerebellum, brain stem, and spinal cord. The LC also receives input from the above mentioned brain areas (Nieuwenhuys, 1984). Thus, the NE system has a widespread effect on various brain regions and thereby on cognition and behaviour.

The number of neurons within in the LC range from 45 000 to 60 000 cells in normal young adult human brains and this number declines up to 50% in the normal aging human brain (Mann et al., 1983). NE levels also seems to be reduced in the aging population compared to younger subjects (Yates et al., 1983).

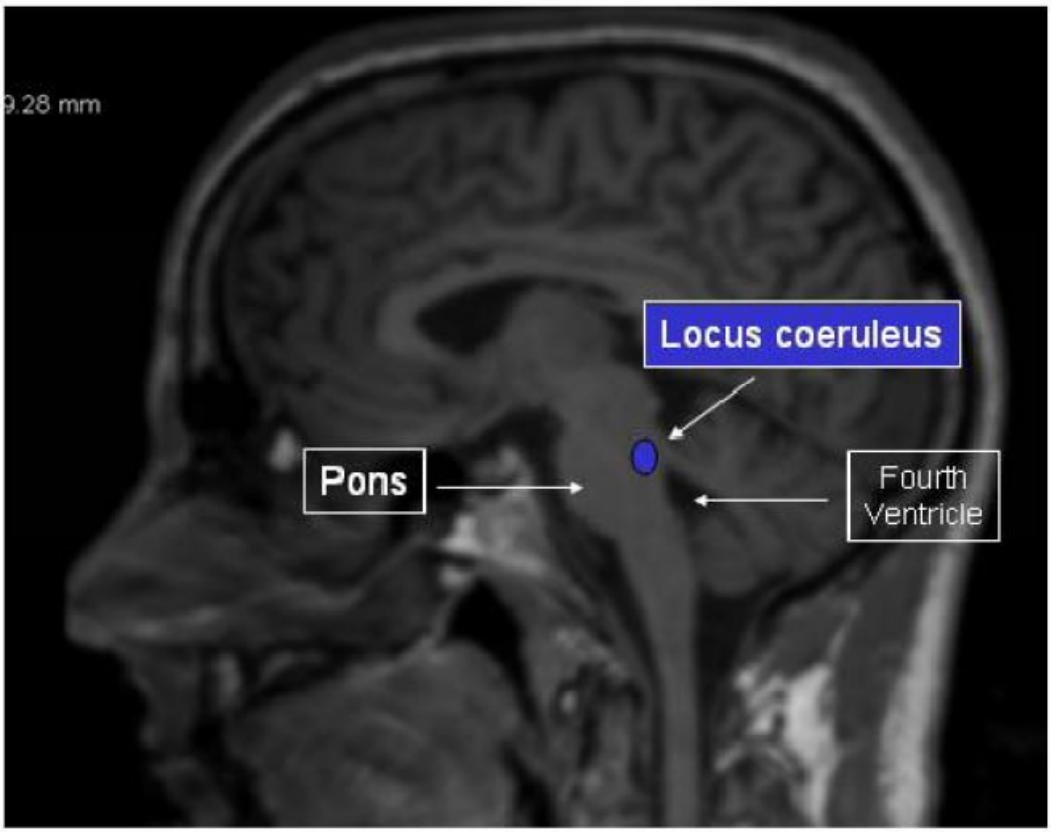

Figure 1. Courtesy of Dr. Lars Frings.

3. Classical Functions of Norepinephrine in the CNS

NE is derived from the essential amino acid L-tyrosine. The tyrosine hydroxylase converts L-tyrosine into L-dihydroxyphenylacetic (L-DOPA), which is then transformed into dopamine by dopa-decarboxylase. The β-hydroxylase converts dopamine into NE. NE is then released into synaptic cleft and exerts its effects via binding adrenergic receptors, which can be divided into α- and β-adrenergic receptors, as discussed later. A role has been described for NE in cognition, emotions, and behaviour (Figure 2). The classical psychiatric disease, in which modulation of NE has been postulated to be of pivotal role, is the major depressive disorder (MDD). The monoamine deficiency hypothesis holds a deficiency in serotonin and NE levels accountable for the pathogenesis of MDD. This is supported by the usage of tricyclic antidepressant drugs or monoamine oxidase inhibitors, which are highly effective in alleviating symptoms of depression (Belmaker and Agam, 2008).

However, there is a strong interplay between the different neurotransmitter systems in the CNS. E.g., NE not only mediates other neurotransmitter system, but also gets modified by others. NE interacts with acetylcholine, serotonin, and dopamine (Beani et al., 1978) (Vizi and Pasztor, 1981) (Bianchi et al., 1979) (Murphy et al., 1998) (Gresch et al., 1995). In addition, NE modulates neurotrophic factors like corticotropin-releasing hormone (Melia and

Duman, 1991). Changes in these neurotransmitter and neurotrophic factor systems may lead to changes in behaviour in normal controls.

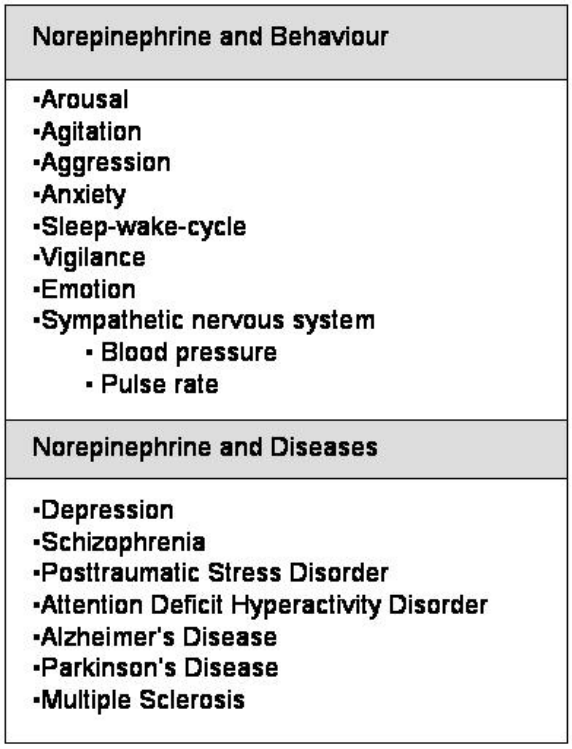

Figure 2.

4. ADRENOCEPTORS

There are two principal groups of receptors for epinephrine and NE, so-called adrenoreceptors, which are divided into α- and β-adrenoreceptors. α-adrenoreceptors are subdivided into α_1 and α_2, whereas the β-adrenoreceptors into β_1, β_2 and β_3. All the adrenoreceptors are coupled to different G protein subtypes. More specifically, α_1-adrenoreceptors is coupled to G_q, α_2-adrenoreceptors to G_i, and all the β-adrenoreceptors to G_s. Briefly, activation of G_s and G_i stimulates and reduces the production of cAMP, respectively. cAMP functions as a second messenger that can activate the protein kinase A (PKA), which in turn, can transfer the signals to the nucleus.

Stimulation of the α_1-adrenoreceptors results in the activation of the $G_{q/11}$ protein, which subsequently activates phospholipase Cβ (PLCβ) and leads to cleavage of phosphatidylinositol-4,5-bisphosphate into inositol-1,4,5-trisphosphate (IP_3) and diacylglycerol (DAG). IP3 induces the release of Ca^{2+} form intracellular stores and DAG functions as a second messenger to activate protein kinase C (PKC) (Hein and Michel, 2007).

On the other hand, α_2-adrenoreceptors mostly mediate their intracellular signalling through G_i. In this case, the signalling through the G_α and $G_{\beta\gamma}$ subunits may be important. Activation of the $G_{\alpha i}$ leads to the inhibition of adenylyl cyclase (AC) with a reduction in cAMP levels, whereas activation of $G_{\beta\gamma}$ leads to inhibition of Ca^{2+} channels and activation of K^+ channels and mitogen-activated protein kinases MAPK (Hein et al., 2006).

Stimulation of β-ARs leads to activation of G_s protein, resulting in a subsequent increase in cAMP. This increase in cAMP induces stimulation of PKA and phosphorylation of the transcription factor cAMP responsive element binding protein (CREB). After this phosphorylation, CREB binds to the cAMP-responsive element in the promoter of many genes (Tan et al., 2007).

Epinephrine and NE have different affinities to the ARs. NE binds to all receptors, although the affinity for β_2 is weaker.

5. Role of NE and Adrenergic Agonists in Peripheral Immune Cells Functions

The immune system is a network of different tools that protects the organism against diseases. The cells of these system are the white blood cells that are produced in the bone marrow that function as the defensive cells of the organisms. There are different immune cells that are involved in the innate or adaptive immunity.

Many studies have been showing some roles for NE and adrenoreceptors agonists and antagonists in the modulation of immune functions. Catecholamines have been identified in different immune cells, like macrophages (Spengler et al., 1994) (Brown et al., 2003) (Flierl et al., 2007), peripheral human (Musso et al., 1996) and cerebrospinalfluid (CSF) lymphocytes (Bergquist et al., 1994), mouse lymphocytes (Josefsson et al., 1996), human peripheral blood mononuclear cells (PBMCs) (Marino et al., 1999) including neutrophils (Cosentino et al., 1999), T and B lymphocytes, monocytes and granulocytes (Cosentino et al., 2000), and murine bone marrow derived mast cells (Freeman et al., 2001). Moreover, these cells also express adrenergic receptors.

NE, at concentrations that preferentially stimulate α_2-adrenoreceptors, has been shown to decrease the capacity of interferon (IFN)γ to activate macrophages to a tumoricidal state (Koff and Dunegan, 1985). NE increases chemotaxis and phagocytosis by macrophages (Javierre et al., 1975) (Garcia et al., 2003). However, these two processes seem to depend on different receptors. To date, low doses of NE, which preferentially binds to α-adrenoreceptors, induce chemotaxis. This is confirmed by the fact that phentolamine, an α antagonist, but not propranolol, a β antagonist, blocks the chemotaxis of macrophages. On the other hand, both drugs inhibited the phagocytosis induced by NE, suggesting a participation of α and β-adrenoreceptors in this process (Garcia et al., 2003).

Almost two decades ago, Spengler and colleagues (Spengler et al., 1990) (Spengler et al., 1994) demonstrated that activation of α_2-adrenoreceptors by NE and UK-14304, a synthetic agonist, can increase the production of tumor necrosis factor (TNF) induced by lipopolysaccharide (LPS) in murine macrophages. In addition, this augmentation in LPS-induced TNF was reduced by yohimbine, an α_2-adrenoreceptors antagonist (Spengler et al.,

1990). On the contrary, activation of β-adrenoreceptors decreased the TNF production induced by LPS (Spengler et al., 1994). Interestingly, co-stimulation of macrophages with LPS and the α_2 or β-adrenoreceptors antagonists in the absence of adrenergic agonists, induced the opposite effects observed after stimulation with the agonists (Spengler et al., 1994), supporting the idea of an endogenous role for NE in macrophages.

Blockade of α_2, β_1 and β_2-adrenoreceptors on LPS-stimulated alveolar macrophages reduces the release of interleukin (IL)-1β, IL-6 and cytokine-induced neutrophil chemoattractant-1. In this same condition, TNFα release is also strongly reduced by α_2 and β_2-adrenoreceptors antagonists. However, the blockade of α_2-adrenoreceptors reached the most consistent suppression of the investigated cytokines (Flierl et al., 2007).

Salmeterol, NE and isoproterenol reduce the secretion of TNFα in LPS-stimulated THP-1 cells, a human monocytic cell line (Severn et al., 1992) (Sekut et al., 1995). The reduction induced by salmeterol can be blocked by oxprenolol, suggesting that this effect might be mediated through β_2-adrenoreceptors. More important, previous oral administration of salmeterol to LPS-injected mice reduces the TNFα in serum and this effect was reversed by propranolol (Sekut et al., 1995). In human whole blood, NE and isoproterenol reduce TNFα and IL-6 expression induced by LPS, an effect that is blocked by metropolol, a β_1 antagonist, but not by phentolamine, an α antagonist (van der Poll et al., 1994). In accordance to this, stimulation of α-adrenoreceptors with phenilephrine also had no effect on cytokine production induced by LPS in human whole blood (van der Poll et al., 1994). In addition to these effects on TNF and IL-6 production, NE also inhibits the IL-1 production induced by LPS and IFN in mouse peritoneal macrophages (Koff and Dunegan, 1985).

Recently, Flierl and colleagues presented important evidences that macrophages and polymorphonuclear cells possess the complete intracellular machinery for the synthesis, release and inactivation of catecholamines (Flierl et al., 2007). By using two models of inflammatory acute lung injury, the authors demonstrated that an increased or decreased production of catecholamine augments or decreases the intensity of the inflammatory injury, respectively. More specifically, *in vivo* blockade of α_2-adrenoreceptors strongly reduces the intensity of the inflammatory injury, measured by the severity of lung damage. These and other evidences allowed the authors and also others to consider the phagocytic system as a diffusely expressed adrenergic organ (Flierl et al., 2007).

Activation of β-ARs by isoproterenol enhances the expression of COX-2 and iNOS in a human urothelial cell line (Harmon et al., 2005). Since activation of β-adrenoreceptors leads to an increase in cAMP and a subsequent PKA activation, the authors investigated whether the increase in these inflammatory markers was due to activation of this pathway. However, this increase is independent of PKA, since PKA inhibitors did not reduce the augmentation in COX-2 and iNOS expression.

The activation of α_1-adrenoreceptors is less studied in inflammatory disorders, since it does not seem to play a major role in immune functions (Hasko, 2001).

6. IMMUNE SYSTEM IN THE CNS

The CNS also contains resident cells that are responsible for the innate immune response. The main cell types responsible for this function are microglia and astrocytes.

Microglia are considered the CNS macrophages that become active after injury or inflammation. These cells share a common monocytic progenitor with macrophages, and similarly are also able to produce and release many inflammatory mediators after activation, like eicosanoids, cytokines, chemokines, complement components, oxidative radicals and others. Moreover, they also present other functions like phagocytosis and antigen presentation. It is believed that microglia play an important role not only in protecting the CNS against infections, but also in the development of neurodegenerative diseases. However, their exact role in many neuroinflammatory conditions remains unclear.

7. ROLE OF NE AND ADRENERGIC AGONISTS IN MICROGLIA FUNCTIONS

Considering the possible contribution of microglia in neuroinflammatory and neurodegenerative disorders, much work has been developed to search for substances or pathways that modulate microglia activation. The agonists of ARs are among these investigated pharmacological targets.

Adrenoreceptors have been identified in microglia and the role of NE has been investigated in microglia activation. *In vitro*, microglia can be activated by different stimuli, like LPS, amyloid-β, IL-1β, TNFα and IFNγ. However, the most used activator of microglia in *in vitro* studies is LPS. Stimulation of microglia with LPS leads to the increase in the production of different inflammatory mediators, like nitric oxide (NO), prostaglandins (PG), cytokines and others.

NO is an important mediator in most brain pathological conditions that possess an inflammatory component, which is produced mainly by the inducible NO synthase (iNOS). Microglia, as well as astrocytes, are able to produce NO. Although NO is important for the innate immune defense against pathogens, it is also implicated in the pathology of different neuroinflammatory and neurodegenerative diseases, being involved, for example, in neuronal cell death (Brown, 2007). Norepinephrine, as well as phenylephrine, an agonist of α-adrenoreceptors and isoproterenol, and agonist of β-adrenoreceptors, reduce the expression of iNOS and the production of NO induced by LPS in murine microglia (Chang and Liu, 2000) (Mori et al., 2002) (Dello Russo et al., 2004) (Farber et al., 2005).

The production of reactive oxygen species (ROS) is associated with cytotoxicity. In the CNS, microglia are an important source of these species. In neonatal hamster microglia stimulated with phorbol myristate acetate, a PKC activator, isoproterenol reduces the production of superoxide anion and this decrease was blocked by a β-adrenoreceptors antagonist (Colton and Chernyshev, 1996).

The so-called pro-inflammatory cytokines, IL-1β, IL-6 and TNFα, may be important for the pathogenesis of diseases that present a neuroinflammatory component. IL-1 is one of the most studied cytokine and it presents different actions in the CNS, such as increase in iNOS

activation, induction of growth factors, reduction of glutamate release, altered N-methyl-D-aspartic acid response and others (Lucas et al., 2006).

Tomozawa et al. (Tomozawa et al., 1995) showed that isoproterenol induces IL-1β mRNA in microglia, but not in astrocytes. This increase was inhibited by propranolol and by a cAMP-dependent protein kinase inhibitor. Similarly, NE, β1- and β2-adrenoreceptors agonists produce an increase in IL-1β mRNA, which is suppressed by β_1- and β_2-adrenoreceptors antagonists (Tanaka et al., 2002). In line with those data, isoproterenol increases IL-1α and IL-1β mRNA in microglia (Hetier et al., 1991). On the other hand, these authors also showed that LPS-induced production of IL-1β protein was inhibited by isoproterenol (Hetier et al., 1991). NE also decreases the production of IL-1β induced by LPS in miroglia (Dello Russo et al., 2004) (Madrigal et al., 2005). However, the reasons for these differences among the studies are still not clear.

Incubation of neurons with media obtained from LPS-treated microglia induces neuronal cell death. However, if microglia are previously treated with NE, IL-1β production and neuronal cell death are reduced. The reduction of neuronal cell death can also be obtained by the treatment of the neurons with an IL-1β antagonist, suggesting an important role of microglial derived-IL-1β in neuronal cytotoxicity (Madrigal et al., 2005).

Since TNFα and IL-6 are also important mediators in inflammatory responses, some work has also been done to investigate whether adrenoreceptors activation influences the production and release of these cytokines. TNFα, acting via two different receptors, p55 and p75, can present deleterious or protective effects in the CNS. There, it can be produced by microglia and astrocytes (Lucas et al., 2006). IL-6 has many functions in the CNS (see (Van Wagoner and Benveniste, 1999)).

Different groups have demonstrated that NE and other ARs agonists reduce LPS-induced TNFα and IL-6 expression and release (Hetier et al., 1991) (Mori et al., 2002) (Farber et al., 2005). However, the role of each adrenoreceptors in this response is still unclear. For example, Mori et al. (Mori et al., 2002) demonstrated that NE, the α_1 agonist phenylephrine, the β_1 agonist dobutamine and the β_2 agonist terbutaline reduces the expression of TNFα and IL-6 mRNA and release, whereas the α_2 agonist clonidine had no effect. This reduction in TNFα and IL-6 was not observed after treatment of microglia with β_1 and β_2 agonists (Prinz et al., 2001). This difference could be explained by the different animal species and different adrenoreceptors agonists used in the studies.

The effect of adrenoreceptors agonists on the production of other important mediators involved in inflammation have also been investigated. Prostaglandins are produced via the metabolism of AA by cyclooxygenases (COX) and subsequently by prostaglandin synthases. There are two main COX isoforms, COX-1 and COX-2. In general, COX-1 is considered to be constitutive, because it is constitutively expressed in many tissues, whereas COX-2 is induced by inflammatory stimuli, but it can also be present in some tissues without stimulation. Although it is still not clear, a role for COX-2 has been suggested for some neurodegenerative diseases (Hoozemans and O'Banion, 2005). Just few studies addressed the influence of adrenoreceptors activation on the AA cascade. Isoproterenol has been shown to increase the expression of COX-2 and PGE_2 synthesis induced by LPS in microglia (Minghetti and Levi, 1995). Our laboratory has also demonstrated that NE is able to increase COX-2 expression in LPS-stimulated microglia (Schlachetzki et al., submitted).

8. ROLE OF NE AND ADRENERGIC AGONISTS IN ASTROCYTES FUNCTIONS

Astrocytes also express adrenoreceptors (Hertz et al., 1984) (Richards et al., 1989) and their activation has been shown to play some role in inflammatory contexts. NE reduces iNOS expression and nitrate accumulation in LPS plus cytokines-stimulated rat primary astrocytes (Feinstein et al., 1993; Feinstein, 1998). The reduction in the nitrate accumulation is attenuated by propranolol, but not by phentolamine, an α antagonist (Feinstein et al., 1993) (Facchinetti et al., 2004).

NE also inhibits the IFNγ-induced major histocompatibility (MHC) class II antigen expression in rat astrocytes, which is reduced by propranolol, but not by phentolamine or propranolol, suggesting that the effect of NE might be mediated through β_2-adrenoreceptors (Frohman et al., 1988).

In astrocytes, isoproterenol reduces TNFα and IL-6 promoter activity induced by LPS, as well as mRNA and protein levels (Nakamura et al., 1998). This effect was blocked by a β_2 antagonist, but not by a β1 antagonist. Similar results were obtained by Facchinetti et al. (Facchinetti et al., 2004), who showed that NE and isoproterenol reduce TNFα release in LPS-stimulated astrocytes and which is reversed by propranolol. The constitutive expression of IL-1 receptor mRNA is also reduced by isoproterenol and blocked by propranolol (Tomozawa et al., 1995).

On the other hand, in the absence of LPS, NE and isoproterenol induce the expression and release of IL-6 in astrocytes (Maimone et al., 1993) (Norris and Benveniste, 1993). Moreover, NE synergizes with IL-1β and TNFα to induce IL-6 release.

Investigating the mechanisms by which NE induces its anti-inflammatory activity, Klotz and colleagues (Klotz et al., 2003) demonstrated that NE and isoproterenol induce the transcription and expression of PPARγ in murine primary astrocytes and neurons. PPARγ is an important nuclear receptor involved in the transcription of different inflammatory mediators. Therefore, it is possible that NE induces some anti-inflammatory effects through increased PPARγ expression.

NE also influences the expression of other genes involved in the inflammatory response in the brain, such as MHC class II antigen and ICAM-1. More specifically, NE has opposite effects on these gene products depending on the cell type, like reducing the expression of MHC class II in glial cells, while enhancing MHC class II in IFNγ-stimulated bovine brain endothelial cells. On the other hand, NE reduces the expression of ICAM in both astrocytes and brain endothelial cells (Feinstein et al., 2002).

9. INTRACELLULAR SIGNALLINGS INDUCED BY ADRENERGIC ACTIVATION

As described previously, activation of β-adrenoreceptors leads to the accumulation of cAMP and activation of PKA. This suggests that the effects of NE and other β-adrenoreceptors agonists are mainly mediated via activation of PKA. This is supported by the fact, that the effects of NE is mimicked by β agonists or by compounds that increase

intracellular concentration of cAMP, like forskolin, dibutyryl cAMP and 8-bromo-cAMP (Feinstein et al., 1993) (Pahan et al., 1997), undelying that NE acts via a cAMP-dependent signalling. However, other signallings might induced in response to NE. E.g. β_2-adrenoreceptors activation reduces the production of cytokines in LPS-stimulated macrophages through inhibition of NF-κB (Farmer and Pugin, 2000) and via increasing the levels of IκB (Feinstein et al., 2002).

Recently, Tan et al. (Tan et al., 2007) demonstrated that activation of β_2-adrenoreceptors in the macrophage cell line (RAW264.7) in the absence of inflammatory stimulus increased the transcription and protein synthesis of IL-1β and IL-6. This increase was not reduced by neither a PKA nor a NF-κB inhibitor, but was dependent on p38 and p42/44 MAPK activation, which in turn, activated activating transcription factor (ATF)1 and ATF2.

10. NOREPINEPHRINE IN ALZHEIMER'S DISEASE

Alzheimer's disease (AD) is the most common neurodegenerative disease in the elderly. Prevalence increases with age and by the year 2050 it has been estimated that world-wide 1 out of 85 persons will suffer from AD (Brookmeyer et al., 2007). AD is clinically characterized by progressive memory deficits, speech problems, and visuospatial orientation. As the disease advances, the patient my develop apraxia (loss of the ability to execute or carry out learned purposeful movements), and requires help in performing activities of daily living. In moderate and severe stages of the disease, AD patients may show signs of neuropsychiatric syndromes like labile affect, aggression, hallucinations, sleep disturbances, and apathy.

Neuropathological hallmarks of the disease are so called plaques, i.e., deposits of aggregated amyloid-β, and intracellular inclusion bodies primarily containing tau, termed neurofibrillary tangles. Nowadays, the "amyloid hypothesis" has reached wide-spread recognition (Hardy and Allsop, 1991) (Hardy and Selkoe, 2002). According to the amyloid hypothesis, amyloid-β aggregation causes altered calcium homeostasis in neurons, and increased oxidative stress as well as a pro-inflammatory environment with microglial activation in the CNS. Eventually, these changes lead to tau dysfunction and neurofibrillar tangle formation within susceptible neurons. This may ultimately end in synaptic and neuronal dysfunction and death (Hardy and Allsop, 1991) (Hardy and Selkoe, 2002). Widely recognized is a neuronal loss of cholinergic neurons, especially of the Nucleus basalis of Meynert (Whitehouse et al., 1982). However, neuronal cell loss is not restricted to neurons of the cholingeric system, but also to other brain regions.

Up to 60% of neuronal cell death has also been described in the LC in post-mortem brains of AD patients (Mann et al., 1980) (Mann et al., 1982) (Wilcock et al., 1988) (Marcyniuk et al., 1986) (Szot et al., 2006) (Matthews et al., 2002) (Yang and Schmitt, 2001) (Ichimiya et al., 1986; Bondareff et al., 1987a) (Burke et al., 1999). In addition, reduced NE content was measured biochemically in different brain regions in post-mortem brains of AD patients (Baker and Reynolds, 1989) (Mann et al., 1980) (Mann et al., 1982) (Adolfsson et al., 1979) (Iversen et al., 1983) (Matthews et al., 2002) (Nazarali and Reynolds, 1992) (Arai et al., 1992) (Palmer et al., 1987; Reinikainen et al., 1988) (Yates et al., 1983; Arai et al., 1984; Ichimiya et al., 1986). In patients with mild cognitive impairment, a "pre-" symptomatic stage of AD, significant reduction of LC neurons has also been shown (Grudzien et al., 2007).

Patients with Lewy body dementia, a disease related to AD and PD also show decreased NE levels (Ohara and Kondo, 1998). These findings with neuronal loss of the LC and reduced levels of NE could not been observed in patients with vascular dementia (Mann et al., 1982) (Haglund et al., 2006) or fronto-temporal dementia (Yang and Schmitt, 2001). In addition, upregulation of adrenergic receptors, especially β_2-adrenoreceptors has been observed in the hippocampus and prefrontal cortex in brains of AD patients (Kalaria et al., 1989). Some studies even suggested that LC cell death or decreased NE brains levels correlate with the severity and duration of dementia in AD (Bondareff et al., 1987b) (Bondareff et al., 1987a) (Matthews et al., 2002). Negative correlation between NE and cognitive function as measured with the mini mental status exam was found in the CSF of AD patients (Oishi et al., 1996). In contrast, another recent study was not able to detect any correlation between LC degeneration and severity of AD pathology (Haglund et al., 2006).

The remaining neurons of the LC seem to dampen NE deficiency by several mechanisms: by increase in tyrosine hydroxylase mRNA expression and metabolic activity, and sprouting of axons into the hippocampus as evidenced by an increase in α_2-adrenoreceptors (Szot et al., 2006) (Hoogendijk et al., 1999). However, an overall decrease in α_2-adrenoreceptor density in the brain of AD patients has been described (Meana et al., 1992). Moreover, a reduced density of NE innervation into the hippocampus has been observed (Powers et al., 1988).

More insights of the role of NE in AD has been obtained by using animal models of AD. A major drawback of most AD animal models is the fact they do not fully mimic the AD pathology as seen in humans. E.g., aged transgenic AD mice do not show reduction of LC cell numbers or cortical NE levels. To investigate the role of NE depletion in AD animal models, a selective NE neurotoxin, DSP-4 or N-(2-chloroethyl-N-ethyl-2 bromobenzylamine, can be injected directly into the LC. DSP4 causes acute loss of LC neurons, degeneration of LC axon terminals and decreased neuronal activity (Grzanna et al., 1989) (Fritschy and Grzanna, 1989) (Olpe et al., 1983). In addition, DSP4 injection leads to impaired electrophysiological functions of the remaining LC neurons (Magnuson et al., 1993).

Depletion of NE may cause deterioration of AD pathology in different animal models (Heneka et al., 2002) (Kalinin et al., 2007) (Heneka et al., 2006). Animals who received amyloid-β injections into the cortex and chronic DSP4 to induce LC neuronal cell death led to induction of inflammatory changes within the CNS of AD animals. An increase in iNOS, IL-1β, and IL-6 expression compared to control animals was measured in the brain. However, COX-2 expression was transiently reduced in the AD animals. Co-injection with NE or the β-adrenoreceptors agonist isoproterenol attenuated the inflammatory response in the amyloid-β and DSP4 injected animals. The inflammatory response caused by NE depletion seems to be due to reduced levels of NF-κB inhibitory IκB proteins and of heat shock protein 70 (Heneka et al., 2003).

Noradrenergic depletion in AD transgenic animals showed an increase in the plaque number and plaque area as well as to an increase in the number of activated microglia and astrocytes (Heneka et al., 2006) (Kalinin et al., 2007).

Heneka and O'Banion proposed the theory that LC loss and noradrenergic depletion of cortical and hippocampal areas may promote neuropathological and inflammatory changes in a vicious, sustained cycle in AD (Heneka and O'Banion, 2007).

Another reason for increased plaque burden may be the decreased capability of microglia to phagocytose and digest amyloid plaques. Microglia have been considered to act as a

double-edged sword: on the hand they are neuroprotective by secreting neurotrophic factors, anti-inflammatory molecules like IL-4 or IL-10 or promote phagocytosis of soluble and insoluble forms of amyloid-β; on the other hand microglia might caue neurotoxic effects by releasing inflammatory mediators such as IL-1β, IL-6, TNF-α or NO. In a study by Kalinin and colleagues, treatment of a primary microglial cell culture with 10 μM NE led to a 12-fold increase in phagocytosis of labelled Aβ *in vitro* (Kalinin et al., 2007). This effect may be due to increased cAMP levels via the activation of β-adrenoreceptors.

Degeneration of LC and NE loss in the brain in AD transgenic mice also showed influence on AD neuropathology applying magnetic resonance imaging and PET nuclear imaging. It has been be shown that AD transgenic animals receiving DSP4 treatment showed significant changes in glucose metabolism, neuronal integrity and cholinergic function *in vivo* compared to control transgenic AD mice (Winkeler et al., 2008).

In AD, neuropsychiatric sequelae of the disease may at least partially explained by degeneration of LC neurons and an altered NE system.

Agitated behaviours are common in the vast majority of patients with AD during the course of the disease. Increased norepinephrine activity has been linked with agitation and aggression (Lindenmayer, 2000). This may be due to an upregulation of α_2- and β-adrenoreceptors in the cerebellum (Russo-Neustadt and Cotman, 1997). In that study, the authors suggested that the cerebellum may have an important role in behavioural control. Another reason that might account for agitated behaviour is an increased sensitivity to NE stimulation in AD patients. Degeneration of the LC has also been postulated to result in aggressive behaviour and a positive correlation between NE cell loss and aggression (Matthews et al., 2002).

Depression is especially found in patients with a mild stage of AD. Depressed AD patients show significantly more LC neuron degeneration compared to non-depressive AD patients (Forstl et al., 1992) (Zubenko and Moossy, 1988). Depressed AD patients also show signs of reduced NE cortical levels (Zubenko et al., 1990). Changes in NE content within the thalamus may explain changes observed in the EEG of AD patients (Soininen et al., 1992).

Thus, NE has to be considered a major factor in the pathogenesis of AD and that treatment options targeting the NE system may be beneficial to the AD patient.

Data from clinical studies suggest that pharmacological inhibition of adrenoreceptors may alter the cognitive function of AD patients. Patients with cognitive impairments deteriorated even more in the delayed memory test when treated with a β-blocker (Gliebus and Lippa, 2007). On the other hand, treatment with a β-adrenoreceptor antagonist AR led to a better outcome in behavioural disturbances, e.g., aggression, in a nursing home for demented patients (Peskind et al., 2005). Another approach is the treatment by augmenting noradrenergic signaling. In a study conducted by Watson and colleagues, insulin treatment in people without dementia increased levels of NE as measured in the CSF and more importantly, better cognitive function was noted in these patients (Watson et al., 2006). However, hyperinsulinemia in another study increased the level of inflammatory markers in the CSF (Fishel et al., 2005).

11. ROLE OF NOREPINEPHRINE IN PARKINSON'S DISEASE

Idiopathic Parkinson's disease (PD) belongs to the group of movement disorders and affects about one percent of the population over the age of 50 years. Patients with PD may present with the cardinal symptoms of tremor, rigidity, bradykinesia, and loss of postural reflexes. Idiopathic PD is characterized neuropathologically by the degeneration of dopaminergic neurons in the substantia nigra pars compacta resulting in reduced levels of dopamine in the striatum. Affected neurons in the substantia nigra show intraneuronal inclusions, termed Lewy bodies. Lewy bodies are mainly composed of aggregated α-synuclein. The cardinal motor symptoms of PD do not become apparent until around 80% of the dopaminergic terminals have been lost.

However, besides symptoms involving the extrapyramidal system, many patients with PD show signs of non-motor symptoms. Neuropsychiatric symptoms like depression, apathy, dementia, hallucinations, and sleep disturbances such as rapid eye movement sleep disorder, restless legs and periodic limb movements and excessive daytime somnolence have also great significance in quality-of-life, hospitalisation rates, or social economic burden (Global Parkinson's Disease Survey Steering Committee , 2002) (Aarsland et al., 2000) (Witjas et al., 2002) (Chaudhuri et al., 2006). These clinical deficits clearly show that also other brain regions and neurotransmitters besides the substantia nigra and dopamine, respectively, may be of relevance in PD. Indeed, neuronal loss and the occurrence of Lewy-bodies have been described in many other brain regions of the brain (Braak et al., 2003).

Regarding the NE system, loss of neurons in the LC and the existence of Lewy bodies have been shown by analysis of post mortem brains of PD patients (Zarow et al., 2003) (Hoogendijk et al., 1995) (Jellinger, 1991) (Chan-Palay and Asan, 1989). Reduced levels of NE in addition to disturbances in other related neurotransmitter system like the serotonergic may account for clinically relevant symptoms like depression, dementia, sleep disorders and autonomic dysfunction seen in PD.

Besides its involvement in behavioural symptoms, there might exist in analogy to AD a direct effect of NE on the dopaminergic system and thereby involvement in the motor symptoms. There is some evidence, that NE neurons of the LC directly innervate midbrain dopaminergic neurons as stimulation of the LC facilitates firing of neurons of the substantia nigra (Grenhoff et al., 1993).

Neuroprotective and Anti-Inflammatory Effects of NE on the Dopaminergic System

Experimental lesions of the LC in animal models of PD exacerbate PD pathology and behavioural symptoms (Marien et al., 1993) (Mavridis et al., 1991) (Fornai et al., 1997) (Srinivasan and Schmidt, 2004a). This could imply, that loss of NE levels in the substantia nigra leads to an abolition of a neuroprotective effect of NE on dopaminergic neurons and render it more susceptible to disturbances in the homeostasis of the substantia nigra. This hypothesis is corroborated by findings in animal mouse models, in which higher NE levels protect dopaminergic neurons from damage (Kilbourn et al., 1998) (Rommelfanger et al., 2004) (Srinivasan and Schmidt, 2004b). Recovery of NE levels after an acute lesion of the LC

leads to a reversal of motor symptoms in an animal model of PD (Srinivasan and Schmidt, 2004c). In human post-mortem PD brains, brain regions with high NE levels showed less dopaminergic cell loss (Tong et al., 2006). The mechanism(s) for the observed neuroprotective effect of NE is unclear. One mechanism may be the role of NE as an endogenous anti-inflammatory agent as described earlier for AD. Microglial activation plays a pivotal role in mediating neuroinflammation and is observed in PD (McGeer et al., 1988) (Imamura et al., 2003) (Ouchi et al., 2005) (Sawada et al., 2006). As mentioned above, NE can downregulate the expression of inflammatory genes and NO (Mori et al., 2002) (Chang and Liu, 2000). Therefore, reduction of NE due to degeneration of NE neurons of the LC may be permissive for enhanced inflammatory responses and eventually resulting in neuronal cell death.

Besides its anti-inflammatory effect, NE might exert anti-oxidant properties. NE promotes survival and function of primary rat dopaminergic cells mesencephalic cells by reducing oxidative stress in vitro (Troadec et al., 2001). It has been proposed that dopaminergic cells are especially susceptive to oxidative stress in PD (Fahn and Sulzer, 2004).

NE may therefore be a target for a symptomatic therapy for some aspects of PD (Rye and DeLong, 2003). Increasing NE levels in the brain has the potential to slow down disease progression by protection of dopaminergic midbrain neurons and thereby improving motor symptoms but also to alleviate non-motor symptoms like depression and sleep disorders. A clinical trial with efaroxan, an α_2-adrenoreceptor antagonists, revealed positive results in management of bradykinesia and rigidity (Rascol et al., 1998). Reboxetin, a selective NE reuptake inhibitor showed good clinical efficacy in the treatment of depression without worsening of motor symptoms (Lemke, 2000). Enhancing NE content with methylphenidate, a dopamine and NE reuptake inhibitor, improved motor symptoms in patients with advanced stages of PD, also pointing at a connectivity between the dopaminergic and the NE systems (Devos et al., 2007). A beneficial effect of NE on L-DOPA induced dyskinesia has been suggested (Colosimo and Craus, 2003). On the other hand, blocking of NE release by administration of clonidin, an α_2-adrenoreceptor agonist, impairs attention in PD patients (Riekkinen et al., 1998).

12. NOREPINEPHRINE IN MULTIPLE SCLEROSIS

Norepinephrine has been suggested to have an immunosuppressive role in the brain as reviewed elsewhere (Feinstein et al., 2002). In *Multiple sclerosis*, the most common demyelinating disease of the CNS, inflammatory cell infiltration with recruitment of peripheral mononuclear cells from the blood, is a major pathological hallmark. In addition, microglia and astrocytes show evidence of immune activation. In this autoimmune disease, NE level alterations may also contribute to the disease pathogenesis. NE concentration in the grey matter regions of spinal cords of experimental autoimmune encephalomyelitis (EAE) rats, an animal model of multiple sclerosis, was found to be depleted (White et al., 1983). Pharmacological studies with β-adrenoreceptor agonists suppressed EAE symptoms (Wiegmann et al., 1995) (Chelmicka-Schorr et al., 1989). However, findings further strengthening a role of NE in patients with MS are scarce. Interestingly, in patients with MS

no β_2-adrenoreceptor was detected on astrocytes in normal appearing white matter and around plaques (De Keyser et al., 1999) (Zeinstra et al., 2000). The reason for this is not known yet. As mentioned above, NE may dampen the inflammatory response of glial cells astrocytes by inhibition of genes involved in the inflammatory response, i.e., iNOS, IL-1 and TNF-α. A down-regulation of the β_2-adrenergic receptor on astrocytes may increase the inflammatory response of astrocytes in brains of patients with multiple sclerosis and thereby contribute to the disease pathogenesis. Indeed, astrocytes in MS plaques express for example high levels of iNOS and NO may mediate demeyelination and axonal injury (Liu et al., 2001) (Smith and Lassmann, 2002). In the EAE mouse model, mice treated with venlafaxine, a serotonin/NE reuptake inhibitor showed down regulation of the inflammatory gene response (TNFα, IL-12) (Vollmar et al., 2008)

13. SUMMARY

As shown in various animal models of neurodegenerative disease, NE may have a direct effect on the pathogenesis of various neurodegenerative disorders. NE seems to exert anti-inflammatory and anti-oxidative effects and thereby influences neuroinflammation. Neuroinflammation emerges as a major player in the disease process of AD and PD. Deterioration of the NE system may increase neuroinflammation, thereby rendering certain neuronal cell population more endangered to degenerative processes. On the other hand, alterations in the NE system, contributes to the development of neuropsychiatric sequelae in patients with neurodegenerative diseases. Thus, development of regimes targeting the NE system may be helpful in the symptomatic treatment of cardinal and neuropsychiatric symptoms as seen in these diseases.

REFERENCES

Global Parkinson's Disease Survey Steering Committee (2002) Factors impacting on quality of life in Parkinson's disease: results from an international survey. *Mov. Disord.* 17:60-67.

Aarsland D, Larsen JP, Tandberg E, Laake K (2000) Predictors of nursing home placement in Parkinson's disease: a population-based, prospective study. *J. Am. Geriatr. Soc.* 48:938-942.

Adolfsson R, Gottfries CG, Roos BE, Winblad B (1979) Changes in the brain catecholamines in patients with dementia of Alzheimer type. *Br. J. Psychiatry* 135:216-223.

Arai H, Kosaka K, Iizuka R (1984) Changes of biogenic amines and their metabolites in postmortem brains from patients with Alzheimer-type dementia. *J. Neurochem.* 43:388-393.

Arai H, Ichimiya Y, Kosaka K, Moroji T, Iizuka R (1992) Neurotransmitter changes in early- and late-onset Alzheimer-type dementia. *Prog. Neuropsychopharmacol. Biol. Psychiatry* 16:883-890.

Baker GB, Reynolds GP (1989) Biogenic amines and their metabolites in Alzheimer's disease: noradrenaline, 5-hydroxytryptamine and 5-hydroxyindole-3-acetic acid depleted in hippocampus but not in substantia innominata. *Neurosci. Lett.* 100:335-339.

Beani L, Bianchi C, Giacomelli A, Tamberi F (1978) Noradrenaline inhibition of acetylcholine release from guinea-pig brain. *Eur. J. Pharmacol*. 48:179-193.

Belmaker RH, Agam G (2008) Major depressive disorder. *N. Engl. J. Med.* 358:55-68.

Bergquist J, Tarkowski A, Ekman R, Ewing A (1994) Discovery of endogenous catecholamines in lymphocytes and evidence for catecholamine regulation of lymphocyte function via an autocrine loop. *Proc. Natl. Acad. Sci. U S A* 91:12912-12916.

Bianchi C, Spidalieri G, Guandalini P, Tanganelli S, Beani L (1979) Inhibition of acetylcholine outflow from guinea-pig cerebral cortex following locus coeruleus stimulation. *Neurosci. Lett* 14:97-100.

Bondareff W, Mountjoy CQ, Roth M, Rossor MN, Iversen LL, Reynolds GP (1987a) Age and histopathologic heterogeneity in Alzheimer's disease. Evidence for subtypes. *Arch. Gen. Psychiatry* 44:412-417.

Bondareff W, Mountjoy CQ, Roth M, Rossor MN, Iversen LL, Reynolds GP, Hauser DL (1987b) Neuronal degeneration in locus ceruleus and cortical correlates of Alzheimer disease. *Alzheimer Dis. Assoc. Disord.* 1:256-262.

Braak H, Del Tredici K, Rub U, de Vos RA, Jansen Steur EN, Braak E (2003) Staging of brain pathology related to sporadic Parkinson's disease. *Neurobiol. Aging* 24:197-211.

Brookmeyer R, Johnson EC, Ziegler-Graham K, Arrighi HM (2007) Forecasting the global burden of Alzheimer's disease. *Alzheimer's and Dementia* 3.

Brown GC (2007) Mechanisms of inflammatory neurodegeneration: iNOS and NADPH oxidase. *Biochem. Soc. Trans*. 35:1119-1121.

Brown SW, Meyers RT, Brennan KM, Rumble JM, Narasimhachari N, Perozzi EF, Ryan JJ, Stewart JK, Fischer-Stenger K (2003) Catecholamines in a macrophage cell line. *J. Neuroimmunol.* 135:47-55.

Burke WJ, Li SW, Schmitt CA, Xia P, Chung HD, Gillespie KN (1999) Accumulation of 3,4-dihydroxyphenylglycolaldehyde, the neurotoxic monoamine oxidase A metabolite of norepinephrine, in locus ceruleus cell bodies in Alzheimer's disease: mechanism of neuron death. *Brain. Res.* 816:633-637.

Chan-Palay V, Asan E (1989) Alterations in catecholamine neurons of the locus coeruleus in senile dementia of the Alzheimer type and in Parkinson's disease with and without dementia and depression. *J. Comp. Neurol*. 287:373-392.

Chang JY, Liu LZ (2000) Catecholamines inhibit microglial nitric oxide production. *Brain Res. Bull.* 52:525-530.

Chaudhuri KR, Healy DG, Schapira AH (2006) Non-motor symptoms of Parkinson's disease: diagnosis and management. *Lancet Neurol.* 5:235-245.

Chelmicka-Schorr E, Kwasniewski MN, Thomas BE, Arnason BG (1989) The beta-adrenergic agonist isoproterenol suppresses experimental allergic encephalomyelitis in Lewis rats. *J. Neuroimmunol.* 25:203-207.

Colosimo C, Craus A (2003) Noradrenergic drugs for levodopa-induced dyskinesia. *Clin. Neuropharmacol.* 26:299-305.

Colton CA, Chernyshev ON (1996) Inhibition of microglial superoxide anion production by isoproterenol and dexamethasone. *Neurochem. Int* 29:43-53.

Cosentino M, Marino F, Bombelli R, Ferrari M, Lecchini S, Frigo G (1999) Endogenous catecholamine synthesis, metabolism, storage and uptake in human neutrophils. *Life Sci.* 64:975-981.

Cosentino M, Bombelli R, Ferrari M, Marino F, Rasini E, Maestroni GJ, Conti A, Boveri M, Lecchini S, Frigo G (2000) HPLC-ED measurement of endogenous catecholamines in human immune cells and hematopoietic cell lines. *Life Sci.* 68:283-295.

De Keyser J, Wilczak N, Leta R, Streetland C (1999) Astrocytes in multiple sclerosis lack beta-2 adrenergic receptors. *Neurology* 53:1628-1633.

Dello Russo C, Boullerne AI, Gavrilyuk V, Feinstein DL (2004) Inhibition of microglial inflammatory responses by norepinephrine: effects on nitric oxide and interleukin-1beta production. *J. Neuroinflammation* 1:9.

Devos D, Krystkowiak P, Clement F, Dujardin K, Cottencin O, Waucquier N, Ajebbar K, Thielemans B, Kroumova M, Duhamel A, Destee A, Bordet R, Defebvre L (2007) Improvement of gait by chronic, high doses of methylphenidate in patients with advanced Parkinson's disease. *J. Neurol. Neurosurg. Psychiatry* 78:470-475.

Elenkov IJ, Wilder RL, Chrousos GP, Vizi ES (2000) The sympathetic nerve--an integrative interface between two supersystems: the brain and the immune system. *Pharmacol. Rev.* 52:595-638.

Facchinetti F, Del Giudice E, Furegato S, Passarotto M, Arcidiacono D, Leon A (2004) Dopamine inhibits responses of astroglia-enriched cultures to lipopolysaccharide via a beta-adrenoreceptor-mediated mechanism. *J. Neuroimmunol*. 150:29-36.

Fahn S, Sulzer D (2004) Neurodegeneration and neuroprotection in Parkinson disease. *NeuroRx* 1:139-154.

Farber K, Pannasch U, Kettenmann H (2005) Dopamine and noradrenaline control distinct functions in rodent microglial cells. *Mol. Cell Neurosci.* 29:128-138.

Farmer P, Pugin J (2000) beta-adrenergic agonists exert their "anti-inflammatory" effects in monocytic cells through the IkappaB/NF-kappaB pathway. *Am. J. Physiol. Lung Cell Mol. Physiol.* 279:L675-682.

Feinstein DL (1998) Suppression of astroglial nitric oxide synthase expression by norepinephrine results from decreased NOS-2 promoter activity. *J. Neurochem.* 70:1484-1496.

Feinstein DL, Galea E, Reis DJ (1993) Norepinephrine suppresses inducible nitric oxide synthase activity in rat astroglial cultures. *J. Neurochem.* 60:1945-1948.

Feinstein DL, Heneka MT, Gavrilyuk V, Dello Russo C, Weinberg G, Galea E (2002) Noradrenergic regulation of inflammatory gene expression in brain. *Neurochem. Int.* 41:357-365.

Fishel MA, Watson GS, Montine TJ, Wang Q, Green PS, Kulstad JJ, Cook DG, Peskind ER, Baker LD, Goldgaber D, Nie W, Asthana S, Plymate SR, Schwartz MW, Craft S (2005) Hyperinsulinemia provokes synchronous increases in central inflammation and beta-amyloid in normal adults. *Arch. Neurol.* 62:1539-1544.

Flierl MA, Rittirsch D, Nadeau BA, Chen AJ, Sarma JV, Zetoune FS, McGuire SR, List RP, Day DE, Hoesel LM, Gao H, Van Rooijen N, Huber-Lang MS, Neubig RR, Ward PA (2007) Phagocyte-derived catecholamines enhance acute inflammatory injury. *Nature* 449:721-725.

Fornai F, Bassi L, Bonaccorsi I, Giorgi F, Corsini GU (1997) Noradrenaline loss selectivity exacerbates nigrostriatal toxicity in different species of rodents. *Funct. Neurol.* 12:193-198.

Forstl H, Burns A, Luthert P, Cairns N, Lantos P, Levy R (1992) Clinical and neuropathological correlates of depression in Alzheimer's disease. *Psychol. Med.* 22:877-884.

Freeman JG, Ryan JJ, Shelburne CP, Bailey DP, Bouton LA, Narasimhachari N, Domen J, Simeon N, Couderc F, Stewart JK (2001) Catecholamines in murine bone marrow derived mast cells. *J. Neuroimmunol.* 119:231-238.

Friedman JI, Adler DN, Davis KL (1999) The role of norepinephrine in the pathophysiology of cognitive disorders: potential applications to the treatment of cognitive dysfunction in schizophrenia and Alzheimer's disease. *Biol. Psychiatry* 46:1243-1252.

Fritschy JM, Grzanna R (1989) Immunohistochemical analysis of the neurotoxic effects of DSP-4 identifies two populations of noradrenergic axon terminals. *Neuroscience* 30:181-197.

Frohman EM, Vayuvegula B, Gupta S, van den Noort S (1988) Norepinephrine inhibits gamma-interferon-induced major histocompatibility class II (Ia) antigen expression on cultured astrocytes via beta-2-adrenergic signal transduction mechanisms. *Proc. Natl. Acad Sci. U S A* 85:1292-1296.

Garcia JJ, del Carmen Saez M, De la Fuente M, Ortega E (2003) Regulation of phagocytic process of macrophages by noradrenaline and its end metabolite 4-hydroxy-3-metoxyphenyl-glycol. Role of alpha- and beta-adrenoreceptors. *Mol. Cell Biochem.* 254:299-304.

Gliebus G, Lippa CF (2007) The influence of beta-blockers on delayed memory function in people with cognitive impairment. *Am. J. Alzheimers Dis. Other Demen*. 22:57-61.

Grenhoff J, Nisell M, Ferre S, Aston-Jones G, Svensson TH (1993) Noradrenergic modulation of midbrain dopamine cell firing elicited by stimulation of the locus coeruleus in the rat. *J. Neural Transm. Gen. Sect* 93:11-25.

Gresch PJ, Sved AF, Zigmond MJ, Finlay JM (1995) Local influence of endogenous norepinephrine on extracellular dopamine in rat medial prefrontal cortex. *J. Neurochem.* 65:111-116.

Grudzien A, Shaw P, Weintraub S, Bigio E, Mash DC, Mesulam MM (2007) Locus coeruleus neurofibrillary degeneration in aging, mild cognitive impairment and early Alzheimer's disease. *Neurobiol. Aging* 28:327-335.

Grzanna R, Berger U, Fritschy JM, Geffard M (1989) Acute action of DSP-4 on central norepinephrine axons: biochemical and immunohistochemical evidence for differential effects. *J. Histochem. Cytochem.* 37:1435-1442.

Haglund M, Sjobeck M, Englund E (2006) Locus ceruleus degeneration is ubiquitous in Alzheimer's disease: possible implications for diagnosis and treatment. *Neuropathology* 26:528-532.

Hardy J, Allsop D (1991) Amyloid deposition as the central event in the aetiology of Alzheimer's disease. *Trends Pharmacol. Sci.* 12:383-388.

Hardy J, Selkoe DJ (2002) The amyloid hypothesis of Alzheimer's disease: progress and problems on the road to therapeutics. *Science* 297:353-356.

Harmon EB, Porter JM, Porter JE (2005) Beta-adrenergic receptor activation in immortalized human urothelial cells stimulates inflammatory responses by PKA-independent mechanisms. *Cell Commun. Signal.* 3:10.

Hasko G (2001) Receptor-mediated interaction between the sympathetic nervous system and immune system in inflammation. *Neurochem. Res*. 26:1039-1044.

Hein P, Michel MC (2007) Signal transduction and regulation: are all alpha1-adrenergic receptor subtypes created equal? *Biochem. Pharmacol.* 73:1097-1106.

Hein P, Rochais F, Hoffmann C, Dorsch S, Nikolaev VO, Engelhardt S, Berlot CH, Lohse MJ, Bunemann M (2006) Gs activation is time-limiting in initiating receptor-mediated signaling. *J. Biol. Chem.* 281:33345-33351.

Heneka MT, O'Banion MK (2007) Inflammatory processes in Alzheimer's disease. *J. Neuroimmunol.* 184:69-91.

Heneka MT, Gavrilyuk V, Landreth GE, O'Banion MK, Weinberg G, Feinstein DL (2003) Noradrenergic depletion increases inflammatory responses in brain: effects on IkappaB and HSP70 expression. *J. Neurochem.* 85:387-398.

Heneka MT, Galea E, Gavriluyk V, Dumitrescu-Ozimek L, Daeschner J, O'Banion MK, Weinberg G, Klockgether T, Feinstein DL (2002) Noradrenergic depletion potentiates beta -amyloid-induced cortical inflammation: implications for Alzheimer's disease. *J. Neurosci.* 22:2434-2442.

Heneka MT, Ramanathan M, Jacobs AH, Dumitrescu-Ozimek L, Bilkei-Gorzo A, Debeir T, Sastre M, Galldiks N, Zimmer A, Hoehn M, Heiss WD, Klockgether T, Staufenbiel M (2006) Locus ceruleus degeneration promotes Alzheimer pathogenesis in amyloid precursor protein 23 transgenic mice. *J. Neurosci.* 26:1343-1354.

Hertz L, Schousboe I, Hertz L, Schousboe A (1984) Receptor expression in primary cultures of neurons or astrocytes. *Prog. Neuropsychopharmacol. Biol. Psychiatry* 8:521-527.

Hetier E, Ayala J, Bousseau A, Prochiantz A (1991) Modulation of interleukin-1 and tumor necrosis factor expression by beta-adrenergic agonists in mouse ameboid microglial cells. *Exp. Brain Res*. 86:407-413.

Hoogendijk WJ, Pool CW, Troost D, van Zwieten E, Swaab DF (1995) Image analyser-assisted morphometry of the locus coeruleus in Alzheimer's disease, Parkinson's disease and amyotrophic lateral sclerosis. *Brain* 118 (Pt 1):131-143.

Hoogendijk WJ, Feenstra MG, Botterblom MH, Gilhuis J, Sommer IE, Kamphorst W, Eikelenboom P, Swaab DF (1999) Increased activity of surviving locus ceruleus neurons in Alzheimer's disease. *Ann. Neurol.* 45:82-91.

Hoozemans JJ, O'Banion MK (2005) The role of COX-1 and COX-2 in Alzheimer's disease pathology and the therapeutic potentials of non-steroidal anti-inflammatory drugs. *Curr. Drug Targets CNS Neurol. Disord*. 4:307-315.

Ichimiya Y, Arai H, Kosaka K, Iizuka R (1986) Morphological and biochemical changes in the cholinergic and monoaminergic systems in Alzheimer-type dementia. *Acta Neuropathol.* 70:112-116.

Imamura K, Hishikawa N, Sawada M, Nagatsu T, Yoshida M, Hashizume Y (2003) Distribution of major histocompatibility complex class II-positive microglia and cytokine profile of Parkinson's disease brains. *Acta Neuropathol.* 106:518-526.

Iversen LL, Rossor MN, Reynolds GP, Hills R, Roth M, Mountjoy CQ, Foote SL, Morrison JH, Bloom FE (1983) Loss of pigmented dopamine-beta-hydroxylase positive cells from locus coeruleus in senile dementia of Alzheimer's type. *Neurosci. Lett.* 39:95-100.

Javierre MQ, Pinto LV, Lima AO, Sassine WA (1975) Immunologic phagocytosis by macrophages: effect by stimulation of alpha adrenergic receptors. *Rev. Bras. Pesqui. Med Biol.* 8:271-274.

Jellinger KA (1991) Pathology of Parkinson's disease. Changes other than the nigrostriatal pathway. *Mol. Chem. Neuropathol.* 14:153-197.

Josefsson E, Bergquist J, Ekman R, Tarkowski A (1996) Catecholamines are synthesized by mouse lymphocytes and regulate function of these cells by induction of apoptosis. *Immunology* 88:140-146.

Kalaria RN, Andorn AC, Tabaton M, Whitehouse PJ, Harik SI, Unnerstall JR (1989) Adrenergic receptors in aging and Alzheimer's disease: increased beta 2-receptors in prefrontal cortex and hippocampus. *J. Neurochem.* 53:1772-1781.

Kalinin S, Gavrilyuk V, Polak PE, Vasser R, Zhao J, Heneka MT, Feinstein DL (2007) Noradrenaline deficiency in brain increases beta-amyloid plaque burden in an animal model of Alzheimer's disease. *Neurobiol. Aging.* 28:1206-1214.

Kilbourn MR, Sherman P, Abbott LC (1998) Reduced MPTP neurotoxicity in striatum of the mutant mouse tottering. *Synapse* 30:205-210.

Klotz L, Sastre M, Kreutz A, Gavrilyuk V, Klockgether T, Feinstein DL, Heneka MT (2003) Noradrenaline induces expression of peroxisome proliferator activated receptor gamma (PPARgamma) in murine primary astrocytes and neurons. *J. Neurochem.* 86:907-916.

Koff WC, Dunegan MA (1985) Modulation of macrophage-mediated tumoricidal activity by neuropeptides and neurohormones. *J. Immunol*. 135:350-354.

Lemke MR (2000) Reboxetine treatment of depression in Parkinson's disease. *J. Clin. Psychiatry* 61:872.

Lindenmayer JP (2000) The pathophysiology of agitation. *J. Clin. Psychiatry* 61 Suppl 14:5-10.

Liu JS, Zhao ML, Brosnan CF, Lee SC (2001) Expression of inducible nitric oxide synthase and nitrotyrosine in multiple sclerosis lesions. *Am. J. Pathol*. 158:2057-2066.

Lucas SM, Rothwell NJ, Gibson RM (2006) The role of inflammation in CNS injury and disease. *Br. J. Pharmacol.* 147 Suppl 1:S232-240.

Madrigal JL, Feinstein DL, Dello Russo C (2005) Norepinephrine protects cortical neurons against microglial-induced cell death. *J. Neurosci. Res.* 81:390-396.

Magnuson DS, Staines WA, Marshall KC (1993) Electrophysiological changes accompanying DSP-4 lesions of rat locus coeruleus neurons. *Brain Res.* 628:317-320.

Maimone D, Cioni C, Rosa S, Macchia G, Aloisi F, Annunziata P (1993) Norepinephrine and vasoactive intestinal peptide induce IL-6 secretion by astrocytes: synergism with IL-1 beta and TNF alpha. *J. Neuroimmunol.* 47:73-81.

Mann DM, Yates PO, Hawkes J (1982) The noradrenergic system in Alzheimer and multi-infarct dementias. *J. Neurol. Neurosurg. Psychiatry* 45:113-119.

Mann DM, Yates PO, Hawkes J (1983) The pathology of the human locus ceruleus. *Clin. Neuropathol*. 2:1-7.

Mann DM, Lincoln J, Yates PO, Stamp JE, Toper S (1980) Changes in the monoamine containing neurones of the human CNS in senile dementia. Br J Psychiatry 136:533-541.

Marcyniuk B, Mann DM, Yates PO (1986) Loss of nerve cells from locus coeruleus in Alzheimer's disease is topographically arranged. *Neurosci. Lett* 64:247-252.

Marien M, Briley M, Colpaert F (1993) Noradrenaline depletion exacerbates MPTP-induced striatal dopamine loss in mice. *Eur.J. Pharmacol.* 236:487-489.

Marino F, Cosentino M, Bombelli R, Ferrari M, Lecchini S, Frigo G (1999) Endogenous catecholamine synthesis, metabolism storage, and uptake in human peripheral blood mononuclear cells. *Exp. Hematol.* 27:489-495.

Matthews KL, Chen CP, Esiri MM, Keene J, Minger SL, Francis PT (2002) Noradrenergic changes, aggressive behavior, and cognition in patients with dementia. *Biol. Psychiatry* 51:407-416.

Mavridis M, Degryse AD, Lategan AJ, Marien MR, Colpaert FC (1991) Effects of locus coeruleus lesions on parkinsonian signs, striatal dopamine and substantia nigra cell loss after 1-methyl-4-phenyl-1,2,3,6-tetrahydropyridine in monkeys: a possible role for the locus coeruleus in the progression of Parkinson's disease. *Neuroscience* 41:507-523.

McGeer PL, Itagaki S, Boyes BE, McGeer EG (1988) Reactive microglia are positive for HLA-DR in the substantia nigra of Parkinson's and Alzheimer's disease brains. *Neurology* 38:1285-1291.

Meana JJ, Barturen F, Garro MA, Garcia-Sevilla JA, Fontan A, Zarranz JJ (1992) Decreased density of presynaptic alpha 2-adrenoceptors in postmortem brains of patients with Alzheimer's disease. *J. Neurochem.* 58:1896-1904.

Melia KR, Duman RS (1991) Involvement of corticotropin-releasing factor in chronic stress regulation of the brain noradrenergic system. *Proc. Natl. Acad. Sci. U S A* 88:8382-8386.

Minghetti L, Levi G (1995) Induction of prostanoid biosynthesis by bacterial lipopolysaccharide and isoproterenol in rat microglial cultures. *J. Neurochem.* 65:2690-2698.

Mori K, Ozaki E, Zhang B, Yang L, Yokoyama A, Takeda I, Maeda N, Sakanaka M, Tanaka J (2002) Effects of norepinephrine on rat cultured microglial cells that express alpha1, alpha2, beta1 and beta2 adrenergic receptors. *Neuropharmacology* 43:1026-1034.

Murphy DL, Andrews AM, Wichems CH, Li Q, Tohda M, Greenberg B (1998) Brain serotonin neurotransmission: an overview and update with an emphasis on serotonin subsystem heterogeneity, multiple receptors, interactions with other neurotransmitter systems, and consequent implications for understanding the actions of serotonergic drugs. *J. Clin. Psychiatry* 59 Suppl 15:4-12.

Musso NR, Brenci S, Setti M, Indiveri F, Lotti G (1996) Catecholamine content and in vitro catecholamine synthesis in peripheral human lymphocytes. *J. Clin. Endocrinol. Metab.* 81:3553-3557.

Nakamura A, Johns EJ, Imaizumi A, Abe T, Kohsaka T (1998) Regulation of tumour necrosis factor and interleukin-6 gene transcription by beta2-adrenoceptor in the rat astrocytes. *J. Neuroimmunol.* 88:144-153.

Nazarali AJ, Reynolds GP (1992) Monoamine neurotransmitters and their metabolites in brain regions in Alzheimer's disease: a postmortem study. *Cell. Mol. Neurobiol.* 12:581-587.

Nieuwenhuys R (1984) Chemoarchitecture of the brain.: Springer Verlag.

Norris JG, Benveniste EN (1993) Interleukin-6 production by astrocytes: induction by the neurotransmitter norepinephrine. *J. Neuroimmunol.* 45:137-145.

Ohara K, Kondo N (1998) Changes of monoamines in post-mortem brains from patients with diffuse Lewy body disease. *Prog. Neuropsychopharmacol. Biol. Psychiatry* 22:311-317.

Oishi M, Mochizuki Y, Yoshihashi H, Takasu T, Nakano E (1996) Laboratory examinations correlated with severity of dementia. *Ann. Clin. Lab. Sci.* 26:340-345.

Olpe HR, Laszlo J, Dooley DJ, Heid J, Steinmann MW (1983) Decreased activity of locus coeruleus neurons in the rat after DSP-4 treatment. *Neurosci. Lett* 40:81-84.

Ouchi Y, Yoshikawa E, Sekine Y, Futatsubashi M, Kanno T, Ogusu T, Torizuka T (2005) Microglial activation and dopamine terminal loss in early Parkinson's disease. *Ann. Neurol*. 57:168-175.

Pahan K, Namboodiri AM, Sheikh FG, Smith BT, Singh I (1997) Increasing cAMP attenuates induction of inducible nitric-oxide synthase in rat primary astrocytes. *J. Biol. Chem.* 272:7786-7791.

Palmer AM, Francis PT, Bowen DM, Benton JS, Neary D, Mann DM, Snowden JS (1987) Catecholaminergic neurones assessed ante-mortem in Alzheimer's disease. *Brain Res.* 414:365-375.

Peskind ER, Tsuang DW, Bonner LT, Pascualy M, Riekse RG, Snowden MB, Thomas R, Raskind MA (2005) Propranolol for disruptive behaviors in nursing home residents with probable or possible Alzheimer disease: a placebo-controlled study. *Alzheimer Dis. Assoc. Disord.* 19:23-28.

Powers RE, Struble RG, Casanova MF, O'Connor DT, Kitt CA, Price DL (1988) Innervation of human hippocampus by noradrenergic systems: normal anatomy and structural abnormalities in aging and in Alzheimer's disease. *Neuroscience* 25:401-417.

Prinz M, Hausler KG, Kettenmann H, Hanisch U (2001) beta-adrenergic receptor stimulation selectively inhibits IL-12p40 release in microglia. *Brain Res.* 899:264-270.

Rascol O, Sieradzan K, Peyro-Saint-Paul H, Thalamas C, Brefel-Courbon C, Senard JM, Ladure P, Montastruc JL, Lees A (1998) Efaroxan, an alpha-2 antagonist, in the treatment of progressive supranuclear palsy. *Mov. Disord.* 13:673-676.

Reinikainen KJ, Paljarvi L, Huuskonen M, Soininen H, Laakso M, Riekkinen PJ (1988) A post-mortem study of noradrenergic, serotonergic and GABAergic neurons in Alzheimer's disease. *J. Neurol. Sci.* 84:101-116.

Richards EM, Sumners C, Chou YC, Raizada MK, Phillips MI (1989) Alpha 2-adrenergic receptors in neuronal and glial cultures: characterization and comparison. *J. Neurochem.* 53:287-296.

Riekkinen M, Kejonen K, Jakala P, Soininen H, Riekkinen P, Jr. (1998) Reduction of noradrenaline impairs attention and dopamine depletion slows responses in Parkinson's disease. *Eur. J. Neurosci.* 10:1429-1435.

Rommelfanger KS, Weinshenker D, Miller GW (2004) Reduced MPTP toxicity in noradrenaline transporter knockout mice. *J. Neurochem.* 91:1116-1124.

Russo-Neustadt A, Cotman CW (1997) Adrenergic receptors in Alzheimer's disease brain: selective increases in the cerebella of aggressive patients. *J. Neurosci.* 17:5573-5580.

Rye D, DeLong MR (2003) Time to focus on the locus. *Arch. Neurol*. 60:320.

Sawada M, Imamura K, Nagatsu T (2006) Role of cytokines in inflammatory process in Parkinson's disease. *J. Neural Transm. Suppl*.:373-381.

Sekut L, Champion BR, Page K, Menius JA, Jr., Connolly KM (1995) Anti-inflammatory activity of salmeterol: down-regulation of cytokine production. *Clin. Exp. Immunol.* 99:461-466.

Severn A, Rapson NT, Hunter CA, Liew FY (1992) Regulation of tumor necrosis factor production by adrenaline and beta-adrenergic agonists. *J. Immunol.* 148:3441-3445.

Smith KJ, Lassmann H (2002) The role of nitric oxide in multiple sclerosis. *Lancet Neurol.* 1:232-241.

Soininen H, Reinikainen K, Partanen J, Mervaala E, Paljarvi L, Helkala EL, Riekkinen P, Sr. (1992) Slowing of the dominant occipital rhythm in electroencephalogram is associated with low concentration of noradrenaline in the thalamus in patients with Alzheimer's disease. *Neurosci. Lett* 137:5-8.

Spengler RN, Allen RM, Remick DG, Strieter RM, Kunkel SL (1990) Stimulation of alpha-adrenergic receptor augments the production of macrophage-derived tumor necrosis factor. *J. Immunol.* 145:1430-1434.

Spengler RN, Chensue SW, Giacherio DA, Blenk N, Kunkel SL (1994) Endogenous norepinephrine regulates tumor necrosis factor-alpha production from macrophages in vitro. *J. Immunol*. 152:3024-3031.

Srinivasan J, Schmidt WJ (2004a) Behavioral and neurochemical effects of noradrenergic depletions with N-(2-chloroethyl)-N-ethyl-2-bromobenzylamine in 6-hydroxydopamine-induced rat model of Parkinson's disease. *Behav. Brain Res.* 151:191-199.

Srinivasan J, Schmidt WJ (2004b) Treatment with alpha2-adrenoceptor antagonist, 2-methoxy idazoxan, protects 6-hydroxydopamine-induced Parkinsonian symptoms in rats: neurochemical and behavioral evidence. *Behav. Brain Res.* 154:353-363.

Srinivasan J, Schmidt WJ (2004c) Functional recovery of locus coeruleus noradrenergic neurons after DSP-4 lesion: effects on dopamine levels and neuroleptic induced-parkinsonian symptoms in rats. *J. Neural Transm.* 111:13-26.

Szot P, White SS, Greenup JL, Leverenz JB, Peskind ER, Raskind MA (2006) Compensatory changes in the noradrenergic nervous system in the locus ceruleus and hippocampus of postmortem subjects with Alzheimer's disease and dementia with Lewy bodies. *J. Neurosci*. 26:467-478.

Tan KS, Nackley AG, Satterfield K, Maixner W, Diatchenko L, Flood PM (2007) Beta2 adrenergic receptor activation stimulates pro-inflammatory cytokine production in macrophages via PKA- and NF-kappaB-independent mechanisms. *Cell Signal* 19:251-260.

Tanaka KF, Kashima H, Suzuki H, Ono K, Sawada M (2002) Existence of functional beta1- and beta2-adrenergic receptors on microglia. *J. Neurosci. Res.* 70:232-237.

Tomozawa Y, Inoue T, Satoh M (1995) Expression of type I interleukin-1 receptor mRNA and its regulation in cultured astrocytes. *Neurosci. Lett.* 195:57-60.

Tong J, Hornykiewicz O, Kish SJ (2006) Inverse relationship between brain noradrenaline level and dopamine loss in Parkinson disease: a possible neuroprotective role for noradrenaline. *Arch. Neurol.* 63:1724-1728.

Troadec JD, Marien M, Darios F, Hartmann A, Ruberg M, Colpaert F, Michel PP (2001) Noradrenaline provides long-term protection to dopaminergic neurons by reducing oxidative stress. *J. Neurochem.* 79:200-210.

van der Poll T, Jansen J, Endert E, Sauerwein HP, van Deventer SJ (1994) Noradrenaline inhibits lipopolysaccharide-induced tumor necrosis factor and interleukin 6 production in human whole blood. *Infect. Immun.* 62:2046-2050.

Van Wagoner NJ, Benveniste EN (1999) Interleukin-6 expression and regulation in astrocytes. *J. Neuroimmunol.* 100:124-139.

Vizi ES, Pasztor E (1981) Release of acetylcholine from isolated human cortical slices: inhibitory effect of norepinephrine and phenytoin. *Exp. Neurol.* 73:144-153.

Vollmar P, Nessler S, Kalluri SR, Hartung HP, Hemmer B (2008) The antidepressant venlafaxine ameliorates murine experimental autoimmune encephalomyelitis by suppression of pro-inflammatory cytokines. *Int J. Neuropsychopharmacol*.:1-12.

Watson GS, Bernhardt T, Reger MA, Cholerton BA, Baker LD, Peskind ER, Asthana S, Plymate SR, Frolich L, Craft S (2006) Insulin effects on CSF norepinephrine and cognition in Alzheimer's disease. *Neurobiol. Aging* 27:38-41.

White SR, Bhatnagar RK, Bardo MT (1983) Norepinephrine depletion in the spinal cord gray matter of rats with experimental allergic encephalomyelitis. *J. Neurochem.* 40:1771-1773.

Whitehouse PJ, Price DL, Struble RG, Clark AW, Coyle JT, Delon MR (1982) Alzheimer's disease and senile dementia: loss of neurons in the basal forebrain. *Science* 215:1237-1239.

Wiegmann K, Muthyala S, Kim DH, Arnason BG, Chelmicka-Schorr E (1995) Beta-adrenergic agonists suppress chronic/relapsing experimental allergic encephalomyelitis (CREAE) in Lewis rats. *J. Neuroimmunol.* 56:201-206.

Wilcock GK, Esiri MM, Bowen DM, Hughes AO (1988) The differential involvement of subcortical nuclei in senile dementia of Alzheimer's type. *J. Neurol. Neurosurg. Psychiatry* 51:842-849.

Winkeler A, Waerzeggers Y, Klose A, Monfared P, Thomas AV, Schubert M, Heneka MT, Jacobs AH (2008) Imaging noradrenergic influence on amyloid pathology in mouse models of Alzheimer's disease. *Eur. J. Nucl. Med. Mol. Imaging* 35 Suppl 1:S107-113.

Witjas T, Kaphan E, Azulay JP, Blin O, Ceccaldi M, Pouget J, Poncet M, Cherif AA (2002) Nonmotor fluctuations in Parkinson's disease: frequent and disabling. *Neurology* 59:408-413.

Yang Y, Schmitt HP (2001) Frontotemporal dementia: evidence for impairment of ascending serotoninergic but not noradrenergic innervation. Immunocytochemical and quantitative study using a graph method. *Acta Neuropathol.* 101:256-270.

Yates CM, Simpson J, Gordon A, Maloney AF, Allison Y, Ritchie IM, Urquhart A (1983) Catecholamines and cholinergic enzymes in pre-senile and senile Alzheimer-type dementia and Down's syndrome. *Brain Res.* 280:119-126.

Zarow C, Lyness SA, Mortimer JA, Chui HC (2003) Neuronal loss is greater in the locus coeruleus than nucleus basalis and substantia nigra in Alzheimer and Parkinson diseases. *Arch. Neurol*. 60:337-341.

Zeinstra E, Wilczak N, Streefland C, De Keyser J (2000) Astrocytes in chronic active multiple sclerosis plaques express MHC class II molecules. *Neuroreport* 11:89-91.

Zubenko GS, Moossy J (1988) Major depression in primary dementia. Clinical and neuropathologic correlates. *Arch. Neurol.* 45:1182-1186.

Zubenko GS, Moossy J, Kopp U (1990) Neurochemical correlates of major depression in primary dementia. *Arch. Neurol.* 47:209-214.

In: Biochemistry and Histocytochemistry… ISBN: 978-1-60876-283-5
Editors: S. Fuchs, M. Auer, pp. 25-44 © 2010 Nova Science Publishers, Inc.

Chapter 2

THE ROLE OF NORADRENALINE ON INTERPERSONAL FUNCTIONING

Wai S. Tse [*] ***and Alyson J. Bond***
Department of Applied Social Studies, City University of Hong Kong,
Tat Chee Ave., Hong Kong, China
National Addiction Centre, Institute of Psychiatry, King's College London,
London, United Kingdom

ABSTRACT

The aim of this chapter is to examine the role of noradrenaline in interpersonal functioning. Healthy interpersonal functioning is important for the development of relationships in both work and personal situations. Many psychiatric disorders including depression are associated with poor interpersonal functioning and less social activity but improvement in interpersonal functioning can be independent of symptom resolution. Noradrenaline may be involved in the adaptive function of human social behaviours.

Concepts relevant to interpersonal behaviours leading to interpersonal rejection and the relationship between social skills and depression will be briefly reviewed. Then the methodology involved in this type of research will be described. This will involve both techniques developed to measure interpersonal functioning, from questionnaires to laboratory tasks, and psychotropic drugs which have been used to study noradrenergic function.

Using these methodologies, experimental results showing specific effects related to noradrenaline in both clinical and experimental studies will be described. Reboxetine has been shown to be associated with increased cooperative behaviour and other socially adaptive behaviours.

It is concluded that noradrenaline modulates cooperation and other socially adaptive behaviours and this action may promote friendship formation and facilitate social support.

[*] Correspondence information: Email-tse.vincent@cityu.edu.hk, Address: Department of Applied Social Studies, City University of Hong Kong, Tat Chee Ave., Kowloon, Hong Kong.

I .WHAT IS INTERPERSONAL FUNCTIONING?

A. Importance of Healthy Interpersonal Functioning for Relationship Formation and Social Support

Having good interpersonal functioning is important for psychological well-being. Interpersonal functioning encompasses the concepts of social support and meaningful close relationships. Good functioning has been suggested to have a stress-buffering function to reduce pressure and tension and protect against the development of serious mental disorders. For example, in an important study (Cohen et al., 1986), 188 university students were asked to fill in questionnaires measuring their social support, depression and social skills in three separate sessions. The interval between sessions was 11 weeks. Those who reported more perceived social support were found to have lower depression scores.

Thus, according to the stress-buffering model, the beneficial effects of social support on depression are exerted by a reduction of stress (Dean and Lin, 1977). In contrast to this hypothesis, other evidence suggests that social support exerts direct positive effects on depression rather than mitigating the negative impact of stress. For example, Dean and Ensel (1982) found that there were no significant interaction effects between social support and stress in predicting depression. Furthermore, Aneshensel and Stone (1982) found that social support did not influence the impact of stress on depression. In their analysis, it was found that depression was independently related to stress and social support. In fact, no significant interaction between social support and stress was found to predict depression. Thus, social support may not principally reduce depressive symptoms by the reduction of stress.

There are two main concepts of interpersonal functioning: the quantitative and qualitative aspects. Quantitative refers to social network size. In some studies, it was found that depressed patients had significantly smaller social network sizes as compared to healthy controls (e.g. Flaherty et al., 1983). However, contradicting results were also found (e.g. Schaefer et al., 1981). It has been pointed out that this aspect of interpersonal functioning may not be an appropriate measure to indicate the positive effects of social support (Leavy, 1983; Brugha, 1984). In fact, increased network size might actually produce some negative influences. For example, Schaefer et al. (1981) and Blazer (1983) suggested that increased social network size could also increase negative interpersonal events, which might counteract the potential positive effects of social support. According to another strand of research, the positive effects of interpersonal functioning are thought to relate more closely to the qualitative aspect e.g. closeness of relationship.

Weiss (1974) proposes six elements of social relationships which are important for maintaining psychological well-being: attachment, social integration, opportunity for nurturance, reassurance of worth, a sense of reliable alliance, and obtaining guidance. Thus, social relationships that provide a sense of worth or attachment would be protective against the development of depression. In the same vein, Oatley and Bolton (1985) suggest that if a person lacks alternative sources of self-definition and at the same time an event occurs that is likely to disrupt the roles by which people define their worth, he/she would be more likely to develop depression. Evidence to support this notion comes from research conducted by Bolton and Oatley (1987). They found that unemployed people were more likely to become depressed if they had little social contact with others. Furthermore, the authors point out that

social contact supplied an alternative source of sense of worth to that which the unemployed person had lost. Similarly, Mallinckrodt and Fretz (1988) found that social support offering reassurance of worth was important in lowering stress symptoms.

The benefit of social support is clear and Vinokur et al. (1987) suggested that social support is an interpersonal transaction. People are therefore able to elicit behaviour from others to assure them of their sense of worth. As suggested by Pearlin et al. (1981) such interpersonal transactions might be dependent on the extent of the relationship. Alternatively, Mallinckrodt and Fretz (1988) proposed that those who share common values and interests provide reassurance between themselves and that these shared values and interests are the key determinants for building a meaningful relationship with others. Therefore, being able to develop a close friendship with others is important in interpersonal functioning. One important factor in friendship formation is the possession of adequate social skills. Cohen et al. (1986) reported that improved social skills were associated with an increase in friendships and perceived social support. In line with this finding, Cole and Milstead (1989), using Structural Equation Modelling, showed that social skills had a strong influence on social support (beta = 0.70). Therefore, social skills are an important determinant of friendship development, which subsequently influence interpersonal functioning.

B. Relationship between Depression and Interpersonal Functioning Deficits

Interpersonal behavioural deficits are common in many psychiatric conditions, including schizophrenia (Haley, 1985), depression (Coyne, 1976a; Libet, and Lewinsohn, 1973; Gurtman, 1987), mania (DSM-IV), attention deficit hyperactivity disorder (ADHD, Alessandri, 1992) and autism (VanMeter et al., 1997). These deficits might contribute to poor interpersonal functioning and they might also result in reduction of social support. Therefore, studying interpersonal behaviours should significantly contribute to our understanding of the micro-mechanism of interpersonal functioning related to different psychiatric illnesses.

According to research conducted in depressed patients, deficits in social skill behaviours can be categorised into two dimensions: activity and involvement. Many research findings have shown that depressed patients are less active: they talk less, show less eye contact, and smile less. This kind of social behaviour has been described as passive and uninvolved and could lead to rejection by the other person in a dyadic social interaction. In contrast, according to one of the major classification system (DSM-IV; APA, 1994), the communication behaviour of manic patients is characterised as joking, punning, and amusing irrelevancies. This behaviour might also negatively affect interpersonal interaction leading to social rejection and poor interpersonal functioning as in the case of depression and could be recognised as the active counterpart of a depressed communication style. Therefore both too little and too much activity are harmful to interpersonal functioning. People with healthy interpersonal behaviours might be warm and sociable and therefore active and involved in conversations with a social partner, or they might be shy and quiet and therefore passive but involved (Sacks and Bugental, 1987).

Much research has focused on the relationship between interpersonal functioning and depression. It has been found that depressed patients show more problems in their interpersonal functioning (Flaherty et al., 1983; Friedman, 1993; Klerman, 1989). They engage less in social activities, such as visiting friends/relatives and they enjoy their work

less. Problems in interpersonal functioning may persist for years, even after symptom resolution (Hirschfeld et al. 2000). In fact, Hammen and Brenman (2002) suggested that interpersonal dysfunction is a stable trait for people with clinical depression. Therefore, it remains unclear whether reduced interpersonal functioning precedes or is a consequence of depression. However, the common consensus is that psychosocial functioning does play a role in the mechanism of depressive disorders.

Flaherty et al. (1983) found that social functioning had a strong negative relationship with the social network of depressed patients; the larger the social network, the less likely patients were to be depressed. On the other hand, poor social functioning might be indicative of more interpersonal stress. However, the detailed mechanism of how the social network affects depressive symptoms is not clear. One of the reasons for this lies in the definition of social functioning. The concept of social functioning encompasses many different facets of social behaviour. Tyrer and Casey (1993) suggest that social functioning contains six features: co-operation, affability, bonding, community, status, and class. These six features could be grouped into two categories. The first three features would be related to interpersonal functioning such as social network and relationships, and the others would be related to societal functioning such as social role or standing within society. These different aspects of interpersonal functioning might affect depressive disorders differently. For example, Plant and Sachs-Ericsson (2004) reported that having stronger social support from a close friend could reduce stress. In the following section, we focus on aspects of interpersonal functioning.

II. HOW TO MEASURE INTERPERSONAL FUNCTIONING?

A. Measures of Global Interpersonal Functioning:

Interpersonal functioning has been a topic of clinical study. The concepts of interpersonal functioning are many and there is no common definition. In general, interpersonal functioning is understood to indicate the ability of a person to form positive social relationships that might be reflected in the social support they receive from friends and family members, the closeness of their relationships with others, and the motivation to form supportive friendly relationships with others.

In this review, we describe 3 questionnaires commonly used to measure an individual's interpersonal functioning: the interview schedule for social interaction, the revised social adjustment scale, and the social adaptation self-evaluation scale. These 3 questionnaires differ both in their theoretical underpinnings and their item structure and so it can be concluded that they measure different aspects of the interpersonal functioning of an individual.

I) Interview Schedule for Social Interaction

Building upon the hypothesis that deep and meaningful social relationships have a protective role against neurosis, Henderson et al. (1980) developed the interview schedule for social interaction (ISSI). Six benefits were believed to be found in a meaningful relationship including: (1) a sense of attachment and security, (2) social integration, (3) provision of reassurance as to one's personal worth, (4) a sense of reliable alliance, (5) the opportunity to

care for others and (6) availability of help and guidance. The interview takes 45 minutes to finish. In their psychometric analysis, Henderson et al. (1980) noted that the reassurance and reliable alliance dimensions could not be measured reliably and that they might be confounded with the concept of friendship. Furthermore, validity of the dimension, the opportunity to care for others, was weak. Despite these psychometric weaknesses, McDowell (1987) recommended this as one of the best scales to measure social support.

Based on Henderson et al.'s work, an abbreviated version of the ISSI has been developed by Unden and Orth-Gomer (1989) which contains two dimensions: availability of social integration (AVSI) and availability of attachment (AVA). The AVSI measures superficial relationships and support. It simply focuses on the quantity or number of relationships which would be a weak predictor of future psychological health. However, the AVA measures the availability of deep relationships: with close friends, family members and spouses who could provide emotional support. The AVA purports to be a good predictor of resistance to psychological stress.

II) Social Adjustment Scale-Revised

Weissman and Paykel (1974) revised a previously developed questionnaire to assess the performance of individuals in different roles, called the social adjustment scale (SAS-R). These roles included: (1) work, (2) housework, (3) parental role, (4) social leisure activities, (5) extended family relationships, (6) marital relationship, and (7) family unit. Functioning in the last four roles is an important indicator of interpersonal functioning. Having deep relationships outside the immediate family helps an individual to draw more social support. Furthermore, the success of relationships outside the family indicates that the person possesses competent social skills and is able to form and maintain meaningful relationships with others. Marital and familial relationships were the resources most easily accessible to the individuals. However, broken marital and familial relationships might generate stress and lead to the development of depression (Weissman, 1997).

While the SAS enjoys a certain amount of success from being widely adopted in many different psychological studies, its evaluation is also dependent on role changes which might be one short-coming. In addition, any reduced social interaction reported from the scale might be confounded with social discomfort.

III) Social Adaptation Self-Evaluation Scale

Based on the social reinforcement model of depression (Libet and Lewinsohn, 1973), the social adaptation and self-evaluation scale (SASS; Bosc, Dubini, and Polin, 1997) is a recently developed drive-based scale for the evaluation of social functioning. The assessment of the motivational aspect of interpersonal functioning may be more apposite than the ability-based aspect (Ranjith et al., 2005). In their social reinforcement model of depression, Libert and Lewinshon (1973) argued that people who do not have the skills to acquire social reinforcement would be vulnerable to the risk of depression. Bosc et al. (1997) proposed that the passivity of depressed people decreases their ability to elicit social reinforcement including social support and favorable attitudes from others, which are important for the maintenance of self-esteem and the reduction of stress. Together, these two groups of authors suggest that the lack of motivation to acquire social reinforcement makes an individual vulnerable to the risk of depression as well as maintaining the depression for a long time.

Thus, the drive-based aspect of social functioning is more sensitive than the ability-based aspect as a way of depicting the role of social functioning in depression.

The SASS assesses the areas of work and leisure, family and extra-family relationships, satisfaction with one's roles and the ability to manage one's environment. These are related to the mediating factors of life stress, family cohesion, social exchange, and social support. One of the advantages of the SASS is that the assessment would not be affected by role changes due to life developments.

B. Questionnaires for Interpersonal Behaviour:

Interpersonal behaviour is an interest of many clinical studies and so some questionnaires have been developed. Due to the context of these questionnaires, many of the behaviours are related to interaction in a psychiatric institute setting and only a few of them are free from the limitation of this context and suitable for a non-clinical population. Despite this limitation, two questionnaires have been used in psychopharmacological studies and have shown promising results indicating the effects of antidepressants on social behaviour.

I) Impact Message Inventory

Based upon his interpersonal theory, Kiesler developed the Impact Message Inventory (IMI: Kiesler et al., 1985). In his theory, he suggested that a person's (sender) own behaviours would impose his/her own self-definition onto another person by interpersonal interaction and this person would receive and decode it covertly. The emotions, cognition of this person would be subjected to the influences of the sender. The IMI is a 90 item self-report inventory to assess 8 different types of covert reactions toward a specified person evoked during interpersonal transactions: dominant, friendly-dominant, friendly, friendly-submissive, submissive, hostile-submissive, hostile, hostile-dominant. In addition, the IMI can assess 15 interpersonal styles: dominant, competitive, hostile, mistrusting, detached, inhibited, submissive, succorant, abasive, deferent, agreeable, nurturant, affiliative, sociable and exhibitionistic. The use of the IMI in drug studies could provide ecologically valid interpersonal behavioural effects relating to specific drug actions. This information could complement the social behavioural information obtained in laboratory studies. Using a different technique, Moskowitz et al. (2001) reported that 14 days tryptophan supplementation enhanced dominant behaviours by the participants. Thus, the IMI could be sensitive to neurotransmitter manipulation.

II) Two Dimensional Social Interaction Scale

In our study of human social behaviour, we have developed a new observer rating scale called the Two Dimensional Social Interaction Scale (2DSIS; Tse and Bond, 2001) to measure social behaviour using a two-dimensional approach. The two dimensions are activity and participation and they are created based on the behavioural description of many common psychiatric disorders including depression, mania, autism and ADHD according to the DSM-IV. In accordance with these considerations, we proposed a two bipolar dimensional categorization system for social behavior: activity-passivity and participation-nonparticipation. A list of 20 adjectives was generated by selecting common social interaction

descriptions e.g. talkative, warm, cool, using a thesaurus (Robert, 1962). The use of an adjective checklist to quantify social behavior and so an observer rating approach was chosen. The scale was validated in a stranger-confederate dyadic social interaction paradigm. The 2DSIS provides a quick method of assessing social behavior which can be used in conjunction with conventional assessment tools to evaluate the social functioning of patients before and after treatment (Tse and Bond, 2001).

C. Laboratory Tasks

The study of social behaviours can be done by asking the participants to report their own social behaviours using a standard rating form or the ratings can be done by an observer who is close to the targeted participants. However, subjective bias cannot be avoided with the use of the rating method. Direct counting of the observable behaviours under a structured setting can provide a meaningful method to measure drug effects on social behaviours. It represents a powerful tool to examine the slightest changes in social behaviours induced by psychoactive drugs. We are going to describe three different laboratory tasks to study interpersonal interaction: dyadic interaction, the mixed motive game and the tangrams game. The two participants could both be volunteers, or one a volunteer and one a confederate. The discussion of the use of confederates is beyond the scope of the present review. Instead of focusing on actual social behaviour, facial emotion perception, which is thought to be one of the most important factors regulating social behaviour, is commonly studied in many psychiatric disorders including depression and schizophrenia. A brief description of this technique will be included.

I) Stranger Dyadic Interaction

Stranger-dyadic interaction has been used in many studies of social behaviour and some have used depressed people. Briefly, a person, who could be another volunteer or a confederate (an actor) who did not know the subject before, is placed with the subject in a room for a brief period of time. They are instructed to interact with each other. Usually, the room is equipped with a camera and microphone to record the movement and conversation of both persons for subsequent analysis. In the depressed-stranger social interaction, the interaction takes place between a normal healthy volunteer and a depressed person. After the social interaction, the stranger is also usually asked to rate how much they would reject their social partner (depressed person) as measured by the Post Encounter Scale (PES; Coyne, 1976b) and this is the end of the experiment. Four major problems were identified with this commonly used depressed-stranger dyadic social interaction paradigm. Therefore, we have designed a modified version of the dyadic social interaction paradigm. The four problems and the way in which we tackled them will now be outlined.

1) A common problem in stranger-dyadic social interaction studies is that the subjects may not act in their normal way. Many factors have caused this problem. One factor is the one way mirror. This might arouse the subjects' suspicions that they are being observed and they will therefore act in a socially desirable way. In order to reduce this kind of suspicion, there was no one-way mirror in the room and the camera and

microphone were hidden in furniture in the room. Subjects were therefore unaware of filming or recording until the debriefing.

2) The second problem is the explicit instruction to socially interact with the other person in the room. This instruction is very artificial and might also arouse subjects' suspicions and lead them to think their social partner might be a confederate and that their behaviour would be recorded. As a result, they might act in a particular way and weaken the validity of the result. In order to overcome this potential problem, the subjects were not asked explicitly to socially interact with their social partner. Instead, they were told that they would be playing a game with another volunteer in a few minutes when the laboratory was ready. Meanwhile, they were taken to the waiting room where the other volunteer was already waiting while the experimenter checked the equipment. The subject therefore believed that he/she and the confederate were both waiting to do the same experiment. This encouraged them to interact.
3) The third factor that might affect the validity of the ordinary dyadic-stranger social interaction is that there is no measurement concerning the behavioural manifestation of rejection. Most experiments finish after the social interaction, as soon as the stranger has filled in the Post Encounter Scale. The direct effects of the interaction or of rejection (on the PES) have not therefore been examined. In the present experiment, an interactive co-operative game was included. The game was played immediately after the social interaction and the PES. The game behaviour of the subjects therefore provided objective information about the effects of interaction with different confederates and rejection as measured by a pencil and paper method.
4) A fourth problem is the use of other volunteers as the social partner in the social interaction paradigm. The social behaviour of different volunteers would vary. In addition their appearance, voice quality, interests could differ considerably and lead to potential differences in attractiveness. These factors might influence the results, especially on the measurement of rejection. Therefore, confederates were used to reduce such variation as recommended by Sacco et al. (1985).

The modified stranger-dyadic paradigm requires two persons to come to a waiting room (equipped with a camera and microphone to collect their social interaction behaviours) where they are kept for 3 minutes. One of the persons is a well-trained confederate who is able to produce reliably a set of pre-determined behaviours. To avoid any expectancy effects, the confederate is blind to the experimental hypothesis. Furthermore, several methods are used to ensure a reliable performance of thepredefined role including intensive training in the use of standardized conversation scripts and nonverbal behaviours rules. These behaviour rules involved, for example, smiling and engaging in eye contact during conversation and speaking little and rarely initiating conversation but keeping the topics relevant to the subjects. The rules were developed based on a study conducted by Sacks and Bugental (1987).This maximizes experimental control and minimizes statistical errors due to individual effects.

In our search for the major dependent variables, five behavioral variables were identified to be sensitive to antidepressant treatment: total duration of speech (SPEECH); proportion of

speech by subject with eye contact (GAZE1)[1]; proportion of speech by subject without any eye contact (NOGAZE2)[2]; proportion of subject eye contact during confederate speech (LOOK3)[3]; and proportion without any eye contact from subject during confederate speech (NOLOOK4)[4]. The absolute amount of these social behaviors could be strongly affected by the role of the confederate and so proportions such as GAZE, NOGAZE, LOOK, and NOLOOK can be used to produce a better inference of the treatment effects. These behaviours have been shown to be reliably influenced by antidepressants (Tse and Bond, 2003). Other behaviours, such as smiling, head nodding, illustrative movement and fiddling, were found to be less reliably influenced by antidepressants (Tse and Bond, 2002).

II) Mixed Motive Game

The Prisoner dilemma (PD) game is one of the standard protocols used to study cooperative behaviour. However, it only involves the option of either cooperation or deflection which is too simple to account for complex human social interactions. A modified version of the Prisoner Dilemma game called the mixed motive game (MMG) has been developed (Hokanson et al., 1980). It allows more choices in the continuum from cooperation to deflection, including ingratiation, punitive moves without self-gain, cooperation and deflection. Furthermore, differently from the PD, the MMG requires participants to select their options in a sequential rather than in a simultaneous manner.

In the MMG, player 1 selects their choice (one of the three rows) first. After knowing the choice of row that player 1 has selected, player 2 has to choose one of the three options of that row (see Figure 1).The sequential selection procedure tries to resemble the cooperation decision process in real live situations in which one person proposes a suggestion and another replies with one of these four cooperative-deflective choices. To enhance the ecological validity of the game, the game is played for 30 trials rather than a one-off trial. Under this selection method, player 2 will always have a higher power to be cooperative, deflective or punitive. Thus, retaliation by player 1 is impossible even if player 2 always plays in a punitive manner. This allows observation of the cooperative/punitive behavioural effects of antidepressant treatment with a minimum disturbance of other psychological influences inherent in the game.

Furthermore, communication between the participants and confederates is allowed by the use of a standardized questionnaire called The Communication Checklist (CCL; Hokanson et al., 1980) to enhance the ecological validity of the game. It is a 24-item inventory which measures 6 different types of communication: extrapunitiveness; cooperativeness; ingratiation; sadness; blaming partner and helplessness. These experimental settings represent daily working situations which require making choices of cooperation and communication with colleagues/ strangers on a longer-term basis. In a study using a serotonergic antidepressant, Tse and Bond (2003) reported that 2weeks of citalopram treatment significantly enhanced cooperative communication and cooperative behaviours in the MMG.

1 GAZE is calculated by measuring the total duration of eye contact while the subject is speaking divided by the total duration of speech (SPEECH).

2 NOGAZE is calculated by summing the duration of each sentence spoken by the subject during which the subject shows no eye contact at all divided by the total duration of speech (SPEECH).

3 LOOK is calculated by measuring the total duration of eye contact while the confederate is speaking divided by the total duration of speech by the confederate.

4 NOLOOK is calculated by summing the duration of each sentence spoken by the confederate during which the subject shows no eye contact at all divided by the total duration of speech by the confederate.

	1	2	3
1	Player 1 Player 2 5 5	Player 1 Player 2 -5 7	Player 1 Player 2 7 5
2	Player 1 Player 2 7 -5	Player 1 Player 2 -5 -5	Player 1 Player 2 5 -3
3	Player 1 Player 2 5 7	Player 1 Player 2 -3 5	Player 1 Player 2 5 5

Figure 1. The 3 possible pay-off schemes in the Mixed-Motive game. Player 1 (confederate) chooses one of the 3 rows, which is indicated by highlighting the row and player 2 (subject) selects one of the three panels on the chosen (highlighted) row.

III) Tangrams Game

A new method to measure cooperative behaviours has been developed by Knutson et al. (1998). They used a standardised dyadic puzzle task called the Tangrams Game (TG) to measure three common social behaviours: cooperation, issuing commands and giving a one-way solution. The authors claimed that the TG can elicit face-valid social behaviours that can be reliably measured within the context of a co-operative and dominant interaction. In the TG, pairs of subjects were given 10 minutes to combine a set of 7 puzzle pieces into configurations that matched as many target shapes as possible (for example, see Figure 2), with the rule that only one partner could touch the puzzle pieces at a time. The game behaviours of the volunteers were video recorded and then coded into three categories: co-operation (i.e. making suggestions while a partner handled the puzzle pieces); issuing commands; and a one-way solution (i.e. grasping the pieces with the intent of arriving at a unilateral solution) by an independent rater. Affiliative behaviour was defined as: cooperation - (command + one-way solution). In their study, Knutson et al. (1998) reported that healthy volunteers who received a week's treatment of paroxetine show significantly more affiliative behaviour than those who received placebo treatment. However, this enhancement of affiliative behaviour was not found after 4 weeks of the treatment.

IV) Facial Emotion Recognition

According to his theory of interpersonal behaviour processes, Trower (1980) proposed that the perception of a social partner's emotion is the first important step in determining how social behaviours are being expressed. Facial expression is one of the rich and reliable sources to detect emotions of social partners. In fact, accurate face perception has an important survival value (Ekman, 1993). Healthy people are able to interpret others' facial expressions accurately. This ability has even been found to extend to the assessment of faces represented by some cartoon pictures consisting of a dot, stroke and circle, rather than photographs of a real human face. On the other hand, depressed patients were not able to judge the meaning of these pictures. When they were asked to judge the facial expression of a special set of these drawings which had no clear distinct expression of sadness or rejection, they rated them to be more sad and rejecting than they actually were (Bouhury, Bloem, and Groothuis, 1995).

Seven puzzle pieces given to the subject pair.

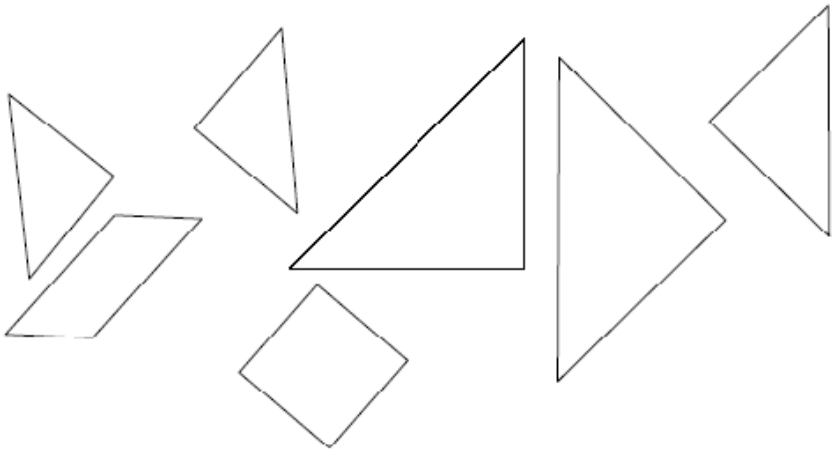

Sample target shape given to the subject pair

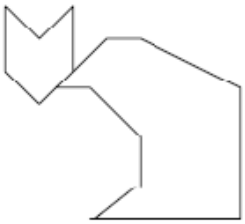

Expected answer from the subject pair.

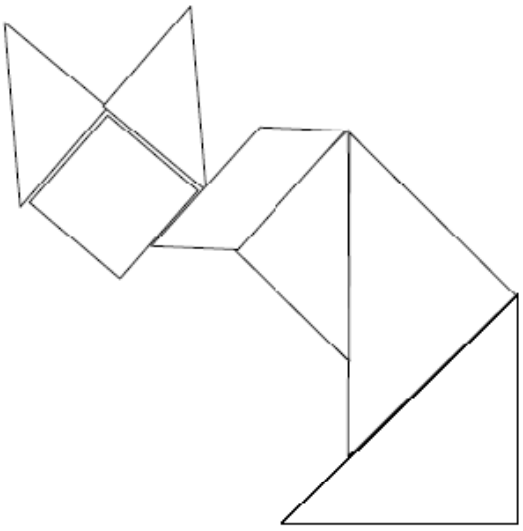

Figure 2. An example of the Tangrams game.

These results confirm that negative cognitions can be influential in the evaluation process so that depressed people judge even ambiguous abstract pictures more negatively.

In a study of the facial emotion recognition effects of an antidepressant, Harmer et al (2001) used a computerized morphed face technique to study how common antidepressants influence the facial emotion recognition ability of healthy volunteers. Using specialized computer software, 7 common facial emotions (sad, fearful, disgusted, angry, happy, surprised and neutral) in their full strength (100%) were morphed with a neutral face in 10% gradient. Thus, each facial emotion will have 10% gradient of strength of that emotion from 10% to 100%. These morphed faces are used as the targets in the facial emotion recognition task. In the task, each face is shown individually for a period of 250ms on a computer screen and participants are asked to identify the faces as quickly as possible by pressing a key corresponding to one of the 7 emotions. The computer registers the correct hit, incorrect hits, missing responses, reaction time, and types of hit for each face for further analysis. The task was found to be sensitive to noradrenaline manipulation (Harmer et al., 2001).

III Evidence to Support the Role of Noradrenaline in Interpersonal Functioning

A. Clinical Study: Global Interpersonal Functioning (SASS Study):

Reboxetine, was the first antidepressant to be developed to work specifically on noradrenaline (Wong et al., 2000). It is a specific noradrenergic reuptake inhibitor (NARI) and in a clinical study, it was found to improve the psycho-social functioning of depressed patients, as measured by the Social Adaptation Self-evaluation Scale (SASS), more than fluoxetine, a specific serotonergic reuptake inhibitor (SSRI) antidepressant (Dubini, Bosc, and Polin, 1997). It has been suggested that social adaptation as measured on the scale used (SASS) is associated with the concept of social motivation (Charles et al., 1999). The improvement, thus, appeared to be associated with enhancement of social motivation which might be important for the therapeutic recovery process (Hirschfeld, et al., 2000). However, the mechanism by which the changes in noradrenaline induced by reboxetine led to improvement on the SASS is unknown.

As pointed out by Healy and Healy (1998), this work was all based on the SASS, a self-report scale, and an improvement in self-perceived social motivation is not an objective measurement of real behavioural improvement. In our study examining the validity of the SASS, however, it was found to relate to observer ratings of social behaviour (Tse and Bond, 2001). The two participant category ratings were significantly positively related to SASS scores, suggesting high social motivation, and the two nonparticipant categories were negatively associated with the SASS scores, confirming that poorer levels of interpersonal functioning are associated with less adaptive social behaviour. People with higher interpersonal functioning are more socially motivated to engage in various social activities, e.g. hobbies, contact with friends. However, the enhancement of social activity is only one aspect of social motivation. This aspect might not be sufficient to explain the improvement in interpersonal functioning. Showing initiative to engage with others in a social circle and co-operating with them on joint ventures are two other important steps involved in social

integration. In behavioural terms, these two steps would mean actions involving a willingness to co-operate with others. Previous research using serotonergic antidepressants found that both fluoxetine and paroxetine, improved nonverbal behaviours in healthy volunteers (Stager et al.; 1995, Knutson et al., 1998). Therefore, noradrenergic antidepressants, such as NARIs, may also affect cooperative behaviour which might contribute to improvements in interpersonal functioning.

B. Experimental Study: Facial Emotion Perception Positive Bias in Healthy Volunteers

In a series of studies of the role of noradrenaline on facial emotion recognition, Harmer and colleagues conducted a series of experiments to examine how noradreanline influences the facial emotion recognition process in healthy volunteers. These well-planned psychopharmacological studies examined the effects of a single dose of a beta-adrenoceptor antagonist, an acute dose of reboxetine and one week's administration of reboxeine.

In the beta-andrenoceptor antagonist study, Harmer et al. (2001) reported that acute administration of propranolol significantly increased reaction time to identify sad faces compared to placebo in the absence of any subjective mood states changes related to the drug. Yet, recognition of fearful faces was not affected by the treatment. This enhancement provided partial support that reduction of noradrenergic transmission increases negative bias to process negative information.

In the acute dose of reboxetine study, Harmer et al. (2003) reported that healthy volunteers who received reboxetine treatment correctly identified happy faces at lower intensity significantly more than those who received placebo. However, reboxetine effects on the enhancement of identification were not observed in happy faces with higher intensity. In the 7-day reboxetine treatment study, Harmer et al. (2004) found that healthy volunteers who received reboxetine showed decreased recognition of fearful and angry faces as compared to those who received placebo. This reduction was not related to subjective mood improvement. In contrast to the previous findings, repeated doses of reboxetine did not facilitate the recognition of the happy faces. Harmer et al. (2003; 2004) interpreted these findings as a reboxetine enhancement of positive information processing which is important for the therapeutic effects of an antidepressant. This helps depressed patients to process negative information in a more positive light.

To further confirm the mechanism of the positive information processing bias produced by reboxetine, Norbury et al. (2007) employed functional magnetic resonance imaging (fMRI) technique to search for changes in neural activation in the facial emotion recognition task related to 7 days reboxetine treatment. In this study, two different types of facial recognition task were employed: covert and overt. In the covert facial recognition task, the target faces were presented for 17ms and masked by neutral faces which were presented for 183ms. In the overt facial recognition task, the faces were presented for 200ms with no mask. They found that healthy volunteers who received 7 day's reboxetine treatment showed increased right fusiform activation in response to covert happy faces. This is opposite to the observation in depressed patients who showed a reduction in right fusiform activation to happy faces (Surguladze et al., 2005). These findings together with those reported by Harmer et al. (2003, 2004) suggest that enhancement of positive information processing would be an

important therapeutic mechanism for noradrenergic antidepressants. This mechanism is comparable to those involved in cognitive behavioural therapy which has been shown to facilitate positive information processing.

Thinking positively might be important for the readiness to make an amicable response in ambiguous social situations where very little social information is available and a response has to be made quickly. The initial positive social behaviours could help to engender positive relationships with others and promote social bonding. This would help someone to start out with a positive relationship as well as maintain already existing relationships by reducing unnecessary conflicts with others.

C. Experimental Study: Cooperative and Dominant Behaviours in Healthy Volunteers

Inspired by the work of Dubini et al. (1997), we investigated the role of noradrenaline on human social behaviours. We hypothesized that enhancement of noradrenaline transmission by reboxeine would increase cooperative behaviours. In addition, based on the work of animal studies, subordinate status in animals like rats and monkey can be seen as an analogue of depression in humans. Subordinate animals show submissive behaviors more often and they also show symptoms of depression like higher cortisol levels, sleeping difficulties and weight loss. Submissive behaviours have been related to brain serotonin levels. Furthermore, antidepressant treatments have been shown to enhance the dominant status of previously subordinate animals. Therefore, we hypothesized that 2 weeks of reboxetine treatment would increase dominant behaviours in human subjects. Three experiments were set up: (1) an acute dose of reboxetine and (2) 2 weeks' treatment with reboxetine using the stranger dyadic interaction. These two experiments aimed to examine how enhancement of noradrenergic transmission might influence cooperative behaviour and other social behaviours related to interpersonal functioning. These two experiments focused on participants' interactions when meeting with strangers. They might behave differently when meeting with a familiar friend. Thus, the third experiment was developed to examine how 2 weeks' reboxetine treatment would influence the interpersonal behaviours of participants when they met their flatmate to play a cooperative game TG,.

In the acute dose of reboxetine study, Tse and Bond (2002) reported that healthy volunteers who received reboxetine treatment sent significantly more cooperative messages as measured by the CCL and they also played an interactive game (MMG) more co-operatively. This indicates prosocial effects. Furthermore, they reduced hand fiddling during the stranger dyadic interaction. This effect might be related to the reduction of self-focussed attention, enhancement of attention to their social partners and increased engagement with others. This hypothesis is consistent with the effects of noradrenaline suggested by Coccaro and Siever (1995) and Healy and McMonagle (1997). The social behavioural changes were independent from moods state changes as reboxetine treatment was not found to have significant effects on the mood states of the participants.

The effects of repeated doses of reboxetine varied with the situation encountered. In the stranger dyadic situation, after receiving 2 weeks' reboxetine, participants showed reductions in eye contact made with the confederate in the dyadic interaction and gave significantly fewer helplessness messages as measured by the CCL during the MMG compared to placebo

(Tse and Bond, 2003). The participants were also rated to be more passive nonparticipant in the 2DSIS by observers. The reduction of eye contact suggested that participants were trying to avoid any potential social confrontation or conflict at first meeting and they were viewed as more passive and uninvolved by an observer. However, they increased their confidence on the game by giving fewer helplessness messages. Thus, this could be a strategy to form new relationships.

In everyday interactions with their flatmates, the effects of 2 weeks' treatment with reboxetine on social behaviours were different from those found in the stranger dyadic interaction. It was found that participants on reboxetine were rated to be less submissive on the IMI and as more passive participant on the 2DSIS by their flatmates (Tse and Bond, 2003). They were generally viewed more positively when on reboxetine and the treatment seemed to result in an enhancement of an already existing friendship. Thus, reboxetine seemed to help both the development and consolidation of social bonds via changes in social behaviours.

Using a different method of measuring social behaviour with a flatmate, Tse and Bond (2006) reported that after receiving 2 weeks' reboxetine, participants issued significantly more commands to their flatmates in a cooperative game (TG) than when they received placebo treatment. This interaction reveals that reboxetine can enhance assertive social behaviour with a familiar person which would not be expressed in the stranger dyadic interaction. Meeting a stranger might inhibit the expression of assertive behaviours to avoid rejection. However, the expression of assertive behavior to their flatmates was not associated with enhancement of aggression which could lead to poor social relationships. Enhancement of assertiveness might help to improve the unbalanced social hierarchy in groups and promote positive dominant status. Furthermore, acting assertively implies higher self-esteem. People with higher self-esteem are more likely to be able to deal with challenges, take responsibility for their actions and less likely to blame others which promotes the development of social relationships.

Volunteers treated with reboxetine might be more co-operative and submissive to strangers which might help them to get on with people who are not known to them. . Social behaviour after reboxetine treatment could therefore be constructive to friendship development. The failure of 2 weeks' reboxetine treatment to increase co-operative social behaviour on the Mixed-Motive game might lie in the fact that the difference between the points which the subjects awarded to themselves and to the confederate was very small. In the repeated dose reboxetine study, the subjects awarded the confederate more after both placebo and reboxetine. The subjects in this study therefore appear to be very co-operative, irrespective of treatment.

After reboxetine treatment, the participants displayed both more co-operative and assertive behaviour towards their flatmates. An increase in assertiveness together with co-operativeness might relate to an increase in both self-confidence and self-expression, which might lead to more positive social communication. An increase in co-operation, in particular, might result in more positive social interaction and encouragement to the other person resulting in a better relationship. Anderson and Martin (1995) found that people with both a high assertive and a high responsive communication style communicated more for affection, inclusion and pleasure than those whose style was high assertive but low responsive. Thus, this distinctive social behaviour pattern after reboxetine treatment might be expected to lead to better interpersonal functioning.

CONCLUSION

The psychopharmacological study of the role of noradrenaline in interpersonal functioning is still in its early development. Few attempts have been made previously to try and discover noradrenergic functions in interpersonal behaviour, and so information regarding to its role is very limited. This is partly due to the limited research tools, with regard to both measures of social behaviour and noradrenergic manipulation, available for the study of interpersonal functioning. There are only a few suitable self-report questionnaires to measure interpersonal functioning and behaviours as described earlier in this chapter. Paradigms to study interpersonal behaviours and facial recognition provide objective measures of the acute and longer term effects of noradrenaline enhancement. These are complementary to the self-report measurements and enable a fuller description of the role of noradrenaline in interpersonal functioning.

Although more psychopharmacological studies should be conducted to examine how noradrenaline regulates interpersonal functioning, this is also restricted by the pharmacological manipulations available. There is only few commercially available noradrenaline reuptake inhibitor which is specific enough to target only noradrenaline activity. When trying to lower noradrenaline levels, a drink containing specifically selected amino acids not only lowers noradrenaline, but also dopamine. Therefore, any observable effects of lowering noradrenaline on interpersonal functioning might also be due to the reduced levels of dopamine.

Despite these limitations, the present chapter has summarized the key results regarding the role of noradrenaline on interpersonal functioning. In a clinical study, it was found that selective noradrenergic antidepressant treatment improved global interpersonal functioning as measured by the SASS significantly more than a selective serotonergic antidepressant. In experimental studies conducted with healthy participants, reboxetine treatment improved positive bias in facial emotion recognition and enhanced social cooperative and dominant behaviours. These results are complementary to those observed in the clinical studies and therefore, suggest that noradrenaline plays an important role in the promotion of affiliative behaviours related to interpersonal functioning.

REFERENCES

Alessandri, S.M. (1992). Attention, play and social behavior in ADHD preschoolers. *Journal of Abnormal Child Psychology*, 20, 289-302.

American Psychiatric Association (1994). Diagnostic and Statistical Manual of Mental Disorders (4th ed). Washington, DC, American Psychiatric Association.

Anderson, C.M., and Martin, M.M. (1995). Communication motives of assertive and responsive communicators. *Communication Research Reports*, 12, 186-191.

Aneshensel, C.S., and Stone, J.D. (1982). Stress and depression: A test of the buffering model of social support. *Archives of General Psychiatry*, 39, 1392-1396.

Blazer, D.G. (1983). Impact of late-life depression on the social network. *American Journal of Psychiatry*, 140, 162-166.

Bloton,W., and Oatley, K. (1987). A longitudinal study of social support and depression in unemployed men. *Psychological Medicine,* 17, 453-460.

Bosc, M., Dubini, A., and Polin, V. (1997). Development and validation of a social functioning scale, the Social Adaptation Self-evaluation Scale. European *Neuropsychopharmacology*, 7, Suppl 1, S57-S70.

Bouhuys, A.L., Bloem, G.M., and Groothuis. T.G.G. (1995). Induction of depressed and elated mood by music influences the perception of facial emotional expressions in healthy subjects. *Journal of Affective Disorders*, 33, 215-226.

Brugha, T.S. (1984). Personal losses and deficiencies in social networks. *Social Psychiatry*, 19, 69-74.

Charles, B.N., Reunette, W.H., and Dennis, S.C. (1999). The role of norepinephrine in the treatment of depression. *Journal of Clinical Psychiatry*, 60, 623-631.

Coccaro, E.F., and Siever, L.J. (1995). The neuropsychopharmacology of personality disorders. In: F.E. Bloom, and D.J. Kupfer (Eds.). Psychopharmacology: The fourth generation of progress. Raven Press, New York, pp 1567-1579.

Cohen, S., Sherrod, D.R., and Clark, M.S. (1986). Social skills and the stress-protective role of social support. *Journal of Personality and Social Psychology,* 50, 963-973.

Cole, D. A., and Milstead, M. (1989). Behavioral correlates of depression: Antecedents or consequences? *Journal of Counseling Psychology*, 36, 408-416.

Coyne, J.C. (1976a). Depression and the response of others. *Journal of Abnormal Psychology*, 85: 186-193.

Coyne, J.C. (1976b). Toward an interactional description of depression. *Psychiatry*, 39, 28-40.

Dean, A., and Ensel, W.M. (1982). Modelling social support, life events, competence, and depression in the context of age and sex. *Journal of Community Psychology,* 10, 392-408.

Dean, A., and Lin, N. (1977). The stress-buffering role of social support. *Journal of Nervous and Mental Disease*, 165, 403-417.

Dubini, A., Bosc, M., and Polin, V. (1997). Do noradrenaline and serotonin differentially affect social motivation and behaviour? *European Neuropsychopharmacology*, 7(suppl), S49-S55.

Ekman, P. (1993). Facial expression and emotion. *American Psychologist*, 48, 384-392.

Flaherty, J.A., Gaviria, F.M., Black, E.M., Altman, E., and Mitchell, T. (1983). The role of social support in the functioning of patients with unipolar depression. *American Journal of Psychiatry*, 140, 473-476.

Friedman, R.A. (1993). Social impairment in dysthymia. Psychiatric Annals, 23, 632-637.

Gurtman, M.B. (1987). Depressive affect and disclosures as factors in interpersonal rejection. *Cognitive Therapy and Research*, 11. 87-99.

Haley, W.E. (1985). Social skills deficits and self-evaluation among depressed and non-depressed psychiatric inpatients. *Journal of Clinical Psychology*, 41, 162-168.

Hammen, C., and Brennan, P. (2002). Interpersonal dysfunction in. depressed women: Impairments independent of depressive. symptoms. *Journal of Affective Disorders*, 72, 145–156.

Harmer, C.J., Perrett, D.I., Cowen, P.J., and Goodwin, G.M. (2001). Administration of the beta-adrenoceptor blocker propranolol impairs the processing of facial expression of sadness. *Psychopharmacology*, 154, 383-389.

Harmer, C.J., Hill, S.A., Taylor, M.J., Cowen, P.J., and Goodwin, G.M. (2003). Toward a neuropsychological theory of antidepressant drug action: increase in positive emotional bias after potentiation of norepinephrine activity. *American Journal of Psychiatry,* 160, 990-992.

Harmer, C.J., Shelley, N.C., Cowen, P.J., and Goodwin, G.M. (2004). Increased positive versus negative affective perception and memory in healthy volunteers following selective serotonin and norepinephrine reuptake inhibition. *American Journal of Psychiatry*, 161, 1256-1263.

Healy, D., and McMonagle, T. (1997). The enhancement of social functioning as a therapeutic principle in the management of depression. *Journal of Psychopharmacology*, 11 (suppl), S25-S31.

Healy, D., and Healy, H. (1998). The clinical pharmacologic profile of reboxetine: Does it involve the putative neurobiological substrates of wellbeing? *Journal of Affective Disorder*, 5, 313-322.

Henderson, S., Duncan-Jones, P., Byrne, D.G., and Scoot, R. (1980). Measuring social relationships: the interview schedule for social interaction. *Psychological Medicine,* 10, 723-734.

Hirschfeld, R.M., Montgomery, S.A., Keller, M.B., Kasper, S., Schatzberg, A.F., Moller, H.J., Healy, D., Baldwin, D., Humble, M., Versiani, M., Montenegro, R., and Bourgeois, M. (2000). Social functioning in depression: a review. *Journal of Clinical Psychiatry*, 61, 268-275.

Hokanson, J.E., Sacco, W.P., Blumberg, S.R., and Landrum, G.C. (1980). Interpersonal behavior of depressive individuals in a mixed-motive game. *Journal of Abnormal Psychology*, 89, 320-332.

Kiesler, D.J., Anchin, J.C., Perkins, M.J., Chirico, B.M., Kyle, E.M., and Federman, E.J. (1985). Impact Message Inventory. Mind Garden: California

Klerman, G.L. (1989). Depressive disorders: Further evidence for increased medical morbidity and impairment of social functioning. *Archives of General Psychiatry*, 46, 856-858.

Knutson, B., Wolkowitz, W.M., Cole, S.W., Chan, T., Moore, E.A., Johnson, R.C., Terpstra, J., Turner, R.A., and Reus, V.I. (1998). Selective alteration of personality and social behavior by serotonergic intervention. *American Journal of Psychiatry*, 155, 373-379.

Leavy, R.L. (1983). Social support and psychological disorder: A review. *Journal of Community Psychology*, 11, 3-21.

Libet, J.M., and Lewinsohn, P.M. (1973). Concept of social skill with special reference to the behavior of depressed persons. *Journal of Consulting and Clinical Psychology,* 40, 304-312.

Mallinckrodt, B., and Fretz, B.R. (1988). Social support and the impact of job loss on older professionals. *Journal of Counseling Psychology*, 35, 281-286.

McDowell, I., and Claire, N. (1987). Measuring Health: a guide to rating scales and questionnaires. New York: Oxford University Press.

Moskowitz, D.S., Pinard, G., Zuroff, D.C., Annable, L., and Young, S.N. (2001). The effect of tryptophan on social interaction in everyday life: a placebo-controlled study. *Neuropsychopharmacology*, 25, 277-289.

Norbury, R., Mackay, C.E., Cowen, P.J., Goodwin, G.M., and Harmer, C.J. (2007). Short-term antidepressant treatment and facial processing. *British Journal of Psychiatry*, 190, 531-532.

Oatley, K., and Bolton, W. (1985). A social-cognitive theory of depression in reaction to life events. *Psychological Review*, 92, 372-388.

Pearlin, L.I., Menaghan, E.G., Lieberman, M.A., and Mullan, J.T. (1981). The stress process. *Journal of Health and Social Behavior*, 22, 337-356.

Plant, E.A., and Sachs-Ericsson, N. (2004). Racial and Ethnic Differences in Depression: The Roles of Social Support and Meeting Basic Needs. *Journal of Consulting and Clinical Psychology*, 72, 41-52.

Ranjith, G., Farmer, A., McGuffin, P., and Cleare. A.J. (2005). Personality as a determinant of social functioning in depression. *Journal of Affective Disorders*, 84, 73-76.

Robert, A. (1962). Roget's Thesaurus of English words and phases. London, Longmans, Green and Co Ltd.

Sacks, C.H., and Bugental, D.B. (1987). Attributions as moderators of affective and behavioral responses to social failure. *Journal of Personality and Social Psychology*, 53, 939-947.

Sacco, W.P., Milana, S., and Dunn, V.K. (1985). Effect of depression level and length of acquaintance on reaction of others to a request for help. *Journal of Personality and Social Psychology*, 49, 1728-1737.

Schaefer, C., Coyne, J.C., and Lazarus, R.S. (1981). The health-related functions of social support. *Journal of Behavioral Medicine*, 4, 381-406.

Stager, S.V., Ludlow, C.L., Gordon, C.T., Cotelingam, M., and Rapoport, J.L. (1995). Fluency changes in persons who stutter following a double blind trial of clomipramine and desipramine. *Journal of Speech and Hearing Research*, 38, 516-525.

Surguladze, S., Brammer, M.J., Keedwell, P., Giampietro, V., Young, A.M., Travis, M.J., Willams, S.C., and Phillips. M.L. (2005). A differential pattern of neural response toward sad versus happy facial expression in major depressive disorder. *Biological Psychiatry*, 57, 21-209.

Trower, P. (1980). How to lose friends and influence nobody: an analysis of social failure. In W.T. Singleton, P. Spurgeon, and R.B. Stammers (Eds.), *The analysis of social skill* (pp. 257-273). NY: Plenum.

Tse, W.S., and Bond, A.J. (2001). Development and validation of the Two-Dimensional Social Interaction Scale (2DSIS). *Psychiatry Research*, 103, 249-260.

Tse, W.S., and Bond ,A .J. (2002). Serotonergic intervention affects both Social Dominance and Affiliative Behaviour. *Psychopharmacology*, 161, 324-330.

Tse, W.S., and Bond, A. J. (2003). Reboxetine promotes social bonding in healthy volunteers. *Journal of Psychopharmacology*, 17, 189-195.

Tse, W.S., and Bond, A.J. (2006). Noradrenaline might enhance assertive human social behaviours: An investigation in a flatmate relationship. *Phamacopsychiatry*, 39, 175-179.

Tyrer, P., and Casey, P. (Ed) (1993). Social function in Psychiatry: The hidden axis of classification exposed. Petersfield, England: Wrightson Biomedical Publishing.

Under, A.L., and Orth-Gomer, K. (1989). Development of social support instrument for use in population survey. *Social Sciences Medicine*, 29, 1387-1392.

VanMeter, L., Fein, D., Morris, R., Waterhouse, L., and Allen, D. (1997). Delay versus deviance in autistic social behavior. *Journal of Autism and Developmental Disorders*, 27, 557-569.

Vinokur, A., Schul, Y., and Caplan, R.D. (1987). Determinants of perceived social support: Interpersonal transactions, personal outlook, and transient affective states. *Journal of Personality and Social Psychology*, 53, 1137-1145.

Weiss, R.S. (1974). The provisions of social relationships. In Z. Rubin (Ed.), Doing unto others: Joining, molding, conforming, helping, loving (pp. 17-26). NJ: Prentice Hall.

Weissman, M.M. (1997). Beyond symptoms: social funcitioning and the new antidepressants. *Journal of Psychopharmacology*, 11 (suppl), S5-S8.

Weissman, M.M., and Paykel, E.S. (1974). The depressed woman: A study of social relationships. Chicago: University of Chicago Press.

Wong, E.H.F., Sonders, M.S., Amara, S.G., Tinholt, P.M., Piecey, M.F.P., and McArthur, R.A. (2000). Reboxetine: A pharmacologically potent, selective, and specific norepinephrine reuptake inhibitor. *Biological Psychiatry*, 47, 818-829.

In: Biochemistry and Histocytochemistry… ISBN: 978-1-60876-283-5
Editors: S. Fuchs, M. Auer, pp. 45-64 © 2010 Nova Science Publishers, Inc.

Chapter 3

THE NEUROTRANSMITTER NOREPINEPHRINE AND ITS ROLE IN AFFECTIVE DISORDERS

Eliyahu Dremencov*
Brains On-Line, BV, and the University of Groningen Institute of Pharmacy, Groningen, Netherlands

I. ABSTRACT

There are number of lines of evidence that the neurotransmitter norepinephrine (NE) might be very important in pathophysiology of anxiety and mood disorders. Firstly, NE projections innervate the limbic system, suggesting the involvement of NE in the regulation of emotions and cognition. Secondly, NE interacts with serotonin (5-HT) and dopamine (DA) systems, which also play very important roles in the regulation of mood. Thirdly, it has been shown that various agents for increasing NE availability, such as NE reuptake inhibitors, are also effective antidepressant drugs. And fourthly, the depletion of NE can result in the relapse of depression after successful treatment with antidepressant drugs. All these pieces of evidence suggest that the stimulation of NE transmission can be beneficial in the treatment of affective disorders. However, different psychiatric medications have distant effects on NE transmission. The current chapter analyses the effect of psychiatric medications on NE system and proposes how the treatment outcome might be improved.

II. INTRODUCTION

a. Neurotransmitter Norepinephrine

Norepinephrine, together with epinephrine and dopamine (DA), belongs to the catecholamine family of hormones and neurotransmitters. DA is synthesized in all catecholamine neurons by decarboxylation of levodopa. This process is catalyzed by aromatic

* Brains On-Line BV, L.J. Zielstraweg 1, 9713 GX Groningen, Netherlands, Tel +31.50.317.1440, Fax +31.50.317.1449, E-mail e.dremencov@brainsonline.org

amino acid decarboxylase and requires the presence of pyridoxal phosphate. Levodopa itself is synthesized by oxidation of the amino acid tyrosine. This oxidation is a rate-limited process and it is catalyzed by tyrosine hydroxylase. In the NE-releasing neurons (spinal neurons of the autonomic system, sympathetic ganglia neurons and brain NE neurons), the enzyme DA beta hydroxylase turns DA into NE. This process requires vitamin C as a cofactor. In the sympathetic ganglia neurons, and especially in the epinephrine-secreting cells of adrenal medulla, NE is partially transformed into epinephrine. This transformation is performed by the enzyme phenylethanolamine N-methyltransferase (PNMT) (Kandel et al., 2000).

NE molecules are made inside into synaptic vesicles by the vesicular monoamine transporter (VMAT). This transport is an active, adenosine triphosphate (ATP)-requiring process. VMAT also transports DA, epinephrine and serotonin (5-HT). These hormones and transmitters are so-called monoamines (MO). Certain drugs, such as reserpine and tetrabenazine, inhibit the VMAT and suppress vesicular MO storage (Reinhard et al., 1988; Russo et al., 1994).

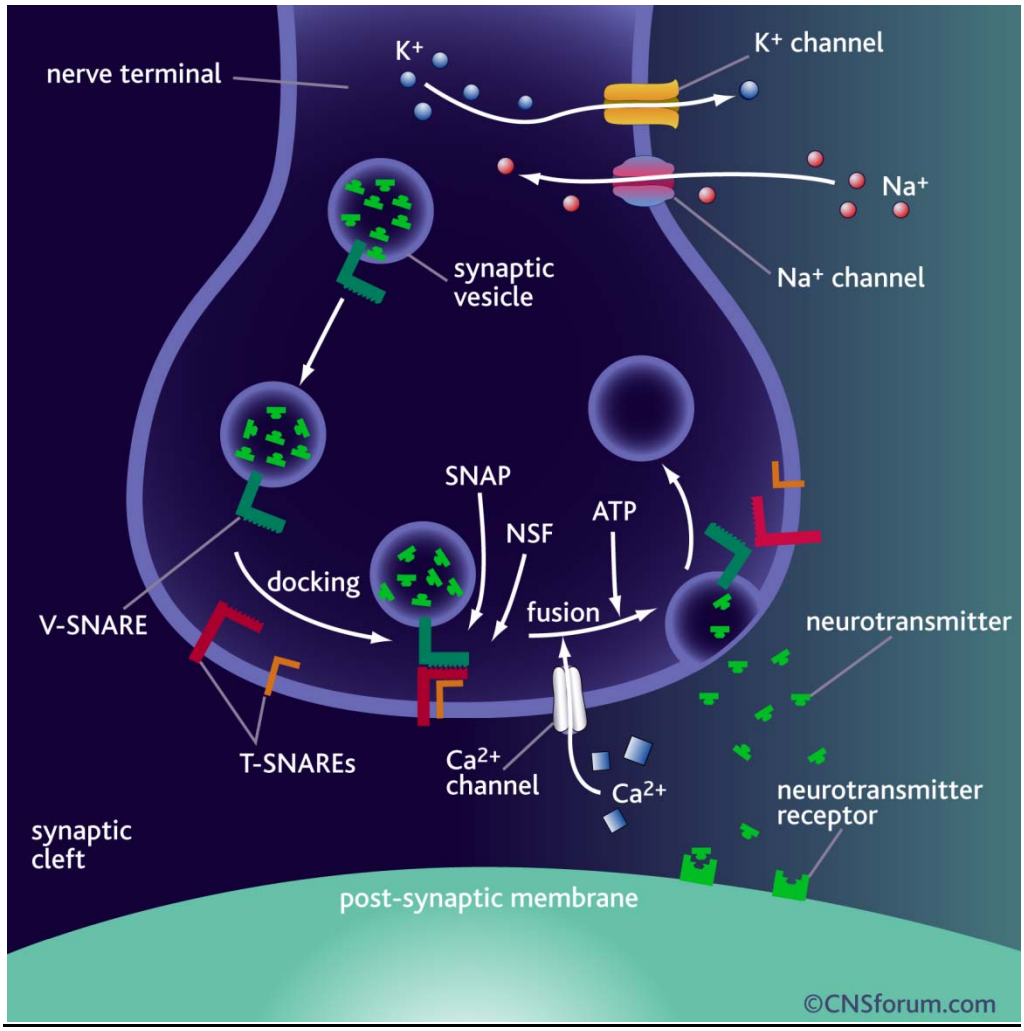

Figure 1. Norepinephrine synapse. Published with permission of Lundbeck Institute.

Neuronal action potentials (APs), when they arrive to the nerve terminal, stimulate the fusion of the synaptic vesicles with the cellular membrane, and NE is released into the synaptic space. Certain compounds, such as methamphetamines or bupropion, increase NE release *via* an AP-independent release mechanism (Dong and Blier 2001; Piacentini et al., 2003).

NE molecules released into the synaptic space are reabsorbed back into the presynaptic neuron by the membrane NE transporter (NET). This process requires ATP. The NET is a target for numerous drugs. Several tricyclic antidepressants (TCA), such as imipramine, non-specifically inhibit both NET and 5-HT (5-HTT) transporters (Corrodi and Fuxe 1968). Other TCAs, called norepinephrine reuptake inhibitors (NRIs), such as desipramine, specifically inhibit the NET (Curet et al., 1992; Lacroix et al., 1991). There are also non-tricyclic selective inhibitors of the NET, called selective norepinephrine reuptake inhibitors (SNeRIs), and dual inhibitors of the NET and 5-HTT (SNRIs). The examples for SneRIs and SNRIs are reboxetine and venlafaxine, respectively (Beique et al., 1998a; Beique et al., 1998b; Beique et al., 1999; Dawson et al., 1999; Szabo and Blier 2001c).

After reuptake of it NE is stored again or it is degraded. The major metabolic pathway of NE is its oxidation into 3,4-dihydroxymandelic acid by the type A of the enzyme monoamine oxidize (MAO). Numerous drugs have MAO as their primary target. Their can be divided into two groups: non-reversible MAO inhibitors (MAOIs) and reversible MAO inhibitors (RIMAs). Respective examples for these groups are phenelzine and moclobemide (Blier and de Montigny 1985; Blier et al., 1986).

The storage, reuptake and release of norepinephrine are shown in Figures 1 and 2. Table 1 summarizes the effect of various drugs on the reuptake and release of norepinephrine.

b. Noradrenergic System

There are several nuclei containing NE neurons in the pons and medulla oblongata (Figures 3). The NE neurons of medulla oblongata are situated in the caudal raphe nuclei and project to the spinal cord (A1, A5 and A7 cell groups in rat) and hypothalamus (A2 group). These NE pathways regulate mostly sensory, motor and autonomic functions. The NE neurons of the pons are concentrated in the area called locus coeruleus (LC, A6 in rat). The NE system of the LC plays an important role in the regulation of sensory, motor, neuroendocrine, and cognitive functions of the brain (Bouret and Sara 2005; Kandel et al., 2000; Kiernan and Barr 1998). In the current chapter only the NE system of LC will be discussed.

LC consists mostly of NE neurons. However, γ-aminobutyric acid (GABA)-secreting neurons are also found in the peripheries of the LC (Iijima and Ohtomo 1988). The NE neurons of LC have local and distant afferent and efferent connections. The local bilateral connections of LC arrive from and project to the GABA cells of periaqueductal gray (PAG) and acetylcholine (ACH) neurons of pontomesencephalic tegmentum (PMT) (Jones, 1991).

The major distant afferents to the LC arrive from the brainstem (nucleus paragigantocellularis, PGI) and telencephalon (central nucleus of amygdala, CEA, and prefrontal cortex, PFC). The efferents of the LC innervate literally all areas of the central neural system (CNS). The majority of the fibers, however, project to the hippocampus, dentate gyrus (DG), prefrontal cortex (PFC) and basolateral nucleus of amygdala (BLA) (Bouret and Sara 2005; Kandel et al., 2000; Kiernan and Barr 1998).

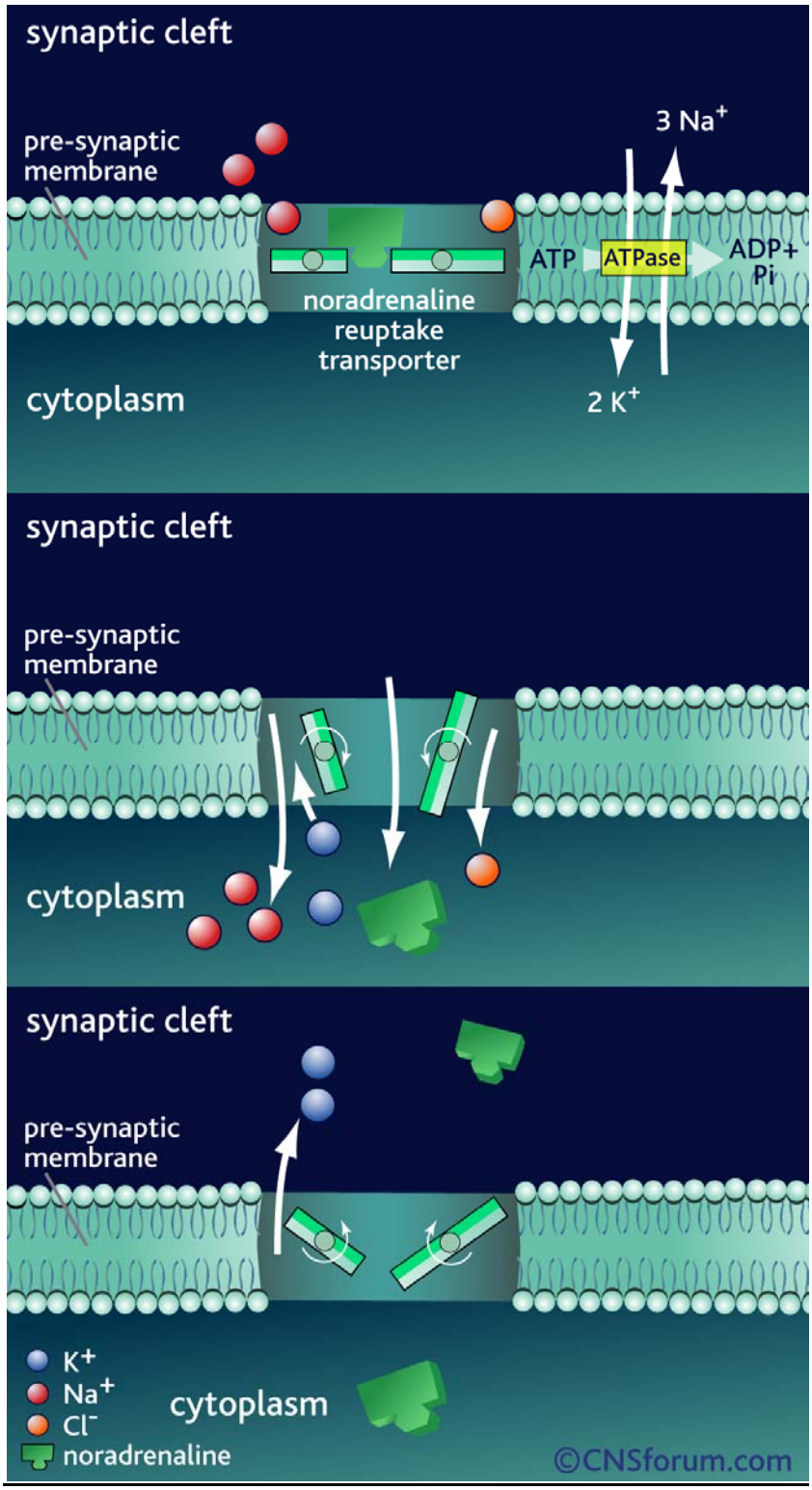

Figure 2. Reuptake of norepinephrine. Published with permission of Lundbeck Institute.

Table 1: Drugs affecting the storage, release, reuptake, autoregulation and metabolism of norepinephrine. (↓), inhibitory effect; (↑), excitatory effect.

Process	Mediator	Drugs
Storage	Vesicular monoamine transporter	Reserpine (↓) Tetrabenazine (↓)
Release	Synaptic proteins	Methamphetamines (↑) Bupropion (↑)
Reuptake	Norepinephrine transporter	Tricyclic antidepressants (imipramine, ↓) Tricyclic norepinephrine reuptake inhibitors (desipramine, ↓) Selective norepinephrine reuptake inhibitors (reboxetine, ↓) Dual serotonin/ norepinephrine reuptake inhibitors (venlafaxine, ↓)
Negative autoregulation of norepinephrine neuronal firing activity	α_2-adrenergic autoreceptor	Idazoxan (↓) Noradrenergic and specific serotonergic antidepressants (Mirtazapine ,↓) Atipical antipsychotic drugs (Risperidone , ↓)
Metabolism	Monoamine oxidize A	(Reversible) monoamine oxidize inhibitors (phenelsine, moclobemide, ↓)

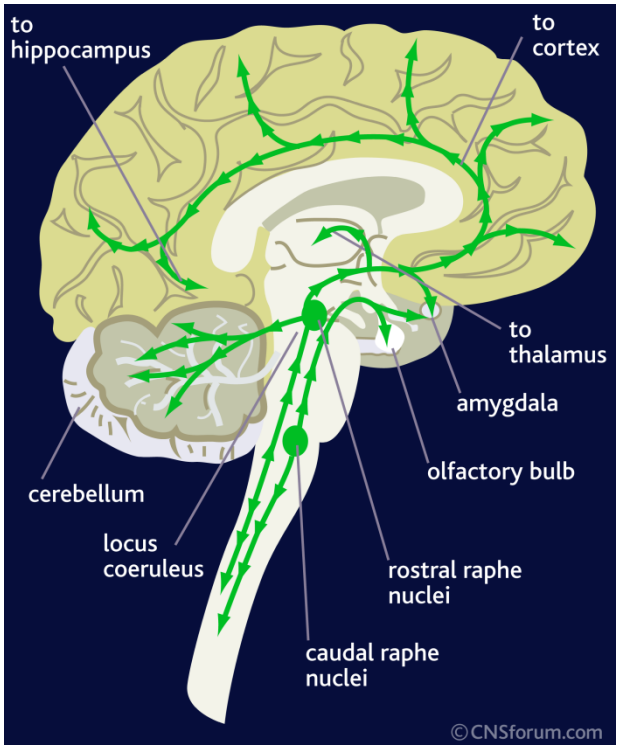

Figure 3. Norepinephrine pathways of human brain. Published with permission of Lundbeck Institute.

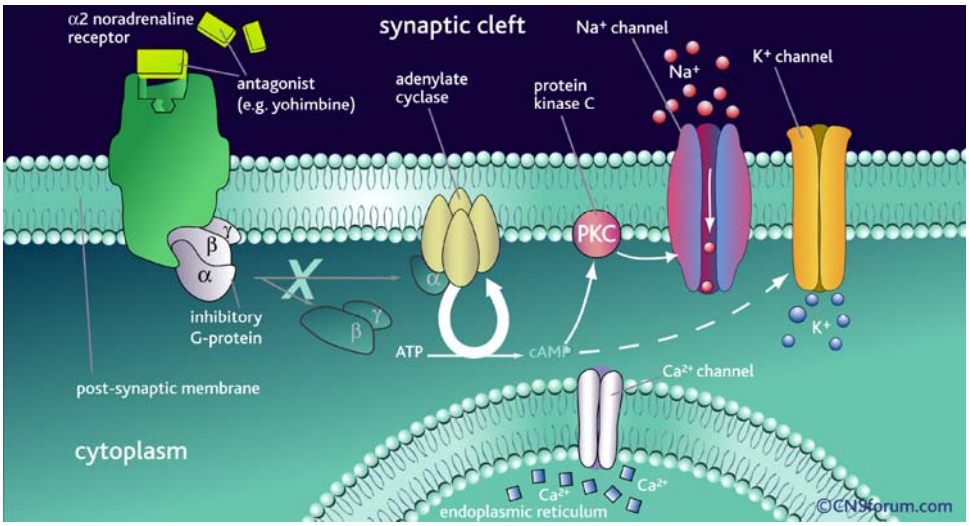

Figure 4. Mechanism of action of an antagonist of α_2-adrenoceptors. Published with permission of Lundbeck Institute.

c. Noradrenergic Receptors

All receptors for NE (adrenoceptors) are G-protein-coupled metabotropic receptors. However, they vary by their location (presynaptic autoreceptors and post-synaptic hetreroreceptors), pharmacology (three families α_1, α_2 and β with three subtypes in each family $\alpha_{1A/B/D}$, $\alpha_{2A/B/D}$ and $\beta_{1/2/3}$), signal transduction (G_{Q11}-α_1 family, G_I-α_2, and G_S-β), and physiology (excitatory of inhibitory effect on the postsynaptic neuron).

The only inhibitory adrenoceptors and only that are located on both pre- and post-synaptic neurons are α_2-adrenoceptors. These receptors are coupled to the G_I protein. Their activation results in $G_{I\alpha}$ dissociation into the $G_{I\alpha}$ and $G_{I\beta\gamma}$. $G_{I\alpha}$ deactivates adenylyl cyclase (AC) and sodium (Ca^{2+}) channels, while $G_{I\beta\gamma}$ opens potassium (K^+) channels. An increase in K^+- and decrease in Ca^{2+}-influx leads to hyperpolarisation. This decreases the rate of AP firing and inhibits NE release. The mechanism of action of α_2-adrenoceptors is shown in Figure 4.

Both α_1 and β adrenoceptors are postsynaptic excitatory heteroreceptors. Their action is mediated via the activation of Ca^{2+} current. However, different mechanisms are involved: G_Q-mediated phospholipase C (PLC) activation and G_S-mediated AC stimulation, respectively (Kandel et al., 2000). When they present on glutamate pyramidal neurons, β-adrenoceptors receptors decrease the Ca^{2+}-activated after-hyperpolarization K^+ influx, making the neurons more responsive for excitatory inputs. The α_1 adrenoceptors, however, increase membrane conductance and make the pyramidal cells less excitable (Devilbiss and Waterhouse 2000).

d. Norepinephrine Neurons

NE neurons express mixed tonic/phasic firing activity. The firing rate is approximately 2 Hertz and it remains relatively constant. Short bursts containing two or three APs occur with a periodicity of one or two per minute (Figures 5) (Aghajanian and Vandermaelen 1982; Dremencov et al., 2007a; Dremencov et al., 2007c). The firing activity of NE neurons is auto-regulated as well as controlled by other transmitters. In the LC, NE the activation of α_2 adrenergic autoreceptors by NE suppresses the firing activity of NE neurons. In the nerve-terminal level, the activation α_2 adrenoceptors attenuates NE release without suppression of the firing activity (Mongeau et al., 1993).

The α_2 adrenoceptors are target for several drugs. Several of them, such as idozaxan, are selective antagonists of α_2-adrenoceptors. Others, such as mirtzapine, risperidone and paliperidone, antagonize α_2-adrenoceptors together with other receptors: α_1 adrenoceptors and 5-$HT_{2A/2C}$ serotonergic receptors (Dremencov et al., 2007c; Haddjeri et al., 1995; Haddjeri et al., 1996; Richelson and Souder 2000). The mechanism of action of an antagonist of α_2-adrenoceptors is presented in Figure 5.

NE neuronal firing activity is controlled by GABA and glutamate. GABA input to the NE neurons comes from both local (LC) and distant (such as PAG) neurons. GABA inhibits the firing activity of NE neurons via a $GABA_A$ receptor-mediated mechanism. The distant afferent inputs into the LC (PGI, CEA and PFC) are exclusively glutamatergic. Glutamate increases the firing activity of NE neurons (Torrecilla et al., 2007).

The firing activity of NE neurons is negatively regulated by 5-HT and DA. The effect of 5-HT on NE neuronal firing activity is mediated *via* the 5-HT_{2A} and 5-HT_{1A} receptors. The 5-HT_{2A} receptors are situated on GABA neurons projecting to the LC. The 5-HT_{1A} receptors are located on the nerve terminals of glutamate afferents (Szabo and Blier 2001b; Szabo and Blier 2002b). Their activation results in an increase of GABA and in a decrease of glutamate influx into the LC (Figure 6) and in inhibition of firing activity of NE neurons (Dremencov et al., 2007a; Dremencov et al., 2007c; Szabo et al., 1999; Szabo and Blier 2001a; Szabo and Blier 2001a; Szabo and Blier 2001c).

Similarly to NE, DA also suppresses the firing activity of NE neurons, *via* the D_2-receptor mediated mechanism. NE however has different effects on the firing activity of 5-HT and DA neurons: the decrease in the brain NE followed by an increase of activity of DA neurons and by suppression of firing of 5-HT neurons (Guiard et al., 2008). Figure 7 summarizes the reciprocal interactions between NE, 5-HT and DA systems.

III. Role of Norepinephrine in Mood and Cognition

a. Pain and Nociception

The NE system plays an important role in the perception, modulation, and response to the pain. Nociceptive stimuli arrive into the LC *via* the PGI pathway. NE neurons respond to the nociceptive stimuli by burst firing followed by silence (Dremencov et al., 2007a; Dremencov et al., 2007c; Szabo and Blier 2001b; Szabo and Blier 2001d; Szabo and Blier 2001g; Szabo

and Blier 2002a). The burst firing of NE results in an increase in NE releases (Sajedianfard et al., 2005).

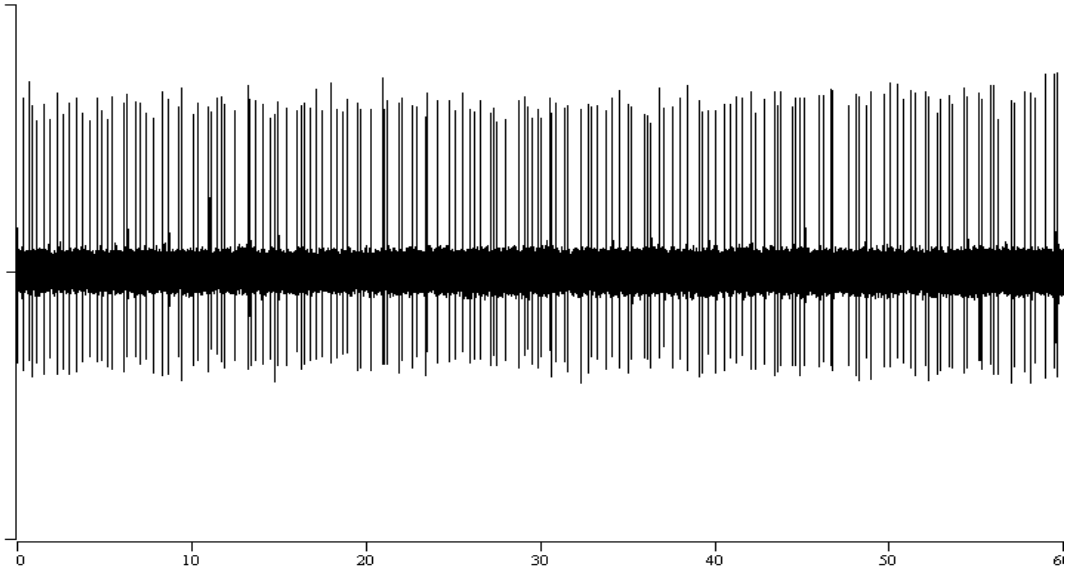

A. Normal firing of a norepinephrine neuron

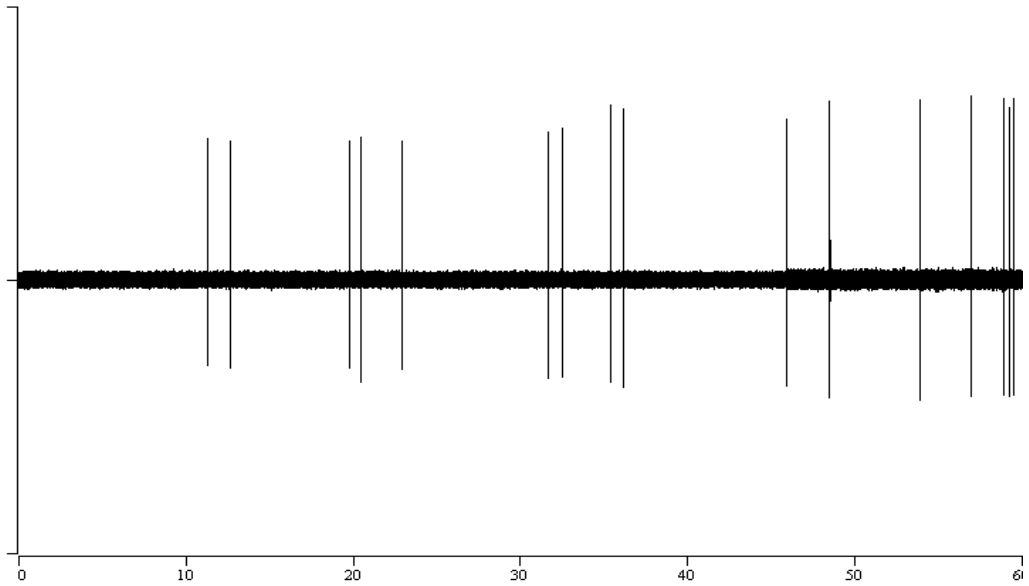

B. Firing of a norepinephrine neuron inhibited by serotonin

Figure 5. The effect of the selective serotonin reuptake inhibitor, escitalopram, on firing activity of norepinephrine neurons. Norepinephrine neurons exhibit tonic-phasic firing activity of 1.5-3.0 Hz, with small (2-3/min) number of short burst (*). Escitalopram inhibits the firing activity of norepinephrine neurons.

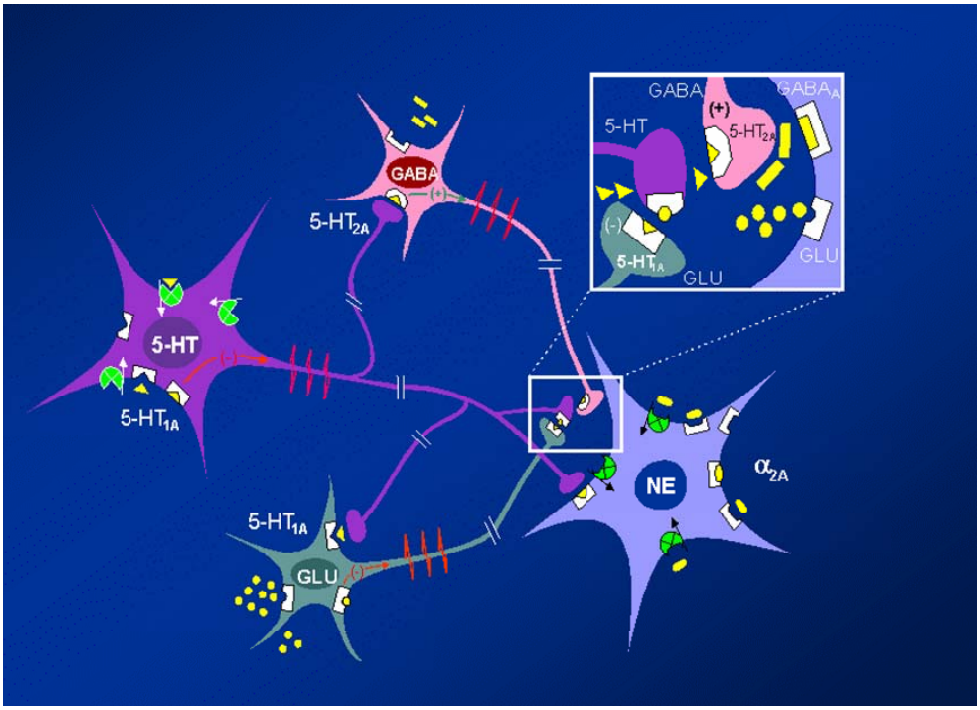

Figure 6. Mechanism of serotonin-induced inhibition of firing activity of norepinephrine neurons. Serotonin increases the GABA and decrease glutamate influx into the locus coeruleus, via 5-HT2A and 5-HT1A receptor-mediated mechanisms, respectively. This increase in GABA and decrease in glutamate influx results in the inhibition of firing activity of norepinephrine neurons. Published with permission of Pierre Blier, M.D., Ph.D., University of Ottawa Institute of Mental Health Research.

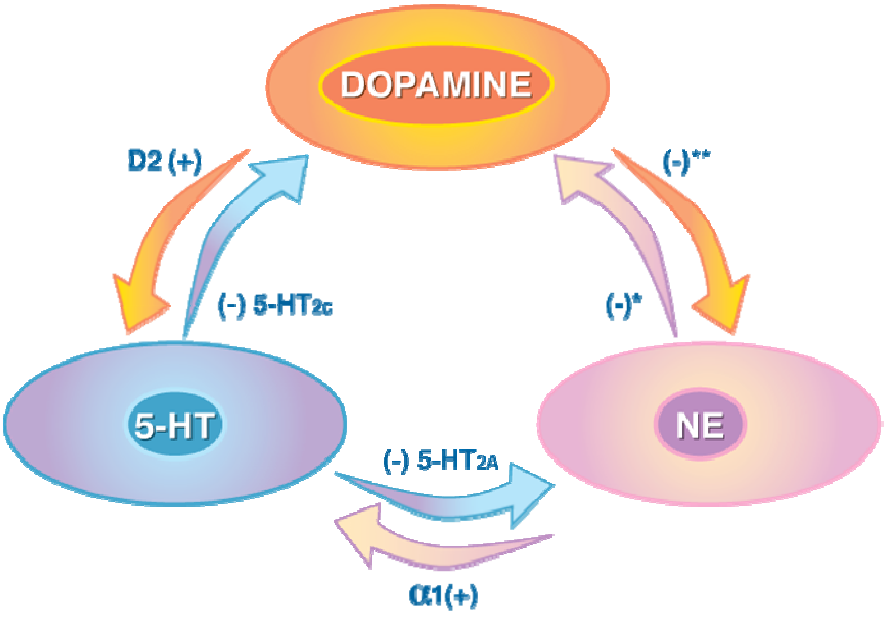

Figure 7. Functional interactions between norepinephrine, serotonin and dopamine systems. Published with permission of Pierre Blier, M.D., Ph.D., University of Ottawa Institute of Mental Health Research.

The role of the NE system in pain response involves both the direct anti-nociception and the triggering on behavioral response to the pain as to an aversive event. The first is probably mediated *via* the NE efferents descending to the brain steam and spinal cord (Clark and Proudfit 1991a; Clark and Proudfit 1991b; Clark and Proudfit 1991c; Clark et al., 1991; Proudfit and Clark 1991). The second might be a function of the reciprocal LC-amygdala network.

The involvement of NE in pain modulation has been demonstrated in several studies. Thus, electrical stimulation of LC or its spinal cord-projecting efferents induces an anti-nociceptive effect in rats (West et al., 1993; Yeomans et al., 1992). Paradoxically, lesioning of NE neurons is also increases the pain threshold (Hammond and Proudfit 1980). Other studies demonstrated as well that NE can either enhance or suppress nociception in the spinal cord and brainstem levels. It has, therefore, been suggested that different receptors mediate nociceptive and anti-nociceptive effects of NE. Pain stimulation is probably mediated via the α_1-, and pain suppression via α_2-adrenoceptors (Wei and Pertovaara 2006). Inflammation and sustained pain induce an increase in α_2-and a decrease in α_1-mediated NE transmission in the spinal cord. Thus, NE probably increases the sensitivity to acute pain and decreases it to chronic pain.

b. Emotions

NE transmission is fundamental in emotions, and in particular in fear and anxiety. Numerous animal and human studies support this paradigm. For example, exposure of rats to stressful stimuli increases NE release in various areas of brain, such as hypothalamus, stria terminalis, and supraoptic nucleus (Fendt et al., 2005; Onaka et al., 2003; Otagiri et al., 2000; Shekhar et al., 1994; Shekhar et al., 2002; Shimizu et al., 1990; Tanaka, 1999; Yokoo et al., 1990a; Yokoo et al., 1990b). This response, however, desensitizes shortly when the stressful stimuli is repeated (Hajos-Korcsok et al., 2003). Neuroimaging studies in human subjects demonstrated that aversive emotional stimuli activate amygdala via a β-adrenoceptor-mediated mechanism (van Stegeren, 2008a). Another study demonstrates that increase in brain NE reduces the taste threshold in humans, which indicates induction of anxiety (Heath et al., 2006).

Stress-related stimuli probably trigger NE neuronal activity, *via* the amygdala and PFC afferents. The activation of NE neurons results in an increase in NE transmission in the hypothalamus and limbic system. The increase in NE levels in hypothalamus results in activation of hypothalamus-hypophysis-adrenal (HPA) axis, *via* a β-adrenergic receptor-mediated mechanism. An increase in NE in the limbic system stimulates neuronal activity of glutamatergic pyramidal neurons and decreases the firing of GABA basket interneurons, *via* α_2- and β-adrenergic mechanisms, respectively.

NE-induced activation of the amygdala is probably involved in the emotional response to stress which includes behavior inhibition and freezing awareness. NE activation of hippocampus and PFC mediates the behavioral response to stress and danger. This response includes awareness, attention and activity.

Somewhat similar to the dual involvement of NE in the modulation of pain, this transmitter also paradoxically increases response to acute stress but decrease it to the chronic.

This different effect on acute and chronic aversions increases the behavioral adaptation to the changing environmental conditions.

c. Cognition

NE system plays an important role in various cognitive functions: attention, concentration, consolidation and retrieval of memory (Berridge and Waterhouse 2003; Harley, 2004; van der Meulen et al., 2007). Studies in human and animal subjects demonstrated that proper NE function is critical for the spatial working memory (Rossetti and Carboni 2005). In rodents, NE plays an important role in the olfactory memory (Veyrac et al., 2007). NA reuptake inhibition improves the learning and behavior flexibility (Seu et al., 2008). In humans, blocking of β_2-adrenoceptor-mediated cortical transmission suppress the numerical memory performance (Muller et al., 2005). On the other hand, there is an increase in cortical NE during the spatial memory performance. There is also evidence for a critical role of cortical α_2-adrenoceptors in memory and cognition (Coull, 1994; Matthews et al., 2002).

There are contradictory reports regarding the role of NE in probabilistic learning and decision making. Several suggest that the NE system involved in decision making (Cohen and Aston-Jones 2005; Nieuwenhuis et al., 2005). However, other studies propose that 5-HT and DA mediate the estimation of probability and decision making rather than NE (Chamberlain et al., 2006). Its was also suggested that NE trigger on the formation and deformation of synchronized activity networks in the PFC. This effect of NE is probably mediated via the β_2-adrenergic receptor-mediated mechanism and mediates behavior adaptation and flexibility (Aston-Jones and Cohen 2005a; Aston-Jones and Cohen 2005b; Bouret and Sara 2005).

Several studies postulate that NE plays a central role in consolidation and retrieval of stress-related memory (Hurlemann et al., 2005; Mueller et al., 2008a; Ouyang and Thomas 2005; van Stegeren, 2008b). The role of this activity is fear conditioning and extinction. These behavioral effects of NE are probably mediated via hippocampal β_2 and α_2 receptors, respectively (Davies et al., 2004; Garelick and Storm 2005). NE pathways and their role in nociception, emotions, cognition and behavior are summarized in table 2.

NE is fundamental in human attention and concentration. It has been demonstrated that idozaxan increase the attention in healthy volunteers (Smith et al., 1992). To contrasy, the administration of α_2-adrenergic agonist clonidine results in attention lapses in humans. These clonidine-induced attention difficulties can be reversed by idozaxan (Smith and Nutt 1996).

IV. NOREPINEPHRINE AND AFFECTIVE DISORDERS

a. Stress and Anxiety Disorders

The important role of NE in stress response suggests that this transmitter might be involved in anxiety disorders (van Stegeren, 2008a). An increased feeling of fear might be explained by hyper-functionality of the NE system, especially in the amygdala (van Stegeren et al., 2008). On the other hand, NE system of the hippocampus mediates fear extinction.

Pathological inability to forget aversive events may be therefore explained by reduced NE transmission in the PFC (Mueller et al., 2008b). Therefore, the NE system might playan important role in the pathology of generalized anxiety disorder (GAD), panic disorder (PD) and post-traumatic stress disorder (PTSD). However, different NE pathways may be involved.

Table *2*. Norepinephrine pathways, their targets and functions.

Target of pathway	Receptor	Physiological effect	Behavioral function
Brain steam and spinal cord	α_1 α_2	Excitation Inhibition	Nociception (acute pain) Anti-nociception (chronic pain)
Hypothalamus	α_2	Activation of HPA axis	Neuroendocrine response to the stress
Amygdala	β_1	Excitation	Fear feeling
Hippocampus	β_1, β_2 α_2	Excitation of pyramidal neurons. Induction of LTP. Inhibition of GABA basket cells	Emotional memory. Fear conditioning and extinction.
Prefrontal cortex	β_1 α_2	Excitation of pyramidal neurons. Inhibition of GABA basket cells	General activity, cognition, behavior flexibility, attention, concentration

Several studies demonstrated that anxiety disorders correlate with changes of NE activity. Fox example, GAD and melancholia are associated with increased plasma NE concentration. Clonidine challenge test studies demonstrated that anxiety associated with decreased activity of α_2-adrenergic autoreceptors, suggesting increased NE transmission. And indeed, increased plasma NE levels were observed in patients with anxiety and melancholia (Nutt, 2001).

On the other side, PTSD does not correlate with an increase in basal NE transmission. However, robust increase in plasma concentrations of NE and its metabolites in PTSD patients are observed after their re-exposure to the traumatic contents. The administration of an α_2-adrenoceptor antagonist, yohimbine, resulted in a panic attack in PTSD patients. These observations suggest that an increased NE tone is involved in acute anxiety and panic attack, rather than in the cognitive aspect of PTSD. Further imaging studies are required to study the role of the hippocampal and/or cortical NE system in neuropathology of PTSD (Newport and Nemeroff 2000).

b. Unipolar Depression and Bipolar Disorder

The NE system is involved in the feeling of energy, fear regulation, general activity, memory and cognition. It is therefore likely that NE is involved in depressive disorder, and in particular in anhedonia, reduced activity and cognition, and in increased anxiety observed in depressed patients. Increased nociception and chronic pain in depression may also be caused, at least in part, by impaired NE transmission (Nutt et al., 2006; Nutt, 2006; Strittmatter et al., 2005).

Indeed, there is a correlation between impaired NE transmission and depressive behavior. Postmortem studies demonstrated increased NE levels in the brains of unipolar and bipolar suicide victims (Juckel et al., 2000; Wiste et al., 2008). One positron emission tomography (PET) study suggested that depressive patients have an increased activity of MAO-A, which might result in reduced catecholamine levels (Meyer et al., 2006). Another imaging study showed correlation between the degree of loss of limbic NE innervation and severity of depressive symptoms in Parkinson patients (Brooks and Piccini 2006; Remy et al., 2005).

Contrary to depression, the manic stage of bipolar disorder is characterized by increased energy and activity. Since the activity and energy feeling mediated by NE, an increase in NE transmission might contribute to manic behavior. Indeed, it has been reported that increased urine NE levels follow the manic episode of bipolar illness (Juckel et al., 2000; Nutt, 2006).

Based on the evidences, mentioned above, it can be concluded that NE is involved in both depression and mania. This involvement is based, at least in part, on the role of NE in the mediation of energy and activity. Decreased activity in depression might results from attenuation in NE transmission, and manic hyperactivity from an increase in NE tone.

V. Effect of Psychiatric Drugs on Noradrenergic System

a. Antidepressant Drugs

There is only one antidepressant drug (AD) that stimulates the firing of NE neurons. This is the noradrenergic and specific serotonregic antidepressant (NaSSA) mirtazapine. It increases NE neuronal firing activity using the blocking of α_2-adrenergic autoreceptors (Haddjeri et al., 1996). Other ADs inhibit the firing of NE neurons, *via* an α_2-adrenergic and/or 5-HT_{2A} receptor-mediated pathway. Catecholamine-acting ADs, such as NaRIs, SNRIs, desipramine or bupropion, elevate the extracellular NE levels in the brain *via* either reuptake inhibition or release stimulation (Fernandez-Pastor et al., 2005; Li et al., 2002; Parini et al., 2005; Piacentini et al., 2003; Sacchetti et al., 1999). This increase results in the activation of α_2-adrenergic autoreceptors, which leads to the activation of α_2-autoreceptors to the inhibition of firing of NE neurons (Curet et al., 1992; Szabo and Blier 2001d).

The 5-HT acting ADs, such as SSRIs or MAOIs, elevate extracellular 5-HT levels in the brain (Mork et al., 2003; Tao et al., 2000). This increase in 5-HT levels results in the activation of GABA neurons, via the 5-TH_{2A} receptor-mediated mechanism. The increase in GABA levels in the LC results in inhibition of NE neuronal firing activity, via a $GABA_A$ receptor-mediated mechanism (Figure 6; Szabo and Blier 2001e; Szabo and Blier 2002a).

The inhibition of firing of NE neurons, produced by catecholamine-acting ADs, appears after sub-acute or chronic administration of these ADs (Curet et al., 1992; Szabo and Blier 2001d). The 5-HT acting ADs inhibit NE neurons only after chronic administration (Dremencov et al., 2007c; Szabo and Blier 2001f; Szabo and Blier 2001h). This is due to the time course needed to achieve a robust and permanent increase in 5-HT levels in the nerve-terminal level of 5-HT neurons (Mongeau et al., 1997; Pineyro and Blier 1999). However, the SSRI escitalopram inhibits the NE neuronal firing activity after three-day administration only (Fig.5) (Dremencov et al., 2007a; Dremencov et al., 2007c). This rapid effect of escitalopram might be explained by its high selectivity and effectiveness as a 5-HT reuptake inhibitor, in

comparison to other SSRIs (Dremencov et al., 2007c; El Mansari et al., 2005; Hyttel, 1982; Mork et al., 2003; Tatsumi et al., 1997).

In contrast to the AD-induced inhibition of 5-HT neurons, which recovers after prolonged administration of an AD, the AD-induced inhibition of NE neurons does not recover over time (Dremencov et al., 2007a; Dremencov et al., 2007c; Mongeau et al., 1997; Parini et al., 2005; Sacchetti et al., 1999; Szabo et al., 2000; Szabo and Blier 2001f). This AD-induced inhibition of NE neurons can be reversed by the antagonists of either α_2-adrenergic and 5-HT_{2A} receptors in the LC and related areas (Dremencov et al., 2007a; Dremencov et al., 2007c). However, chronic administration of idozaxan or of the SSRI sertaline results in the desensitization of α_2-adrenergic autoreceptors in the rat PFC (Thomas et al., 1994; Thomas et al., 1998). This desensitization might explain the increase in NE levels in the rat PFC after chronic sertaline (Thomas et al., 1998).

The beneficial effect of mirtazapine in the treatment of depression might be explained by its α_2-adrenoceptor antagonistic property. Bupropion and desipramine might be also beneficial in depression because of their ability to increase extracellular NE levels (Fernandez-Pastor et al., 2005; Li et al., 2002; Parini et al., 2005; Sacchetti et al., 1999). The beneficial effect of NE in depression can be explained by the excitatory effect of NE on 5-HT neurotransmission and by the direct involvement of NE transmission in anxiety, energy feeling and motivation (Guiard et al., 2008; Stahl, 2000).

b. Mood Stabilizers and Atypical Antipsychotic Drugs

Lithium (Li) is a common mood stabilizer and it used in the treatment of bipolar disorder. There are numerous evidences that the therapeutic effect of Li is mediated via an inositol triphosphate (IP_3) and protein kynase C (PKC)-mediated mechanism (Arnsten, 2008). Since the IP_3 and PKC are involved the signal transduction pathway of α_1-adrenoceptors, it is possible that there receptor are target of Li treatment. Indeed, it has been observed that chronic Li suppress the a1-mediated IP_3 formation and PKC activation. It has been also observed that chronic Li deregulates α_1, α_2 and β-adrenoceptors in the brain (Devaki et al., 2006).

It has been observed that Li potentiates the SSRI milnacipran-induced elevation of extracellular NE levels in the rat PFC (Kitaichi et al., 2005). However, several studies suggest that Li might decrease the NE transmission when it is given alone. Chronic Li decreases the cAMP response to NE administration (Masana et al., 1991). Another study demonstrated that iontophoretic administration of Li antagonizes the action of NE on rat PFC neurons (Kovacs and Hernadi 2002). Based on the hypothesis that increased NE transmission is involved in manic episodes, it can be suggested that anti-manic effect of Li ix explained by its suppressive effect on the NE system.

Atypical antipsychotic drugs (AADs), in addition to their application as a first-line treatment in schizophrenia, are also effective mood stabilizers. AADs are successfully used in unipolar and bipolar mood disorders, either as solo treatment or as adjuncts to SSRIs (Blier et al., 2005; Kennedy et al., 2001; Kennedy and Lam 2003; Papakostas et al., 2007; Simon and Nemeroff 2005; Tremblay and Blier 2006; Uzun et al., 2005). It has been suggested that the beneficial effect of AADs as adjuncts to SSRIs is explained, at least in part, by their ability to

reverse the SSRI-induced inhibition of NE neuronal firing activity in the LC (Blier and Szabo 2005; Dremencov et al., 2007a; Dremencov et al., 2007b). The SSRI-induced inhibition of NE neuronal firing activity is mediated via 5-HT_{2A} receptors . Thus, antagonists of these receptors might reverse the inhibitory effect of SSRIs on the firing of NE neurons. Indeed, it has been observed with the AADs risperidone and olanzapine co-administered with the SSRIs escitalopram and fluoxetine, respectively (Dremencov et al., 2007c; Seager et al., 2005). One study demonstrated that the AAD olanzapine not only reverses fluoxetine-induced inhibition of NE neuronal firing activity, but also stimulates the firing of NE neurons on its own (Dawe et al., 2001).

In 1989, t was reported for the fist time that idozaxan is benefitial as a mood stabilizer (Osman et al., 1989). It has been therefore suggested that α_2-adrenergic autoreceptors could be an important target for antipsychotic and mood-stabilizing treatments (Nutt, 1994). Indeed, ertain AADs, such as risperidone, are potent antagonists of α_2-adrenoceptors (Janssen et al., 1988; Richelson and Souder 2000). As a result, risperidone not only reserve the SSRI-induced inhibition of NE neuronal firing activity but also increases it above the value observed in control animals (Dremencov et al., 2007c). The electrophysiological findings, demonstrating that the AADs increase and/or prevent the SSRI-induced decrease in the firing activity of NE neurons are consistent with an AAD-induced elevation in extracellular levels of NE, observed in microdialysis studies. The ability of AADs to stimulate the NE transmission might explain, at least in part, their beneficial effect in mood disorders.

Electroconvulsive therapy has been used as antidepressive, mood-stabilizing and antipsychotic treatments (Eitan and Lerer 2006; Shapira et al., 1991). It is reported that electroconvulsive shocks (ECS), an animal model for the ECT, affect the NE system. Thus, both acute and chronic ECS increase cortical and hippocampal NE release. Chronic ECS also desensitize α_2-adrenergic autoreceptors in the PFC (Thomas et al., 1992). Paradoxically, electrophysiological studies report that chronic ECS suppress the firing activity of NE neurons in the ECS (Grant and Weiss 2001). Based on the evidences of ECS-induced increase in brain NE levels, it can be concluded that the benefitial effect of the ECT is mediated, at least in part, via NE system.

VI. CONCLUSIONS

The NE system mediates various autonomic, neuroendocrine, emotional and cognitive functions. One of the central roles of NE is response to stress and aversion. This role can be summarized as an activation of response to the acute stress and aversion, followed by decreased reaction to repeated or chronic aversion. Since the response to stress and aversion is a basic part in pathology of mood disorder, NE should play an important role in anxiety, depression and mania. Indeed, this role has been demonstrated in numerous animal and human studies. Majority of antidepressant drugs and mood stabilizers affect NE system as their direct or indirect target. Various medications have different effects on NE neuronal activity. The majority of antidepressants, Li and benzodiazepines suppress NE transmission. Other medications, such as AADs, activate NE neuronal firing activity and NE release. Appropriate combination of different medications, based on the consideration of their effect on NE system, might be critical to obtain good treatment outcome. The combination of SSRIs

and AADs in bipolar or treatment-resistant depression is an example for such treatment strategies.

ACKNOWLEDGMENTS

The author thanks Drs. Pierre Blier and Xia Zhang (University of Ottawa Institute of Mental Health Research) for their guidance and mentorship, Dr. Martin G. de Vries (Brains On-Line BV) carefull reading of this chapter, Novo Science for their kind invitation to write this chapter, and Lundbeck Institute for the illustrations. Especial acknowledgments should be given to the reviewers, Dr. Anthony A. Grace (University of Pittsburgh, PA, USA) and Dr. David J. Nutt (University of Bristol, UK).

REFERENCES

Aston-Jones, G. & Cohen, J. D. (2005a). Adaptive gain and the role of the locus coeruleus-norepinephrine system in optimal performance. *J. Comp. Neurol.*, *493*, 99-110.

Aston-Jones, G. & Cohen, J. D. (2005b). An integrative theory of locus coeruleus-norepinephrine function: Adaptive gain and optimal performance. *Annu. Rev. Neurosci.*, *28*, 403-450.

Berridge, C. W. & Waterhouse, B. D. (2003). The locus coeruleus-noradrenergic system: Modulation of behavioral state and state-dependent cognitive processes. *Brain Res. Brain Res. Rev.*, *42*, 33-84.

Blier, P. (2005). Medication combination and augmentation strategies in the treatment of major depression. In D. J. Stein, D. J. Kupfer, & Schatzberg, A. F. (Eds.), *The American Textbook of Mood Disorders.* American Psychiatric Publishing Inc., Washington DC, 509-524.

Blier, P. & Szabo, S. T. (2005). Potential mechanisms of action of atypical antipsychotic medications in treatment-resistant depression and anxiety. *J. Clin. Psychiatry*, *66 Suppl 8*, 30-40.

Bouret, S. & Sara, S. J. (2005). Network reset: A simplified overarching theory of locus coeruleus noradrenaline function. *Trends Neurosci.*, *28*, 574-582.

Brooks, D. J. & Piccini, P. (2006). Imaging in parkinson's disease: The role of monoamines in behavior. *Biol. Psychiatry*, *59*, 908-918.

Celada, P., Puig, M., Amargos-Bosch, M., Adell, A. & Artigas, F. (2004). The therapeutic role of 5-HT1A and 5-HT2A receptors in depression. *J. Psychiatry Neurosci.*, *29*, 252-265.

Chamberlain, S. R., Muller, U., Blackwell, A. D., Clark, L., Robbins, T. W. & Sahakian, B. J. (2006). Neurochemical modulation of response inhibition and probabilistic learning in humans. *Science*, *311*, 861-863.

Cohen, J. D. & Aston-Jones, G. (2005). Cognitive neuroscience: Decision amid uncertainty. *Nature*, *436*, 471-472.

Coull, J. T. (1994). Pharmacological manipulations of the alpha 2-noradrenergic system. effects on cognition. *Drugs Aging*, *5*, 116-126.

Davies, M. F., Tsui, J., Flannery, J. A., Li, X., DeLorey, T. M. & Hoffman, B. B. (2004). Activation of alpha2 adrenergic receptors suppresses fear conditioning: Expression of c-fos and phosphorylated CREB in mouse amygdala. *Neuropsychopharmacology*, *29*, 229-239.

Dremencov, E., El Mansari, M. & Blier, P. (2007a). Distinct electrophysiological effect of paliperidone and risperidone on the firing activity of rat serotonin and norepinephrine neurons. *Psychopharmacology (Berl)*, *194*, 63-72.

Dremencov, E., El Mansari, M. & Blier, P. (2007b). Noradrenergic augmentation of escitalopram response by risperidone: Electrophysiologic studies in the rat brain. *Biol. Psychiatry*, *61*, 671-678.

El Mansari, M. & Blier, P. (2005). Responsiveness of 5-HT(1A) and 5-HT2 receptors in the rat orbitofrontal cortex after long-term serotonin reuptake inhibition. *J. Psychiatry Neurosci.*, *30*, 268-274.

Fendt, M., Siegl, S. & Steiniger-Brach, B. (2005). Noradrenaline transmission within the ventral bed nucleus of the stria terminalis is critical for fear behavior induced by trimethylthiazoline, a component of fox odor. *J. Neurosci.*, *25*, 5998-6004.

Garelick, M. G. & Storm, D.R. (2005). The relationship between memory retrieval and memory extinction. *Proc. Natl. Acad. Sci.*, U. S. A., *102*, 9091-9092.

Guiard, B. P., El Mansari, M., Merali, Z. & Blier, P. (2008). Functional interactions between dopamine, serotonin and norepinephrine neurons: An in-vivo electrophysiological study in rats with monoaminergic lesions. *Int. J. Neuropsychopharmacol.*, 1-15.

Hajos-Korcsok, E., Robinson, D. D., Yu, J. H., Fitch, C. S., Walker, E. & Merchant, K. M. (2003). Rapid habituation of hippocampal serotonin and norepinephrine release and anxiety-related behaviors, but not plasma corticosterone levels, to repeated footshock stress in rats. *Pharmacol. Biochem. Behav.*, *74*, 609-616.

Hammond, D. L. & Proudfit, H. K. (1980). Effects of locus coeruleus lesions on morphine-induced antinociception. *Brain Res.*, *188*, 79-91.

Harley, C. W. (2004). Norepinephrine and dopamine as learning signals. *Neural Plast.*, *11*, 191-204.

Hurlemann, R., Hawellek, B., Matusch, A., Kolsch, H., Wollersen, H., Madea, B., Vogeley, K., Maier, W. & Dolan, R. J. (2005). Noradrenergic modulation of emotion-induced forgetting and remembering. *J. Neurosci.*, *25*, 6343-6349.

Janssen, P. A., Niemegeers, C. J., Awouters, F., Schellekens, K. H., Megens, A. A. & Meert, T. F. (1988). Pharmacology of risperidone (R 64 766), a new antipsychotic with serotonin-S2 and dopamine-D2 antagonistic properties. *J. Pharmacol. Exp. Ther.*, *244*, 685-693.

Juckel, G., Hegerl, U., Mavrogiorgou, P., Gallinat, J., Mager, T., Tigges, P., Dresel, S., Schroter, A., Stotz, G., Meller, I., Greil, W. & Moller, H. J. (2000). Clinical and biological findings in a case with 48-hour bipolar ultrarapid cycling before and during valproate treatment. *J. Clin. Psychiatry*, *61*, 585-593.

Kennedy, S. H. & Lam, R. W. (2003). Enhancing outcomes in the management of treatment resistant depression: A focus on atypical antipsychotics. Bipolar Disord., *5 Suppl 2*, 36-47.

Kennedy, S. H., Lam, R. W., Cohen, N. L. & Ravindran, A. V. (2001). Clinical guidelines for the treatment of depressive disorders. IV. medications and other biological treatments. *Can. J. Psychiatry*, *46 Suppl 1*, 38S-58S.

Kitaichi, Y., Inoue, T., Nakagawa, S., Izumi, T. & Koyama, T. (2005). Effect of milnacipran on extracellular monoamine concentrations in the medial prefrontal cortex of rats pre-treated with lithium. *Eur. J. Pharmacol.*, *516*, 219-226.

Kovacs, P. & Hernadi, I. (2002). Iontophoresis of lithium antagonizes noradrenergic action on prefrontal neurons of the rat. *Brain Res.*, *947*, 150-156.

Marek, G. J., Martin-Ruiz, R., Abo, A. & Artigas, F. (2005). The selective 5-HT2A receptor antagonist M100907 enhances antidepressant-like behavioral effects of the SSRI fluoxetine. *Neuropsychopharmacology*, *30*, 2205-2215.

Masana, M. I., Bitran, J. A., Hsiao, J. K., Mefford, I. N. & Potter, W. Z. (1991). Lithium effects on noradrenergic-linked adenylate cyclase activity in intact rat brain: An in vivo microdialysis study. *Brain Res.*, *538*, 333-336.

Matthews, K. L., Chen, C. P., Esiri, M. M., Keene, J., Minger, S. L. & Francis, P. T. (2002). Noradrenergic changes, aggressive behavior, and cognition in patients with dementia. *Biol. Psychiatry*, *51*, 407-416.

Meyer, J. H., Ginovart, N., Boovariwala, A., Sagrati, S., Hussey, D., Garcia, A., Young, T., Praschak-Rieder, N., Wilson, A. A. & Houle, S. (2006). Elevated monoamine oxidase a levels in the brain: An explanation for the monoamine imbalance of major depression. *Arch. Gen. Psychiatry*, *63*, 1209-1216.

Mueller, D., Porter, J. T. & Quirk, G. J. (2008). Noradrenergic signaling in infralimbic cortex increases cell excitability and strengthens memory for fear extinction. *J. Neurosci.*, *28*, 369-375.

Muller, U., Mottweiler, E. & Bublak, P. (2005). Noradrenergic blockade and numeric working memory in humans. *J. Psychopharmacol.*, *19*, 21-28.

Newport, D. J. & Nemeroff, C. B. (2000). Neurobiology of posttraumatic stress disorder. *Curr. Opin. Neurobiol.*, *10*, 211-218.

Nieuwenhuis, S., Aston-Jones, G. & Cohen, J. D. (2005). Decision making, the P3, and the locus coeruleus-norepinephrine system. *Psychol. Bull.*, *131*, 510-532.

Nutt, D. J. (2001). Neurobiological mechanisms in generalized anxiety disorder. *J. Clin. Psychiatry*, *62 Suppl 11*, 22-7; discussion 28.

O'Carroll, R. E. & Papps, B. P. (2003). Decision making in humans: The effect of manipulating the central noradrenergic system. *J. Neurol. Neurosurg. Psychiatry.*, *74*, 376-378.

Onaka, T., Ikeda, K., Yamashita, T. & Honda, K. (2003). Facilitative role of endogenous oxytocin in noradrenaline release in the rat supraoptic nucleus. *Eur. J. Neurosci.*, *18*, 3018-3026.

Otagiri, A., Wakabayashi, I. & Shibasaki, T. (2000). Selective corticotropin-releasing factor type 1 receptor antagonist blocks conditioned fear-induced release of noradrenaline in the hypothalamic paraventricular nucleus of rats. *J. Neuroendocrinol.*, *12*, 1022-1026.

Ouyang, M. & Thomas, S. A. (2005). A requirement for memory retrieval during and after long-term extinction learning. *Proc. Natl. Acad. Sci.*, U. S. A., *102*, 9347-9352.

Papakostas, G. I., Petersen, T. J., Kinrys, G., Burns, A. M., Worthington, J. J., Alpert, J. E., Fava, M. & Nierenberg, A. A. (2005). Aripiprazole augmentation of selective serotonin reuptake inhibitors for treatment-resistant major depressive disorder. *J. Clin. Psychiatry*, *66*, 1326-1330.

Remy, P., Doder, M., Lees, A., Turjanski, N. & Brooks, D. (2005). Depression in parkinson's disease: Loss of dopamine and noradrenaline innervation in the limbic system. *Brain*, *128*, 1314-1322.

Richelson, E. & Souder, T. (2000). Binding of antipsychotic drugs to human brain receptors focus on newer generation compounds. *Life Sci.*, *68*, 29-39.

Rossetti, Z. L. & Carboni, S. (2005). Noradrenaline and dopamine elevations in the rat prefrontal cortex in spatial working memory. *J. Neurosci.*, *25*, 2322-2329.

Seager, M. A., Barth, V. N., Phebus, L. A. & Rasmussen, K. (2005). Chronic coadministration of olanzapine and fluoxetine activates locus coeruleus neurons in rats: Implications for bipolar disorder. *Psychopharmacology (Berl)*, *181*, 126-133.

Seu, E., Lang, A., Rivera, R. J. & Jentsch, J. D. (2008). Inhibition of the norepinephrine transporter improves behavioral flexibility in rats and monkeys. *Psychopharmacology (Berl)*.

Shekhar, A., Katner, J. S., Sajdyk, T. J. & Kohl, R. R. (2002). Role of norepinephrine in the dorsomedial hypothalamic panic response: An in vivo microdialysis study. *Pharmacol. Biochem. Behav.*, *71*, 493-500.

Shekhar, A., Katner, J. S., Rusche, W. P., Sajdyk, T. J. & Simon, J. R. (1994). Fear-potentiated startle elevates catecholamine levels in the dorsomedial hypothalamus of rats. *Pharmacol. Biochem. Behav.*, *48*, 525-529.

Shimizu, T., Tsuda, A., Yokoo, H., Mizoguchi, K., Gondoh, Y., Matsuguchi, N. & Tanaka, M. (1990). Effects of stress, non-stress cyclicity on hypothalamic noradrenaline release in rats. *Kurume Med. J.*, *37*, 49-53.

Simon, J. S. & Nemeroff, C. B. (2005). Aripiprazole augmentation of antidepressants for the treatment of partially responding and nonresponding patients with major depressive disorder. *J. Clin. Psychiatry*, *66*, 1216-1220.

Szabo, S. T. & Blier, P. (2002a). Effects of serotonin (5-hydroxytryptamine, 5-HT) reuptake inhibition plus 5-HT(2A) receptor antagonism on the firing activity of norepinephrine neurons. *J. Pharmacol. Exp. Ther.*, *302*, 983-991.

Szabo, S. T. & Blier, P. (2002b). Effects of serotonin (5-hydroxytryptamine, 5-HT) reuptake inhibition plus 5-HT(2A) receptor antagonism on the firing activity of norepinephrine neurons. *J. Pharmacol. Exp. Ther.*, *302*, 983-991.

Szabo, S. T. & Blier, P. (2001a). Serotonin (1A) receptor ligands act on norepinephrine neuron firing through excitatory amino acid and GABA(A) receptors: A microiontophoretic study in the rat locus coeruleus. *Synapse*, *42*, 203-212.

Szabo, S. T. & Blier, P. (2001b). Response of the norepinephrine system to antidepressant drugs. *CNS Spectr.*, *6*, 679-684.

Szabo, S. T. & Blier, P. (2001c). Functional and pharmacological characterization of the modulatory role of serotonin on the firing activity of locus coeruleus norepinephrine neurons. Brain Res., *922*, 9-20.

Szabo, S. T., de Montigny, C. & Blier, P. (1999). Modulation of noradrenergic neuronal firing by selective serotonin reuptake blockers. *Br. J. Pharmacol.*, *126*, 568-571.

Tanaka, M. (1999). Emotional stress and characteristics of brain noradrenaline release in the rat. *Ind. Health*, *37*, 143-156.

Tigges, P., Juckel, G., Schroter, A., Moller, H. J. & Hegerl, U. (2000). Periodic motor impairments in a case of 48-hour bipolar ultrarapid cycling before and under treatment with valproate. *Neuropsychobiology*, *42 Suppl 1*, 38-42.

Torrecilla, M., Ruiz-Ortega, J. A., Ugedo, L. & Pineda, J. (2007). Excitatory regulation of noradrenergic neurons by L-arginine/nitric oxide pathway in the rat locus coeruleus in vivo. Naunyn Schmiedebergs Arch. *Pharmacol.*, *375*, 337-347.

Tremblay, P. & Blier, P. (2006). Catecholaminergic strategies for the treatment of major depression. *Curr. Drug Targets*, *7*, 149-158.

Uzun, S., Kozumplik, O., Mimica, N. & Folnegovic-Smalc, V. (2005). Aripiprazole: An overview of a novel antipsychotic. *Psychiatr. Danub*, *17*, 67-75.

van der Meulen, J. A., Joosten, R. N., de Bruin, J. P. & Feenstra, M. G. (2007). Dopamine and noradrenaline efflux in the medial prefrontal cortex during serial reversals and extinction of instrumental goal-directed behavior. *Cereb. Cortex*, *17*, 1444-1453.

van Stegeren, A. H. (2008a). The role of the noradrenergic system in emotional memory. *Acta Psychol. (Amst)*, *127*, 532-541.

van Stegeren, A. H. (2008b). The role of the noradrenergic system in emotional memory. *Acta Psychol. (Amst)*, *127*, 532-541.

van Stegeren, A. H., Wolf, O. T., Everaerd, W. & Rombouts, S. A. (2008). Interaction of endogenous cortisol and noradrenaline in the human amygdala. *Prog. Brain Res.*, *167*, 263-268.

Veyrac, A., Nguyen, V., Marien, M., Didier, A. & Jourdan, F. (2007). Noradrenergic control of odor recognition in a nonassociative olfactory learning task in the mouse. *Learn. Mem.*, *14*, 847-854.

Wei, H. & Pertovaara, A. (2006). Spinal and pontine alpha2-adrenoceptors have opposite effects on pain-related behavior in the neuropathic rat. *Eur. J. Pharmacol.*, *551*, 41-49.

West, W. L., Yeomans, D. C. & Proudfit, H. K. (1993). The function of noradrenergic neurons in mediating antinociception induced by electrical stimulation of the locus coeruleus in two different sources of sprague-dawley rats. *Brain Res.*, *626*, 127-135.

Wiste, A. K., Arango, V., Ellis, S. P., Mann, J. J. & Underwood, M. D. (2008). Norepinephrine and serotonin imbalance in the locus coeruleus in bipolar disorder. *Bipolar Disord.*, *10*, 349-359.

Yeomans, D. C., Clark, F. M., Paice, J. A. & Proudfit, H. K. (1992). Antinociception induced by electrical stimulation of spinally projecting noradrenergic neurons in the A7 catecholamine cell group of the rat. *Pain*, *48*, 449-461.

Yokoo, H., Tanaka, M., Tanaka, T. & Tsuda, A. (1990a). Stress-induced increase in noradrenaline release in the rat hypothalamus assessed by intracranial microdialysis. *Experientia*, *46*, 290-292.

Yokoo, H., Tanaka, M., Yoshida, M., Tsuda, A., Tanaka, T. & Mizoguchi, K. (1990b). Direct evidence of conditioned fear-elicited enhancement of noradrenaline release in the rat hypothalamus assessed by intracranial microdialysis. *Brain Res.*, *536*, 305-308.

In: Biochemistry and Histocytochemistry… ISBN: 978-1-60876-283-5
Editors: S. Fuchs, M. Auer, pp. 65-80 © 2010 Nova Science Publishers, Inc.

Chapter 4

THE ROLE OF SYMPATHETIC NERVE ACTIVITY IN RENAL INJURY

***Kazuko Masuo*[*1,2], *Gavin W. Lambert*[2] *and Murray D. Esler*[2]**
[1]Nucleus Network Ltd. and [2]Human Neurotransmitter Laboratory,
Baker IDI Heart & Diabetes Research Institute,
Melbourne, Victoria 3004, Australia

ABSTRACT

Renal injury, chronic renal disease and end-stage renal disease are often associated with obesity, hypertension, and diabetes mellitus. Heightened sympathetic nerve activity is observed in patients with renal injury, renovascular hypertension, chronic renal disease and end-stage renal disease (ESRD). Further, heightened sympathetic nerve activity as observed in plasma norepinephrine concentrations predicts survival and the incidence of cardiovascular events in patients with end-stage renal disease, and future renal injury in normotensive healthy subjects with a normal range of renal function. Hypertension, obesity and diabetes are currently among the World Health Organization's top 10 global health risks. Hypertension and diabetes mellitus, which occur often with obesity, together account for approximately 70% of end-stage renal diseases in the United States and Japan. Obesity also leads to increases in the incidence of cardiovascular diseases including renal injury. Many clinical and epidemiological studies have also documented that heightened sympathetic nerve activity plays an important role in obesity and hypertension. Thus, one could speculate that heightened sympathetic nerve activity might be an important mechanism of the onset and maintenance of renal injury, and that obesity and hypertension might emphasize the relationship between heightened sympathetic nerve activity and renal injury.

Human obesity and hypertension have strong genetic as well as environmental determinants. Several observations show associations of β2- and β3-adrenoceptor polymorphisms with hypertension and obesity, although these findings have not been confirmed. In addition, relationships between adrenoceptor polymorphisms, plasma

* Correspondence: Kazuko Masuo, MD, PhD, 1Nucleus Network Ltd., 2 Human Neurotransmitter Laboratory Baker IDI Heart & Diabetes Research Institute 89 Commercial Road, Melbourne Victoria 3004, Australia, Phone: +61-3-8532-1111 Fax: +61-3-8532-1100 E-mail: kmasuo@baker.edu.au.

norepinephrine levels, and renal function have not been fully studied. Understanding the contribution of plasma norepinephrine and β-adrenoceptor polymorphisms with the onset and maintenance of renal injury might aid in the prevention of renal injury, chronic renal disease and end-stage renal disease in obesity and hypertension. It may theoretically help rational, pharmacological treatments for renal injury in obesity and hypertension.

The purpose of this review is to provide the current findings on the relationships between sympathetic nerve activity, β-adrenoceptor polymorphisms and renal function. Also, to further understand the precise roles of sympathetic nerve activity in renal injury in the context of obesity and hypertension, which may lead to the prevention and treatment of renal injury in these patients.

Keywords: *plasma norepinephrine, sympathetic nerve activity, renal injury, end-stage renal disease, hypertension*

INTRODUCTION

Currently heightened sympathetic nerve activity is recognized as an important mechanisms involved in cardiovascular complications in humans [1]. Heightened sympathetic nerve activity leads to arterial blood pressure elevation, triggers arterial damage, and results in cardiovascular events. There is consistent evidence that high plasma norepinephrine levels as an index of heightened sympathetic nerve activity, predicts mortality in cardiovascular disease such as chronic congestive heart failure [2], asymptomatic left ventricular dysfunction [3] and end-stage renal disease (ESRD) [4]. Renal injury predicts the development of cardiovascular disease [5]. Therefore, the early stage of renal injury may be used as one of the markers for future serious cardiovascular events.

The association between hypertension, obesity and chronic renal disease is well recognized [6-8]. Obesity and hypertension also lead to increases in the incidence of metabolic diseases such as diabetes mellitus, and diabetes mellitus is frequently associated with renal injury (proteinuria/microalubuminuria). More than 70% of patients with ESRD has recently been attributed to complications of diabetes or hypertension [5]. The incidence of hypertension, one of the primary etiological factors for chronic renal failure, is significantly higher with obesity, suggesting that obesity is an independent factor for chronic renal disease [7]. Obesity is also frequently observed with diabetes mellitus [9, 10] and hypertension [11], and both diabetes and hypertension together account for approximately 70% of ESRD in the United States [5]. Further, obesity is an important factor to the onset of renal disease [12]. Heightened sympathetic nerve activity is documented in both obesity and hypertension in many clinical and epidemiological studies [13-18]. Thus, one could speculate that heightened sympathetic nerve activity associated with obesity and hypertension might play an important role in the onset and maintenance of renal injury regardless of its severity [17-19].

Many investigators have shown heightened sympathetic nerve activity observed in plasma norepinephrine or microneurography in patients with ESRD in cross-sectional studies [20, 21]. These observations show renal injury or ESRD is a consequence of hypertension and obesity, however, most of previous studies regarding the relationships between sympathetic nerve activity and renal function have investigated proteinuria or microalbuminuria as a maker for renal injury. Few investigations have simultaneously taken into account

sympathetic nerve activity and renal function in the same study population followed longitudinally for several years [19]. Only one study is available to show that heightened sympathetic nerve activity (high plasma norepinephrine) predicts future renal injury in normotensive, healthy subjects [19]. Further, this study suggested that the β2- adrenoceptor polymorphisms that is recognized with the strong linkage of the pathogenesis of obesity and hypertension [22-26] relates to future renal injury [19]. These findings may indicate a vicious triangle between sympathetic nerve activation, renal injury (ESRD), obesity and hypertension, and those states may be determined by genetic background through heightened sympathetic nerve activity.

The purpose of this article is to provide the current findings on the important, but not fully clarified topics, including the relationships between sympathetic nerve activity and renal injury in hypertension and obesity. To better understand the contribution of the sympathetic nervous system to the onset and the development of renal injury might prevent future ESRD especially in patients with obesity, hypertension and diabetes, and help theoretically rational treatments on those patients with renal injury.

PLASMA NOREPINEPHRINE AS A PREDICTOR FOR FUTURE CARDIOVASCULAR AND RENAL EVENTS

(1)Plasma Norepinephrine Levels Predicts Cardiovascular Events in Patients with ESRD (Figure 1)

Heightened sympathetic nerve activity has an important role in cardiovascular complications in humans [1]. Sympathetic nerve activity is consistently elevated in patients with ESRD [25, 26] (Figure 1). Zoccali *et al.* [8, 20] examined the relationships between sympathetic nerve activity (plasma norepinephrine levels) and mortality and cardiovascular events in 228 patients undergoing chronic hemodialysis without originally heart failure. They found 45% of dialysis subjects had significantly high plasma norepinephrine levels located in the upper limit of the normal range. One-hundred and twenty four (124) fatal and nonfatal cardiovascular events occurred in 85 patients during the follow-up period (34±15 months). Plasma norepinephrine levels proved to be an independent predictor of fatal and nonfatal cardiovascular events in a multivariate Cox regression model.

(2)Plasma Norepinephrine Levels Predicts Future Renal Injury in Normotensive Healthy Subjects (Figures 2 And 3)

Masuo *et al*. [19] measured renal function (creatinine, BUN, creatinine clearance) and plasma norepinephrine levels over a 5-year period in nonobese, normotensive men with normal renal function. Subjects who had a significant deterioration of renal function (≥10% increases from baseline of creatinine and BUN or decrease in creatinine clearance) over a 5-year period had higher plasma norepinephrine at the entry period and greater increases in plasma norepinephrine over 5 years (Figure 2)**.** In this study, subjects who had significant changes in body weight or blood pressure were excluded.

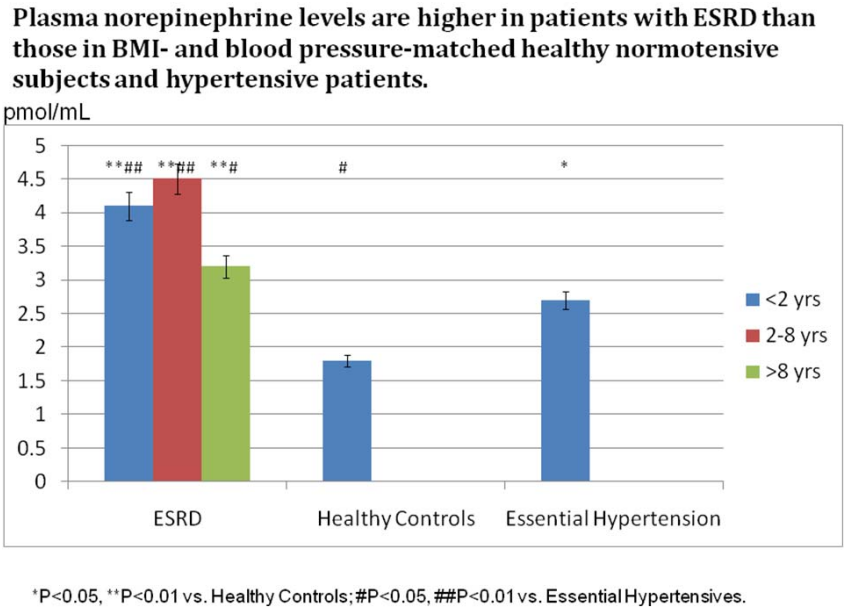

Figure 1. ESRD; patients with end-stage renal disease. Plasma norepinephrine levels decreased with the duration of hemodyalisis. Plasma norepinephrine levels were significantly higher in patients with ESRD with hemodialysis than BMI-matched normotensive subjects or BMI- and blood pressure-matched essential hypertensive patients. [Reference 21, Masuo K, et al. 2008]

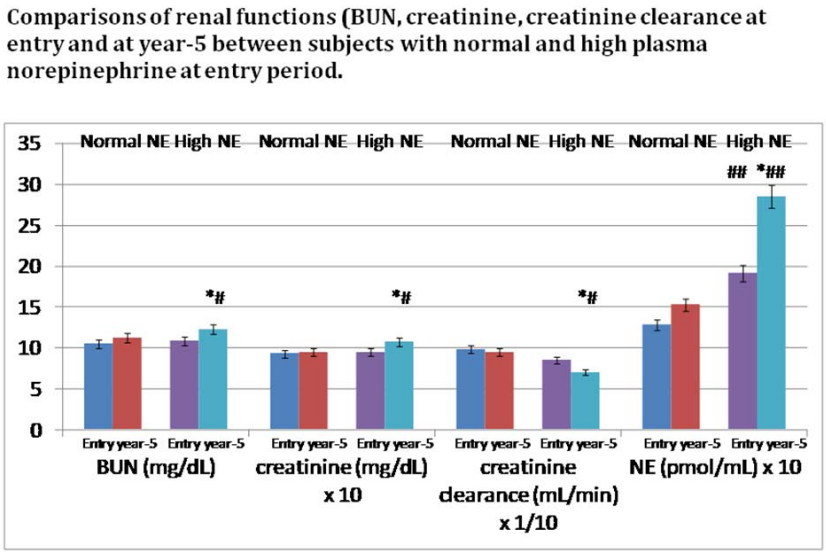

Figure 2. NE, norepinephrine; Normal NE, normal plasma norepinephrine concentrations at entry period; High NE, high (>mean +2SD) plasma norepinephrine concentrations at entry period. [Reference 19, Masuo K, et al.2007].

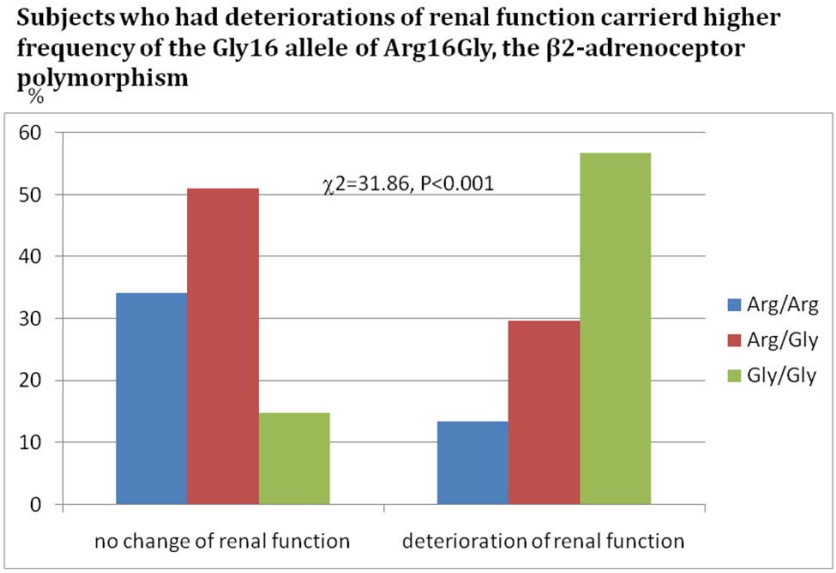

Figure 3. Subjects who had deteriorations of renal function carried higher frequency of the Gly16 allele of Arg16Gly, the β 2-adrenoceptor polymorphism.[Reference 19, Masuo K, et al. 2007].

Further, subjects who had significantly higher levels of plasma norepinephrine carried higher frequency of the Gly16 allele of β2-adrenoceptor polymorphism [20] (Figure 3). The Gly16 allele of β2-adrenoceptor polymorphism is also known to be associated with obesity [23, 25, 26], hypertension [23, 26], and metabolic syndrome [24]. Thus, high plasma norepinephrine might be a predictor determined genetically by the β2-adrenoceptor polymorphism (Arg16Gly) for renal injury, obesity, hypertension, and metabolic syndrome.

These observations demonstrate that plasma norepinephrine as an index of sympathetic nerve activity has strong linkage with the onset and development of renal injury. Plasma norepinephrine (a neurotransmitter) measurements represent a useful marker to assess sympathetic nerve activity in a cohort studies, although the amount of norepinephrine in the plasma is only a fraction of the amount released into the synaptic clefts and may be influenced by several factors, such as the rate of reuptake into the nerve endings or into extra neuronal cells, the density of neuroeffector junctions, and the metabolic clearance rate. However, in our experience, plasma norepinephrine concentrations from forearm venous sampling correlate closely with whole-body norepinephrine spillover measured by the isotope dilution technique (Figure 4) and muscle sympathetic nervous activity using microneurography [27, 28]. This suggests that forearm venous plasma norepinephrine levels are still practical for population-based studies.

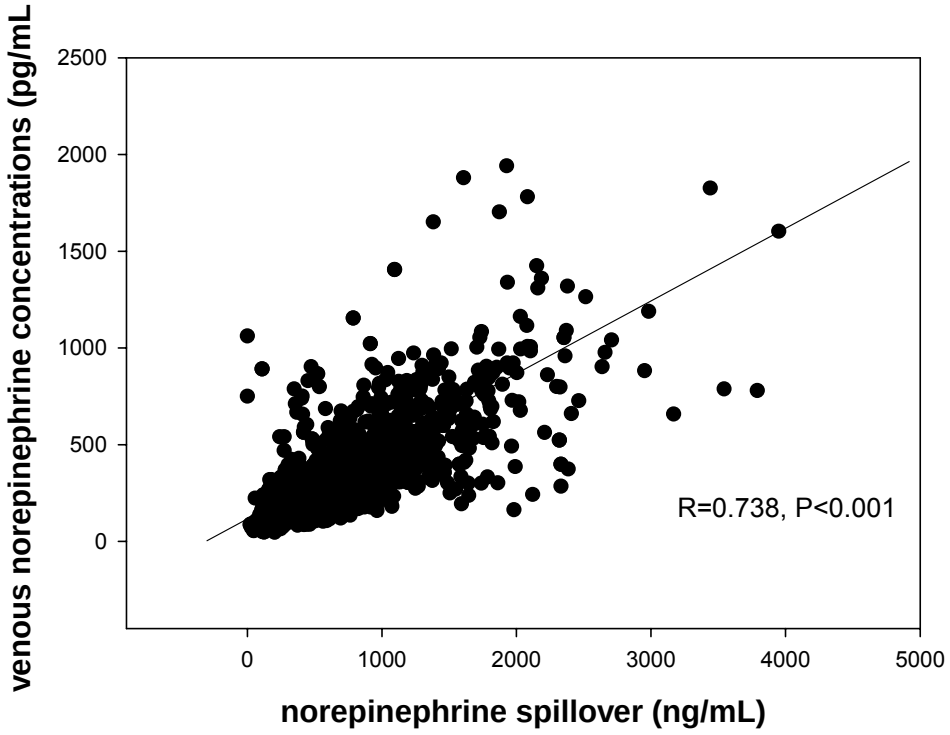

Figure 4. Correlation between whole-body plasma norepinephrine spillover and venous plasma norepinephine concentrations .[Reference 29, Masuo K, et al. 2008].

THE ROLE OF THE KIDNEYS IN HYPERTENSION AND OBESITY

Hypertension and obesity are important causes for renal injury, chronic renal disease and ESRD. The association between hypertension, obesity and heightened sympathetic nerve activity is well documented [18, 22-29]. Rumantir *et al.* [30] found when compared with healthy nonobese normotensive subjects, norepinephrine spillover from the heart and kidneys is increased in lean hypertensive patients. In the obese population, renal norepinephrine spillover was increased in both normotensive and hypertensive obese, independent of blood pressure, while cardiac norepinephrine spillover was significantly reduced in obese normotensive individuals. Hall *et al.* [7, 31] reviewed the importance in the kidneys for the pathogenesis of obesity-related hypertension as obesity raises blood pressure by increasing renal tubular reabsorption, impairing pressure natriuresis, causing volume expansion due to activation of the sympathetic nervous system and renin-angiotensin system, and by physical compression of the kidneys, especially when visceral obesity is present. Long-term obesity may cause an increasing urinary protein excretion and a gradual loss of nephron function that worsens with time and exacerbates hypertension. These investigations demonstrate that the kidney and renal sympathetic nerve activity play important roles in the pathogenesis of hypertension, obesity, and obesity-related hypertension.

Renal Sympathetic Nerve Activity in Hypertension

There is growing evidence that the renal sympathetic nerves may contribute to the pathogenesis of several types of experimental hypertension in animal models and that the defect in renal excretory function in hypertension is an increase in renal sympathetic nerve activity [32]. Increased renal sympathetic nerve activity is found in animal models of hypertension and hypertensive humans as mentioned above [30]. Renal denervation can either attenuate the severity or delay the development of hypertension in spontaneously hypertensive rats (SHR), in DOCA-salt treated rats and in renovascular hypertensive rats [33-35]. On the other hand, increased renal sympathetic nerve activity results in reduced renal excretory function by virtue of effects on the renal vasculature, the tubules, and the juxtaglomerular granular cells, and impaired arterial baroreflex regulation. Intra-renal administration of catecholamines has been shown to elicit an increase in systemic arterial pressure as long as the infusion is continued. Blood pressure is directly influenced either by several manoeuvres applied to the kidney or by the electrical stimulation of afferent renal nerve fibers. It is known that efferent renal sympathetic nerve activity, by exerting a direct influence on renal arteriolar tone, renin release and sodium and water excretion, can interfere with the control of arterial pressure by modifying peripheral resistance, circulating angiotensin II and volume balance. These investigations showed that the renal sympathetic nerves may contribute to the development of hypertension through the renal excretory defect as well as vascular tone either directly or indirectly via the renin-angiotensin system.

On the other hand, Burke *et al.* [36] observed that the sympathetic nerve activity modulates peripheral vasoconstriction in angiotensin II-induced hypertension. Renal sympathetic nerve activity was not altered by angiotensin II-induced hypertension nor blood pressure levels (hypertension) was not altered by renal denervation. The greater depressor effect of acute ganglion blockade was observed in angiotensin II-induced hypertensive rabbits. The findings suggest that renal sympathetic nerve activity does not contribute to hypertension, but the renal sympathetic nerve activity exerts increased vasoconstriction in the peripheral vasculature in angiotensin II-induced hypertension. Lohmeier *et al.* [37] reported that renal denervation did not abolish sustained baroreflex-mediated reductions in arterial pressure, and does not affect mean arterial pressure, plasma norepinephrine concentration, plasma rennin activity, and sodium excretion chronically (14 days after renal denervation), although those were recognized at the early stage (1 day after renal denervation). Their findings are important to evaluate the long-term efficacy of renal denervation of refractory hypertension.

Conflicting results have been published with regards to the effects of renal denervation on hypertension. Further studies are needed to clarify these relationships and the mechanisms of the renal sympathetic nervous system in hypertension.

Sympathetic Nerve Activity and Abnormal Renal-Pressure Natriuresis in Hypertension (Figure 4)

Long-term control of arterial pressure has been attributed to the kidney by virtue of its ability to couple the regulation of blood volume to the maintenance of sodium and water balance by the mechanisms of pressure natriuresis and dieresis [31]. In the presence of a

defect in renal excretory function, hypertension arises as the consequence of the need for an increase in arterial pressure to offset the abnormal pressure natriuresis and diuresis mechanisms, and to maintain sodium and water balance (Figure 5). One of the most important of abnormal renal-pressure natriuresis proved to be the renin-angiotensin system. When the renin-angiotensin system is fully functional, the chronic relationship between arterial pressure and sodium excretion is extremely steep, and sodium balance can be maintained over a wide range of intakes with minimal changes in arterial pressure. Another important neurohormonal modulation of renal-pressure natriuresis is the sympathetic nervous system. In obese subjects, impaired pressure natriuresis is initially due to increased renal sodium reabsorption because glomerular filtration rate (GFR) and renal plasma flow are actually increased. With prolonged obesity, increased arterial pressure, renal vasodilation and glomerular hyperfiltration, neurohormonal activations on the sympathetic nervous system and renin-angiotensin system, and metabolic changes may cause glomerular injury and further impairment of renal-pressure natriuresis, resulting in more severe hypertension and a gradual loss of kidney function [38]. Relatively small changes in renal artery pressure may cause large alterations in sodium and water excretions that persisted as long as renal artery pressure is altered.

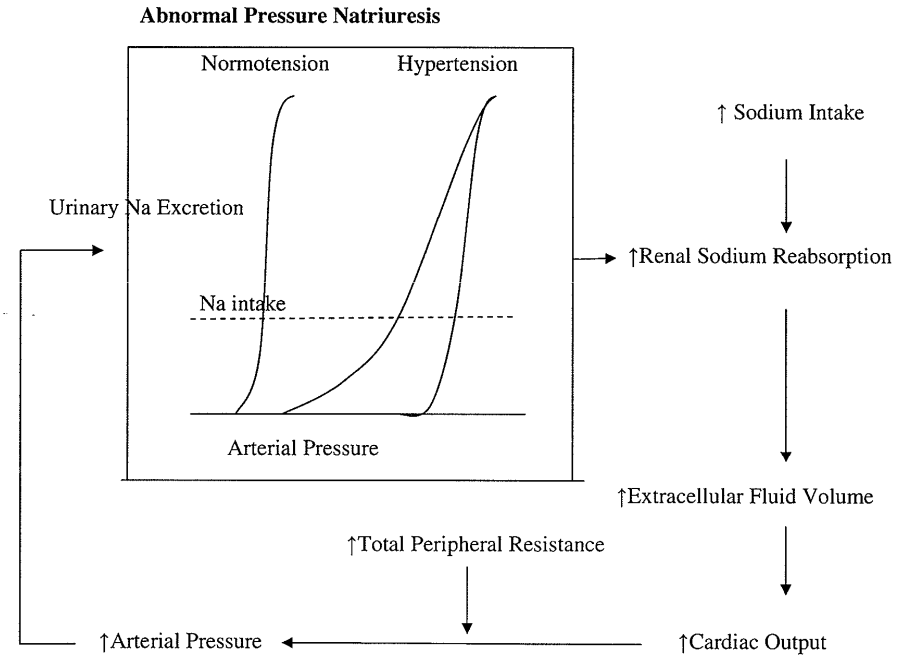

Figure 5. Abnormal pressure-natriuresis causes high blood pressure .

Leptin Causes Hypertension through Sympathetic Nerve Activation in the Kidney

Leptin, a 16-kDa protein derived principally from adipose tissue, has been implicated in body weight homeostasis (weight loss) by reducing appetite and by increasing energy

expenditure through sympathetic nerve stimulation to thermogenic tissue [39, 40]. In the kidney, leptin may affect blood pressure mainly by two opposing ways: the first, leptin stimulates renal sympathetic nerve activity [41-43], thus renal denervation attenuates the anti-natriuretic and hypotensive effect of obesity in rats [44]. The second is related to nitric oxide (NO) synthesis [45] and endothelial mechanisms [46]. The renal effect of leptin also depends on the exposure time of the hormone. Leptin infusion for short periods of time (bolus infusion) produces increased sodium excretion and urine output with no changes in blood pressure in lean Sprague-Dawley normotensive rats, but the natriuretic effect of leptin was attenuated significantly in obese Zucker rats [47]. The increased natriuresis and fractional sodium excretion are not accompanied by substantial exchanges in glomerular filtration rate or the renin-angiotensin axis suggesting decreased sodium tubular transport. Sodium-potassium exchange (Na/K-ATPase) activity in the renal medulla decreased significantly following acute leptin administration [48]. Further, several observations suggest hypotensive effects of leptin, itself, through stimulation of systemic NO release [49] and leptin-mediated vasorelaxant effects [46] when sympathetic nerve activity was blocked pharmacologically [45].

SYMPATHETIC NERVE ACTIVITY IN RENAL DISEASE

Sympathetic Nerve Activity in Patients with Renal Parenchymal Disease (Renal Injury)

Intravascular volume expansion is a major pathogenic factor in renal parenchymal hypertension. In these patients, excessive renin secretion relative to volume status and heightened sympathetic nerve activity are observed, and those contribute to hypertension in patients with renal injury. Potential mechanisms include afferent stimuli from the injured kidneys to the brain, reduced central dopaminergic tone, reduced baroreceptor sensitivity, abnormal vagal function and endothelial dysfunction in patients with renal dysfunction [45, 46, 49].

Early glomerular changes in obesity may be the precursors of more severe glomerular injury and progressive impairment of pressure natriuresis. For example, studies in obese humans have shown that obesity is associated with proteinuria even before they had major histological changes in the kidneys [50]. Obese subjects have glomerulomegary and focal segmental glomerulosclerosis even in the absence of diabetes [50], and the prevalence significantly increases more than 10 times following with increases in the frequency of obesity.

Sympathetic Nerve Activity in Patients with End-Stage Renal Disease (ESRD)

Evidence now strongly indicates a role for the sympathetic nerve activity in the pathogenesis of hypertension in renal failure (ESRD). Hypertension occurs commonly and early in renal disease and is paralleled by increases in sympathetic nerve activity, as indicated

by increased muscle sympathetic nerve activity and circulating norepinephrine (Figure 1). This appears to be driven by the diseased kidneys, because nephrectomy or denervation has been shown to correct blood pressure and sympathetic nerve activity in human and animal studies [51]. One of the important mechanisms of the sympathetic nerve activity in hypertension in patients with ESRD is due to abnormal renal sodium excretion in patients with ESRD. In the normal state, interactions between the kidney and sympathetic nervous system serve to maintain blood pressure and glomerular filtration rate within tightly controlled levels, but in renal failure, a defect in renal sodium excretory function leads to an abnormal pressure natriuresis relationship and activation of the renin-angiotensin system, contributing to the development of hypertension (Figure 5) and progression of kidney disease [33, 34, 52, 53]. Another mechanism is that the sympathetic nerve activity may modulate baroreflex regulation and vasulature tone through the central nervous system and angiotensin II [36]. Afferent signals from the kidney, detected by chemoreceptors and mechanoreceptors, feed directly into central nuclei of the sympathetic nerve activity by circulating and brain-derived angiotensin II [54]. Therefore, the pathogenesis of hypertension in renal failure (ESRD) is complex and arises from the interaction of hemodynamic and neuroendocrine factors. At least, we can find that sympathetic nerve activity has strong relationships with regards to increased risk of cardiovascular disease [8, 20] in patients with ESRD and survival rate in chronic heart failure with renal injury, suggesting that we have to pay attention to sympathetic nerve activation to treat patients with ESRD.

Sympathetic Nerve Activity in Renovascular Hypertension

Although there is general agreement with regards the renin-angiotensin system for elevated blood pressure in the early phase of renovascular hypertension, other mechanisms such as sodium retention and the sympathetic nerve activation may contribute to the progress of the disorder [55, 56]. Miyajima *et al.* [57] reported increased muscle sympathetic nerve activity in renovascular hypertensive patients. Johnson *et al.* [58] found increased muscle sympathetic nerve activity and whole-body norepinephrine spillover in long-term renovascular hypertensive patients compared to normotensive subjects as well as primary hypertensive patients, and they reported sympathetic nerve activity 2 times higher in renovascular hypertensive patients compared to normotensive subjects. Esler *et al.* [59] reported a 38% increase in whole-body norepinephrine spillover in renovascular hypertensive patients compared to healthy normotensive subjects due to mainly higher norepinephrine release. Increased muscle sympathetic nerve activity is normalized after successful angioplasty of a renal artery, suggesting that restoration of blood flow to the ischemic kidneys may have eliminated the afferent stimulus that provoked the increased sympathetic nerve drive.

CLINICAL IMPLICATIONS

We discussed the importance of heightened sympathetic nerve activity, especially heightened renal sympathetic nerve activity, for the pathogenesis of renal disease and ESRD

in hypertension because the kidneys play a prominent role in fluid and electrolyte regulation and resultant arterial pressure homeostasis through renal sympathetic nerve activity and the renin-angiotensin system.

Renal Denervation as a Therapy for Hypertension

Many investigations have implicated sympathetically mediated mechanisms in the development of hypertension in animal models and in humans [1, 18, 22]. Accordingly, in some models of hypertension, complete renal denervation delayed the development of hypertension [33-35]. Renal denervation attenuates long-term hypertensive effects of angiotensin II [60]. Renal denervation changes baroreceptor function to attenuate chronic blood pressure elevation [33]. Further, renal sympathetic nerve activity is modulated by changes in baroreceptor afferent nerve activity under long-term high sodium diet [52] and low sodium diet represented by angiotensin II stimulation [34] in animal models. Disruption of the negative feedback loop between baroreceptor afferents and renal sympathetic nerve activity may lead to impaired regulation of fluid balances, resulting in an elevation in arterial pressure.

Jacob *et al.* [33] reported renal denervation chronically (10 days) lowered arterial pressure regardless of amount of sodium intakes in Sprague-Dawley rats. Another study was examined by Veelken *et al.* [53] to show that renal denervation prevent the onset of glomerulonephritis. Complete surgical bilateral renal denervation was performed 2 days before glomerulonephritis induced by injecting the monoclonal antibody. Denervation significantly reduced albuminuria, mesangiolysis, formation of microaneurysms, deposition of glomerular collagen IV, and expression of TGF-beta compared with sham-operated controls. Accordingly, inflammation, identified by accumulation of interstitial macrophages and renal expression of TNF-alpha, and mesangial cell proliferation were significantly reduced. These findings indicate that renal denervation ameliorates acute inflammation of glomerulonephritis in the kidney. They also speculated neurotransmitters or neuropeptides and their receptors might represent novel targets for the treatment of acute glomerulonephritis. Ojenda *et al.* [35] have proposed that early renal denervation may prevent the development of hypertension in intrauterine growth-restricted offspring who develop hypertension at the pre-pubertal age. They compared blood pressure and renal norepinephrine contents with intrauterine growth-restriction in animal models with and without renal denervation. Blood pressure and norepinephrine contents in the kidneys were significantly lower in those with renal denervation compared with sham operation after 2 weeks of renal denervation. The results indicate the effectiveness to prevent hypertension in low-birth weight babies who frequently had hypertension accompanied with a high risk of cardiovascular events.

In addition, currently the investigation of patients with refractory hypertension associated with end-stage renal disease are continuing to confirm the efficacy and safety of renal denervation by Ardian Inc (NCT00664638) [61]. Catheter-based renal denervation has been reported as an effective and safe, without serious adverse events, treatment to reduce blod pressure in 45 patients with resistant hypertension for 12 months in a multicenter trial [62, 63].

SUMMARY

The role of the sympathetic nervous system in renal injury, end-stage renal disease, and renovascular hypertension are discussed through a literature review accompanying sympathetic nerve mechanisms in hypertension and obesity. Relevant studies of sympathetic nerve activity and β2-adrenoceptor polymorphism might contribute to the onset and maintenance of renal injury in healthy subjects and in patients with chronic heart failure and cardiovascular events in ESRD patients. A better understanding of the relationships of sympathetic nerve activity with renal injury might help clinical implications (treatment) for renal injury in hypertensive patients and hypertension in patients with ESRD. Recently, the role of denervation of renal sympathetic nerve in refractory hypertension has been examined and showed its efficacy in humans. The outcome from the study have not been established, but a number of animal studies show theoretical benefits for those patients in the acute phase. Further studies are needed to clarify the relationships between the sympathetic nerve activity and renal injury.

REFERENCES

[1] Mancia G, Grassi G, Giannattasio C, Seravalle G. Sympathetic activation in the pathogenesis of hypertension and progression of organ damage. *Hypertension.* 1999; 34: 724-728.

[2] Cohn JN, Levine TB, Olivari MT, Garberg V, Lura D, Francis GS, Simon AB, Rector T. Plasma norepinephrine as a guide to prognosis in patients with chronic congestive heart failure. *N. Engl J Med.* 1984; 31: 819-823.

[3] Benedict CR, Shelton B, Johnstone DE, Francis G, Greenberg B, Koustam M, Probstfield JL, Yusuf S. for the SOLVD Investigators. Prognostic significance of plasma norepinephrine in patients with asymptomatic left ventricular dysfunction. *Circulation.* 1996; 94: 690-697.

[4] Ksiazek A, Zatuska W. Sympathetic overactivity in uremia. *J. Ren. Nutr.* 2008; 18: 118-121.

[5] Report of a WHO Expert Committee. Physiological status: the use and interpretation of anthropometry. *World Health Organ. Tech. Rep. Ser.* 1995; 854: 1-452.

[6] White SL, Caas A, Atkins RC, Chadban SJ. Chronic kidney disease in the general population. *Adv. Chronic. Dis.* 2005; 12: 5-13.

[7] Hall JE, Jones DW, Kuo JJ, de Silva A, Tallam LS, Liu J. Impact of the obesity epidemic on hypertension and renal disease. *Curr .Hypertens. Rep.* 2003; 5: 386-392.

[8] Zoccali C, Mallamaci F, Parlongo S, Cutrupi S, Benedetto AB, Tripepi G, Bonanno G, Rapisarda F, Fatuzzo P, seminara G, Cateliotti A, Stancanelli B, Malatino S. Plasma norepinephrine predicts survival and incident cardiovascular events in patients with end-stage renal disease. *Circulation.* 2002; 105: 1354-1359.

[9] Colditz GA, Willett WC, Rotnizky A, Manson JE. Weight gain as a risk for clinical diabetes mellitus in women. *Ann. Intern. Med.* 1995; 122: 481-486.

[10] Chen J, Muntner P, Hamm LL, Jones DW, Batuman V, Fonseca V, Whelton PK, He J. The metabolic syndrome and chronic kidney disease in U.S. adults. *Ann. Intern. Med.* 2004; 140: 167-174.

[11] Garrison RJ, Kannel WB, Stokes J 3rd, Castelli WP. Incidence and precursors of hypertension in young adults: the Framingham offspring study. *Prev. Med*. 1987; 16: 235-251.

[12] Iseki K, Ikemiya Y, Kinjo K, Inoue T, Iseki C, Takishita S. Body mass index and the risk of development of end-stage renal disease in a screened cohort. *Kidney Int.* 2004; 65: 1870-1876.

[13] Masuo K, Mikami H, Ogihara T, Tuck ML. Weight gain-induced blood pressure elevation. *Hypertension*. 2000; 35: 1135-1140.

[14] Masuo K, Kawaguchi H, Mikami H, Ogihara T, Tuck ML. Serum uric acid and plasma norepinephrine concentrations predict subsequent weight gain and blood pressure elevation. *Hypertension.* 2003; 42: 474-480.

[15] Masuo K, Mikami H, Ogihara T, Tuck ML. Sympathetic nerve hyperactivity precedes hyperinsulinemia and blood pressure elevation in young, nonobese Japanese population. *Am. J. Hypertens.* 1997; 10: 77-83.

[16] Masuo K, Mikaki H, Ogihara T, Tuck ML. Familial hypertension, insulin, sympathetic activity and blood pressure elevation. *Hypertension.* 1998; 32: 96-100.

[17] Masuo K, Mikami H, Ogihara T, Tuck ML. Familial obesity, sympathetic activation and blood pressure level. *Blood Press.* 2001; 10: 199-204.

[18] Masuo K. Obesity-related hypertension: Role of the sympathetic nervous system ,insulin, asnd leptin. *Curr. Hypertens. Rep.* 2002; 4: 112-118.

[19] Masuo K, Katsuya T, Sugimoto K, Kawaguchi H, Rakugi H, Ogihara T, Tuck ML. High plasma norepinephrine levels associated with β2-adrenoceptor polymorphisms predict future renal damage in nonobese normotensive individuals. *Hypertens. Res.* 2007; 30: 503-511.

[20] Zoccali C, Mallamaci F, Tripepi G, Parlongo S, Cutrupi S, Benedetto FA, Cataliotti A, Malatino S. Norepinephrine and concentric hypertrophy in patients with end-stage renal disease. *Hypertension.* 2002; 40: 41-46.

[21] Masuo K, Kawaguchi H, Katsuya T, Rakugi H, Ogihara T. Higher plasma norepinephrine, but lower plasma leptin concentrations in patients with end-stage renal disease. *Hypertens. Res.* (in press).

[22] Masuo K, Lambert GW, Rakugi H, Ogihara T, Esler MD. Neurovascular role of sympathetic nervous system and beta-adrenoceptor polymorphisms in obesity and hypertension. *Curr. Hypertens. Rev.* 2008; 4: 121-130.

[23] Masuo K, Katsuya T, Fu Y, Rakugi H, Ogihara T, Tuck ML. Beta2- and beta3-adrenergic receptor polymorphisms are related to the onset of weight gain and blood pressure elevation over 5 years. *Circulation.* 2005; 111: 3429-3434. .

[24] Masuo K, Katsuya T, Fu Y, Rakugi H, Ogihara T, Tuck ML. Beta2-adrenoceptor polymorphisms relate to insulin resistance and sympathetic overactivity as early markers of metabolic disease in nonobese, normotensive individuals. *Am. J. Hypertens.*2005; 8: 1009-1014.

[25] Masuo K, Katsuya T, Kawaguchi H, Fu Y, Rakugi H, Ogihara T, Tuck ML. Beta2-adrenoceptor polymorphisms relate to obesity through blunted leptin-mediated sympathetic activation. *Am. J. Hypertens.* 2006; 19: 1084-1091.

[26] Masuo K, Katsuya T, Kawaguchi H, Sugimoto K, Rakugi H, Ogihara T, Tuck ML. Beta2- and beta3-adrenoceptor polymorphisms relate to subsequent weight gain and blood pressure elevation in obese normotensive individuals. *Hypertens. Res.* 2006; 29: 951-959.

[27] Straznicky NE, Lambert EA, Lambert GW, Masuo K, Esler MD, Nestle PJ. Effects of dietary weight loss on sympathetic activity and cardiac risk factors associated with the metabolic syndrome. *J. Clin. Endocrinol. Metab.* 2005; 90: 5998-6005.

[28] Esler M, Straznicky N, Eikelis N, Masuo K, Lambert G, Lambert E. Mechanisms of sympathetic activation in obesity-related hypertension. *Hypertension*. 2006; 48: 787-796.

[29] Masuo K, Straznicky NE, Lambert GW, Esler MD. Obesity and obesity-related hypertension: Role of the sympathetic nervous system and β-adrenoceptor polymorphisms. In: Sympathetic Nervousd System Research Developments. Nova Science Publishers Inc. New York, USA., Editor, Kaneko M., pp67-92.

[30] Rumantir MS, Vaz M, Jennings GL, Collier G, Keye DM, Seals DR, Wiesner GH, Brunner-La Rocca HD, Esler MD. Neural mechanisms in human obesity-related hypertension. *J. Hypertens.* 1999; 17: 1125-1133.

[31] Hall JE. The kidney, hypertension, and obesity. Hypertension. 2003; 41[part 2]: 625-633.

[32] Deka-Starosta A, Garty M, Zukowska-Grojec Z, Keise HR, Kopin IJ, Goldstein DS. Renal sympathetic nerve activity and norepinephrine release in rats. *Am. J. Physiol.* 1989; 257: R229-R236.

[33] Jacob P, Ariza P, Osborn JW. Renal denervation chronically lower arterial pressure independent of dietary sodium intake in normal rats. *Am. J. Physiol. Heart Circ.* Physiol. 2003; 284: H2302-2310.

[34] Lohmeier TE, Lohmeier JR, Reckelhoff JF, Hildebrandt DA. Sustained influence of the renal nerves to attenuate sodium intake retention in angiotensin hypertension. *Am. J. Physiol. Regul. Interg .Comp. Physiol.* 2001; 281: R434-R443.

[35] Ojeda NB, Johnson WR, Dwyer TM, Alexander BT. Early renal denervation prevents development of hypertension in growth-restricted offspring. *Clin. Exp. Pharmacol. Physiol.* 2007; 34: 1212-1216.

[36] Burke SL, Evans RG, Moretti JL, Head GA. Levels of renal and extrarenal sympathetic drive in angiotensin II-induced hypertension. *Hypertension.* 2008; 51: 878-883.

[37] Lohmeier TE, Hildebrandt DA, Dwyer TM, Barrett AM, Irwin ED, Rossing MA, Kieval RS. Renal denervation does not abolish sustained baroreflex-mediated reductions in arterial pressure. *Hypertension*. 2007; 49: 373-379.

[38] Hall JE. Mechanisms of abnormal renal sodium handling in obesity hypertension. *Am. J. Hypertens*. 1997; 10: S49-S55.

[39] Correia ML, Haynes WG. Obesity-related hypertension: Is there a role for selective leptin resistance? *Curr. Hypertens. Rep*. 2004;6:230-235.

[40] Rahmouni K, Haynes WG. Leptin and the central neural mechanisms of obesity hypertension. Drugs Today (Barc). 2002;38:807-817.

[41] Haynes WG, Sivitz WI, Morgan DA, Walsh SA, Mark AL. Sympathetic and cardiorenal actions of leptin. *Hypertension.* 1997; 30: 619-623.

[42] Haynes WG, Morgan DA, Walsh SA, Mark AL, Sivitz WI. Receptor-mediated regional sympathetic nerve activation by leptin. *J. Clin. Invest.* 1997; 100: 270-278.

[43] Rahmouni K, Haynes WG, Morgan DA, Mark AL. Intracellular mechanisms involved in leptin regulation of sympathetic outflow. *Hypertension.* 2003; 41: 763-767.

[44] Villarreal D, Reams G, Freeman RH. Effects of renal denervation on the sodium excretory actions of leptin in hypertensive rats. *Kidney Int.* 2000; 58: 989-994.

[45] Vecchione C, Maffei A, Colella S, Aretini A, Poulet R, Frati G, Gentile MT, Fratta L, Trimarco V, Trimarco B, Lembo G. Leptin effects on endothelial nitric oxide is mediated through Akt-endothelial nitric oxide synthase phosphorylation pathway. Diabetes. 2002; 51: 168-173. Diabetes. 2002; 51: 168-173.

[46] Lembo G, vecchione C, Fratta L, Marino G, Trimarco V, d'Amati G, Trimarco B. Leptin induces direct vasodilation through distinct endothelial mechanisms. *Diabetes.* 2000; 49: 293-297.

[47] Villarreal D, Reams G, Freeman RH, Taraban A. Renal effects of leptin in normotensive, hypertensive, and obese rats. *Am. J. Physiol.* 1998; 275: R2056-R2060.

[48] Beltowski J, Marciniak A, Wojcicka G, Gorny D. The opposite effects of cyclic AMP-protein kinase a signal transduction pathway on renal cortical and medullary Na+, K+-ATPase activity. *J. Physiol. Pharmacol.* 2002; 53: 211;231.

[49] Beltowski J, Wojcicka G, Borkowska E. Human leptin stimulates systemic nitric oxide production in the rat. *Obes. Res.* 2002; 10: 939-946.

[50] Wesson DE, Kurtzman NA, Prommer JP. Massive obesity and nephrotic proteinuria with a normal renal biopsy. *Nephron.* 1985; 40: 235-237.

[51] Hausberg M, kosch M, Hamelink P, Barenbrock M, Hohage H, Kisters K, Dietl KH, Dahn KH. Sympathetic nerve activity in end-stage renal disease. *Circulation*. 2002; 106: 1974-1979.

[52] Lohmeier TE, Hildebrandt DA, Hood WA. Renal nerves promote sodium excretion during long-term increases in salt intake. *Hypertension.* 1999; 33: 487-492.

[53] Veelken R, Vogel EM, Hilgers K, Amann K, Hartner A, Sass G, Neuhuber W, Tiegs G. Autonomic renal denervation ameliorates experimental glomerulonephritis. *J. Am. Soc. Nephrol.* 2008; 19: 1371-1378.

[54] Philips JK. Pathogenesis of hypertension in renal failure: role of the sympathetic nervous system and renal afferents. *Clin. Exp. Pharmacol. Physiol.* 2005; 32: 415-418.

[55] Brown JJ, Davies DL, Morton JJ, Robertson JI, Cuesta V, Lever AF, Padfield PL, Trust P. Mechanism of renal hypertension. *Lancet.* 1976. 1; 1219-1221.

[56] Suzuki H, Ferrario CM, Speth RC, Brosnihan KB, Smeby RR, de Silva P. Alterations in plasma and cerebrospinal fluid norepinephrine and angiotensin II during the development of renal hypertension in conscious dogs. *Hypertension.* 1983; 5: I-139-I-148.

[57] Miyajima E, Yamada Y, Toshida Y, Matsuoka T, Shionoiri H, Tochikubo O, Ishi M. Muscle sympathetic nerve activity in renovascular hypertension and primary aldosteronism. *Hypertension.* 1997; 17: 1057-1062.

[58] Johnson M, Elam M, Rundqvist B, Eisenhofer G, Herlitz H, Lambert G, Friberg P. Increased sympathetic nerve activity in renovascular hypertension. *Circulation.* 1999; 99: 2357-2542.

[59] Esler M, Jennings G, Biviano B, Lambert G, Haking G. Mechanism of elevated plasma noradrenaline in the course of essential hypertension. *J. Cardiovasc. Pharmacol.* 1986; 8: 539-544.

[60] Hendel MD, Collister JP. Renal denervation attenuates long-term hypertensive effects of angiotensin II in the rat. *Clin. Exp. Pharmacol. Physiol.* 2006; 33: 1225-1230.

[61] Clinical Trials.gov. A service of the U.S. National Institute of Health. Renal denervation in refractory hypertension. http://clinicaltrials.gov/ct2/show/NCT00664638?spons=%22Ardian+Inc%22andspons_ex=Yandrank=3

[62] Krum H, Schlaich M, Whitbourn P, et al. Catheter-based renal sympathetic denervation for resistant hypertension; a multiplecentre safety and proof-of-principle cohort study. *Lancet.* 2009; 373: 1275-1281.

[63] Schlaich MP, Sobotka PA, Krum H, Lambert E, Esler MD. Renal sympathetic nerve ablation for uncontrolled hypertension. *N Engl J Med*. 2009; 361: 932-934.

In: Biochemistry and Histocytochemistry… ISBN: 978-1-60876-283-5
Editors: S. Fuchs, M. Auer, pp. 81-116 © 2010 Nova Science Publishers, Inc.

Chapter 5

QUANTITATIVE IMMUNOHISTOLOGY - PROBLEMS AND SOLUTIONS

***Anthony S.Y. Leong*[*1] *and Trishe Y.M. Leong*[†2]**

[1]Medical Director, Hunter Area Pathology Service; Chair Discipline of Anatomical Pathology, University of Newcastle, Australia; Adjunct Professor, Peking University, Beijing, China

[2]Deputy Managing Pathologist, Victorian Cytology Service, Melbourne, Australia

ABSTRACT

As immunohistochemistry enters its fourth decade as a diagnostic tool this analytical procedure continues to experience poor reproducibility, albeit in specific situations. The problem becomes more important with the mounting pressure to employ the assay in a quantitative manner for the assessment of therapeutic and prognostic markers in a number of neoplasms. Qualitative applications of immunohistochemistry are well established and continue to increase with the range of sensitive antibodies and detection systems available, however, numerous variables that influence the immunoexpression of proteins in formalin-fixed tissue continue to exist in the pre-analytical and analytical phases of the test procedure. Many pre-analytical variables are currently beyond the control of the laboratory. Tissue fixation is critical but the exposure to fixative prior to accessioning by the laboratory is not controlled. Antigen retrieval, another pivotal procedure in immunohistology, continues to be employed in an empirical manner with the actual mechanism of action remaining elusive. There is great variation in reagents, method, and duration of tissue processing and immunostaining procedure, and detection system employed is not standardized between laboratories. While many of these variables are offset by the application of antigen retrieval, which enables the detection of a wide variety of antigens in fixed tissue, the method itself is not standardized. This myriad of variables makes it inappropriate to provide meaningful comparisons of results obtained in

* Address for Correspondence: Professor Anthony S-Y Leong, MD, Hunter Area Pathology Service, Locked Bag 1, HRMC, Newcastle 2310, Australia, Email: aleong@mail.newcastle.edu.au, FAX: 612 4921 4440.

† Trishe Y-M Leong, M.D. Victorian Cytology Service, 752 Swanston Street (Cnr Faraday St) Carlton, VIC 3052, AUSTRALIA.

different laboratories and even in the same laboratory as in current practice each specimen experiences different pre-analytical variables. Importantly, it calls into question the use of immunohistochemistry as a quantitative assay. Furthermore, variables in interpretation exist and cutoff thresholds for positivity differ. Failure to recognize false positive and false-negative stains leads to further errors of quatitative measurement. Many of the problems relating to the technology and interpretation of immunostaining originate from failure to recognize that this procedure is different from other histological stains and involves many more steps that cannot be monitored until the end result is attained. While several remedial measures can be suggested to address some of these problems, accurate and reproducible quantitative assessment of immunostains presently remains elusive as important variables that impact on antigen preservation in the paraffin-embedded biopsy cannot be standardized.

Keywords: immunohistochemistry, variables, antibodies, controls, quantitation, pitfalls

INTRODUCTION

Immunohistochemistry was first introduced as a fluorescence-based technique in the mid 1940s. The development of the peroxidase-anti-peroxidase and avidin-biotin-peroxidase techniques enabled application to formalin-fixed, paraffin-embedded tissues (FFPT), facilitating its usefulness in tissue diagnosis. With the development of hybridoma technology, the technique rapidly became entrenched as an invaluable adjunct to morphologic diagnosis and through the introduction of antigen retrieval techniques; an ever-increasing range of diagnostic proteins could be identified in FFPT.

The ability to work with FFPT sections, the most common medium in which histological diagnosis is rendered, and the increasing sensitivity of the technique enabled exquisite localization of staining to specific cell structures and organelles. As such, we proposed 'immunohistology' as a more appropriate term for this morphology-based investigation in order to emphasize this fundamental attribute (Leong et al, 1997a). Alternative appellations like 'immunohistopathology' (Elias, 2005), and 'immunomicroscopy' (Taylor and Cote, 2005) were subsequently proffered in recognition of the importance of correlating morphologic features with the immunological assay.

Immunohistology has wide applications in both research and diagnosis. Through the identification of proteins expressed in the cell and connective tissues, the assay has been employed for a myriad of diagnostic purposes (Leong and Wright, 1987; Leong and Leong, 2006) that include tumor diagnosis, (Leong 1992; Leong and Leong 1997, Taylor and Cote, 2005), identification of infective organisms, phenotyping of lymphomas and leukemias, the identification of hormones and peptides, and the demonstration of diagnostic morphological patterns and structures that are normally not visible in routinely stained sections such as basal lamina for the identification of soft tissue tumors (Leong et al, 1997b) and microvilli (Leong et al, 1990; 1992). Immunohistological markers have been employed for prognostication in a wide range of neoplasms (Leong and Lee, 1995; Leong 2001). The immunohistological identification of cellular proteins serves as a surrogate technique for molecular analysis in the identification of genetic alterations, normal expression, overexpression, aberrant expression, and loss of expression of genes. For example, the absence of E-cadherin distinguishes

infiltrating lobular breast carcinoma from infiltrating ductal carcinoma (Bratthauer et al, 2002; Wood and Leong, 2003), and the loss of mismatch repair gene proteins is useful for the screening of microsatellite instability (Ribic et al, 2003; Popat et al, 2005). There have even been proposals that some tumors such as gastrointestinal stromal tumors and lobular carcinoma of the breast be defined by their immunohistological phenotype (Fletcher et al, 2003; Acs et al, 2001) and the assay can also be employed for the identification of carrier states. Antibodies have been raised to chimeric proteins that result from the translocation of certain genes that are recognized to be specific for certain tumors. For example, the immunoexpression of the chimeric NPM-ALK protein that represents the fusion of the nucleophosmin (*NPM*) gene on chromosome 5q35 to the anaplastic lymphoma kinase (*ALK*) gene on chromosome 2p23 is diagnostic of anaplastic large cell lymphoma (Stein et al, 2000). When immunohistological assays are employed in this manner it is a cheaper and more rapid test that serves as a useful screening procedure for several genetic abnormalities.

The foregoing applications of immunohistology are largely qualitative but individualized cancer treatment has resulted in the immunohistological evaluation of many prognostic markers often with attempts at quantitation. A contemporary trend in cancer therapy is the targeting of specific molecules expressed by cancer cells; these commonly being molecules on the cell surface that are involved in the regulation of growth and proliferation (Leong and Leong, 2006). Humanized or chimeric monoclonal antibodies have been produced to a handful of these target molecules and the best therapeutic response generally occurs in those tumors expressing large amounts of the target molecules. As such, there has been an increasing push, largely driven by medical oncologists, for the quantitation of such expressed molecules as detected by immunohistochemical stains.

This article examines the validity of quantitative values assigned to the immunohistological assay and the variables that potentially affect such values.

THE IMMUNOHISTOLOGICAL ASSAY – A TOTAL TEST APPROACH

Earlier in the development of immunohistology when the assay lacked sensitivity and specificity, the problems of reproducibility and consistency were very evident because many stains were capricious. The advent of sensitive antibodies and enhanced detection systems, together with the development of the antigen retrieval procedure made it possible for most laboratories to consistently stain for a large variety of antigens in FFPT so that such initial problems with reproducibility were forgotten or relegated to the background. However, the proliferation of reagents and procedures resulted in a wide variation in adopted practice and it was soon realized that this diversity could be a potential issue in immunohistology giving rise to calls for standardization (Taylor 1994; O'Leary 2001, Taylor and Levenson, 2006; Goldstein et al, 2007). The concern largely focused on reagents and procedures without much attention paid to fixation and other variables that influence antigen preservation. The drive for quantitation of therapeutic and prognostic markers in a variety of tumors has resulted in a renewed necessity to address the problems of reproducibility and standardization.

Immunohistology should not be regarded as an empirical procedure similar to other histological stains. Immunohistology is different in that it entails many more steps to perform and success cannot be monitored until completion of the entire procedure. It is more akin to a

biochemical assay. As such, this analytical procedure is more appropriately viewed as a total test comprising pre-analytical, analytical, and post-analytical phases. A systematic detailed examination of the many variables that influence each of these analytical phases will serve well our desire to attain reproducible quantitative immunohistology.

PRE-ANALYTICAL VARIABLES: TISSUE PRESERVATION, TRANSPORTATION, FIXATION AND TISSUE PROCESSING

The variables that influence this phase of the analytical process are particularly difficult or currently impossible to control because tissue samples are obtained in different ways by different clinicians, and in diverse hospital and clinical settings.

Intrinsic Properties of the Sample

In the routine setting, tissue samples may be obtained by fine needle aspiration, as needle cores, endoscopic biopsies, superficial biopsies of skin or mucosa, or by more extensive excisional procedures. The state of the biopsy, which may be intrinsically necrotic, or ischemic, and the duration between removal of the tissue and placement into fixative will determine the amount of detectable antigen.

Immediately after death or removal of the biopsy sample, degradation and autolysis commences, and delays in fixation affect the preservation of tissue antigens. Some antigens appear to withstand adverse conditions, e.g., blood group antigens can still be immunohistochemically detected in minute spots of dried blood, but many other antigens do not. Degradation rates differ between organs and tissues (Pelstring et al, 1991) and biochemical changes occur very rapidly within seconds after death (Pearse 1980). Biopsy specimens should be immersed in formalin soon after removal. They must not be allowed to dry out during the clinician's zealous examination (often under hot lights) for gross changes that are invariably not visible to the naked eye, or for other reasons including photography of the unfixed specimen (Figure 1a and 1b). Large specimens such as mastectomies are often immersed whole in fixative, delaying fixation to the deeper tissues and adversely affecting antigen preservation.

Fixation and Fixatives

Fixatives can vary in type and composition. Ten per cent formalin (4% formaldehyde) is the universal fixative, being inexpensive and producing morphological detail that pathologists are most accustomed. However, formalin penetrates tissues slowly and it was a commonly held belief that formalin preserves antigens poorly. Furthermore, formalin deteriorates with storage. Aqueous solutions of formaldehyde contain equilibrium of its monohydrate methylene glycol, formaldehyde, and water. Methylene glycol, in turn, forms various oligomers including low molecular weight polymeric hydrates or polyoxymethylene glycols.

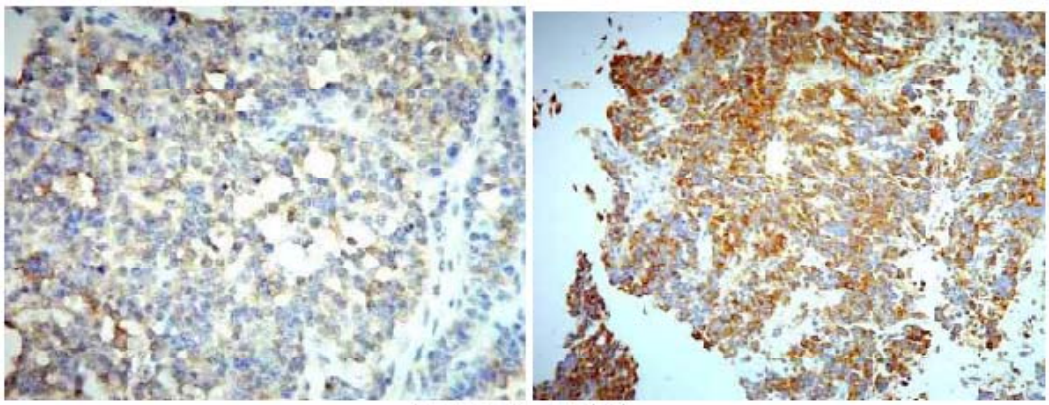

Figure 1. Polyphenotypic small round cell tumor from the abdomen of a 4-year-old boy. (a) The biopsied material stained weakly for CD99, whereas (b) the excised tumor showed diffuse and strong positivity for the same antigen. The staining procedure used was identical.

Formalydehyde appears to be the active component and effective fixation results from the formation of cross-links between proteins end groups that include amino, imino, amido, peptide, guanidyl, hydroxyl, carboxyl, SH, and aromatic rings. The formation of such methylene bridges between amino groups on adjacent molecules is thought to be the basis of formaldehyde-based fixation (Pearse, 1980). It has been clearly demonstrated that the ability to demonstrate a wide range of tissue antigens varies inversely with the duration of exposure to formaldehyde (Leong and Gilham, 1989)). Tissues fixed in formaldehyde displayed a distinct and progressive loss of staining of many antigens, frequently proportional to the duration of exposure to the fixative. There was an appreciable loss of staining of some antigens after 3 days; many antigens were lost after 7 days and most were not demonstrable after 14 days of fixation. Interestingly, enzymatic predigestion per se was useful for the unmasking of only some antigens, ineffective and even deleterious in others (Leong and Gilham, 1989).

Unfortunately, formalin fixation is not a single uniform procedure but varies from laboratory to laboratory with respect to concentration, pH and buffers, and temperature and duration of exposure. All these parameters strongly impact on the outcome of immunostaining. Furthermore, exposure to formalin occurs in several stages, after removal of the specimen and before receipt by the laboratory, during the interim period in the laboratory before tissue processing, and again during tissue processing. All these durations vary between laboratories, and for different specimens accessioned by the same laboratory (Figure 2a and 2b).

It is also likely that certain antigens have optimal durations of fixation. It has been shown that for the immunohistological demonstration of estrogen receptor, a minimum fixation time of 6-8 hrs in formalin is required for consistent results (Goldstein et al 2003). This minimum time is particularly critical in small biopsies and needle cores which tend to receive insufficient or weak initial formaldehyde fixation followed by extraction/fixation in ethanols used for dehydration in the tissue processor, resulting in inconsistent demonstration of some tissue antigens.

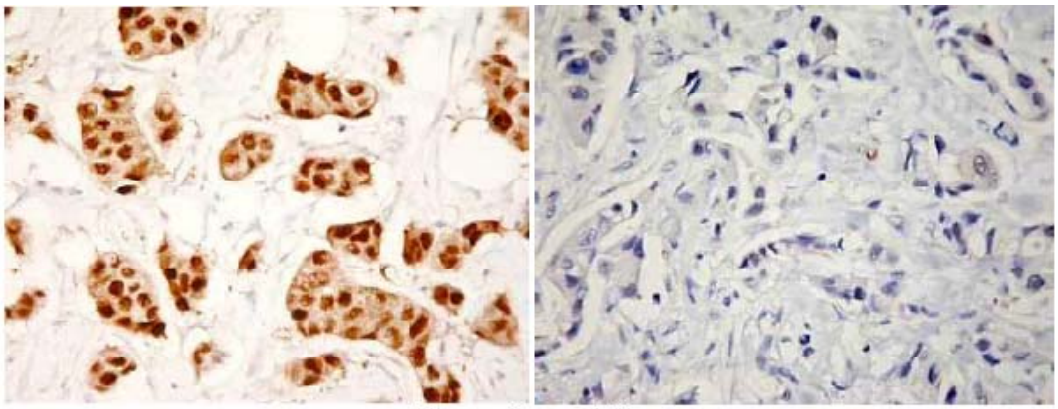

Figure 2. (a) Needle core biopsy of infiltrating ductal carcinoma of the breast fixed for 8 hours in buffered formalin stained strongly for estrogen receptor. (b) The same tumor in the mastectomy specimen that was immersed in buffered formalin for 48 hours failed to stain for the same antigen.

Capricious epitopes of antigens that cannot be demonstrated following routine formalin fixation can be successfully stained if only exposed to the fixative for a short duration (Raymond and Leong, 1990), or by using a physical fixation agent such as microwaves (MWs) (Leong and Milios, 1993a, 1993b). Antigen preservation in tissues fixed by MW irradiation in normal saline was clearly superior to formalin fixation and some antigens not demonstrable in formalin-fixed tissues were readily labeled in MW-fixed sections (Leong et al, 1988). Similarly, immunolabelling of cytological preparations has been shown to be optimal with 0.1% formal saline as the fixative and air-drying as the best method of preparation of such material (Supinthawong et al, 1996).

The various fixation and tissue preparation methods for light microscopic immunohistochemistry have been reviewed (Larsson 1993) but in routine practice immersion in 10% buffered formalin is the most common method of fixation, with coagulant fixatives less frequently employed (Leong 1994). Alcohol-based fixatives appear not to react covalently with amino acids and therefore leave the primary protein structure unaltered although aspects of the tertiary structure may be changed (Pearse 1980). Earlier reports suggested methacarn (a mixture of methanol and acetic acid) as a useful fixative for preservation of tissue antigens (Gown and Vogel, 1984), and a variety of other fixatives and mixtures of alcohol with other reagents has been used (Larsson 1993). Shrinkage of tissue and extraction of small antigens remains a problem with alcoholic fixatives so that formalin has remained the universal fixative for routine morphologic examination and immunohistology.

The dehydration process may also affect antigen preservation and various special dehydration procedures have claimed improved tissue antigenicity. Similarly, certain types of paraffin, celloidin, and polyethylene glycol have been shown to be useful for immunohistology (Larsson 1993).

Other aspects of the fixation procedure, including pH and temperature, have an impact on antigen preservation, more severely for some antigens compared to others. The pH of formalin affects the type of cross-linking that occurs. With 10% neutral buffered formalin, hydrogen sites in peptide molecules are available for linkage as they are in the uncharged state. Lowering of the pH induces formation of charged amino groups (NH_3^+) that lack

reactive hydrogen sites and favors interactions with amide ($CO\text{-}NH_2$) groups. The formation of methylol bridges can theoretically alter the native conformation of a protein substantially and the configuration of covalent cross-links may alter the structure of important epitopes (Leong 1994). In addition to inducing cross-linking, formalin also disrupts hydrogen bonds and other electrostatic interactions that affect the configuration of proteins, further increasing the possibility of important alterations to epitopic targets. As antibodies are mostly raised to proteins in their native conformation state, they may not bind as effectively to target polypeptides that have such structural transmogrification, so-called "antigen masking". The extent of this antigen masking is proportional to the duration of fixation (Leong and Gilham, 1989; Leong 1994). The antigen masking effects of formalin and concerns about its toxicity has prompted the use of formalin substitutes, which are generally either alcohol- or water-based. Several commercial fixatives have been produced including Histochoice (Amresco, Soron, OH, USA), FineFix (Milestone, Bergamo, Italy), NoToX (Earth Sate Technologies, Lumberton, NC, USA), and Ominfix (An-Con Genetics Inc, Melville, NY, USA) but their efficacy in antigen preservation remains to be proven particularly in the case of some predictive and prognostic factors such as hormone receptors and HER2/neu for which alcohol-based fixative have been shown to be detrimental.

Fresh acetone-fixed tissue sections have traditionally been held as the 'gold standard' for reference purposes in immunohistochemistry as it was assumed that fresh tissue had unadulterated nuclear, membranous, and cytoplasmic epitopes, which when exposed to fixative, were altered or lost forever. However, it was recently shown that more than half of the 26 antibodies tested in a study showed better immunohistological signals following fixation in neutral buffered formalin and antigen retrieval; and only two antibodies displayed better results in fresh acetone-fixed sections (Shi et al, 2008) In particular, nuclear antigens showed better staining in tissue fixed by neutral buffered formalin. It thus appears that neutral buffered formalin performs well; not only as a convenient and cheap universal fixative for cytomorphology but also for antigen preservation and that a better alternative is yet to be found. Heat-induced antigen retrieval appeared to improve immunohistochemical staining of unfixed frozen sections and dot-blot protein extracts suggesting that natural steric barriers exist even in the fresh state (Kakimoto et al, 2008).

Tissue Processing

While it is possible to control the duration of exposure to formaldehyde after the accession by the laboratory, it is difficult or not possible to control the events preceding. Furthermore, the exact duration between excision of tissue and placement in formalin is invariably not known. This factor is a major obstacle to standardization of fixation, a pivotal influence on antigen preservation. There is another period of exposure to formalin when the specimen is in transit in the laboratory awaiting examination, dissection, and sampling before final tissue processing. This duration of exposure will vary between different specimens in the same laboratory. Further exposure to formalin in the tissue processor will affect antigen preservation and tissue-processing cycles can vary considerably in composition and duration, with newer tissue processors employing reagents different to the conventional formalin, ethanol and xylene (Visinoni et al, 1998; Morales et al, 2004).

There are major differences in tissue processing protocols with variations in the time of immersion in formalin and alcohols. These variables can be controlled and standardized for the individual laboratory but in the case of tissue blocks prepared in other laboratories such variations may significantly affect the staining of tissue antigens.

Tissues previously subjected freezing or decalcification show poor and inconsistent preservation of some antigens.

Storage of Tissue Sections

There is evidence that exposure to the elements can affect tissue antigens. Tissues sections that are left on the bench at room temperature have shown deterioration of antigenicity (Jacobs et al, 1996; Wester et al, 2000; Divito et al, 2004) and stored tissue blocks displayed degradation of target antigens (Blind et al, 2008)**.** Temperature, drying, and exposure to ultra-violet light have been implicated as significant factors contributing to this loss (Blind et al, 2008). It is not an uncommon practice to have control sections cut well in advance of immunostaining and unless optimally stored, such controls will affect the optimization of new antibodies and other reagents. Should delays in staining be anticipated, FFPT sections should be wrapped in aluminum foil and stored at minus 20^{o}C for optimal antigen preservation (Figure 3a and 3b).

ANALYTICAL VARIABLES – ANTIGEN RETRIEVAL, ANTIBODIES, DETECTION SYSTEMS AND CONTROLS

Unlike the pre-analytical factors, analytical factors are more readily controlled within the individual laboratory. Analytical variables that are associated with the demonstration of the antigen include antibody specificity and sensitivity, dilution, detection system, and antigen retrieval.

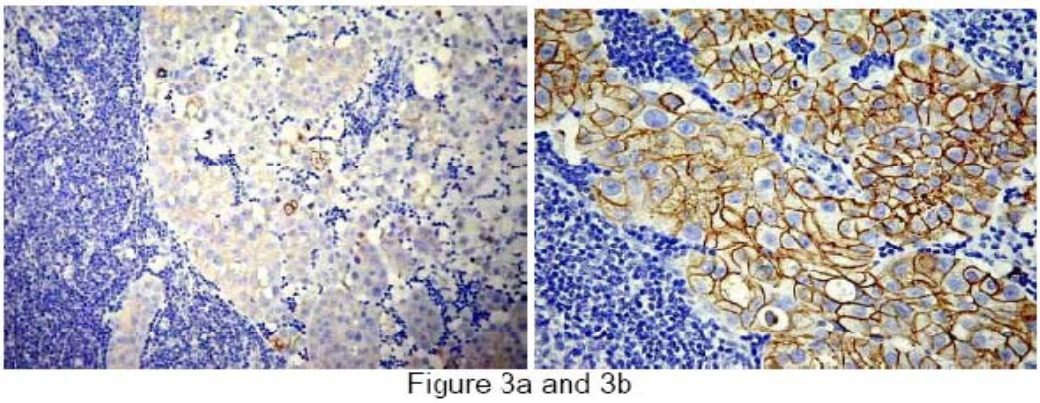

Figure 3: (a) Staining for Her2 in a control section of breast carcinoma. The section had been prepared some 30 days earlier and stored at 4oC. There was barely any staining in the material. (b) A freshly prepared section from the same tissue block showed 3+ staining for Her2 protein.

THE IMMUNOHISTOLOGICAL ASSAY

The immunohistological test is the application of an antibody to label a protein in tissues or cells based on antibody-antigen recognition. The cells may be fixed and embedded in paraffin, or unfixed as in frozen sections, or as intact cells in cytological preparations. The basic aim of the procedure is the distinct localization of signal to specific cell and tissue components in the section, at the same time retaining good morphological visualization. Amplifying the signal without increasing the non-specific background staining or noise is a major strategy to allow application of the assay to routinely processed diagnostic tissues.

The direct immunofluorescence technique in which a fluorescein-labeled primary antibody is employed to detect the protein of interest represents the most basic immunohistological test. However, despite the simplicity of this one-step stain, the insensitivity of this assay that provided a 1:1 antigen to signal ratio and the poor morphologic visualization and preservation of frozen sections, restricted its application. The development of two- and three-step techniques that amplified the antigen to signal ratio, and permanent chromogen systems such as horseradish-peroxidase and diaminobenzidine were important milestones in the evolution of the immunohistological assay as they allowed the procedure to be applied to fixed-paraffin-embedded tissue sections, discussed in detail elsewhere (Leong et al, 1994; 1997a). Additional developments such as the use of polymers (Sabattini et al, 1998) and tyramide (King et al, 1998) further amplified the antigen to signal ratios, and antigen retrieval methods including enzyme digestion and post-fixation in heavy metal solutions improved the detection of antigens in fixed tissues (Leong 1994; Leong et al, 1997a), however, it was the introduction of the so-called heat-induced antigen retrieval method that had the greatest impact (Shi et al, 1991; Leong and Milios, 1993a; Gown et al, 1993; Cuevas et al, 1994). *Pari-pasu* with these developments, the range of antibodies and their specificity and sensitivity continued to improve, all contributing to consolidate the pivotal role of the immunohistological assay in both research and diagnosis.

SUBSTRATE AND CHROMOGEN SYSTEMS

Antibody molecules cannot be seen with the light microscope unless they are labeled. A variety of labels have been used including fluorescent compounds and their active enzymes, all with the property of inducing the formation of a colored reaction product from a suitable substrate system to allow visualization. Some of these systems can be employed in electron microscopy by rendering the reaction product electron dense through appropriate treatment. Alternatively, particulate labels such as gold, ferritin, or viral particles can be used (Leong 1993).

Common chromogen systems currently in use include diaminobenzidine (DAB), 3-amino-9-ethyl-carbazole (AEC), Hanker-Yates reagent, alpha-naphthol pyronin used with peroxidase as substrate; fast blue, fast red, BCIP- (5-bromo-4-chloro-3-indolyl phosphate) NBT (nitroblue tetrazolium) used with alkaline phosphatase as substrate; tetrazolium, tetranitroblue tetrazolium used with glucose oxidase as substrate, and immunogold with silver enhancement (Leong, 1993; Leong et al, 1997a).

AEC is alcohol soluble and its crisp red color contrasts well against hematoxylin. To avoid removal of the alcohol-soluble product, a non-alcohol based stain like Mayer's hematoxylin should be used. AEC has two reactive sites so that when one is converted it turns red but when both are saturated a green-brown color results. Aquamount causes slow loss of the stain and glycerol mounting is required, rendered permanent by sealing the edges of the cover slip. AEC may be chosen because it may be a lower-risk carcinogen compared to DAB.

Clearly, a number of chromogenic systems are available and may be varied between laboratories. The horseradish peroxidase-DAB system is probably the most widely favored as the brown reaction product contrasts well against a wide range of counterstains and mountants. DAB is not only alcohol resistant but can be visualized in the electron microscope. Osmification can produce a more intense dark brown-black color and a similar effect is achieved by post-treatment with nickel sulphate or cobalt chloride but such enhancement is seldom necessary. The reaction product is relatively stable with fading occurring only after years in routine storage.

Antigen Retrieval

One of the earliest methods of antigen retrieval was proteolytic digestion of tissue sections employed prior to the application of the primary antibodies. A number of proteolytic enzymes served this purpose, including trypsin, proteinase K, pronase, pepsin, ficin, DNase, and others (Leong 1993, Leong et al, 1997a; Miller et al 2000). Not only are the enzymes different but there is also variation in concentration, duration, and temperature of digestion. Furthermore, not all antigens benefit from proteolytic digestion, and some show deleterious effects with loss of staining (Leong and Gilham, 1989). In addition, inappropriate protocols result in tissue breakdown and loss of morphology with high levels of background and false-positive staining.

The introduction of heat-induced antigen retrieval signified a major milestone in immunohistology, greatly enhancing our ability to demonstrate antigens in FFPT with greater consistency (Shi et al, 1991; Leong et al, 1993a, 1993b; Gown et al, 1993; Cuevas et al, 1994). The initial technique was achieved with MWs, which has remained the most convenient method for antigen retrieval, but a variety of other methods of generating heat have since been spawned including water baths, hot plates, wet autoclaves, pressure cookers, and vegetable steamers. Shi et al (1991) described MW heating of FFPT in the presence of heavy metal solutions, such as lead thiocyanate, up to temperatures of 100^{o} C to "unmask" a wide variety of antigens for immunostaining. It was subsequently shown that MW-irradiation of deparaffinised-rehydrated sections in 10 mmol citrate buffer at pH 6.0 produced, with few exceptions, increased intensity and extent of immunostaining of a wide variety of tissue antigens (Leong et al, 1993a; Gown et al, 1993; Cuevas et al, 1994). The use of citrate buffer eliminated the need to employ heavy metal solutions which, when heated, generate toxic fumes. Several commercial antigen retrieval reagents are available but they mostly do not produce any better results than that obtained with citrate buffer (Leong et al, 1996).

MWs are a form of non-ionizing radiation with a typically standard frequency of 2.45 GHz, a wavelength of 12.2 cm and photon energy of 10^{-5} electron volts. When dipolar molecules such as water or the polar side chains of proteins are exposed to the rapidly alternating electromagnetic fields, they oscillate through 180^{o} at the rate of 2.45 billion cycles

per second. The molecular movement or kinetics so induced results in the generation of instantaneous heat that is proportional to the energy flux and continues until radiation ceases. It was only recently recognized that molecules other than water and the polar side chains of proteins may oscillate in the electromagnetic field generated by MWs. Molecules with an uneven distribution of electrical charge such as inorganic material and copper oxides can also be rotated (Leong 2005).

All methods of heat generation listed above suffer from problems with accurate temperature and time control. These two variables have been shown to be critical to the process of heat-induced antigen retrieval. They are inversely related so that antigen retrieval at lower temperatures requires longer durations to achieve the same results as that obtained with higher temperatures (Chaiwun et al, 2000). The time taken to attain the desired temperature from variable starting temperatures, time required to cool to room temperature, and actual temperature attained are variables that cannot be controlled with most methods of heating. Furthermore, there is the problem of unevenness of heating within microwave cavities, making the entire process impossible to standardize with resulting inconsistencies in methodology. Computerized control of time and temperature that is available with some commercial MW instruments takes the guesswork out of heat-induced antigen retrieval. Accurate time and temperature control not only produces superior antigen retrieval across the spectrum of diagnostic antigens but accurate heating to 120^{o}C or "superheating" has proven to produce notably better antigen staining (Figure 4a and 4b) (Leong et al, 2002a).

Our understanding of the effects of formaldehyde on proteins dates back to work done in the 1940s (Fraenkel-Conrat et al, 1947; Fraenkel-Conrat and Olcott, 1948a, 1948b). A recent comprehensive review of the fixative action of formaldehyde and antigen masking is available (Shi 2000). The amino acid side chain of proteins includes many groups that may react with aldehydes that contribute to the stabilization of proteins. However, despite the vast literature on the subject of protein modification by formaldehyde, there is no clear consensus as to which are the predominant molecular species resulting from this method of fixation. There is no doubt that some of the cross-linked adducts are very stable and remain irreversibly changed even after extensive washing, while others revert under varying conditions to free formaldehyde and the amino acid (Pearce 1980). Without a complete understanding of the actions of formaldehyde on proteins, it is not surprising that we do not fully understand the mechanisms of antigen retrieval.

Heat appears to be a common denominator in antigen retrieval produced by a variety of methods including MWs. Heat is hypothesized to cause protein denaturation based on the observation that some antigens or endogenous enzymatic activities may be lost after heat treatment (Cattoretti et al, 1993) and heat induces reversal of various chemical modifications of the protein structure that result from formalin fixation. Other actions that produce antigen retrieval include the loosening or breakage of the cross-linkages caused by formalin fixation, hydrolysis of Schiff bases, and multiple pathways including extraction of diffusible blocking proteins, precipitation of proteins, and dehydration of the tissue sections to allow better penetration of antibody and increased accessibility to epitopes (Suuurmeijier et al, 1993), all or some of which may be achieved by other methods of retrieval including enzyme digestion and changes in pH. MW energy may itself mobilize the last traces of paraffin that may not have been extractable by standard techniques, thereby improving antibody penetration (Gown et al, 1993).

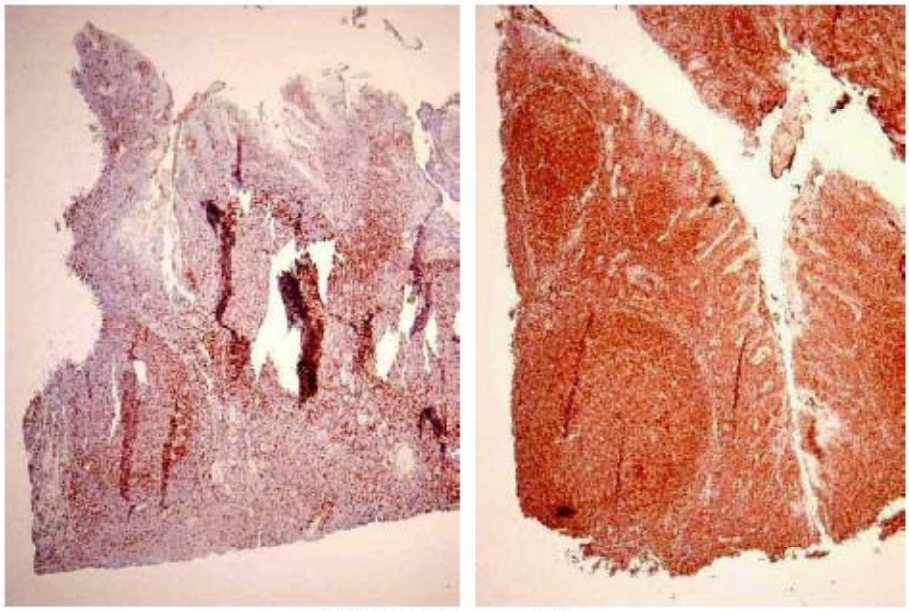

Figure 4a and 4b

Figure 4. (a) A section of tonsil stained for CD45 following antigen retrieval in citrate buffer pH6.0 at 98^{o}C. (b) The adjacent section stained for the same antigen following antigen retrieval in citrate buffer pH6.0 at 110^{o}C showed visibly stronger staining.

It was proposed that the calcium complex formation that occurs with formalin fixation may mask antigens and that the release of calcium from this cage-like complex may require a considerable amount of energy such as high temperature heating and calcium chelation by citrate (Morgan et al, 1997). However, it has been argued that while this calcium effect may be acting with some antigens it may not be sufficient to explain the loss of immunoreactivity for many other antigens and is unlikely to represent the general mechanism of antigen retrieval (Shi et al, 2000).

The role of kinetics in antigen retrieval is also not known. While the focus has been on heat as the responsible factor in MW retrieval, the rapidly oscillating electromagnetic field of MWs may itself have an effect on chemical reactions and proteins. While heat or thermal energy will increase molecular kinetics and hasten chemical reactions, the rapid rotation of molecules directly induced by the MWs will give rise to greatly increased collision of molecules, which will in turn accelerate chemical reactions. The heat generated may represent only an epiphenomenon secondary only to the kinetics. One study that examined MW stimulation of CEA/anti-CEA reaction in an enzyme-linked immunosorbent assay system found that despite continuous cooling by ice MW stimulation increased reaction rates by a factor of 1000, allowing the investigators to conclude that such rate increases were far too large to be explained solely by the modest increase in temperature (Hjerpe et al, 1988). Another study went further to elucidate the existence of a “microwave effect” (Choi et al, 1997) The authors showed that the rate of droplet temperature increase obtained in a thermal cycler was similar to that achieved by MW irradiation. However, the immunostaining obtained from a 3-minute incubation at 37^{o}C in the thermal cycler followed by 2-minute incubation without heating was much weaker than that seen with MWs. Similarly it was

demonstrated that 7-s MW irradiation followed by 5-min room temperature incubation for each step of the avidin-biotin peroxidase complex procedure produced good immunolabelling (Takes et al, 1989). The droplet temperature raised no more than 5^{o}C following 7-s irradiation at 100% power in a 850-watt oven (Choi et al, 1997) so that temperature was not a significant component of the accelerated reaction. Others have argued that there is no significant MW effect and the accelerated reactions are a function of heat. It has been concluded that MW irradiation did not produce cleavage or polymerisation of proteins and irradiation resulted an electrophoretic pattern that was similar to that obtained when lysozyme and hemoglobin was heated in formaldehyde to 60^{o} C for 30 min (Hopwood et al, 1988). Interestingly, results to the contrary have been shown in a study of S-adenosylhomocysteine hydrolase and 5'-methylthioadenosine phosphorylase, two thermophilic and thermostable enzymes, where exposure to MWs caused a non-thermal, irreversible and time-dependent inactivation of both enzymes (Porcelli et al, 1997),

In a model immunostaining system using short synthetic peptides to mimic the antibody-binding site of common diagnostic protein targets, Sompuran et al (2006), found that not all of the peptides studies exhibited the formalin-fixation and antigen retrieval phenomenon. One group of peptides was recognized by antibody even after prolonged exposure to formalin while another group exhibited the formalin-fixation and antigen-retrieval phenomenon only after another irrelevant protein was mixed with the peptide before fixation. Amino acid sequence analysis indicated that fixation and antigen retrieval were associated with a tyrosine in or near the antibody-binding site bound covalently to a nearby arginine implicating the Mannich reaction as an important factor in the process.

The Mannich reaction is a complicated, multistep interaction, which firstly involves a reaction between formaldehyde and an amine to produce an iminium ion. The iminium ion may then react with another carbonyl-containing molecule to form an intermediate product and for this to occur, the carbonyl-containing molecule must be in an enol configuration. In the final step of the reaction, the iminium ion and the enol react together to form a stable product. The findings of Sompuran et al (2004) concurred with those of Fraenkel-Conrat et al (1947, 1948) who had indicated that of all the protein cross-linking reactions that occur as a result of formalin fixation, the Mannich reaction is different, in that the cross-linkages can be hydrolysed with heat or alkaline treatment. Antibodies appear to recognize linear protein epitopes in FFPT and antigen retrieval may simply remove cross-linked proteins that are sterically interfering with antibody binding (Sompuran et al, 2004; 2006). The recent demonstration that antigen retrieval produces immunohistological staining results in FFPT that are comparable or better than that in acetone-fixed fresh frozen section (Shi et al, 2008) and that heat-induced antigen retrieval enhances immunostaining in unfixed fresh frozen sections and dot-blot protein extracts (Kakimoto et al, 2008) is further support of the concept that intrinsic natural steric barriers exist and interfere with antibody binding. The demonstration that MWs can also be employed to enhance the demonstration of HER2/neu gene in chromogenic in-situ hybridization (CISH) is particularly interesting and it suggests that similar mechanisms may be operative in the 'masking' of DNA (Leong et al, 2007). However, it would seem that these observations provide some insights into the action of antigen retrieval with some peptides but answers to the majority still remain unknown.

The demonstration that exposure to ultrasound (Portiansky et al, 1996) can significantly increase antibody-antigen reaction in immunostaining lends further support to the relevance of molecular movement as an important factor in the acceleration of the chemical reaction as

the amount of heat generated by this physical modality is negligible (Leong 2005). A number of other hypothetical physical mechanisms may also play a role in the actions of MWs. Although the proton energy generated in MW fields is too small to alter covalent bonding, they may readily affect the integrity of non-covalent secondary bonding, including hydrophobic interactions, hydrogen bonds and van der Waal's interactions that make up the precise steric interactions at the cell membrane.

The combination of heat retrieval with enzymatic digestion has allowed enhanced demonstration and localization of a number of antigens including the immunoglobulins (Leong et al, 2002). Proteolytic digestion can be performed with a number of enzymes, and at varying concentrations and for varying durations. It can precede or follow heat induced antigen retrieval with different results. For optimal outcomes, it is necessary to explore all possible combinations and permutations of these variables with the realization that excesses can result in loss of antigen and cell morphology.

The chemical composition of the retrieval solution may affect the efficacy of the process and a wide variety of solutions have been advocated including citrate buffer, Tris buffer, glycine-hydrochloric acid, EDTA, urea, heavy metal solutions, and other proprietary reagents. The molarity of the solution may also significantly influence immunostaining (Taylor et al, 1996).

The pH of the retrieval solution has been shown to be one of the most important factors in antigen retrieval (Figure 5a and 5b). Three patterns of staining reflect the influence of pH. Some antigens (CD20, AE1, EMA, NSE and PCNA) showed no variation at pH values ranging from 1.0 to 10.0, other antigens (MIB1, ER) displayed a dramatic decrease in staining intensity at middle pH values (pH 3.0-6.0) with strong staining above and below the range, and a third pattern was demonstrated by other antigens (CD43, HMB45) which were weakly stained at low pH (1.0-2.0) and displayed a sharp rise in intensity with increasing pH (Shi et al, 1995).

We have previously demonstrated the use of MWs to accelerate antibody-antigen reactions in the staining of labile lymphocyte membrane antigens in cryostat sections and the exposure of cryostat sections briefly to MWs before the commencement of immunolabelling produced better quality cytomorphology and staining (Leong and Milios, 1986). A similar procedure has been adopted for freshly frozen brain sections with notable enhancement of immunostaining, without affecting the integrity of cytomorphology (Boon et al, 1988). MWs have been successfully used to accelerate immunolabelling in paraffin-embedded sections (Leong et al, 1990) and the same technique has been applied for immunofluorescence labeling (Chiu et al, 1987).

MWs have been applied between sequential rounds of a three-layer immunoenzyme staining (mouse Mab, goat anti-mouse IgG and mouse PAP or mouse APAAP) and color development technique for multiple antigen detection (Lan et al, 1995). The MWs denatured bound antibody molecules resulting in the blocking of cross reactivity between the sequential staining steps, allowing the use of primary and other antibodies raised in the same species. Besides serving a role in antigen retrieval, MWs also inactivated peroxidase and alkaline phosphatase enzymes present in PAP and APAAP complexes, which would otherwise have led to inappropriate color development.

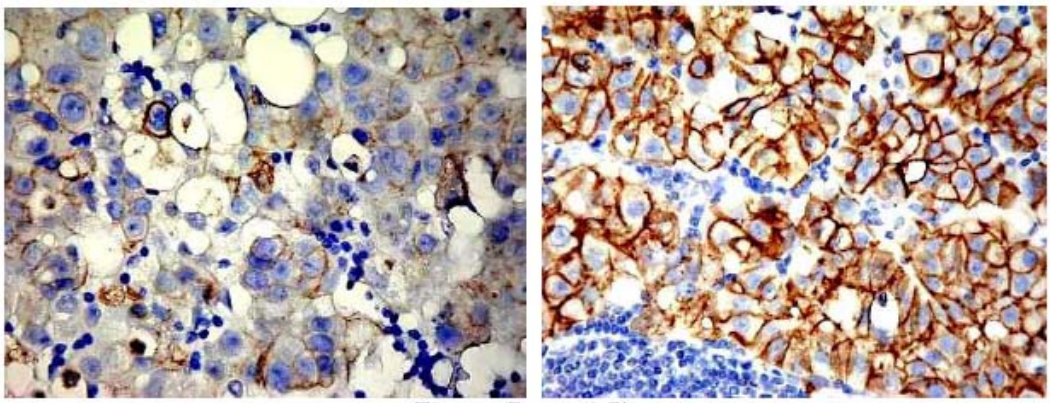

Figure 5. Staining for Her2 protein following antigen retrieval performed at different pH. (a) Following antigen retrieval in citrate buffer pH6.0 there was only focal staining compared to (b) diffuse staining when retrieval was performed in citrate/EDTA buffer at pH8.0.

Antibodies and Detection Systems

While the ever-increasing range of antibodies is a boon to diagnostic immunohistology, it can be confusing, as one needs to be familiar with the specificity and sensitivity of the reagent that is used. There is also an increasing choice of antibodies that are purported to detect the same antigen but, in fact, detect different epitopes, albeit of the same antigen. For example, in the case of the antibodies to estrogen receptor (ER) H222 and ID5, the former labels ER only in frozen sections and not in fixed paraffin-embedded sections, whereas, the latter displays the reverse properties, suggesting that they detect different epitopes on the same antigen. The sensitivity of different antibody clones directed to the same antigen may also vary significantly (Figure 6a and 6b). It has been shown that two antibodies to proliferating cell nuclear antigen (PCNA), namely 19A2 and PC10, show vastly different sensitivities (Leong et al, 1993), and proliferation indices obtained with these two markers are significantly different to other markers of cycling cells such as MIB1, Ki-67, KiS1, and KiS5 (Leong et al, 1995).

The manufacturer's antibody concentration and methodology serve as useful guides but each new antibody has to be carefully optimized as the vagaries of pre-analytical and analytical variables differ between laboratories. Antibodies produce a positive reaction over a range of concentrations and selection of the optimal concentration is largely one of individual choice (Figure 7a and 7b). Many laboratories and quality assurance programs favor an intense dark brown to almost black diaminobenzidine reaction product. We recommend a golden brown color, which does not obscure the cytomorphological features in the section, an all-important attribute in immunohistology.

Care should also be taken to store antibodies at the appropriate temperature. After aliquoting required working amounts of primary antibody for dilution, the antibody concentrate should be stored at -20^{o}C or preferably -70^{o}C. Antibody concentrates stored at the latter temperature can remain effective indefinitely despite their 'use by date'. When stored at 4^{o}C, antibodies have a shorter shelf life.

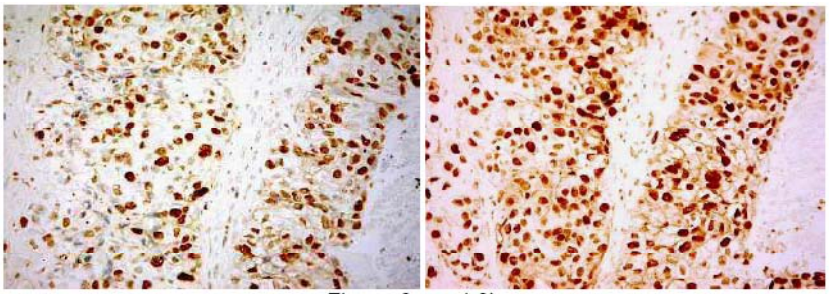

Figure 6. Staining obtained with two antibody clones to proliferating cell nuclear antigen (PCNA). Antigen retrieval and staining procedures were identical for the two antibodies. (a) Clone 19A2 showed a proliferating index of 75% compared to (b) to a 98% proliferating index in the adjacent section of breast cancer when stained with clone PC10.

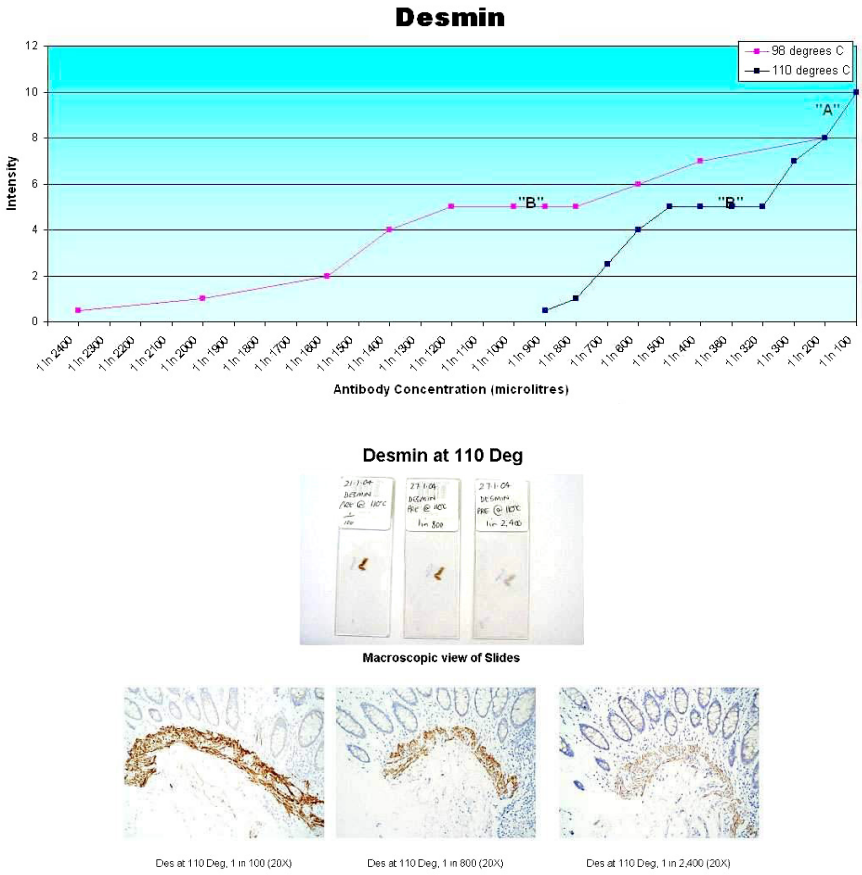

Figure 7. (a) Optimization graph for anti-desmin antibody at 98oC and 110oC. With increasing concentrations of the antibody a plateau is attained where the target antigen is positively labelled, identified as “B”. Antibody concentrations above this plateau resulted in background staining, indicated as “A” on the graphs. Corresponding stains obtained with three dilutions from the plateau are shown in (b) after antigen retrieval at 110oC. There is clearly a choice of dilutions that are ‘positive’ and the choice is subjective

The process of antibody optimization also requires that different temperatures of antigen retrieval be explored, and although citrate buffer at 10 mMol/litre is a good universal retrieval solution, a higher pH may be required for more capricious antigens as previously discussed (Shi et al, 1995). In addition, the synergistic action of proteolytic digestion should be routinely explored as a pre-MW and post-MW procedure.

Antigen detection systems vary significantly in sensitivity. The ability to detect small amounts of antigen not detectable by previous less sensitive techniques requires that we must continually adjust our diagnostic criteria to incorporate new immunohistological information. In some situations, the markedly increased sensitivity of the detection system can result in a high background and accurate localization of the signal can be lost when the signal to antigen ratio is increased considerably. This is demonstrated in the staining for C4d where localization of the antigen to peritubular capillaries is not discernable with ultrasensitive polymer detection systems like the EPOS (DakoCytomation, Sydney, Australia) because of extension of the staining beyond the capillaries into the inter-tubular interstitium (Figure 8a and 8b).

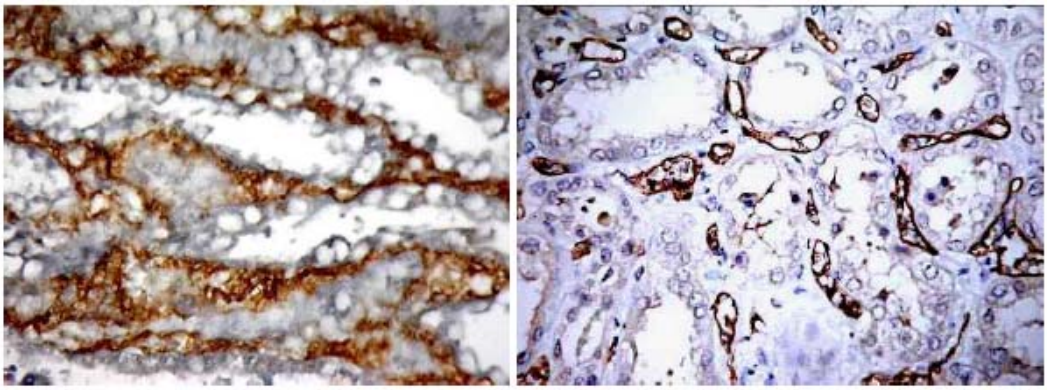

Figure 8a and 8b

Figure 8. Transplanted kidney stained for C4d using (a) an ultrasensitive polymer detection system (EnVision) and (b) standard strepavidin-biotin peroxidase system. There was clear staining of peritubular capillaries in (b) compared to the polymer system where the stain extended into the intertubular interstitium masking the capillaries.

AUTOMATED IMMUNOSTAINING

With the adoption of immunohistochemistry as an integral component of morphologic diagnosis, there has been a proliferation of automated immunostaining devices. These devices serve to produce timely results and consistency of staining within the individual laboratories. Importantly, they performed the many slow and repetitive steps of application of reagents and antibodies, monitoring of incubation times, and washing and wiping of slides after each step that are otherwise operator-dependent in the manual procedure and may be prone to error. While automation has been embraced with enthusiasm, it comes with its own price in that each device employs a different system, especially in the antibody concentration, duration of incubation and method of antibody incubation. Capillary gap stainers employ surface tension for the antibodies and reagents to ascend to immerse the tissue section, whereas other devices

'blow' a fixed aliquot of reagent over the tissue section or drop the reagent over the section. Some devices are 'closed' systems that require specific proprietary reagents, whereas others are 'open' and can be used with reagents from other sources although the detection system remains fixed. Importantly, some systems employ polymer detection systems, whereas the majority use variations of the conventional avidin-biotin peroxidase system. The temperature at which incubation is performed can vary with each device. Thus although automated immunostaining devices are useful they introduce a further set of variables that will differ between laboratories. Within the same laboratory, automated devices can produce inconsistencies that often cannot be accounted for (Figure 9).

Controls

As with all laboratory procedures positive and negative controls must be employed in immunohistology. Negative controls take the form of tissues that are known not to contain the antigen of interest. Another form of negative control includes the substitution of the primary antibody with antibody diluent, non-immune immunoglobulin or an antibody of irrelevant specificity derived from the same species and at the same dilution.

It used to be thought that absorbing the primary antibody with highly purified protein or the peptide antigen employed to generate the primary antibody produced an ideal negative control. This eliminated the binding of the antibody to the protein in the section. However, it has been shown that the absorption control may not bind to the same protein that was used to generate the primary antibody, which, furthermore, may recognize a similar epitope of unrelated protein, especially after tissue fixation (Willingham 1999; Burry 2000).

The most appropriate control for any immunostain would be an internal control because it would have been subjected to identical pre-analytical and analytical variables as the test tissue. However, such controls are invariably non-lesional or benign cells that express the antigen of interest at levels different to the tumor cells and are thus not ideal controls. Nonetheless, they are currently the best controls available.

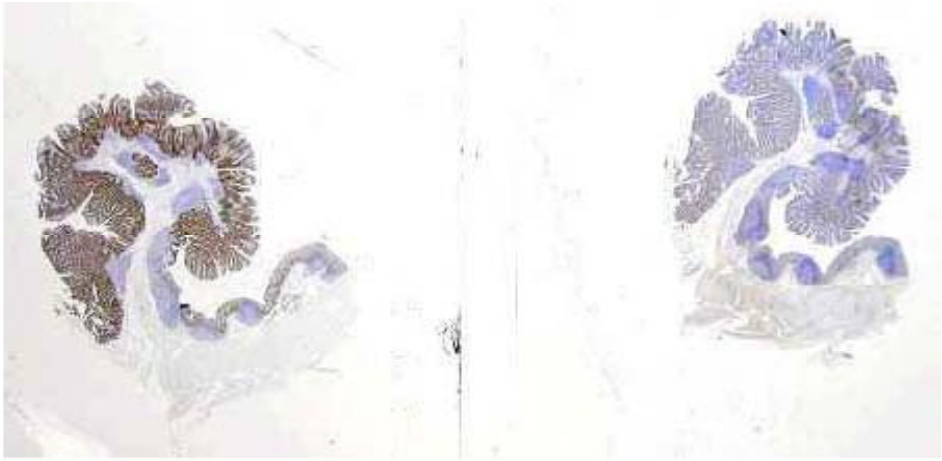

Figure 9. A section of colonic adenomatous polyp stained for CDX2 in an automated device. Despite identical conditions, in one run (right image), the staining was inexplicably weak.

The alternative, an external control of similar tumor tissue known to express the antigen of interest, would have been subjected to an entirely different set of pre-analytical variables. It is inappropriate to use benign tissue as external controls when examining tumor cells.

Reference standards for quality control of reagents and tests in the clinical laboratory are well established. Such standards can be obtained from pooled serum but the development of reference standard controls for immunohistology is subjected to many more obstacles. Unlike serum samples, pathological tissues cannot be pooled and their supply is not limitless. Furthermore, morphologically similar tumors are not necessarily antigenically identical. The use of multitissue blocks provides a solution to some of these problems. Multi-tissue blocks are prepared by binding together with sausage skin many slivers of a wide range of different tumors to serve as both positive and negative controls. Similar blocks can also be made of non-tumor tissue, however, but all such blocks also contain a limited amount of material. When testing for tumor antigen, it is more appropriate to employ multi-tumor blocks as controls as the level of antigen is more likely to correspond to that in the test section than if multi-non tumor blocks were the control.

Microtissue arrays are a possible solution to the limited supply of control tissue. Microarray blocks allow the incorporation of 200-300 fine tissue cores into blocks that can be used for controls against a wide variety of antibodies and as the cores are small (0.5-1.5 mm diameter) much of the original tissue block remains preserved. Microtissue arrays should be used with the recognition that each core of tissue has been subjected to different fixation and processing so that the level of antigen preservation in each of the 200-300 tissue samples are different and by no means standardized.

Recognition of this deficiency in controls led to the development of the ‘Quicgel’ control which was an artificial tissue control block using a breast cancer cell line which was added to the tissue cassette containing the test sample (Riera et al, 1999). This method requires the availability of suitable cell lines expressing the antigen in question, which needs to display consistent behavior under cell culture and storage. An extension of the ‘Quicgel’ method is ‘histoids’ in which three-dimensional pellets are grown in centrifugal cell culture to produce, in theory, an unlimited supply of ‘faux tissue’ controls. If three or more cell lines are co-cultured, the faux tissue can be employed as controls for many of the commonly employed antibodies including controls for fixation and the processing steps. Alternatively, it has been suggested that it may be possible to develop preparations of purified protein that can be diluted to produce a series of known reference standards for both Western blotting and immunohistochemistry (Taylor 2006).

In quantitative procedures, a validated control expressing the range of scores is included alongside the test section so that it is subjected to the identical staining procedure. Closer examination of this common practice reveals that such ‘controls’ are not optimal simply because they have been subjected to different pre-analytical variables, e.g., fixation and tissue processing may be quite different to the test tissue. As such, titrating the staining procedure to such ‘controls’ can be misleading and inappropriate. Ideally, both controls and test must be subjected to identical pre-analytical and analytical conditions so that the state of antigen preservation in both tissues is identical.

It is clear from the foregoing discussion that the question of appropriate controls has not been satisfactorily answered. As a consequence, this deficiency and the fact that variables cannot presently be standardized between laboratories and between specimens, all quantitative measures in immunohistology, many of which are subjective, should be viewed

with skepticism and caution especially if therapeutic decisions are based on assigned scores (Leong 2004a; 2004b).

TEST VALIDATION

As the immunohistological assay becomes more frequently employed as a prognostic as well as predictive tool in cancer, there is a gradual realization that the test requires careful validation. All too often an antibody is purchased that is claimed by the vendor to be specific for a cancer and this is run against a few such cancers that are high expressors of the protein. Titration and optimization of the antibody may be performed, although even these procedures are may not be done and the manufacturer's recommendation are simply followed without regard for the variations in pre-analytical and analytical factors operative for the individual laboratory. Such testing is not the same as validation, which requires that the testing be done against a large number of both positive and negative specimens. While all the criteria for clinical validation that include a definitive clinical study with a sample size that is adequate for statistical analysis, methodological validation, and optimized cutoff value cannot be adhered to, immunohistological prognostic and predictive markers must reliably predict outcomes or response to treatment in the patient samples used for validation (McGuire 1991). Indeed, the arguments for validation of prognostic and predictive markers can also be extended to all other diagnostic markers as identification and specific typing of a neoplasm can rise to the level of a predictive test as specific chemotherapeutic agents and regimens have been developed to many tumors and treatment becomes highly individualized.

This requirement for appropriate validation was first imposed in the recent guidelines for HER2 testing in breast cancer (Wolff et al, 2007). Both technical and clinical validation should be performed for the immunohistological assay. Ideally, a valid method should show substantial equivalence with protein expression or a clinically relevant surrogate or methodological identity to the original clinical validation assay. This is easier said than done. Validation against the original clinical validation assay is difficult or even impossible and the alternative is validation against a recognized 'gold standard'. In the case of HER2, there is in reality no such 'gold standard', neither FISH nor immunohistology is accurate in predicting outcome in 100 per cent of cases (Leong and Leong, 2006; Vogel et al, 2002) and we have to settle for substantial methodological or analytical equivalence to the original study using a validated sample set or cross-validation with an alternative validated method, in this case either FISH or immunohistology.

Another method of validation is through interlaboratory comparison or comparison with a reference laboratory whose testing has been validated. In the latter situation the question arises as to 'what constitutes a reference laboratory?' Even large-volume, so-called central laboratories, can fall short of required standards. Concordance between two such laboratories for FISH was 92% and between FISH and IHC was 82% (Dybdal et al, 2005), figures that fall short of the 95% recommended by the recent HER2 Testing Guidelines (Wolff et al, 2007). When results from a peripheral laboratory were compared with those obtained in a central reference laboratory the concordance for FISH and IHC were 88.1 and 81.6% respectively (Perez et al, 2006). Reproducibility and concordance between laboratories is clearly a problem that extends to other prognostic and predictive markers as exemplified by inter-

laboratory comparisons of estrogen and progesterone receptor assays where reliable assays were found in only 36% of participating laboratories in Europe (Rhodes et al, 2001).

It has been suggested that validation exercises may not be necessary if a validated commercial method is employed and the vendor's protocol carefully followed. This clearly is not true as pre-analytical factors are so different between laboratories that standardization of the staining method is not a guarantee of uniformity of sensitivity.

Another method of validation is the use of standard samples from an approved source but such sources and tissue are not currently available. The use of consensus positive and negative tissue in the form of tissue microarrays is a possible substitute (Fitzgibbons et al, 2006). Alternatively, tissue samples from cases accessioned by your own laboratory known to harbor the target protein by non-IHC means can be used, but in all these situations it has to be remembered that there is no fixation or processing standard so that agreement between laboratories and between samples is subject to pre-analytical variables discussed previously. Clearly the ideal validation procedure would be against patient outcome but this is a costly exercise and often not practical as they require appropriate numbers of patients and a prospective study.

The recent HER2 testing guidelines suggest 25 to 100 samples as sufficient numbers for validation. However, 25 samples may not be sufficient to achieve concordance between laboratories or methods in any validation exercise as the probability of making the 95% concordance standard is significantly less than 0.5 according to the Table A8 of the Guidelines (Wolff et al, 2007).

The setting of rigorous performance standards in prognostic and predictive testing (with potential extension to all IHC staining) will have consequences. If proficiency is regulated, those laboratories not meeting the required 95% concordance benchmark may have to cease testing in the United States and elsewhere where proficiency is regulated. This raises again the previous question of what is a validated method as currently there is no objective arbiter of what is valid.

POST-ANALYTICAL PHASE

While the post-analytical phase also includes generation and delivery of the results/reports, these aspects will not be discussed here.

INTERPRETATION

Some of the problems encountered in this area result from the lack of well-defined standards of what constitutes a positive result and if there are grades or degrees of positivity. There is no consensus of what is an adequate threshold or cut-off. What percentage of cells displaying immunoexpression is required to for a lesion to be positive? Undoubtedly, this figure varies among observers and is very much influenced by the quality and sensitivity of the staining procedure in different laboratories. If the cells that take up stain are cytomorphologically atypical and correspond to the tumor population, then no more than a few definitely stained tumor cells are necessary for a positive result. Often, larger numbers of

positive tumor cells can be demonstrated in this situation by simply increasing the primary antibody concentration or increasing the duration and/or temperature of the antigen retrieval process. It should be borne in mind that when the cutoff is set at 10% the highest degree of interobserver concordance is achieved and concordance falls to unacceptable levels when the cutoff for some immunohistological stains is set higher (see below).

In a way, the selection of a cutoff level for any immunostain represented an excursion into some form of quantitation. Pathologists often report immunohistological stains in some semiquantitative manner by grading the intensity of staining as 'negative', 'weak', 'moderate' or 'strong'; or numerically as '0', '1+', '2+' or '3+', and would assess the extent of staining in the tumor as 'focal' or 'extensive', sometimes based on a percentage of tumor cell staining. Such methods have not been standardized and cut-off values, intensities, and extent of staining carry little relevance when immunohistology is employed in a qualitative manner as the question asked 'is the tumor positive?' for a specific antigen and not 'how positive is the tumor?' However standardization becomes immensely relevant when some quantitative value has to be assigned to the results. Problems associated with quantitative immunohistology have been discussed elsewhere (Leong 2004a). Essentially, because it is virtually impossible to control or standardize the pre-analytical factors that influence the preservation of antigens in FFPT, quantitation becomes farcical. In the ideal situation, clinicopathological validation for each laboratory's staining procedure and results should be conducted but even so, it has been argued that such retrospective studies are usually conducted on selected material from one institution where fixation and tissue processing are relatively uniform and staining is batched to a single run, further minimizing variation. This is very different to the situation in routine diagnostic practice. Simple variation in chromogen incubation times can produce vast differences in stain intensity that can severely affect visual quantitation. Indeed, one widely acknowledged expert has observed that even with automated immunostaining there can be a "daily variation in optical density of as much as 30% for estrogen receptor, when the same block of tissue was used as a daily control" (Seidal et al, 2001). There have been recommendations that quantitative immunohistology be conducted only after validation procedures are carried out by comparing results with those achieved by another technology such as FISH, or by comparing with an external control such as cell lines calibrated by immunohistology or FISH. Even if reference cell lines are stained alongside the test material, it must be remembered that the ability to stain the control tissues appropriately only serves to control the staining procedure. Only when controls and test materials are subjected to the same pre-analytical and analytical variables are they truly comparable but such conditions will be almost impossible to achieve. Until both controls and test are subject to identical conditions of preparation all results obtained by visual quantitation of immunohistological stains are, at best, approximations (Leong 2004b).

Other variables that are relevant to quantitative immunohistology include the area of the tissue section to assess: random versus peripheral versus central versus invasive tumor versus in situ tumor. With assessments such as the Ki-67 proliferative index, should areas of highest activity be counted or should counts be conducted randomly? With counts for vessels, should values be based on the relative area (hence volume) occupied by the vessels or density? Interpretation of positive staining can be particularly difficult in the case of some nuclear antigens such as Ki-67, p53, and ER due to nucleolar staining, resulting in significant interobserver variation. While stain enhancement techniques using metallic ions or organic

compounds have been employed to assist visualization, many of these only change the color of the chromogen and do not truly enhance staining.

FALSE-POSITIVE, FALSE-NEGATIVE, CROSS-REACTIVITY AND ABERRANT EXPRESSION

Familiarity with the characteristics and specificity of the antibody used will avert incorrect interpretation. A positive stain is heterogenous in the section and heterogenous in the cell. Antigens often show specific organelle localization. For example, cyclin D1 is a nuclear antigen and cytoplasmic or membrane staining should not be read as a positive result. On the other hand, the ALK protein is commonly located to the nucleus and cytoplasm of anaplastic large cell lymphoma as a result of t(2;5). However, in as many as 28% of cases where there is a variant translocation, staining is confined to the cytoplasm and/or cell membrane. This cytoplasmic and membrane localization should not be interpreted as a false-positive reaction as it represents the true distribution of a variant form of the ALK fusion protein (Stein et al, 2000).

A large number of cell types and their corresponding tumors may display positive staining for proteins that are not anticipated. In this context the staining is called false positive, aberrant or cross-reactive and can potentially lead to incorrect diagnosis.

Cross reactivity may occur with some antibodies. Polyclonal CEA cross reacts with non-specific cross-reactive antigens in granulocytes whereas the monoclonal version of this antibody does not. Some antibodies may cross react with common epitopes on different intermediate filaments such as cytokeratin antibodies with GFAP-expressing glial cells.

When cells express proteins that are not expected, the phenomenon has been described as “aberrant” expression. In many cases the expression has been shown to be true expression by molecular analysis, such as the staining of cytokeratin in some mesenchymal cells and their corresponding tumors such as leiomyosarcoma, rhabdomyosarcoma, and angiosarcoma.

True false positive staining may occur in a variety of situations. In the assessment of immunostains, an “edge effect” may be observed whereby cells in the periphery of the tissue section stain more strongly than the rest of the section. Often this is seen as a distinct peripheral band and may reflect better fixation of tissue in the periphery because of the slow penetration of fixative to the central parts of the tissue block. It may also be the result of reagents seeping beneath the section at the edges so that both surfaces of the section are stained. In any event this edge effect is more often than not true staining, albeit, enhanced in comparison to the rest of the section. In a somewhat similar vein, cracks and spaces in the tissue section can show non specific entrapment of reagents so that there is false positive staining of cells lining such spaces.

A number of cell types may display false positive staining and these can be readily recognized as they clearly stand out against the otherwise negative staining cells of interest. Necrotic and apoptotic cells often show false staining because of increased oxidative enzymes, and areas of necrosis, in particular should be avoided when assessing immunostains or when attempting to quantitate. The stratum granulosum of the epidermis may show non-specific staining as do RNA-rich cells. Interestingly, cells rich in mitochondria may also stain non-specifically and in oncocytomas, the abundance of mitochondria can pose a problem in

the assessment of immunostaining. The same occurs with cells rich in lysosomes such as granular cell tumors, because of the abundance of oxidative enzymes within the lysosomal bodies.

Certain tissues are rich in endogenous biotin and staining systems that employ avidin will produce non-specific staining unless the endogenous biotin is blocked. In particular tissues such as renal, liver and large bowel may routinely require blocking because of endogenous biotin. Alternatively, a detection system that does not use avidin may be employed. Gestational endometrial glands represent a potential pitfall as endogenous biotin may produce prominent intranuclear inclusions that mimic viral inclusions and are mistaken as such when they show false positive staining for viral antigens. In such situations, most irrelevant antibodies are likely to produce staining of the biotin inclusions that can be reduced with biotin blocking procedures or more conveniently eliminated by employing a system that does not use avidin such as the alkaline-phosphatase-peroxidase or EPOS (Dako, Santa Barbara, Calif, USA) systems (Cooper et al, 1997).

Lastly, antigens may be phagocytosed by macrophages such as in the case of myoglobin. Myoglobin released from necrotic skeletal muscle in the vicinity of soft tissue tumors may be phagocytosed by macrophages that should not be mistaken for myoglobin immuno-expressing tumor cells.

RECEPTOR DETECTION FOR TARGETED THERAPIES

The drive for quantitation of immunohistological stains has largely escalated because of target therapies in an increasing number of cancers, as there is evidence to suggest that the response to such treatments is dependent on the amount of receptors expressed by the tumor cells. Currently, the number of tumors that can be treated in this manner is small but this form of therapy has potential to increase.

Targeted therapy with humanized antibodies that have been validated include those to HER2/neu (Trastuzumab) in breast cancer, CD117 (Imatinib, Glivec, STI571) in chronic myeloid leukemia and gastrointestinal stromal tumor, CD20 (Retuximab, Retuxam) in aggressive B cell lymphomas including mantle cell lymphoma and diffuse large cell lymphoma, CD33 (Gemtuzumab ozogamicin, Myotarg) in myeloblastic leukemia, Epidermal Growth Factor Receptor (EGFR) in colorectal cancer (Cetuximab, Erbitux) and non small cell lung cancer (Gefitinin, Iressa, Erlotinib, Tarceva), and the somatostatin receptors (Sandostatin, Octreotide) in pituitary and gastroenteropancreatic endocrine tumors.

CD20 and CD33 staining are enumerated in the flow cytometer so that scores are based on the percentage of positive cells. Cutoff values are generally set at 90% and above. With immunohistological methods of receptor detection a variety of methods of scoring have been devised based on the percentage of positivity and intensity of staining of tumor cells.

For the immunohistological scoring of EGFR in colorectal cancer and non-small cell lung cancer (NSCLC) at least three Food and Drug Administration (FDA) approved EGFR kits have been employed in clinical trials of monoclonal antibody based targeted treatment. These have included the Dako EGFR pharmaDx, Zymed EGFR kit and Ventana EGFR 3C6 antibody.

One study comparing the sensitivity of these kits for EGFR detection in metastatic colorectal carcinoma found Zymed and Ventana kits to be more sensitive but a high concordance was observed for all three kits in the evaluation of intensely stained tumor cells (Penault-Llorca et al, 2006). Interestingly, when the authors examined scoring systems that combined the percentage of positive cells and staining intensity they found it to be not useful as staining intensity correlated with the percentage of positive cells. They also found that fixatives and the nature of the specimen did not influence staining results. Other studies have suggested that the Dako kit may be more sensitive especially for the prediction of survival with Gefitinib in NSCLC (Hirsch 2008) and that the percentage of positive tumor cells predicted benefit from gefitinib and not the intensity of staining (Hirsch 2008; Cappuzzo 2005). Cutoff values have been chosen arbitrarily with some trials employing a cutoff of 1% or more positivity irrespective of membrane staining being complete or incomplete (Cunningham 2004; Saltz 2004), while others have adopted different values, reflecting the lack of a consensus concerning scoring for EGFR immunostaining (Goldstein and Amin, 2001; Tos and Ellis, 2005). The conflicting results obtained with different reagents and cutoff values has raised question as to the reliability of immunohistochemical assessment of EGFR (Sabourin et al, 2005).

HORMONE RECEPTORS AND HER2/*NEU* IN BREAST CANCER

One of the earliest immunohistological stains to be subjected to some form of quantitative evaluation was the staining of hormone receptors in breast cancer. In the case of estrogen and progesterone receptors, when the initial reluctance to accept immunohistological staining in place of cytosolic assays was overcome, there was pressure to adopt some method of quantitation to replace the quantitative results obtains from cytosolic assays. In our study, we found that 10% positivity corresponded to the 10 fmol cutoff adopted for the cytosolic assay of estrogen receptor (Raymond and Leong, 1990). Because of pressure to provide numbers to the stains we reported on two parameters for estrogen and progesterone immunohistological stains, namely intensity of stain, i.e., negative, weak, moderate and strong (or 0, 1+, 2+ and 3+, respectively) and the extent of staining, i.e., <10%, 11-25%, 26-50%, 51-75%, and >75%. The latter were chosen for convenience as they could, with experience, be assessed by examination with a low-power objective lens. Several methods of quantitation for hormone receptors have been proposed, and one of the more widely used methods employs both the intensive and extent of staining in a combined fashion (Barnes et al, 1996; Allred et al, 1998; Hervey et al, 1999). The scores are employed clinically to predict response to hormone therapy and for prognosis, despite the observation that a clinical response was obtained with tumors displaying as low as 1% of estrogen receptor positivity (Hervey et al, 1999) which led to the National Institutes of Health recommendation that any positive staining for estrogen receptor is considered to be a definitive result and indication for anti-estrogen therapy. More recently, it was demonstrated in a large number of patients that the distribution of estrogen and progesterone receptors is bimodal as is the distribution of Allred scores (Collins et al, 2005). This finding implies that these parameters predictive of response to hormonal therapy are generally either negative or positive, with only small number falling in between (Nadji 2008).

Immunostaining for HER2/neu protein has been a widespread method assessment in breast cancer. The overexpression of this protein has been confirmed to be an independent prognostic marker in node-positive and more recently, also in node-negative patients. More importantly, HER2/neu positive status predicts positive response to adriamycin-based therapies and poor response to tamoxiphen, even in estrogen receptor-positive tumors. The recommended scoring for HER2 is a 4-tiered system, where 0 = no staining; 1+ = faint/barely perceptible membrane staining in more than 10% of tumor cells, which only stain in part of their membrane; 2+ = weak to moderate complete membrane staining in >10% of tumor cells; 3+ = strong complete membrane staining in >10% of tumor cells (Jacobs et al, 1987; Allred and Swanson, 2000). As with other quantitative scores in immunohistology these cutoffs are have been arbitrarily set and the 10% value was recently revised to 30%, again arbitrarily (Wolff et al, 2007).

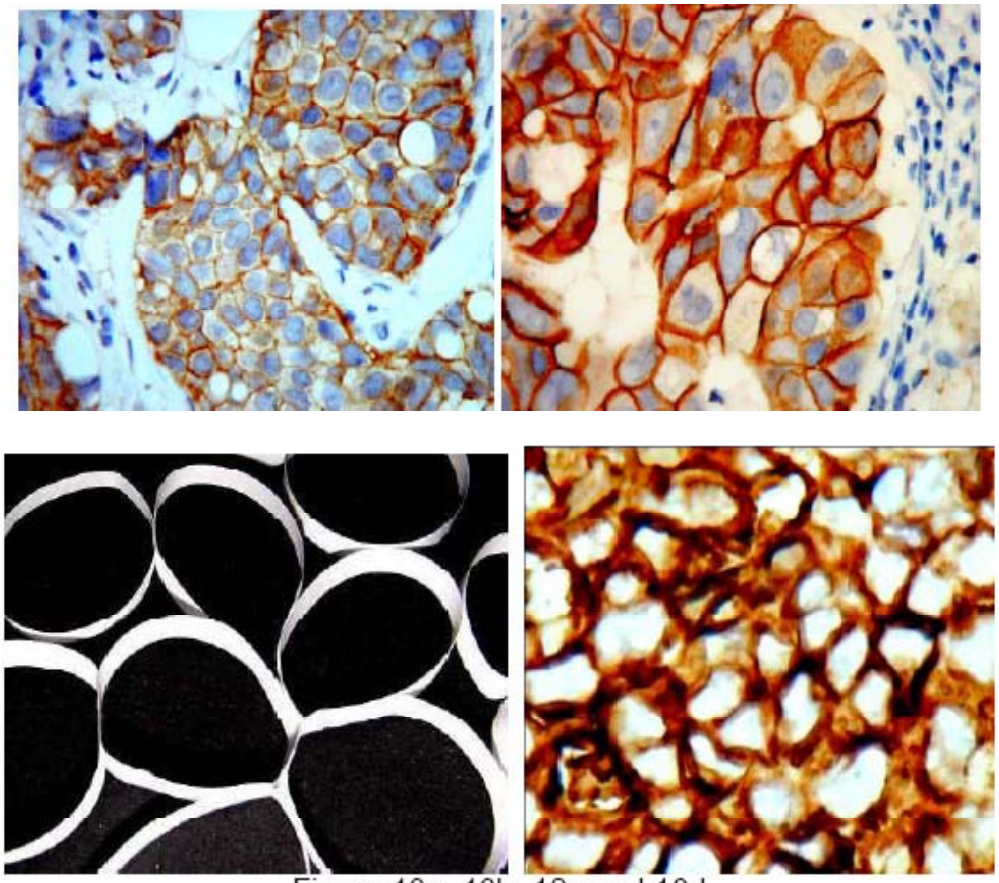

Figure 10. (a) There was strong and complete membranous staining in >10% of tumor cells for Her2 in this tumor attaining a 3+ score. However, Her2 was not found to be amplified by FISH. In contrast, the staining in another tumor (b) displayed a distinct 'band', which corresponded to amplification of the gene. (c) Depicts the reason for the band pattern of labeling as a 3-5 micron slice of cell is present in the tissue section. (d) Staining for CD79a a lymphocyte membrane protein also showed the distinctive band pattern as would be seen with other membrane proteins.

Scores 0 and 3+ are easy to identify, but it is more difficult to discriminate between 1+ and 2+, and between 2+ and 3+ as the distinction is largely based on subjective perception of the intensity of staining. Another issue of contention is the use of the 10% cutoff for a positive result (Leong and Leong, 2006). This value is entirely arbitrary and did not take into account the significance of heterogeneity in Her2 staining. When the cutoff was arbitrary raised to 60% in a multicenter study, a concordance of 95% was obtained with fluorescence in situ hybridization (FISH) (Vincent-Salomon et al, 2003). In the National Surgical Adjuvant Breast and Bowel Project studies, when 3+ cases were retested in a central laboratory 18 and 26% were found to be negative (Paik et al, 2002; Roche et al, 2002). In one quality assurance program, it was found that when using an approved test kit for HER2, only 56% of participating laboratories attained acceptable staining (Miller et al, 2004).

In view of the demonstrated subjectivity involved in adjudicating staining intensity and therefore percentages of positive-stained cells, it would be more accurate to associate immunohistochemical labeling with specific cell structures. For example, when Her2 immunoexpression was linked to a specific pattern of membrane localization in that positivity was assigned only when the entire thickness of the section of cell membrane was labeled to produce a band-like staining pattern, a significantly greater degree of concordance with FISH was achieved (Leong et al, 2006) (Figure 10a, 10b, 10c and 10d). The HER2 protein is synthesized in the cytoplasm and transported to the cell membrane; so cytoplasmic staining is not an artifact. At the membrane in normal breast epithelium, HER2 aggregates in clusters, located predominantly in the basolateral aspect of the cells (Leong et al, 2006; Nagy et al, 1999). When HER2 is upregulated, these aggregates become larger and eventually coalesce to give the appearance of linear membrane expression (Nagy et al, 1999). As the tissue section includes 3-5 micron-thick slices of cell membrane, the appearance of positive staining for HER2 should be visualized as a band (Leong et al, 2006), a pattern also seen with the staining of other cell-membrane localized antigens like epithelial membrane antigen, CD79a, CD20, and CD3.

INTEROBSERVER VARIABILITY IN QUANTITATIVE IMMUNOHISTOLOGY

In one published study of interobserver reliability in the scoring of four markers used in colorectal cancer the authors suggested that interclass correlation coefficients for p53 and VEGF indicated substantial agreement between six observers when based on a ‘positive’ score with a predetermined cutoff (Zlobec et al, 2006). Closer examination of the results reveal that the interclass correlation coefficient was ‘strong’ (>0.75%) only for p53, an intranuclear marker when a cutoff of 10% was applied and ‘excellent’ (Kappa coefficient 0.831) when no positivity versus any positivity was evaluated but fell significantly when other cutoff values were used. With the cytoplasmic markers VEGF, Bcl-2 and APAF-1 Kappa coefficients were all <0.50 or ‘poor’ when values above 10% cutoff were used. Thus excellent or strong agreement was achieved when no positivity versus any positivity was evaluated and when 10% cutoff was employed. In other words, correlation was good for a ‘yes’ or ‘no’ result or at a 10% cutoff, but when cutoffs were based on different values, correlation was weak suggesting that quantitation of immunohistology is unreliable and

expose the subjectivity of quantitative scoring. Interestingly, in subsequent publications from the same group, it was recommended that a 'scoring method based on percentage of positive tumor cells, rather than on staining intensity' be adopted (Zlobec et al, 2007). Furthermore, results from such studies reveal that nuclear staining is easier to assess compared to cytoplasmic staining where weak staining can pose difficulties in assessment (Kay et al, 1996). It is for these reasons that we advocate localization of staining to specific anatomical structures as the most accurate method of assessing immunostains.

CONCLUSION

From the forgoing discussion it should be abundantly clear that many variables exist in the different analytical phases of the immunohistological assay (Leong and Leong, 2007). Some of these variables are critical to the preservation of tissue antigens in fixed paraffin-embedded sections and to attain reproducible quantitative results of immunostaining that are meaningful, these variables need to be standardized between laboratories and between different specimens accessioned by the same laboratory. The variables, particularly those in the pre-analytical phase are not within the control of the pathology laboratory and currently pose insurmountable obstacles to standardization.

Antigen retrieval has been a major milestone in alleviating many of the problems related to the demonstration of cellular and tissue proteins in FFPT but careful consideration must be given to all the variables discussed previously and these need to be standardized. For this to happen international and national consensus groups can play an important role in their recommendations of optimal methods and procedures. The recent guidelines from the College of American Pathologists and American Society of Clinical Oncology for human epidermal growth factor receptor 2 testing in breast cancer is one such example (Wolff et al, 2007) although it is still a long way from enforcing standardization of the technology and methodology.

Standardization of the significant differences in the variables that occur before accessioning by the pathology laboratory requires co-operation of the clinicians responsible for obtaining the specimens. One way of achieving this end is through some form of enforcement by peer groups. Delays in fixation should be minimized and the time placed into formalin should be recorded so that the total duration of fixation can be controlled. Specimens that do not conform to recommended optimal conditions cannot be regarded to produce acceptable quantitative results especially if all other laboratory procedures are standardized. For consistency, the laboratory should, as far as possible, adopt standard procedures for fixation, tissue processing, sectioning, and staining. Automated immunostaining devices provide a means of standardization of the staining protocol within the laboratory but the availability of several such commercial devices using different protocols makes uniformity between laboratories difficult. Antibodies should be stored in the appropriate manner at $-70^{o}C$, with only aliquots of working dilutions stored at $4^{o}C$. Sections should be subjected to immunostaining as soon as possible after preparation. If delays are anticipated, the cut sections should be wrapped in foil and kept in a dark container at $-20^{0}C$. As it is not possible to standardize the many variables that can influence antigen preservation in the sample, the

best alternative at present is to optimize the staining procedure in order to obtain the best results, and this is done against known positive controls of appropriate tissues.

New antibodies require appropriate validation. All too often the claims of the antibody distributor/manufacturer as regards sensitivity and specificity are accepted without in-house validation, sometimes leading to inappropriate interpretation of the staining results. The antibody should be validated and optimized to known positive controls of similar tissue. Optimization should be performed against known positive controls of appropriate tissues that have been fixed and processed in a similar if not identical manner to the test tissue. In addition, the antigen retrieval method and performance of immunohistochemical staining should also be similar. To ascertain the most optimal method of antigen retrieval the following methods should be routinely tested for each new antibody. Antigen retrieval should be tested with citrate buffer, 10 mmol/l at pH6.0, and citrate/EDTA at pH8.0 as retrieval solutions. This should be performed at both 98^0C and 110^0C, with varying concentrations of primary antibody, starting with that suggested by the product manufacturer. If satisfactory results are not obtained, enzyme digestion (with protease or similar) should be introduced as an additional step before and after the heat-induced antigen retrieval. Assessment is based on the signal to noise ratio and the integrity of tissue morphology. It may be necessary, with less sensitive antibodies, to experiment with different buffers of varying pH as retrieval solutions. Another variable that may require manipulation is the duration of heating. Optimization of the antigen retrieval procedure for each antibody is, at present, the most important step towards standardization. The optimization process merely ensures that the procedure is at its greatest sensitivity but cannot verify proper tissue fixation or processing and does not amount to standardization. Validation of the antibody and methodology against benchmark standards is a more complex issue that has been discussed.

Similarly, for the post-analytical phase appropriate scoring methods have to be developed. Scoring methods need to be evidence-based; the best form of validation being patient outcome. Such validation would require collaborative or international studies. In is clear that scores based on intensity produce variable results that are often not reproducible. When the target antigen is confined to a known anatomical structure, scoring becomes easier with greater concordance and reproducibility as demonstrated with nuclear antigens like Ki67 (Zlobec et al, 2006; 2007) and even then when it is applied as percentage of staining cells without concern for intensity. Cytoplasmic staining is more difficult to score as the target antigen can be localized in a several or one specific organelle. As such cytoplasmic staining should be assessed on the basis of specific antigen localization. Similarly with cell membrane staining as with Her2/neu antigen, the entire thickness of the cell membrane in the tissue section should be stained before being assigned a positive score. The assessment of partial membrane staining is prone to poor concordance and reproducibility.

Other factors in the post-analytical phase are dependent on the experience of the reporting pathologist. Selection of the appropriate antibodies to be used and the appropriate area in the section for assessment is dependant on pathologists' expertise. Cut-off numbers are mostly arbitrary and when scoring, should assessment be made in the areas of highest intensity or is a mean value more appropriate? Some of these issues can be standardized through the use of automated cellular imaging systems that can evaluate the target cells using a large number of different morphologic parameters. Despite all these measures it is clear that there will remain a number of variables that can significantly influence antigen preservation that are beyond the control of the laboratory so that even among specimens accessioned by

the same laboratory, many pre-analytical factors are different and no two specimens are subjected to identical conditions. The realization of these variables and the acknowledgment of the need for standardization, however, is a large step closer to attaining the goal of quantitative immunohistology.

REFERENCES

Acs G, Lawton TJ, Rebbeck TR, et al. Differential expression of E-cadherin in lobular and ductal neoplasms of the breast and its biologic and diagnostic implications. *Am. J. Clin. Pathol.* 2001;115:85-98.

Allred DC, Harvey JM, Berardo M, et al. Prognostic and predictive factors in breast cancer by immunohistochemical analysis. *Mod. Pathol.* 1998;11:155-168.

Allred DC, Swanson PE. Testing for erbB-2 by immunohistochemistry in breast cancer. *Am. J. Clin. Pathol.* 2000;113:171-175.

Barnes DM, Harris WH, Smith P, et al. Immunohistochemical determination of oestrogen receptor: comparison of different methods of assessment of staining and correlation with clinical outcome of breast cancer patients. *Br. J. Cancer* 1996;74:1445-1451.

Blind C, Koepenik A, Pacyna-Gengelbach M, et al. Antigenicity testing by immunohistochemistry after tissue oxidation. *J. Clin. Pathol* .2008;61:79-83.

Boon ME, Marani E, Adriolo PJM, et al. Microwave irradiation of brain tissue: production of microscopic slides within one day. *J. Clin. Pathol.* 1988;41:590-593.

Bratthauer GL Combined E-cadherin and high molecular weight cytokeratin immunoprofile differentiates lobular, ductal, and hybrid mammary intraepithelial neoplasias. *Hum. Pathol.* 2002;33:620-627

Burry RW. Specificity controls for immunocytochemical methods. *J. Histochem. Cytochem.* 2000;48:163-168.

Cappuzzo F, Finocchiaro G, Rossi E, et al. EGFR FISH assay predicts for response to cetuximab in chemotherapy refractory colorectal cancer patients. *Ann. Oncol.* 2008;19:717-723.

Cattoretti G, Peleri S, Parravicini C, et al. Antigen unmasking on formalin-fixed, paraffin-embedded tissue sections. *J. Pathol.* 1993;171:83-98

Chaiwun B, Shi SR, Cote RJ, Taylor CR. Major factors influencing the effectiveness of antigen retrieval immunohistochemistry. IN: Shi SR, Gu J, Taylor CR, eds. *Antigen. Retrieval. Techniques*. Natick, MA: Eaton Publishing; 2000;41-53.

Chiu KY, Chin KW. Rapid immunofluorescence staining of human renal biopsy specimens using microwave irradiation. *J. Clin. Pathol.* 1987;40**:** 689-692

Choi T-S, Whittlesey M, Slap SE, Anderson VM, Gu J. Microwave immunocytochemistry: advances in temperature control. IN: Gu J, ed. *Analytical morphology: Theory, Applications, and Protocols.* Natick, MA, USA: Eaton Publishing; 1997; 91-114.

Collins LC, Botero ML, Schnitt SJ. Bimodal frequency distribution of estrogen receptor immunohistochemical staining results in breast cancer: an analysis of 825 cases. *Am. J. Clin. Pathol.* 2005;123:16-20

Cooper K, Haffajee Z, Taylor L. Comparative analysis of biotin intranuclear inclusions of gestational endometrium using the APAAP, ABC and PAP immunodetection systems. *J. Clin. Pathol.* 1997*;* 50:153-156.

Cuevas EC, Bateman AC, Wilkins BS. Johnson PA et al. Microwave antigen retrieval in immunocytochemistry: a study of 80 antibodies. *J. Clin. Pathol.* 1994*;* 47**,** 448-452.

Cunningham D, Humblet Y, Siena S, et al. Cetuximab monotherapy and cetuximab plus irinotecan in irinotecan-refractory metastatic colorectal cancer. *N. Engl. J. Med.* 2004;351:337-345.

DiVito KA, Charette LA, Rimm DL, Camp RL. Long-term preservation of antigenicity on tissue microarrays. *Lab. Investig.* 2004;84:1071-1078.

Dybdal N, Leiberman G, Anderson S, et al. Determination of HER2 gene amplification by fluorescence in situ hybridization and concordance with the clinical trials immunohistochemical assay in women with metastatic breast cancer evaluated for treatment with trastuzumab. *Breast Cancer Res. Treat* .2005;93:3-11.

Elias JM. Immunohistopathology. A practical approach to diagnosis. Chicago: ASCP Press, 2003.

Fitzgibbons PL, Murphy DA, Dorfman DM, et al. Interlaboratory comparison of immunohistochemical testing for HER2: results of the 2004 and 2005 College of American Pathologists HER2 Immunohistochemistry Tissue Microarray Survey. *Arch. Pathol. Lab. Med.* 2006;130:1440-1445.

Fletcher CD, Berman JJ, Corless C, et al: Diagnosis of gastrointestinal stromal tumors: A consensus approach. *Hum. Pathol.* 2003;33:459-465.

Fraenkel-Conrat H, Brandon B Olcott H. The reaction of formaldehyde with proteins. IV: Participation of indole groups: gramicidin. *J. Biol. Chem.* 1947*;*168: 99-118.

Fraenkel-Conrat H, Olcott H. Reaction of formaldehyde with proteins. VI: Crosslinking between amino groups with phenol, imidazole, or indole groups. *J. Biol. Chem.* 1948a*;* 174: 827-843.

Fraenkel-Conrat H, Olcott H. The reaction of formaldehyde with proteins. V: crosslinking between amino and primary amide or guanidyl groups. *J. Am. Chem. Soc.* 1948b*;* 70: 2673-2684.

Goldstein NS, Hewitt SM, Taylor CR, et al. Recommendations for improved standardization of immunohistochemistry. *Appl. Immunohistochem. Mol .Morph.* 2007;15:124-33.

Goldstein NS, Amin M. Epidermal growth factor receptor immunohistochemical reactivity in patients with American Joint Committee on Cancer Stage IV colon adenocarcinoma: implications for a standardized scoring system. *Cancer* 2001;92:1331-1346

Goldstein NS, Ferkowicz M, Odish E, Mani A, Hastah F. Minimum formalin fixation time for consistent estrogen receptor immunohistochemical staining of invasive breast carcinoma. *Am. J. Clin. Pathol.* 2003*;*120:86-92.

Gown AM, de Wever N, Battifora H. Microwave-basd antigenic unmasking: A revolutionary new technique for routine immunohistochemistry. *Appl. Immunohistochem.* 1993;1:256-266.

Gown AM, Vogel AM. Monoclonal antibodies to human intermediate filament proteins. II. Distribution of filament proteins in normal human tissues. *Am. J. Pathol.* 1984*;*114:309-321.

Hervey JM, Clark GM, Osborne CK, et al. Estrogen receptor status by immunohistochemistry is superior to the ligand-binding assay for predicting response to adjuvant endocrine therapy in breast cancer. *J. Clin. Oncol.* 1999;17:1474-1481.

Hirsch FR, Dziadziuszko R, Thacher N, et al. Epidermal growth factor receptor immunohistochemistry: comparison of antibodies and cutoff points to predict benefit from gefitinib in a phase 3 placebo-controlled study in advanced nonsmall-cell lung cancer. *Cancer* 2008;112:1114-21.

Hjerpe A, Boon ME, Kok LP. 1988. Microwave stimulation of an immunological reaction (CEA/anti-CEA) and its use in immunohistochemistry. *Histochem J* 1988*;* 20, 388-396.

Hopwood D, Yeaman G, Milne G. 1988. Differentiating the effects of microwave and heat on tissue proteins and their cross linking by formaldehyde. *Histochem J* 1988*;* 20, 341-346.

Jacobs TW, Gown AM, Yazji H, et al. Specificity of HercepTest in determining HER-2/neu status of breast cancers using the United States Food and Drug Administration-approved scoring system. *J. Clin .Oncol.* 1999;17:1983-1987.

Lan HY, Mu W, Nikolic-Paterson DJ, Atkins RC. A novel, simple, reliable, and sensitive method for multiple immunoenzyme staining: use of microwave oven heating to block antibody cross reactivity and retrieve antigens. *J. Histochem. Cytochem.* 1995*;* 43, 97-102.

Jacobs TW, Prioleau JE, Stillman IE, et al. Loss of tumor marker-immunostaining intensity on stored paraffin slides of breast cancer. *J. Natl. Cancer Inst.* 1996;88:1054-1060.

Kay EW, Walsh CJ, Whelan D, et al. Interobserver variation of p53 immunohistochemistry – an assessment of a practical problem and comparison with other studies. *Br. J. Biomed. Sci.* 1996;53:101-107

King G, Payne S, Walker F, et al. A highly sensitive detection method for immunohistochemistry using biotinylated tyramine. *J. Pathol.* 1998;183;237-241.

Kakimoto K, Takekoshi S, Miyajima K, Osamura RY. Hypothesis for the mechanism for heat-induced antigen retrieval occurring on fresh frozen sections without formalin fixation in immunohistochemistry. *J. Mol. Hist.* 2008 (in press)

Larsson L. Tissue preparation methods for light microscopic immunohistochemistry. *Appl Immunohistochem* 1993*;*1:2-16.

Leong AS-Y. New vistas in the histopathological assessment of cancer. *Med. J. Aust.* 1992;157:699-701.

Leong AS-Y. Immunohistochemistry – theoretical and practical aspects. IN: Leong AS-Y, editor. *Applied Immunohistochemistry for the Surgical Pathologist*. London; Edward Arnold; 1993;1-22.

Leong AS-Y. Fixation and Fixatives. IN: Woods AE, Ellis RC, editors. *Laboratory Histopathology - A Complete Reference.* London; Churchill Livingstone; 1994;4.1-26.

Leong AS-Y. Immunohistological markers for tumor prognostication. *Curr. Diagn. Pathol.* 2001:7:176-186

Leong AS-Y. Pitfalls in diagnostic immunohistology. *Adv. Anat. Pathol.* 2004a*;*11:86-93.

Leong AS-Y. Quantitation in immunohistology: Fact or fiction? A discussion of variables that influence results. *Appl. Immunohistochem. Mol. Morph.* 2004b;12:1-7.

Leong AS-Y. Microwave Technology for Light Microscopy and Ultrastructural Studies. Bangkok, Thailand; Amarin Printing and Publishing Company Ltd; 2005.

Leong AS-Y, Leong TY-M. Invited Review: Newer developments in immunohistology. *J. Clin. Pathol.* 2006; 59:1117-1126.

Leong AS-Y, Leong FJ: Immunohistochemistry in the Diagnosis of Solid Tumours. IN*:* Nakamura R (ed). *Manual of Clinical Laboratory Immunology, 5th Edition.* Washington DC; ASM Press; 1997, 380-387

Leong AS-Y, Gilham PN. The effects of progressive formaldehyde fixation on the preservation of tissue antigens. *Pathology* 1989;21:81-9.

Leong AS-Y, Lee AKC. Biological indices in the assessment of breast cancer. *J. Clin. Pathol: Mol. Pathol.* 1995;48:M221-38.

Leong AS-Y, Milios J. Rapid immunoperoxidase staining of lymphocyte antigens using microwave irradiation. *J. Pathol.* 1986*;*148: 183-187.

Leong AS-Y, Milios J. Accelerated immunohistochemical staining by microwaves. *J. Pathol*.1990;161: 327-334.

Leong AS-Y, Milios J. An assessment of the efficacy of the microwave-antigen retrieval procedure on a range of tissue antigens. *Appl. Immunohistochem.* 1993a;1:267-274.

Leong AS-Y, Milios J. Comparison of antibodies to oestrogen and progesterone receptors and the influence on microwave-antigen retrieval. *Appl. Immunohistochem.* 1993b;1:2-88.

Leong AS-Y, Milios, Duncis CG. Antigen preservation in microwave-irradiated tissues. A comparison with routine formalin fixation. *J. Pathol.* 1988;156:275-82.

Leong AS-Y, Milios J, Leong FJ. Epitope retrieval with microwaves: A comparison of citrate buffer and EDTA with three commercial retrieval solutions. *Applied Immunohistochemistry* 1996;4: 201-207.

Leong AS-Y, Milios J, Tang SK. Is immunolocalisation of proliferating cell nuclear antigen (PCNA) in paraffin sections a valid index of cell proliferation? *Appl. Immunohistochem.*;1993;1:127-35.

Leong AS-Y, Wright J. The contributions of immunohistochemical staining in tumour diagnosis. *Histopathology* 1987*;*11:1295-1305.

Leong AS-Y, Lee ES, Yin H, et al. Superheating antigen retrieval. *Appl. Immunohistochem.* 2002a;10:263-8.

Leong AS-Y, Parkinson R, Milios J. 'Thick' cell membranes revealed by immunocytochemical staining. A clue to the diagnosis of malignant mesothelioma. *Diagn. Cytopathol.* 1990;6:9-13.

Leong AS-Y, Stevens MW, Mukherjee TM. Malignant mesothelioma: cytologic diagnosis with histologic, immunohistochemical and ultrastructural correlation*. Sem. Diagn. Pathol.* 1992;9:141-150.

Leong AS-Y, Vinyuvat S, Suthipintawong C, Milios J. A comparative study of cell proliferation markers in breast carcinomas. *J. Clin. Pathol: Mol. Pathol.* 1995;48:M83-87

Leong AS-Y, Wick MR, Swanson PE. Immunohistology and Electron Microscopy of Anaplastic and Pleomorphic Tumours*.* Cambridge: Cambridge University Press;1997a; 2-35.

Leong A S-Y, Vinyuvat S, Suthipintawong C, Leong FJ: Patterns of basal lamina immunostaining in soft tissue tumours. *Applied Immunohistochemistry* 1997b;5:1-7.

Leong AS-Y, Yin H, Haffajee Z. Patterns of immunostaining of immunoglobulin in formalin-fixed, paraffin-embedded sections. *Appl. Immunohistochem. Mol. Morph.* 2002;10:110-4.

Leong AS-Y, Formby M, Haffajee Z, Morey A. Refinement of immunohistologica parameters for Her2/neu scoring. Validation by FISH and CISH. *Appl. Immunohistochem. Mol. Morph.* 2006;14:384-389.

Leong AS-Y, Haffajee Z, Clark M. Microwave enhancement of CISH for Her2 oncogene. *Appl. Immunohistochem. Mol. Morph.* 2007;15:88-93.

Leong TY-M, Leong AS-Y. Controversies in the assessment of HER-2. More questions than answers. *Adv Anat Pathol* 2006;13:263-269.

Leong TY-M, Leong AS-Y. Variables that influence outcomes in immunohistology. *Aust. J. Med. Sci.* 2007;28:47-59.

McGuire WL. Breast cancer prognostic factors: evaluation guidelines. *J. Natl. Cancer Inst.* 1991;83:154-155.

Miller RT, Swanson PE, Wick MR. Fixation and epitope retrieval in diagnostic immunohistochemistry: a concise review with practical considerations. *Appl Immunohistochem Mol. Morph* .2000;8:228-35.

Miller K, Ibrahim M. The breast HER-2 module. *Immunocytochemistry* 2004;3:147-150.

Morales AR, Nassiri M, Kanhoush R, et al. Experience with an automated microwave assisted rapid tissue processing method: Effect on histology and timeliness of diagnostic surgical pathology. *Am. J. Clin. Path.;* 2004;121:528-36.

Morgan JM, Navabi H, Jasani B. Role of calcium chelation in high-temperature antigen retrieval at different pH values. *J. Pathol. 1997;* 182: 233-7.

Nadji M: Quantitative immunohistochemistry of estrogen receptor in breast cancer. Much ado about nothing. *Appl Immunohistochem Mol. Morph.* 2008;16:105-07.

Nagy P, Jenei A, Kirsch AK, et al. Activation-dependent clustering of the erbB2 receptor tyrosine kinase detected by scanning near-field optica. l microscopy. *J. Cell Sci.* 1999;112:1733-41.

O'Leary TJ (2001). Standardization in immunohistochemistry. *Appl. Immunohistochem. Mol. Morph.* 2001;9:3-8.

Paik S, Bryant J, Tan-Chiu E, et al. Real-world performance of HER2 testing – National Surgical Adjuvant Breast and Bowel Project experience. *J. Natl. Can. Inst.* 2002;94:852-854.

Pearse AGE. Histochemistry. Theoretical and Applied, 4th ed, vol 1. Edinburgh; Churchill Livingstone; 1980; 95.

Pelstring RJ, Allred DC, Esther RJ, et al. Differential antigen preservation during autolysis. *Hum. Pathol.* 1991;22:237-41.

Penault-Llorca F, Cayre A, Arnould L, et al. Is there an immunohistochemical technique definitely valid in epidermal growth factor assessment? *Oncol. Rep* .2006;16:1173-1179.

Perez EA, Suman VJ, Davidson NE, et al. HER2 testing by local, central, and reference laboratories in specimens from the North Central Cancer Treatment Group N9831 intergroup adjuvant trial. *J. Clin. Oncol.* 2006;24:3032-3038.

Popat S, Hubner R, Houlston RS. Systematic review of microsatellite instability and colorectal cancer prognosis. *J. Clin. Oncol.* 2005;23:609-18.

Porcelli, M., Cacciapuoti, G., Fusco, S., et al. Non-thermal effects of microwaves on proteins: thermophilic enzymes as model system. *FEBS Letters* 1997; 402, 102-6.

Portiansky EL, Gimeno EJ. A new epitope retrieval method for the detection of structural cytokeratins in the bovine prostate tissue. *Appl. Immunohistohcem.*1996; 4:208-14.

Raymond W, Leong AS-Y. Oestrogen receptor staining of paraffin-embedded breast carcinomas following short fixation in formalin: A comparison with cytosolic and frozen section receptor analyses. *J. Pathol.* 1990;160:295-303.

Rhodes A, Jasani B, Balaton AJ, et al. Study of interlaboratory reliability and reproducibility of estrogen and progesterone receptor assays in Europe. Documentation of poor reliability and identification of insufficient microwave antigen retrieval time as a major contributory element of unreliable results. *Am. J. Clin. Pathol.* 2001;115:44-58.

Ribic CM, Sargent DJ, Moore MJ, et al. Tumor microsatellite-instability status as a predictor of benefit from fluorouracil-based adjuvant chemotherapy for colon cancer. *N. Engl. J. Med.* 2003;349:247-257.

Riera J, Simpson JF, Tamayo R, et al. Use of cultured cells as a control for quantitative immunocytochemical analysis of estrogen receptor in breast cancer. The Quicgel method. *Am. J. Clin. Pathol* .1999;111:329-332.

Roche PC, Suman VJ, Jenkins RB, et al. Concordance between local and central laboratory HER2 testing in the Breast Integroup Trial N9831. *J Natl Cancer Inst* 2002;94:855-857.

Saltz LB, Meropol NJ, Loehrer PJ, et al. Phase II trial of cetuximab in patients with refractory colorectal cancer that expresses the epidermal growth factor receptor. *J. Clin. Oncol*.2004;22:1201-1208.

Sabattini E, Bisgaard K, Ascani S, et al. The EnVision system. A new immunohistochemical method for diagnostics and research: Critical comparison with the APAAP, ChemMate, CSA, LABC, and SABC techniques. *J. Clin. Pathol.* 1998;51:506-510..

Sabourin JC, Cayre A, Arnould L, et al. Comparison of three commercially available immunohistochemical tests for EGFR expression in clorectal cancers. Is immunohistochemistry (IHC) reliable? *J. Clin. Oncol.* 2005;23 (June Suppl):9705-9710.

Seidal T, Balaton AJ, Battifora H. Interpretation and quantification of immunostains. *Am. J. Surg. Pathol.* 2001;25:1204-1207.

Shi SR, Key ME, Kalra KL. Antigen retrieval in formalin-fixed, paraffin-embedded tissues: an enhancement method for immunohistochemical staining based upon microwave oven heating of tissue section. *J. Histochem. Cytochem.* 1991;39:741-8.

Shi SR, Imam SA, Young L, Cote RJ, Taylor CR. Antigen retrieval immunohistochemistry under the influence of pH using monoclonal antibodies. *J. Histochem. Cytochem.* 1995; 43:193-201.

Shi SR, Key ME, Kalra KL. Antigen retrieval in formalin-fixed, paraffin-embedded tissues: An enhancement method for immunohistochemical staining based on microwave oven heating of tissue sections. *J. Histochem. Cytochem.* 1991;39:741-748.

Shi SR, Liu C, Pootrakul L, et al. Evaluation of the value of frozen tissue section used as 'gold standard" for immunohistochemistry. *Am. J. Clin. Pathol.* 2008; 129:358-366.

Shi S-R, Gu J, Turrens J, et al. Development of the antigen retrieval technique: Philosophical and theoretical bases. IN: Shi S-R, Gu J, Taylor CR. Eds. *Antigen Retrieval Techniques: Immunohistochemical and Molecular Morphology.* Natick, MA: Eaton Publishing, 200;17-40.

Sompuram SR, Vani K, Messana E, Bogen SA. A molecular mechanism of formalin fixation and antigen retrieval. *Am. J. Clin. Pathol.* 2004*;*121: 190-199.

Sompuram SR, Vani K, Bogen SA. A molecular model of antigen retrieval using a peptide array. *Am. J. Clin. Pathol.* 2006;125:91-98.

Stein H, Foss HD, Durkop H, et al. CD30+ anaplastic large cell lymphoma: a review of its histopathologic, genetic, and clinical features. *Blood* 2000;96:3681-3695.

Suurmeijer AJH, Boon ME. Notes on the application of microwaves for antigen retrieval in paraffin and plastic tissue sections. *Eur. J. Morph.* 1993*;* 31, 144-150.

Suthipintawong C, Vinyuvat S, Leong AS-Y. Immunostaining of cell preparations: A comparative evaluation of common fixatives and protocols. *Diagn. Cytopathol.* 1996;15:167-174.

Takes PA, Kohrs J, Krug R, Kewley S. Microwave technology in immunohistochemistry: application to avidin-biotin staining of diverse antigens. *J. Histotech.* 1989*;*12, 95-98.

Taylor CR. An exaltation of experts: Concerted efforts in the standardization of immunohistochemistry. *Hum. Pathol.* 1994;25:2-4.

Taylor CR, Shi SR, Chen C, et al. Comparative study of antigen retrieval heating methods: microwave, microwave and pressure cooker, autoclave and steamer. *Biotech. Histochem.* 1996;71:263-70.

Taylor CR, Levenson RM: Quantification of immunohistochemical – issues concerning methods, utility and semi-quantitative assessment II. *Histopathology* 49:411-24,2006.

Taylor CR, Cote RJ. Immunomicroscopy, A Tool for the Surgical Pathology, 3rd Edition, Edinburgh: Elsevier, 2005

Taylor CR. Personal communication. 2006.

Tos AP, Ellis I. Assessing epidermal growth factor receptor expression in tumours: What is the value of current test methods? *Eur. J. Cancer.* 2005;41:1383-92

Vincent-Salomon A, MacGrogan G, Couturier J, et al. Calibration of immunohistochemistry for assessment of Her2/neu in breast cancer: results of the French Multicentre GEFPICS Study. *Histopathology* 2003;42:337-347.

Visinoni F, Milios J, Leong AS-Y, *et al*. Ultra-rapid microwave/variable pressure induced histoprocessing: Description of a new tissue processor. *J. Histotechnol.* 1998;21: 219-224.

Vogel CL, Cobleigh MA, Tripathy D, et al. Efficacy and safety of trastuzumab as a single agent in first-line treatment of HER2-overexpressing metastatic breast cancer. *J. Clin. Oncol.* 2002;20:719-726.

Wester K, Wahlund E, Sundstrom C, et al. Paraffin section storage and immunohistochemistry. Effects of time, temperature, fixation, and retrieval protocol with emphasis on p53 protein and MIB1 antigen. *Appl. Immunohistochem. Mol. Morph.* 2000;8:61-70.

Willingham MC. Conditional epitopes: Is your antibody always specific*? J. Histochem. Cytochem.* 1999;47:1233-1239.

Wolff AC, Hammond ME, Schwartz JN, et al. American Society of Clinical Oncology/College of American Pathologists guideline recommendations for human epidermal growth factor receptor 2 testing in breast cancer. *J. Clin. Oncol.* 2007;25:118-145

Wood B, Leong AS-Y. Cell adhesion proteins – Biology, detection and applications. *Pathology* 2003;35:101-105.

Zlobec I, Steele R, Michel RP, et al. Scoring of p53, VEGF, Bcl-2 and APAF-1 immunohistochemistry and interobserver reliability in colorectal cancer. *Mod. Pathol.* 2006;19:1236-1242.

Zlobec I, Terracciano L, Jass JR, Lugli A. Value of staining intensity in the interpretation of immunohistochemistry for tumor markers in colorectal cancer. *Virchows Arch*.2007;451:763-9.

In: Biochemistry and Histocytochemistry… ISBN: 978-1-60876-283-5
Editors: S. Fuchs, M. Auer, pp. 117-141 © 2010 Nova Science Publishers, Inc.

Chapter 6

IMMUNOHISTOCHEMICAL BASIS FOR ORTHODONTIC TREATMENT

***Toshiyuki Kawakami*[*1,2,3], *Keisuke Nakano*[1,2,3], *Takako Shimizu*[4], *Takehiro Watanabe*[1], *Rina Muraoka*[1], *Akihiro Kimura*[1,3] *and Hiromasa Hasegawa*[1,3]**

[1]Hard Tissue Pathology Unit, Matsumoto Dental University Graduate School of Oral Medicine, Shiojiri, 399-0781 Japan

[2]Hard Tissue Pathology Unit, Matsumoto Dental University Institute for Oral Science, Shiojiri, 399-0781 Japan

[3]Department of Oral Pathology, Matsumoto Dental University School of Dentistry, Shiojiri, 399-0781 Japan

[4]Department of Dental Diagnostic Sciences, Matsumoto Dental University Hospital, Shiojiri, 399-0781 Japan

ABSTRACT

It is important to establish the biological basis of immunohistochemical characteristics of mandibular bone and cartilage, as well as periodontal tissue reaction to mechanical stress for orthodontic treatment.

The mandible is composed of mandibular bone and cartilage. This cartilage is classified as secondary, together with condylar, coronoid and angular cartilages. The mandibular bone formation pattern attracts many researchers because it suggests large possibilities for orthodontic treatment. Mandibular condylar cartilage has bone characteristics which are more significant than cartilaginous characteristics. In general, Runx2 is a transcription factor necessary for osteoblast differentiation and bone formation. Therefore, we focused on Runx2 and investigated the distribution of Runx2 in developing mouse mandibular condylar cartilage, with Jagged-Notch signaling, using immunohistochemistry (IHC) and in situ hybridization (ISH) techniques. These IHC and ISH results suggest that Runx2 plays an

* Address for Correspondence: Professor Toshiyuki Kawakami, Hard Tissue Pathology Unit, Department of Hard Tissue Research, Matsumoto Dental University Graduate School of Oral Medicine, Shiojiri, 399-0781 Japan, Phone and Fax: +81-263-51-2035, E-mail: kawakami@po.mdu.ac.jp

essential role for mandibular condylar cartilage development, especially that Runx2 is essential for the onset of secondary cartilage differentiation.

In addition, to establish an immunohistochemical basis for orthodontic treatment, we examined early changes of Runx2 and Msx2 immunohistochemical expressions by immunohistochemistry in mouse periodontal ligament exposed to mechanical stress. At 20 minutes, 1 hour, 3 hours, 9 hours and 24 hours, relevant parts of the mouse tissues were histopathologically evaluated, and they were examined for Runx2, Msx2 and alkaline phosphatase (ALP) expressions. Strong expressions of Runx2 and Msx2 were seen in periodontal fibroblasts of the tension side at 20 minutes after mechanical stress. Expressions of Runx2 and Msx2 became stronger in parallel with time, and at 24 hours after mechanical stress, the periodontal fibroblasts, cementoblasts, and osteoblasts showed strong expression. Moreover, ALP has also demonstrated similar strong expression. All these results strongly suggested that Runx2 promoted differentiation of osteoblasts at an early stage and Msx2 worked as an activator of Runx2 function. Furthermore, because Heat Shock Proteins (HSPs) serve as molecular chaperones to maintain homeostasis in tissues, we examined the immunohistochemical profile change of one such protein, HSP70, in periodontal ligament cells after receiving mechanical stress during orthodontic treatment in the course of up to 24 hours. We thought that the mechanical stress for orthodontic treatment might cause dynamic histological change occurred within a short time and might also cause expression of HSP70 in periodontal ligament tissue.

INTRODUCTION

For orthodontic treatment, it is important not only to examine the tissue reaction of periodontal tissues to the orthodontic mechanical stress, but also to examine the physiological characteristics of the mandibular body bone and cartilages. Therefore, in this chapter, we describe both the biological and immunohistochemical basis.

At first, we should mention the specialty of the mandible, mandibular body bone and cartilages. It is well known that the mandible is formed mainly of mandibular body bone and three cartilages. The mandibular body bone is formed by intramembranous ossification mode, which is called by other names such as membranous ossification mode, fibrous ossification mode, and direct ossification mode. Human developing mandibular bone has chondrocyte-like cells, shown in histopathological specimens (Figure 1) [46]. In this figure, chondrocites-like cells are observed during the mandibular osteogenetic process. This phenomenon is described as “chondroid-bone” in Orban’s Oral Histology and Embryology [3]. But there is no further description in other histology and embryology text books. This phenomenon is slightly different from direct osteogenesis mode. So we are investigated the physiological characteristics of mandibular bone formation.

Regarding the cartilages, they are displaced by bone tissue through the course of intrachondral ossification, also known as cartilaginous ossification mode, intracartilagenous ossification mode and indirect ossification mode. Regarding this ossification mode, there are some slightly different features from those of joint cartilages in descriptions in the following pivot in many histology and embryology text books.

Third, we examined tissue reactions of the periodontal tissues to the mechanical stress of orthodontic force in the orthodontic treatment courses. This was carried out histopathologically and immunohistochemically using animal experiment design models. In

recent years, the examination of transcriptional factors related with bone remodellings, bone formation and resorption. Therefore, we describe our immunohistochemical examination results of mainly related transcription, regulation and morphogenesis factors in animal experiments. Furthermore, we will describe the immunohistochemical profile change of Heat Shock Proteins (HSPs) in the periodontal tissue due to the mechanical stress from experimental orthodontic treatment in mice.

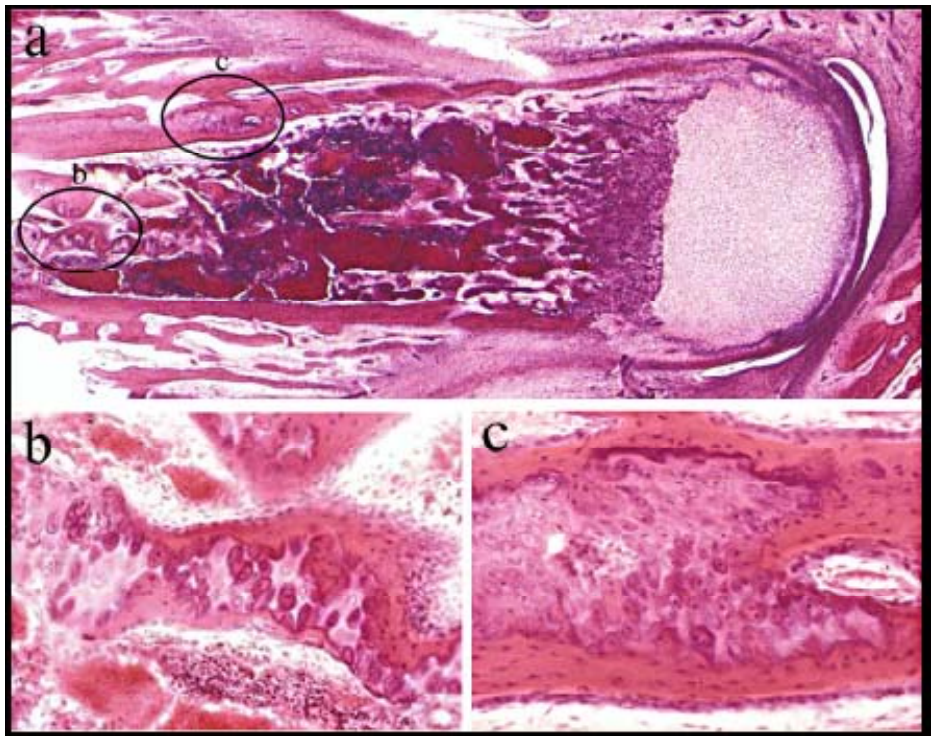

Figure 1. Human developing mandible (a) containing chondrocyte-like cells (b and c: enlarged photos) (HE, from Professor Noriyuki Sahara, Matsumoto Dental University Graduate School of Oral Medicine)

DEVELOPING MANDIBULAR BODY BONE

It is well known that mandibular bone is formed by intramembraneous ossification mode. That is, osteoblasts directly form bone structure in the matrices without cartilaginous formation of structural outline. The mandibular bone formation pattern attracts many researchers because it suggests large possibilities for orthodontic treatment. In the course of morphogenesis of mandibular body bone, chondroid bone occurs (Figure 1). To clarify the nature of chondroid bone, matrix protein production and gene expression were investigated in the anterior ends of developing mandibular bone of mice from the embryonic day 15 (E15) to the 7th neonatal day. Immature bone formation occurred in E15 and chondroid bone was observed histologically in the 2nd neonatal day. Immunohistochemically, bone-forming cells showed positive reaction for type 1 collagen, osteocalcin and type 10 collagen. Type 2 collagen production was detected in E18. Both type 1 and type 2 collagen co-existing in

chondroid bone matrix, as well as bone forming cells, expressed type 1, 2 and 10 collagen and osteocalcin mRNA signals from E15 to the 7th neonatal day (Figure 2). These results indicate that some bone forming cells have characteristics of cartilage cells, and that chondroid bone formation intermingles with osteogenesis in the early phase of mandibular formation [24].

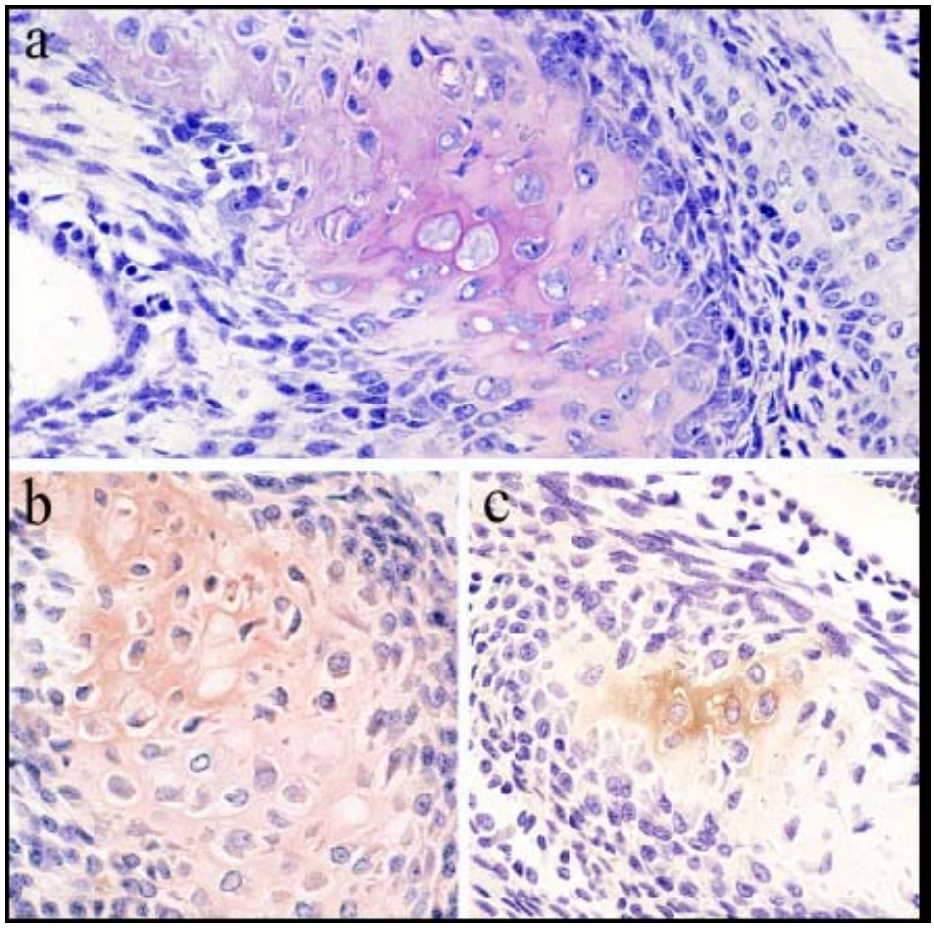

Figure 2. Chondrocye-like cells in developing mouse mandibular body bone showing metachromasia to TB (a), which immunohistochemically react positively to type 2 collagen (b) and type 1 collagen (c).

DEVELOPING MANDIBULAR CARTILAGES

Mandibular cartilages are classified as secondary, including condylar, coronoid and angular cartilages. They differ from primary cartilage in morphological and immunohistochemical organization. Especially, our examination results suggest that mandibular condylar and angular cartilages has bone characteristics which are more significant than cartilaginous characteristics. Furthermore, mandibular condylar cartilage is recognized as an important growth site, for orthodontic treatment [16, 20, 46].

At first, we describe the physiological histology of developmental mouse mandibular condylar cartilage. At E14, there were no development features of mandibular condyle,

although there was some osteoblastic cell proliferation and a small amount of mandibular body bone matrices. At the distal upper portion of the developmental mandibular bone, round, oval and/or spindle-shaped mesenchymal cell proliferation and condensation with no metacholomatic reaction to toluidine blue (TB) were seen at E14 (Figure 3). At E15, mandibular condylar cartilage was clearly evident as TB metacholomasia, which was first expressed at a middle zone of proliferating mass. At E16, it can be classified as consisting of 4 different cell layers on the basis of the cellular morphological changes: fibrous, proliferative, maturative and hypertrophic. These proliferating chondrocytes showed a metacholomatic reaction. Furthermore, the volume of condylar cartilage grew both in length and width. In this stage, articulation occured between the mandibular bone and the condylar cartilage. At E17, the mandibular condylar cartilage further grew both in length and width, especially in the hypertrophic layer. At the connection area of the mandibular trabecular bone and the hypertrophic layer of the condylar cartilage, endochondral ossification occurred. Perichondral ossification had also begun within the sheath of condyle; that is, direct bone formation. At E18, endochondral ossification further progressed and the mandibular condyle increased in volume. At just after birth (E19), the condylar cartilage grew further. No metacholomatic reactions were observed in fibrous layers, but weakly positive reactions were seen in proliferative layers. A metacholomasia reaction was clearly detected in both maturative and hypertrophic layers.

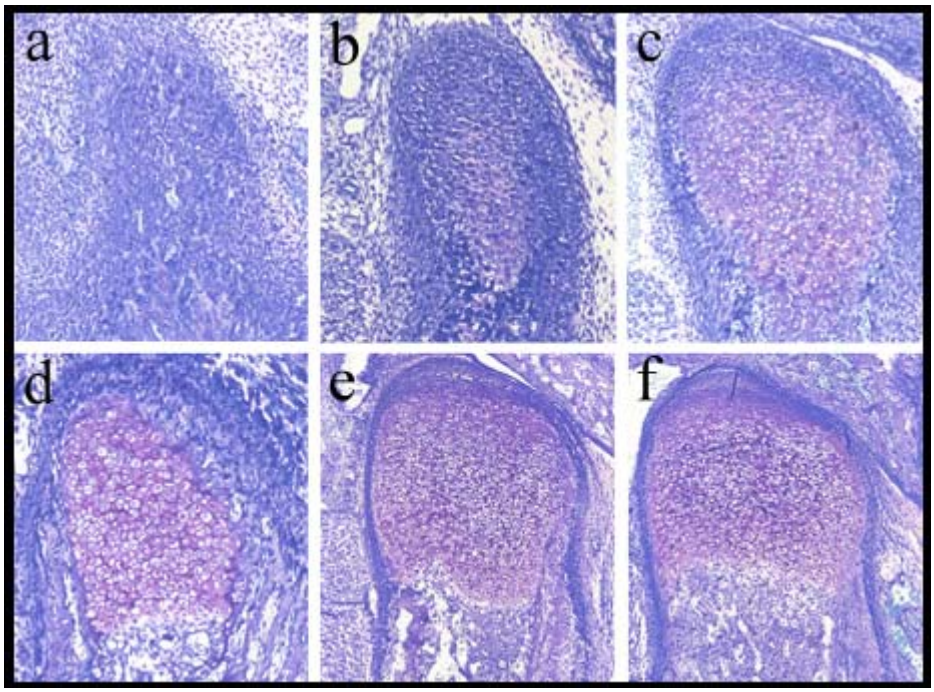

Figure 3. Developing mandibular condylar carilage from E14 (a), E15 (b), E16 (c), E17 (d), E18 (d), and just after birth: E19 (f) in TB stained specimens.

Regarding angular cartilage, histologically, there were no developmental features of mandiblar angle, with some osteoblastic cell proliferation and a little bone matrices with mesencymal cell proliferation, in E14. Mouse mandiblar angle development started as a

coagulation of mesenchymal cells at the end of the developmental mandible in E15, although there was no metachromasia reaction to TB. At E16, cells of the central portion of the cell coagulation showed metachromasia to TB (Figure 4). After that, the mandiblar angular cartilage developed through a similar course of intrachondral ossification with invasion of capillaries. At E17, direct (perichondral) bone formation was observed at the anterior portion. Immunohistochemically, at E16, type 2 collagen positive chondrocytes were detected, although there was no positive reaction at E14 and E15. Furthermore, these proliferating chondrocytes showed positive reactions to type 1 collagen and osteopontin (OPN) through the examination period.

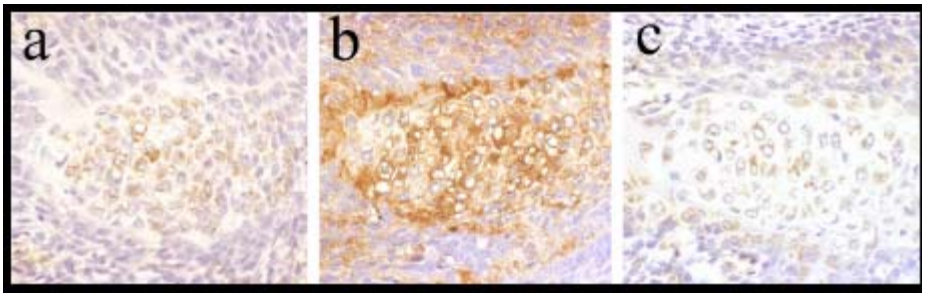

Figure 4. Chondrocyte-like cells react immunohistochemically positive to collagen type 2 (a), type 1 (b), and OPN (c) in developing mouse mandibular angular cartilage of E16.

Among the numerous papers on the mandiblar angular and condylar cartilages, Tengan [57] reported the examination results of developmental aspects of mandiblar condylar and angular cartilages. In a report using C57BL/6N mice, the developmental start of the mandiblar angular cartilage was observed as a coagulation of mesenchymal cell proliferation in the end of the mandibular bone at the 14.5th fetal day. Our examination results of histological findings and TB reactions of ddY mice mandiblar angular cartilage suggest that the development starts nearly the same fetal day. Histologically and histochemically (TB), after the 17th fetal day, endochondral ossification occurred with invasion of capillaries, and perichondral ossification occurred in the periphery of the cartilage mass.

In the immunohistochemical examination, the proliferating chondrocytes of the mandiblar angular cartilage showed positive reactions to type 2 collagen, as well as to type 1 collagen and OPN. In an examination of mandibular chondylar cartilage, Mizoguchi [29] reported the same immunohistochemical aspects, and Ishiwari et al. [19] reported the gene expression using in situ hybridization technique. Therefore, present immunohistochemical results of mandiblar angular cartilage show that the characteristics of proliferating mandibular angular cartilage are nearly the same as mandiblar condylar cartilage, and slightly different from normal physiological articular cartilage.

On the developmental start of the condylar cartilage of the our examination, the findings from TB specimens of the early developmental stage of mandibular condylar cartilage indicated the following. At the distal upper portion of the developmental mandibular bone, mesenchymal cell proliferation and condensation without metacholomasia were seen at E14. At E15, mandibular condylar cartilage was clearly evident as a metacholomatic reaction to TB. This developmental process was mostly in accord with other researchers' data [18, 30, 40, 42]. Such mesemchymal cell changes were demonstrated in the mandibular angular

cartilage, as reported by Tengan et al.[57]. In their report using C57 BL/6N mice, the developmental start of the mandibular angular cartilage was observed as a coagulation of mesenchymal cell proliferation in the end of the mandibular bone fetal day at 14.5. As mentioned above, we [21, 45] reported histological findings and TB reactions of ddY mouse mandibular angular cartilage. These results suggest both angular and condylar cartilage development starts nearly the same fetal day as Tengan reported [57]. These data suggest that chondrocytic differentiation had started from E14, and this area had turned into cartilaginous tissue at E15.

There are some different components of the extracellular matrix between the primary and secondary cartilage [29, 32]. Immunohistochemical studies for the expression pattern of type 1 and 2 collagens [18, 19, 29] revealed that both types of collagen were simultaneously produced in chondrocytes at this area. Moreover, simultaneous expression of type 1 and 2 collagen genes have been confirmed. These findings enable us to accumulate different characteristics and aspects of this cartilage than general endochondral ossification ones. We have reported that immunohistochemical-positive reactions to OPN were detected in almost all layers of the cytoplasms of the condylar chondrocytes [51]. This result is consistent with a number of findings by other researchers. In an examination of mandibular chondylar cartilage, Mizoguchi [29] reported that the proliferating chondrocytes were positive for type 1 collagen, as well as for type 2 collagen and OPN. Ishiwari et al.[19] reported these gene expressions and localization of that type 1 collagen gene expression in the proliferative and maturative layers of the condylar cartilage using in situ hybridization techniques.

Furthermore, on angular cartilage in our previous IHC examination [21, 45], the proliferating chondrocytes of the mandibular angular cartilage showed positive reactions to type 1 collagen and OPN, as well as to type 2 collagen. Therefore, IHC results of mandibular angular cartilage show that the characteristics of proliferating mandibular angular cartilage are nearly the same as mandibular condylar cartilage. Type 2 positive cells and OPN expressions indicated that the bone factor, in addition to the cartilaginous generative factor, have participated in the matrix, since bone characteristics are more significant than cartilaginous characteristics. Our data for angular cartilage indicates that it presumably applies to condylar cartilage examination.

REGULATION FACTORS IN MORPHOGENESIS OF MANDIBULAR CONDYLAR CARTILAGE

Recently, various studies have shown that mandibular condylar cartilage formation is regulated by many morphogenesis factors and their signaling, such as fibroblast growth factor receptor, and platetet-derived growth factor receptor [13, 28]. Therefore we have investigated these factors in the mandibular condylar cartilage [51, 70].

In general, Runx2 is a transcription factor necessarily for osteoblast differentiation [11, 46] and bone formation [26, 31]. Furthermore, it has been reported that Runx2 regulates chondrocyte hypertrophy during chondrogenesis in long bones [55]. Runx2 is responsible for signaling chondrocyte maturation and endochondral ossification during mandibular condyle advancement [56]. As we have reported previously [21, 46], we have conducted research to prove our presumption that there is a strong association between Runx2 for this generation

pattern, since Runx2 is an essential factor for differentiation to osteoblast [26, 31, 33]. Because matrix protein that characterizes bone, such as type 1 collagen and OPN, has often been expressed, mandibular condylar cartilage has intense bone characteristics.

As a result, at E14, Runx2 expression was detected by means of IHC and ISH examination, which indicates that the Runx2 expression leads to the secondary chondrocytes differentiation, with examination of type 2 collagen by IHC and TB stain. Shibata et al.[39, 41, 43] had reported that Runx2 is essential for the onset of formation of the mandibular condylar cartilage, as well as for the normal development of Meckel's cartilage. Their result supports our above-mentioned result that Runx2 controls the initial differentiation for mandibular condylar condrocyte at the E14 stage in mice. In condylar cartilage as a secondary cartilage, the development onset was regulated by Runx2. Therefore, it was considered that the characteristics of Runx2 regulated condylar secondary cartilage show the co-expression of bone and cartilage matrix proteins, as mentioned in the beginning of this session.

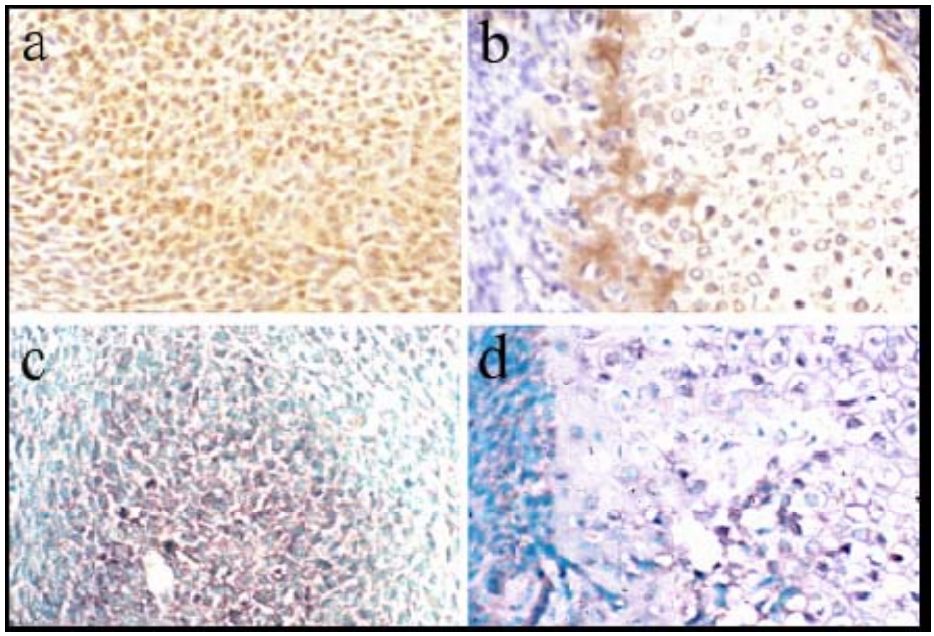

Figure 5. Runx2 immunohistochemical expression is visible in coagulating cells in E14 (a) and the positive reaction is also detected at the sheath of condylar cells in E17 (b) in IHC. Expression of Runx2 mRNA appear in the cytoplasm of proliferating chondrocytes in E14 (c) and the gene signals are throughout most all layers in E18 (d) in ISH.

At E17 and E18, Runx2 expression strongly appeared in hypertrophic cartilage in ISH specimens, which might relate to the differentiation to osteoblasts [5, 28, 52]. This agrees with reports [33, 56] which explains that the Runx2 expression of IHC and ISH had been identified in the hypertrophic layer, and also takes part in the endochondral ossification mode. Shibata [41] has reported that Runx2 deficient mice lack mandibular condylar cartilage and mandibular bone. The results of the present examination clearly show the distribution of Runx2 expression for ISH and IHC at the cartilage inside of the sheath of mandibular condyle where direct bone formation occurs. Runx2 expression is evidence for Runx2 control over perichondral ossification. Runx2 expression at E14/E15 and E17/E18 results in cartilaginous

differentiation and osseous displacement in the condyle, respectively. Finally, Runx2 gene is continuously expressed at almost the same level in ISH specimens throughout the examination period of condylar cartilage. However, in IHC specimens at E14/E15 and E17/E18, Runx2 peptide is observed at high levels in specific parts and their localization is uniform. Further study is required to explain this phenomenon, and reveal the difference between the peptide and gene level.

Thus, the purpose of this study was to investigate the participation of Runx2 in mandibular condylar cartilage. There were no development features of mandibular condyle (E14). At the distal upper portion of developmental mandibular bone, mesenchymal cell proliferation and condensation with no metacholomasia reaction to TB were seen at E14. At E15, mandibular condylar cartilage was clearly evident as a metachlomasia to TB. In IHC specimens at E14, expression of Runx2 peptide was observed in the nuclei and the cytoplasm of coagulating mesenchymal cells. After E17, Runx2 factors appeared in the cells of the condylar cartilage sheath, and they were also distinct in the cytoplasm and nucleus. In ISH specimens at E14 and E15, expressions of Runx2 mRNA appeared in the cytoplasm of proliferating chondrocytes. From E16 up to E18, the mRNA was detected throughout almost all cytoplasm in all layers. These IHC and ISH results suggest that Runx2 plays an essential role for mandibular condylar cartilage development, especially that Runx2 is essential for the onset of the secondary cartilage differentiation.

Generally, Notch1 and Math1 are important regulation factors of morphogenesis [9, 10, 51, 68]. There are no reports on mandibular condylar cartilage, although there is a report on their distribution of articular cartilage [12].

Next, we describe the results of Jagged-Notch signaling in the mandibular condylar cartilage. As we have reported, these expression patterns were different from each other in the articular cartilage, and the Notch1 reactions only localized in the hypertrophic cells. Math1 was distributed mainly in the hypertrophic layer and partially in the proliferative layer. These results suggest that regulation factors of morphogenesis --Notch1 and Math1-- may play some essential role in mandibular condylar cartilage [51]. The inconstant distribution of both factors presumed that the generation of the condylar cartilage does not correspond with morphogenesis mechanism in articular cartilage. It is strongly suggested that mandibular condylar and angular cartilages differ slightly different from physiological articular cartilage.

Concerning our recent paper on mouse mandibular bone formation [51], the Notch1 reactions were localized only in the hypertrophic cells, and these expression patterns were different from each other in the articular cartilage. Math1 is also a regulation factor of morphogenesis [68], and it was distributed mainly in the hypertrophic layer and partially in the proliferative layer [51]. Moreover, Hayes et al. have reported that NICD expression becomes restricted to deeper layers of articular cartilage after birth in the mouse [14]. As a result, the inconstant distribution of Notch1 factors suggests that the generation of the condylar cartilage does not correspond with morphogene mechanism in articular cartilage. It is strongly suggested that mandibular condylar and articular cartilage differ slightly from physiological articular cartilage. In this examination, we investigated only mandibular condyle cartilage for a short period. In the future, we hope to investigate further for longer periods after birth.

In general, Notch signaling is necessary for cell fate determination, cell proliferation and differentiation. Therefore, we focused on Notch signaling in the developing mouse mandibular condylar cartilage. The examination results are summarized as follows. At E14, in

the mandibular condylar cartilage forming area, expression of Notch1 intracelllar domain (NICD) was observed in the nuclei of coagulating mesenchymal cells. After E15, NICD appeared in the nuclei and the cytoplasms of cells. In ISH examination at E14, expressions of Notch1 mRNA appeared in cytoplasm of proliferating chondrocites. From E15 to E19, Notch1 mRNA was detected throughout almost all cytoplasm in all layers.

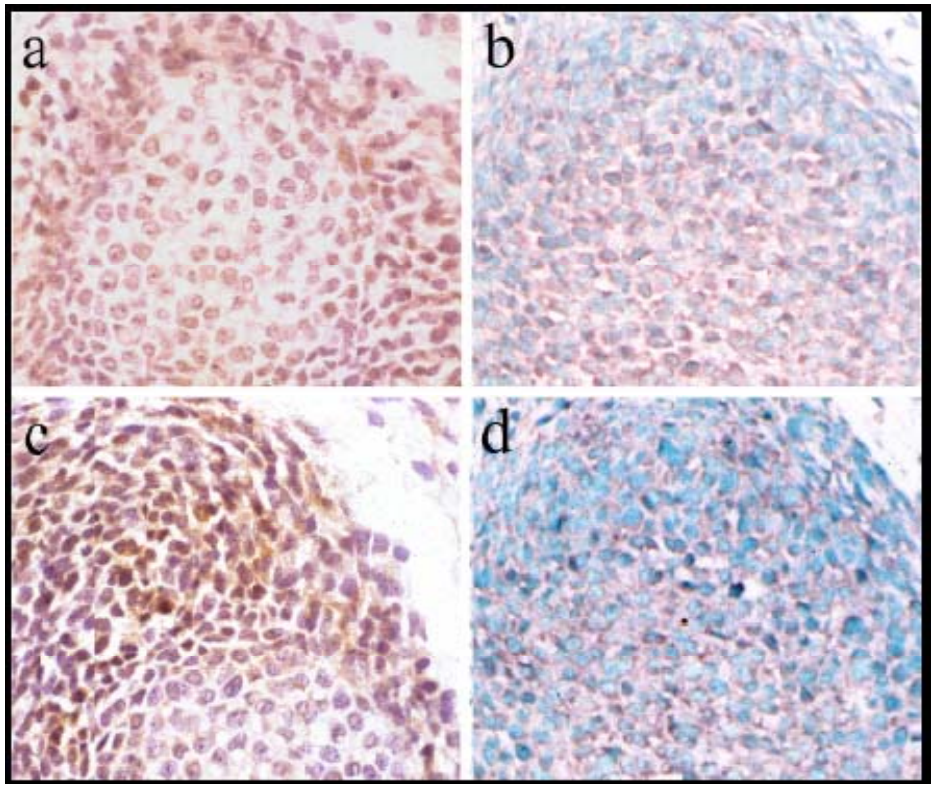

Figure 6. Proliferating cells have NICD positive products in E15 by IHC (a) and the mRNA are detected by ISH (b). Jagged, the ligand of Notch, is also detected in E15 (c) and Jagged genes are also expressed in cytoplasms of the cells in E15 (d).

Next lokking at Jagged, the ligand of Notch, at E15 we see that the proliferating cells had positive products of Jagged in their cytoplasms and cell membrane of almost all coagulating cells. At E16, Jagged positive reactions were detected in cells of the proliferative, maturative and hypertrophic layers, and weakly labeled in cells of the fibrous layer. Furthermore, cytoplasmic and membranous reactions were observed in the cells just inside of the condylar cartilage sheath. At E17, cytoplasmic and membranous reactions of Jagged appeared strongly in the cells just inside the condylar cartilage sheath. At E18, Jagged immunohistochemical-positive products were observed in almost all cells of the layers, and they were mostly distinct in the sheath of the condyle. At just after birth (E19), Jagged peptide was observed in a portion of almost all layer cells in their cytoplasm and membrane. Through the examination period, the pattern of distribution and intensity of expression of Jagged peptides were not uniform. By ISH, At E14, expressions of Jagged mRNA appeared in cytoplasms of proliferating chondrocytes. Their distribution intensity was not uniform. At E15, cytoplasmic and membranous reactions of Jagged gene appeared in the cells of chondrocytes. After E16

and up to just after birth (E19), cytoplasmic positivities for Jagged mRNA were detected throughout almost all condylar cells. However, positive signals for Jagged mRNA were reduced at the rim of condyle. Their distribution pattern was not uniform.

Disruption of Notch ligands and receptors, as well as downstream signaling components of the Notch pathway, have been implicated in many developmental defects and pathological conditions [69]. Notch functions in all progenitor cells give rise to the limb bone, cartilage, muscles and progenitor [1]. It has also been reported that Notch1 is not required to form the limb skeleton, musculature, or vasculature [12]. Furthermore, the Notch family is a highly-conserved family of cell surface signaling molecules [60]. In the developmental stage, Notch1 takes part in the representative three major phenomena, namely lateral inhibition, induction and asymmetric cell division [7, 38]. Notch signaling has been implicated in bone development and it is expressed in osteoblasts [10, 60]. With reference to cartilage, the Delta-Notch signaling pathway has been reported to be important in regulating the progression of prehypertrophic chondrocytes to hypertrophic chondrocytes in examinations using chicks [9]. Furthermore, Hayes et al.[14] described that Notch signalling is closely related to the formation of articular cartilage and allows for co-oriented ossification in the growth plate in mice experiments.

In this examination, expression of NICD at the cell membrane might relate to cell-to-cell intercommunication from E15 up to just after birth. NICD translocates from the cell membrane to the nucleus, which act as a transcriptional activator and regulating gene expression through the examination period. At E14, Notch1 expression was detected by means of IHC and ISH examination, which indicates that Notch1 expression leads to mesenchymal cells further differentiating into chondrocytes as a secondary cartilage. We have previously reported that Runx2 is essential for the onset of mandibular condylar cartilage development, with examination of type 2 collagen by IHC and TB stain [47]. We expected NICD also to be essential for the onset of mandibular condylar cartilage development. At E17 and E18, NICD expression appeared in hypertrophic cartilage in IHC specimens. This agrees with our past research which explained that the Runx2 expression of IHC and ISH is present in the hypertrophic layer and also takes part in the endochondral ossification mode [47]. Yasui et al. have reported three modes of ossification during distraction osteogenesis in the rabbits [64, 65], and have been suggested that some hypertrophic chondrocytes undergo further differentiation into osteoblast-like cells and participate in initial bone formation. The results of the present study support that hypertrophic chondrocytes further differentiate into osteoblasts. At E17 and E18, our examination results showed the distribution of NICD expression for IHC at the cartilage inside of the sheath of mandibular condylar cartilage development, where direct bone formation occurs. NICD expression might relate to perichondral ossification in which mesemchymal cells differentiate into osteoblasts. On the other hand, the Notch1 gene was expressed at weak levels in the cartilage cytoplasm inside the sheath of mandibular condylar cartilage. Finally, Notch1 gene was continuously expressed in the cartilage cytoplasm in ISH specimens throughout the examination period. Notch1 was detected by means of IHC and ISH examination, which indicates that the Notch1 expression leads to secondary chondrocyte differentiation, especially in morphogenesis during embryonic stage. Furthermore, Notch1 distribution intensity is not uniform; thus, it is suggested that there is some reason for the role at mandible condylar cartilage development. The examination of the expression of these factors in developing mandibular condylar cartilage in embryonic mice is now progressing.

Our present result demonstrated that NICD and Jagged were both detected by IHC, and their distribution patterns were very similar. This phenomenon means Notch signaling is activated by Jagged [48, 49, 50]. Furthermore, Hayes et al.[14] have reported that Jagged peptides were absent from developing articular cartilage but were present in deeper layers from after one month. Therefore, the expression patterns of mandibular condylar cartilage and articular cartilage were different. It is strongly suggested that mandibular condylar and articular cartilages differ slightly from physiological articular cartilage.

PERIODONTAL TISSUE REACTIONS IN ORTHODONTIC TREATMENT

To establish a biological base of periodontal tissues, such as alveolar bone tissue, periodontal ligament fibroblasts, osteoblasts, cementoblasts and osteoclasts, for orthodontic treatment, research using animal experiment models has been performed in the last several decades [61]. Reitan [34, 35] examined the tissue reactions during orthodontic tooth movement. The author pointed out the histopathological findings of bone formation and/or resorption of alveolar bone of both tension and expression sides in these experiments. However, recently periodontal fibroblast cell lines are also being used in this kind of research. Regarding with tissue reaction occurring in orthodontic treatment, osteoblasts at the surface of the tension side and osteoclasts at the pressure side of the relevant periodontal space of the alveolar bone appear, and they play some roles in resorption and addition of bone; these are well-known facts. Takano-Yamamoto et al.[54] and Cho [8] examined the histological, immunohistochemical and in situ hybridization findings of both tension and pressure sides of the periodontal tissues during the orthodontic tooth movement in an animal model.

Recently research related to periodontal fibroblasts has advanced, and the cells have now been shown to possess characteristic features other than what fibroblasts are generally known to have. Saito et al.[36] showed expression of Runx2 in a fibroblast cell line. However, calcification does not occur in periodontium even though Runx2 expression is detected in periodontal fibroblasts. This result suggests that a mechanism, which inhibits action of Runx2, exists. In fact, Yoshizawa et al.[66] recently reported that homeobox factor Msx2 suppressed differentiation of osteoblasts by inactivating Runx2 transcription. In the paper of Yoshizawa et al., the following is described [66]. Ligaments are comprised of tough yet flexible connective soft tissue. Little is known, however, about the precise characteristics of the periodontal fibroblasts due to the absence of specific markers and cell lines. Therefore, they established a periodontal ligament cell line, PDL-L2, with suppressed Runx2 transcriptional activity and an inability to form calcified nodules. They used the cell lines and demonstrated that endogenous Msx2 provents ligament fibroblasts from undergoing osteoblastic differentiation by repressing Runx2 activity.

Thus, we examined the periodontal tissue reaction of mice due to mechanical stress according to the Waldo method [61], before examination of the transcription factor profile change [62]. In the examination group, the arrangement of the periodontal ligament was irregular on specimen day 1. The extension and compression sites were observed at the opposite side of the roots. In day 1 and 3 specimens, the osteoclasts appeared in the compression sites. In day 7 specimens, the number of osteoclasts was reduced to fewer than that of day 3.

Figure 7. Diagram and histopathological photograph of design of experimental orthodontic tooth movement using mice.

Immunohistochemical examination revealed that the expression patterns of Runx2 and Msx2 were clearly dynamically changed compared to the control specimens. These results suggest that the appearance of transcription factors related to cell differentiation of periodontal ligament, which was due to the mechanical stress of insertion of elastic separator, happened within 24 hours. Next, we applied mechanical stress to periodontal tissue of the mouse and examined protein expressions of Runx2 and Msx2 by immunohistochemistry in a time period up to 24 hours [59].

In control specimens, when distal buccal root of the upper first molar was horizontally examined, the alveolar bone socket was in an oval shape with a long diameter of 320μm and a short diameter of 250μm, though a small variation of size between the samples existed (Figure 8). Although localization of the root in the alveolar bone socket showed a slight deviation to the mesial direction, the root with periodontal tissue was mainly localized in the center with a diameter of 50μm. Periodontium was basically arranged between the alveolar bone and cemental surface of the root with radiated as well as bundle-shaped fibers. However, in some parts, direction of the arrangement was slightly different in the mesial side. In these parts, fibroblasts between the roots localized in a transverse direction possibly to be able to keep continuity with the roots after branching. On the other hand in the distal side of the root, vertical or oblique images were observed. Capillaries between bundles of the periodontium were seen. The fibroblasts, with a long elliptical nucleus within spindle shaped cytoplasm, were detected in the periodontium through the running direction of the periodontium. On the other hand, cementoblasts were localized at the cemental surface as one layer with an elliptical nucleus and scanty cytoplasm. Osteoblasts with a nucleus in an oval shape and scanty cytoplasm showed slight flatness, andthey were arranged on the surface of the alveolar bone. In addition, remodeling lines representing resorption and addition of the bone were seen. In some parts of the alveolar bone, a resorption-like structure with osteoclasts was observed. Osteoclasts were also detected in the cemental surface.

Regarding the findings of the experimental group, differences from the control group will be emphasized. With the 20-minute group, the root clearly moved about 20μm in the mesial direction representing the pressure side. The root was enlarged about 70μm on the distal side (Figure 8). Thus at the tension side, the radiated arrangement of the periodontium became clear, and the periodontal fibroblasts showed an appearance of spindle shape cytoplasm and long oval or flat-like nucleus. On the other hand, disorder in arrangement of the periodontal fibroblasts was recognized on the pressure side.

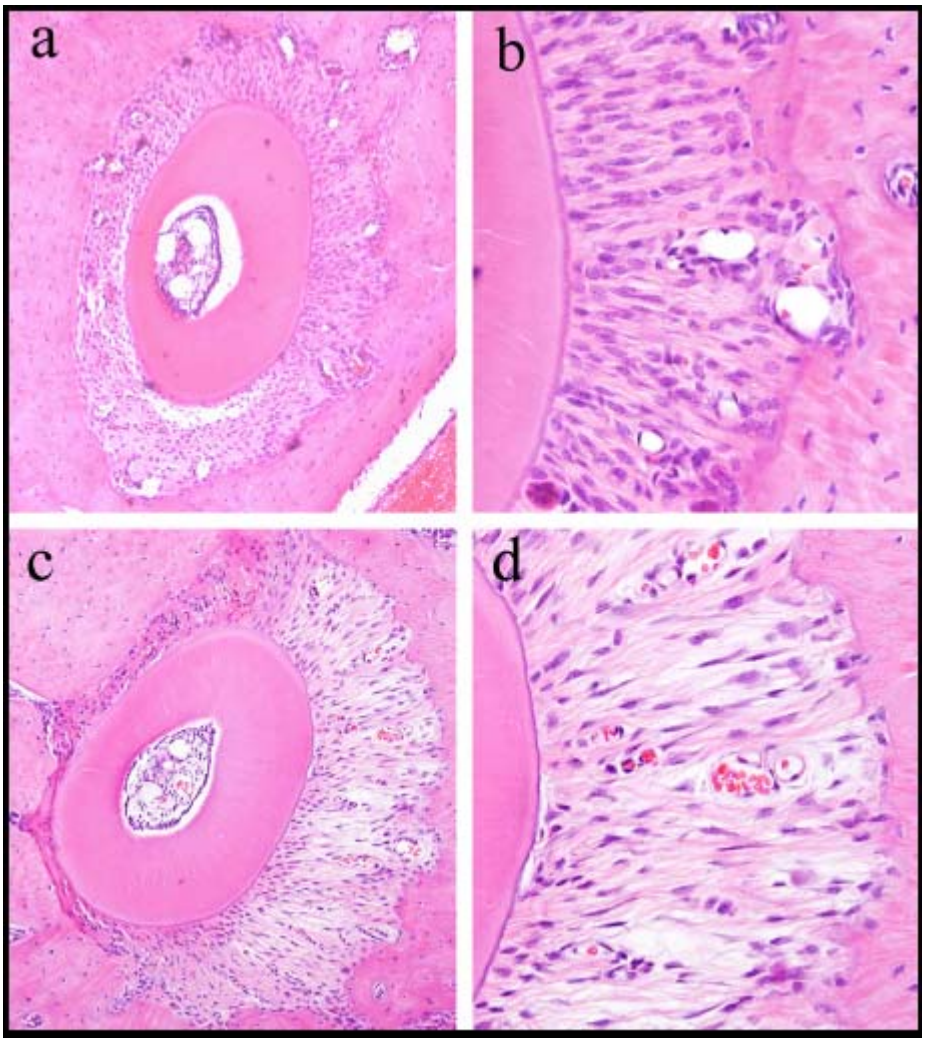

Figure 8. Histopathological features of control specimens (a, b) and experimental 1-hour specimens (c, d).

In the 1-hour group, the relative location of the root in the alveolar bone further moved mesially, and the width of the periodontium of the same part was narrow with a diameter of about 10 μm. On the other hand the periodontal space of the opposite distal tension side enlarged to a width of 90 μm. The periodontium of the same part was considerably stretched and the interfibrillar area became loose. Cytoplasm and nucleus of the periodontal fibroblasts were in a long spindle shape. At the pressure side, various degenerative changes in the cells, which formed the periodontium, were recognized. Many osteoblasts and cementoblasts distributed at the alveolar bone surface were confirmed as elliptical shape cells.

In the 3-hour group, the width of the periodontium at the distal tension side enlarged to a size of 100 μm, resulting in relative mobility of the root and stretching of the periodontal fibers with the formation of interfiber space. The root on the pressure side approached further toward the alveolar bone. On the tension side, cytoplasms of the periodontal fibroblasts were

in long spindle shape and their nuclei showed a shape from long oval to long spindle. Many osteoblasts on the alveolar bone surface with a shape of oval or cylinder were observed.

In the 9-hour group, the periodontal space on the distal tension side was about 100 μm due to relative movement of the root in the alveolar bone. On the mesial pressure side, the root extremely approached the alveolar bone, resulting in degeneration and atrophy of the tissue. Thus the cells were almost not recognizedon this side. On the tension side, the space of the periodontium decreased. Cytoplasms of the periodontal fibroblasts were in a short spindle shape and their nuclei were in a long elliptical shape. On the other hand, cementoblasts on the root surface were also in an elliptical or a cylindrical shape. Osteoblasts coming in contact with the alveolar bone revealed an elliptical or cylindrical shape, and an increase in their number was recognized.

In the 24-hour group, the periodontal tissue on the pressure side approached further toward the alveolar bone and the cell components were almost not recognized. On the other hand, on the tension side, the cytoplasms of the periodontal fibroblasts were in a spindle shape, and their nuclei were in a slight thick elliptical shape. Osteoblasts on the alveolar bone surface were mostly in a cylindrical or short elliptical shape. A similar appearance was also detected in the cementoblasts.

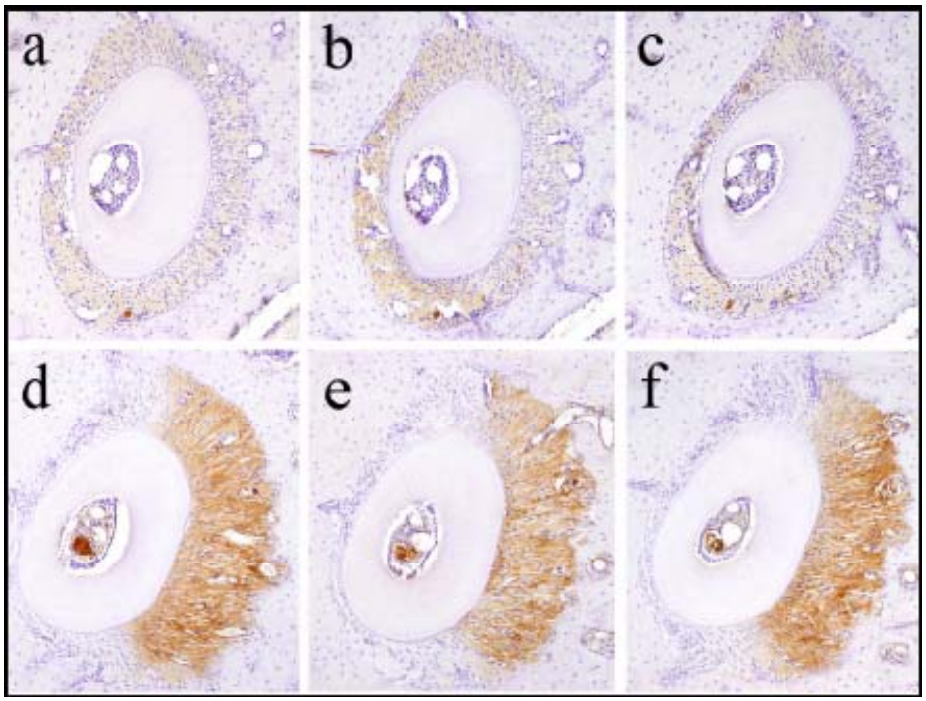

Figure 9. Immunohistochemical findings of control specimens, Runx2 (a), Msx2 (b) and ALP (c), and experimental 1-hour specimens (d: Runx2, e: Msx2 and f: ALP).

Immunohistochemically, in the control group, weak expression of Runx2 peptide was observed at the periodontium of the distal buccal side of the first molar root during all mechanical stress time intervals. This expression was slightly stronger on the mesial side. When observed in detail, this expression was mainly attributed to cytoplasm of the fibroblasts (Figure 9). Msx2 expression was also similar to the expression pattern of Runx2. However,

Msx2 expression was stronger on the mesial side when compared to Runx2 expression. Again weak expression of ALP was also detected at all mechanical stimulus times similar to Runx2 expression.

In the experimental group (Figure 9), regarding with Runx2 expression, strong reaction in cytoplasms of the periodontal fibroblasts at the tension side was detected. On the other hand, on the pressure side, slightly weak staining as compared to the control group was observed. Although positive staining of ALP expression similar to Runx2 pattern was observed on the tension side, density was stronger when compared to Runx2 expression.

In the 1-hour group, strongly stretched cytoplasms of the periodontal fibroblasts and the cementoblasts showed Runx2 protein, and this expression was stronger compared to the 20-minute group. Also, Runx2 expression almost disappeared at all areas of the pressure side. Expression and distribution of Msx2 protein were identical to Runx2 protein expression. The ALP expression state was similar to Runx2 expression pattern. However, ALP expression was much strongeon the tension side of the periodontal fibroblasts compared to Runx2 expression.

In the 3-hour group, Runx2 demonstrated positive expression in cytoplasms of the pretty stretched and enlarged periodontal fibroblasts and cementoblasts. The positive staining area extended to the pressure side compared with 1-hour group. This expression state was also detected in cytoplasms of the osteoblasts. Positive Msx2 expression at the periodontal fibroblasts and cementoblasts was slightly weaker than Runx2 expression. ALP expression findings were also similar to Msx2 expression.

In the 9-hour group, Runx2 revealed a positive reaction in cytoplasm of the strongly stretched periodontal fibroblasts, cementoblasts and osteoblasts. This immunoreaction further extended to the pressure side as compared with the 3-hour group. At this period, Msx2 expression result was similar to Runx2 expression. ALP expression was also confirmed to be similar with Runx2 expression findings.

In the 24-hour group, Runx2 revealed a strong positive reaction in all areas of the root periodontal fibroblasts, cementoblasts and osteoblasts except the areas of the root closely attached to the alveolar bone on the pressure side. The reaction was strongest during this period. The Msx2 result was also similar to the Runx2 findings. Furthermore, ALP findings were also similar to the staining of the others. However, strong expression of ALP was also shown in the osteoclasts located on the alveolar bone surface.

To understand the biological mechanism in orthodontic treatment, research using animal experiments has been performed in the last several decades. Thereafter, efforts have focused on all aspects of tissue change upon mechanical stress. Especially research has focused on bone resorption and addition at the tension side after mechanical stimulus by showing existence of osteoclasts and osteoblasts, respectively. Because there has recently been considerable attention to tissue changes in the early period, examination of tissue type shifted from hard to soft, i.e. periodontal tissue. Recently an increasing number of research studies investigating cell differentiation and morphogenesis, which are regulated by mediators such as cytokines and transcription factors, have been conducted. Osteoblasts and osteoclasts have a major role for cell differentiation in orthodontic dental treatment, and much research using these cells has also been performed [5, 28, 52]. Thus, we planned the current research based on the recent success of Saito et al.[36] and Yoshizawa et al.[66] as mentioned in the introduction section.

Before discussing the results of the present findings,our experimental system will be verified. Based on the method established by Waldo [61], a rubber dam sheet was placed between mouse molars, and degeneration of the periodontal tissue was observed. Insertion of a rubber dam sheet between the mouse molars provides easy and simple application of the method. Thus, mastering this technique will allow examination of the many animals to be performed in a short time. However, one shortcoming of this technique is the possibility that the tooth can move over time and the power enforced to rubber dam sheet cannot be fixed. Another method described by Andrade et al.[37] used a coil string between the anterior teeth and first molars for mechanical stress. Although a fixed power can be applied using this method, its application is extremely difficult and it is impossible to use many experimental animals in a short time. This time we examined expression and distribution of the factors related with bone formation in the periodontium by immunohistochemistry. To increase reliability of the current examination, the use of many samples was needed. Therefore, we used the Waldo method [61] in this examination. Regarding experiment time, we limited the time up to 24 hours based on our recent report, confirming the changes of Runx2 and Msx2 proteins within 24 hours in mechanically-stimulated periodontium [62]. Reitan [35] reported that acute cellular remodeling reaction in mechanically-stimulated bone is the start of bone formation within 1-2 days. In the current research, changes of osteoblast differentiation-related factors, such as Runx2 and Msx2 expressions within 24 hours, were considered to reflect this kind of reaction. Kawarizadeh et al.[23] applied mechanical stress to rat molar for 15 minutes and observed increased expression of Runx2 in the relevant periodontal fibroblasts. In our study, we used a long range of time intervals from 20 minutes to 24 hours.

The mesial side of the second molar root was observed in our previous study [62]. However, the root was relatively thin and its rotation occurred due to insertion of the rubber dam sheet, and fixation at the tension as well as pressure sides was not properly done. Due to these reasons, time-dependent observation was quite difficult. To overcome these difficulties, the mesial distal side of the first molar root was observed in the current study. In the results of histopathological observation in the current study, early morphological changes of the periodontal fibroblasts were observed in the 20-minute group. The periodontium showed enlargement on the tension side and constriction at the pressure side, and the periodontal space enlargement was in the highest state in the 3-hour group. The results demonstrated prominent alteration of the periodontal fibroblasts. The nucleus was in a spindle shape, and the cytoplasm was strongly pulled out. Proliferation of the osteoblasts distributed on the tension side surface of the alveolar bone was confirmed in the groups from 3 to 9 hours. On the other hand, the cementoblasts localized at cementum surface did not show a major change. In the 24-hour group, the width of the periodontal space was enlarged to a maximum state. Cells with thick elliptical nuclei and rich cytoplasm increased. Reitan [34] stated that during bone formation of the alveolar bone, precursor cells of the osteoblasts at the periodontium differentiated into osteoblasts and appeared at the surface of the alveolar bone, followed by active bone formation. In the results of our current research, within 24 hours the cells from the periodontium were considered to proliferate and differentiate into osteoblasts.

Several facts about Runx2 and Msx2 are mentioned. Komori [52] clearly showed that Runx2 promoted the differentiation process of osteoblasts at an early stage but oppositely suppressed the differentiation at a later stage. That is, although Runx2 induces differentiation of mesenchymal stem cells into osteoblasts at an early stage, it keeps the osteoblasts in an immature differentiated state by suppressing the process at later stages. Runx2 was mentioned

to inhibit differentiation of osteoblasts into osteocytes. On the other hand, Msx2, a transcription regulatory factor with homeodomain, was identified as a mammalian homolog of the drosophila cell cycle related gene, Msh [4, 43]. Msx was identified to have two variants in humans (Msx1 and Msx 2) and 3 variants in mice (additional Msx3). A high expression of Msx2 was shown in bone and joint. Homeobox gene product is known to activate or inactivate transcription of other genes, and it is considered as one of the genes with an inhibitory function for morphogenesis. Satokata et al.[37] reported that the Msx2 knockout mouse is born alive but that abnormality of multiple ectodermal tissues is seen. Similar to human diseases, incomplete formation of calvaria, abnormal tooth formation and cartilage hypoplasia were detected. Thus Msx2 was considered to play an important role in the early differentiation process including activation as well as inactivation states. Ichida et al.[23] investigated the role of Msx2 in differentiation of pluripotent mesenchymal stem cells of C3H10T1/2 and C2C12 as well as mouse first generation cultured osteoblasts, and showed an ALP increase in C3H10T1/2 and C2C12 cells and promotion of calcification in mouse first generation cultured osteoblasts by Msx2. That result strongly suggests that Msx2 plays a crucial role as a transcription factor for osteoblast differentiation. Cheng et al.[6] similarly showed that Msx2 functioned as an inhibitory factor for lipocyte differentiation and as an acceleration factor for osteoblast differentiation. This result shows that Msx2, in addition to its dedifferentiation induction function, induces osteoblasts in priority depending on change of its amount. Furthermore, Ishii et al.[17] reported that Msx2 and Twist, by cooperating with each other, are involved in the differentiation and proliferation of osteoblasts. Yanagisawa et al.[63] examined expression of transcription factors in osteoblasts by western blotting and confirmed increased expression of Runx2 and Msx2, suggesting that they play important roles in osteoblast differentiation.

As mentioned in the earlier section, regarding with characteristics of the periodontal fibroblasts, Yoshizawa et al.[66] examined mRNAs of the periodontal cells PDL-L2 and the osteoblast cells MC3T3-E1 by microarray method for comparison of gene expressions. Their results showed that Msx2 is expressed in high amount in PDL-L2 cells. When the change of Msx2 expression was examined over time, although Msx2 expression did not display any alteration in PDL-L2 cells, its expression in MC3T3 cells decreased by differentiation of the cells and finally disappeared with formation of evident calcification. When Msx2 in PDL-L2 cells was deleted, the cells showed calcification. Oppositely, when Msx2 was forced to be expressed in MC3T3 cells, calcification was unable to occur, and stimulation with BMP2 results in only a small amount of calcification. Thus, Msx2 is the gene responsible for inhibition of calcification, and calcification ability of the cells can be regulated in vitro by adjusting the expression of Msx2. In another study, Liu et al.[27] suggested that Msx2 suppressed differentiation of osteoblast precursor cells as well as immature osteoblasts, and promoted proliferation of osteocytes. Moreover, Shirakabe et al.[53] reported that Msx2 functioned as an inhibitory factor for Runx2 activity during morphological formation of human cranial bones.

From the results of the current examination, Runx2 showed weak activity in periodontal fibroblasts of the control group at all the time intervals. This result was compatible with the report of Saito et al.[36], which mentioned the low transcriptional activity of Runx2 expression in PDL-L2 cells. In our results, Msx2 revealed also weak expression in the periodontium space during all the experiment time intervals similar to Runx2 expression

pattern. Our data was an in vivo confirmation of the in vitro results of Yoshizawa et al.[66], in which Msx2 expression was reported to block differentiation of osteoblasts.

After application of mechanical stress, Runx2 expression disappeared on the pressure side at 1 hour. However, at the tension side, Runx2 protein expression appeared in the periodontal fibroblasts as early as 20 minutes after mechanical stress, and became stronger in parallel with the time. This result suggests that this process is even faster than its appearance in osteoblasts in alveolar bone at the tension side. Our results support the opinion of Komori [52], who reported that Runx2 promoted differentiation of osteoblasts at an early stage. Also, Msx2 protein reaction similar to Runx2 appeared in the periodontal fibroblasts as early as 20 minutes and became stronger over time. Expression of the osteoblast marker ALP also showed strong expression with parallel to Msx2 expression. Thus, our results suggest that Msx2 activates Runx2 function as similarly reported by Ichida et al.[23] but opposite to results of Yoshizawa et al.[66], which mentioned Msx2 as an inhibitory factor for osteoblast differentiation.

In conclusion, application of mechanical stress on the periodontal fibroblasts resulted in strong expressions of ALP, Runx2 and Msx2 on the tension side over time, which were found to be in low level in the control group. Our results suggest that Runx2 induces differentiation of osteoblasts, and Msx2 functions as a promoting factor for Runx2 activity on the tension side in cells exposed to mechanical stress.

PERIODONTAL TISSUE REACTION TO CELL INJURY STIMULATION

In general, Heat Shock Proteins (HSPs) serve as a molecular chaperone to maintain homeostasis in tissues. Therefore, HSPs are expressed physiologically in response to some kind of mechanical stresses. In orthodontic treatment, they are also expressed in the related periodontal tissues, especially in periodontal ligament. Furthermore, the induction of this stress protein, HSP, has also been observed in the pulp cells after experimental tooth movement in animal experiments by Shigehara et al.[44]. Next, Yoshimatsu et al.[67] reported the expression of HSP in periodontal ligament during orthodontic tooth movement, but the experimental time course was from 2 up to 10 days. The results showed that HSP expression was significantly higher on the tension side 2 days after application of the appliance, whereas no significant change was observed on the pressure side at any given time point. Furthermore, the PCNA labelling indices of PDL cells were increased significantly on the tension side 6 and 10 days after application of the appliance, and on the pressure side 2, 6 and 10 days after application of the appliance. These data suggest that collagen is metabolised predominantly on the tension side, and that PDL cells actively proliferate on both the tension and pressure sides during orthodontic tooth movement.

Thus, we examined the immunohistochemical profile change of the HSP70 in periodontal ligament cells after receiving mechanical stress during orthodontic treatment in the course of up to 24 hours. In histopathologically, in the experimental specimens, the extension and compression portions were observed on the opposite side of the root. In 24h specimens, the compression site of the periodontal ligament of the related tooth root was narrow due to tissue degeneration. Furthermore, specimens showed the presence of some osteoclasts. Expansion of blood vessels was seen in the area of the extension site.

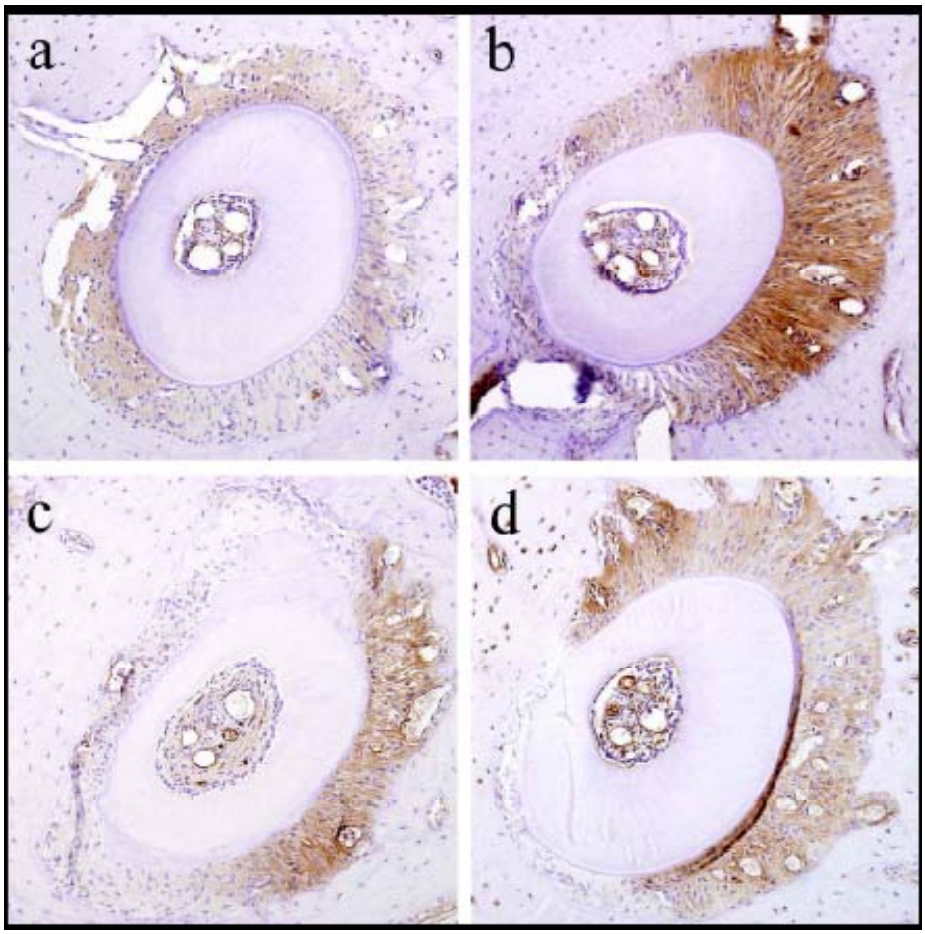

Figure 10. Immunohistochemical features of HSP in control (a), and 1-hour (b), 3-hour (c) and 24-hour (d) experimental specimens.

In experimental specimens, immunostaining of HSP70 was observed in the periodontal fibroblasts, cementoblasts and vascular endothelial cells of the extension site. Through all experimental groups, there were no IHC reactions in osteoblasts of periodontal ligament. In the dental pulp tissue, positive reactions were seen and were stronger than in control specimens. In control specimens, almost all periodontal ligament cells showed a negative reaction, except for a few fibloblasts. In conclusion, we thought that the mechanical stress for orthodontic treatment might cause dynamic histological change within a short time as well as expression of HSP70 in periodontal ligament tissue.

REFERENCES

[1] Akiyama H, Chaboissier MC, Martin JF, Schedl A and de Crombrugghe B (2002) The transcription factor Sox9 has essential roles in successive steps of the chondrocyte differentiation pathway and is required for expression of Sox5 and Sox6. *Genes. Dev.* 16: 2813-2828.

[2] Andrade I Jr, Silva TA, Silva GAB, Teixeira AL and Teixeira MM (2007) The role of tumor necrosis factor receptor type 1 in orthodontic tooth movement. *J. Dent. Res.* 86: 1089-1094.

[3] Baska SN (1980) Orban's Oral Histology and Embryology, 9th ed, 240-260, CV Mosby Co, St Luis.

[4] Bendall AJ and Abate-Shen C (2000) Roles for Msx2 and Dix homeoproteins in vertebrate development. *Gene* 247: 17-31.

[5] Boyle WJ, Simonet WS and Lacey DL (2003) Osteoclast differentiation and activation. *Nature* 423: 337-342.

[6] Cheng SL, Shao JS, Charlton-Kachigian N, Loewy AP, and Towler DA (2003) Msx2 promotes osteogenesis and suppresses adipogenic differentiation of multipotent mesenchymal progenitors. *J. Biol. Chem.* 278: 45969-45977.

[7] Chiba S.(2006) Notch signaling in stem cell systems. *Stem Cell* 24: 2437-2447.

[8] Cho Y (1995) A histologic study of the alveolar bone remodeling on the periosteal side incident to experimental tooth movement. *Jpn. J. Orthodont.* 54: 369-384.

[9] Crowe R, Zikherman J and Niswander L (1999) Delta-1 negatively regulates the transition from prehypertrophic to hypertrophic chondrocytes during cartilage formation. *Development* 126: 987-998.

[10] Deregowski V, Gazzerro E, Priest L, Rydziel S and Canalis E (2006) Notch1 overexpression inhibits osteoblastogenesis by suppressing Wnt/beta-catenin but not bone morphogenetic protein signaling. *J. Biol. Chem.* 281: 6203-6210.

[11] Ducy P, Zhang R, Geoffroy V, Ridall AL and Karsenty G (1997) Osf2/Cbfa1: a transcriptional activator of osteoblast differentiation. *Cell* 89: 747-754.

[12] Francis JC, Radtke F and Logan MP (2005) Notch1 signals through Jagged2 to regulate apoptosis in the apical ectodermal ridge of the developing limb bud. *Dev. Dyn.* 234: 1006-15.

[13] Hamada T, Suda N and Takayuki K (1999) Immunohistochemical localization of fibroblast growth factor receptors in the rat mandibular condylar cartilage and tibial cartilage. *J. Bone Mine.r Metab.* 17: 274-282.

[14] Hayes AJ, Dowthwaite GP, Webster SV and Archer CW (2003) The distribution of Notch receptors and their ligands during articular cartilage development. *J. Anat.* 202: 495-502.

[15] Ichida F, Nishimura R, Hata K, Matsubara T, Ikeda F, Hisada K, Yatani H, Cao X, Komori T, Yamaguchi A and Yoneda T (2004) Reciprocal roles of Msx2 in regulation of osteoblast and adipocyte differentiation. *J. Biol. Chem.* 279: 34015-34022.

[16] Ishii M (1995) An immunohistochemical study on fetal mouse condylar cartilage. *J Tokyo Med. Dent. Univ.* 62: 16-28.

[17] Ishii M, Merrill AE, Chan YS, Gitelman I, Rice DPC, Sucov HM and Maxson RE Jr (2003) Msx2 and Twist cooperatively control the development of the neural crest-derived skeletogenic mesenchyme of the murine skull vault. *Development* 130: 6131-6142.

[18] Ishii M, Suda N, Toshimoto T, Shoichi S and Kuroda T (1998) Immunohistochemical findings type I and type II collagen in prenatal mouse mandibular condylar cartilage compared with the tibial anlage. *Arch. Oral Biol*. 43: 545-55.

[19] Ishiwari Y, Nagatsuka H, Inoue M and Nagai N (1999) Localized expression of type I, II and X collagen genes in the mandibular condyle of immature mice. *Okayama Dent. J.* 723: 688-698.

[20] Kawakami T, Nagatsuka H, Nakano K, Shimizu T, Tsujigiwa H, Hasegawa H and Nagai N (2008) Cell differentiation of neoplastic cells originating in the oral and craniofacial regions. In "Cell Differentiation Research Developments". Ivanova LB ed., Nova Science Publishers, Inc., New York, 1-30.

[21] Kawakami T, Shimizu M and Shimizu T (2005) Immunohistochemical characteristics of developing mandibular angle in fetal mice. *Eur. J. Med. Res*.10: 547-548.

[22] Kawakami T, Shimizu M and Shimizu T (2005) Immnohistochemical Characteristics of developing mandibular angle in fetal mice. *Eur. J. Med. Res.* 10: 547-548.

[23] Kawarizadeh A, Bourauel C, Gotz W and Jager A (2005) Early responses of periodontal ligament cells to mechanical stimulus in vivo. *J. Dent. Res.* 84:902-906.

[24] Kimura A (2003) Matrix protein production and gene expression in bone forming cells on mandibular bone formation of mouse. J. Tokyo Dent. Coll. Soc. 103: 335-345.

[25] Komori T (2005) Regulation of skeletal development by the Runx family of transcription factors. *J. Cell Biochem.* 95: 445-453.

[26] Kuboki T, Kanyama M, Nakanishi T, Akiyama K, Nawachi K, Yatani H, Yamashita K, Takano-Yamamoto T and Takigawa M (2003) Cbfa1/Runx2 gene expression in articular chondrocytes of the mice temporomandibular and knee joints in vivo. *Arch. Oral Biol* .48: 519-525.

[27] Liu YH, Tang Z, Kundu RK, Wu L, Luo W, Zhu D, Sangiorgi F, Snead ML and Maxson RE Jr (1999) Msx2 gene dosage influences the number of proliferative osteogenic cells in growth centers of the developing murine skull: A possible mechanism for MSX2-mediated craniosynostosis in humans. *Dev. Biol*. 205: 260-274.

[28] Nakashima K, Zhou X, Kunkel G, Zhang Z, Deng JM, Behringer RR and de Crombrugghe B (2002) The novel zinc finger-containing transcription factor osterix is required for osteoblast differentiation and bone formation. *Cell* 108: 17-29.

[29] Mizoguchi I (1999) Growth behavior of the mandible condylar cartilage. *Tohoku Univ. Dent. J.* 8: 1-21.

[30] Mizoguchi I, Nakamura M, Takahashi I, Kagayama M and Mitani H (1990) An immunohistochemical study of localization of type I and type II collagens in mandibular condylar cartilage compared with tibial growth plate. *Histochemistry* 93: 593-599.

[31] Papachristou DJ, Pirttiniemi P, Kantomaa T, Papavassiliou AG and Basdra EK (2005) JNK/ERK-AP-1/Runx2 induction "paves the way" to cartilage load-ignited chondroblastic differentiation. *Histochem. Cell Biol.* 124: 215-223.

[32] Rabie ABM and Hagg U (2002) Factors regulating mandibular condylar growth. *Am. J. Orthod. Dentofac. Orthop.* 22: 401-409

[33] Rabie ABM, Tang GH and Hägg U (2004) Cbfa1 couples chondrocytes maturation and endochondral ossification in rat mandibular condylar cartilage. *Arch. Oral Biol.* 49: 109-118.

[34] Reitan K (1953) Tissue changes following experimental tooth movement as related to the time factor. *Dent. Rec.* 73: 559-568.

[35] Reitan K (1960) Tissue behavior during orthodontic tooth movement. *Am. J. Orthodont.* 46: 881-900.

[36] Saito Y, Yoshizawa T, Takizawa F, Ikegami M, Ishibashi O, Okuda K, Hara K, Ishibashi K, Obinata M andKawashima H (2002) A cell line with characteristics of the periodontal ligament fibroblasts is negatively regulated for mineralization and Runx2/Cbfa1/Osf2 activity, part of which can be overcome by bone morphogenetic protein-2. *J. Cell Sci.* 115: 4191-4200.

[37] Satokata I, Ma L, Ohshima H, Bei M, Woo I, Nishizawa K, Maeda T, Takano Y, Uchiyama M, Heaney S, Peters H, Tang Z, Maxson R and Maas R (2000) Msx2 deficiency in mice causes pleiotropic defects in bone growth and ectodermal organ formation. *Nat. Genet.* 24: 391-395.

[38] Sciaudone M, Gazzerro E, Priest L, Anne MD and Canalis E (2003) Notch 1 impairs osteoblastic cell differentiation. *Endocrinology* 144: 5631-5639.

[39] Shibata S, Fukuda K, Suzuki S, Ogawa T and Yamashita Y (2006) An in situ hybridization study of Runx2, Osterix, and Sox9 at the onset of condylar cartilage formation in fetal mouse mandible. *J. Anat.* 208: 169-177.

[40] Shibata S, Suda N, Suzuki S, Fukuoka H and Yamasita Y (2006) An in situ hybridization study of Runx2, Osterix, and Sox9 at the onset of condylar cartilage formation in fetal mouse mandible. *J. Anat.* 208: 169-177.

[41] Shibata S, Suda N, Yoda S, Fukuoka H, Ohyama K, Yamashita Y and Komori T (2004) Runx2-deficient mice lack mandibular condylar carilage. *Anat Embriol* 208: 273-208.

[42] Shibata S, Suzuki S, Tengan T, Ishii M and Kuroda T (1996) A histological study of the developing condylar cartilage of the fetal mouse mandible using coronal sections. *Arch. Oral. Biol.* 41: 47-54.

[43] Shibata S, Suzuki S, Tengan T, Ishii M and Kuroda T (1996) A hitological study of the developing condylar cartlage of the fetal mouse mandible using coronal sections. *Arch. Oral. Biol.* 41: 47-54.

[44] Shigehara S, Matsuzaka K and Inoue T (2006) Morphological changes and expression of HSP70, osteopontin and osteocalcin mRNAs in rat dental pulp cells with orthodontic tooth movement. *Bull. Tokyo Den. Coll.* 478: 117-124.

[45] Shimizu M (2005) Histological and immunohistochemical observations of developing mandibular angle in mice. *J. Hard Tissue Biol.* 14: 346-350.

[46] Shimizu T (2005) Histological characteristics of mandible in fetal mice. *J Hard Tissue Biol.* 14: 67-68.

[47] Shimizu T (2006) Participation of Runx2 in mandibular condylar cartilage development. *Eur. J. Med. Res.* 11: 455-461.

[48] Shimizu T, Nakano K, Tsujigiwa H, Nagatsuka H, Watanabe T, Okafuji N, Kurihara S, Hasegawa H, Nagai N and Kawakami T (2007) Notch signaling in mandibular condylar cartilage development. *Eur. J. Med. Res.* 12: 515-519.

[49] Shimizu T, Okafuji N, Nakano K, Kurihara S and Kawakami T (2008) Jagged1 peptide appearing in mandibular condylar cartilage development. *Eur. J. Med. Res.* 13: 4-6.

[50] Shimizu T, Tsujigiwa H, Nagatsuka H, Nakano K, Okafuji N, Kurihara S, Nagai N and Kawakami T (2008) Gene expression of Jagged 2 in mandibular condylar cartilage development. *Eur. J. Med. Res.* 13: 1-3.

[51] Shimizu T, Tsujigiwa H, Nagatsuka H, Okafuji N, Kurihara S, Nagai N and Kawakami T (2005) Expression of Notch1 and Math1 in mandibular condyle cartilage in neonatal mice. *Angle Orthodont.* 75: 993-995.

[52] Simonet WS, Lacey DL, Dunstan CR, Kelley M, Chang MS, Luthy R, Nguyen HQ, Wooden S, Bennett L, Boone T, Shimamoto G, DeRose M, Elliott R, Colombero A, Tan HL, Trail G, Sullivan J, Davy E, Bucay N, Renshaw-Gegg L, Hughes TM, Hill D, Pattison W, Campbell P, Sander S, Van G, Tarpley J, Derby P, Lee R and Boyle WJ (1997) Osteoprotegerin: A novel secreted protein involved in the regulation of bone density. *Cell* 89: 309-319.

[53] Shirakabe K, Terasawa K, Miyama K, Shibuya H, Nishida E (2001) Regulation of the activity of the trascription factor Runx2 by two homeobox proteins, Msx2 and Dlx5. Gene Cell 6: 851-856.

[54] Takano-Yamamoto T, Takemura T, Kitamura Y and Nomura S (1994) Site-specific expression of mRNAs for osteonectin, osteocalcin, and osteopontin revealed by in situ hybridization in rat periodontal ligament during physiological tooth movement. *J. Histochem. Cytochem.* 42: 885-896.

[55] Takeda S, Bonnamy JP, Owen MJ, Ducy P and Karsenty G (2001) Continuous expression of Cbfa1 in nonhypertrophic chondrocytes uncovers its ability to induce hypertrophic chondrocyte differentiation and partially rescues Cbfa1-deficient mice. *Genes Dev.* 15: 467-481.

[56] Tang GH and Rabie ABM (2005) Runx2 Regulates Endochondral Ossification in Condyle during Mandibular Advancement. *J. Dent. Res.* 84: 166-171.

[57] Tengan T (1990) Histogenesis and three-dimensional observation on condylar cartilage in prenatal mice. *J. Tokyo Med. Dent. Univ.* 57: 32-57.

[58] Visnapuu V, Peltomäki T, Rönning O, Vahlberg T and Helenius H (2002) Distribution of fibrobalast growth factors (FGFR-1 and -3) and platelet-derived growth factor receptors (PDGFR) in rat mandibular condyle during growth. *Orthod. Craniofac. Res.* 5: 147-153.

[59] Watanabe T, Nakano K, Muraoka R, Shimizu T, Okafuji N, Kurihara S, Yamada K and Kawakami T (2008) Role of Msx2 as a promoting factor for Runx2 at the periodontal tension sides elicited by mechanical stress. *Eur. J. Med. Res.* 13: 425-431.

[60] Watanabe N, Tezuka Y, Matsuno K, Miyatani S, Morimura N, Yasuda M, Fujimaki R, Kuroda K, Hiraki Y, Hozumi N and Tezuka K (2003) Suppression of differentiation and proliferation of early chondrogenic cells by Notch. *J. Bone Miner. Metab.* 21: 344-352.

[61] Waldo CM (1953) Method for the study of tissue response to tooth movement. *J. Dent. Res.* 32: 690-691.

[62] Watanabe T, Okafuji N, Nakano K, Shimizu T, Muraoka R, Kurihara S, Yamada K and KawakamiT (2007) Periodontal tissue reaction to mechanical stress in mice. *J. Hard Tissue Biol.* 16: 71-74.

[63] Yanagisawa M, Suzuki N, Mitsui N, Koyama Y, Otsuka K and Shimizu N (2008) Compressive force stimulates the expression of osteogenesis-related transcription factor in ROS 17/2.8 cells. *Arch. Oral Biol*. 53: 214-219.

[64] Yasui N, Ono K, Konomi H and Nagai Y (1984) Transitions in collagen types during endochondral ossification in human growth cartilage. *Clin. Orthop. Relat. Res.* 183: 215-218.

[65] Yasui N, Sato M, Ochi T, Kimura T, Kawahata H, Kitamura Y and Nomura S (1997) Three modes of ossification during distraction osteogenesis in the rat. *J. Bone Joint. Surg. Br* . 79: 824-830.

[66] Yoshizawa T, Takizawa F, Iizawa F, Ishibashi O, Kawashima H, Matsuda A, Endo N and Kawashima H (2004) Homeobox protein Msx2 acts as a molecular defense mechanism for preventing ossification in ligament fibroblasts. *Mol. Cell Biol.* 24: 3460-3472.

[67] Yoshimatsu M, Uehara M and Yoshida N (2008) Expression of heat shock protein 47 in the periodontal ligament during orthodontic tooth movement. *Arch. Oral Biol.*

[68] Zine A and de Ribaupierre F (2002) Notch/Notch ligands and Math1 expression patterns in the organ of Corti of wild-type and Hes1 and Hes5 mutant mice. *Hear Res.* 170: 22-31.

[69] Zine A, Van De Water TR and de Ribaupierre F (2000) Notch signaling regulates the pattern of auditory hair cell differentiation in mammals. *Development* 127: 3373-3383.

[70] Kawakami T and Shimizu T (2009) Role of Notch signaling in mouse mandibular condylat cartilage development. *Acta. Anat. Nipponica* 84(S): 69.

In: Biochemistry and Histocytochemistry… ISBN: 978-1-60876-283-5
Editors: S. Fuchs, M. Auer, pp. 143-151 © 2010 Nova Science Publishers, Inc.

Chapter 7

PATHOLOGICAL RESEARCH ON MOLECULAR-TARGETED THERAPY AND ADVANCED IMMUNOHISTOCHEMICAL APPROACHES

***Yutaka Hatanaka*[*1,2], *Yuki Imaoka*[1], *Kaoru Hashizume*[1], *and Robert Y Osamura*[2]**

[1] Dako Japan Inc., Kakkyoyama 18, Shijo-Nishinotoin-higashiiru, Shimogyo, Kyoto 600-8493, Japan

[2] Department of Pathology, Tokai University School of Medicine, 143 Shimokasuya, Boseidai Isehara Kanagawa, 259-1193, Japan

ABSTRACT

With the development of highly specific antibodies and improvements in detection systems, immunohistochemistry has become a common analytical technique, and detection techniques such as the avidin/biotin- and polymer-based methods are widely used in pathological research and diagnosis. Meanwhile, the development of molecular-targeted agents that make attacks against proteins and their sites via kinase activity has led to increasing demand for a next generation IHC approach. Here, we outline recent methodologies that are useful for advanced IHC analysis in pathological research into therapeutic agents.

INTRODUCTION

Immunohistochemistry (IHC) is an integral part of both diagnostic and research processes. The history of IHC started in 1941 when bacteria were identified using a direct fluorescent method, and then followed the indirect method, the enzyme-based method with

* Correspondence: Yutaka Hatanaka, PhD, Dako Japan Inc., 18 Kakkyoyama, Nishinotoin-higashiiru, Shijo-dori, Shimogyo, Kyoto 600-8493, Japan, Phone: 81-75-211-3675, Fax: 81-75-211-3675, E-mail: yutaka.hatanaka@dako.com.

horseradish peroxidase (HRP) conjugates, the peroxidase anti-peroxidase (PAP) method in the 1970s, methods based on the avidin-biotin reaction in the early 1980s, and the use of dextran polymer technology in the mid-1990s [1-3]. These advances led to more sophisticated and sensitive IHC techniques, and prototypes of the currently used IHC techniques were almost complete by the late 1990s. With respect to diagnostic processes, IHC has become an indispensable tool for pathological testing, and detection techniques such as the avidin/biotin-based and polymer-based methods are performed on automated platforms in many pathology laboratories (Figure 1) [3,4]. On the other hand, for research purposes, there is an increasing demand for advanced IHC approaches because of the recent emergence of new types of molecular-targeted agents, for which understanding of the therapeutic mechanism is important, and antibodies that allow for the visualization of small molecular structures including phosphorylated sites on proteins and hapten conjugates such as fluorescent dyes. In recent years, therefore, several strategies have been developed to help researchers better comprehend tissue information, especially on formalin-fixed paraffin-embedded tissues, which provide a lot of useful information during IHC analysis.

IMMUNOHISTOCHEMICAL ANALYSIS WITH PHOSPHO-SPECIFIC ANTIBODY TO MONITOR PROTEIN PHOSPHORYLATION STATE IN TISSUE

In pathologic research related to molecular-targeted agents, in particular that related to small molecule-type kinase inhibitors such as gefitinib and erlotinib, IHC for phosphorylated proteins is a key technique. Whether the phosphorylation state of a protein is determined by the above-described conventional detection methods depends upon the titer and reactivity (i.e. sensitivity and specificity) of the primary antibody employed and the molecular number of the phosphorylated protein. Higher detection sensitivity is often needed for the determination of phosphorylation state in formalin-fixed, paraffin-embedded tissue. The catalyzed signal amplification (CSA) system, which is based on the peroxidase-mediated deposition of haptenized tyramide and is also known as the tyramide signal amplification (TSA) and the catalyzed reporter deposition (CARD) system, is widely accepted as a highly sensitive detection method for IHC and *in situ* hybridization [5-7], and a ready-to-use type detection kit that employs biotinyl-tyramide and avidin-biotin complex reactions (BT-CSA) is commonly used in pathologic research with archival tissue [7,8]. However, until relatively recently, the practicality of the existing BT-CSA method was limited because of its complex staining procedure with multiple reaction steps and its enhancement by BT, which results in undesirable staining caused by endogenous biotin in the tissue.

Recently, a biotin-free simplified CSA method, employing fluorescyl-tyramide and an anti-fluorescein antibody reaction (FT-CSA), has been developed [9] and allows for quick, reproducible detection (Figure 2). Our data concerning detection sensitivity shows that both CSA methods are 100-fold more sensitive than the conventional methods, while the total detection time required for the FT-CSA is almost the same as that of conventional methods (70-80 minutes) and much shorter than that of the time-consuming BT-CSA method (120 minutes) [9]. Thus, this improved CSA technology is simplified to the level where it can be used in routine testing and large-scale tissue based-clinicopathologic research.

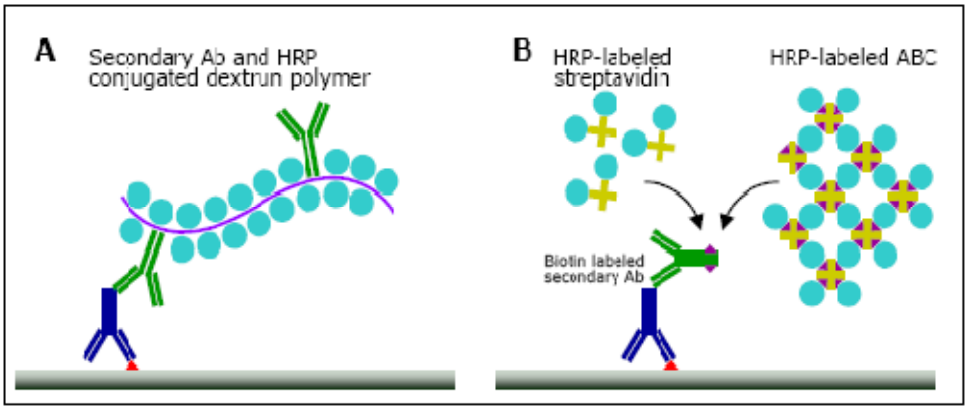

Figure 1. Conventional immunohistochemical detection methods. Horseradish peroxidase (HRP) and alkaline phosphatase are commonly employed as enzymes for visualization with chromogen. A: The polymer -based method in which dextran polymer is commonly used. B: Streptavidin/biotin reaction-based methods including the labeled streptavidin (LSAB) and streptavidin-biotin complex (sABC) methods.

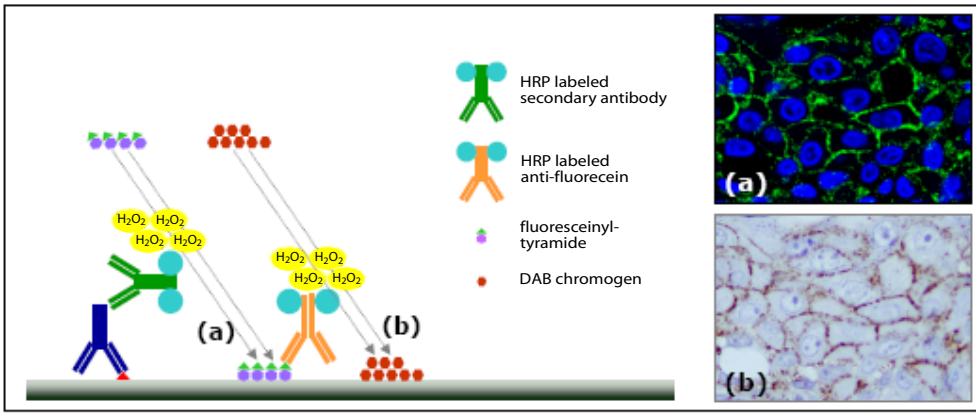

Figure 2. Highly sensitive immunohistochemical detection method. The catalyzed signal amplification system, which employs fluoresceinyl tyramide (FT-CSA), is a representative enhancement technique that is suitable for pathological research with archival tissue sections. The method consists of two steps, an amplification step by first-step peroxidase-labeled antibody and fluoresceinyltyramide (a), and a visualization step by second-step peroxidase-labeled antibody and chromogen (b), in both of which microscopic observation of immunosignals is possible (inset photos; HER4 IHC analysis in A431 epidermoid cell lines).

In our previous study on IHC analysis of phosphorylated EGFR (pEGFR) proteins in archival NSCLC tissues, we found a significant difference in the staining results obtained using the FT-CSA and those obtained via conventional methods. Also, the results from an EGFR mutation assay exhibited a substantially higher correlation with the results from the FT-CSA than with those produced by conventional methods. Thus, it is important to carefully select a suitable detection method. Moreover, when several specific antibodies against different phosphorylated sites of a protein are available, the phosphorylation level of each site can be analyzed with their antibodies as well as by Western blot analysis. Such an approach

provides information on which phosphorylation sites on a protein correlate with clinical outcomes and the histological tissue distribution of activation in each phosphorylation site.

When phosphorylation-specific antibodies are employed for IHC analysis, validating them in a pilot study is a key factor for accurate monitoring of phosphorylated protein in tissue [9,10]. Among the commercially available phosphorylation-specific antibodies, some have insufficient specificity and react with non-phosphorylated target protein or phosphorylated family protein of target other than phosphorylated target proteins. Therefore, it is preferable to confirm the specificity of each antibody using biochemical analysis such as western blotting with a purified phosphorylated target as well as proteins and peptides from the same family. However, it is often difficult to obtain the appropriate standard proteins and peptides for performing method validation. A dephosphorylation assay by phosphatase treatment is an effective way of doing this and at least it can be readily confirmed whether an antibody binds to only phosphorylated tissue or to both phosphorylated and non-phosphorylated targets. In this assay, calf intestinal alkaline phosphatase and lambda phosphatase are commonly used, and are applied to deparaffinized, antigen-retrieved tissue sections when archival materials are subjected to analysis [9,10].

In summary, for monitoring the phosphorylation state of a tissue, highly sensitive detection provides an effective alternative to conventional detection, especially for archival material in which the fixation process is not controlled sufficiently compared with experimental material such as xenografts. The selection and validation of the phosphorylation-specific antibody used are also key processes for obtaining reliable histological information.

IMMUNOHISTOCHEMICAL ANALYSIS WITH THERAPEUTIC ANTIBODY FOR IDENTIFICATION OF A DIRECT TARGET IN TISSUE

Since trastuzumab-based therapy started in the late 1990s, there has been growing interest in pathological research relating to therapeutic antibodies against solid tumors. At present, three types of recombinant human monoclonal antibodies (rh-mAb) are used: i) human–mouse chimeric antibodies as represented by cetuximab, ii) humanized antibody as represented by trastuzumab, and iii) completely human antibody as represented by panitumumab have already been approved as therapeutic antibodies, and quite a number of other candidates are undergoing clinical trials. To understand the biochemical binding properties of these therapeutic rh-mAbs and the intratumoral localization of the target proteins that are bound by these agents in tissue, an IHC approach that uses them as primary antibodies is very useful. Prior to the development of the rh-mAb, IHC analysis with human antibodies such as serum autoantibody had been tried, but there were major technical difficulties in the analytical method. In general, using rh-mAb as the primary antibody makes it impossible to use a conventional detection system because anti-human secondary antibodies bind to endogenous antibodies that are present in human tissues, resulting in undesirable background staining.

To overcome this, two progressive methodologies have recently been established by Bussolati et al. [11] and Glazyrin et al. [12] (Figure 3). One is a method that is based on masking endogenous antibodies using blocking reagent [12].

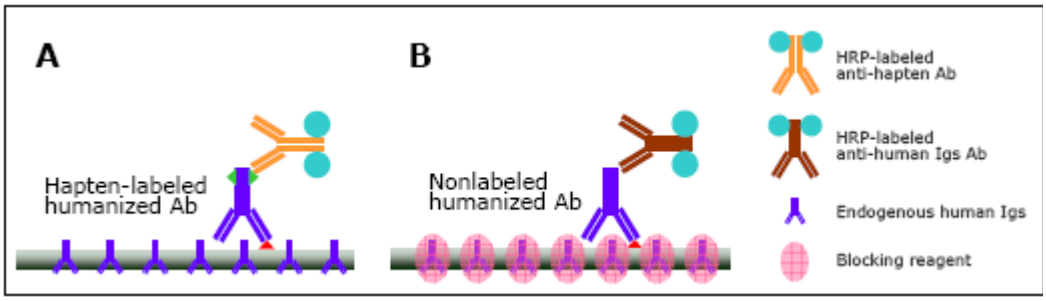

Figure 3. Immunohistochemical detection methods with therapeutic antibodies for analysis of human tissues. Therapeutic antibodies such as human–mouse chimeric antibody, humanized antibody, and completely human antibody are used as the primary antibody in these methods. A: A method with hapten-labeled therapeutic antibody. B: A method with non-labeled therapeutic antibody using a reagent that blocks endogenous human Igs.

This method allows for enhancement of rh-mAb-derived signals using a conventional detection system without any modification. The other is a method that is based on the haptenization of rh-mAb, and biotin is commonly used as the hapten molecule [11,12]. This method allows for complete elimination of the background staining caused by endogenous antibodies in human tissues. In our study, fluorescein-conjugated rh-mAb was employed for IHC analysis (Figure 3). Use of this hapten conjugate has several advantages including removal of the background staining that results from endogenous biotin, direct applicability to flow cytometry and immunofluorescence analyses, and the possibility of further enhancement using the above-mentioned FT-CSA system. These two methods can both be performed on an automated platform.

CHROMOGENIC VISUALIZATION OF DUAL-COLOR FISH SIGNALS WITH ANTI-HAPTEN ANTIBODIES

The fluorescence in situ hybridization (FISH) technique has become a powerful tool for genetic analysis in pathological testing and research. In routine genetic testing with formalin-fixed, paraffin-embedded tissues, FISH is mainly used in the differential diagnosis for lymphoid and soft tissue tumors in which chromosomal abnormalities such as translocation are involved [13]. It is also used to predict the responsiveness to molecular-targeted therapy of solid tumors in which the gene copy number has changed due to amplifications, deletions, or aneusomies [14]. In particular, in HER2 testing to select suitable patients for trastuzumab therapy, FISH is commonly used to determine the status of gene amplification in breast cancer cells as is the IHC method [15,16], because results produced by these two methods correlate well with each other, and both provide clinical benefits. However, because of its limitations, FISH is not as widely available as IHC in spite of its superiority as a quantitative test. In general, FISH analysis is more expensive and time-consuming than IHC analysis and also requires specialized expertise and equipment for fluorescence observation.

Under such circumstances, the chromogenic in situ hybridization (CISH) technique has been attracting attention in recent years. It is a well-known technique and has already been approved for HER2 testing [15,16]. There are two major CISH methods used in HER2

testing, the diaminobenzidine (DAB)-based and silver-based visualization systems, both of which are used in a single-color manner, unlike the dual-color FISH method that is commonly used in pathological testing and research. Recently, a new type dual-color CISH system was developed with an improved chromogen [17]. The CISH system converts the green and red fluorescent signals that are detected by the FITC- and Texas Red-labeled FISH probe mix into long-time stable blue and red chromogenic signals by immunostaining with a mixture of two different anti-hapten antibodies against the fluorescent dyes (Figure 4). This chromogenic visualization can be used to identify gene amplification and deletion and chromosomal translocation. We have introduced a method for analyzing the tissue heterogeneity of gene alterations, for which the FISH method isn't really suitable, and obtained a good staining pattern with both a commercially available probe and an in-house BAC clone probe. We have also succeeded in converting more than 70 FISH stained tissues that had been stored at low temperature (4°C) for three years into CISH stained tissues, which can be stored semi-permanently. With the development of translational research via array-based comparative genomic hybridization, there is a growing need to further analyze the identified cancer-related gene alterations in archival tissues. We believe that the approach outlined above will be accepted as an alternative to FISH analysis in future pathological research.

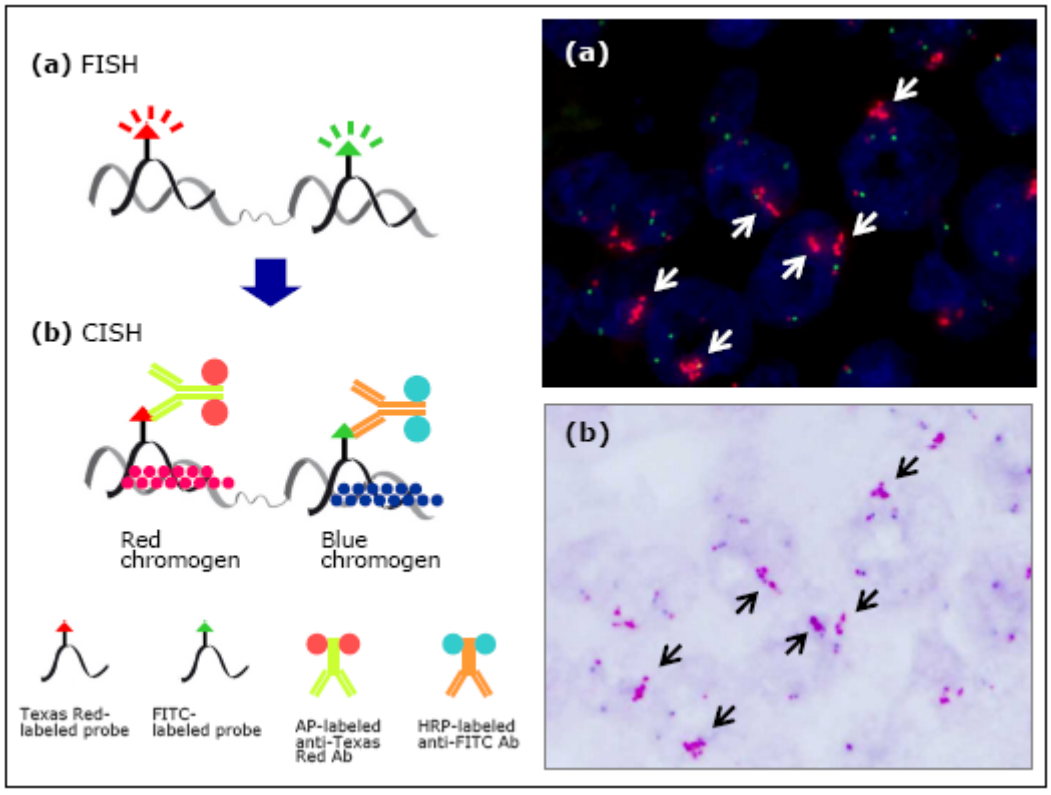

Figure 4. A detection method for chromogenic visualization of dual-color FISH signals with anti-hapten antibody. After FISH-staining with two different fluorochromes such as FITC and Texas Red (a and inset photo a; HER2 FISH analysis in breast carcinoma), archival tissue can be immunohistochemically detected using the corresponding anti-fluorochrome antibodies and two different chromogens (b and inset photo b; HER2 CISH analysis in the same lesion as in the upper photo).

ADVANCED IMMUNOHISTOCHEMICAL TECHNIQUES AND THEIR METHOD VALIDATION

The importance of biomarkers in anti-cancer drug development has been strongly emphasized in several studies [18-20]. To extend our understanding of the molecular basis of cancer, anti-cancer drug development now focuses on targeting the specific molecular alterations present in cancer cells and finding biomarkers for them. The advanced IHC approaches for archival tissues shown in this review are often required in biomarker research. During these processes, method validation is a crucial step that researchers must take when they establish a new IHC method. IHC approaches sometimes fail to demonstrate diagnostic, prognostic, and/or predictive significance. This is not because of an error in the underlying scientific rationale but rather due to poor method validation. Among the key elements involved in validating an IHC approach, the reference tissue material used during the validation phase is one of the most important, and cell line based sections are a powerful tool for verifying the results analyzed. We often employ formalin-fixed, paraffin-embedded tissues prepared from *in vivo* cell line xenograft materials [21] and *in vitro* cell line material cultured three-dimensionally in gel matrix materials [22] (Figure 5) as these materials allow us to verify IHC techniques and to ensure the reliability of the data obtained from them due to their well-characterized cellular information regarding biochemical and molecular alterations.

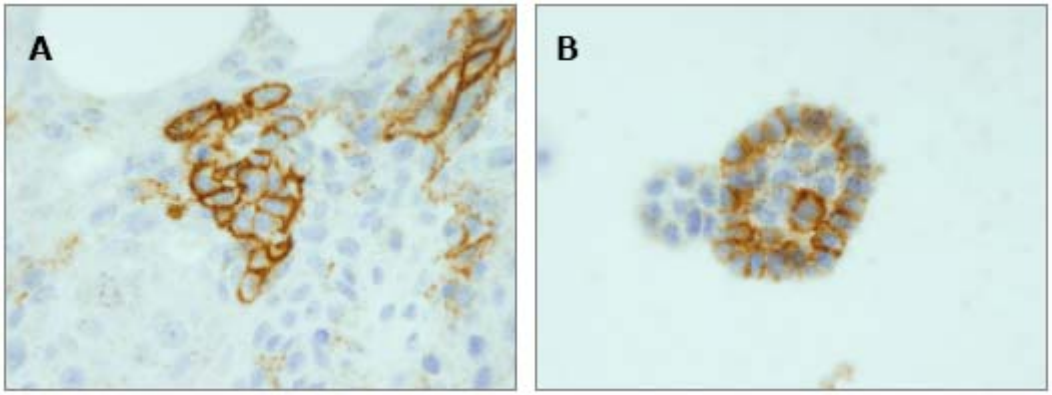

Figure 5. Immunohistochemical staining of phosphorylated EGFR in A431 epidermoid cell lines. Tissues from A431 xenograft bearing SCID mouse (A) and 3D-cultured A431 cells in collagen gel (B) were formalin-fixed, paraffin-embedded, and used for method validation.

CONCLUSION

This commentary has focused on recent methodologies for advanced IHC in pathological research for molecular-therapeutic agents. With cutting-edge innovations including antibody production technologies, there are increasingly powerful tools for research available. Furthermore, while these can be employed for emerging IHC analysis, method validation is also important to ensure the reliability of the data obtained.

REFERENCES

[1] Taylor CR, Shi SR, Barr NJ, et al. Techniques of immunohistochemistry: principles, pitfalls and standardization. In: Dabbs D, ed. Diagnostic Immunohistochemistry. 2nd ed, Philadelphia: Churchill Livingstone; 2006: 1-42.

[2] Key ME. Trends in immunohistochemistry: The integration of tissue-based analysis and molecular profiling*., J. Histotechnol.*, 2002; 25: 243-245.

[3] Sabattini E, Bisgaard K, Ascani S, et al. The EnVision™+ system: a new immunohistochemical method for diagnostics and research. Critical comparison with the APAAP, ChemMateTM, CSA, LABC, and SABC techniques., *J. Clin. Pathol.* 1998; 51: 506–511.

[4] Goldstein NS, Hewitt SM, Taylor CR, et al. Recommendations for improved standardization of immunohistochemistry., Appl Immunohistochem *Mol. Morphol.* 2007; 15: 124–133.

[5] Bobrow MN, Harris TD, Shaughnessy KJ, et al. Catalyzed reporter deposition, a novel method of signal amplification. Application to immunoassays. *J. Immunol. Methods.* 1989; 125: 279–285.

[6] Bobrow MN, Shaughnessy KJ, Litt GJ. Catalyzed reporter deposition, a novel method of signal amplification. II. Application to membrane immunoassays. *J. Immunol. Methods.* 1991; 137: 103–112.

[7] Adams JC. Biotin amplification of biotin and horseradish peroxidase signals in histochemical stains. *J. Histochem. Cytochem.* 1992; 40: 1457–1463.

[8] Hashizume K, Hatanaka Y, Kamihara Y, et al. Automated immunohistochemical staining of formalin-fixed and paraffinembedded tissues using a catalyzed signal amplification method. *Appl. Immunohistochem. Mol. Morphol*. 2001; 9: 54–60.

[9] Hatanaka Y, Imaoka Y, Torisu K, et al. A simplified, sensitive immunohistochemical detection system employing signal amplification based on fluorescyl-tyramide/antifluorescein antibody reaction: its application to pathologic testing and research. *Appl. Immunohistochem. Mol. Morphol.* 2008; 16: 87-93.

[10] Shapiro C, Crosby K, Lewis M et al. Optimization and Validation of Activation-State Specific Antibodies for the Immunohistochemical Analysis of Fresh Frozen Tissues and Cells. Proc Am Assoc Cancer Res. 2006.

[11] Bussolati G, Montemurro F, Righi L, et al. A modified Trastuzumab antibody for the immunohistochemical detection of HER-2 overexpression in breast cancer. *Br. J. Cancer*. 2005; 92: 1261-1267.

[12] [Glazyrin A, Shen X, Blanc V, et al. Direct detection of herceptin/trastuzumab binding on breast tissue sections. *J. Histochem. Cytochem.* 2007; 55: 25-33.

[13] Ventura RA, Martin-Subero JI, Jones M, et al. FISH analysis for the detection of lymphoma-associated chromosomal abnormalities in routine paraffin-embedded tissue. *J. Mol. Diagn.* 2006; 8: 141-151.

[14] Popescu NC, Zimonjic DB. Molecular cytogenetic characterization of cancer cell alterations. *Cancer Genet. Cytogenet*. 1997; 93:10-21.

[15] Wolff AC, Hammond ME, Schwartz JN, et al. American Society of Clinical Oncology/College of American Pathologists guideline recommendations for human

epidermal growth factor receptor 2 testing in breast cancer. *J. Clin. Oncol.* 2007; 25: 118-145.

[16] Laudadio J, Quigley DI, Tubbs R, et al. HER2 testing: a review of detection methodologies and their clinical performance. *Expert Rev. Mol. Diagn.* 2007; 7: 53-64.

[17] Lacroix-Triki M, Mounie E, Charafe-Jauffret E, et al. Double staining chromogenic in situ hybridization is a useful alternative to fluorescent in situ hybridization: first comparative study of HER2 and TOP2A gene amplification in breast cancer. *Proc. San. Antonio Breast Cancer Symp.* 2007.

[18] Kelloff GJ, Bast RC Jr, Coffey DS, et al., Biomarkers, surrogate end points, and the acceleration of drug development for cancer prevention and treatment: an update prologue. *Clin. Cancer Res.* 2004; 10: 3881-3884.

[19] Cummings J, Ward TH, Greystoke A, et al. Biomarker method validation in anticancer drug development. *Br. J. Pharmacol.* 2008; 153: 646-656.

[20] Ludwig JA, Weinstein JN. Biomarkers in cancer staging, prognosis and treatment selection. *Nat. Rev. Cancer.* 2005; 5: 845-56.

[21] Takikita M, Chung JY and Hewitt SM. Tissue microarrays enabling high-throughput molecular pathology. *Curr. Opin. Biotechnol.* 2007; 18: 318-325.

[22] Kobayashi H, Higashiyama M, Minamigawa K, et al. Examination of in vitro chemosensitivity test using collagen gel droplet culture method with colorimetric endpoint quantification. *Jpn. J. Cancer Res.* 2001; 92: 203-210.

In: Biochemistry and Histocytochemistry… ISBN: 978-1-60876-283-5
Editors: S. Fuchs, M. Auer, pp. 153-157 © 2010 Nova Science Publishers, Inc.

Chapter 8

PRE-EMBEDDING SCARCE BIOLOGICAL SPECIMENS FOR LIGHT AND ELECTRON MICROSCOPY

Philippe Taupin [*1,2]
[1] Fighting Blindness Vision Research Institute, Dublin, Ireland
[2] School of Biotechnology, Dublin City University, Ireland

ABSTRACT

Processing biological specimens for light microscopy (LM) and electron microscopy (EM) requires a critical amount of samples. We report a pre-embedding technique for processing scarce biological specimens for LM and EM. The technique is based on immobilizing the samples in bovine serum albumin (BSA) and bis-acrylamide (BA), cross-linked and polymerized. The preparation is compatible with a broad range of histological and electron microscopy protocols and procedures. It presents several advantages over other pre-embedding techniques; it is rapid, simple, and permits efficient and reproducible analysis of scarce biological specimens by LM and EM. The technique may be particularly useful for processing specimens, like biopsies, cystic and amniotic-fluid cells.

INTRODUCTION

Light microscopy and electron microscopy are powerful techniques for studying the structure and ultrastructure of tissues, cells, particles and organisms (Leapman, 2004). New types of software allow three-dimensional re-construction of the structure and ultrastructure of specimens, providing further information on the organization of the biological samples (Radermacher and Ruiz, 2006). Results from these studies are correlated with other investigations, like immunological, biochemical and physiological studies, to unravel the relationship structure-function of the specimens (Mannello et al., 1998; Malatesta et al., 1999).

* Corresponding author: Philippe Taupin. Fighting Blindness Vision Research Institute. School of Biotechnology, Dublin City University. Glasnevin. Dublin 9. Ireland. Tel. (01) 700 - 5284. Email philippe.taupin@dcu.ie.

Processing biological specimens for LM and EM requires a critical amount of material, to go through multiple steps of dehydration, infiltration and embedding, before they can be studied under the microscope (Wang and Minassian, 1987; Mascorro and Bozzola, 2007). For some samples, like biopsies, cystic and amniotic-fluid cells, barely enough material can be obtained to be processed safely, requiring them to be pre-embedded in a solidified matrix, of agarose or gelatin, prior to processing (Malatesta et al., 1998). However, the difficulty in identifying the samples in the solidified gel and the fragility of the gel limit the efficiency and reliability of these techniques. We report a simple and direct pre-embedding technique for processing scarce biological specimens for LM and EM. It is based on pre-embedding the samples in BSA and BA, cross-linked and polymerized with paraformaldehyde (PF), glutaraldehyde (GA) and ammonium persulfate (AP).

PRE-EMBEDDING BIOLOGICAL SPECIMENS IN BSA AND BA

Pre-embedding scarce biological specimens in BSA and BA requires the preparation of two solutions: a pre-embedding mix, and a cross-linking and polymerizing mix. The pre-embedding mix is prepared by mixing, per sample: 6.6 µl of 30% BSA, 5 µl of 40% BA and 1 µl of Temed, corresponding to a volume of 12.6 µl per sample (Table 1). The cross-linking and polymerizing mix is prepared, by mixing: 24 µl of 12.5% PF, 2 µl of 25% GA and 5 µl of 10% AP (Table 1). The pre-embedding, and cross-linking and polymerizing mixes are prepared aside. The cross-linking and polymerizing mix is prepared immediately before use.

Table 1. Pre-embedding biological specimens in BSA and BA

Pre-embedding mix		
Reagents	Stock solution (%)	µl stock solution per sample
BSA BA Temed	30 40 100	6.6 µl 5 µl 1 µl
Cross-linking and polymerizing mix		
Reagents	Stock solution (%)	µl stock solution
PF GA AP	12.5 25 10	24 µl 2 µl 5 µl

Abbreviations: AP, ammonium persulfate; BA, bis-acrylamide; BSA, bovine serum albumin; GA, glutaraldehyde; PF, paraformaldehyde.

The technique reported, for pre-embedding scarce biological specimens in BSA and BA, applies to tissues or cells, prepared as pellet or suspension. Prior to pre-embedding, the biological specimens are fixed in 4% PF for 10 min for processing for LM, or 2.5% GA for 10 min for processing for EM. The biological specimens are prepared in 23.1 µl of phosphate buffer saline (PBS), by immersion for tissues or cell pellets, or resuspension for cell

suspensions. The pre-embedding solution is prepared by adding 6.2 µl of the cross-linking and polymerizing mix, per sample, to the pre-embedding mix. The pre-embedding solution is gently mixed, prior to adding to the samples; 18.8 µl of the pre-embedding solution are added per sample. The pre-embedding solution must be carefully added and mixed into the samples prepared in PBS, not to disrupt it, particularly when handling cell pellets. The final volume for each sample is 41.9 µl. The final concentration of BSA and BA are 4.7 and 4.8 %, respectively. The samples are left at room temperature, for 1 to 1 h 30 min, for cross-linking and polymerization of the pre-embedding solution. The samples are then transferred in PBS, for further processing.

PROCESSING BIOLOGICAL SAMPLES PRE-EMBEDDED IN BSA AND BA FOR LM AND EM

For LM processing, the biological samples, pre-embedded in BSA and BA cross-linked and polymerized, are transferred in sucrose 30%, in phosphate buffer and left at 4°C, overnight. The samples are embedded in OCT-tissue tek or paraffin, for example, and processed for histological protocols and procedures, like sectioning on microtome or cryostat. Sections are stained with histological stains, like cresyl violet, and processed for immuno-histology or -cytology (Taupin, 2008).

For EM processing, the biological samples, pre-embedded in BSA and BA, are cut into 1 x 2 x 2 mm pieces. When processing tissues or cell pellets, the samples, pre-embedded in BSA and BA, are observed under light microscope to visualize, cut out and isolate the pieces of gel containing the biological material. The samples are dehydrated through graded concentrations of ethanol, and embedded in araldite or LR White. Semi-thin and thin sections are prepared using an ultramicrotome. Semi-thin sections are mounted on glass slides and stained with methylene blue, to visualize the samples. Thin sections are mounted on formvar-coated grids. The grids are stained with uranyl acetate, at room temperature for 10 min., followed by lead citrate, at room temperature for 10 min. (Taupin, 2008).

DISCUSSION

We report a simple and direct pre-embedding technique for processing scarce biological specimens for LM and EM. It is based on pre-embedding the samples in BSA and BA, cross-linked and polymerized. The technique is compatible with a broad range of LM and EM protocols and procedures.

Processing scarce biological specimens for LM and EM requires the samples to be pre-embedded in a solidified gel, to be processed safely. We report that a mixture of approximately 5% BSA and 5% BA, cross-linked with PF and GA, and polymerized with AP, produce a gel-like matrix, suitable for pre-embedding tissues and cells, as pellets or a suspension. Biological samples, pre-embedded in BSA and BA, can be processed using a broad range of protocols and procedures for LM and EM. For LM, the samples can be processed for cryostat and paraffin sectioning, and cresyl violet staining. For EM, they can be processed for LR White and araldite embedding, as well as staining with uranyl acetate and

lead citrate. Osmium post-fixation is a usual procedure for staining samples for EM, as it enhances the contrast when viewing under an electron microscope (Mascorro and Bozzola 2007). Osmium post-fixation is not performed when processing scarce biological samples, before or after pre-embedment in BSA and BA. On the one hand, before pre-embedment, it would result in loss of samples, particularly when processing cells, as pellet or suspension. On the other hand, it would result in samples contaminated with osmium, when performed after pre-embedment.

The technique has been developed and validated using HEK 293 cells, fibroblasts and brain tissue samples. It can be applied to a broad range of tissues and cells, originating from diverse sources. Studies reveal that the structure and ultrastructure of cells and tissues, pre-embedded in BSA and BA, are well preserved when processed for LM and EM, despite the samples not being post-fixed with osmium. Uranyl acetate and lead citrate staining of thin sections mounted on formvar coated grids prove to efficiently stain the biological specimens for EM (Taupin, 2008).

The use of BSA coupled with BA offers several advantages and benefits for processing scarce biological samples, over other techniques for pre-embedment. The gel-like matrix formed with BSA and BA is translucent, making it possible to identify the tissues or cells, prepared as pellet, in the cross-linked and polymerized gel and cut them out, as opposed to agarose or gelatin that are opaque once solidified. Further, the use of BA to polymerize the gel-like matrix offers a more resistant matrix for processing samples, throughout the histological procedures, particularly for EM processing that requires multiple and longer steps.

In all, pre-embedment of scarce biological specimens, in BSA and BA, results in efficient and reproducible processing and analysis of the samples by LM and EM. It also represents an improvement over most commonly used techniques for pre-embedding biological samples. Processing tissues and cells for cryostat and paraffin sectioning allows performing immuno-histological and -cytological staining and analysis of the samples. LR White is used when investigators aim at performing post-embedding immunological reactions for EM (Timms 1986). However, the conditions for performing immunostaining, on samples pre-embedded in BSA and BA, remain to be established and validated. BSA has been previously reported as a clinical sealant and for derived applications, like spinal cord disc repair (Fürst and Banerjee, 2005; Pursifull and Morey, 2007). Investigations will need to be conducted to evaluate the merit of the gel-like substance of BSA and BA, cross-linked and polymerized, for surgical applications.

CONCLUSION

We report a simple and direct pre-embedding technique for processing scarce biological specimens for LM and EM; the samples are pre-embedded in BSA and BA, cross-linked and polymerized. The technique is compatible with a broad range of LM and EM protocols and procedures. It is applicable to tissues and cells, prepared as pellet or suspension. The technique represents an improvement over others, like the ability to visualize the samples once pre-embedded and a better resistance to histological processing. It allows a more efficient and reproducible analysis of the samples by LM and EM. The technique is

particularly suitable for studying scarce isolated cells and rare human material, like biopsies, cystic and amniotic fluid cells. As such, it will contribute to advances in cell biology. Further investigations must be carried out to evaluate the merit of the gel-like substance of BSA and BA, cross-linked and polymerized, for other applications, like immunological staining of the samples and for surgical applications.

REFERENCES

Fürst W, Banerjee A. (2005) Release of glutaraldehyde from an albumin-glutaraldehyde tissue adhesive causes significant in vitro and in vivo toxicity. *Ann. Thorac. Surg.* 79, 1522- 8.

Leapman RD. (2004) Novel techniques in electron microscopy. *Curr. Opin. Neurobiol.* 14, 591-98.

Malatesta M, Mannello F, Sebastiani M, Cardinali A, Marcheggiani F, Renò F, Gazzanelli G. (1998) Ultrastructural characterization and biochemical profile of human gross cystic breast disease. *Breast Cancer Res. Treat.* 48, 211-9.

Malatesta M, Mannello F, Sebastiani M, Bianchi G, Gazzanelli G. (1999) Prostate-specific antigen found in type I breast cyst fluids is a secretory product of the apocrine cells lining breast gross cysts. *Breast Cancer Res. Treat.* 57, 157-63.

Mannello F, Malatesta M, Fusco E, Bianchi G, Cardinali A, Gazzanelli G. (1998) Biochemical characterization and immunolocalization of prostate-specific antigen in human term placenta. *Clin. Chem.* 44, 1735-7.

Mascorro JA, Bozzola JJ. (2007) Processing biological tissues for ultrastructural study.*Methods Mol Biol.* 369, 19-34.

Pursifull NF, Morey AF. (2007) Tissue glues and nonsuturing techniques. *Curr. Opin. Urol.* 17, 396-401.

Radermacher M, Ruiz T. (2006) Three-dimensional reconstruction of single particles in electron microscopy image processing. *Methods Mol. Biol.* 319, 427-61.

Taupin P. (2008) Processing scarce biological samples for light and transmission electron Microscopy. *Eur. J. Hist.* 52, 135-9.

Timms BG. (1989) Postembedding immunogold labeling for electron microscopy using "LR White" resin. *Am. J. Anat.* 175, 267-75.

Wang NS, Minassian H. (1987) The formaldehyde-fixed and paraffin-embedded tissues for diagnostic transmission electron microscopy: a retrospective and prospective study.*Hum. Pathol*. 18, 715-27.

In: Biochemistry and Histocytochemistry…
Editors: S. Fuchs, M. Auer, pp. 159-180
ISBN: 978-1-60876-283-5
© 2010 Nova Science Publishers, Inc.

Chapter 9

ROLE OF SURROGATE LIGHT CHAIN EXPRESSING B CELLS IN THE FORMATION OF SELF-REACTIVE ANTIBODIES

Pieter Fokko van Loo, Laurens P. Kil and Rudi W. Hendriks*
Department of Pulmonary Medicine, Room Ee2251, Erasmus MC Rotterdam,
PO Box 2040, NL 3000 CA Rotterdam, the Netherlands

ABSTRACT

Autoimmune diseases, such as rheumatoid arthritis (RA) and systemic lupus erythematosus (SLE) are facilitated by B cells that have lost self-tolerance. B cells contribute to autoimmune diseases by production of autoantibodies, by presenting autoantigens or by secreting proinflammatory cytokines. For that reason, it is important to understand the origin of autoreactive B cells and their role in the pathogenesis of autoimmune disease. Many autoreactive B cell receptors (BCR) are normally generated during B cell development, but in healthy individuals most of the B cells carrying an autoreactive BCR are silenced by deletion, receptor editing, inclusion or anergy. Interestingly, in humans a unique self-reactive $VpreB^+LC^+$ B cell subset was identified, which comprises 0.5-1% of circulating B cells and co-expresses conventional immunoglobulin light chain (Ig LC) and the non-rearranging surrogate light chain (SLC), which was previously thought to be exclusively expressed during early B cell development. These $VpreB^+LC^+$ B cells are present in healthy individuals and accumulate in the joints of some patients with RA. They manifest an unusual Ig heavy chain (HC) and LC repertoire, which displays evidence for receptor editing and is associated with autoimmunity. To elucidate the role of these autoreactive $VpreB^+LC^+$ B cells in the development of autoimmunity, we have recently generated a novel SLC-transgenic mouse model in which all B cells coexpress SLC components. Here we review the characteristics of the unique subset of $VpreB^+LC^+$ B cells identified in human and discuss our findings in the SLC-transgenic mouse model in the context of the involvement of $VpreB^+LC^+$ B cells in the etiology of autoimmune disease.

* Department of Pulmonary Medicine, Room Ee2251, Erasmus MC Rotterdam, PO Box 2040, NL 3000 CA Rotterdam, the Netherlands; Phone: ++31-10-7043700; E-mail: r.hendriks@erasmusmc.ml.

INTRODUCTION

Autoimmune diseases are characterized by a breakdown of tolerance of the immune system to self-antigens. An immune reaction against self-antigens is cooperatively established by antigen presenting cells, T lymphocytes and B lymphocytes. B cells do not only contribute to autoimmune pathology through the production of autoreactive antibodies, but also via the production of proinflammatory cytokines or by presenting auto-antigens to T cells. That B cells play a key role in driving autoimmune responses is clearly illustrated by the continuously expanding group of autoimmune diseases that can be treated by B cell depletion therapy (reviewed in Ref. [1]). In several auto-immune diseases up to ~40% of all mature B cells in patients are self-reactive [2,3]. Nevertheless, high fractions of self-reactive B cells per se do not directly explain the contribution of B cells to auto-immune disease, since even in healthy individuals ~20% of mature B cells have affinity for self-antigens [4]. Therefore, it is evident that in autoimmune disease silencing or control of the activation of autoreactive B cells is severely hampered. To understand how self-reactive B cells contribute to autoimmunity it is of vital importance to know how self-reactive B cells can emerge, differentiate and survive, and how they are controlled once they have fully matured (see Ref. [5,6] for recent reviews). In this review, we focus on a recently identified interesting subset of B cells that co-express immunoglobulin (Ig) light chain and the non-rearranging surrogate light chain (SLC), which manifests an unusual self-reactive Ig repertoire.

INDUCTION OF SELF-TOLERANCE DURING B CELL DEVELOPMENT

Each B cell assembles during its differentiation a unique B cell receptor (BCR) through recombination of V, D, and J gene segments that encode the antigen-recognizing variable parts of the BCR Ig heavy chain (HC) and light chain (LC)(reviewed in Ref. [6,7]). Successful V(D)J rearrangement at the pro-B cell stage of the Ig HC locus leads to surface expression of the precursor-B cell receptor (pre-BCR), composed of a Ig μ HC and the non-rearranging λ5 and VpreB SLC components [8-11] (Figure 1). The pre-BCR signals for proliferation of the now called large pre-B cells and induces further cellular differentiation. Next to the induction of surface markers such as CD2, the IL-2 receptor and MHC class II, this includes termination of SLC expression and redirection of the V(D)J recombination machinery from Ig HC to the Ig κ and λ LC loci (reviewed in Ref. (12-14). Upon successful rearrangement of the Ig κ or λ locus, small pre-B cells differentiate into immature B cells that express a fully rearranged BCR of the IgM isotype on the cell membrane.

The random nature of the V(D)J recombination process generates a diverse BCR repertoire, including potential autoreactive BCRs [4]. Indeed, ~50-75% of early B cells carry an autoreactive BCR that is polyreactive to several antigens, including DNA, lipopolysaccharide (LPS) or insulin [15]. To ensure self-tolerance, B cells carrying an autoreactive BCR are counterselected or silenced at multiple checkpoints throughout B cell differentiation (Figure 1). There are three major mechanisms that shape the repertoire of developing B cells and thereby silence autoreactive B cells: clonal deletion, receptor editing (including inclusion) and anergy.

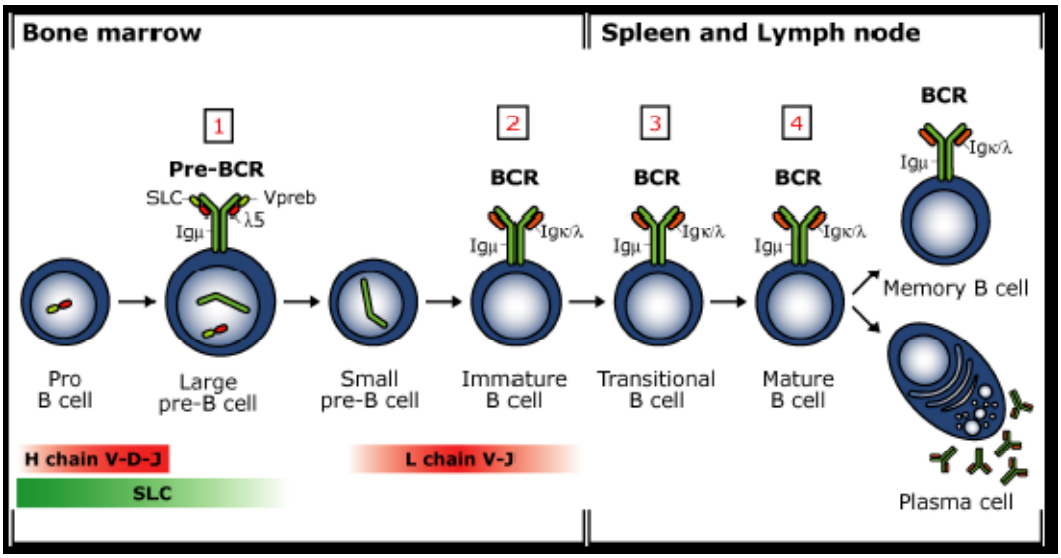

Figure 1. Overview of B cell development. B cells are classified into different stages based on rearrangement status of the Ig HC and LC loci. Four major checkpoints for BCR repertoire selection and silencing of autoreactive B cells are indicated: 1= pre-BCR checkpoint; 2= immature B cell/receptor editing; 3= peripheral transitional B cell; 4= (lack of) second activation signal.

A fourth mechanism controls the activation of mature B cells by preventing B cell activation in the absence of a second activation signal, *i.e.* T cell help or Toll like receptor (TLR) signaling.

(1) Clonal Deletion

The pre-BCR, expressed at the large pre-B cell stage, is the first checkpoint to test functionality of the newly arranged Ig HC. As a large fraction of the initial formed Ig μ HC cannot pair with the SLC complex, this checkpoint accounts for a substantial change in Ig HC repertoire [16]. Very recently, it was proposed that the pre-BCR also serves as a checkpoint to eliminate potential autoreactive Ig HCs, as mice deficient for the SLC components exhibit a relative increase in activated B cell numbers and elevated serum concentrations of antinuclear autoantibodies [17]. The Ig HC repertoire in SLC-deficient mice displayed prototypical autoantibody features, including an increase of length and basic amino acid content of the complementarity-determining region 3 (CDR3). Similar features were overrepresented in cloned Ig HCs from human λ5-deficient bone marrow B cells, implicating that negative selection of such Ig HCs also occurs in human pre-B cells [18]. Striking is the finding that SLC-deficient mice showed a clear enrichment beyond the pre-B cell stage of Ig HC CDR3 regions containing multiple basic amino acids, indicating that in SLC-deficient mice self-tolerance is lost beyond the pre-BCR checkpoint [17]. Because SLC-deficient mice have a strongly reduced peripheral B cells fraction due to a severe pre-B cell arrest, it cannot be excluded that the enrichment of autoreactive B cells beyond the pre-B cell stage in SLC-deficient mice is a direct result of the lymphopenia. B cell lymphopenia relieves the competition between autoreactive and non-autoreactive B cells for survival factors, such as B

cell activating factor (BAFF), in peripheral niches [19,20]. Therefore, the autoreactive BCR repertoire in SLC-deficient mice might reflect a less stringent counterselection of autoreactive B cells in the periphery. Additional research should elucidate the true significance of the pre-BCR checkpoint in inducing self-tolerance.

(2) Receptor Editing

A second major checkpoint during B cell development is the immature B cell stage. At this stage, the newly formed BCR becomes for the first time membrane expressed, allowing to sense whether it binds self-antigens. Immature B cells expressing an auto-reactive BCR are at this point silenced by apoptosis, unless they manage to alter the BCR specificity by receptor editing (Figure 2) [21-23]. Receptor editing is a process of continued V(D)J rearrangement of productively recombined Ig LC loci, to generate a new, non-autoreactive BCR. The ongoing V(D)J rearrangement results in the joining of more upstream V segments to more downstream J segments. Once the recombination possibilities of the used Ig LC locus are exhausted, V(D)J recombination may continue at different Ig LC loci after inactivation of the autoreactive locus (24). Successful abolishment of BCR self-reactivity by receptor editing prevents central deletion of autoreactive immature B cells and allows their migration to secondary lymphoid organs to continue their differentiation [22, 23] Receptor editing is a major mechanism to shape the BCR repertoire, since studies in Ig LC transgenic mice demonstrated that ~25% of peripheral B cells in these mice express edited LCs [25, 26].

Although receptor editing is intended to delete autoreactive specificities from the BCR repertoire, V(D)J recombination of a second Ig LC locus without recombinatorial deletion of the originally autoreactive Ig LC allele may lead to preservation of this autoreactive allele throughout further B cell differentiation. This then gives rise to peripheral B cells expressing dual BCRs, a phenomenon referred to as allelic inclusion [27-29]. Co-expression of an innocuous and an autoreactive Ig LC, both competing for binding to the same Ig HC, will dilute out the self-reactive BCR on the cell surface, thereby allowing the originally autoreactive B cell to escape elimination or silencing. The persistence of B cells that encode dual BCRs poses a threat to self-tolerance, as these cells can produce autoantibodies that have the potential to participate in autoimmune disease [28, 29].

(3) Anergy

Those immature B cells that successfully pass the first major autoreactivity checkpoint in the bone marrow fully upregulate surface BCR expression and migrate to secondary lymphoid organs. When these immature B cells arrive in a new antigenic environment containing self-antigens that are absent in the bone marrow, they are reassessed at a next BCR checkpoint. At the transition from short-lived immature into long-lived mature B cell, B cells carrying a self-reactive BCR are silenced either by apoptosis or by functional inactivation, a mechanism referred to as anergy.

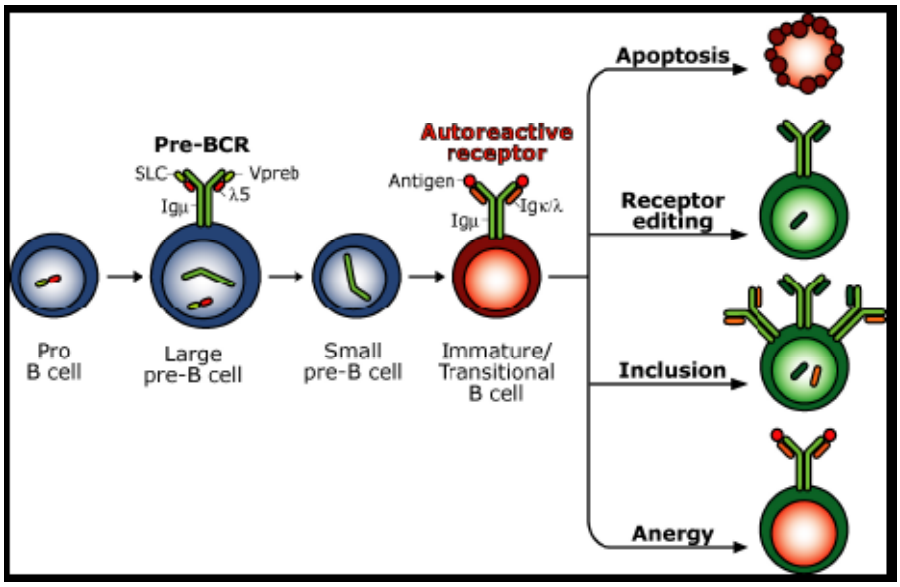

Figure 2. Four mechanisms to achieve B cell tolerance. B cells with an auto-reactive BCR can (i) be driven into apoptosis, (ii) undergo receptor editing of the Ig LC, (iii) dilute out the self-reactive BCR by co-expression of an innocuous conventional LC, or (iv) become anergic.

Anergic B cells have become unresponsive to their cognate antigen, a condition which is induced by changes in their gene expression profile [30, 31] Anergic/autoreactive B cells depend for their survival on BAFF. During maturation of weakly autoreactive transitional B cells, BAFF counterregulates the activation of apoptosis signaling pathways upon self-antigen recognition by the BCR. Since in peripheral lymphoid organs BAFF availability is normally limited, this anti-apoptotic cytokine preferentially sustains the survival of non-autoreactive B cells in which BCR mediated pro-apoptotic signaling is minimal. As anergic B cells poorly compete with normal B cells for the limited amounts of BAFF present, this survival factor controls the life span and thereby the number of anergic B cells (See Ref. [32] for a recent review on the role of BAFF in peripheral B cell selection and survival). Either increased BAFF production or decreased BAFF consumption due to low B cell numbers can relax the competitive pressure between non-autoreactive and autoreactive B cell clones, thereby allowing more autoreactive transitional B cells to survive and differentiate in peripheral lymphoid organs [19, 20].

Anergic B cells frequently exhibit a shortened life-span and are often restricted in their differentiation and activation. As a result, anergic B cells normally do not participate in auto-immune responses. However, the anergic state of autoreactive B cells is reversible, as removal self-antigen allows further differentiation and activation of the anergic B cell. Thus, chronic BCR stimulation by the self-antigen is required to maintain anergy of these cells [33,34]. Therefore defects in the induction or maintenance of anergy might contribute to the pathogenesis of autoimmune disease. For example, it has been demonstrated that transgenic self-reactive BCRs fail to induce B cell anergy in autoimmune prone MRL/lpr mice [35,36], while in non-susceptible mouse strains these transgenic B cells are restrained in their differentiation into mature B cells and plasma cells.

The mechanism by which an autoreactive B cell is silenced is determined by the developmental stage at which the BCR is exposed to the self-antigen, the nature of the self-antigen, as well as the avidity of its BCR for the autoantigen. While auto-antigens that extensively crosslink BCR's evoke a strong BCR signal that prefentially instructs apoptosis of the transitional B cell stage, self-antigens that weakly crosslink autoreactive BCRs are more prone to render the B cell anergic [34].

(4) Lack of Second Activation Signal

Despite stringent counterselection of self-reactive B cells during B cell development, still ~20% mature B cell compartment is autoreactive [4]. This fraction of self-recognizing B cells includes marginal zone (MZ) and B-1 B cells, which are known to produce antibodies to blood-borne pathogens and so-called "natural antibodies", respectively [37]. Nevertheless, the fraction of self-reactive B cells has to be tightly regulated to prevent uncontrolled immune reactions to self-antigens. To avoid that binding of the BCR to its cognate antigen would on itself be sufficient to elicit a B cell response, a second signal - which is only provided if recognized antigen is truly exogenous - is obligatory to permit mature B cell activation. Would B cell activation solely depend on a BCR stimulus, this would enable an autoreactive B cell to mount an uncontrolled auto-reactive immune response. The antigen-specific B cell can receive this second signal from T helper lymphocytes, or directly via TLRs that recognize pathogen associated molecular patterns (PAMPs) of the antigen. In auto-immunity, parallel recognition of a self-antigen by the BCR and TLR, resulting in simultaneous BCR- and TLRs signaling, might therefore provide a mechanism to break tolerance of autoreactive B cells.

As T cell help provides the second signal to activated B cells, B cells that have a potential for autoreactivity can be kept in check by the absence of appropriate T cell help. Indeed, T-cell tolerance is an important mechanism for maintaining B-cell tolerance, since defective T-cell tolerance and activation is a major underlying cause of autoimmune disease in many animal models and patients. For example, in healthy Balb/c mice, the anergic status of anti-double-stranded DNA B cells can readily be reversed by provision of T cell help by autoreactive T cells [40, 41]. Moreover, it has been shown that anti-chromatin B cells secrete autoantibodies in vivo upon provision of $CD4^+$ T cell help, whereby $CD4^+$ $CD25^+$ regulatory T cells act to inhibit maturation of autoantibody responses (42). Furthermore, inhibition of T-B cell interaction (e.g. by anti-CD40 ligand antibodies) is effective in the treatment of SLE nephritis [38, 39].

The final stage of B cell differentiation where the BCR repertoire is shaped is the germinal centre (GC) reaction. In the T cell dependent GC reaction, the BCR is adapted for its cognate antigen by somatic hypermutation (SMH) and class switch recombination (CSR), both of which are driven by activation induced cytidine deaminase (AID). Since AID induces targeted point mutations in the CDRs of the Ig HCs and Ig LCs, this can dramatically alter the BCR affinity or even its specificity. As AID activity may also result in the formation of an autoreactive BCR, a stringent counterselection of such self-reactive B cells is required. By analysis in human of the BCR repertoire of post-GC IgG^+ memory B cells, it was demonstrated that indeed new auto-reactive B cells develop by SHM: whereas ~20% of naive B cells is self-reactive, up to ~40% of the IgG^+ memory B cells expressed a true de novo created self-reactive BCR. Apparently, lack of T cell help prevents activation of these self-

reactive IgG^+ memory B cells [43]. It has also been found that AID overexpression in B cells is associated with production of highly pathogenic multireactive autoantibodies [44]. Autoreactive IgG^+ memory B cells were found in similar frequencies in healthy individuals and most SLE-patients [45]. Although these autoreactive IgG^+ memory B cells may contribute to auto-immune disease, their role remains unsolved. Likewise, it is unclear whether an additional checkpoint does exist to eliminate self-reactive memory B cells.

BCR REPERTOIRE SELECTION IN AUTOIMMUNE DISEASES

Signaling from the BCR is critical in the counterselection of self-recognizing B cells. Attenuation of BCR signaling might dramatically affect the BCR repertoire composition, leading to accumulation of autoreactive mature B cells, as has been found in mouse models [46-48] and in several human diseases, including X-linked agammaglobulinemia (XLA) [49-52]. XLA is caused by mutations in the gene encoding the critical (pre-)BCR signaling molecule Bruton's tyrosine kinase (BTK). It is characterized by an almost complete block of B cell development at the pre-B cell stage, resulting in very low numbers of circulating B cells [53,54]. It was found that the majority (~60%) of the few residual B cells carry a self-reactive or polyreactive BCR. The antibodies expressed by XLA B cells were reactive to self-antigens, including DNA, insulin and LPS. This finding demonstrates that BTK-deficiency leads to impaired silencing of autoreactive immature B cells, most likely by impaired sensing of auto-antigens at the immature B cell stage [55]. In agreement with this finding several cases of XLA patients with autoimmune pathology have been described [56-58]. Taken together, this demonstrates that attenuated BCR signaling might provide a mechanism of breakdown of central tolerance in certain autoimmune diseases, including RA.

Many autoimmune diseases are characterized by a distinct signature of disease-specific autoantibodies. Prevalent autoantibodies in RA include rheumatoid factors (RF), recognizing the constant regions of IgG subclasses and antibodies against cyclic citrullinated proteins/peptides [59,60]. In SLE anti-nuclear antigen autoantibodies (ANAs) are found that are directed against dsDNA, ssRNA, chromatin, or ribonucleoproteins [61]. Nevertheless most of the autoantibodies are not exclusively found in one autoimmune disease, and especially RF as well as ANAs can be detected in a variety of autoimmune disorders, including Sjögren's syndrome (SS) [62, 63]. The serology of SS patients is illustrative for this, since 75-95% of these patients are positive for RF, ~50% are positive for ANAs, and the classical SS auto-antibodies anti-Ro/SSA and anti-La/SSB are also directed against nuclear antigens and are frequently detected in SLE patients as well [64, 65].

The serology of autoimmune patients therefore clearly illustrates that in systemic auto-immune diseases the tolerance of B cells to multiple self-antigens is breached. Despite this general breakdown of B cell tolerance, still differences in BCR repertoire characteristics between RA, SLE and SS patients do exist, indicating that the emergence and selection of autoreactive B cells differ considerably between these disorders. Apart from antigen driven selection of the BCR repertoire, the BCR in these diseases probably are the result of different defects at several tolerance checkpoints during B cell differentiation, including survival factors.

Rheumatoid Arthritis

In RA patients the silencing of autoreactive B cells is clearly hampered at the immature B cell tolerance checkpoint [3]. As a result, their mature naive B cell compartment contains increased proportions of autoreactive B cells that can produce classic RA autoantibodies (~35-50%, compared with ~20% in healthy controls). Moreover, in a fraction of patients, RA B cells express an increased proportion of polyreactive BCRs. This shift in BCR repertoire specificities in RA patients is clearly reflected by altered Ig HC and LC characteristics of the new bone marrow emigrant B cells, e.g. an increase in Ig κ CDR3 length and differences in Vκ and Jκ segment usage. In 3 out of 9 patients, these differences comprised a decrease in downstream Jκ and upstream Vκ usage, coherent to a decrease in receptor editing at the immature B cell stage. However, as 1 RA patient clearly displayed an increase in receptor editing, it is unlikely that a single mechanism affects receptor editing in all these RA patients.

In addition to the observed defect in central B cell silencing, deletion of peripheral autoreactive and polyreactive B cells is clearly defective. In fact, in most RA patients no significant decline in the fraction of autoreactive or polyreactive B cells has been observed during transitional B cell differentiation. In conclusion, both a defect at central and peripheral B cell tolerance contributes to the increased fraction of autoreactive and polyreactive mature B cells in RA patients.

Systemic Lupus Erythematosus

Also SLE patients show an increase in autoreactive and polyreactive antibodies in the mature naive B cell compartment. But in contrast to the clear defect in central tolerance in RA, neither the number of Ig HC CDR3-positive charges nor their lengths or specific Ig gene usage was sufficient to predict polyreactivity in SLE patients [2]. In new bone marrow emigrant B cells from SLE patients, Ig HC and Ig LC features such as V and J segment usage and CDR3 length were not significantly different from those observed in healthy controls. Although investigation of the peripheral B cell BCR repertoire in various studies did not yield entirely consistent results regarding Vκ and Jκ usage, it appears that receptor editing a the Ig κ locus is increased, when compared with healthy controls [2, 66, 67].

Importantly, auto-antibodies in SLE specifically recognize DNA and ssRNA, which may well act as TLR-ligands. DNA-containing immune complexes from SLE patients can therefore activate various immune cells, e.g. dendritic cells and macrophages, in a TLR-dependent way. Moreover, BCR and TLR signaling is concomitantly trigged on self-reactive B cells that recognize the Fc-region on an immune complex composed of IgG auto-antibodies bound to DNA or ssRNA [68,69]. Such anti-IgG auto-antibodies known as rheumatoid factors (RFs), that are found in SLE, RA and SS, may well catalyze the pathogenesis of these immune disorders [70]. On the other hand, TLR signaling can also contribute to B cell silencing. In particular, it has been shown that signaling from TLR7 and TLR9, recognizing ssRNA or CpG motif DNA respectively, have opposing inflammatory and regulatory effects on the development of autoimmune pathology [71].

IDENTIFICATION OF THE VPREB$^+$LC$^+$ B CELL SUBSET

Although it is has become evident that loss of self-tolerance is a key step in the initiation of autoimmune diseases [46, 72, 73], the origin of self-reactive B cells is still poorly understood. Therefore, the finding in human by Meffre et al. of the unique self-reactive VpreB$^+$LC$^+$-B cell subset that is associated with antibodies found in SLE and RA [74-76], is of great interest.

The identified VpreB$^+$LC$^+$ B cell population differs from conventional B cells in that they have surface co-expression of the conventional Ig LC and the non-rearranging surrogate light chain (SLC) component VpreB [75]. Expression of the SLC complex, which is composed of the λ-like (λ5 in mouse) and VpreB proteins, is normally restricted to the pro-B and pre-B cell stage. Upon productive Ig HC gene rearrangement, the SLC forms – together with an Ig μHC - the pre-BCR that is then expressed on the cell surface (Figure 1) [8-13]. Pre-BCR signaling induces proliferation and further cellular differentiation of the pre-B cell [13], including termination of SLC expression, thereby ensuring that SLC and conventional LC are expressed in a mutually exclusive manner [77, 78].

VpreB$^+$LC$^+$ B cells are present in the circulation, where they make up 0.5-1% of B cell population, independent from the age of the healthy individual. In addition, the cells are also found in tonsils. Further characterization of the VpreB$^+$LC$^+$ B cell subset revealed that they express, next to VpreB, also other genes whose expression is restricted to early B cell development, including recombination activating gene-1 (RAG1), RAG2, terminal deoxinucleotidyl transferase (TdT) and λ5 at the mRNA level. The expression level of all these genes, including VpreB, is at least ~5 fold lower compared to the expression found in pre-B cells, and for λ5 even much lower [75]. The identified gene expression profile would indicate that VpreB$^+$LC$^+$ B cells might reflect early immature B cells that have rapidly emigrated to the periphery and are still in the process of downregulating VpreB and the other pre-B cell associated genes. However, they cannot simply be regarded as an immature B cell population, because VpreB$^+$LC$^+$ B cells are found among immature, mature and memory B cells and express many of the same markers as conventional B cells.

VPREB$^+$LC$^+$ B CELLS HAVE AN AUTO-REACTIVE IG REPERTOIRE

Interestingly, the Ig repertoire of VpreB$^+$LC$^+$ B cells differs significantly from that found in conventional B cells [74-76]. Cloning and sequencing of the Ig HC VH1, VH3, VH4 and VH5 families from sorted VpreB$^+$LC$^+$ B cells revealed that VH1, VH4 and VH5 gene segment usage was altered in VpreB$^+$LC$^+$ B cells. The VH1, VH3 and VH5 genes, but not the VH4 genes, expressed in these cells had a longer CDR3 length with more aromatic amino residues. This was the result of increased usage of the long JH6 segment, more D-D fusions and long N-nucleotide insertions. Furthermore, the Ig repertoire of the VpreB$^+$LC$^+$ B cells expressing VH1, VH3, and VH5 gene segments showed a biased D-segments usage, with an overrepresentation of reading frames (RF) encoding hydrophobic amino acids. Nevertheless, the VpreB$^+$LC$^+$ B cells encoding VH4 BCRs had normal CDR3 length and composition. As it has been suggested that VH4 genes are prone to generate auto-reactive B cells, this might explain the normal VH4 usage by VpreB$^+$LC$^+$ B cells. Overall these findings showed that

VH1, VH3, and VH5 BCRs on VpreB$^+$LC$^+$ B cells are enriched for characteristics that are normally counterselected in conventional B cells.

Also Ig κ and λ LC genes expressed by VpreB$^+$LC$^+$ B cells had a longer CDR3 length. Analysis of the Ig κ repertoire revealed increased usage of downstream Jκ4- and Jκ5-segments, whereas Ig κ$^+$ conventional B cells mainly used Jκ1 and Jκ2. This skewed Jκ-segment usage by VpreB$^+$LC$^+$ B cells was accompanied with a biased usage of more upstream Vk gene segments. Upstream Vκ segments and downstream Jκ segments usage are both signs of receptor editing [22, 23]. In addition, Ig κ$^+$ VpreB$^+$LC$^+$ B cells displayed enrichment for the usage of Vκ4 family member B3. This specific Vκ4 family member is thought to encode a DNA-recognizing antibody that is overrepresented in SLE patients [67].

The presence of Ig LCs with evidence for receptor editing at the Ig κ locus, a process that is frequently induced by autoreactive BCRs, links the VpreB$^+$LC$^+$ B cells to autoimmunity. Moreover, the finding of an Ig repertoire in VpreB$^+$LC$^+$ B cells with long CDR3 regions is intriguing. Normally, B cells encoding a BCR with long CDR3 regions are eliminated during B cell development, but long CDR3 regions are frequently found among auto-reactive and poly-reactive antibodies, including those present in joints of RA patients [79-81]. In this regard it is striking that VpreB$^+$LC$^+$ B cells did not only comprise a small proportion of the circulating B cell population of healthy donors, but were also found to be enriched in synovium of RA patients [75]. Namely, in the synovium of 4 out of 12 RA patients analyzed, 5-15% of the B cells present were VpreB$^+$LC$^+$ B cells, which implied a ~10-20-fold induction compared to percentages found in the circulation. A large fraction of these synovial VpreB$^+$LC$^+$ B cells expressed CD10 and CD38, which are markers found on GC B cells, indicating that these VpreB$^+$LC$^+$ B cells take part in GC reactions. Taken together, the localization and the BCR repertoire of the VpreB$^+$LC$^+$ B cells link these cells to autoimmunity.

Indeed, it turned out that the majority of the VpreB$^+$LC$^+$ B cells had a self-reactive Ig. By cloning and expressing Ig HC and LC from single sorted VpreB$^+$LC$^+$ B cells it was shown that ~70% of VpreB$^+$LC$^+$ B cells produced an Ig that was reactive to Hep2 cell lysate in ELISA assays, compared to ~15% of conventional B cells. Moreover, up to 50% of the Igs expressed by VpreB$^+$LC$^+$ B cells, versus less than 5% of those expressed by conventional B cells, were true ANAs that recognize a diverse pattern of cellular antigens. Further characterization of the antigen specificity revealed that a large fraction (~43%) of the Igs from VpreB$^+$LC$^+$ B cells recognized at least ssDNA, dsDNA, IgM, insulin or LPS and even 23% (less than 5% among conventional B cells) of these Igs were polyreactive, as they recognized more than two of these analyzed antigens. All polyreactive Igs from VpreB$^+$LC$^+$ B cells used JH6, had long CDR3 regions with hydrophobic and aromatic residues that were encoded by abnormal D segment reading frame usage.

Taken together, the majority of VpreB$^+$LC$^+$ B cells present in human express self-reactive Igs, including true ANAs and polyreactive Igs. Normally, B cells expressing self-reactive Igs are eliminated during B cell development to maintain self-tolerance. Nevertheless, the majority of the VpreB$^+$LC$^+$ B cells, present in immature, mature and memory B cell subpopulations in the periphery express self-reactive Igs. This suggests that co-expression of the SLC component VpreB, next to a conventional LC, rescues the self-reactive VpreB$^+$LC$^+$ B cells from deletion. Furthermore, as anti-DNA and anti-Ig self-antibodies are associated with SLE and RA, respectively, this indicates that VpreB$^+$LC$^+$ B cells can produce self-

reactive antibodies that are known to play a key role in the etiology of these autoimmune diseases (Figure 3).

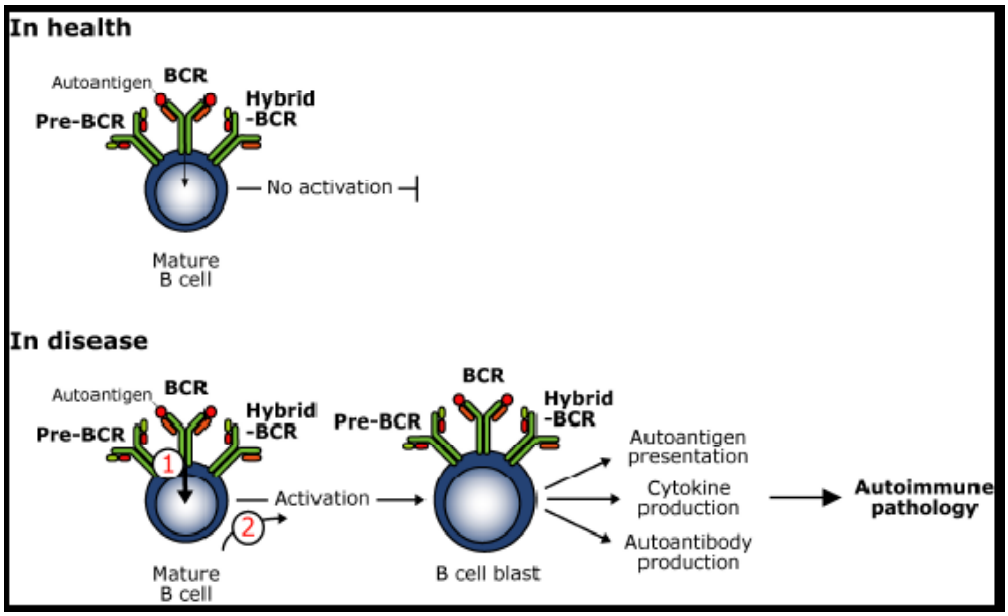

Figure 3. Model for the contribution of VpreB+LC+ B cells to autoimmune pathology. Although most VpreB+LC+ B cells present in human express self-reactive BCRs, they are normally kept in check. The presence of VpreB protein rescues such self-reactive B cells from deletion, but also precludes their activation and differentiation into memory B cells or plasma cells (because of reduced BCR signals). Only under specific disease conditions, the VpreB+LC+ B cells may become activated, e.g. because of (1) enhanced BCR signaling, or (2) additional signals originating from TLR or helper T cells. The resulting activated autoreactive B cells contribute to autoimmune pathology by multiple mechanisms.

ANALYZING THE VPREB$^+$LC$^+$ B CELLS WITH SLC-TG MOUSE MODEL

To elucidate the effect of prolonged expression of the SLC components during B cell development, we have recently generated a new SLC-transgenic (Tg) mouse model in which all B cells are SLC$^+$ [82]. To this end, we have individually cloned genomic constructs of λ5 and VpreB$_1$ (together forming the SLC) under the control of the human CD19 promoter region, which targets expression of transgenes to all stages of B cell development. We obtained independent λ5 and VpreB$_1$ Tg mouse lines expressing high and low levels of these SLC components.

Normally, expression of the SLC components λ5 and VpreB is restricted to pro-B and large pre-B cell stage. The SLC forms at this developmental stage with the newly arranged Ig μHC the pre-BCR, which induces a proliferative burst of the large pre-B cells and signals for cellular maturation. It has been assumed that the large pre-B cells lose their proliferative capacity due to the termination of pre-BCR signaling as a result of down regulation of the expression of the SLC components at the pre-B cell stage [12, 13]. Remarkably, we found that enforced SLC expression at the pre-B cell stage did not result in increased proliferation

of the large pre-B cells, did not affect the generation of small pre-B cells nor induced small pre-B cell to undergo proliferation [82].

However, presence of SLC proteins beyond the pre-B cell stage severely hampered B cell development. At the immature B cell stage the SLC components had the capacity - in the presence of conventional Ig LC - to induce constitutive BCR internalization. The internalization was dependent on the adapter protein SLP65 (SH2 domain-containing leukocyte-specific phosphoprotein of 65 kDa, or BASH/BLNK) that is downstream of the (pre-)BCR. Internalization of the BCR at the immature B cell stage resulted in secondary Ig LC rearrangements, reflected by increased fractions of Ig λ^+ cells and a severe developmental arrest of immature B cells.

The effects of SLC expression on mature B cells in the periphery were dose-dependent. Low-level expressing SLC-Tg mice did not exhibit reduced splenic B cell numbers but had significantly increased proportions of $CD21^{hi}CD23^{low}$ MZ B cells. In contrast, high-level expressing SLC-Tg mice had severely reduced numbers of splenic B cells with increased fractions of surface $CD5^+$ B-1 B cells [82]. It has been shown that increasing BCR signaling strength directs developing B cells from the default follicular B cell fate into the MZ B cell and eventually into the B1 cell lineage [83-86].Therefore, the dose-dependent effect of SLC on MZ and $CD5^+$ B-1 B cell development is consistent with the notion that SLC increases basal BCR signaling. MZ and $CD5^+$ B-1 B cell fractions, which typically produce polyreactive low affinity antibodies with recurrent specificities, are thought to be positively selected on the basis of their BCR [84, 85]. Therefore, the increased fraction of these B cells in the SLC-Tg mice might be indicative for an autoreactive BCR repertoire of the SLC^+ B cells.

Analysis of B cell activation in the high-level SLC-Tg mice demonstrated that SLC^+ B cells resemble anergic B cells, as they displayed impaired BCR-induced phosphorylation and reduced in vitro responses to anti-IgM stimulation [82]. Nevertheless, in low- and high-level SLC-Tg mice, SLC^+ B cells were spontaneously driven into IgM^+ plasma cell differentiation [82]. A significant fraction of these plasma cells produced self-reactive antibodies, because we detected elevated levels of anti-nucleosome IgM in the serum of SLC-Tg mice. However, the mice did not develop overt spontaneous autoimmune pathology, which may be related to the fact that the SLC-Tg B cells did not undergo sufficient activation, Ig HC class switch recombination (CSR) or affinity maturation. The finding that the SLC^+LC^+ B cells in the SLC-Tg mice did not contribute to autoimmune pathology is consistent with the situation in human, where the self-reactive $VpreB^+LC^+$-B cells are present in healthy individuals, but are kept in check by self-tolerance mechanisms.

DYSREGULATED SLC EXPRESSION IN AUTOIMMUNITY

It has been assumed that in the small subset of SLC^+LC^+-B cells in human the sustained expression of SLC components was simply a result of the expression of a BCR with particular antigen specificity. However, our SLC-Tg model unexpectedly demonstrated for the first time that dysregulated SLC expression can be one of the primary causes of defective BCR repertoire selection and the formation of auto-antibodies [82].

This raises the question how dysregulated SLC expression affects BCR repertoire selection. Most likely the answer to this question may lie in the dual expression of the BCR along with the pre-BCR. During normal B cell development the initially produced autoreactive B cells are silenced by the mechanisms discussed above, namely induction of apoptosis, anergy, or by receptor editing of the BCR with possible outcome the expression of a dual BCR (Figure 2). Possible, dysregulated SLC expression affects BCR repertoire selection by the induction of anergy. Indeed we have found in the SLC-Tg mice that $SLC^{+}LC^{+}$ B cells resemble anergic B cells [82]. The pre-BCR signals in a cell-autonomous and constitutive fashion [87] and it has been demonstrated that constitutive pre-BCR signaling reduces Ig-alpha phosphorylation and Ca^{2+} influx [77]. Therefore, it is likely that constitutive signaling from the pre-BCR might induce the anergic status of the $VpreB^{+}LC^{+}$ B cells. Alternatively, also the autoreactive nature of the BCR might induce the anergic status of the $VpreB^{+}LC^{+}$ B cells [34].

A possible second mechanism by which dysregulated SLC expression interferes with BCR repertoire selection might be that dual expression of pre-BCR and BCR mimics the Ig L chain allelic/isotype inclusion situation where an innocuous Ig LC silences an autoreactive Ig LC (27, 88). In this case, in $VpreB^{+}LC^{+}$ B cells the SLC component might substitute for an innocuous Ig LC and competes with the potential autoreactive Ig LC, thereby reducing surface expression of this autoreactive Ig LC, resulting in silencing of the autoreactive $VpreB^{+}LC^{+}$ B cells.

It has been reported that B cells silenced by either induction or by dual BCR expression still have the capacity to eventually secrete auto-reactive antibodies [27], [28] ,[29]. In the situation of anergy, it has been demonstrated that B cells carrying a transgenic anti-DNA BCR on a BALB/c background do not give rise to auto-antibodies, indicating that when self-tolerance is maintained these B cells are anergic. However, the anergic phenotype is lost when the transgenic anti-DNA BCR is crossed on the autoimmune prone MRL/lpr background, as these mice had high titers of transgenic anti-DNA antibodies, already at the age of 10 weeks [35, 89, 90]. Moreover, it has been shown that the anergic status of B cell is reversible. In particular, when anergic B cells were transferred into mice lacking their specific auto-antigen, the initial anergic B cells lost their anergic characteristics and proceeded normal B cell development [30]. Also the inclusion of an auto-reactive BCR by predominant expression of an innocuous BCR can eventually give rise to production of the auto-antibody, as has been shown by Lui et al., using the 3-83-Tg model [28]. This model expresses the prearranged 3-83 BCR that recognizes MHC class I H-$2K^{k,b}$ [91]. Mice carrying this 3-83 Tg on the autoreactive MHC class I H-$2K^{k,b}$ background expressed - due to receptor editing of the 3-83 BCR - only non-autoreactive BCRs without 3-83 specificity in the periphery. Nevertheless, when these mice were aged, 3-83 specific IgM antibodies were found in the serum [28]. This indicates that - although B cells have undergone receptor editing of the 3-83 BCR - at least a significant fraction of these B cells expressed (next to the innocuous BCR) also intracellularly the autoreactive 3-83 BCR. Taken together, this demonstrates that B cells expressing dual BCRs still have the capacity to produce potential harmful antibodies.

It was shown by Bankovich et al. that the SLC heterodimer binds to the Ig HC CDR3 in such a way that the antigen binding site of the Ig HC is covered by the C-terminal unique region of VpreB [92]. This would imply that the pre-BCR complex cannot recognize an antigen. Indeed, the same authors show that an Ig HC from an antibody specific for ovalbumin (OVA) did not bind to OVA-protein when expressed together SLC as a pre-BCR

complex [92]. In contrast, a another group showed that a so-called surrobody, which is a pre-BCR-like complex composed a specific Ig HC and a fusion protein of the SLC complex (λ5 and VpreB expressed as one protein), binds with high affinity to the antigen the Ig HC was directed against [93]. The usage of truncated SLC proteins in the former study and fusion proteins of truncated SLC components in the latter precludes a direct comparison of the results obtained. Nevertheless, the possibility that VpreB binds to the antigen binding domain of the Ig HC would imply that in $VpreB^+LC^+$ B cells the binding of VpreB to the Ig HC can mask the autoreactivity of the Ig HC and thus may interfere with the elimination of autoreactive B cells. Yet, it remains to be elucidated whether the binding of a SLC component can physically mask the true autoreactive potential of an Ig HC.

The silencing of the $VpreB^+LC^+$ B cells might be exclusively dependent on the VpreB protein or on the complete SLC complex. It has been shown that in the absence of λ5, the VpreB protein is able to pair *in vitro* to a number of Ig HCs [94, 95]. Nevertheless, the $VpreB^+LC^+$ B cells express, next to VpreB, low levels of λ5 mRNA, suggesting the possibility that they may co-express λ5 protein [75]. So, it is unclear whether silencing of $VpreB^+LC^+$ B cells is only dependent on surface expression of VpreB, or whether low amounts of λ5 protein support VpreB surface expression.

STUDYING THE ROLE OF SLC^+LC^+ B CELLS IN AUTOIMMUNITY

Various data from the $VpreB^+LC^+$ B cells in human, together with our findings in the SLC-Tg mouse model point to a role of dysregulated SLC expression in the development of auto-reactive B cells. The presence of significantly increased proportions of $VpreB^+LC^+$ B cells in the synovium of a fraction of RA patients suggests that the $VpreB^+LC^+$ B cells are involved in RA. However, because $VpreB^+LC^+$ B cells are also present in healthy individuals and the SLC-Tg mice did not spontaneously develop autoimmune pathology, under normal conditions these autoreactive B cells are apparently kept in check by self-tolerance mechanisms. We therefore hypothesized that $VpreB^+LC^+$ B cells might break through self-tolerance in an autoimmune prone condition to contribute to autoimmune pathology. To test this hypothesis we crossed the SLC-Tg models, expressing low or high levels of the SLC components, on two autoimmune prone genetic backgrounds, Eμ-Bcl2-Tg and Fc γ Receptor IIb-deficient ($FcγRIIb^{-/-}$) mice.

The Eμ-Bcl2-Tg mice [96] have B cell-specific overexpression of the anti-apoptotic protein Bcl2, which interferes with the formation of a self-tolerant BCR repertoire. Bcl2 overexpression allows autoreactive B cells, which are normally negatively selected, to escape self-tolerance mechanisms, resulting in an increasing pool of autoreactive B cells. We analyzed the effect the $λ5^{high}$-Tg, $VpreB^{high}$-Tg and $λ5^{high}$-$VpreB^{high}$ double-Tg and found that 10-week-old SLC^{high}-Tg;Eμ-Bcl2-Tg mice have an increased splenic pool of potential harmful activated SLC^+LC^+ B cells and Ig isotype-switched plasma cells, which may enhance autoimmunity (P.F. van Loo, unpublished results). Preliminary analyses suggest increased levels of autoreactive antibodies in the serum. The phenotype was also present – even more pronounced – in the $VpreB^{high}$-Tg;Eμ-Bcl2-Tg group (P.F. van Loo, unpublished results).

FcγRIIb-deficiency results in loss of self-tolerance, causing spontaneous development of systemic vasculitis, at the age of 4-5 months [47, 97-99]. The SLC-Tg mice on the FcγRIIb-

deficient background demonstrated a phenotype that was quite similar to SLC-Tg;Eμ-Bcl2-Tg mice. SLC^{high}-Tg;$Fc\gamma RIIb^{-/-}$mice displayed enhanced spontaneous GC formation, which was most pronounced in the $VpreB^{high}$ single Tg group. Analysis of 10-week old SLC^{low}-Tg;$Fc\gamma RIIb^{-/-}$ mice revealed that exclusively the $VpreB^{low}$ single Tg;$Fc\gamma RIIb^{-/-}$ mice had a ~5-10 fold increase in the number of IgG2a/$2b^{+}$ plasma cells. Interestingly, IgG2a/2b are the most pathogenic subclasses and activate both FcγRIII and IV [100]. Finally, we found that the onset of collagen induced arthritis [101] appeared to be accelerated in $VpreB^{high}$-Tg;$Fc\gamma RIIb^{-/-}$ mice, when compared with the $Fc\gamma RIIb^{-/-}$ group (P.F. Van Loo, unpublished results).

Taken together, analyses in SLC-Tg mice demonstrate that $SLC^{+}LC^{+}$ B cells can contribute to the etiology of autoimmune disease, as dysregulated expression of SLC components, in particular VpreB, can drive B cells in the direction of autoimmunity. As the identified SLC-expressing B cells in human express predominantly VpreB protein - and much lower levels of λ5 protein - , our data in the mouse support the hypothesis that persistent VpreB expression in human results in the formation of autoreactive $VpreB^{+}LC^{+}$ B cells.

CONCLUSION

To maintain self-tolerance, B cells expressing self-reactive Igs are eliminated by various central and peripheral mechanisms, like deletion, receptor editing and anergy. Nevertheless, the majority of $VpreB^{+}LC^{+}$ B cells present in human express self-reactive Igs, including true ANAs and polyreactive Igs, suggesting that expression of VpreB proteins parallels dual receptor expression in the mouse (Figure 2; Ref. [27]) and rescues self-reactive $VpreB^{+}LC^{+}$ B cells from deletion. Our preliminary characterization of the phenotype of VpreB transgenic mice on the autoimmune prone $Fc\gamma RIIb^{-/-}$ background, including (i) enhanced GC development, (ii) increased Ig class switched plasma cells, (iii) accelerated disease progression in collagen induced arthritis, indicates that $VpreB^{+}LC^{+}$ B cells contribute to autoimmune pathology. At the moment, it is unclear whether activation of $VpreB^{+}LC^{+}$ B cells and their subsequent differentiation into antibody producing cells precedes or establishes the onset of autoimmunity, or whether it simply reflects the breakdown of B cell tolerance once the autoimmune disease has developed. Understanding the details of autoreactive B cell regulation may improve the management of autoimmune disease. As B-cell ablative therapy with anti-CD20 antibody, which efficiently depletes naive and memory B cells (but not long-lived plasma cells) is effective in patients with SLE and RA, it is attractive to develop strategies to specifically target $VpreB^{+}LC^{+}$ B cells.

ACKNOWLEDGMENTS

This work was partly supported by the Reumafonds grant DAA 08-1-103, the Dutch Cancer Foundation KWF/NKB grant EMCR 2006-3547 and AICR grant 04-343.

REFERENCES

[1] Sanz, I., J. H. Anolik, and R. J. Looney. 2007. B cell depletion therapy in autoimmune diseases. *Front Biosci.* 12:2546-2567.

[2] Yurasov, S., H. Wardemann, J. Hammersen, M. Tsuiji, E. Meffre, V. Pascual, and M. C. Nussenzweig. 2005. Defective B cell tolerance checkpoints in systemic lupus erythematosus. *The Journal of experimental medicine* 201:703-711.

[3] Samuels, J., Y. S. Ng, C. Coupillaud, D. Paget, and E. Meffre. 2005. Impaired early B cell tolerance in patients with rheumatoid arthritis. *The Journal of experimental medicine* 201:1659-1667.

[4] Wardemann, H., S. Yurasov, A. Schaefer, J. W. Young, E. Meffre, and M. C. Nussenzweig. 2003. Predominant autoantibody production by early human B cell precursors. *Science* 301:1374-1377.

[5] Shlomchik, M. J. 2008. Sites and Stages of Autoreactive B Cell Activation and Regulation. *Immunity* 28:18-26.

[6] Schlissel, M. S. 2003. Regulating antigen-receptor gene assembly. *Nat. Rev. Immunol.* 3:890-899.

[7] Jung, D., C. Giallourakis, R. Mostoslavsky, and F. W. Alt. 2006. Mechanism and control of V(D)J recombination at the immunoglobulin heavy chain locus. *Annual review of immunology* 24:541-570.

[8] Sakaguchi, N., and F. Melchers. 1986. Lambda 5, a new light-chain-related locus selectively expressed in pre-B lymphocytes. *Nature* 324:579-582.

[9] Kudo, A., and F. Melchers. 1987. A second gene, VpreB in the lambda 5 locus of the mouse, which appears to be selectively expressed in pre-B lymphocytes. *Embo. J.* 6:2267-2272.

[10] Karasuyama, H., A. Kudo, and F. Melchers. 1990. The proteins encoded by the VpreB and lambda 5 pre-B cell-specific genes can associate with each other and with mu heavy chain. *J. Exp. Med.* 172:969-972.

[11] Tsubata, T., and M. Reth. 1990. The products of pre-B cell-specific genes (lambda 5 and VpreB) and the immunoglobulin mu chain form a complex that is transported onto the cell surface. *J. Exp. Med.* 172:973-976.

[12] Hendriks, R. W., and S. Middendorp. 2004. The pre-BCR checkpoint as a cell-autonomous proliferation switch. *Trends Immunol.* 25:249-256.

[13] Melchers, F. 2005. The pre-B-cell receptor: selector of fitting immunoglobulin heavy chains for the B-cell repertoire. *Nat .Rev. Immunol.* 5:578-584.

[14] Martensson, I. L., R. A. Keenan, and S. Licence. 2007. The pre-B-cell receptor. *Current opinion in immunology* 19:137-142.

[15] Nemazee, D. 1995. Does immunological tolerance explain the waste in the B-lymphocyte immune system? Experiment and theory. *Annals of the New York Academy of Sciences* 764:397-401.

[16] ten Boekel, E., F. Melchers, and A. G. Rolink. 1998. Precursor B cells showing H chain allelic inclusion display allelic exclusion at the level of pre-B cell receptor surface expression. *Immunity* 8:199-207.

[17] Keenan, R. A., A. De Riva, B. Corleis, L. Hepburn, S. Licence, T. H. Winkler, and I. L. Martensson. 2008. Censoring of autoreactive B cell development by the pre-B cell receptor. *Science (New York, N.Y* 321:696-699.

[18] Minegishi, Y., and M. E. Conley. 2001. Negative selection at the pre-BCR checkpoint elicited by human mu heavy chains with unusual CDR3 regions. *Immunity* 14:631-641.

[19] Lesley, R., Y. Xu, S. L. Kalled, D. M. Hess, S. R. Schwab, H. B. Shu, and J. G. Cyster. 2004. Reduced competitiveness of autoantigen-engaged B cells due to increased dependence on BAFF. *Immunity* 20:441-453.

[20] Thien, M., T. G. Phan, S. Gardam, M. Amesbury, A. Basten, F. Mackay, and R. Brink. 2004. Excess BAFF rescues self-reactive B cells from peripheral deletion and allows them to enter forbidden follicular and marginal zone niches. *Immunity* 20:785-798.

[21] Nemazee, D. A., and K. Burki. 1989. Clonal deletion of B lymphocytes in a transgenic mouse bearing anti-MHC class I antibody genes. *Nature* 337:562-566.

[22] Tiegs, S. L., D. M. Russell, and D. Nemazee. 1993. Receptor editing in self-reactive bone marrow B cells. *The Journal of experimental medicine* 177:1009-1020.

[23] Gay, D., T. Saunders, S. Camper, and M. Weigert. 1993. Receptor editing: an approach by autoreactive B cells to escape tolerance. *J. Exp. Med.* 177:999-1008.

[24] Vela, J. L., D. Ait-Azzouzene, B. H. Duong, T. Ota, and D. Nemazee. 2008. Rearrangement of mouse immunoglobulin kappa deleting element recombining sequence promotes immune tolerance and lambda B cell production. *Immunity* 28:161-170.

[25] Retter, M. W., and D. Nemazee. 1998. Receptor editing occurs frequently during normal B cell development. *The Journal of experimental medicine* 188:1231-1238.

[26] Casellas, R., T. A. Shih, M. Kleinewietfeld, J. Rakonjac, D. Nemazee, K. Rajewsky, and M. C. Nussenzweig. 2001. Contribution of receptor editing to the antibody repertoire. *Science (New York, N.Y* 291:1541-1544.

[27] Li, Y., H. Li, and M. Weigert. 2002. Autoreactive B cells in the marginal zone that express dual receptors. *J. Exp. Med* .195:181-188.

[28] Liu, S., M. G. Velez, J. Humann, S. Rowland, F. J. Conrad, R. Halverson, R. M. Torres, and R. Pelanda. 2005. Receptor editing can lead to allelic inclusion and development of B cells that retain antibodies reacting with high avidity autoantigens. *J. Immunol.* 175:5067-5076.

[29] Casellas, R., Q. Zhang, N. Y. Zheng, M. D. Mathias, K. Smith, and P. C. Wilson. 2007. Igkappa allelic inclusion is a consequence of receptor editing. *J. Exp. Med.* 204:153-160.

[30] Merrell, K. T., R. J. Benschop, S. B. Gauld, K. Aviszus, D. Decote-Ricardo, L. J. Wysocki, and J. C. Cambier. 2006. Identification of anergic B cells within a wild-type repertoire. *Immunity* 25:953-962.

[31] Nemazee, D. 2006. Receptor editing in lymphocyte development and central tolerance. *Nat. Rev. Immunol.* 6:728-740.

[32] Stadanlick, J. E., and M. P. Cancro. 2008. BAFF and the plasticity of peripheral B cell tolerance. *Current opinion in immunology* 20:158-161.

[33] Gauld, S. B., R. J. Benschop, K. T. Merrell, and J. C. Cambier. 2005. Maintenance of B cell anergy requires constant antigen receptor occupancy and signaling. *Nature immunology* 6:1160-1167.

[34] Cambier, J. C., S. B. Gauld, K. T. Merrell, and B. J. Vilen. 2007. B-cell anergy: from transgenic models to naturally occurring anergic B cells? *Nat. Rev. Immunol.* 7:633-643.

[35] Mandik-Nayak, L., S. J. Seo, C. Sokol, K. M. Potts, A. Bui, and J. Erikson. 1999. MRL-lpr/lpr mice exhibit a defect in maintaining developmental arrest and follicular exclusion of anti-double-stranded DNA B cells. *J. Exp. Med.* 189:1799-1814.

[36] Culton, D. A., B. P. O'Conner, K. L. Conway, R. Diz, J. Rutan, B. J. Vilen, and S. H. Clarke. 2006. Early preplasma cells define a tolerance checkpoint for autoreactive B cells. *J. Immunol.* 176:790-802.

[37] Lopes-Carvalho, T., and J. F. Kearney. 2004. Development and selection of marginal zone B cells. *Immunol. Rev.* 197:192-205.

[38] Wang, X., W. Huang, L. E. Schiffer, M. Mihara, A. Akkerman, K. Hiromatsu, and A. Davidson. 2003. Effects of anti-CD154 treatment on B cells in murine systemic lupus erythematosus. *Arthritis and rheumatism* 48:495-506.

[39] Kalled, S. L., A. H. Cutler, S. K. Datta, and D. W. Thomas. 1998. Anti-CD40 ligand antibody treatment of SNF1 mice with established nephritis: preservation of kidney function. *J. Immunol.* 160:2158-2165.

[40] Seo, S. J., M. L. Fields, J. L. Buckler, A. J. Reed, L. Mandik-Nayak, S. A. Nish, R. J. Noelle, L. A. Turka, F. D. Finkelman, A. J. Caton, and J. Erikson. 2002. The impact of T helper and T regulatory cells on the regulation of anti-double-stranded DNA B cells. *Immunity* 16:535-546.

[41] Singh, R. R., F. M. Ebling, D. A. Albuquerque, V. Saxena, V. Kumar, E. H. Giannini, T. N. Marion, F. D. Finkelman, and B. H. Hahn. 2002. Induction of autoantibody production is limited in nonautoimmune mice. *J. Immunol.* 169:587-594.

[42] Fields, M. L., B. D. Hondowicz, M. H. Metzgar, S. A. Nish, G. N. Wharton, C. C. Picca, A. J. Caton, and J. Erikson. 2005. CD4+ CD25+ regulatory T cells inhibit the maturation but not the initiation of an autoantibody response. *J. Immunol.* 175:4255-4264.

[43] Tiller, T., M. Tsuiji, S. Yurasov, K. Velinzon, M. C. Nussenzweig, and H. Wardemann. 2007. Autoreactivity in human IgG+ memory B cells. *Immunity* 26:205-213.

[44] Hsu, H. C., Y. Wu, P. Yang, Q. Wu, G. Job, J. Chen, J. Wang, M. A. Accavitti-Loper, W. E. Grizzle, R. H. Carter, and J. D. Mountz. 2007. Overexpression of activation-induced cytidine deaminase in B cells is associated with production of highly pathogenic autoantibodies. *J. Immunol.* 178:5357-5365.

[45] Mietzner, B., M. Tsuiji, J. Scheid, K. Velinzon, T. Tiller, K. Abraham, J. B. Gonzalez, V. Pascual, D. Stichweh, H. Wardemann, and M. C. Nussenzweig. 2008. Autoreactive IgG memory antibodies in patients with systemic lupus erythematosus arise from nonreactive and polyreactive precursors. *Proceedings of the National Academy of Sciences of the United States of America* 105:9727-9732.

[46] Hibbs, M. L., D. M. Tarlinton, J. Armes, D. Grail, G. Hodgson, R. Maglitto, S. A. Stacker, and A. R. Dunn. 1995. Multiple defects in the immune system of Lyn-deficient mice, culminating in autoimmune disease. *Cell* 83:301-311.

[47] Bolland, S., and J. V. Ravetch. 2000. Spontaneous autoimmune disease in Fc(gamma)RIIB-deficient mice results from strain-specific epistasis. *Immunity* 13:277-285.

[48] Nishimura, H., M. Nose, H. Hiai, N. Minato, and T. Honjo. 1999. Development of lupus-like autoimmune diseases by disruption of the PD-1 gene encoding an ITIM motif-carrying immunoreceptor. *Immunity* 11:141-151.

[49] Nimmerjahn, F., and J. V. Ravetch. 2007. Fc-receptors as regulators of immunity. *Adv. Immunol.* 96:179-204.

[50] Tarasenko, T., J. A. Dean, and S. Bolland. 2007. FcgammaRIIB as a modulator of autoimmune disease susceptibility. *Autoimmunity* 40:409-417.

[51] Thomas, J. D., P. Sideras, C. I. Smith, I. Vorechovsky, V. Chapman, and W. E. Paul. 1993. Colocalization of X-linked agammaglobulinemia and X-linked immunodeficiency genes. *Science* 261:355-358.

[52] Vetrie, D., I. Vorechovsky, P. Sideras, J. Holland, A. Davies, F. Flinter, L. Hammarstrom, C. Kinnon, R. Levinsky, M. Bobrow, and et al. 1993. The gene involved in X-linked agammaglobulinaemia is a member of the src family of protein-tyrosine kinases. *Nature* 361:226-233.

[53] Conley, M. E. 1985. B cells in patients with X-linked agammaglobulinemia. *J. Immunol.* 134:3070-3074.

[54] Nomura, K., H. Kanegane, H. Karasuyama, S. Tsukada, K. Agematsu, G. Murakami, S. Sakazume, M. Sako, R. Tanaka, Y. Kuniya, T. Komeno, S. Ishihara, K. Hayashi, T. Kishimoto, and T. Miyawaki. 2000. Genetic defect in human X-linked agammaglobulinemia impedes a maturational evolution of pro-B cells into a later stage of pre-B cells in the B-cell differentiation pathway. *Blood* 96:610-617.

[55] Ng, Y. S., H. Wardemann, J. Chelnis, C. Cunningham-Rundles, and E. Meffre. 2004. Bruton's tyrosine kinase is essential for human B cell tolerance. *J. Exp. Med.* 200:927-934.

[56] Fu, J. L., S. D. Shyur, H. Y. Lin, and Y. C. Lai. 1999. X-linked agammaglobulinemia presenting as juvenile chronic arthritis: report of one case. *Acta paediatrica Taiwanica = Taiwan er ke yi xue hui za zhi* 40:280-283.

[57] Martin, S., D. Wolf-Eichbaum, G. Duinkerken, W. A. Scherbaum, H. Kolb, J. G. Noordzij, and B. O. Roep. 2001. Development of type 1 diabetes despite severe hereditary B-lymphocyte deficiency. *The New England journal of medicine* 345:1036-1040.

[58] Verbruggen, G., S. De Backer, D. Deforce, P. Demetter, C. Cuvelier, E. Veys, and D. Elewaut. 2005. X linked agammaglobulinaemia and rheumatoid arthritis. *Annals of the rheumatic diseases* 64:1075-1078.

[59] Kuhn, K. A., L. Kulik, B. Tomooka, K. J. Braschler, W. P. Arend, W. H. Robinson, and V. M. Holers. 2006. Antibodies against citrullinated proteins enhance tissue injury in experimental autoimmune arthritis. *J. Clin. Invest.* 116:961-973.

[60] Schellekens, G. A., H. Visser, B. A. de Jong, F. H. van den Hoogen, J. M. Hazes, F. C. Breedveld, and W. J. van Venrooij. 2000. The diagnostic properties of rheumatoid arthritis antibodies recognizing a cyclic citrullinated peptide. *Arthritis Rheum.* 43:155-163.

[61] Smeenk, R., K. Brinkman, H. van den Brink, R. M. Termaat, J. Berden, H. Nossent, and T. Swaak. 1990. Antibodies to DNA in patients with systemic lupus erythematosus. Their role in the diagnosis, the follow-up and the pathogenesis of the disease. *Clinical rheumatology* 9:100-110.

[62] Shmerling, R. H., and T. L. Delbanco. 1991. The rheumatoid factor: an analysis of clinical utility. *The American journal of medicine* 91:528-534.

[63] Solomon, B. 2002. Anti-aggregating antibodies, a new approach towards treatment of conformational diseases. *Current medicinal chemistry* 9:1737-1749.

[64] Harley, J. B., E. L. Alexander, W. B. Bias, O. F. Fox, T. T. Provost, M. Reichlin, H. Yamagata, and F. C. Arnett. 1986. Anti-Ro (SS-A) and anti-La (SS-B) in patients with Sjogren's syndrome. *Arthritis and rheumatism* 29:196-206.

[65] Phan, T. G., R. C. Wong, and S. Adelstein. 2002. Autoantibodies to extractable nuclear antigens: making detection and interpretation more meaningful. *Clinical and diagnostic laboratory immunology* 9:1-7.

[66] Bensimon, C., P. Chastagner, and M. Zouali. 1994. Human lupus anti-DNA autoantibodies undergo essentially primary V kappa gene rearrangements. *The EMBO journal* 13:2951-2962.

[67] Dorner, T., S. J. Foster, N. L. Farner, and P. E. Lipsky. 1998. Immunoglobulin kappa chain receptor editing in systemic lupus erythematosus. *J. Clin. Invest.* 102:688-694.

[68] Leadbetter, E. A., I. R. Rifkin, A. M. Hohlbaum, B. C. Beaudette, M. J. Shlomchik, and A. Marshak-Rothstein. 2002. Chromatin-IgG complexes activate B cells by dual engagement of IgM and Toll-like receptors. *Nature* 416:603-607.

[69] Lau, C. M., C. Broughton, A. S. Tabor, S. Akira, R. A. Flavell, M. J. Mamula, S. R. Christensen, M. J. Shlomchik, G. A. Viglianti, I. R. Rifkin, and A. Marshak-Rothstein. 2005. RNA-associated autoantigens activate B cells by combined B cell antigen receptor/Toll-like receptor 7 engagement. *The Journal of experimental medicine* 202:1171-1177.

[70] Vinuesa, C. G., and C. C. Goodnow. 2002. Immunology: DNA drives autoimmunity. *Nature* 416:595-598.

[71] Christensen, S. R., J. Shupe, K. Nickerson, M. Kashgarian, R. A. Flavell, and M. J. Shlomchik. 2006. Toll-like receptor 7 and TLR9 dictate autoantibody specificity and have opposing inflammatory and regulatory roles in a murine model of lupus. *Immunity* 25:417-428.

[72] O'Keefe, T. L., G. T. Williams, F. D. Batista, and M. S. Neuberger. 1999. Deficiency in CD22, a B cell-specific inhibitory receptor, is sufficient to predispose to development of high affinity autoantibodies. *J. Exp. Med.* 189:1307-1313.

[73] Pao, L. I., K. P. Lam, J. M. Henderson, J. L. Kutok, M. Alimzhanov, L. Nitschke, M. L. Thomas, B. G. Neel, and K. Rajewsky. 2007. B cell-specific deletion of protein-tyrosine phosphatase shp1 promotes B-1a cell development and causes systemic autoimmunity. *Immunity* 27:35-48.

[74] Meffre, E., M. Chiorazzi, and M. C. Nussenzweig. 2001. Circulating human B cells that express surrogate light chains display a unique antibody repertoire. *J. Immunol.* 167:2151-2156.

[75] Meffre, E., E. Davis, C. Schiff, C. Cunningham-Rundles, L. B. Ivashkiv, L. M. Staudt, J. W. Young, and M. C. Nussenzweig. 2000. Circulating human B cells that express surrogate light chains and edited receptors. *Nat. Immunol.* 1:207-213.

[76] Meffre, E., A. Schaefer, H. Wardemann, P. Wilson, E. Davis, and M. C. Nussenzweig. 2004. Surrogate light chain expressing human peripheral B cells produce self-reactive antibodies. *J. Exp. Med.* 199:145-150.

[77] Meixlsperger, S., F. Kohler, T. Wossning, M. Reppel, M. Muschen, and H. Jumaa. 2007. Conventional light chains inhibit the autonomous signaling capacity of the B cell receptor. *Immunity* 26:323-333.

[78] Thompson, E. C., B. S. Cobb, P. Sabbattini, S. Meixlsperger, V. Parelho, D. Liberg, B. Taylor, N. Dillon, K. Georgopoulos, H. Jumaa, S. T. Smale, A. G. Fisher, and M. Merkenschlager. 2007. Ikaros DNA-binding proteins as integral components of B cell developmental-stage-specific regulatory circuits. *Immunity* 26:335-344.

[79] Ichiyoshi, Y., and P. Casali. 1994. Analysis of the structural correlates for antibody polyreactivity by multiple reassortments of chimeric human immunoglobulin heavy and light chain V segments. *J. Exp. Med.* 180:885-895.

[80] Bridges, S. L., Jr., S. K. Lee, M. L. Johnson, J. C. Lavelle, P. G. Fowler, W. J. Koopman, and H. W. Schroeder, Jr. 1995. Somatic mutation and CDR3 lengths of immunoglobulin kappa light chains expressed in patients with rheumatoid arthritis and in normal individuals. *J. Clin .Invest.* 96:831-841.

[81] Crouzier, R., T. Martin, and J. L. Pasquali. 1995. Heavy chain variable region, light chain variable region, and heavy chain CDR3 influences on the mono- and polyreactivity and on the affinity of human monoclonal rheumatoid factors. *J. Immunol.* 154:4526-4535.

[82] van Loo, P. F., G. M. Dingjan, A. Maas, and R. W. Hendriks. 2007. Surrogate-light-chain silencing is not critical for the limitation of pre-B cell expansion but is for the termination of constitutive signaling. *Immunity* 27:468-480.

[83] Tze, L. E., B. R. Schram, K. P. Lam, K. A. Hogquist, K. L. Hippen, J. Liu, S. A. Shinton, K. L. Otipoby, P. R. Rodine, A. L. Vegoe, M. Kraus, R. R. Hardy, M. S. Schlissel, K. Rajewsky, and T. W. Behrens. 2005. Basal immunoglobulin signaling actively maintains developmental stage in immature B cells. *PLoS Biol.* 3:e82.

[84] Hayakawa, K., M. Asano, S. A. Shinton, M. Gui, D. Allman, C. L. Stewart, J. Silver, and R. R. Hardy. 1999. Positive selection of natural autoreactive B cells. *Science* 285:113-116.

[85] Wen, L., J. Brill-Dashoff, S. A. Shinton, M. Asano, R. R. Hardy, and K. Hayakawa. 2005. Evidence of marginal-zone B cell-positive selection in spleen. *Immunity* 23:297-308.

[86] Lam, K. P., R. Kuhn, and K. Rajewsky. 1997. In vivo ablation of surface immunoglobulin on mature B cells by inducible gene targeting results in rapid cell death. *Cell* 90:1073-1083.

[87] Ohnishi, K., and F. Melchers. 2003. The nonimmunoglobulin portion of lambda5 mediates cell-autonomous pre-B cell receptor signaling. *Nat. Immunol.* 4:849-856.

[88] Huang, H., J. F. Kearney, M. J. Grusby, C. Benoist, and D. Mathis. 2006. Induction of tolerance in arthritogenic B cells with receptors of differing affinity for self-antigen. *Proc. Natl. Acad. Sci. U S A* 103:3734-3739.

[89] Roark, J. H., A. Bui, K. A. Nguyen, L. Mandik, and J. Erikson. 1997. Persistence of functionally compromised anti-double-stranded DNA B cells in the periphery of non-autoimmune mice. *International immunology* 9:1615-1626.

[90] Nguyen, K. A., L. Mandik, A. Bui, J. Kavaler, A. Norvell, J. G. Monroe, J. H. Roark, and J. Erikson. 1997. Characterization of anti-single-stranded DNA B cells in a non-autoimmune background. *J. Immunol.* 159:2633-2644.

[91] Russell, D. M., Z. Dembic, G. Morahan, J. F. Miller, K. Burki, and D. Nemazee. 1991. Peripheral deletion of self-reactive B cells. *Nature* 354:308-311.

[92] Bankovich, A. J., S. Raunser, Z. S. Juo, T. Walz, M. M. Davis, and K. C. Garcia. 2007. Structural insight into pre-B cell receptor function. *Science* 316:291-294.

[93] Xu, L., H. Yee, C. Chan, A. K. Kashyap, L. Horowitz, M. Horowitz, R. R. Bhatt, and R. A. Lerner. 2008. Combinatorial surrobody libraries. *Proc. Natl. Acad. Sci. U S A* 105:10756-10761.

[94] Seidl, T., A. Rolink, and F. Melchers. 2001. The VpreB protein of the surrogate light-chain can pair with some mu heavy-chains in the absence of the lambda 5 protein. *Eur. J. Immunol.* 31:1999-2006.

[95] Minegishi, Y., L. M. Hendershot, and M. E. Conley. 1999. Novel mechanisms control the folding and assembly of lambda5/14.1 and VpreB to produce an intact surrogate light chain. *Proc. Natl. Acad. Sci. U S A* 96:3041-3046.

[96] Strasser, A., S. Whittingham, D. L. Vaux, M. L. Bath, J. M. Adams, S. Cory, and A. W. Harris. 1991. Enforced BCL2 expression in B-lymphoid cells prolongs antibody responses and elicits autoimmune disease. *Proc. Natl. Acad. Sci .U S A* 88:8661-8665.

[97] Bolland, S., Y. S. Yim, K. Tus, E. K. Wakeland, and J. V. Ravetch. 2002. Genetic modifiers of systemic lupus erythematosus in FcgammaRIIB(-/-) mice. *J. Exp. Med.* 195:1167-1174.

[98] Nakamura, A., T. Yuasa, A. Ujike, M. Ono, T. Nukiwa, J. V. Ravetch, and T. Takai. 2000. Fcgamma receptor IIB-deficient mice develop Goodpasture's syndrome upon immunization with type IV collagen: a novel murine model for autoimmune glomerular basement membrane disease. *J. Exp. Med.* 191:899-906.

[99] Yuasa, T., S. Kubo, T. Yoshino, A. Ujike, K. Matsumura, M. Ono, J. V. Ravetch, and T. Takai. 1999. Deletion of fcgamma receptor IIB renders H-2(b) mice susceptible to collagen-induced arthritis. *J. Exp. Med.* 189:187-194.

[100] Baudino, L., S. Azeredo da Silveira, M. Nakata, and S. Izui. 2006. Molecular and cellular basis for pathogenicity of autoantibodies: lessons from murine monoclonal autoantibodies. *Springer seminars in immunopathology* 28:175-184.

[101] Lubberts, E., L. A. Joosten, M. Chabaud, L. van Den Bersselaar, B. Oppers, C. J. Coenen-De Roo, C. D. Richards, P. Miossec, and W. B. van Den Berg. 2000. IL-4 gene therapy for collagen arthritis suppresses synovial IL-17 and osteoprotegerin ligand and prevents bone erosion. *J. Clin. Invest.* 105:1697-1710.

In: Biochemistry and Histocytochemistry… ISBN: 978-1-60876-283-5
Editors: S. Fuchs, M. Auer, pp. 181-273 © 2010 Nova Science Publishers, Inc.

Chapter 10

UNIQUE ENZYMES OF ASPERGILLUS FUNGI USED IN JAPANESE BIOINDUSTRIES

Eiji Ichishima[1]*
Laboratory of Molecular Enzymology, Graduate School of Bioengineering,
Soka University, Tokyo, Japan

1. INTRODUCTION

The most widely used organisms are fungi, and several enzymes and organic acids are synthesized by species of *Aspergillus*. Over than the past 1,000 years the use of hydrolytic enzymes from fungi has become more prevalent in Japanese fermentation industries. The molds *Aspergillus oryzae* (Figure 1), *A. sojae*, *A. awamori*, and *A. saitoi* are of great practical importance in the fermentation industries, enzyme technologies, food industries, and civilization in Japan [1, 2]. In the eastern world rice is used instead of malt or mashed grapes for fermentation. Here a mold, usually *A. oryzae*, initiates the fermentation process by hydrolyzing rice starch to fermentable sugars. Later on the sugar is converted to change by spontaneous fermentation by either yeast or bacteria leading to products such as ‘Sake’, Japanese rice wine [3]. Other examples of the traditional use of fungi in food production are in the making of soy sauce and miso paste. In the fermented vegetable protein, soy sauce, the cooked soybeans are mixed with equal amounts of roasted wheat and then inoculated with a pure cultured ‘Koji’ starter or ‘seed mold’ [4].

Another important field for the early industrial application of fungi was the production of enzymes, and enzymes are now being used in a wide variety of processes. The invention and production of ‘Takadiastase’ for *A. oryzae* by Takamine J. in 1894 became an enzyme industry from the late nineteen century [5]. After Takadiastase was discovered it was produced in appreciable amounts during the Second World War, initially with *A. oryzae*, *A. sojae*, *A. awamori*, and *A. niger*. *Aspergillus saitoi*, which is a food microorganism, a black *Aspergillus* used in ‘Shochu’, a traditional Japanese spirit, was described taxonomically by Sakaguchi *et al*. [6]. An acid stable proteolytic enzyme ‘Molsin’ from *A. saitoi* produced on

1 Kasuya 3-15-17-101, Setagaya, Tokyo 157-0063, Japan, e-mail: ichie@cb3.so-net.ne.jp.

an industrial scale by us used in the preparation of a human digestant (Fujisawa Pharmaceutical Co., Osaka) [7, 8].

The genome of *Aspergillus oryzae* has been sequenced in 2005 [9]. The ability to secrete large amounts of proteins and the development of a transformation system have facilitated the use of *A. oryzae* in modern biotechnology. In 2006, the Brewing Society of Japan gave its seal of approval to the decision: '*Aspergillus oryzae* and related food *Aspergilli* are the national microorganisms of Japan'.

In this review, catalytic and molecular properties of unique and characteristic enzymes obtained from *Aspergillus* fungi used in Japanese bioindustries are described.

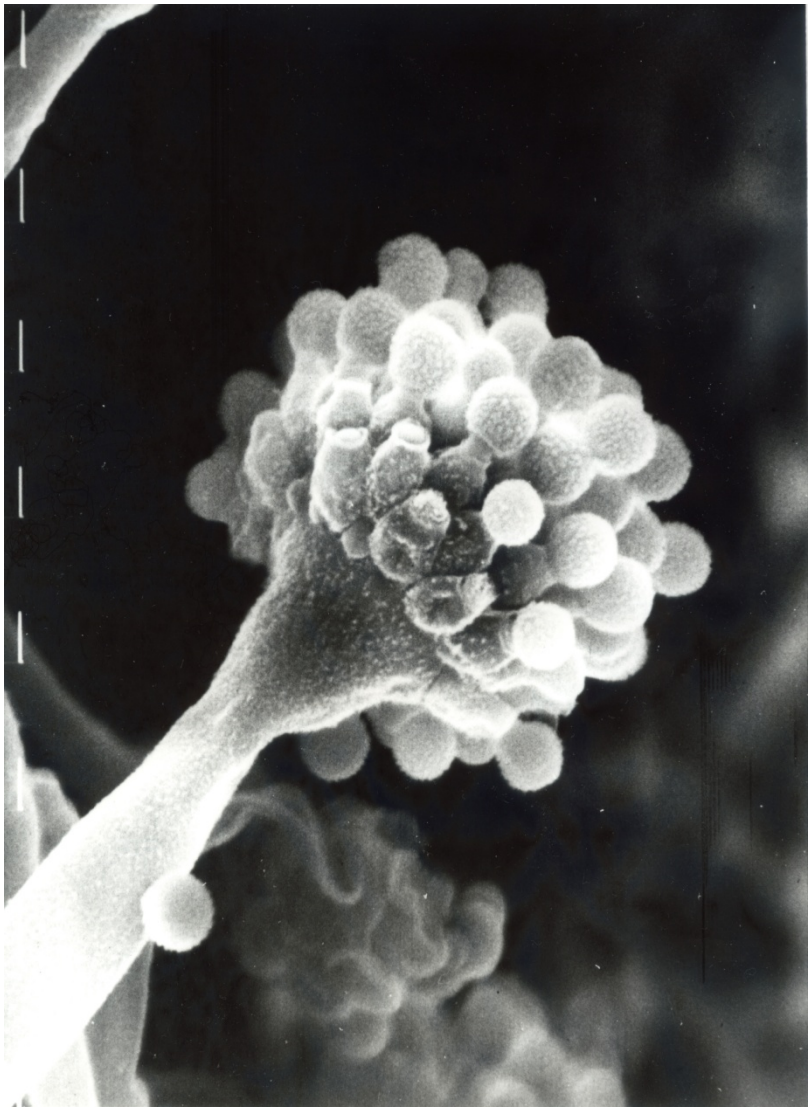

(Reproduced with kind permission of Dr. Kazuya Hayashi, Kikkoman Coop.)

Figure 1. Electronmicroscopic photograph of conidia, phialides, and conidiophore of the filamentous fungus Aspergillus oryzae.

2 THE THIRD ACTIVE SITE RESIDUE OF ASPARTIC PROTEINASE FROM *ASPERGILLUS* IS ESSENTIAL FOR TRYPSINOGEN ACTIVATION AT PH 3-4.5

2.1. Aspartic Proteinase

The aspartic proteinases (EC 3.4.23.−) from mammalian and fungi are all characterized by a molecular mass of 35,000, and pH optima for catalytic action in the range of 1.5-5.0. They include the mammalian enzymes, pepsin (EC 3.4.23.1), cathepsin D (EC 3.4.23.5), renin (EC 3.4.23.15), and chymosin (EC 3.4.23.4), and a number of fungal enzymes such as those from *Aspergillus saitoi* , *A. oryzae* and *A. sojae* (EC 3.4.23.18), *Penicillium janthienllum* (EC 3.4.23.20), *Rhizopus chinensis* (EC 3.4.23.21), and *Rhizomucor* (formerly *Mucor*) *pusillus* (EC 3.4.23.23), *Endothia parasitica* (EC 3.4.23.22), and a viral enzyme from a human immunodeficiency virus (HIV-I) (retropepsin, EC 3.4.23.16). They share the property of being inhibited by epoxy-compound, 1,2-epoxy-3-(*p*-nitrophenoxy)-propanne (EPNP), and by a diazonium compound, diazoacetyl-DL-norleucine-methylester (DAN), in the presence of Cu^{2+} ions.

Aspartic proteinases comprise a group of enzymes whose proteolytic activities are dependent on two aspartic acid residues, Asp32 and Asp215, in pepsin numbering ([10]. There is good evidence that most of them belong to a family of enzymes similar in sequence and structure. These enzymes are bilobal, each lobe having a similar fold, with a deep and extended cleft that can accommodate at least seven amino acid residues of substrate in the S_4-S_3' subsites [11]. The abbreviations used are: S_1, S_2, S_3, etc. and S_1', S_2', S_3', etc., corresponding subsites of the proteinase [12]; P_1, P_2, P_3, etc. and P_1', P_2', P_3', etc., amino acid residues of substrate on the amino-terminal and carboxyl sides of the scissile peptide bond, respectively. Each domain contributes one aspartyl residue, corresponding to Asp32 and Asp215 of pepsin, to the catalytic center of the extended binding site [13].

The 'flap', an antipararell β-hairpin comprising residues 73 to 83 [penicillopepsin [14] numbering], projects across the cleft forming a channel into which a substrate binds. Although the enzymes are quite similar in their three-dimensional structures, there are drastic differences in the catalytic properties, especially in substrate specificities. While, these enzymes show distinct preferences for cleaving the bonds between hydrophobic residues occupying the P_1-P_1' subsites. For example, renin [15] is characterized by very specific hydrolysis of angiotensin at Leu10-Leu11 and chymosin [16] digests *κ*-casein at Phe105-Met106 for milk clotting.

Thus, the differences in substrate specificity may be the result of alteration in the structure of substrate binding sites.

2.2. Aspergillopepsin I

An aspartic proteinase from *A. saitoi* ATCC 14332 (now designated *A. phoenicis* [17]), aspergillopepsin I (formerly aspergillopeptidase A), is a monomeric protein with a molecular mass of 34,302 Da [7, 8]. Aspergillopepsin I primarily hydrolyzes two bonds in the oxidized

B chain of insulin: Leu15-Tyr16 and Phe24-Phe25 [18]. Minor cleavages are noted at His10-Leu11, Ala14-Leu15 and Tyr16-Leu17.

Aspergillopepsin I favours hydrophobic residues at P_1 and P_1' [18, 19] but also accepts a Lys residue in the P_1 position, which leads to activation of trypsinogen by cleavage of the Lys6-Ile7 bond [20, 21]. Furthermore, penicillopepsin also has preference for a Lys residue in the P_1 position, which leads to activation of trypsinogen by cleavage of the Lys6-Ile7 bond [22]. The S_1 subsite is formed by several hydrophobic residues in the neighborhood of the catalytic Asp-32 and by the residues on the active site flap.

For trypsinogen activation, enteropeptidase (enterokinase, EC 3.4.21.9) [23] is a key enzyme for mammalian protein digestion. The selective cleavage site of trypsinogen by enteropeptidase initiates Lys6-Ile7 bond. Then trypsin (EC 3.4.21.4) activates other zymogens. Thus, the formation of trypsin by enteropeptidase is the master activation step.

Aspartic proteinases generally have broad primary specificity, but the fungal and mammalian enzymes can differ dramatically from each other in catalytic efficiency against substrates containing a Lys residue at P_1 position [24]. Based on the sequence alignment and structure of aspartic proteinases, the major differences in the S_1 subsite between the fungal and mammalian enzymes can be located at position [76 77] where the number in square brankets denotes penicillopepsin numbering] and 78 [79] on the active site flap (Table 1). These residues may be involved in the recognition of basic amino acid residues at the P_1 potition of substrates.

Aspergillopepsin I and the fungal aspartic proteinases, penicilllopepsin, rhizopuspepsin, and endothiapepsin, display significant similarities in their amino acid sequences. Although no three-dimentional structure of aspergillopepsin I is available, the substrate binding sites may be identical by analogy with those aspartic proteinases, penicillopepsin [14, 25, 26], endothiapepsin [27], and rhizopuspepsin [28].

Table 1. Comparison of the amino acid sequence of the active-site flap in the aspartic proteinase family

Aspartic proteinase 83	Residue number
Class I	
Aspergillopepsin I	WDISYG**D**G**S**SASGD
Penicillopepsin	WSISYG**D**G**S**SASGN
Rhizopuspepsin	WSISYG**D**G**S**SASGI
Endothiapepsin	WSISYG**D**G**S**SSSGD
Candidapepsin	FYIGYG**D**G**S**SSQGT
Class II	
Mucorpepsin	LNITYG**T**G-GANGI
Porcine pepsin	LSITYG**T**G-SMTGI
Human cathepsin D	FDIHYG**S**G-SLSGY

(Shintani,T. et al., J. Biochem. (Tokyo), 120, 974-981 (1996)).

The amino acid sequences of aspergillopepsin I, penicillopepsin, rhizopuspepsin, endothiapepsin, candidapepsin, mucorpepsin, porcine pepsin, and human cathepsin D are aligned. These enzymes are classified into two groups (class I and II). Class I enzymes have

the ability to activate trypsinogen and class II enzymes have no activity for trypsinogen activation. The mutated positions are indicated in boldface characters.

2.3. D76S-Aspergillopepsin I Abolished Trypsinogen Activation

We isolated and characterized its genomic DNA (D25318) and cDNA of aspergillopepsin I gene (*apnS*) and expressed it in yeast *S. cerevisiae* cells [29]. By altering a single substituted amino acid in aspergillopepsin I by site-directed mutagenesis to the corresponding residue in pepsin, renin, or chymosin, we obtained a mutant enzyme denoted D76S-aspergillopepsin I [29] in Figure 2. These mammalian aspartyl proteinases have no capacity of trypsinogen activation and have threonine residue instead of Asp76 in aspergillopepsin I. Expression products of mutant D76S-aspergillopepsin I and wild-type enzyme were observed by SDS-PAGE and Western blotting. These results strongly suggest that active D76S-aspergillopepsin I was secreted from the yeast cells harboring a plasmid designated to express prepro-D76S-aspergillopepsin I in the cells. The cultured filtrates of recombinant wild-type and mutant enzymes were isolated and were salted out with 60% $(NH_4)_2SO_4$. Then, the precipitates were dialyzed against 10 mM acetate buffer (pH 5.0). The activities of the two recombinant enzymes for casein hydrolysis [7] were 0.35 and 0.37 nkatal/ml, respectively. After activation of trypsinogen at pH 3.0, the fluorogenic activity of activated trypsin was measured at pH 8.0 with benzoyl-L-arginyl-4-methylcoumaryl-7-amide (Bz-Arg-MCA). Trypsinogen activating activity of the wild-type enzyme was determined to be $(1.08 \pm 0.03) \cdot 10^{-2}$ nkatal/ml, while none was found for the mutant enzyme.

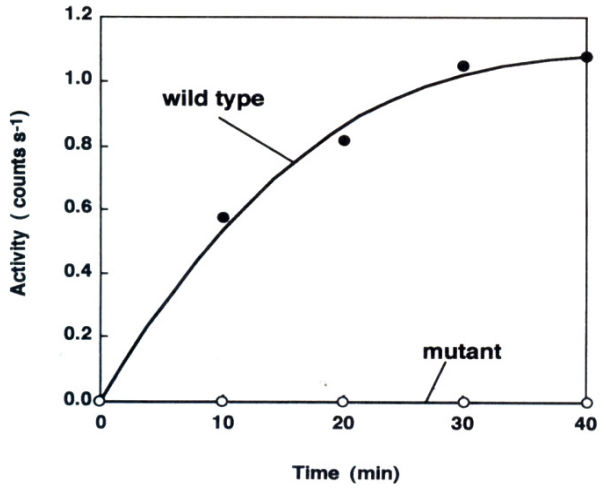

Figure 2. Activities of trypsinogen activation of the mutated D76S-aspergillopepsinI and aspergillopepsin I.

To explore the contribution of an unpaired charged residue to substrate binding and catalysis in the binding pocket of D76S-aspergillopepsin I, we were interested in how interaction of the ε-amino group of lysyl substrate, trypsinogen, affects the catalytic efficiency. As shown in Figure 2, the activity of D76S-aspergillopepsin I on trypsinogen was

completely abolished. Hydrolysis of casein sustrate by the D76S-aspergillopepsin I mutant is not altered within this pH range.

This suggests that the activity is quantitatively influenced by the electrostatic interaction between ε-amino group in the basic substrate of trypsinogen and acidic Asp76 in aspergillopepsin I.

Thus, we concluded that Asp76 is the binding site for the basic substrate, trypsinogen, and that a single amino acid mutation (Asp76 → Ser76) is sufficient to alter the substrate specificity of the enzyme for trypsinogen activation [29].

2.4. Characterization of the S_1 Subsite Specificity

In order to obtain further information about the primary specificity of aspergillopepsin I, we constructed an aspergillopepsin I expression system in *Escherichia coli*, prepared mutants at positions 76 and 78 of aspergillopepsin I by site-directed mutagenesis, and compared their molecular and enzymatic properties [30]. We showed that the nature of the active site flap is important for deciding the S_1 substrate specificity of aspartic proteinases [30].

For overexpression, the ATG codon was added in front of the putative pro-sequence of aspergillopepsin I cDNA by the PCR technique. The cDNA fragment was cloned into pET12a, and the resulting plasmid, pETAP was introduced into *E. coli* BL21 (DE3) cells. The cells harboring pETAP produced pro-aspergillopepsin I under the control of T7 promoter, and the enzyme was not active and was mostly insoluble. We therefore developed a procedure for the renaturation of recombinant pro-aspergillopepsin I into the correctly refolded zymogen, as described in "EXPERIMENTAL PROCEDURES" of the ref. [30]. The inclusion bodies were solubilized with 8 M urea, and dialyzed under alkaline pH. The active proenzyme was purified to homogeneity by two chromatography steps on a Toyopearl HW-55F column and a RESOURCE Q column. The purity of protein was judged by SDS-PAGE (Figure 3, lane 1). The yields of purified pro-aspergillopepsin I from inclusion bodies were routinely 10-20%. The amino acid sequence of the NH_2-terminal region was determined as Met-Ala-Pro-Ala-Pro-Thr-Arg-Lys-Gly-, identical to the expected from the construction. Pro-aspergillopepsin I was converted to the mature form within 5 min by incubating at pH 2.7, 0^oC (Figure 3, lane 3). The conversion was inhibitd by pepstatin, an aspartic proteinase inhibitor (Figure 3, lane 2). These results indicate that aspergillopepsin I was generated from pro-aspergillopepsin I by autoactivation.

Purified aspergillopepsin I was prepared from the crude pro-aspergillopepsin I preparation by acidification and subsequent chromatography on a RESOURCE Q column, and gave a single band on SDS-PAGE (Figure 3, lane 4). The NH_2-terminal sequence of recombinant aspergillopepsin I was found to be Glu-Ala-Ala-Ser-Lys-Gly-Ser-Ala-, which was three amino acid residues longer than that of native aspergillopepsin I from *Aspergillus saitoi* (Ser-Lys-Gly-Ser-Ala-). These results suggested that autocatalytic cleavage of the propeptide (Lys-Glu) may be occurring in front of glutamic acid and the product is terminated by aminopeptidase(s) in the fungal culture or that the activation of the zymogen *in vitro* may be basically different from that *in vivo*. In spite of the difference of NH_2-terminal sequences of the authentic and recombinant aspergillopepsin Is, these two enzymes were almost equal in specific activity for hydrolysis of casein (0.138 and 0.139 katal/kg, respectively) and kinetic

parameters for hydrolysis of a peptide substrate, Pro-Thr-Glu-Phe-Phe(4-NO_2)-Arg-Leu, at pH 3.0 (K_m = 0.01 mM and k_{cat} = 15.5 s^{-1} for both enzymes).

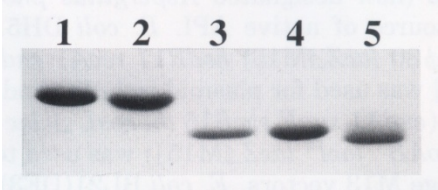

Figure 3. Conversion of proaspergilopepsin I to mature aspergillopepsin I.

The mutant aspergillopepsin Is were purified by the same method as the wild-type aspergillopepsin I. The purities of the enzymes were judged by SDS-PSGE. The mobilities of mutant aspergillopepsin Is were the same as that of the wild-type enzyme from *E. coli*. Furthermore, the effects of the maturation on the secondary structures of the enzymes were investigated by CD. The CD spectra (from 190 to 260 nm) of the enzymes were essentially identical, and contents of α-helix and β-structure of the wild-type and mutant enzymes were very similar. These results indicated that there was no significant conformational difference between the wild-type and mutant aspergillopepsin Is.

Table 2 shows a comparison of the specific activities of wild-type and mutant aspergillopepsin Is for the hydrolyses of casein, hemoglobin and the activation of bovine trypsinogen by cleaving the Lys6-Ile7 bond. The activity of trypsinogen activation fell below the detectable level in the D76S-mutant without any change in the proteinase activities for casein and hemoglobin. However, in the D76N-mutant both hydrolytic and trypsinogen activating activities were approximately half those of wild-type. In the D76E and S78A mutants there are significant decreases in the activity of trypsinogen activation, with very little effect on the proteinase activities for casein and hemoglobin. The catalytic activities of D76T and ΔS78 (deletion mutant) were generally decreased, but there were larger reductions in trypsinogen activating activity, as with D76S- and S78A-aspergillopepsin Is. These results strongly suggest that Asp76 [Asp77 in penicillopepsin numbering] and Ser78 of aspergillopepsin I play an important role in the recognition of the basic amino acid residue at the P_1 position.

The wild-type (19) and D76N-aspergillopepsin Is cleaved the Tyr4-Ile5 and His6-Pro7 bonds of angiotensin I (Asp-Arg-Val-Tyr-Ile-His-Pro-Phe-His-Leu), while only the Tyr4-Ile5 bond was hydrolyzed by D76E, D76S, D76T, S78A, and ΔS78 aspergillopepsin Is. Thus, the mutations of Asp76 and Ser78 caused changes in the substrate specificities of aspergillopepsin I, decreasing the affinity for basic residues at the P_1 position, and making the specificity more restrictive so that only hydrophobic residues are acceptable at the P_1 and P_1' position, as in mammalian aspartic proteinases.

To probe the effects of the mutations on specificity at the P_1 position, we used peptide substrates, Pro-Thr-Glu-Phe-Phe(4-NO_2)-Arg-Leu (PTEFF(4-NO_2)RL, 'peptide A'), Pro-Thr-Glu-Lys-Phe(4-NO_2)-Arg-Leu (PTEKF(4-NO_2)RL, 'peptide B'), and Ac-Ala-Ala-Lys-Phe(4-NO_2)-Ala-Ala-amide (Ac-AAKF(4-NO_2)AA-NH_2, 'peptide C'). Peptide A was cleaved Phe-Phe(4-NO_2) bond, which represents pepsin-like activity, and peptide B and peptide C were cleaved at the Lys-Phe(4-NO_2) bond, which is equivalent to trypsinogen activation. No other bond in these peptides was hydrolyzed by any of the enzymes. From kinetic determination of

the k_{cat}/K_m (catalytic efficiency) one can obtain the second-order rate constant for convertion of substrate to product.

Table 2. Specific activities of wild-type and mutant aspergillopepsin Is for the hydrolyses of casein and hemoglobin and the activation of bovine trypinogen

Mutant aspergillopepsin I	Specific activity		
	Casein (katal/kg)	Hemoglobin (katal/kg)	Trypsinogen activation (katal/kg)
Wild type	0.139 (100)	0.75 (100)	5.1 (100)
D76N	0.060 (43)	0.38 (51)	2.3 (45)
D76E	0.041 (29)	0.45 (60)	0.02 (0.4)
D76S	0.103 (74)	0.40 (53)	N.D.
D76T	0.023 (17)	0.12 (16)	N.D.
S78A	0.142 (102)	0.53 (71)	0.37 (7)
ΔS78	0.010 (7)	0.077(10)	N.D.

(Shintani,T. et al., J. Biochem. (Tokyo), 120, 974-981 (1996))

Proteolytic activities were assayed in 50 mM sodium acetate, pH 2.7, 1% casein or hemoglobin at 30°C. The activation of bovine trypsinogen was done with 5 mM trypsinogen in 50 mM sodium citrate, pH 3.0 at 30°C. Parentheses indicate the percentages of the activities of wild-type aspergillopepsin I.

Combining the effects due to substrate binding and transition state stabilization, this parameter is useful for assessing altered substrate specificity. Differences in $\log(k_{cat}/K_m)$ provide an accurate measure of the lowering of the transition state activation energy ($\Delta G_T^{\neq}$). The k_{cat}, K_m, and k_{cat}/K_m values were determined from the initial rate measurements and the results are listed in Table 3 and graphically represented in Figure 4.

The effects of individual mutations on the activity of aspergillopepsin I towards the substrate that contain Phe at P_1 were considerably less dramatic. The mutations at Asp76 and Ser78 led to a 2- to 30-fold lowering of k_{cat}/K_m compared to the wild-type aspergillopepsin I for this substrate. The decrease in k_{cat}/K_m was largely due to the effect of the mutation on K_m. There was a significant effect of the mutations on activity towards the substrate containing Lys at P_1. For peptide B, the D76E, D76S, D76T, and ΔS78 mutations caused 130-, 430-, 2,600-, and 650-fold decreases in k_{cat}/K_m value compared to the wild-type aspergillopepsin I, respectively, whereas the D76N mutant effectively hydrolyzed this substrate. Peptide B has the same sequence except for the substitution of P_1 Phe to Lys. The effect of each mutation on K_m was similar to that in the case of peptide A, indicating that the changes of K_m value caused by the mutation may be independent of the interaction with the P_1 side chain. The decreases in catalytic efficiencies mainly reflect decreases in k_{cat} for the Lys side chain of the substrate. The effects of each mutation on activity towards peptide C were similar to those in the case of peptide B, although there was no detectable cleavage with D76S and D76T mutant aspergillopepsin Is.

We have mutated the Asp76 [77, penicillopepsin numbering] and Ser78 [79] residues of aspergillopepsin I to test their roles in determining the primary specificity. These residues are conserved only in the enzymes with the ability to activate trypsinogen, such as penicillopepsin and rhizopuspepsin.

Table 3. Kinetic parameters for wild-type and mutant aspergillopepsin Is towards the peptide substrates containing phenylalanine or lysine residue at the P_1 position

Mutant aspergillopepsin I	K_m (mM)	k_{cat} (s^{-1})	k_{cat}/K_m ($mM^{-1} \cdot s^{-1}$)
PTEF↓F(4-NO_2)RL			
Wild type	0.007	15.7	2,240
D76N	0.010	8.3	830
D76E	0.057	10.9	191
D76S	0.061	10.8	177
D76T	0.073	5.9	81
S78A	0.017	20.3	1,190
ΔS78	0.107	10.8	101
PTEK↓F(4-NO_2)RL			
Wild type	0.009	4.5	500
D76N	0.027	3.2	119
D76E	0.050	0.20	4
D76S	0.034	0.040	1.2
D76T	0.065	0.014	0.2
S78A	0.017	0.61	36
ΔS78	0.046	0.036	0.8
Ac-AAK↓F(4-NO_2)AA-NH_2			
Wild type	0.092	6.8	74
D76N	0.103	3.5	34
D76E	0.171	0.039	0.2
D76S	ND		
D76T	ND		
S78A	0.130	0.93	7
ΔS78	0.094	0.001	0.01

Arrows (↓) indicate the scissible bonds.
ND, not ditected.
(Shintani,T. et al., J. Biochem. (Tokyo), 120, 974-981 (1996)).

Reactions were carried out in 0.1 M sodium acetate, pH 4.5 at 30°C. The kinetic parameters were determined from plots of initial rates *versus* substrate concentration (0.002-0.300 mM for all substrates).

The three-dimensional enzyme-inhibitor complex structutres have been analyzed for penicillopepsin and rhizopuspepsin. According to these analyses, the side-chain carboxylate and amide nitrogen of Asp77 are hydrogen bonded to P_2 amide nitrogen and carbonyl of the inhibitor, respectively, and there is a hydrogen bond between the P_2 carbonyl oxygen and amide nitrogen of Gly76 (Figure 5A). When a hydrophobic amino acid occupies the P_1 position of a ligand, the hydrophobic side chain is accommodated in the hydrophobic S_1

poket, which consists of Asp31, Tyr75, Phe112, and Leu121 [26, 28]. Three-dimentional structure of the penicillopepsin/Iva-Val-Val-LySta-OEt (Iva: isovaleryl; LySta: 4*S*,3*S*-4,8-diamino-3-hydroxyloctanoic acid) complex revealed that the ε-amino group of the LySta side chain forms a tight ion pair with the carboxylate of Asp77 and hydrogen bonds with the carboxylate of Asp77 and hydroxyl group of Ser79 (Figure 5A).

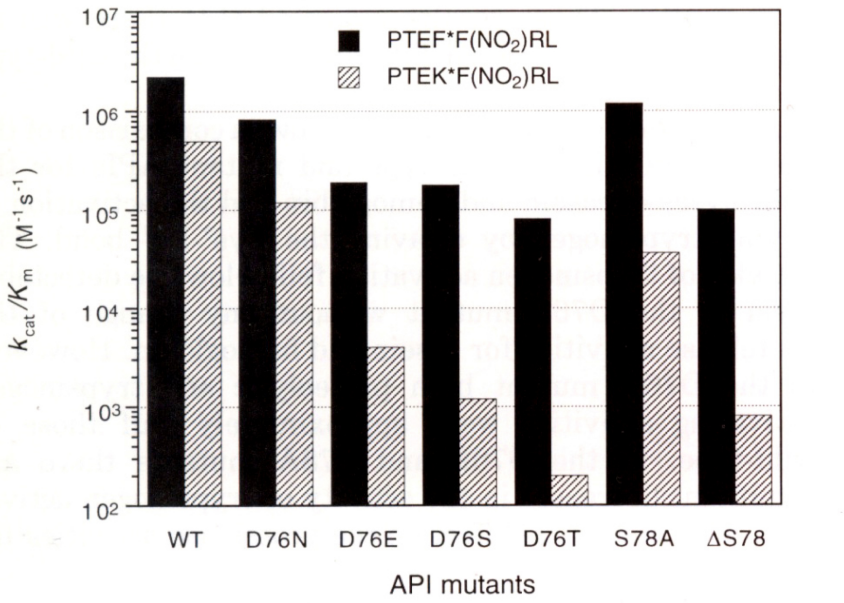

Figure 4. Catalytic efficiencies (kcat/Km) for mutant aspergillopepsin I against peptide substrates having Phe or Lys at the P1 positions.

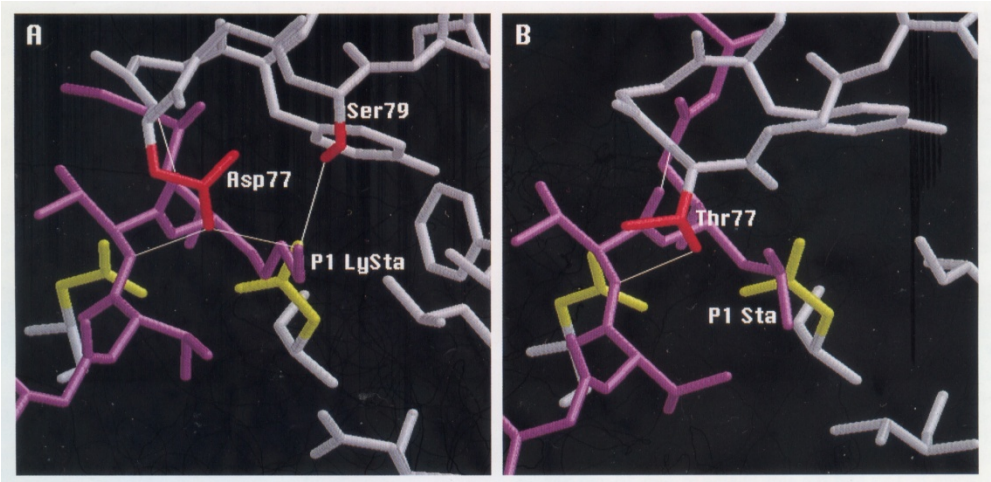

Figure 5. Representations of S_1 subsites of penicillopepsin (A) and porcine pepsin (B) with inhibitors.

We therefore altered Asp76 of aspergillopepsin I to Asn in order to replace the carboxyl group with an uncharged side chain very similar in size to that of Asp, and to Glu so that the

carboxyl group would retained but the effective distance to the side chian of the P_1 residue of a substrate would change. The substitution of Ser78 to Ala was made to examine the effect of hydrogen bonding on P_1 Lys specificity by the removal of the hydroxyl group of the Ser side chain.

The D76S and D76T substituted and Ser78 deleted (ΔS78) aspergillopepsin Is corresponding to mammalian aspartic proteinases were also constructed. The deletion of Ser78 (ΔS78) in aspergillopepsin I, corresponding to mammalian aspartic proteinases such as pepsin (Figure 5B), renin, and cathepsin D, would give rise to a shorter and warped flap, which may change the direction of the Asp76 side chain to bind to the main chain of the substrate and/or cause steric hindrance between the resulting flap and the ε–amino group of P_1 Lys. Thus, in the recognition of P_1 Lys of substrate, Asp76 [Asp77 in penicillopepsin numbering] and Ser78 of aspergillopepsin I appear to contribute complex by forming a hydrogen bond network between P_1 Lys and the side chain of Asp76 and Ser78, which may be supported by the unique flap structure of aspergillopepsin I.

Furthermore, Asp77 is shown to be the binding site to P_1 Lys in a substrate by crystallographic study of penicillopepsin [25, 26] and site-directed mutagenesis studies of rhizopuspepsin (31). Using the *S. cerevisiae* expression system, Tyr77 on the flap of mucorpepsin (32) has been shown to enhance catalytic efficiency of this fungal aspartic proteinase.

A comparison of the Michaelis-Menten kinetic parameters for the hydrolysis of peptide A and B by the site directed mutants of aspergillopepsin Is that Asp76 and Ser78 play important roles in aspergillopepsin I activity when substrates contain Lys at the P_1 position. The inhibition analysis of D77T mutated rhizopuspepsin using Lys-Pro-Ala-Ala-[X]-Ala-Leu-Gly-NH2, where [X] is LySta (4*S*,3*S*-4,8-diamino-3-hydroxyloctanoic acid) or As-LysSta, showed that rhizopuspepsin is able to bind substrate containing Lys at the P_1 position through the electrostatic interaction of Asp77 with P_1 Lys [31]. However, D76N mutant aspergillopepsin I retained sufficient activities towards peptides B and C containing Lys at the P_1 position, as well as trypsinogen activation, which indicated that that the negative charge of Asp76 may be dispensable for the recognition of P_1 Lys. On the basis of the data in Table 3, although the changes of K_m value by the mutations may be independent of the interaction with the P_1 side chain, the D76S, D76T, and Δ78 mutations result in large reductions in k_{cat} value *versus* the substrates containing Lys at the P_1 position. It appears that these residues on the active site flap have important roles in the stabilization of the transition state complex. This effect can be explained simply by one or both of the mechanisms: (i) a disturbance of the hydrogen bond network between P_1 Lys and the side chains of Asp76 and Ser78, and/or (ii) steric hindrance of substrate binding resulting from the change of flap structure. When D76S or D76T mutant aspergillopepsin I binds to a substrate containing Lys at the P_1 position, the hydroxyl group of Ser or Thr would be hydrogen bonded to P_2 amide nitrogen of the main chain as in mammalian enzyme (Figure 5 B) [33, 34], which may cause an alteration of the side-chain torsion angle of Ser or Thr in order to hydrogen bond to the substrate and disable this group from binding to the ε-amino group of P_1 Lys. The substitution of Ser-78 [79] to alanine removes the hydrogen bond between Ser78 and the ε-amino group of P_1 Lys. The deletion of Ser78 in aspergillopepsin I, corresponding to mammalian aspartic proteinases such as pepsin (Figure 5 B), renin and cathepsin D, would give rise to a shorter and warped flap, which may change the direction to the Asp76 side chain to bind to the main chain of the substrate and/or cause steric hindrance between the resulting flap and the ε-amino group of P_1

Lys. Thus, in the recognition of P_1 Lys of a substrate, Asp76 and Ser78 of aspergillopepsin I appear to contribute to the stabilization of the transition-state complex by forming a hydrogen bond network between P_1 Lys and the side chains of Asp76 and Ser78, which may be supported by the unique flap structure of aspergillopepsin I.

3 ENGINEERING OF PORCINE PEPSIN

3.1. Pepsin

Pepsin (EC 3.4.23.1) is a typical aspartic proteinase produced in the gastric mucosa of vertebrates as a zymogen form [10]. This enzyme has been extensively characterized, and its three-dimensional structure has been determined at high resolution. Porcine pepsin, in particular, has been studied as model to analyze the structure-function relationship of the aspartic proteinases. Although the aspartic proteinases including mammalian and fungal enzymes are quite similar in their three-dimentional structures, there are drastic differences in the catalytic properties, especially in substrate specificities.

There also have been many studies on the tertiary structures of aspartic proteinases with peptide-derived inhibitors, and the relationship between their structures and substrate specificities has been demonstrated. Although the hydrogen bonding pattern between the main chain of inhibitor and enzyme is well conserved in all inhibitor-enzyme complexes, the differences in the size of substrates, of which residues make van der Waals contacts with the side chain of inhibitor, may control the substrate specificities in aspartic proteinases. The attempts to examine the structural determinations of substrate specificities of aspergillopepsin I by site-directed mutagenesis have been made [29, 30]. And, Asp77 is shown to be the binding site to P_1 Lys in a substrate by crystallographic study of penicillopepsin [25, 26].

The present chapter described the investigation whether the active site flap controls the S_1 subsite specificity of aspartic proteinases, and for this we generated several mutants of porcine pepsin by site-directed mutagenesis and analyzed their enzymatic properties [35]. The substitution of Thr77 by Asp and the insertion of Ser between Gly78 and Ser79, corresponding to the fungal enzymes, conferred upon porcine pepsin the ability to hydrolyze the substrate containing a Lys residue at the P_1 position. These experiments provide positive evidence of the importance of the active site flap of aspartic proteinases in the S_1 subsite specificity.

3.2. Alteration of S_1 Substrate Specificity of Pepsin to those of Fungal Aspartic Proteinase

The structure of porcine pepsinogen cDNA was reported earlier by Lin *et al*. [36]. Therefore, porcine pepsinogen cDNA was cloned by reverse transcriptase-PCR, using total RNA from porcine gastric mucosa as a template. PCR primers were designated for direct expression in the *E. coli* pET system. The *Nde*I/*Sal*I fragment was inserted into pET12a, which was designated as pETPP, to express porsine pepsinogen under the control of a T7 promoter. The amplified cDNA was dideoxy-sequenced to verify whether it was synthesized

correctly. The sequence was identical with that reported by Lin *et al*. [36] except for the substitution of Tyr-242 by Asp. Porcine pepsin has been sequenced in several laboratories by protein and cDNA sequencing [37, 38], and these studies indicated that there are two variants at position 242 of amino acid sequence (Asp or Tyr). The electrospray mass spectrometry of porcine pepsin also demonstrated the existence of two variants [39]. Hence, the cDNA obtained in this study seemed to correct and available for expression studies.

The *E. coli* cells harboring pETPP produced pepsinogen as an inclusion body under the control of the T7 promoter. The inclusion body was purified by washing with buffer and then refolded by solubilization with 8 M urea and subsequent dialysis under alkaline pH as described "Experimental Procedures" of ref. [35]. Porcine pepsin was purified from the refolded pepsinogen preparation by acidification and subsequent chromatogaraphy on a RESOURCE Q column and gave a single band on SDS-PAGE. The NH_2-terminal sequence of recombinant pepsin was found to be predominatly Ile-Gly-Asp-Glu-Pro-Leu-Glu-Asn-, which is known as the NH_2-terminal sequence of porcine pepsin [37], and a minor sequence of Ala-Ala-Leu-Ile-Gly-Asp-Glu-Pro- was also detected; the same results were reported in the activation of native porcine pepsinogen by Kageyama and Takahashi [40]. The secondary structure of native and recombinant porcine pepsins was analyzed by CD spectrometry. The CD spectral data showed that the spectrum of the recombinant enzyme was essentially superimposable on that of the native enzyme. The native and recombinant enzymes were almost equal in specific activity for hydrolysis of acid-denatured hemoglobin (82 and 83 milikatals/kg, respectively).

The mutant porcine pepsins, T77D, G78(S)S79, and T77D/G78(S)S79, were purified by the same method as wild-type pepsin, and the purities of the enzymes were judged by SDS-PAGE. The NH_2-terminal sequences of the mutants were the same as that of wild-type enzyme. The secondary structures of recombinant wild-type and mutant pepsins were analyzed by CD spectrometry to determine whether localized or global changes of structures were induced by the mutations. The CD spectral data showed that the spectra of the mutants were essentially superimposable on that of the wild-type enzyme. These results suggest that no major conformational alterations occurred in the mutant enzymes.

Proteolytic activities for acid-denatured hemoglobin and trypsinogen-activating activities due to limited protelysis of the Lys6-Ile7 bond of trypsinogen were measured with wild-type and mutant pepsins. The specific activities of mutant enzymes, T77D, G78(S)S79, and T77D/G78(S)S79, for hemoglobin hydrolysis were determined to be 53.8, and 50 millikatals/kg, respectively. Each mutant enzyme effectively hydrolyzed hemoglobin although the activity of G78(S)S79 mutant was 10 times lower than that of wild-type enzyme. The specific activities of wild-type, T77D, and T77D/G78(S)S79 enzymes for trypsinogen activation were 0.04, 0.01, and 18.5 micro-katals/ml, respectively, and no detectable activity was found for G78(S)S79 enzyme, which indicates that the activity of trypsinogen activation was significantly increased only by the double mutant. However, it was still 300-fold less than the activity of aspergillopepsin I. SDS-PAGE analysis showed that trypsinogen was converted to trypsin by T77D/G78(S)S79 mutant alone (Figure 6, lane 5) and the cleavage site was found to be Lys6-Ile7 by NH_2-terminal sequencing. These results indicated that the double mutation, T77D/G78(S)S79, in the active site flap altered substrate specificity of porcine pepsin to those of fungal aspartic proteinases, aspergillopepsin I, penicillopepsin, and rhizopuspepsin.

Peptide A (PTEFF(4-NO_2)RL) was cleaved at the Phe-Phe(4-NO_2) bond by each enzyme, which indicated that mutant enzymes also prefer hydrophobic residues in P_1 and P_1' in the

substrate. The T77D/G78(S)S79 mutant hydrolyzed Lys-Phe(4-NO_2) bond in peptide B (PTEKF(4-NO_2)RL) and C (Ac-AAKF(4-NO_2)AA-NH_2), which is equivalent to trypsinogen activation. While, for wild-type enzyme no hydrolyses at Glu-Lys and Phe(4-NO_2)-Ala bonds in peptide B and peptide C were observed (Table 4). The T77D mutant cleaved at the Lys-Phe(4-NO_2) bond in peptide B, but at the Phe(4-NO_2)-Ala bond in peptide C. There was no cleavage in peptide B and peptideC by G78(S)S79 mutant.

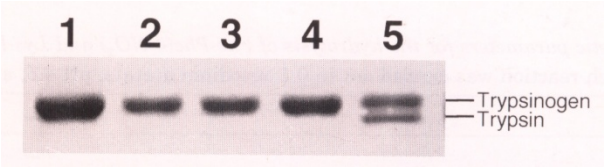

Figure 6. Conversion of trypsinogen to trypsin by mutant pepsins.

Table 4. Kinetic parameters for the hydrolysis of Phe-Phe(4-NO2) and Lys-Phe(4-NO2) bonds in the peptide substrates by wild-type and mutant pepsins

Mutant pepsin	K_m	k_{cat}	k_{cat}/K_m	Ratio[a]
	mM	s^{-1}	$mM^{-1} \cdot s^{-1}$	
PTEF↓F(4-NO_2)RL				
Wild type	0.04	61	1500	1.0
T77D	0.20	20	100	1.0
G78(S)S79	0.17	2.0	12	1.0
T77D/ G78(S)S79	0.06	23	380	1.0
Aspergillopepsin I	0.01	18	1800	1.0
PTEK↓F(4-NO_2)RL				
Wild type	—[b]			
T77D	0.18	0.10	0.56	0.0056
G78(S)S79	ND[c]			
T77D/G78(S)S79	0.15	1.1	7.3	0.019
Aspergillopepsin I	0.02	13	650	0.36
Ac-AAK↓F(4-NO_2)AA-NH_2				
Wild type	—[d]			
T77D	—[d]			
G78(S)S79	ND[c]			
T77D/G78(S)S79	0.16	2.1	13	0.034
Aspergillopepsin I	0.10	8.0	80	0.044

[a] Ratio is k_{cat}/K_m value relative to that with Pro-Thr-Glu-Phe-Phe(4-NO_2)-Arg-Leu as substrate in each enzyme.
[b] Cleavage occurred between Glu-Lys bond.
[c] No detectable cleavage was observed.
[d] Cleavage occurred between Phe(4-NO_2)-Ala bond.
Arrows (↓) indicate the scissible bonds.
(Shintani,T. *et al., J. Biol. Chem., 272,* 18855-18861 (1997))

Each reaction was carried out in 0.1 M sodium acetate, pH 4.5, at 37°C.

These results indicate that the T77D/G78(S)S79 mutant acquired the ability to recognize a Lys residue at the P_1 position although the enzyme still exhibited a preference for hydrophobic residues at the P_1 position (Table 4).

From kinetic determination of the k_{cat}/K_m (catalytic efficiency) one can obtain the second-order rate constant for conservation of a substrate to a product. Combining effects due to substrate binding and transition state stabilization, this parameter is useful for assessing altered substrate specificity. Differences in $\log(k_{cat}/K_m)$ provide an accurate measure of the lowering of the transition state activation energy ($\Delta G_T^{\neq}$). The kinetic parameters for hydrolysis of Phe-Phe(4-NO_2) and Lys-Phe(4-NO_2) bonds were determined from the initial rate measurements, and the results are listed in Table 4. The mutations led to a 4- to 130-fold decrease of k_{cat}/K_m compared to wild-type enzyme for peptide A. However, the k_{cat}/K_m value for the double mutant was larger than those of single mutants. Although the k_{cat}/K_m values of the double mutant for peptide B and C were 50 and 30 times smaller than for peptide A, respectively, the double mutation led to hydrolysis of the Lys-Phe(4-NO_2) bonds in the former two peptides. The double mutant showed a similar ratio of k_{cat}/K_m for peptide C over peptide A to aspergillopepsin I, although the preference for peptide B was significantly different between the double mutated pepsin and aspergillopepsin I. These results indicated that fungal aspartic proteinase-like specificity of the T77D/G78(S)S79 mutant can be introduced into porcine pepsin (Table 4).

To obtain information on recognition of a Lys residue at the P_1 position by the T77D/G78(S)S79 double mutant, the kinetic parameters for this double mutant were determined at various pH values using three peptide subsrates containing a Phe or Lys in P_1 (Figure 7). In all substrates, the K_m values were pH independent, and above pH 4 the values of k_{cat} and k_{cat}/K_m were controlled by the dissociation of carboxyl group with a pK_a of about 5. Below pH 4, however, the k_{cat} and k_{cat}/K_m values for the P_1 Lys substrates (peptides B and C) decreased as pH declined, while there was no significant change in k_{cat} and k_{cat}/K_m values for the P_1 Phe substrate (peptide A).

The pH-dependent changes of substrate preference are shown in Figure 8. The P_1 Lys/Phe preference increased as pH rose, which indicates that the dissociation of a carboxyl group as Asp77 may affect the preference of a Lys residue at the P_1 position.

In this study, the insertion of Ser between Gly78 and Ser79 of porcine pepsin may have caused an alteration in the direction of the Thr77 side chain and have disabled the side chain of Thr77 from hydrogen bonding to the main chain of the substrate (Figure 5). These would result in overall decreases in catalytic efficiencies for all substrates in the G78(S)S79 mutant. In the T77D mutant, the presence of the longer Asp77 side chain may allow the flap to bind more loosely to the substrate and result in a decrease in the number of van der Waals contacts between enzyme and substrate; this would lead to a reduction in catalytic efficiency. However, the T77D mutant enzyme hydrolyzed the Lys-Phe(4-NO_2) bond in Pro-Thr-Glu-Phe(4-NO_2)-Arg-Leu (peptide B) although its catalytic efficiency was very low, whereas the Glu-Lys bond was the main cleavage site in wild-type pepsin. This would be due to the electrostatic repulsion between Glu of the substrate and Asp77 of the T77D mutant enzyme, and it would not be positive recognition of anionic Lys residue in P_1. The wild-type and T77D mutant enzymes cleaved the Phe(4-NO_2)-Ala bond in Ac-Ala-Ala-Lys-Phe(4-NO_2)-Ala-Ala-NH_2 (peptide C) due to the strong interaction between the Phe(4-NO_2) residue of the substrate and S_1 hydrophobic poket of the mutants. The double mutated pepsin exhibited higher

catalytic efficiency (k_{cat}/K_m) for the P_1 Phe substrate than did the single mutants. The double mutant would have a flap structure and hydrogen bond network between Asp77 and the main chian of a substrate similar to those of the fungal aspartic proteinases. In the double mutant, the scissible peptide bond of the substrate may lie at a more stable position.

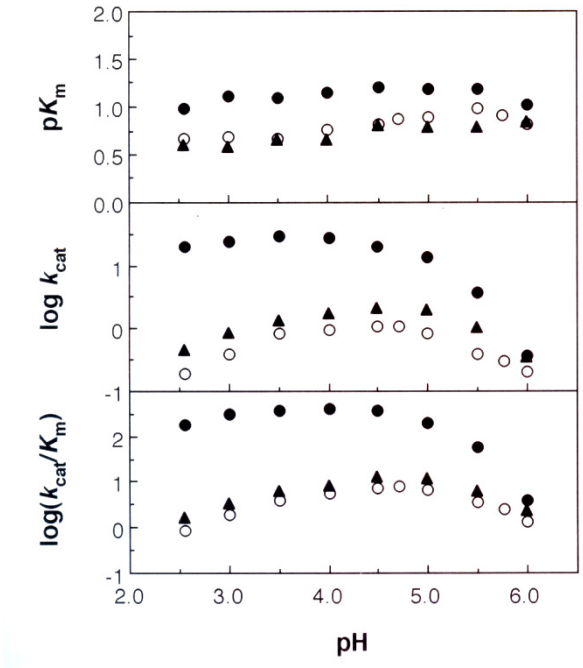

Figure 7. pH dependence of pKm. logkcat, amd log(kcat/Km) by mutant pepsins.

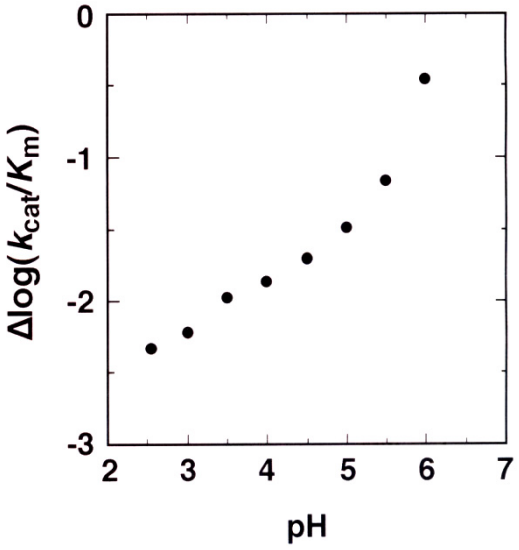

Figure 8. pH dependent substrate preference of double mutated pepsin.

Furthermore, the double mutant effectively hydrolyzed the Lys-Phe(4-NO_2) bond in peptide B and C, due to the additional two hydrogen bonds; the side chain of Asp77 and inserted Ser in the mutant may be hydrogen-bonded to the ε-amino group of the Lys residue in P_1 as fungal enzymes. In a previous study on aspergillopepsin I [30], the effect of the substitution of Ser79 by Ala (S79A) and the deletion of Ser79 (ΔS79; corresponding to porcine pepsin) on the substrate spscificity were analyzed. The P_1 Lys/Phe preference of the ΔS79 mutant was reduced more significantly than the S79A enzyme. Therefore, in mutant pepsins the insertion of Ser is important for the orientation of the side chian at position 77, although this Ser may also contribute to the hydrogen acceptor in the hydrogen-bonding interaction.

The effect of the dissociation of the β-carboxyl group of Asp77 in double mutated pepsin on the recognition of Lys residue at the P_1 position were examined by pH-dependent hydrolysis of two type of peptide substrates containing Phe or Lys at P_1. The major differences in pH activity profiles were the k_{cat}/K_m values below pH 4. These values for P_1 substrates (peptide B and C) decreased as the pH dropped, while there was no significant change for P_1 substrate (peptide A). The K_m values were pH independent in all cases. These results are different from those of the studies that the existence of Lys or Arg residues at the P_4, P_3, P_2, P_3', P_4', and P_5' positions in the substrates influences the K_m values with little effect on k_{cat} in porcine pepsin [41]; the ionic interactions between the basic residues in the substrate and the side-chain carboxylates in the S_4, S_3, S_2, S_3', S_4', and S_5' subsites contribute to substrate affinity.

In double mutated pepsin, it is likely that the dissociation of Asp77 side chain contributes to the stabilization of the transition state when substrates contain Lys residue at the P_1 position rather than substrate affinity. The electrostatic interaction between Asp77 side chain and P_1 Lys of the substrates could play an important role in recognition of Lys residue at the P_1 position. In aspergillopepsin I, however, the substitution of Asp77 by Asn hardly affected the P_1 Lys/Phe preference compared with wild-type enzyme, whereas the substitution of Asp77 by other amino acids (Glu, Ser, and Thr) and the deletion of Ser79 reduced the P_1 Lys/Phe preference with the decrease in the k_{cat} values for the P_1 Lys substrates. This indicates that the recognition of basic P_1 side chain is not dependent on the specific electrostatic interactions between P_1 side chain and Asp77 side chain of the enzyme [30]. From a site-directed mutagenesis study of rhizopuspepsin, Lowther *et al*. (31) concluded that the presence of Asp at position 77 has the potential to establish an extensive hydrogen-bonding network between the enzyme and the substrate containing Lys residue at the P_1 position. In double mutated pepsin, although the dissociation of the β-carboxyl group of Asp77 would be dispensable to accommodate the Lys residue in the S_1 pocket, it enhances the stabilization of the transition state complex when substrates contain a Lys residue at the P_1 position. This may be due to the formation of the electrostatic interaction or the changes of the hydrogen-bonding pattern between Lys residue in P_1 and Asp77 of the mutant pepsin as the pH is higher.

In conclusion, the double mutant pepsin T77D/G78(S)S79 was also able to activate bovine trypsinogen to trypsin by the selective cleavage of the Lys6-Ile7 bond of trypsinogen. Results of this study suggest that the structure of the active site flap contribute to the S_1 substrate specificity for basic amino acid residues in aspartic proteinases.

4 AORSIN FROM ASPERGILLUS ORYZAE, A NOVEL SERINE PROTEINASE WITH TRYPSINOGEN ACTIVATING SPECIFICITY AT ACIDIC PH

4.1. Sedolisin

In addition to these above described aspartic proteinases, there exist some other distinct families that do not contain the consensus sequence of Asp-Thr/Ser-Gly. These are called non-pepsin-type aspartic proteinases and include aspergillopepsin II (EC 3.3.23.19) [42], scytalidiopepsin B (EC 3.4.23.32) [43], pseudomonapepsin (EC 3.4.23.37) [44] and xanthomonapepsin (EC 3.4.23.33) [45, 46]. These families of aspartic proteinases are not sensitive to pepstatin, hence they are also called pepstatin-insensitive carboxyl proteinases.

However, another important member of the aspartic proteinase (of family A7) is the classical late-infantile neuronal ceroid lipofuscinosis (LINCL) protein, CLN2p (ceroid lipofuscinosis, neuronal 2 protein), a human lysosomal enzyme that, when mutated, leads to the fatal neurodegenerative disease, LINCL (47-49). CLN2p has both tripeptidyl-peptidase I and endopeptidase activity at acidic pH [50, 51]. The sequence of CLN2p is significantly similar to the two bacterial pepstatin-insensitive carboxyl proteinases, pseudomonapepsin and xanthomonapepsin [43-46]. Within the sequences of these enzymes, Rawlings and Barrett (50) identified a significant conserved sequence, Gly-Xaa-Ser, which is characteristic of the active-site motif of many serine peptidases. More recently, Lin *et al*. [52] have shown that Ser475, Asp360 and Asp517 are essential for the activity of CLN2p/tripeptidyl-peptidase I, and also that a diisopropyl fluorophosphates (DFP) specifically reacts with CLN2p at Ser475. Furthermore, the crystal structure of psedomonapepsin has been determined [53]. On the basis of its three-dimentional structure, Wlodawer *et al*. [53] have proposed that a family containing psedomonapepsin can be defined as novel family of serine-like enzymes that have a unique catalytic triad, Glu80, Asp84 and Ser287, and that the enzymes in this family are called serine-carboxyl proteinase [pseudomonapepsin is thus also known as *Psedomonas* serine-carboxyl proteinase (PSCP)]. This new family, 'sedolisin', was classified as S53 in the MEROPS database [54]. Consequently, the EC numbers for pseudomonapepsin and xanthomonapepsin have been reassigned as EC 3.4.21.100 and EC 3.4.21.101, respectively.

4.2. Aorsin from *A. oryzae*

An enzyme that hydrolyses Z-Arg-Arg-MCA at acidic pH was found in commercial protease M powder that was drained from a solid culture filtrate of *A. oryza*e [55]. We called the enzyme aorsin. The specific activity of the purified aorsin was 12.8 mkat/kg of protein for Z-Arg-Arg-MCA at 30^{o}C and pH 4.0. Aorsin also hydrolysed clupeine and salmine as well as some fluorogenic peptide substrates, Boc-Gln-Arg-Arg-MCA and Boc-Leu-Lys-Arg-MCA, at an optimum pH of 4.0. Some enzymic and physicochemical properties are summarized in Table 5. The molecular mass of the enzyme was estimated to be 90 kDa and 70-120 kDa by gel filtration and SDS-PAGE (10% gel), previously. Protein that was deglycosylated by *Flabobacterium* N-glycosidase F migrated as a sharp single 61 kDa band using SDS-PAGE (10% gel).

Table 5. Some enzymic and physicochemical properties of aorsin

Property	Method, symbol of condition	Value
Molecular mass	Gel filtration	90 kDa
	SDS-PAGE	7—120 kDa
	SDS-PAGE (deglycosylated)	61 kDa
	Deduced from nucleotide sequence	46,522 Da
Isoelectric point	p*I*	3-4
Ca^{2+} content	Atomic absorption spectrophotometer	1 mol/mol
Melting temperature (T_m)	Differntial scanning calorimeter	66.7°C
Optimum pH	pH	4.0
Specific activity	Z-Arg-Arg-MCA, 30°C, pH 4.0	12.8 mkat/kg
Half-life ($t_{1/2}$) for tolelance of pH	30°C, pH 6.6	150 min
	30°C, pH 6.8	5.5 min
	30°C, pH 2.4	14 min
Half-life ($t_{1/2}$) for tolerance of temperature	60°C, pH 4.0	3.5 min
Inhibitor	Antipain, leupeptin	

(Lee, B. R., et al., Biochem. J., 371, 541-548 (2003)).

The results indicated that the enzyme is a monomer with hetero-N-gycosidases. The enzyme lost activity irreversibly at pH values of > 6.5 and < 3 during incubation at 30°C. The half-life ($t_{1/2}$) values for activity loss at 30°C were 150 min at pH 6.6, and 5.5 min at pH 6.8 and 14 min at pH 2.4. Although the enzyme that was treated at 50°C and pH 4.0 for 10 min remained full active, the residual activity of the enzyme treated at 55°C for 10 min was 65%. The $t_{1/2}$ value for loss of activity at 60°C and pH 4.0 was 3.5 min. The isoelectric point was judged to be 3-4 due to diffuse migration. Aorsin contained 1 mol of calcium per mol. The T_m was 66.7°C. To investigate the inhibitor of aorsin, the enzyme was treated with various inhibitors at 30°C and pH 4.0 for 30 min and the remaining activity was measured. The enzyme activity was inhibited neither by pepstatin nor the standard inhibitors of peptidases of various type, such as diazoacetyl-DL-norleucine methyl ester (DAN) (0.0% nM), E-64 (0.1 mM), iodoacetamide (1 mM), PMSF (10 mM), pefabloc SC (10 mM), EDTA (5 mM), EGTA (5 mM) or o-phenathroline (2 mM), at the final concentration indicated. This inhibition pattern resembled that of psedomonapepsin (or PSCP), a pepstatin-insensitive carboxylproteinase. Only antipain and leupeptin completely inhibited the aorsin at 0.01 mM, but aorsin was not inhibited by tyrostatin [56], which is specific inhibitor of PSCP.

To investigate the substrate specificity of aorsin, 45 types of fluorogenic peptide substrates were used. Aorsin hydrolysed the substrates containing the basic amino acid residues arginine or lysine at P_1 position, but did not hydrolyse any other substrates possessing non-basic amino acids at the P_1 position, indicating that the enzyme has trypsin-like activity. Several good fluorogenic substrates and their kinetic parameters are shown in Table 6.

Table 6. Kinetic parameters of aorsin towards fluorogenic peptide substrates at pH 4.0.

The parameters were determined as described in the Expreimental section of ref. (55). The k_{cat} value was calculated using molecular mass 46,522 Da. The values of k_{cat}t, K_m and k_{cat}/K_m are the means ± S.D. for three to five independent experiments.

Substrate	K_m (μM)	k_{cat} (s^{-1})	k_{cat}/K_m ($M^{-1} \cdot s^{-1}$)
Boc-Gln-Arg-Arg-MCA	0.7 ± 0.03	0.10 ± 0.01	(1.45 ± 0.06) x 10^5
Boc-Leu-Arg-Arg-MCA	3.9 ± 0.25	0.24 ± 0.02	(6.12 ± 0.45) x 10^4
Boc-Gly-Arg-Arg-MCA	2.8 ± 0.22	0.25 ± 0.02	(9.01 ± 0.47) x 10^4
Boc-Leu-Lys-Arg-MCA	10.0 ± 0.51	5.80 ± 0.37	(5.79 ± 0.38) x 10^5
Boc-Gly-Lys-Arg-MCA	26.8 ± 1.33	2.69 ± 0.18	(1.00 ± 0.07) x 10^5
Boc-Leu-Tyr-Arg-MCA	58.0 ± 2.47	4.11 ± 0.12	(7.09 ± 0.38) x 10^4
Boc-Leu-Gly-Arg-MCA	84.5 ± 3.75	1.26 ± 0.04	(1.49 ± 0.09) x 10^4
Boc-Gln-Gly-Arg-MCA	88.3 ± 4.06	0.84 ± 0.05	(9.46 ± 0.07) x 10^3

(Lee, B. R., *et al., Biochem. J., 371*, 541-548 (2003))

Although no significant diference in k_{cat}/K_m values was observed between the substrates, relatively low k_{cat}/K_m values and high K_m values were observed for Boc-Gln-Gly-Arg-MCA and Boc-Leu-Gly-Arg-MCA in which the P_2 positions are occupied by glycine. Low K_m values were also observed for substrates having dibasic amino acids at the P_1 and P_2 positions, such as Boc-Gln-Arg-Arg-MCA, Boc-Leu-Arg-Arg-MCA and Boc-Gly-Arg-Arg-MCA. The highest k_{cat}/K_m value was observed for Boc-Leu-Lys-Arg-MCA. On the other hand, aorsin hydrolysed a peptide hormone dynorphin A (Tyr-Gly-Gly-Phe-Leu-Arg-Arg-Ile-Arg-Pro-Lys-Leu-Lys) at the peptide bond between Arg7 and Ile8, but other peptide bonds were not cleaved despite the presence of several basic residues. These findings indicate that aorsin has a unique, specific requirement for basic residue at P_1 and to prefer paired basic residues. In terms of cleavage, aorsin is closer to a processing enzyme than it is to trypsin.

Plasminogen that was treated with aorsin hydrolysed a Boc-Val-Leu-Lys-MCA substrate, which is a substrate of plasmin, whereas aorsin or plasminogen alone did not hydrolyse the substrate. However, we failed to determine the processing site because activated plasmin could not be purified, probably due to further degradation. Trypsinogen was also activated by being treated with aorsin, and the generated trypsin hydrolysed Z-Phe-Arg-MCA, which was not cleaved by aorsin. The NH_2-terminal sequence of the activated trypsin was determined to be Ile-Val-Gly-Gly-Tyr-, indiating that accurate processing had occurred by aorsin as shown in Figure 9.

A gene (*aorO*) was cloned from *A. oryzae* genomic library. To confirm whether the gene is functional, a plasmid containing a 4 kb *Xba*I fragment was used to transform the *A. oryza*e niaD300 mutant strain.

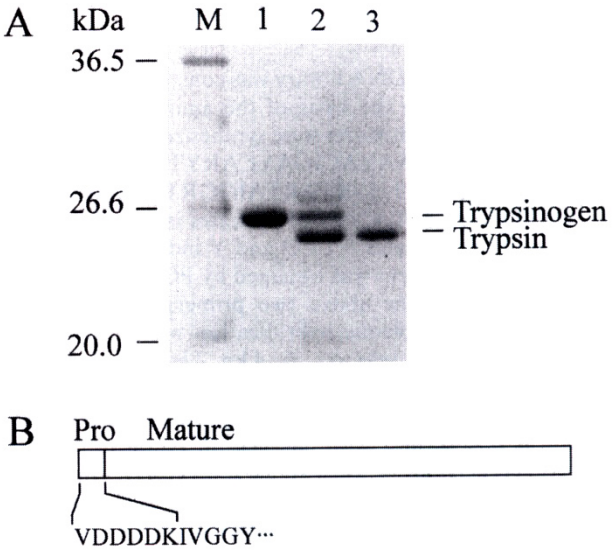

Figure 9. Conversion of trypsinogen into trypsin by aorsin.

Consequently the enzyme activity of the transformant was observed to be about 10-fold higher than that of the recipient strain in the solid culture, but neither demonstrated any activity in the submerged culture. This finding indicates that the cloned gene is functional and expressed only in the solid culture state.

A 4 kb *Xba*I fragment of the cloned *aorO* gene and cDNA were sequenced and compared. Eight introns with short sequences of 50-75 nucleotides were found in the gene. The complete structural gene encoded a protein of 652 amino acids. The amino acid sequences of the lysyl-endopeptidase-digested peptides were verified at positions Asp516 to Leu530 and Asn604 to Thr612. The NH_2-terminal amino acid sequence of the mature enzyme was found at positions Gly216 to Pro244. Consequently the pre-propeptide consisted of 215 amino acid residues from Met1 to Lys215, and the mature form of the enzyme was composed of 437 amino acid residues. The deduced amino acid sequence of the mature protein contained six potential sites for aspargine-linked glycosylation at positions 218, 247, 331, 445, 604 and 613. A protein identify search revealed that the mature aorsin protein was 35% identical with CLN2p [47], 23% identical with PSCP (44) and 22% identical with *Xanthomonas* pepstatin-insensitive carboxyl proteinase (XCP) [46], all of which are pepstatin-insensitive carboxyl proteinases. Several significant amino acids were conserved in aorsin, at Glu86, Asp90, Asp211, Ser354 and Asp395, each of which was equivalent to Glu80, Asp84, Asp170, Ser287 and Asp328 in PSCP respectively, all of which have previously been described as residues essential for enzyme activity [53, 57].

To identify the catalytic residues, the *aorO* gene was mutated at the site of encoding Glu86, Asp90, Asp211, Ser354 or Asp395. Since we confirmed that an authentic *aorO* gene product, aorsin, was not detected in submerged culture broth of *A. oryzae*, we employed *A. oryzae* as a host for recombinant aorsin production. Purified recombinant enzymes showed that they have the same patterns as authentic aorsin in terms of molecular mass, carbohydrate moiety and NH_2-terminal sequence. The results of site-directed mutagenesis of aorsin are shown in Table 7.

Table 7. Kinetic parameters for hydrolysis of fluorogenic peptide substrate Boc-Leu-Lys-Arg-MCA catalysed by aorsin and its mutants at pH 4.0

Mutant aorsin	K_m (μM)	k_{cat} (s^{-1})	k_{cat}/K_m ($M^{-1} \cdot s^{-1}$)	Relative k_{cat}/K_m
Wild type	10.0 ± 0.51	(5.80 ± 0.37)	(5.79 ± 0.38) x 10^5	1
E86D	63.6 ± 4.80	(3.74 ± 0.22) x 10^{-2}	(5.89 ± 0.27) x 10^2	1 x 10^{-3}
E86Q	19.7 ± 0.23	(1.55 ± 0.02) x 10^{-3}	(7.87 ± 0.34) x 10	1.4 x 10^{-4}
D90E	117.0 ± 5.85	(3.52 ± 0.14) x 10^{-2}	(3.00 ± 0.17) x 10^2	5.2 x 10^{-4}
D90N	22.5 ± 1.87	(6.15 ± 0.31) x 10^{-1}	(2.75 ± 0.19) x 10^4	0.048
D211E	23.6 ± 1.51	(3.23 ± 0.21) x 10-^{4}	(1.37 ± 0.05) x 10	2.4 x 10^{-5}
D211N	16.1 ± 1.38	(1.19 ± 0.05) x 10^{-3}	(7.41 ± 0.42) x 10	1.3 x 10^{-4}
S354T	19.3 ± 1.23	(6.45 ± 0.11) x 10^{-4}	(3.34 ± 0.25) x 10	5.8 x 10^{-5}
D395E	10.6 ± 0.92	(5.26 ± 0.26)	(4.97 ± 0.33) x 10^5	0.86
D395N	9.6 ± 0.62	(4.49 ± 0.09)	(4.68 ± 0.26) x 10^5	0.81

(Lee, B. R., *et al., Biochem. J., 371*, 541-548 (2003))

An aspartic acid residue, Asp328 in PSCP and Asp517 in CLN2p, has been identified as catalytic residue [52, 57] or a ligand of calcium binding (53). However, mutant aorsins Asp395→Asn (D395N) and Asp395→Gln (D395Q) had full activity and lost their calcium-binding ability completely. This finding indicates that Asp395 is a calcium-binding site and is not related to the catalytic function. A mutant enzyme replacing Asp211, equivalent to Asp170 in PSCP and Asp360 in CLN2p, with either asparagines (Asp211→Asn, D211N) or glutamic acid (Asp211→Glu, D211E) showed that the k_{cat}/K_m values were remarkably reduced by 7800-42000-fold. Mutation of Ser354, which is equivalent to Ser287 in PSCP and Ser475 in CLN2p, with threonine (Ser354→Thr, S354T) reduced the k_{cat}/K_m value by 17000-fold. Substitution of Glu86, equivalent to Glu80 in PSCP, with either aspartic acid (Glu86→Asp, E86D) or glutamine (Glu86→Gln, E86Q) also reduced the k_{cat}/K_m value by 1000-7400-fold. Surprisingly, however, the k_{cat}/K_m value of the replacement of Asp90, equivalent to Asp84 in PSCP, with asparagine (Asp90→Asn, D90N) was only 21-fold lower than the k_{cat}/K_m value of the wild-type enzyme.

Consequently, the k_{cat}/K_m values of the mutant enzymes Glu86→Gln (E86Q), Asp211→Asn (D211N), and Ser354→Thr (S354T) were 3-4 orders of magnitude lower and Asp90→Asn (D90N) was 21-fold lower than that of wild-type aorsin, indicating that the positions are important for catalysis. Aorsin is another of the S53 family serine-carboxyl proteinases that are not inhibited by pepstatin.

5. DEUTEROLYSIN FROM *ASPERGILLUS*, A MEMBER OF ASPZINCIN FAMILY WITH A NEW ZINC-BINDING MOTIF (HEXXH + D)

5.1. Deuterolysin – Extreamly Heat Stable 19 Kda Zn^{2+}-Protease –

Deuterolysin (EC 3.4.24.39) is extremely stable at 100°C, but unstable around 75°C [58-61]. Deuterolysin shows unique thermal stability. It is most unstable after 10 min at about 65-

75°C, but it regains stability beyond this temperature, and it is relatively stable at 100°C. This phenomenon is attributed to unique properties of deuterolysin in regard to reversible thermal unfolding and resistance for autoproteolysis [61].

Metalloendopeptidases are physiologically important proteinases for processing proteins in eukaryotes and prokaryotes. Hooper attempted to present a scheme based on the zinc-binding site, and this has been extended to classify zinc metalloproteinases into distinct families [62]. There are gluzincins, matazincins, inverzincins, the carboxypeptidase family, and the DD-carboxypeptidase family. Rawlings and Barrett divided the families of metallopeptidases into five groups based on the zinc-binding motif: "HEXXH + E", "HEXX + H", "HEXXH + ?", heterogenous other than HEXXH, and unknown [63]. In the clan MX, the identity of the third ligand to the zinc is unknown.

Site-directed mutagenesis on deuterolysin (EC 3.4.24.39, neutral proteinase II) from *A. oryzae* confirmed that His128 and His132 are zinc lignads and that Glu129 is a catalytically crucial resudue [64]. These studies also identified as aspartic acid residue (Asp164) as the third zinc rigand and, as a consequence, a new family name for deuterolysin containing the zinc-binding motif HEXXH + D was proposed: the 'aspzincin'.

For the crystallographic analysis of McAuley and coworkers [65], deuterolysin is an αβ protein with a zincin-like fold. It comprises eight α-helices and four strands of β-sheet (Figure 10). There are three disulfide bridges between residues Cys6-Cys78, Cys85-Cys103, and Cys117-Cys177; the last of these involves the C-terminal residue, which bridges to a cysteine residue located on a loop region between helices *D* and *E*. The secondary structure of deutrolysin is shown in the text [65]. The structure of another aspzincin with 21% sequence homology to deuterolysin, a peptidyl-Lys-metalloendopeptidase from the fungus *Grifola frondosa*, has determined [66]. This enzyme is closely related in structure to deuterolysin, with an r.m.s. difference in C^{α} positions of 1.2 Å and a topological diversity score of 8.4, yet it is still a poor molecular replacement search model.

The active site of deuterolysin is located in a large cleft on the protein surface formed by β-sheets and an α-helix. The histidine residues coordinating the zinc are located on this helix (α*E*). The Zn^{2+} atom is liganded by two histidine residues (His128 and His132), an aspartic acid residue (Asp143) and two water molecules, folding a distoted octahedral geography as shown in the reference [66]. The metal-ligand distances range from 2.05 and 2.35 Å, falling into the expected range for zinc metal geometry. Several of the angles within the octahedron deviate by more than 10° from ideal value and this distortion is a consequence of accommodation of the bidentate carboxylate group of Asp143 [65]. The catalytic residue which promotes the nucleophilic attack of a water molecule on the carbonyl C atom of the substrate is Glu129.

From the indication of McAurey [65], the structure confirms that deuterolysin is an aspzincin as proposed by Fushimi *et al.* [64], but there is a disagreement in the identitity of the aspartic acid that ligands the zinc. Fushimi and coworkers deduced this was Asp164 after their studies showed mutating this to an asparagines residue led to loss of the zinc ion, whereas the Asp143→Asn mutant retained the zinc. It is not clear why the Asp143 mutant retained the zinc; however, a suggestion as to why mutating Asp146 led to loss of the zinc can be made. Asp146 is located close to His128, with a distance of 2.86 Å between the carboxylate oxygen OD1 of Asp164 and nitrogen ND1 of the histidine.

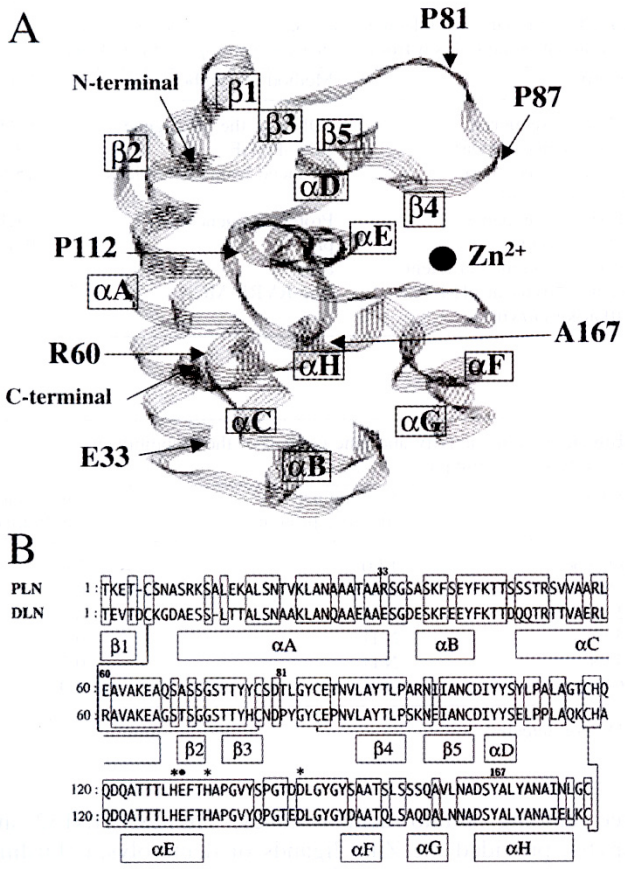

Figure 10. Secondary structure of deuterolysin reported by McAuley et al. (2001) (A) and sequence alignment of penicillolysin (PLN) and deuterolysin (DLN) (B).

The loss of this interaction after mutation to asparagines leads to a change in the orientation or position of this histidine, resulting in loss of zinc-binding ability [65].

5.2. Specificity of Deuterolysin

Deuterolysin shows high activity on basic nuclear proteins such as histone and protamine but has low activities on substrates routinely used in the laboratory, such as casein, hemoglobin, albumin and gelatin [58, 59]. The action of deuterolysin on calf thymus histone H4 was studied [67]. Deuterolysin hydrolyzed histone with various amino acid residues at the P_1 position including basic arginine and lysine, acidic aspartic and glutamic acids, and proline. Deuterolysin had high activity towards peptides next to a pair of basic residues (Lys-Arg, Arg-His, Arg-Lys, and Arg-Arg) in the calf thymus histone H4 (Figure 11). Deuterolysin hydrolyzed bonds between Arg17-His18, His18-Arg19, Arg23-Asp24, and Arg36-Leu37. On the other hand, deuterolysin also hydrolyzed Pro32-Arg33, Glu63-Asn64, Asp68-Ala69, and Met84-Asp83. The specificity of deuterolysin was different from the specificity of microbial metalloendopeptidases such as thermolysin (EC 3.4.24.27) and *A. sojae* neutral proteinase I.

Cleavage sites following pairs of basic residues:

GAKR^{17}↓H^{18}RKVLRDNIQGITKPA
AKRH^{18}↓R^{19}KVLRDNIQGITKPA
AIRR^{36}↓L^{37}ARRGGVK

Other cleavage sites:

KVLR^{23}↓D^{24}NIQGITKQ
ITKP^{32}↓A^{33}IRRLA
VFLE^{63}↓N^{64}VIRD
VIRD^{68}↓A^{69}VTYTEHAKRKTVTAMVV
VTAM^{84}↓D^{85}VVY

The arrows () indicate cleavage sites. The right hand sequences of the arrows indicate the N-terminal amino acid sequences of the small peptide obtained with an Applied Biosystems 743 protein sequencer.

Figure 11. Summary of cleavage specificity of deuterolysin from A. oryzae toward calf thymus histone H14.

Deutrolysin had strong hydrolytic activity toward Boc-Arg-Val-Ar-Arg-MCA, with optimal activity at pH 9.0 (Table 8). The k_{cat}/K_m value of 833 s^{-1} M^{-1} was obtained for Boc-Arg-Val-Ar-Arg-MCA. The enzyme hydrolyzed other dibasic-MCA derivatives: Pyr-Arg-The-Lys-Arg-MCA, Boc-Leu-Lys-Arg-MCA, Boc-Leu-Arg-Arg-MCA, and Z-Arg-Arg—MCA. However, almost no hydrolysis by the enzyme was found toward mono or certain dibasic peptide-MCAs. The findings indicate that deuterolysin had substrate specificity toward paired dibasic amino acid residues at the P_2-P_1 positions.

Table 8. Kinetic parameters of deuterolysin and Co-deuterolysin toward fluorogenic MCA substrates

Substrate	Deuterolysin			Co-deuterolysin		
	K_m (μM)	k_{cat} (s^{-1})	k_{cat}/K_m (s^{-1} · M^{-1})	K_m (μM)	k_{cat} (s^{-1})	k_{cat}/K_m (s^{-1} · M^{-1})
Boc-RVRR-MCA	26.4 ± 4.0	2.2×10^{-2}	833 (100*)	27.5 ± 10.0	1.7×10^{-2}	618 (74)
Pyr-RTKR-MCA	23.7 ± 7.4	2.2×10^{-3}	84 (10)	11.9 ± 1.8	8.2×10^{-4}	69 (8)
Boc-LKR-MCA	146.0 ± 21.0	9.0×10^{-3}	62 (7)	157.3 ± 26.2	3.5×10^{-3}	22 (3)
Boc-LRR-MCA	70.0 ± 3.5	4.5×10^{-3}	71 (9)	63.8 ± 5.7	1.7×10^{-3}	27 (3)
Z-RR-MCA	47.3 ± 10.0	9.0×10^{-4}	19 (2)	52.2 ± 5.7	6.5×10^{-4}	12 (1)

*The rate of hydrolysis of Boc-RVRR-MCA by deuterolysin is taken to be 100, and other such values are relative to that. Results are shown as means ± S.D. of three determinations.

MCA, 4-methylcoumacyl-7-amide.

(Doi, Y., *et al., Biosci. Biotechnol. Biochem., 67*, 264-270 (2003))

5.3. Co-Deuterolysin

The value of electron paramagnetic resonance (EPR) spectroscopy in establishing structures and their dependence on metal coordination-sphere composition and geometry has been illustrated by its application to several aspects of cobalt bioinorganic chemistry. Deuterolysin from *A. oryzae* has a zinc-binding motif, but, the zinc is not detected EPR. Removal of the zinc ion from *A. oryzae* deuterolysin yields the inactive apo-enzyme, which can also be reactivatd by stoichiometric amounts of zinc ions. Moreover, the addition of cobalt ions to the apo-enzyme results in an enzymatically active species. We purified Co-deuterolysin to examine cobalt coordination and geometry by EPR [67]. Kinetic parameters toward fluorogenic MCA substrates (Table 8) and the CD spectrum of cobalt-substituted deuterolysin (Co-deutrolysin) were similar to that of the native deuterolysin.

In Figure 12 we show the Q-band EPR spectra of Co-deuterolysin measured at 10 to 5 K. Preliminary observation of the X- and S-band EPR (9 and 3 GHz, respectively) showed an axial feature but line-broadening prevented us from identifying the *g* principal values from the spectrum. Resolution improvement with the respect to *g* values is one advantage of use of a high microwave frequency. From the spectra at 33.9570 GHz, *g* principal values could be unambiguously measured.

The dominant line-broading mechanism of Co-deuterolysin was unresolved hyperfine splitting of cobalt nucleus and *g*-strain. The line width from a *g*-strain mechanism increases with increasing microwave frequency, but the contribution from hyperfine splitting is independent of the microwave frequency.

On the basis of the Q-band spectrum giving better resolution than that the X- and S-bands, we concluded that the dominant line-broadening mechanism at Q-band EPR was *g*-strain and that there was broadening in the X- and S- band spectra. From spectra simulation in the Q-band spectrum, we obtained the *g* principal values of g_{xx} = 5.20, g_{yy} = 4.75, and g_{zz} = 2.24, and the *g*-strain tensor principal values dg_{xx} = 1.11 (0.2), dg_{yy} = 1.11 (0.2), and dg_{zz} = 0.19 (0.01).

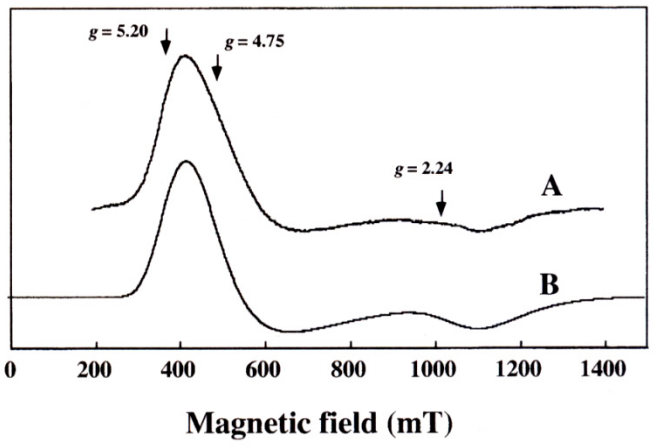

Figure 12. Q-band EPR spectra of Co-deuterolysin.

The absorption spectrum of Co-deuterolysin indicates that the number of coordinating ligands can be four or five, that is, tetrahedral or trigonal-bipyramid, respectively. As a four coordinate site, the absorption energy of Co-deuterolysin is a little high, and the absorption coefficient ε is small. On the other hand, the spectrum lacks the characteristic band (16,000 cm-1) of a five-coordinate site.

It can be concluded that a distorted tetrahedral or a two-triangular pyramidal environment has been assigned to the Co-deuterolysin from the correlation of the *g* principal values, g_{xx} = 5.20, g_{yy} = 4.75, and g_{zz} = 2.24 (67).

5.4. Penicillolysin – Thermolabile 19 Kda Zn^{2+}-Protease –

Penicillolysin is a member of the clan MX and the family of M35 proteases [68-71]. Penicillolysin is a single-chain protein of 177 amino acid residues with a calculated molecular mass of 18525 Da and p*I* of 9.6, which contains three disulfide bonds (Cys6-Cys78, Cys85-Cys103, and Cys117-Cys177) (Figure 10). The enzyme is a thermolabile Zn^{2+}-protease from *Penicillium citrinum* with a unique substrate profile.

Penicillolysin showed a high affinity toward the Pro-X (= Gln, Lys, Leu or Arg) bonds of substance P, dynorphin A [1-13], neurotensin and chicken brain pentapeptide, and the R-R bonds in dynorphin A and neurotensin (Figure 13) [69]. Preferential cleavages of bonds by the enzyme with hydrophobic amino acid residues at the P_1 position were observed on the peptides used (Figure 13). The specificity of penicillolysin differs from that of other metalloprotinases.

The specific activities of penicillolysin for clupeine and casein hydrolysates were 3.04 x 10^{-1} and 5.23 x 10^{-3} katal/kg protein at pH 7.0, respectively (Table 9) [69]. The rate of clupeine hydrolysis was 60-fold greater than that for casein hydrolysis. When zinc is removed, the enzyme is completely inactive, and readdition of zinc restores the dual activities towards clupeine and casein (Table 9). Depending on the casein substrate, the cobalt-penicillolysin (Co-penicillolysin) could be up to ca 1.6 times more active than the native zinc enzyme. On the other hand, in clupeine-hydrolysis, the cobalt enzyme is about 70% as active as the native enzyme. Thus, replacement of the zinc-penicillolysin with cobalt markedly decreases the activity towards clupeins while increases it towards casein.

The curve in Figure 14 shows the CD spectrum of penicillolysin [69]. The α-heix and β-structure content of penicillolysin were ca 19 and 58%, respectively. The CD curve of the apoenzyme is in Figure 14B and is notably different from the native one. The α-helix and the β-structure content of the apoenzyme were ca 9 and 61%, respectively. About 50% of the α-helix was destroyed in the conformational changes from the native to apoenzyme. The CD curve of Co^{2+}-reconstructed enzyme, Co-penicillolysin, is shown in Figure 14C. The contents of α-helix and β-structure were ca 20% and 58%, respectively. This CD curve was almost the same as that the native enzyme. Parameters of the secondary structure of penicillolysin are shown in Table10.

Several candidates for zinc ligands of penicillolysin were mutated and confirmed [72]. Substitutions of His128 and His 132 with Arg, of Glu129 with Gln, of Asp143 with Asn and of Asp164 with Asn resulted in a complete loss of both the enzyme activity and zinc binding ability of all mutant enzymes except D164N. As for the mutant D164N, the zinc content was determined as 1.0 mol/mol of the enzyme and the specific activity was found to be 53%.

Substance P	RPKP↓QQFF↓G↓LM
Dynorphin-A	YGGFLR↓RIRP↓KLK
Neurotensin	<QL↓YENKP↓R↓RPYIL
Chicken brain pentapeptide	LP↓LRFNH_2
Bradykinin	RPPGF↓SPFR
LHRH	<QHW↓SY↓GLRPGNH_2
α-Melanotropin	AcSY↓SMEHF↓ RW↓GKPVNH_2
α-Neoendorphin	YGGF↓L↓RKYPK
Angiotensin II	DRVYIHPF
Angiotensin I	DRVYIHPFHL
CCK-octapeptide (26-33)	DYMGWMDFNH_2

The arrows in the sequences indicate cleavages for 1 h hydrolysis by the enzyme. The degree of hydrolysis being: ↓ > ↓ > ↓.

Figure 13. Summary of cleavage specificity of penicillolysin towards various oligopeptides.

Table 9. Specific activities of penicillolysin, and Zn^{2+}- and Co^{2+}-penicillolysin at pH 7.0

Enzyme	Specific activity (katal・kg^{-1} protein)	
	Clupeine	Casein
Native	3.04 x 10^{-1} (100)	5.23 x 10^{-3} (100)
Zn^{2+}-penicillolysin	2.85 x 10^{-1} (94)	5.20 x 10^{-3} (99)
Co^{2+}-penicillolysin	2.10 x 10^{-1} (69)	8.26 x 10^{-3} (158)

(Yamaguchi, M., *et al., Phytochemistry, 33*, 1317-1321 (1993)).

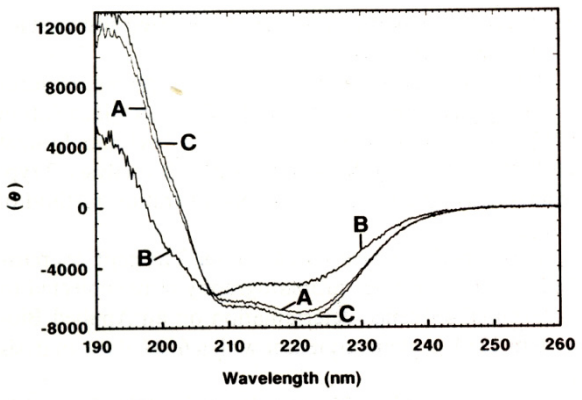

Figure 14. CD spectrea of (A) Penicillolysin(A), apoenzyme (B), and Co2+-penicillolysin (C).

Table 10. Secondary structure content (%) in penicillolysin, apoenzyme and Co2+-penicillolysin

Enzyme	α-Helix	β-Structure	Turn	Random
Penicillolysin	19	58	3	21
Apoenzyme	9	61	2	28
Co^{2+}-penicillolysin	20	58	2	20

(Yamaguchi, M., *et al., Phytochemistry, 33*, 1317-1321 (1993))

This finding indicates that the Zn^{2+} atom is bound by two histidine residues (His128 and His 132) and an aspartic acid residue (Asp143). Substitution of Glu129, a catalytically crucial residue in penicillolysin, with glutamine resulted in a mutant enzyme (E129Q) which exhibited no activity.

A full-length cDNA encoding the penicillolysin, an 18 kDa metalloendopeptidase from *Penicillium citrinum*, was cloned [70]. Analysis of the 1284 base pair nucleotide sequence of the cDNA revealed a single open reading frame coding for 351 amino acid residues. The coding region of penicillolysin gene, *plnC*, occupies 1053 base pairs of the cDNA. The sequence consists of a putative 19-residue signal sequence, a 155-residue propeptide segment, and the 177-residues of penicillolysin with a molecular mass of 18529. Penicillolysin has a sequence of 68% with that of deuterolysin from *A. oryzae*.

Penicillolysin is thermolabile and its activity is almost completely lost above 66°C. It is interesting that, despite having a highly similar identity to and the same number, three, of disulfide bonds as deuterolysin, penicillolysin is thermolabile. Of the substitutions involving residues with largely identical structural environments in penicillolysin and deuterolysin, those for which the deuterolysin situation could be favorable for thermal stability were selected [72].

We designed and constructed two different mutants (R33E/E60R and A167E) for the connection between the two α-helices (A, and C helices or E, and H helices) in the folded penicillolysin [72]. The approximate average content of α-helices and β-structures in a protein can be estimated from the CD spectrum, by comparison to a database of spectra of proteins of known structure. Although the CD spectra of the wild-type and mutants have slight differences, the enzyme activity of the mutants was not largely affected. Kinetic parameters of the mutant R33E/E60R are similar to those of the wild-type enzyme. Similar k_{cat}/K_m parameters were obtained for the two mutants, R33E/E60R (18.2 $M^{-1} \cdot s^{-1}$) and T81P (16.8 $M^{-1} \cdot s^{-1}$). The k_{cat}/K_m value of the A167E mutant (29.8 $M^{-1} \cdot s^{-1}$) was 1.6-fold higher than that of the wild-type enzyme (18.2 $M^{-1} \cdot s^{-1}$).

The stability of both the wild-type and mutant proteins is expressed as the melting temperature, T_m, which is the temperature at which 50% of the enzyme is denatures during irreversible heat denaturation. To prevent the self-digestion of penicillolysin, heat treatment was carried out at pH 5.0 because the proteolytic activity is substantially reduced at this pH and the active form of the enzyme is stable. For the wild-type enzyme and the three mutants, the thermal stabilities and the T_m changes were assayed at pH 5.0 by measuring the far-UV CD spectrum at 222 nm as a function of temperature. For the wild-type penicillolysin, the T_m

value was determined as 68°C at pH 5.0. The chosen mutation in penicillolysin was T81P, which caused in increase in the melting temperature to 71°C at pH 5.0. Unfortunately, we could not obtain thermal stable forms for the two mutants, T78P and A112P, of penicillolysin. The two single mutants, T78P and A112P, were found to fairly unstable enzymes. The destabilizing effect of T87P is probably due to the location of Thr87, which is near the disulfide bridge, Cys85 and Cys103. Ala112 is located in a loop between αD and αE. The αE helix includes a catalytic residue, Glu129, and Zn^{2+}-binding residue, His128. When Ala112 is substituted with a more rigid residue, Pro, a minor structural change to the loop and the αE helix regions might occur. The chosen mutations in penicillolysin, R33E/E60R and A167E, caused an increase in the T_m to 70°C at pH 5.0.

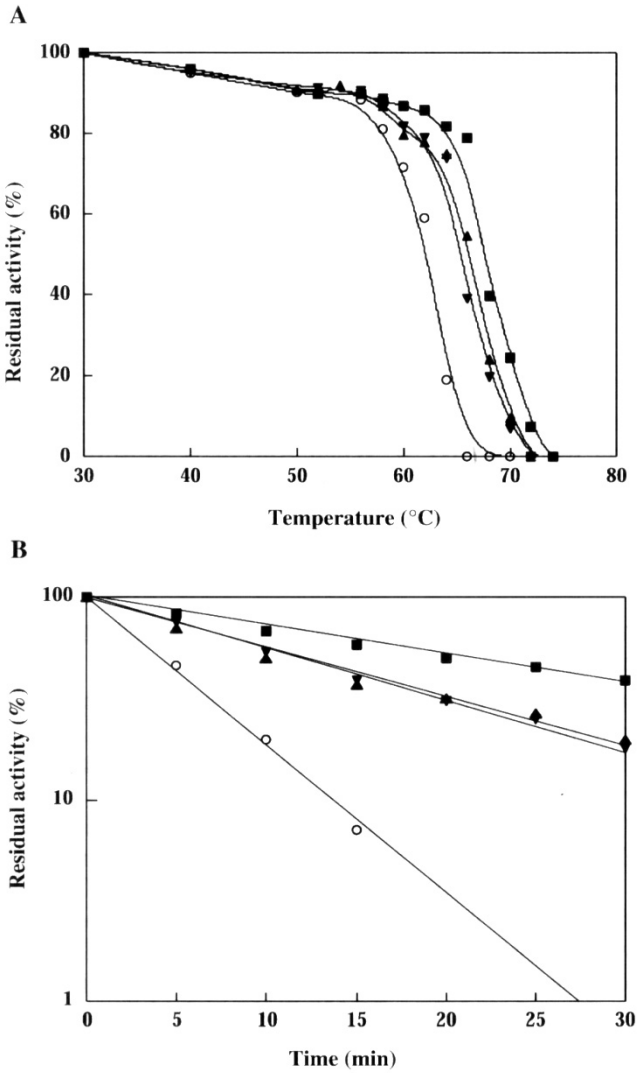

Figure 15. (A) Determination of the half-life of activity, T_{50}, for wild-type penicillolysin (○) and mutants R33E/E60R (▲), A167E (▼) and T81P (■). (B) Stability at 65°C of wild-type of penicillolysin (○), R33E/E60R (▲), A167E (▼) and T81P (■).

When the rate of denaturation of enzyme is measured, it is more common to express the result in terms of the half-life of enzyme activity, $t_{1/2}$, rather than in terms of the rate constant, k_d. For a first-order reaction the relationship is $t_{1/2} = \ln 2/k_d = 0.69/k_d$ [73]. In our study, thermal stability was quantified as $t_{1/2}$, being the temperature at which 50% of the initial activity was retained for 10 min. The thermal stability of the mutants also depended on temperature, as shown in Figure 15. The double mutant R33E/E60R was found to be fairly thermally stable, as shown in Figure 15. The half-life ($t_{1/2}$) value, 66°C, of R33E/E60R was higher than that of the wild-type penicillolysin. It is interesting that two mutations probably due to favorable interactions between the two α-helices (A and C helices) were generated and these interactions are important in the thermal stability of the mutant enzyme R33E/E60R. The A167E mutant showed the same thermal stability as R33E/E60R. The A167E mutation was also sufficient to increase the $t_{1/2}$ value from 62 to 65°C. The single A167E mutation was useful for the thermal stabilization of penicillolysin, indicating that the connection between the αE and αH helices may be important. Among the three proline mutants, the T81P mutant significantly increased the $t_{1/2}$ value from 62 to 68°C, whereas T87P and A112P had no clear stabilizing effects. For the 50% residual activity, the thermal stability at 65°C was 4, 12, 12 and 21 min for the wild-type, R33E/E60R, A167E and T81P, respectively (Figure 15B). When the T81P mutation was introduced, the enzyme was found to be more thermally stable than the two mutants, R33E/E60R and A167E. It is interesting that T81P similarly enhanced the thermal stability of penicillolysin; however, the other two mutants, T87P and A112P, showed decreased thermal stability. The T81P mutant of penicillolysin may have a structure essentially identical to that of the wild-type of deuterolysin. There are indications that the proline residues contribute to enzyme thermal stability [74, 75]. The contribution can be explained in terms of entropic effects (or chain flexibility) since proline is more restricted conformationally in the unfolded state than any other amino acid. Since proline residues are restricted with respect to their φ-ψ angles, their introduction can easily cause conformational strain in the backborne. Suzuki *et al*. [76] demonstrated that an increase in the frequency of proline in β-turns and in the total number of hydrophobic residues can enhance proline thermal stability.

For further investigation, the triple mutant R33E/E60R/T81P was constructed. Surprisingly, the triple mutation was found to produce a fairly thermally unstable enzyme. The half-life ($t_{1/2}$) value of the triple mutant was determined as 58°C.

The thermal stability of an enzyme is influenced by many factors, including amino acid sequence, three-dimensional structure, cofactors and pH. However, at present we cannot explain the results obtained. The present findings described in the ref. (72) show that the thermal stability of penicillolysin is increased dramatically by just a few mutations in one particular region of the protein.

6. ACID ARBOXYPEPTIDASE FROM *ASPERGILLUS SAITOI*

6.1. Acid Carboxypeptidase

Carboxypeptidase A (EC 3.4.17.1) that cleaves carboxy-terminal aromatic or neutral amino acid from peptides and proteins has been extensively characterized [77], and

carboxypeptidase B (EC 3.4.17.2) that cleaves carboxy-terminal arginine or lysine from the peptides and proteins has been studied for many years [78]. Both pancreatic carboxypeptidases A and B are Zn^{2+}-metalloenzymes with an alkaline pH optimum.

While establishing purifying for aspartic proteinase (aspergillopepsin I, EC 3.4.23.18) [7, 8] of *Aspergillus saitoi*, which is a food microorganism strain, it was discovered to be a rich source of acid carboxypeptidase (EC 3.4.16.5), which removes acidic, neutral, and basic amino acids as well as proline from the carboxyterminal position at pH around 3 [79, 80]. The optimum pH with Z-Tyr-Leu (Z- = bebzyloxycarbonyl-) of the acid carboxypeptidase from *A. saitoi* was 3.5. The optimum with Z-Glu-Tyr was 3.1, and that with Z-Gly-Pro-Leu-Gly, 3.2.

The acid carboxypeptidase is stable at temperatures of about 50°C for 10 min, but rapid inactivation occurred at temperatures of about 60°C for 10 min.

Competitive inhibition of the carboxypeptidase from *A. saitoi* by small substrates was found with hydrocinnamic acid, indole-3-propionic acid, and 4-phenylbutyric acid [80]. The K_i for hydrocinnamic acid inhibition was 4 x 10^{-4} M. Diisopropylfluorophosphate (DFP) and tosyl-L-phenylalanylchloromethane (TPCK) were also powerful inhibitors of the carboxypeptidase from *A. oryzae* (80). *p*-Chloromercuribenzoate (PCMB) and iodoacetic acid were also powerful inhibitors of the carboxypeptidase from *A. saitoi*, while the inhibitors of DFP, TPCK, PCMB, and iodoacetic acid on the carboxypeptidase from *A. saitoi* were less than that of *A. oryzae* [80]. As the carboxypeptidase activity of *A. saitoi* has no effect when used with ethylenediaminetetraacetate (EDTA) and *o*-phenanthroline, the enzyme is a different type of carboxypeptidase from those of the pancreatic sources, carboxypeptidase A and carboxypeptidase B [80].

Cultivation of fungi of the genus *Aspergillus* is carried out both in solid ('Koji') culture and liquid (submerged) culture. The first extracellular acid carboxypeptidase from *Aspergillus saitoi* was discovered by Ichishima [79]. Using the method of Yphantis, the extrapolated molecular mass was determined to be 139,000 as shown in Figure 16 [79].

According to the gel filtration molecular mass of 155,000 for the larger form or polymer and 51,000 for the smaller form or monomer were obtained in the absence of NaCl, and in the presence of 0.2 M NaCl a value of 135,000 was obtained (Figure 17) [79].

The interdependence of protein surface and hydration of Sephadex has implications for confusion of the molecular mass experiments. The acid carboxypeptidase from *A. saitoi* is a glycoprotein, containing approximately 30% carbohydrate by weight [81, 82]. Furthermore, a single protein band with molecular mass of 72,000 was detected in SDS-PAGE [79]. This indicates that the carboxypeptidase is a homologous dimmer [79].

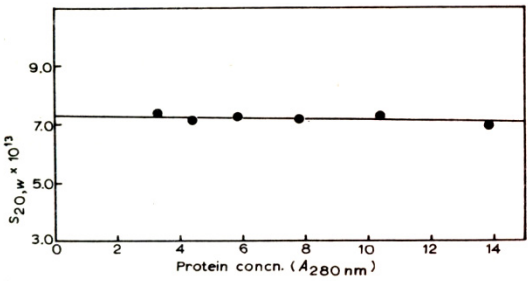

Figure 16. Sedimentation constant, S20,w, of *Aspergillus* acid carboxypeptidase.

6.2. Specificity of Acid Carboxypeptidase

The relative rates of hydrolysis of a series of peptides by the enzyme are shown in Table11.

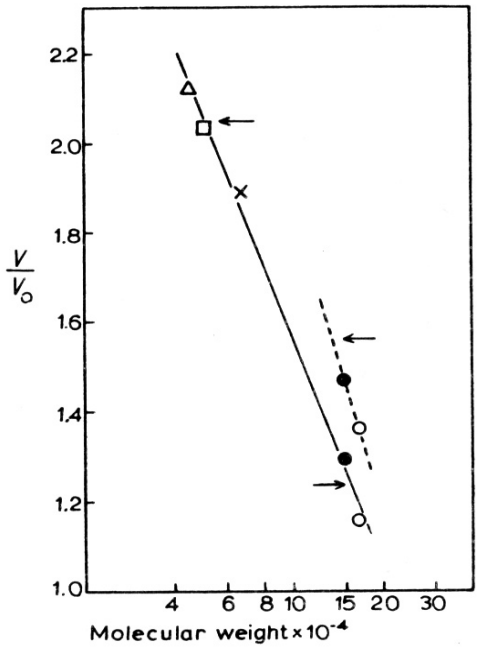

Figure 17. Molecular mass determination of Aspergillus acid carboxypeptidase.

The specificity of the acid carboxypeptidase displays the features typical of all pancreatic carboxypeptidases, hydrolysis of the specific substrate R-X-Y between X and Y (R = peptide residue, Z-, Bz-, Ac-). The amino acid in position Y must have a free carboxyl group; dipeptides (having free amino group) are not hydrolyzed. The enzyme hydrolyzes most of the α-amino substituted peptides. The carboxypeptidase was inactive on a number of small amides tried at pH 3.0. A peculiarity of its specificity, however, was its inability to hydrolyze the peptide bond of tripeptides tried in the Table 11.

Several qualitative conclusions can be drawn from the results. The acid carboxypeptidase splits off neutral and basic amino acids from the substrates and has the ability to hydrolyze the peptide bond, ---X-Pro in oligopeptides.

Significant enzymatic hydrolysis has been found for substrates in which the penultimate position ($X=P_1$ site (12)) of the carboxyterminal is occupied by an aromatic or acidic amino acid residue. It will be noted that, for substrates of the type Z-X-Y, a change in the X position from tyrosine to glycine, from phenylalanine to glutamic acid, or from glutamic acid to glycine leads to a marked decrease in the velocity rate. The favorable effect of the aromatic and carboxyl substituents at the side chain of the X residue is emphasized by the finding that where X is an aromatic amino acid residue and glutamic acid the values of the velocity rate are approximately one-sixhundredth and one-tenth that for X = glycine, respectively.

Table 11. Comparative rate of hydrolysis for *Aspergillus* acid carboxypeptidase on a range of peptides and amides

The rate of hydrolysis of benzyoxycarbonyl-L-Glu-L-Tyr (Z-Glu-Tyr) is arbitrarily taken to be 100. C-terminal amino acid residues of the substrates are expressed as R-X-Y.

Peptides	Relative activity	Peptides	Relative activity
α-Amino-substituted peptides		Tripeptides	
		Gly-Gly-Gly	0
(1) X =aromatic amino acid		Ala-Gly-Gly	0
Z-Tyr-Leu	2502	Leu-Gly-Gly	0
Z-Tyr-D-Leu	0	Gly-Gly-Leu	0
Z-Phe-Leu*	1968	Dipeptides	
Z-Phe-Tyr*	916	Tyr-Leu	0
Z-Phe-Tyr-Leu*	1025	Gly-Gly	0
Ac-Phe-TyrI_2*	1	Gly-Asp	0
(2) X = acidic amino acid		Leu-Gly	0
Z-Glu-Phe*	184	Gly-D-Asp	0
Z-Glu-Tyr	100	Amides	
(3) X = leucine		Z-Tyr-Leu-NH_2*	0
Z-Gly-Pro-Leu-Gly	30	Z-Trp-Phe-NH_2*	0
(4) X = glycine		Z-Gly-Phe-NH_2*	0
Z-Gly-Leu	4	Z-Gly-Leu-NH_2*	0
Z-Gly-Phe	2	Z-Ala-Phe-NH_2*	0
Z-Gly-Trp	0.2		
Z-Gly-Pro	0		
Z-Gly-Pro-Leu-Gly-Pro	0.2		
Bz-Gly-Lys	1		
(5) X = valine			
Z-Val-Glu	0.4		
(6) X = proline			
Z-Gly-Pro-Leu	trace		

*Partially insoluble at pH 3.0.

(Ichishima, E., *Biochim. Biophys. Acta, 56*, 1371-1372 (1992))

It may be concluded, therefore, that with samall synthetic substrates of the type Z-X-Y, where the X-Y bond is broken, the acid carboxypeptidase exhibits a preference for aromatic or carboxyl in the X position. Only limited data are available on the effect of changing the X and Y groups on the side chain specificity of the enzyme, but it would appear that this conclusion holds for substrates in which the X group is changed from tyrosine or phenylalanine to glycine.

Thus Z-Tyr-Leu, Z-Glu-Tyr and Z-Gly-Pro-Leu-Gly are good substrates. Z-Phe-Tyr-Leu, Z-Phe-Leu, Z-Phe-Tyr and Z-Glu-Phe were cleaved very easily by the enzyme, however,

they are extremely insoluble at the acid end of the pH range of carboxypeptidase activity (pH 2-4).

The pH dependence of the acid carboxypeptidase from *A. saitoi* catalyzed hydrolysis of Z-Glu-Tyr was determined, and the main conclusions derived from analysis of the data were that two catalytically active groups on the enzyme with pK_{e1} = 2.3 and pK_{e2} = 4.9 were important in the enzymatic action at pH 3.1 (80). The pK_{e1} of 2.3 could represent participitation of anionozed carboxyl group, whereas the pK_{e2} = 4.9 could be in accord with the ionization of an imidazole group or a carboxyl group [80].

A. saitoi carboxypeptidase has been used for automatic C-terminal amino acid sequence analyses of anticoagulant decapeptide (SQLQEAPLEK) [83] and α-amylase (-LR) from cultured rice (*Oryza sativa*) cells [84], and a recombinant *Serratia marcesence* serine proteinase [85].

The acid carboxypeptidase from *A. saitoi* releases the carboxyterminal phenenylalanine-amide (-Phe-NH_2) from the carboxy-terminal amidated peptides, such as gastrin-related peptide (*t*-amyloxycarbonyl (Aoc)-Trp-Met-Asp-Phe-NH_2, Aoc-WMDF-NH_2) and molluscan cardioexcitatory neuropeptide (Phe-Met-Arg-Phe-NH_2, FMRF-NH_2) [86]. The summarized data are shown in Table 12. When gastrin-related peptide was used as a substrate, the enzyme acted only as a carboxyamidase, because of the presence of the hydrophobic amino acid residue, tryptophan, in the P_3 [12] position.

Table 12. Hydrophobicity of side chains of amino acid residue adjacent to carboxy-terminal bond to be split by the carboxypeptidase from *A. saitoi*

Substrate	Amino acid residues adjacent to carboxy terminal bond to be split by the enzyme[a] $\frac{S_4\ S_3\ S_2\ S_1\ S_1'}{P_4\ P_3\ P_2\ P_1\ P_1'}$ ↓ ↑	Hydrophobicities of side chain of amino acid residues[b] Δgt (kcal/mol)	Relative rate of hydrolysis	Recovery of carboxy terminal amino acid residue (%)
Z-Ala–Phe–NH_2	Z–A–F–NH_2	?–0.5–2.5–?	0	0
	Z–A–FNH_2	?–0.5–2.5	0	0
Gastrin-related peptide	–W–M–D–F–NH_2	3.4–1.3–0.5–2.5–?	0	0
	Aoc–W–M–D–FNH_2	?–3.4–1.3–0.5–2.5	1.0	100
FMRF-amide	F–M–R–F–NH_2	2.5–1.3–?–2.5–?	0.84	76
	F–M–R–FNH_2	2.5–1.3–?–2.5	0.16	14
[D-Ala[2], Met[5]]-enkephalinamide	–DA–G–F–M–NH_2	–0.5–0–2.5–1.3–?	1.0	71
	Y–DA–G–F–MNH_2	2.3–0.5–0–2.5–1.3	0	0
Eledoisin-related peptide	–I–G–L–M–NH_2	–2.9–0–1.8–1.3–?	0.35	31
	–F–I–G–L–MNH_2	–2.5–2.9–0–1.8–1.3	0.65	57

Arrow indicates position of the splitting position.
[a] One-letter amino acid abbreviations were used.
[b] Data are from References [25] and [26].

(Takeuchi, M., *et al., Agric. Biol. Chem., 53*, 2301-2306 (1989))

When eledoisin-related peptide was used as a substrate, the enzyme quickly released methionine-amide rather than methionine from the carboxy-terminus of –FIGLM-NH_2. In this case, the P_3 position was occupied by the hydrophobic amino acid isoleucine. Furthermore, when D-amino acid occupied the P_3 position of the substrate, as in enkepharin-amide, the enzyme did not liberate a carboxy-terminal methionine-amide but acted only as amidase for this substrate. It can be concluded that the S_3-P_3 interaction is important in increasing

enzyme-substrate affinity and turnover rate for the release of carboxy-terminal amino acid amide from the carboxyterminal amidated peptides [86]. When FMRF-NH_2 was used as the substrate, approximately 16% of the carboxyterminal peptide bond in terminal arginyl-phenylalanine was cleaved. Therefore, the enzyme acted not only as a carboxyamidase but also as an amidase for the carboxy-terminal peptide bond (FMRF-NH_2). The carboxypeptidase from *A. saitoi* did not act as amidase for a P_4-lacking substrate such as Z-X-Y-NH_2. Thus, the P_4 position is important for the enzyme to bind and act as an amidase [86]. *Aspergillus* acid carboxypeptidase can hydrolyze the amide bond between the amino acid and 7-amino-4-methylcoumarin (AMC) in the peptide-4-methylcoumaryl-7amide (peptide-MCA) such as Pro-Phe-Arg-MCA (PFR-MCA) at pH 4.9 [87]. In the MCA-substrates, the P_3 position was occupied by a hydrophobic amino acid such as proline or valine.

6.3. Cloning and Expression of Acid Carboxypeptidase Gene (*CPDS*)

Screening of *A. saitoi* cDNA library with synthetic oligonucleotide identified five clones by colony hybridization. One of these colonies was sequenced completely and was found to contain a 1812 bp cDNA that encoded a complete nucleotide sequence of the caboxypeptidase [88]. The cDNA sequence contains a single open reading frame of 532 amino acids starting at position 46 and ending at 1617. The sequence around the proposed methionine start codon closely matches the consensus sequence for eukaryotic translational initiation sites and the stop codon is found in the frame at position 22. Codon usage of the coding region leads the choice of C in the third codon position (C : 53%; G : 20%; T : 18%; A : 9%).

The putative mature *A. saitoi* arboxypeptidase consists of 471 amino acids (molecular mass of 52453 Da). The underlined sequences of amino acid residues in Figure 18 correspond to the sequences found by amino acid sequencing analyses of native caboxypeptidase from *A. saitoi*. Hydropathy analysis by the algorithm of Kyte and Doolittle indicates that the NH_2-terminal portion of the polypeptide is hydrophobic, and analysis based on the signal sequence cleavage prediction method of von Heijne indicates possible cleavage sites after the 18th amino acid. Since *A. saitoi* carboxypeptidase is secreted into the medium, the NH_2-terminal sequence is thought to function as a signal sequence.

Comparison of the deduced sequence of *A. saitoi* carboxypeptidase with other known serine carboxypeptidase sequences shows that they share a low degree of similarity: 32% with wheat carboxypeptidase II, 32.3% with malt carboxypeptidase II and 26.2% with yeast carboxypeptidase Y (Figure 19) [88]. However, all of the sequences conserve the catalytic domains (indicated by boxes II to IV in Figure 19) and the domain (box I in the Figure 19) which contains the amino acid residues recognizing the C-terminal carboxylate group of peptide substrates. There are also present in the sequence ten potential sites for N-linked glycosylation.

The *A. saitoi* carboxypeptidase cDNA was cloned downstream of a GDP promoter, and the resulting plasmid, pGCP13, was used to generate recombinant *A. saitoi* carboxypeptidase protein. No enzymatic activity was detected in the culture supernatant. We detected the *A. saitoi* carboxypeptidase activity of the extract obtained from yeast cells transfected with *A. saitoi* carboxypeptidase cDNA in forward orientation (pGCP13), although no activity was observed with the vector alone at pH 3.1. The recombinant *A. saitoi* carboxypeptidase activity

is not affected by whether the ZPCK, which is an inhibitor of yeast carboxypeptidase Y, is present or not.

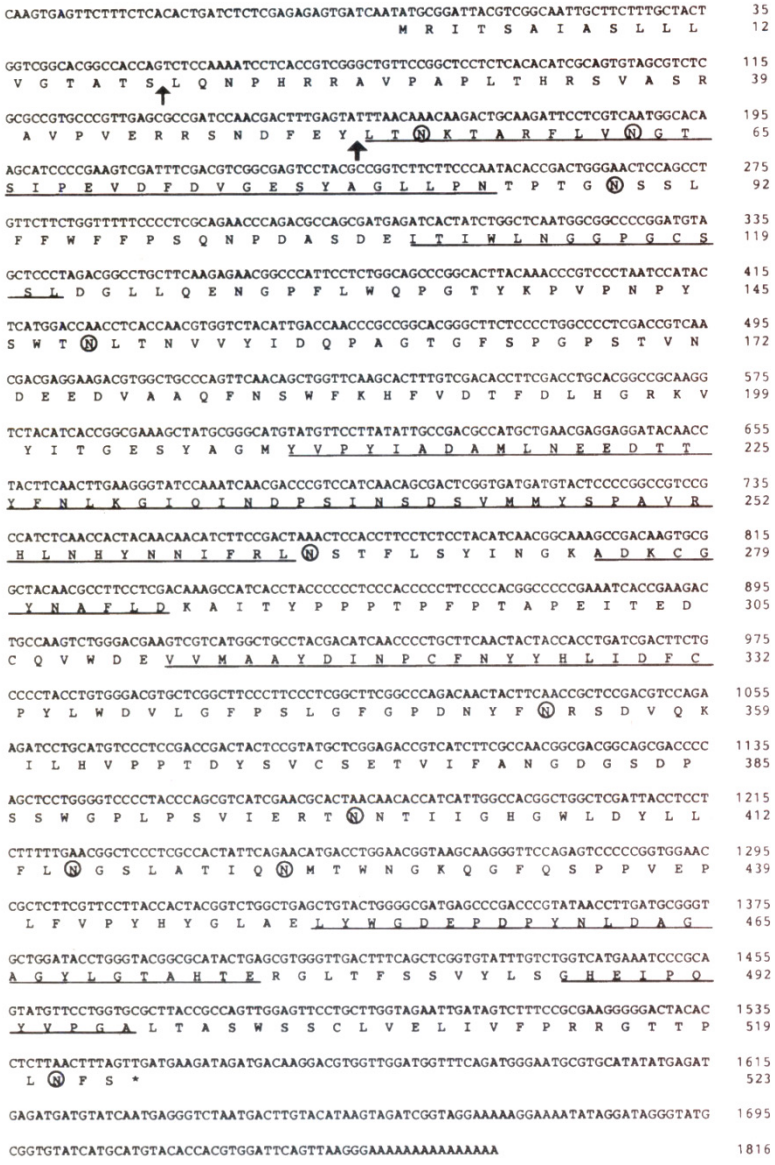

Figure 18. cDNA sequence of A. saitoi carboxypeptidase and deduced amino acid sequence.

Western-blot analysis of yeast cell extracts shows a 72 kDa protein with rabbit anti-(*A. saitoi* carboxypeptidase) serum, which is consistent with the apparent molecular mass of the native *A. saitoi* carboxypeptidase. Conversely, the extracts obtained from yeast cells transfected with the vector (pG-3) alone or with cDNA in reverse orientation (pGP31), as negative controls, yielded no stainable protein.

The recombinant carboxypeptidase was treated with glycopeptidase F and was subjected to SDS-PAGE. De-N-glycosylated recombinant enzymes migrated with apparent molecular masses of 62 kDa, a little larger or equivalent to that of de-N-glycosylated carboxypeptidase from *A. saitoi*.

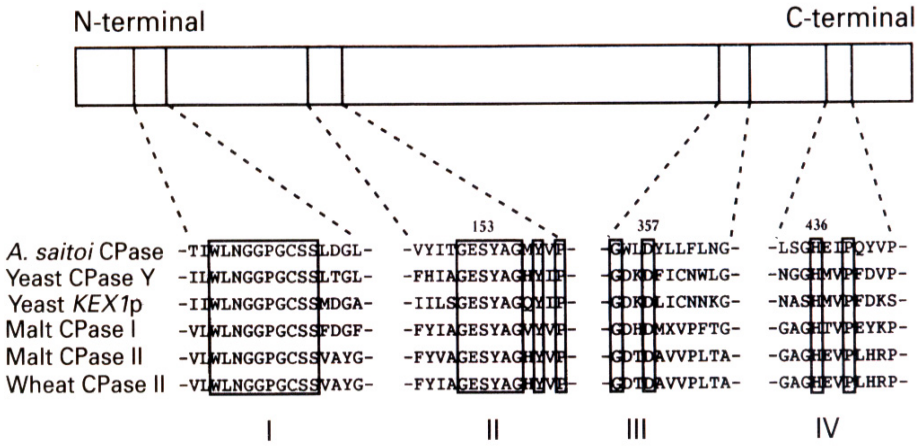

Figure 19. Comparison of the peptide domains reportedly required for enzyme catalysis in eukaryotic serine carboxypeptidases.

The recombinant carboxypeptidase was purified using gel-filtration and cation-exchange chromatography. The purified recombinant enzyme was homogeneous after SDS-PAGE and had a subunit electrophoretic mobility slightly greater than that of the carboxypeptidase from *A. saitoi*. The recombinant carboxypeptidase was subjected to gel filtration on a TSKgel G3000W XL column in comparison with standard proteins of known size.

The estimated molecular mass of the recombinant carboxypeptidase was 135 kDa, which is expected for a dimmer.

The specific activity of the recombinant carboxypeptidase towards Z-Tyr-Leu was measured at pH 3.1. The value for recombinant carboxypeptidase was 4.1 katal/kg, which was almost the same as that of *A. saitoi* carboxypeptidase, 4.5 katal/kg.

As shown in Figure 19, four conserved regions were observed in the *A. saitoi* carboxypeptidase sequence. To establish whether the Ser153, Asp357, and His436 residues in the conserved regions were essential for activity of the *A. saitoi* carboxypeptidase, we generated point mutations that changed each residue to alanine, by oligonucleotide site-directed mutagenesis. The mutated *cpdS* genes were cloned into the pG-3 plasmid and introduced into yeast YPH250 cells. Mutant catboxypeptidases (S153A, D357A, and H436A) were then produced in 5-day cultures. Attempts to detect an inactive protein were made by Western blotting, with the wild-type enzyme as molecular-mass standard. Responses were obtained in all mutants. Next, each extract was assayed with Z-Tyr-Leu at pH 3.1; however, no carboxypeptidase activity was detected from any mutant protein. The Asp138 mutant protein (D138A), as a positive control, completely retained the carboxypeptidase activity. These results suggest that the *A. saitoi* carboxypeptidase functionally conserves the catalytic residues (Ser153, Asp357, and His436) of any other carboxypeptidase, and strongly imply that the *A. saitoi* caeboxypeptidase is a serine proteinase with a catalytic triad comprising

Asp-His-Ser. It can be concluded that *A. saioti* carboxypeptidase is a member of the serine carboxypeptidase C family (EC 3.4.16.5) [89].

6.4. Debittering of the Bitter Peptides

Enzymatic hydrolysates of various proteins have a bitter taste, which may be one of the main drawbacks to their use in food. Arai *et al*. [90] showed that the bitterness of peptides from soybean protein hydrolysates was reduced by treatment of *Aspergillus* acid carboxypeptidase from *A. saitoi*. Significant amounts of free leucine and phenylalanine were liberated by *Aspergillus* carboxypeptidase from the tetracosapeptide of the peptic hydrolysate of soybean as a compound having a bitter taste. Furthermore, the bitter peptide fractions obtained from peptic hydrolysates of casein, fish protein, and soybean protein were treated with wheat carboxypeptidase W [91]. The bitterness of the peptides lessened with an increase in free amino acids. Carboxypeptidase W can eliminate bitter tastes in enzymatic proteins and is commercially available for food processing.

6.5 A new high-mannose type N-linked oligosaccharide

A saitoi acid carboxypeptidase is a glycoprotein that contains both *N*- and *O*-linked sugar chains [81, 82]. Glycosylation of the *A. saitoi* carboxypeptidase suggests the stability of this enzyme against proteinase and proteolysis. In this chapter, the characterization of a new N-linked high-mannose type oligosaccharide from *A. saitoi* acid carboxypeptidase is described.

The sugar chain was cleaved by N-glycanase (Seikagaku Kogyo, Tokyo) from heat-denatured carboxypeptidase with SDS that was purified to homogeneity from the commercial enzyme preparation of *Aspergillus saitoi* ('Molsin', Seisin Pharmaceutical Co., Ltd., Chiba). The cleaved oligosaccharides were purified by gel filtration on a Bio-Gel P 4 column. One major oligosaccharide fraction eluted from the column was used for further structural analyses. The ^{1}H-NMR spectrum of the anomeric proton region of the intact oligosaccharide (Figure 20) was compared with that of the reference oligosaccharide of $Man_9GlcNAc$ [92, 93] from yeast mannoprotein (Table 13). The set of chemical shift values of the intact oligosaccharide was almost identical to that of the yeast $Man_9GlcNAc$ [92, 93] except for the addition of the signal at 5.386 ppm which was assigned to the Man-7 of $Man_{10}GlcNAc_2$ (Figure 20B). Owing to the O-2 substitution of Man-7 in $Man_9GlcNAc_2$ by Man-10, the signals at 5.077 ppm and 5.096 ppm of Man-7 showed a downfield shift (Table13). Chemical shifts appearing around 4.8 ppm and 5.1 ppm should be assigned to the unsubstituted Man-6 and Ma-7, respectively. There must be some contaminanting sugar chains in $Man_{10}GlcNAc_2$. To confirm the mode of the linkage of terminal mannose, the oligosaccharide was digested with the exo-α1→2-mannosidase from *Aspergillus saitoi* [94, 95] at pH 5.0. The ^{1}H-NMR spectrum of the exo-α1→2-mannosidase resistant fragment indicates the structure identification to that of the standard $Man_5GlcNAc_2$. On the other hand, the ^{1}H-NMR spectrum of core oligosaccharide from yeast mannoprotein earlier digested with exo- 1,2-α-mannosidase gave one additional signal at 4,917 ppm, indicating the structure of $Man_6GlcNAc$ (Table 13).

The FAB-MS spectrum of the N-linked oligosaccharide from *A. saitoi* carboxypeptidase gave the *m/z* ion as $(M + Na)^+ = 2067$, which is consistent with the molecular mass of $Man_{10}GlcNAc_2 + 23$. The secondary fragments are formed by elimination of Man and Man_2, to give the ions with *m/z* 1905 and 1743, respectively.

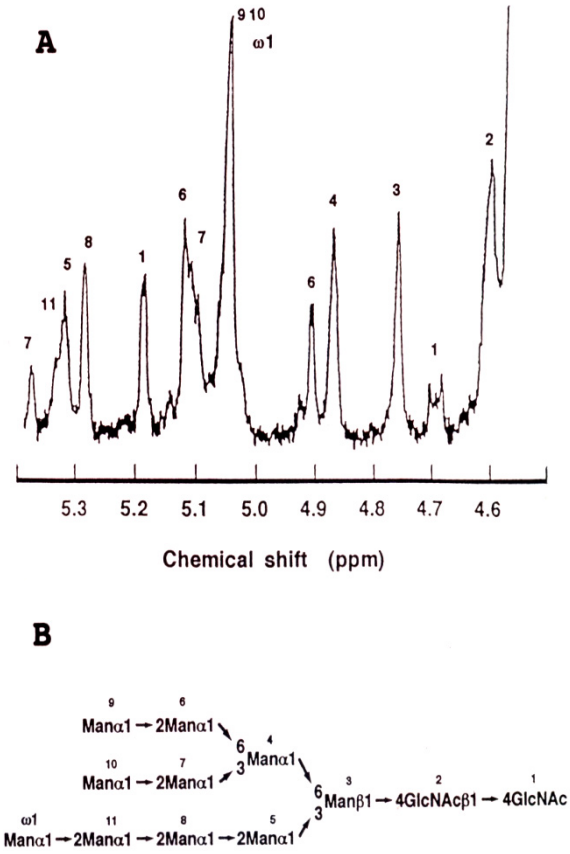

Figure 20. 400 MHz 1H-NMR spectrum of anomeric region at 50oC (A) and proposed structure (B) of the oligosaccharaide from Aspergillus saitoi carboxypeptidase.

To analyze the detailed structure of the oligosaccharide, we used partial acetolysis using the pyridylaminated (PA) derivative $Man_5GlcNAc_2$-PA was derived by partial acetolysis, indicating the oligosaccharide had an extra mannose residue (ω1) substituting for Man-11 in the lower arm of $Man_9GlcNAc_2$. On the bases of the above results, the sugar chain structure of *A. saitoi* carboxypeptidase is proposed as Manα1→2Manα→6(Manα1→2Manα1→3)Manα1→6(Manα1→2Manα1→2Manα1→2Manα1→3)Manβ1→4GlcNAcβ1→4GlcNAc (Figure 20 B), which has not been found in yeast glycoproteins (96) as well as in animal glycoproteins [97].

Table 13. 1H-NMR analysis of Man10GlcNAc2 from CPase 200dpi

Compound	Sugar residue and structure					δ				
	D	C	B	A	A′	D	C	B	A	A
								ppm		
Sugar chain of *A. saitoi* CPase (**I**)	αM →^{6} αM →^{6} βM →^{4}			βGlcNAc →^{4}	αβGlcNAc	5.128	4.877	4.767	4.619	5.192 4.693
	αM ↑^{2}	αM ↑^{3}	βM ↑^{3}							
	αM	αM ↑^{2}	αM ↑^{2}			5.051	5.386	5.328		
		αM	αM ↑^{2}				5.051	5.294		
			αM ↑^{2}					5.335		
			αM					5.051		
Exo-α1→2-mannosidase product of **I**	αM →^{6}	αM →^{6}	βM →^{4}	βGlcNAc →^{4}	αβGlcNAc	4.900	4.876	4.762	4.650	5.178 4.699
		αM ↑^{3}	βM ↑^{3}							
		αM	αM				5.098	5.101		
Yeast mannoprotein inner core fragment	αM →^{6}	αM →^{6}	βM →^{4}	αβGlcNAc		5.146	4.876	4.774	5.197 4.675	
	αM ↑^{2}	αM ↑^{3}	βM ↑^{3}				5.077			
	αM	αM	αM ←^{6}	αM		5.043	5.096	5.340	4.913	
			αM ↑^{2}					5.286		
			αM ↑^{2}							
			αM					5.043		

A number of experiments on the biosynthesis of N-linked oligosaccharides have shown that the maximum length of the high-mannose type structure was $Man_9GlcNAc_2$ which was synthesized in the rough endoplasmic reticulum. Then, the glycoprotein is transferred to the Golgi apparatus and stepwise transfer of mannose takes place. Processing of the N-linked sugar chain of fungal glycoproteins in the Golgi apparatus is not known in contrast to the case of animal glycoproteins [97]. Therefore, the formation process of the unusual structure of $Man_{10}GlcNAc_2$ in *A. saitoi* carboxypeptidase is further problem.

6.6. Carbohydrate Moiety of Acid Carboxypeptidase

The carbohydrate was determined to be 29.1% of the molecular mass of the carboxypeptidase [82]. Mild alkali treatment of the enzyme, under conditions that effect β-elimination of the sugar-substituted serine or threonine, caused a reduction of the carbohydrate content from 29.1% to 19.3%. This suggests that O-linked sugar chains account for about 10% of the total mass, while another 19% must be N-linked sugar chains. The neutral sugar composition analysis of the hydrolysates of the carboxypeptidase showed only D-mannnose, including the presence of high-mannose type sugar chains.

The partially purified N-linked oligosaccharides were pyridylaminated (PA), and the resulting PA-derivatives were analyzed by size-fractionation HPLC (Figure 21). At least eight peaks were detected. The main peaks were eluted at the eluted position of $M8.1^3$ and M9.1; however, three peaks (terminated fractions M10, M11, and M12 respectively) were eluted behind M9.1. All eight peaks were collected together, and the mixture of the peaks was digested with 1,2-α-D-mannosidase (94, 95) from *A. saitoi*. Digestion of the PA-derivatives with1,2-α-D-mannosidase gave one peak cooresponding to the elution position of M5.1, indicating that all of the N-linkd oligosaccharides from *A. saitoi* acid carboxypeptidase had

M5.1 as a "core" fragment, and several extra mannose were attached to the M5.1 core through α-1,2 linkages.

The structure of the PA-oligosaccharide derived from the fraction M10 was analyzed previously (81). In this study, we purified the PA-oligosaccharide derived from the fraction M11 by HPLC, using reverse phase chromatography column (Cosmosil 5C18-P). One major peak (termed fraction 11-C) and two minor peaks (fraction 11-A and B) of PA-oligosaccharides were obtained from fraction M11. The small yield of fractions 11-A and B were not analyzed further. Fraction 11-C was further purified by the size-fractionation HPLC. To analyze the mannosyl linkage of fraction M11, the sequential exoglycosidases digestions were carried out. Digestion of fraction 11-C by 1,2-α-D-mannosidase (*A. saitoi*) [94, 95] at pH 5.0 yielded a new peak corresponding to the elution position of M5.1.

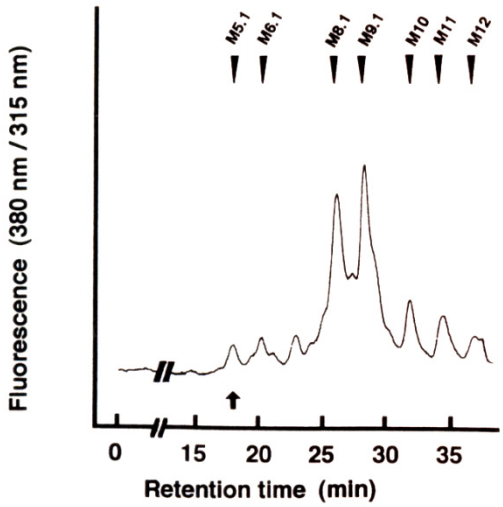

Figure 21. Elution patterns of PA-oligosaccharides derived from A. saioti acid carboxypeptidease.

This product was successively digested with α-mannosidase (Jack Bean), then four mannose residues were released. These results indicate that fraction 11-C has four mannose residues with α-1,2- or α-1,6-linkages and another six mannose residues with α-1,2-linkages located outside of the core.

Partial acetolysis of the fraction 11-C under conditions in which α-1,6-mannosidic linkages are cleaved preferentially gave $Man_6GlcNAc_2$-PA. The $Man_6GlcNAc_2$-PA was digested with 1,2-α-D-mannosidase (*A. saitoi*) [94, 95], resulting in a new product which was eluted at the elution position of M2. It suggested that the lower arm of this oligosaccharide had a structure as follows; Manα1-2Manα1-2Manα1-2Manα1-2Manα1-3Manβ1-4GlcNAcβ1-4GlcNAc. From these results, the structure of Fraction 11-C was proposed to be M11 ($Man_{11}GlcNAc_2$) as shown in Figure 22.

The O-linked sugar chains were prepared by alkaline treatment from the acid carboxypeptidase, and β-elimination products were separated from the polypeptide by precipitation with 7% ethanol. The liberated oligosaccharides (70% ethanol-soluble fraction) were analyzed by HPLC. Only one peak was found at a position corresponding to a monosaccharide (Figure 23). On paperchromatographic analysis, only one spot was also

obtained at the position of mannitol. The O-linked sugar chains were also analyzed by gas chromatography as alditol trifluoroacetate. Only one peak was detected as a mannitol derivative (Figure 23 A). These results indicate the O-linked sugars of *A. saitoi* acid carboxypeptidase are composed of single mannose residues.

Incubation of the purified acid carboxypepidase with Endo H and α-mannosidase (Jack Bean) effected a decrease in its molecular mass and in the width of the protein band on SDS-PAGE. Molecular masses of 136 kDa (dimeric form) and 72 kDa (monomeric form) were estimated for the native (glycosylated) acid carboxypeptidase by low-angle laser lightscattering photoenergy and SDS-PAGE, respectively. The deglycosylated enzyme migrated under identical conditions with an apparent molecular mass of 129 kDa (dimmer) and 60 kDa (monomer), respectively.

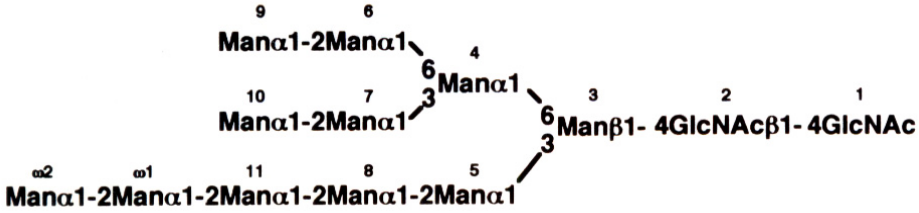

Figure 22. Proposed structure of N-linked oligosaccharide of the fraction 11-C from A. saitoi acid carboxypeptidase.

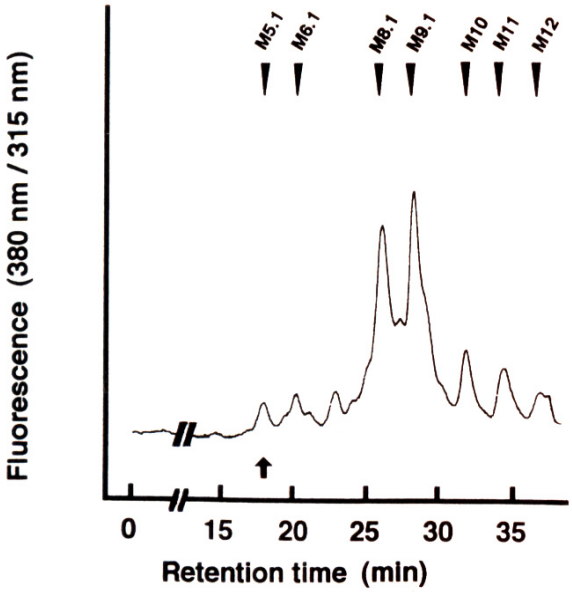

Figure 23. (A) Gas chromatography of trifluoroacetate ---- from A.saitoi acid CPase. (B) HPLC profile of alkali-treatment products from A. saitoi CPase.

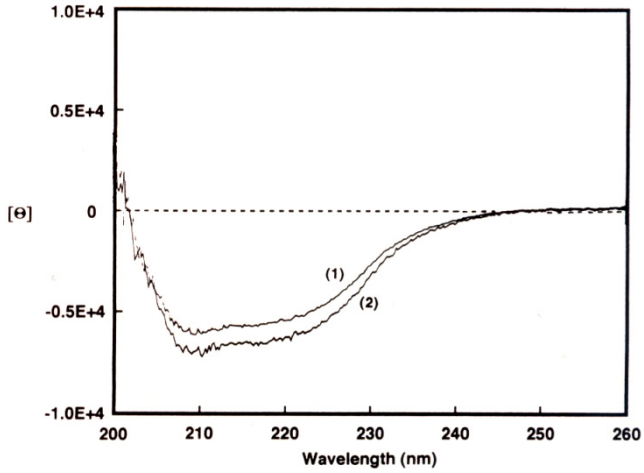

Figure 24. Molecular ellipticity [θ] of native and deglycosylated *A. saitoi* acid carboxypeptidase.

Table 14. Secondary structures of native and deglycosylated acid carboxypeptidases from *Aspergillus saitoi*

Enzyme	α-Helix (%)	β-Sheet (%)	β-Turn (%)	Random (%)
Deglycosylated carboxypeptidase	21.2	30.5	21.8	26.5
Native carboxypeptidase	19.1	23.5	27.1	30.3

(Chiba, Y., et al., Curr. Microbiol., 27, 281-288 (1993))

To investigate whether the oligosaccharide chain influenced protein conformation, the CD and absorption spectra of glycosylated and deglycosylated forms were measured. Slight differences were found between them (Figure 24). From the CD spectra, the contents of α-helix, β-structure, and random coil were calculated (Table 14). The contents of α-helix in the enzymes were almost the same, whereas the contents of β-structure increased in the deglycosylated enzyme. The absorption spectra of the two forms showed no apparent changes. The specific activity of the enzyme decreased slightly from 0.32 katal/kg to 0.31 katal/kg upon deglycosylation. The K_m and k_{cat} values of the native and the deglycosylated enzymes showed no differences (Table 15). The pH and temperature optimum were unaffected by the deglycosylation process. Both forms of the acid carboxypeptidases were most active at pH 3.0-3.5 towards Z-Glu-Tyr. Native acid carboxypeptidaswe was fully active below 50°C but gradually became inactivated above 55°C and denatured completely at 70°C. The temperature activity profile of the deglycosylated enzyme showed a pattern similar to that of the native enzyme.

Deglycosylation had no marked effect on the stability of the acid carboxypeptidase. Both native and deglycosylated enzymes were stable up to 50°C and active in the presence of 4 M urea after 24 h. The molecular structures of both enzymes were not impaired by pepsin at pH 2.5 (Figure 25). These two enzymes had similarly great resistance to peptic digestion after 24h.

The mycelial wet weight and the protein contents of the mycerial extracts and of the culture filtrates were determined at intervals during growth of mycelia. Addition of tunicamycin (final concentration 5 μg/ml) to the culture medium at the beginning of the culture period had little effect on the growth of the fungus, and the protein concentration of the culture filtrate was slightly decreased. On the other hand, a marked decrease of the acid carboxypeptidase activity in the culture filtrate was found (Figure 26 A).

To examine whether unglycosylated acid carboxypeptidase can secreted into the medium, we assayed medium in the presence or absence of tunicamycin by Western blotting analysis. The results indicate that the acid carboxypeptidase was not secreted into the culture medium when tunicamycin was added (Figure 26 B). This suggests that the decrease of enzymatic activity in culture filtrates of mycelia grown in the presence of tunicamycin is largely owing to the decrease of the concentration of the enzyme.

Table 15. Kinetic parameters of active and deglycosylated acid carboxypeptidases from *Aspergillus saitoi* toward Z-Glu-Tyr at pH 3.1 and 30°C

Enzyme	K_m (mM)	k_{cat} (s^{-1})	k_{cat}/K_m ($s^{-1} \cdot mM^{-1}$)
Deglycosylated carboxypeptidase	3.8	97.6	25.7
Native carboxypeptidase	3.6	93.6	26.0

(Chiba, Y., et al., Curr. Microbiol., 27, 281-288 (1993))

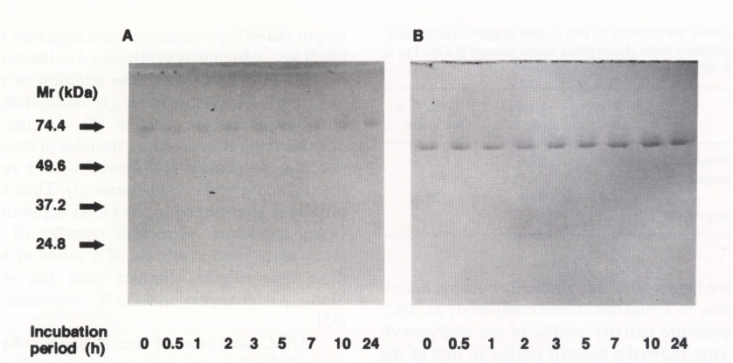

Figure 25. Effect of pepsin treatment on the MW of (A) native and (B) deglycosylated A.saitoi CPase.

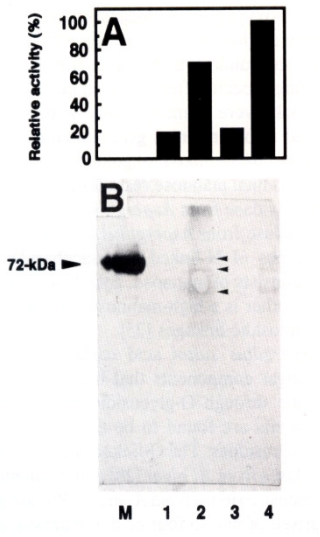

Figure 26. Relative activity of A. saitoi acid carboxypeptidase produced in the culture filtrate in the presence and absence of tunicamysin (A). Western blot analysis of the culture filtrate against the anti-acid carboxypeptidase antibody on SDS-PAGE (B).

7. 1,2-A-D-MANNOSIDASE FROM *ASPERGILLUS SAITOI*

7.1. 1,2-A-D-Mannosidase

The importance of α-mannosidase (EC 3.2.1.24) in the processing system of glycoprotiens in higher eukaryotic cells is well known (98-101). In mammalian cells, 1,2-α-mannosidases are an essential in the early steps of N-linked oligosaccharaide maturation (102). In the Enzyme Nomenclature Recommendations [103], three types of α-mannosidases, namely α-D-mannoside mannohydrolase (EC 3.2.1.24), 1,2-α-mannosyl-oligosaccharide-α-D-mannohydrolase (EC 3.2.1.1.113) and 1,3-(1,6)-mannosyl-oligosaccharide α-D-mannohydrolyase (EC 3.2.1.114), are given as systematic names.

We have described the purification to homogeneity of 1,2-α-D-mannosidases from fungi *Aspergillus saioti* (*A. phoenicis*) [94, 95], *Penicillium citrinum* [104, 105] and *Pycnoporus coccineus* [106] specifically capable of releasing α(1-2)-linked mannose residues from oligosaccharides derived from asparagines-linked glycans of glycoproteins. Ballou [107] isolated characterized the exo-1,2-α-mannosidase from *A. saitoi* and examined its proerties.

The predicted amino acid sequence of the 1,2-α-D-mannosidase from *A. saitoi* (107) is 70, 26, and 35% identical with those of *P. citrunum* 1,2-α-D-mannosidase [108], yeast (*S. cerevisiae*) Man_9-specific mannosidase [109, 110] and mouse Golgi 1,2-α-D-mannosidase from [111], respectively.

7.2. Expression of *A. Saitoi* 1,2-A-D-Mannosidase Gene (*Msds*) in *A. Oryzae* Cells

For the construction of an overexpression system of the intracellular 1,2-α-mannosidase (EC 3.2.1.113) gene (*msdS*) from *A. saitoi* (*A. phonenicis*), the NH_2-terminal signal sequence of the gene was replaced with that of the aspergillopepsin I (EC 3.4.23.18) gene (*apnS*) signal [112]. Then the fused 1,2-α-mannosidase gene (f-*msdS*) was inserted into the *Not*I site between P-No8142 and T-*agdA* in the plasmid pNAN 8142 (9.5 kbp) and thus the *Aspergillus oryzae* expression plasmid pNAN-AM1 (11.2 kbp) was constructed. The fused f-*msdS* gene has been overexpressed in a transformant *A. oryzae niaD* AM1 cell. The recombinant enzyme expressed in *A. oryzae* cells was purified to homogeneity in two steps. The system is capable of making as much as about 320 mg of the enzyme/liter of culture.

The recombinant enzyme has activity with methyl-2-*O*-α-D-mannopyranosyl α-D-mannopyranoside (Man-α1,2-Man-OMe) at pH 5.0, while no activity was determined with methyl-3-*O*-α-D-mannopyranosyl α-D-mannopyranoside (Man-α1,3-Man-OMe) or methyl-6-*O*-α-D-mannopyranosyl α-D-mannopyranoside (Man-α1,6-Man-OMe). The substrate specificity of the enzyme was analysed by using pyridylaminated (PA)-oligomannose-type sugar chains, $Man_{9\text{-}6}(GlcNAc)_2$-PA (Man is mannose; GlcNAc is N-acetylglucosamine). The enzyme hydrolysed $Man_8GlcNAc_2$-PA (type 'M8A', Manα1-2Manα1-2Manα1-3[Manα1-3(Manα1-2Manα1-6)Manα1-6]Manβ1-4GlcNAcβ1-4

GlcNAc-PA) fastest. While, the results showed that the poorest substrate among the PA-sugar chains was 'M6C' (Manα1-3[Manα1-2Manα1-3(Manα1-6)Manα1-6]Manβ1-4GlcNAcβ1-4GlcNAc-PA) for the *A. saitoi* 1,2-α-D-mannosidase, and it was assumed that the Manα1-2 residue in M6C interfered with the hydrolysis of other Manα1-2 residues.

Molecular mass values of the enzyme were determined to be 63 kDa by SDS/PAGE and 65 kDa by gel filtration on Superose 12 respectively. The p*I* value of the enzyme was 4.6. The NH_2-terminal amino acid sequence of the enzyme was GSTQSRADAIKAAFSHAWDGYLQY, and sequence analysis indicated that the signal peptide from aspergillopepsin I gene (*apnS*) gave was removed. The molar absorption coefficient, ε, at 280 nm was determined as 91539 $M^{-1} \cdot cm^{-1}$. Contents of the secondary structure (α-helix, β-structure and the remainder of the enzyme) by far-UV CD determination were about 55, 38 and 7%, respectively. The melting temperature, T_m, of the enzyme was 71°C by differential scanning calorimetry. The calorimetric enthalpy, ΔH_{cal}, of the enzyme was calculated as 13.3 kJ • kg of $protein^{-1}$.

7.3. Catalytic Residues of Ca^{2+}-Independent 1,2-A-D-Mannosidas from *A. Saioi*

Preliminary site-directed mutagenesis experiments of the fused 1,2-α-D-mannosidase gene (f-*msdS*) on the expression vector, pGAM-1, were done previously to identify the functional role of catalytic residues in the 1,2-α-D-mannosidase from *A. saitoi* expressed in yeast cells [113].

Seven carboxylic acid residues to be studied were constructed in the cloned *A. saitoi* 1,2-α-D-mannosidase gene (*msdS*) by site-directed mutagenesis. The roles of six conserved active

carboxylic acids in the catalytic mechanism of *A. saitoi* 1,2-α-D-mannosidase were identified by site-directed mutagenesis and kinetic analyses [114]. Recombinant enzymes were purified homogeneously on SDS-PAGE gels (Figure 27A) and identified as *A. saitoi* 1,2-α-D-mannosidase by Western blot analysis (Figure 27B). Purified forms of all recombinant enzymes were assayed by the Somogyi-Nelson method with Man-α1,2-Man-OMe as a substrate. No activity was detected under standard assay conditions for any of the mutant enzyme except E504Q, and the specific activity could only be determined after extended incubation, typically at 60-90 min (Table 16). From Table 16, it appears obvious that the mutations generated resulted in enzymes with significantly reduced ability to hydrolyze Man-α1,2-Man-OMe, as their specific activity is at least 10^3-fold less than that of the wild type enzyme. The specific activities of D269N and E411Q mutants in particular were not detected completely. The results of several experiments suggest that there is no significant contamination by wild type 1,2-α-D-mannosidase in the low activity of mutant enzymes (D269N and E411Q).

Kinetic characterization of E124Q, E124D, D269E, E273D, E411D, E414D, and E474D mutants and wild type 1,2-α-D-mannosidase was perfomed at pH 5.0 using Man-α1,2-Man-OMe as a substrate. Results of these kinetic experiments are in Table 17. Kinetic parameters for D269N and E411Q mutants could not be measured, since the reaction rates were below the detectable limit. The k_{cat} value for E124Q mutant was 0.0078 s^{-1}, almost 0.3% that of the wild type enzyme. E124D mutant enzyme also decreased the k_{cat} value (0.9% of wild type enzyme). The K_m values of E124Q and E124D mutant enzymes were essentially unchanged.

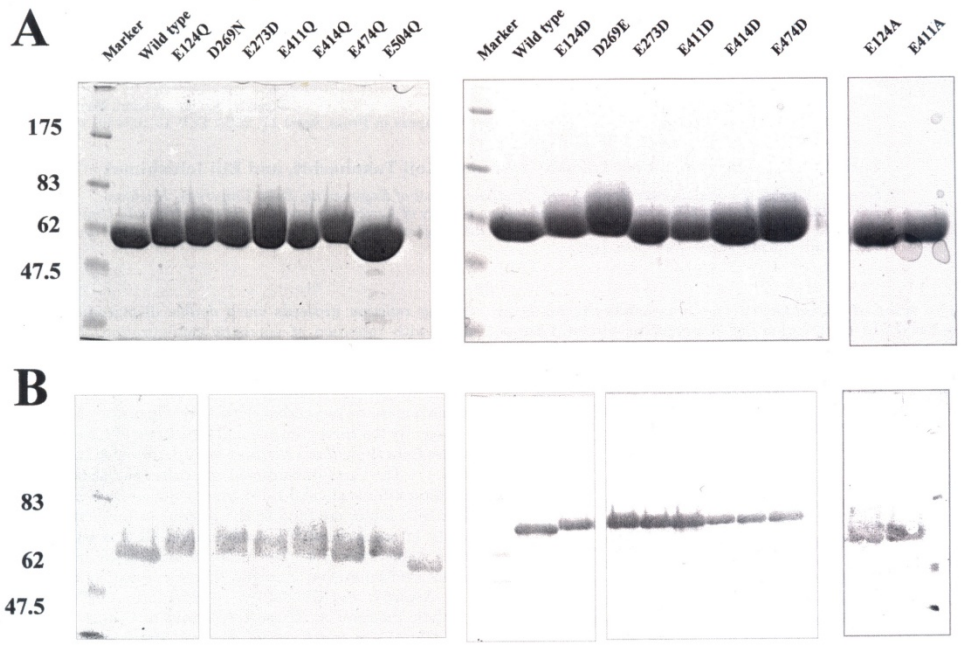

Figure 27. SDS-PAGE (A) and Western blot analysis (B) of the A. saitoi 1,2-α-D-mannosidase and mutants.

Table 16. Specific activities of purified wild type and mutant 1,2-α-D-mannosidases from *A. saitoi*

Mutant 1,2-α-D-mannosidase	Specific activity mkatal/kg[a]	Relarive activity %
Wild type	47.3	100
E124Q	0.009	0.020
E124D	0.096	0.20
D269N	ND[b]	
D269E	0.92	1.9
E273Q	0.007	0.015
E273D	0.30	0.63
E411Q	ND[b]	
E411D	0.35	0.74
E414Q	0.004	0.009
E414D	0.19	0.40
E474Q	0.003	0.006
E474D	0.25	0.53
E504Q	7.0	15

[a]Using Manα1,2Man-OMe as substrate. One katal releases 1 mol of reducing group (calculated as mannose) per second at 30°C, pH 5.0.
[b]ND, not detected.
(Tatara, Y., *et al., J. Biol. Chem., 278*, 25289-25294 (2003)).

Table 17. Kinetic parameters of wild type and mutant 1,2-α-D-mannosidases from *A. saitoi*

Mutant 1,2-α-D-mannosidase	K_m (mM)	k_{cat} (s^{-1})	k_{cat}/K_m $s^{-1} \cdot mM^{-1}$	%
Wild type	0.28	2.5	9.04	100
E124Q	0.13	0.0078	0.062	0.7
E124D	0.49	0.022	0.044	0.49
D269N	ND[a]	ND[a]	ND[a]	
D269E	4.8	0.51	0.11	1.2
E273D	7.0	0.37	0.054	0.6
E411Q	ND[a]	ND[a]	ND[a]	
E411D	8.0	1.4	0.18	2.0
E414D	8.6	0.037	0.0043	0.05
E474D	6.4	0.023	0.0036	0.04

[a]ND, not detected.
(Tatara, Y., *et al., J. Biol. Chem., 278*, 25289-25294 (2003)).

Compared with wild type 1,2-α-D-mannosidase, the D269E and E411D mutant enzymes showed 17- and 28-fold increases in K_m values, respectively, whereas the k_{cat} values were

slightly lower than that of wild type enzyme. The K_m values of E273D, E414D, and E474D mutant enzymes were greatly increased to 23-31 fold that of wild type enzyme, and the k_{cat} values were decreased (1-15% wild type enzyme).

pH-activity profiles of E124A and E124D mutant 1,2-α-D-mannosidases for Manα1,2-Man-OMe hydrolysis are shown in Figure 28. The optimum pH of E124D and E124A mutant enzymes shifted from 5.0 to 4.0 and 4.5, respectively. The activity of E124A mutant enzyme was found to be lower than that of wild type enzyme over the whole pH range studied, but the effect was more pronounced for the basic limb.

Effects of an external nucleophile on alanine mutant enzymes were studied. Mutation (Glu or Asp to Ala) at the general base catalyst creates a cavity in the active site that can accommodate a small external nucleophile. Sodium salts of azide at 3 M were used as external nucleophiles in the enzyme-catalyzed hydrolysis of $Man_6GlcNAc_2$-PA sugar chain. The reaction mixture was analyzed by HPLC (Figure 29). The activity of wild type 1,2-α-D-mannosidase was inhibited by a high concentration of azide. The E124A, D269N, and E411A mutant enzymes were inactive in the absebce of azide, as a peak corresponding to a $Man_5GlcNAc_2$-PA was not detected. In the presence of azide, these mutant enzymes could not be reactivated.

Atomic absorption spectrophotometric analysis and kinetic analysis of wild-type 1,2-α-D-mannosidase were performed. Concentrations of Ca^{2+} were determined by atomic absorption spectrophotometric analysis. The purified recombinant wild type 1,2-α-D-mannosidase almost completely did not contain Ca^{2+}. Other divalent metal cations including Mg^{2+}, Mn^{2+}, Co^{2+}, Cu^{2+}, and Zn^{2+} were also not detected.

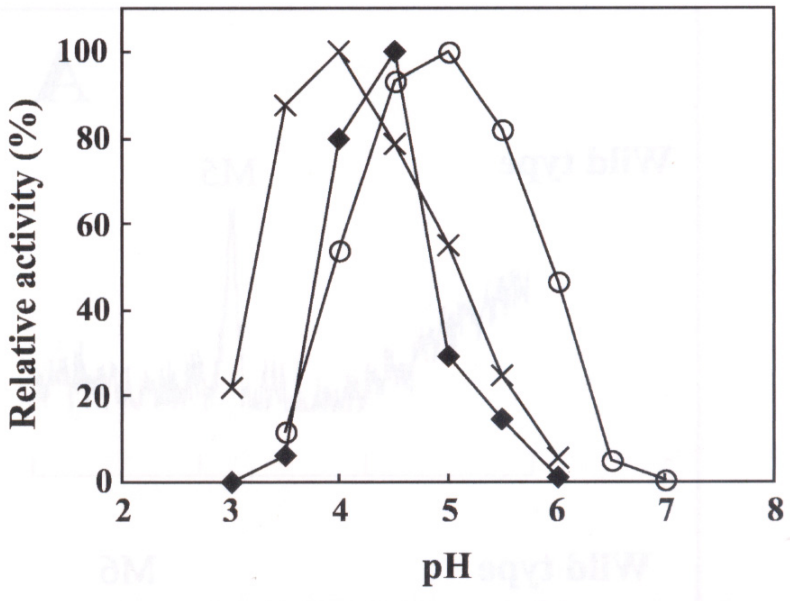

Figure 28. pH-activity profiles of wild type A. saitoi 1,2-α-D-mannosidase and mutants.

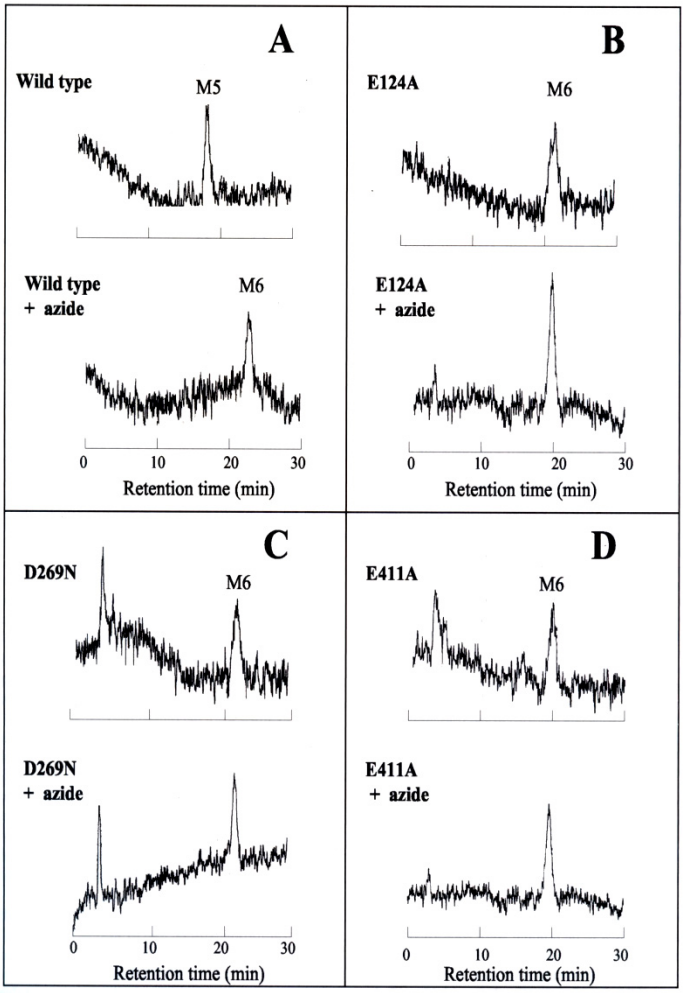

Figure 29. Effect of an external nucleophile on catalytic residue mutants of A. saitoi 1,2-α-D-mannosidase using Man6GlcNAc2-PA as a substrate.

Table 18. Kinetic parameters of wild type and Ca^{2+} biding 1,2-α-D-mannosidase from *A. saitoi*

1,2-α-D-mannosidase	Ca^{2+} binding	K_m	k_{cat}	k_{cat}/K_m
	mol/mol	mM	s^{-1}	$s^{-1} \cdot mM^{-1}$
Wild type	0	0.28	2.53	9.04
Ca^{2+}-treated[a]	0.9	0.29	1.95	6.84

[a]The Ca^{2+}-free wild type enzyme was treated with $CaCl_2$ as described under "Experimental Procedures" of ref. (114).
(Tatara, Y., *et al., J. Biol. Chem., 278*, 25289-25294 (2003))

After Ca^{2+} treatment (see "Experimental Procedures" of ref. [114], Ca^{2+} content was determined as 0.9 mol/mol of wild type 1,2-α-D-mannosidase. Kinetic parameters of Ca^{2+}-free and Ca^{2+} binding 1,2-α-D-mannosidase were determined (Table 18); the k_{cat} and K_m values were little affected by the Ca^{2+} binding.

EDTA inhibited the Ca^{2+}-free wild type 1,2-α-D-mannosidase. The inhibition was investigated by fixed concentrations of EDTA in the assay buffer and by varying the concentrations of substrate. A Lineweaver-Burk plot showed a pattern consistent with competitive inhibition (Figure 30) and gave a K_i of 0.91 mM for EDTA.

For Ca^{2+} binding properties of mutant 1,2-α-D-mannosidase, Ca^{2+} concentration of the mutant 1,2-α-D-mannosidase was determined by atomic absorption spectrophotometry after Ca^{2+} binding treatment. As shown in Table 18, the Ca^{2+}-free wild type enzyme bound 0.9 mol of calcium/mol of protein, ~1 mol/mol. E124D, E411D, and E504Q mutants also contained 0.8, 1.1, and 0.9 mol of calcium/mol of protein, respectively. E124Q, D269E, E269N, E474D contained less calcium than 1 mol of calcium/mol of protein. E411Q, E273Q, E273D, E414Q, and E414D mutants demonstrated an almost complete loss of binding of Ca^{2+}.

Effects of Ca^{2+} binding on 1,2-α-D-mannosidase thermal stability were determined. The spectra of Ca^{2+}-free and Ca^{2+}-bound 1,2-α-D-mannosidase at far and near UV region were consistent with each other. The Ca^{2+} binding did not undergo a large conformational change. Thermally induced loss of secondary and tertiary structure was monitored at 222 and 291 nm, respectively (Figure 31). T_m, the temperature at which half of the molecules are unfolded, for Ca^{2+}-free 1,2-α-D-mannosidase was 56°C and 58°C at 222 and 291 nm, respectively. The Ca^{2+} binding contributed to the thermal stability increasing T_m to 58 °C and 62°C at 222 and 291 nm, respectively.

For identification of catalytic amino acid residues, drastic reductions in the values of the catalytic coefficient (k_{cat}) were observed in the E124Q and E124D mutant enzymes (Table 17). This may result from significant impairment of the chemical steps in the catalytic reaction. The K_m value was essentially unchanged from wild type enzyme. It is, thus, clear that Glu124 participates in glucosidic bond hydrolysis. E124D shifted the optimum pH to be more acidic (Figure 28). This result is shown the lower pK_a of Asp than that of Glu and supports the assumption that Glu124 is directly involved in the catalytic mechanism. It could not be determined whether the Glu124 residue is a carboxylate group (COO^-) or carboxyl group (COOH).

The pH dependence of E124A affected the basic limb, which was generally assumed to be due to the general acid catalyst. An external nucleophile sodium azide did not reactivate the E124A mutant enzyme (Figure 28). Thus the Glu124 may act as an acid catalyst. The mechanism of the all carbohydrate hydrolases usually involves a pair of carboxylic acid residues. In *Penicillium* 1,2-α-D-mannosidase, two of the three residues (Glu124, Asp269, and Glu411 in *A. saitoi* enzyme) are believed to be potentially catalytic residues (115). Glu124 was suggested to act as an acid catalyst as discussed above. The most likely candidates for other catalytic residues are Asp269 and Glu411. However, D269E and E411D did not show a considerable decrease in the k_{cat} values (Table 17).

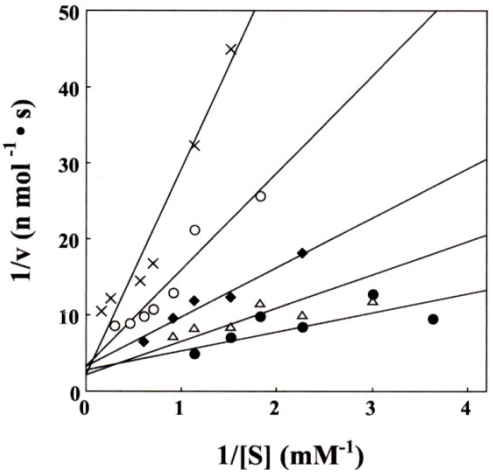

Figure 30. Lineweaver-Burk plot of A. saitoi 1,2-α-D-mannosidase in the presence of EDTA.

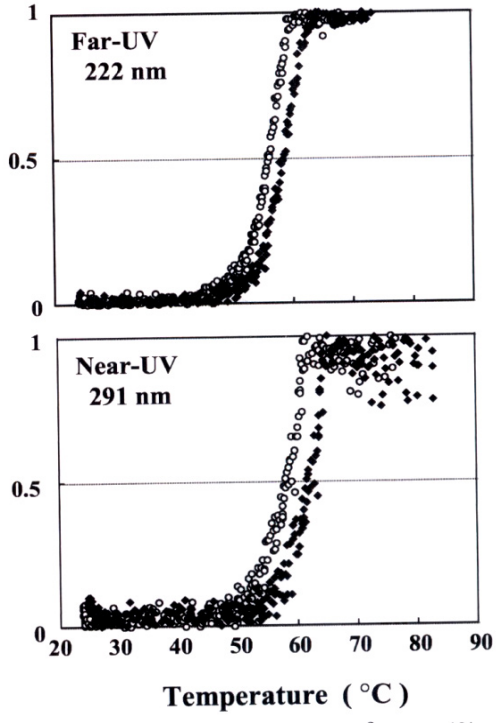

Figure 31. Thermal transition curves of Ca-free and Ca-bound A. saitoi 1,2-α-D-mannosidase.

Recently, a base catalyst of an inverting β-amylase (EC 3.2.1.2) from *Bacillus cereus* var. *mycoides* was determined by the chemical rescue methodology for a catalytic site mutant (E367A) by azide [116]. In the case of *A. saitoi* 1,2-α-D-mannosidase an external nucleophile did not reactivate the D269N and E411A mutant enzymes (Figure 29). Neither Asp269 nor Glu411 residues can be a base catalyst in the normal sense. Although the D269N and E411Q mutant enzymes were catalytically inactive, the D269E and E411D mutant enzymes showed considerable activity. The results indicate that the carboxyl groups at these positions may be

required for the 1,2-α-D-mannosidase activity. Structural and modeling studies on cellobiohydrolase Ce16A (EC 3.2.1.91) from *Trichoderma reesei* suggest that the catalytic mechanism may not directly involve a catalytic base [117]. The catalytic mechanism of 1,2-α-D-mannosidase deviates from the typical glycosyl hydrolase.

E273D, E414D, and E474D mutant enzymes decreased k_{cat} values and increased K_m values (Table 17). The reduction of the k_{cat} value is assumed to be due to the destabilization of the sugar ring. It has become increasingly clear that ring distortion at the −1 site is crucial in the catalytic mechanism of cellobiohydrolase [118, 119]. The catalytic reaction of α-amylase from *Pseudomonas stuzeri* involves three acidic residues; two residues act as a proton donor and a proton acceptor. The other residue works to tightly bind the substrate, giving a twisted and deformed conformation of the glucose ring at position −1 [120]. Glu273, Glu414, and Glu474 of *A. saitoi* 1,2-α-D-mannosidase may bind the substrate to change the conformation of the mannose ring into more reactive one. The three-dimensional structure of *P. citrinum* 1,2-α-D-mannosidase indicates that Glu271, Glu412, and Glu472 residues (Glu273, Glu414, an Glu474 in *A. saitoi* enzyme) in the active site are located at the bottom of the cavity and are not directly involved in the catalytic mechanism. It is demonstrated that these residues are hydrogen-bounded to the Ca^{2+} via water molecule, and the Ca^{2+} is involved in the stability of a substrate. But the recombinant wild type *A. saitoi* 1,2-α-D-mannosidase contained no Ca^{2+} and other divalent metal cations. Despite the Ca^{2+} having no effect on the 1,2-α-D-mannosidase activity (Table 18), its binding sites were conserved in *A. saitoi* 1,2-α-D-mannosidase. This also indicates that the drastic decrease of the activities of E273D, E414D, and E474D mutants (Table 19) did not parallel the loss of the Ca^{2+} binding ability. These residues are involved in the substrate binding sites.

Table 19. Ca^{2+} binding properties of wild type and mutant *A. saitoi* 1,2-α-D-mannosidases after Ca^{2+}-treatment determined by atomic absorption spectrophotometry

Mutant 1,2-α-D-mannosidase	Bound Ca^{2+} mol/mol
Wild type	0.9
E124Q	0.44
E124D	0.8
D269N	0.12
D269E	0.2
D273Q	0
E273D	0
E411Q	0.06
E411D	1.1
E414Q	0
E414D	0
E474Q	0.45
E474D	0.5
E504Q	0.9

(Tatara, Y., *et al., J. Biol. Chem., 278*, 25289-25294 (2003))

It was reported earlier that the recombinant *A. saitoi* 1,2-α-D-mannosidase has a molecule of Ca^{2+} [112]. In this study [114], the recombinant wild type *A. saitoi* 1,2-α-D-mannosidase contained no Ca^{2+}. The purified wild type enzyme did not bind Ca^{2+} with an addition of $CaCl_2$. We found that the Ca^{2+}-free enzyme bound 1 mol of Ca^{2+} per 1 mol of protein after the addition of high concentration of NaCl. It was also demonstrated that the Ca^{2+} binding site is conserved (Table 19). 1,2-α-D-Mannosidase generally requires a divalent metal cation for the activity [121-125]. In the case of *A. saitoi* 1,2-α-D-mannosidase, the Ca^{2+} had no effect on either the k_{cat} or K_m value (Table 18). Thus, it is clear that Ca^{2+} is not essential for the activity of *A. saitoi* 1,2-α-D-mannosidase, although the Ca^{2+} binding site is conserved. EDTA was shown to behave as a competitive inhibitor of *A. saitoi* 1,2-α-D-mannosidase (Figure 30); this indicates that the enzyme contains no divalent metal cation, 1-Deoxymannojirimycin inhibits 1,2-α-D-mannosidase as a substrate analog. However, EDTA is not a analog. Tris is a competitive inhibitor for 1,2-α-D-mannosidase from rabbit river [122].

Tris and other buffers contamining primary hydroxyl group substantially decreased its activity [126, 127]. Carboxyl groups of EDTA may have an affinity for the addition of *A. saitoi* 1,2-α-D-mannosidase. A molecule of Ca^{2+} contributed to thermal stabiliy (Figure 31). The role of Ca^{2+} for *A. saitoi* 1,2-α-D-mannosidase is to protect the enzyme against thermal denaturation, and it was observed to have the same role in *Saccharomyces cerevisiae*-processing 1,2-α-D-mannosidase [128]. Although Ca^{2+} is essential for *S. cerevisiae* enzyme activity [125, 128], *A. saitoi* 1,2-α-D-mannosidase did not require Ca^{2+} for the activity (Table 18). This is the first report demonstrating that 1,2-α-D-mannosidase requires no divalent metal cation for its activity [114].

7.4 A Single Cysteine Residue and Disulfide Bond of 1,2-A-D-Mannosidase

A saitoi 1,2-α-D-mannosidase contains three conserved cysteine residues (Cys334, Cys364, and Cys443). We showed that Cys334 and Cys363 are involved in a disulfide bond, and that Cys443 contains a free thiol group [129].

For identification of a cysteine residue containing a free thiol group, trypsin-digested peptides of *A. saitoi* 1,2-α-D-mannosidase were reacted with 4-fluoro-7-sulfamoylbenzofurazan (ABD-F) and separated by reverse-phase HPLC. A single peak was detected based on fluorescence intensity and was analyzed N-terminal sequencing, and identified as ^{430}DWIWSAFSAV^{439}. The trypsin-digested peptide labeled by ABD-F contained Cys443. The result indicates that Cyss443 contains free thiol group and that Cys334 and Cys363 are involved in a disulfide bond.

Kinetic characterization of wild-type enzyme (WT), C334A, C363A, and C443A was performed at pH 5.0 using Man-α1,2Man-OMe as a substrate. The results are shown in Table 20. Although the K_m and k_{cat} values of C334A were lower than the WT values, no significant differences in catalytic efficiency (k_{cat}/K_m) were observed between the WT and its variants, C334A, C363A, and C443A. Hence it was concluded that the mutations at three cysteine residues did not affect the catalytic performance of 1,2-α-D-mannosidase. Hence, it was concluded that the mutations at Cys334, Cys363, and Cys443 did not affect the catalytic performance of *A. saitoi* 1,2-α-mannosidase.

Table 20. Kinetic parameters, Ca^{2+}-binding properties, and thermostabilities of wild-type (WT) and cysteine mutants of *A. saitoi* 1,2-α-mannnosidase

Enzyme	K_m (mM)	k_{cat} (s^{-1})	k_{cat}/K_m ($s^{-1} \cdot M^{-1}$)	Ca^{2+}-binding[a] (mol/mol)	$t_{1/2}$[b] (min)	T_m[c] (^oC)
Wild type	0.719 ± 0.013	8.51 ± 0.09	11.8	0.0	119	55.8
				1.1	125	
C334A	0.296 ± 0.006	3.87 ± 0.12	13.0	0.0	5.2	49.6
					6.8	
C363A	0.780 ± 0.007	9.48 ± 0.03	12.3	0.0	11.3	49.6
					18.8	
C443A	0.719 ± 0.007	6.67 ± 0.04	9.3	0.0	24.4	51.9
				1.2	38.3	

[a] *A. saitoi* 1,2-α-mannnosidase binds one mole of Ca^{2+} per mole of protein after Ca^{2+}-binding treatment (129).

[b] $t_{1/2}$ is the half-life time (min) when the residual activity of 1,2-α-mannnosidase is 50% after incubation at 55°C.

[c] T_m is a transition midpoint (°C), which is an apparent value because the thermal denaturation is not reversible.

(Tatara, Y., *et al., Biosci. Biotechnol. Biochem., 69*, 2101-2108 (2005))

For thermostability of cysteine mutants, wild-type (WT), C334A, C363A, and C443A were incubated at 55°C, and the half-lives of residual activity ($t_{1/2}$) at 30°C were 119, 5.2, 11.3, and 24.4 min respectively (Table 20). Mutation at Cys334, Cys363, and Cys443 drastically decreased the thermostability of 1,2-α-D-mannosidase. It is evident that the thermostability of *A. saitoi* 1,2-α-D-mannosidase is significantly influenced by mutations.

The wild-type (WT) and cysteine mutants bound about one mole of Ca^{2+} per mole of protein after Ca^{2+}-binding treatment (Table 20). The Ca^{2+}-bound forms were also examined for thermostability, as shown in Figure 32. The half lives of the Ca^{2+}-bound enzymes increased slightly, as compared to those of the Ca^{2+}-free enzyme.

Ca^{2+} is essential for the activity of 1,2-α-D-mannosidase family members, such as *S. cerevisiae* [128] and human endoplasmic reticulum [121], but the *A. saitoi* 1,2-α-D-mannosidase is not dependent on Ca^{2+} and has no divalent metal cation (114). Previously we found that it bound one mol of Ca^{2+} per mol of protein at the active center, which contributed to thermostability (112).

The cysteine mutants also bound Ca^{2+} and were stabilize to some extent (Table 20, Figure 32), though the binding of Ca^{2+} did not fully recover the drastic decrease in thermostability caused by the cysteine mutations [129].

Twelve kinds of mutations at position 443 replacing the Cys443 with alanine, asparagine, aspartic acid, glycine, isoleucine, leucine, methinine, phenylalanine, serine, threonine, tyrosine, and valine were constructed in the *msdS* gene and expressed by *A. oryzae*. Seven mutant enzymes, C443A, C443D, C443G, C443L, C443S, C443T, and C443V, were purified and assayed for 1,2-α-D-mannosidase activity at pH 5.0 using Man-α1,2Man-OMe as a substrate. The specific activity of each mutant enzyme is shown in Table 21. The specific

activities of C443A, C443G, C443S, and C443T were almost the equal of that of the WT. The relative activities of C443D, C443L, C443M, and C443V were less than 50%, as compared to the WT. The other four mutant enzymes, C443F, C443I, C443N, and C443Y, were undetectable or slightly detectable by Western blot analysis of the culture medium.

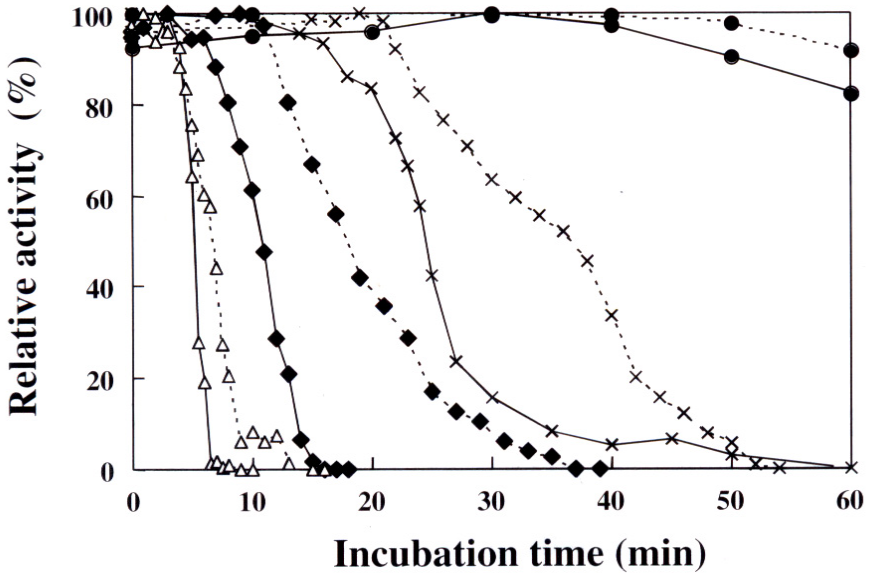

Figure. 32. Thermostability of wild type and cysteine mutants of A. saitoi 1,2-α-D-mannosidasess.

Far-UV and near-UV spectra were measured to analyze the secondary and tertiary structures respectively. The polypeptide backborn is optically active in the far-UV (250-170 nm), and different secondary structures produce characteristic spectra. Tryptophan, tyrosine, and phenylalanine can give CD signals in the near-UV (300-270 nm). The constructed free rotation of the side chains exhibits the absorption band. The spectra revealed that WT, C334A, and C363A had the same minima and maxima, indicating that they had similar secondary and tertiary structures. Consequently, the disulfide bond (C334 and C363) does not contribute significantly to the structure of the enzyme. The far-UV and near-UV spectra of the WT and Cys443 variants (C443A, C443D, C443G, C443L, C443S, C443T, and C443V) are determined. The spectra of the WT, C443A, C443G, C443S, and C443T presented the same waveform and mean residue ellipticity, indicating similar secondary and tertiary structures. Meanwhile, large decreases in the CD intensity of C443D, C443L, C443M, and C443V were observed over the whole range of wavelengths. These results might be ascribed to the partial unfolding of the mutant enzyme.

The CD signal at 222 nm as a function of temperature was collected and fitted to two-state models for WT, C334A, and C363A (Figure 33). The parameters from those fits were used to calculate a curve representing the apparent fraction of unfolded enzyme, F_{app}. The apparent denaturation midpoint (T_m) was determined. Both C334A and C363A exhibited T_m of 49.6^{o}C, 6.2^{o}C lower than that of the WT. The thermal unfolding curves of the Cys443 variants were determined. As compared to the wild type 1,2-α-D-mannosidase (WT), the T_m values decreased by 3.9, 5.6, 5.8, and 30^{o}C for C443A, C443G, and C443S, respectively,

(Table 21). The C443T mutant retained the most stability. The thermostability of C443D, C443L, C443M, and C443V was not analyzed because these mutants would have very little tertiary and secondary conformation.

Table 21. Specific activities and melting temperatures (T_m) of wilt type (WT) and Cys443 variants of *A. saitoi* 1,2-α-mannnosidase, and comparison of amino acid properties

Amino acids at position 443	Specific activity (m katal/kg)	T_m[a] (^oC)	Van der Waals volume[b] (Å^3)	Hydrophobicity[c]
Cys (WT)	47.4	55.8	86	+2.5
Thr	44.9	52.8	93	-0.7
Ala	38.3	51.9	67	+1.8
Gly	44.0	50.2	48	-0.4
Ser	47.1	50.0	73	-0.8
Asp	19.8	ND[d]	91	-3.5
Val	20.7	ND	105	+4.2
Met	14.5	ND	124	+1.9
Leu	11.7	ND	124	+3.8
Asn	NA[e]	NA	96	-3.5
Ile	NA	NA	124	+4.5
Phe	NA	NA	135	+2.8
Tyr	NA	NA	141	-1.3

[a]The midpoint of the transition is an apparent value because thermal denaturation is not reversible.
[b]The van der Waals volumes are from Richars, F. N., *J. Mol. Biol*., 82, 1-14(1974).
[c]Hydrophobicity indices are from Kyte, J. & Doolittle, R. F. A., *J. Mol. Biol*., 157,105-132(1982).
[d]ND means that the values are not determined, because the mutant enzymes from denatured structure.
[e]NA means that the mutant enzymes were not analyzed, because they were not secreted in the culture medium.
(Tatara, Y., *et al., Biosci. Biotechnol. Biochem., 69*, 2101-2108 (2005))

We demonstrated with *Aspergillus* 1,2-α-D-mannosidase that Cys334 and Cys363 forms a disulfide bond and that Cys443 contains a free thiol group. These results are consistent with the crystallographic data on *Penicillium* 1,2-α-D-mannosidase in that the corresponding cysteine residues are involved in the formation of disulfide bond [115].

The structure of *A. saitoi* 1,2-α-D-mannosidase was constructed and viewed with a Swiss-Pdb Viewer. Figure 34 shows the Cys443 and its surrounding amino acid residues. The hydrophobic side chains of Ile375, Leu408, Ala438, Val439, Phe449, and Leu452 are present within 6 Å of the S^{γ} atom of C443. The free thiol group of Cys443 is not involved in a hydrogen bond to any amino acid residues.

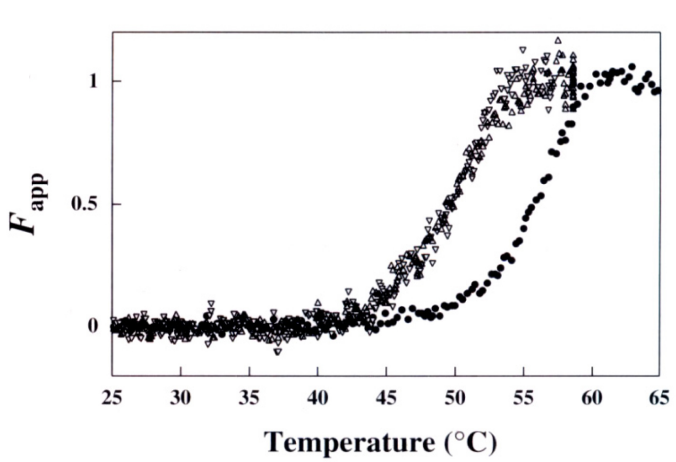

Figure 33. Thermal unfolding curves of WT and cysteine mutants, C334A and C363A, of A. saitoi 12,-α-D-mannosidase.

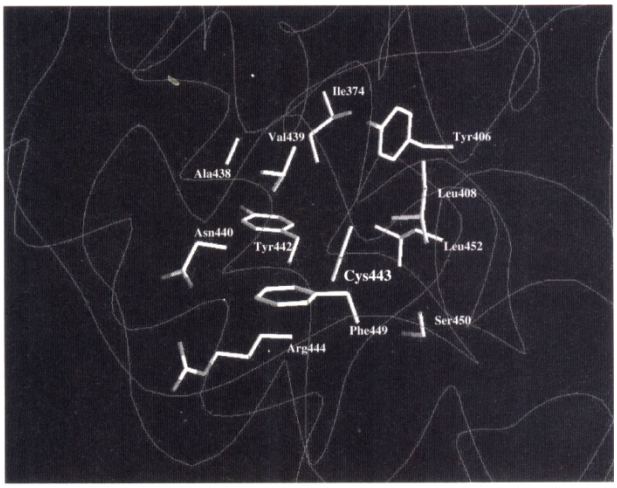

Figure 34. Structural model of *A.saitoi* 1,2-α-D-mannosidase focused on the side chain of C443 and its surrounding amino acids.

Twelve mutant enzymes of Cys443 that contained a large side chian at position 443, such as C443F, C443I, and C443Y, were not secreted into the culture medium. The van der Waals volumes of phenylalanine, isoleucine, tyrosine, and cysteine are 135, 124, 141, and 86 Å^3 respectively (Table 21). It is suggested that large amino acids are not preferred at position 443 because they cause a failure of protein folding *in vivo*. In eukaryotic cells, misfolded proteins are selectively degraded to prevent the accumulation of non-functional, potentially toxic proteins (130-132). Mutant enzymes such as C443F, C443I, and C443Y expressed in *A. oryzae* are recognized as misfolded proteins by the quality control system in the endoplasmic reticulum. The C443N, mutant was not secreted into the culture medium either, even though the van der Waals volume of asparagine is comparatively small (96 Å). The introduction of asparagine at position 443 might give rise to a potential asparagine-linked glycosylation site

(Asn443-Arg444-Thr445). The asparagine residue at position 443 was possibly glycosylated. Oligosaccharides linked to asparagine residues in the context of Asn-Xaa-Ser/Thr are known to have essential roles as carriers of biological information [133]. The unfavorable asparagine-linked sugar chain probably caused the disturbance of protein folding of secretion.

The specific activity of C443D, C443L, C443M, and C443V was less than 50%, compared to that of the WT (Table 21). The CD spectra of these mutants indicated that they were partly unfolded. The van der Waals volumes of aspartic acid (91 Å^3) and valine (105 Å^3) are close to that of cysteine (86 Å^3). Aspartic acid and valine have bifurcated side chains at the C^{γ} and C^{β} atoms respectively. The bifurcated side chains are assumed to causes denaturation of the enzyme.

Leucine and isoleucine have the same van der Waals volume (124 Å^3), and have bifurcated side chains at the C^{γ} and C^{β} atoms respectively. The C443L mutant was secreted as demonstrated structure, while C443I was not secreted. These results suggest that the bifurcated side chain at C^{β} of isoleucine has a large side steric hindrance for the current protein folding and cause the degradation of C443I. Methinine is a sulfur-containing amino acid like cysteine. The C443M mutant also had a partly unfolded structure, which was thought to be due to the large van der Waals volume of methioine (124 Å^3).

When the cysteine443 was replaced with Ala, Gly, Ser, or Thr, the mutant enzymes folded the current conformations. Cys443T was the most thermostable mutant enzyme (Table 21). In this case the van der Waals volume of threonine is 93 Å^3, slightly larger than that of cysteine (86 Å^3). On the other hand, the hydrophobicities of cysteine and threonine are +2.5 and -0.7 respectively [134]. The decrease in the T_m value of the C443T mutant is thought to be due to the low hydrophobicity of threonine.

The C443A mutant is the second most thermostable mutant enzyme. Cysteine and alanine are hydrophobic amino acids (the hydrophobicity of alanine is +1.8). C443A was more thermostable than C443S, although the van der Waals volume of serine (73 Å^3) was closer to that of cysteine (86 Å^3) than alanine (67 Å^3). These results indicate that hydrophobicity at position 443 is crucial to the thermostability of the enzyme. The C443G mutant was also thermolabile. The replacement of cysteine with glycine introduces a void in the space at position 443, which appears to destabilize the enzyme. From these results, we deduced that Cys443 of *A. saitoi* 1,2-α-D-mannosidase is involved in a hydrophobic interaction with the surrounding residues to stabilize the enzyme, and that the van der Waals volume of the amino acid is important to retain a stable interaction.

Molecular modeling of *A. saitoi* 1,2-α-D-mannosidase showed that Cys443 was located in the loop connecting the α13 and α14 helices as well as Cys441 of *Penicillilum* 1,2-α-D-mannosidase. The side chain of Cys443 was buried and surrounded by a hydrophobic environment (Figure 34). When the hydrophobic interaction around C443 was disrupted by site-directed mutagenesis, the normal folding of the enzyme was disturbed. The misfolded and partly denatured mutants were degraded (C443I, C443F, C443Y) and secreted (C443D, C443V, C443M, and C443L) respectively. It is suggested the alteration of the local structure around Cys 443 affects normal folding and determines the destination of the protein.

It is thought that Cys443 is buried to avoid exposure of its highly reactive free thiol group. Further, it is suggested that Cys443 greatly contributes to the thermostability of the enzyme by increasing hydrophobic packing.

7.5. Production of Human Compatible High Mannose-Type ($Man_5GlcNAc_2$) Sugar Chain in Yeast Cells

A yeast mutant capable of producing $Man_5GlcNAc_2$ human compatible sugar chains on glycoproteins was constructed [135]. An expression vector for 1,2-α-D-mannosidase with the "HDEL" endoplasmic reticulum retention/retrieval tag was designed and expressed in *Saccharomyces cerevisiae*. An *in vitro* 1,2-α-D-mannosidase assay and Western blot analysis showed that it was successfully localized in the endoplasmic reticulum. A triple mutant yeast lacking three glycosyltransferase activities was then transformed with an 1,2-α-D-mannosidase expression vector. The oligosaccharides structure of carboxypeptidase Y as well as surface glycoproteins were analyzed, and the recombinant yeast was shown to produce a series of high mannose-type sugar chains including $Man_5GlcNAc_2$. This is the first report of a recombinant *S. cerevisiae* able to produce $Man_5GlcNAc_2$-oligosaccharides, the intermediate for hybrid-type and complex-type sugar chains.

8. ACID ACTIVATION OF PROTYROSINASE FROM *ASPERGILLUS ORYZAE*

8.1. Acid Activation of Protyrosinase from *A. Oryzae*

Tyrosinase (monophenol monooxygenase or monophenol dihydroxy-L-phenyalanine: oxygen oxidoreductase, EC 1.14.18.1) is the only known enzyme participating in the process of melanin biosynthesis (136). The first two steps in the pathway are the oxygenation of monophenol to *o*-diphenol and the oxidation of diphenol to *o*-quinones (catechol oxidase or 1,2-benzenediol : oxygen oxidoreductase, EC 1.10.3.1), both using molecular oxygen. It is copper-containing monooxygenase catalyzing both *o*-hydroxylation of monophenol and the oxidation of *o*-diphenol to *o*-quinones.

Copper ions in the (I) and (II) oxidation states are biologically important. Basically, three different types of copper centre are shown. 'Blue' of type I copper occurs in the blue electron carrying proteins such as stellacyanin, plastocyanin and azurin. There is also 'non-blue' or type II copper and a type III copper centre that is 'non-detectable' by EPR, apparently containing a pair of contiguous copper atoms. Tyrosinase is a type III protein that is not detected EPR because of antiferromagnetism of a pair of copper in it [137].

Our previous paper (138) described the unique process of activation of intracellular protyrosinase from *A. oryzae* by acidifying treatment at pH 3.0 and conformational differences between protyrosinase and tyrosinase. The molecular mass values of the protyrosinase purified by the previous paper (138) were 280,000 by HPLC gel with Shodex WS-803F and 67,000 by SDS-PAGE, respectively. The protyrosinase was found to contain 2 mols of copper per mol of the subunits with the molecular mass of 67,000. It was shown that the protyrosinase was a tetrameric enzyme with identical subunits. NH_2-Terminal sequence analysis indicated the NH_2-terminus of protyrosinase was blocked. Our Western blots showed that the molecular mass of the tyrosinase activated with acidifying treatment at pH 3.0 was 67,000 by SDS-PAGE with or without 2-mercaptoethanol. These results assumed that

protyrosinase and tyrosinase have different conformation, different stabilities and some different properties.

The coding region of the protyrosinase gene, *melO*, from *Aspergillus oryzae* occupies 1671 base pairs of the genomic DNA and is separated into two exons by one intron [139. The full-length cDNA of the *melO* gene was cloned. Analysis of the 1671 base pairs nucleotide sequence revealed a single open reading frame coding 539 amino acid residues. The cDNA has been expressed in yeast cells. The predicted protein product derived from the *melO* gene is identified by Western blotting and activity determination. The predicted amino acid sequence of the gene product was compared with that of *Neurospora crassa* tyrosinase [140]. A coupled pair of three histidine residues in the tyrosinase was assumed to correcspond to Cu(II) ligands in the homologous tyrosinase from *Streptomyces glaucescens* [141, 142] and *Homo sapiens* [143]. A coupled pair of three histidine residues (His-63, His-84 and His-93 for Cu(A)); His-290, His-294 and His-333 for Cu(B) of the protyrosinase from *A. oryzae* was assumed. A covalent –Cys82-Xaa-His84- may be important for the enzymatic activity as described for the thioether bridge, Cys94-Xaa-His96-, of *N. crassa* tyrosinase [144]. The predicted amino acid sequence of the *melO* gene product has 17% and 15% homologous with those from *N. crassa* [144] and *Homo sapiens* [143], respectively.

The expression product of pG3TY was also isolated by PAGE at pH 9.4 gel [139]. The activity band of tyrosinase was stained with dihydroxy-L-phenylalanine (L-DOPA) after acidifying at pH 3. Tyrosinase activity of the pG3YT product was determined to be 0.018 nkat/kg protein. Without acidifying treatment at pH 3.0, no tyrosinase activity was observed. It can be concluded that the expression product of the *melO* gene is the protyrosinase of *A. oryzae*.

8.2. Copper Ligands of Tyrosinase from *A. Oryzae*

Copper ligands of the recombinant tyrosinase from *A. oryzae* expressed in *Saccharomyces cerevisiae* or *Escherichia coli* were identified by site-directed mutagenesis [145].

From a crystallographic analysis of *Palinurus interruptus* haemocyanin [146], one of the pair of copper ions, Cu(A), is surrounded by residues 196, 200 and 226; the other, Cu(B), is surrounded by residues 346, 350 and 386. Mutation positions were selected on the basis of a sequence comparison of the tyrosinase from *A. oryzae* [145] with the other tyrosinases from *N. crassa* [144], *S. antibioticus* [147] and *H. sapiens* [143]. For the cysteine residue it is also assumed that a covalent Cys82-Xaa-His84 might be important for enzymatic activity, as described for the thioether bridge between Cys94 and His96 in the Cys94-Xaa-His96 peptide of *N. crassa* tyrosinase (144). Mutations were focused at positions of 18 histidine residues (His63, His76, His83, His84, His93, His193, His266, His290, His294, His332, His333, His347, His462, His479, His489, His510, His518 and His520) and two cysteine residues (Cys82 and Cys334).

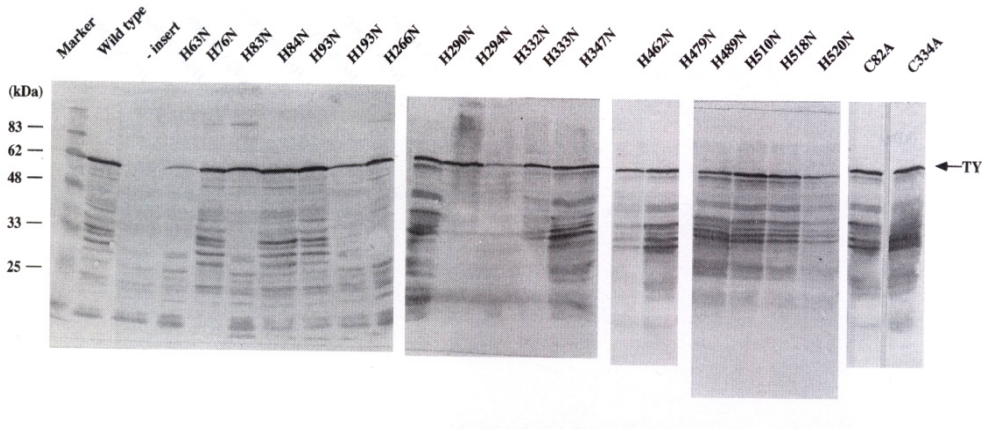

Figure 35. Western blot analyses of the wild type and activated tyrosinases from A. oryzae expressed in S. cerevisiae.

Table 22. Relative activities of wild-type and mutant tyrosinases from *A. oryzae* expressed in *S. cerevisiae* for the monooxygenase with L-tyrosine, and oxidase activity with L-DOPA at pH 5.5

Mutant tyrosinase	Relative activity (%)	
	Monooxygenase with L-tyrosine	Oxidase with L-DOPA
Wild type	100	100
His63Asn	0	0
His76Asn	120	147
His83Asn	122	109
His84Asn	0	0
His93Asn	0	0
His193Asn	0	38
His266Asn	132	105
His290Asn	0	0
His294Asn	0	0
His332Asn	0	0
His333Asn	0	0
His347Asn	82	89
His462Asn	8	16
His479Asn	3	21
His489Asn	7	25
His510Asn	141	104
His518Asn	10	63
His520Asn	29	53
Cys82Ala	0	0
Cys33Ala	79	72

(Nakamura, M., *et al., Biochem. J., 350*, 537-545 (2000)).

A Western blot analysis of the mutant products of the *melO* gene expressed in *S. cerevisiae* showed proteins with molecular masses of approx. 67 kDa that reacted with rabbit anti-(*A. oryzae* protyrosinase) serum, which is consistent with the apparent molecular mass of the native proenzyme, as shown in Figure 35. The activities of activated tyrosinases of the mutant enzymes from *A. oryzae* after acid shock are summarized in Table 22. A number of the mutant enzymes (His63Asn, His84Asn, His93Asn, His290Asn, His294Asn, His332Asn, His333Asn and Cys82Ala) had no detectable activity, indicating that the mutated residues are essential for activity. A second group of mutant enzymes (His76Asn, His83Asn, His193Asn, His266Asn, His347Asn, His462Asn, His479Asn, His489Asn, His510Asn, His518Asn, His520Asn and Cys334Ala) retained full or partial activity. However, one single-residue mutant, His193Asn, exhibited complete destruction of the catalytic activity of mono-oxygenase for L-tyrosine and a partial destruction of oxidase for L-DOPA. It is assumed that the His193 residue might be a binding site of the enzyme for the aromatic substrate L-tyrosine.

We succeeded in overproducing the recombinant protyrosinase from *A. oryza*e as a thioredoxin fusion protein in *E. coli*. The protyrosinases were accumulated as a soluble fraction in these cells. The expressed recombinant fusion protyrosinases have no copper ions. As described for the purification of the recombinant protyrosinase in the Experimental section in the ref. (145), the recombinant protyrosinases were added to make a final concentration of 10 μM $CuSO_4$ and the mixture was incubated at 4°C for 14 h; the binding of copper ions to the active sites of protyrosinase was then performed. In our simplified purification method, the protyrosinases were purified with a single step of Chelating Sepharose FF, which trapped the histidine tag in the anchor region to the C-terminal end of thioredoxin. The wild-type protyrosinase was purified 102-fold over the crude extract. Approximately 20 mg of wild-type protyrosinase was obtained from 1 liter of the culture of *E. coli*; the yield of protyrosinase was 53% for a single-step purification.

Activation of the fusion protyrosinases expressed in *E. coli* was accomplished by acid shock at pH 3.0 for 20 min. The engineered thioredoxin-fusion tyrosinases expressed in *E. coli* were revealed after SDS-PAGE (Figure 36). The molecular masses of the subunits of activated tyrosinases after acid shock were determined as 83 kDa on SDS-PAGE. Gel filtration of the activated tyrosinase on a Superose 8 column gave an estimated molecular mass of 330 kDa. The results suggested that the activated tyrosinase was composed of four identical subunits, each with a molecular mass of 83 kDa.

The NH_2-terminal amino acid sequence of the activated wild-type tyrosinase precipitated with 5% (w/v) trichloroacetic acid was SDKIHLTDD (single-letter amino acid codes), which is known to be the NH_2-terminal sequence of thioredoxin including the 10 residues from the Ser2 to Asp11. Although the initiating methinine residue was encoded in the construct, it seems to have disappeared after cleavage of the protein.

The specific activity of the activated wild-type tyrosinase towards L-tyrosine mono-oxygenation, as determined by the HPLC method, was 1.69 katal/ kg of protein. A K_m of 0.82 mM and a k_{cat} of 23.6 s^{-1} for L-tyrosine mono-oxygenation were calculated from Hanes-Woolf plots.

An atomic absorption spectrophotometric determination of copper contents of the activated site-directed mutant tyrosinases His63Asn, His84Asn, His93Asn, His290Asn, His294Asn, His332Asn, His333Asn, expressed in *E. coli*, demonstrated the loss of binding of

1 mol of copper per mol of subunit as a consequence of the mutagenesis of histidine residues (Table 23).

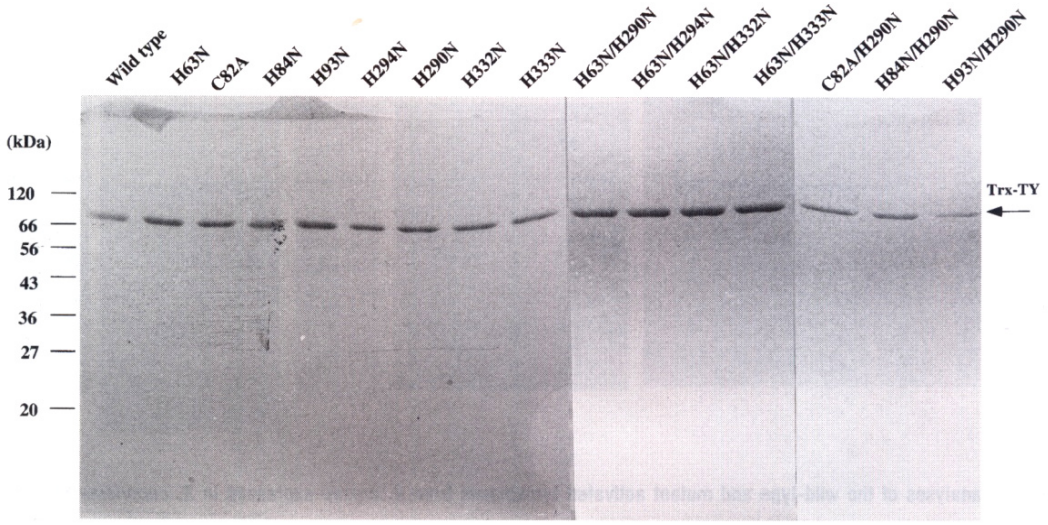

Figure 36. SDS-PAGE of purified wild-type and mutant thioredoxin-fused tyrosinases from A. oryzae expressed in E. coli.

The activation of protyrosinase expressed in *E. coli* was accomplished by incubation with an acidic buffer at ph 3.0 for 20 min. The copper contents of wild-type and mutant protyrosinases are shown in parentheses; the values without parentheses show the copper content of wild-type and mutant tyrosinase after acid activation. Abbreviation: PCMB, *p*-chloromercuribenzoate.

The copper content of the mutant tyrosinase Cys82Ala was also determined as 1 mol per mol of subunit. The copper content of the activated tyrosinase was somewhat lower than that of the protyrosinase (Table 23). Some of the single copper ions might have been removed from the mutant tyrosinases by the acid shock at pH 3.0. As expected from melanin formation, the eight mutant tyrosinases were devoid of any enzymatic activity after acid shock at pH 3.0. An almost complete loss of the copper content was determined by atomic absorption spectrophotometry for seven double mutants, His63Asn/His290Asn, His63Asn/His294Asn, His63Asn/His332Asn, His63Asn/His333Asn, Cys82Ala/His290Asn, His84Asn/His290Asn and His93Asn/His290Asn.

The contents of secondary structures (α-helix, β-structure and random coil of mutant enzymes) by CD spectrophotometry are shown in Table 24. The results for major global changes indicate that the increases in the content of α-helix were 4.4% for His63Asn, 3.3% for His93Asn, 3.3% for His290Asn and 4.2% for His333Asn compared with that of the control of the wild-type enzyme, and the decreases in the content were 4% for Cys82Ala, 2.4% for His84Asn and 2.3% for His294Asn. The results also indicated that the increases in the amount of β-structure were 3.4% for His84Asn and 7.3% for His93Asn; decrease in β-structure of 5.1% for His63Asn, 4.2% for His290Asn and 8.2% for His294Asn were also identified. Despite this, the results for α-helices and β-structures of the mutant enzyme

His84Asn and His332Asn indicated that no substantial changes in the secondary structure occurred.

Table 23. Atomic absorption spectrophotometric determination of copper content for wild-type and mutant tyrosinases from *A. oryzae* expressed in *E. coli*

Mutant tyrosinase	Copper content (mole/mol subunit)	
	Acid activated tyrosinase	Protyrosinase
Wild type	1.7	(1.9)
Wild type after treatment with PCMB	0.02*	$(1.6)^{+}$
His63Asn	0.2	(0.9)
Cys82Ala	0.4	(0.6)
His84Asn	0.2	(0.7)
His93Asn	0.9	(1.0)
His290Asn	0.2	(0.6)
His294Asn	0.3	(0.8)
His332Asn	0.4	(0.4)
His333Asn	0.7	(0.8)
His63Asn/His290Asn	0.01	(0.01)
His63Asn/His294Asn	0	(0.05)
His63Asn/His332Asn	0.03	(0.03)
His63Asn/His333Asn	0.03	(0.08)
Cys82Ala/His290Asn	0.05	(0.07)
His84Asn/His290Asn	0.01	(0.03)
His93Asn/His290Asn	0.01	(0.05)
Apoenzyme	0.01	(0.02)

*After treatment with 0.1 mM PCMB at pH 3.5, activated tyrosinase was dialysed against 5 mM sodium acetate buffer, pH 3.5.

+After treatment with 0.1 mM PCMB at pH 7.0, protyrosinase was dialysed against 5 mM phosphate buffer, pH 7.0.

(Nakamura, M., et al., Biochem. J., 350, 537-545 (2000))

The value of EPR spectroscopy in establishing electronic structures and their dependence on metal co-ordination-sphere composition and geometry can be illustrated by its application to several aspects of copper bio-inorganic chemistry [137]. In the wild-type tyrosinase from *A. oryzae*, the third type of copper (Type III) is silent towards EPR because of antiferromagnetic exchange coupling and/or rapid electron-spin relaxation between two neighbouring Cu(II) centres (Figure 37 and Table 25). The EPR spectra of the five mutant tyrosinases His63Asn, His93Asn, His290Asn, His294Asn and Cys82Ala are shown in Figure 37. Some of their EPR properties of copper, the anisotropic perpendicular and parallel *g*-values ($g_{\perp}$ and $g_{\parallel}$) of copper, and the hyperfine coupling constant parallel, $^{Cu}A_{\parallel}$, of the six mutants are shown in Table 25 and compared with that of the wild-type tyrosinase.

Table 24. Estimated secondary structure for CD determination of the activated tyrosinases from *A. oryzae* after acid shock at pH 3.0

Enzyme	Secondary structure (%)			
	Variant	α-Helix	β-Structure	Random
Activated tyrosinase	Wild type	25.7	41.7	32.6
	His63Asn	30.1	36.6	33.3
	Cys82Ala	21.7	43.0	35.3
	His84Asn	23.3	45.1	31.6
	His93Asn	29.0	49.0	31.1
	His290Asn	29.0	37.5	33.5
	His294Asn	23.4	33.5	33.0
	His332Asn	24.7	43.0	32.3
	His333Asn	29.9	39.1	30.9
Protyrosinase	Wild type	26.7	41.1	32.2

(Nakamura, M., *et al., Biochem. J., 350*, 537-545 (2000))

These results clearly indicate that the five mutants (His63Asn, Cys82Ala, His93Asn, His290Asn and His294Asn) in which the signal copper site is empty contain only 1 mol of copper per mol of subunit of tyrosinase. This information might be valuable in deducing the locations of sites of reactivity on bound substrate molecules. They have a more or less axially symmetrical appearance with the parameters given. The values are very similar for the five mutant tyrosinases, suggesting that the remaining copper is in a similar ligand environment.

In a detailed analysis of copper ligand geometry, the correlations between $g_{\|}$ of copper(II) complexes and ${}^{Cu}A_{\|}$ arising from various factors have been given for copper(II) complexes. The authors noted that a reported complex with a thioether donor at the apex of a square pyramid whose base was the donor set N_2O_2 has $g_{\|} = 2.240$ and $A_{\|} = 0.0178$ cm^{-1}, which placed this complex in the normal square-planar CuN_2O_2 region. Tetrahedral distortion of a square-planar chromatophore with any of the biomimetic (N, O, S) donors decreased $A_{\|}$ and increased $g_{\|}$, lowering the ($g_{\|}$, $A_{\|}$) point for that CuX_4 core. From the geometrical analysis if EPR by Sakaguchi and Addison (147), we deduced that the nitrogen or sulphur donors in the Cu(B) or Cu(A) ligand geometry of the three mutants His63Asn, Cys82Ala and His294Asn should be on a square-tetrahedral geometry and also that the nitrogen or sulphur donors in the Cu(B) or Cu(A) of the two mutants His93Asn and His290Asn should be on a distorted tetrahedral geometry, as shown in Table 25.

We deduced the copper ligand geometry environment from the correlation between $g_{\|}$ and $A_{\|}$ values reported previously (147). Abbreviation: n.d, not determined, because the preparations were partly insoluble at high concentration.

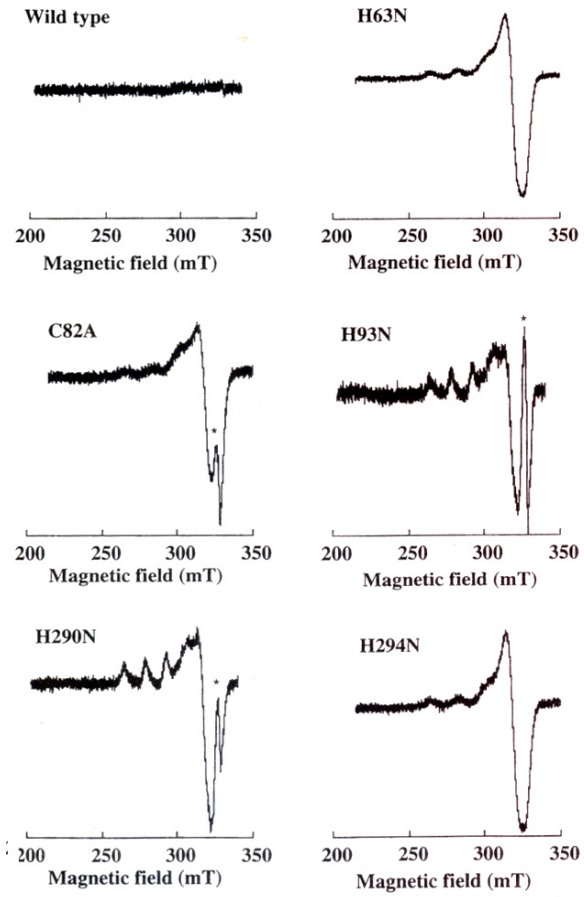

Figure 37. EPR spectra of the wild-type and mutant tyrosinases from *A. oryzae* expressed in *E. coli*.

Table 25. Parameters of EPR spectra for wild-type and mutant tyrosinases from *A. oryzae* expressed in *E. coli*

	EPR spectra obtained			
Enzyme	$g_{\perp}$	$g_{\parallel}$	$A_{\parallel}$ (10^{-4} · cm^{-1})	Copper ligand geometry
Wild type	EPR silent	EPR silent	EPR silent	
His63Asn	2.06	2.256	185	Square tetrahedral
Cys82Ala	2.07	2.253	190	Square tetrahedral
His 84Asn	n.d.	n.d.	n.d.	
His93Asn	2.06	2.301	152	Distorted tetrahedral
His290Asn	2.08	2.301	150	Distorted tetrahedral
His294Asn	2.06	2.251	190	Square tetrahedral

(Nakamura, M., *et al., Biochem. J., 350*, 537-545 (2000))

The EPR spectra of two mutants, His62Asn and His189Asn, of *S. glaucescence* were measured by Huber and Lerch [142]. The mutants had a more or less axially symmetrical appearance by these parameters. The values were similar for both materials, suggesting that the remaining copper atom was in a very similar ligand environment. They noted that the amide nitrogen group was not a good ligand for either Cu(I) or Cu(II). Both mutants of *S. glaucescens* showed dramatically changed physicochemical properties: [1] no enzymatic activity, [2] no reaction with H_2O_2 and [3] only one copper atom bound per molecule. The fact that most of this copper was detectable by EPR confirmed that one copper atom from either the Cu(A) site (Asn62) or Cu(B) site (Asn189) had been selectively removed. From the $g_{\parallel}$ and $A_{\parallel}$ values and the energies of the d-d transition, the copper in both mutants could be defined as being in a slightly distorted tetragonal ligand environment. Applying the correlation between $A_{\parallel}/ g_{\parallel}$, ligand type and geometry in copper complexes, possible copper ligands in *S. glaucescense* were either three nitrogen atoms and one oxygen atom or two nitrogen atoms and two oxygen atoms.

Spitz *et al.* (148) described the Cu(B) motif of all hnown tyrosinases and polyphenol oxidases as differing from those of hemocyanin in that they contain four rather than three absolutely conserved histidine residues; in human tyrosinase these occur at His363, His367, His389 and His390. His363 and His367 are clearly similar to the copper-binding histidine residues of the hemocyanin Cu(B) motif. The His390Ala mutant abolished catalytic activity did not decrease copper binding, whereas the His389 substitution abolished it. These results indicate that it is His389, rather than His390, that has a critical role in copper binding by human tyrosinase, even though it is His390 that has been conserved in all of the putative copper-binding positions.

On the basis of the study of *Neurospora tyrosinase* with a molecular mass of 46 kDa including 2 mol of copper per mol [140, 149], it is conceivable that the activation of protyrosinase takes place by the active conformation of the thioether linkage between Cys94 and His96 [144]. However, the absence of a similar structure in the tyrosinase from *S. antibioticus* [150] makes such a function rather unlikely. After dye-sensitized photo-oxidation of the apoenzyme of *Neurospora* tyrosinase, three histidine residues (His188, His193 and His 289) were destroyed [149]. Copper measurements of photo-oxidized, reconstituted apoenzyme demonstrated the loss of binding of one mol of copper per mol of enzyme as a concequence of the photo-oxidation of histidine residues [149]. Lerch suggested that the three histidine residues destroyed might be ligands of one of the two active-site copper ions; His306 of *Neurospora* tyrosinase was indicated as an active site by active-site-directed modification with cathecol [149]. His306 of *Neurospora* tyrosinase is an essential residue and corresponds to the active His333 of the tyrosinase from *A. oryzae*. His193 of *A. oryzae* tyrosinase, corresponding to the photo-inactivated His188 of *N. crassa* tyrosinase, might not be an essential residue but a binding one for catalysis in the *A. oryzae* enzyme.

For Cu(A), we confirmed that three histidine residues, His63, His84 and His93, are essential residues of the tyrosinase from *A.oryzae* as determined by site-directed mutagenesis (145). In this report we also found that Cys82 is an essential residue for the catalytic activity of the tyrosinase activated at pH 3.0. *A. oryzae* tyrosinase was inhibited completely by *p*-chloromercuribenzoate. The most likely binding sites of the tyrosinase from *A. oryzae* for Cu(A) are His63, His84 and His93, with the remaining conserved Cys82 providing the fourth ligand. We confirmed by atomic absorption spectrophotometry for copper incorporation that Cu(A) is liganded by three histidine residues (His63, His84 and His93) and one cysteine

residue (Cys82). Confirmation was obtained that the two mutants His290Asn and His294Asn contain one copper ion that is fully detectable by EPR (Figure 37 and Table 25). We deduced that the nitrogen or sulphur donors in the copper-ligand geometry of His290Asn and His294Asn should be in a square tetrahedral geometry and a distorted tetrahedral geometry respectively. The results of atomic absorption spectrophotometric determination on the double mutant Cys82Ala/His290Asn confirmed that there was no copper atom. We propose a new binding motif of Cu(A) of tyrosinase from *A. oryzae* in which the Cu(A) ion is co-ordinated by three histidine side chains, His63, His84 and His93, and a single thiol group of Cys82.

In *Aspergillus* tyrosinase, His290, His294 and His333 are clearly similar to the copper-binding histidine residues of the haemocyanin Cu(B) motif. The His332Ala mutant abolished catalytic activity and decreased copper binding. These results indicate that His332 has a critical role in copper binding by *Aspergillus* tyrosinase. We confirmed that three histidine residues, His290, His284 and His333 for Cu(B), are essential residues for catalytic activity and copper ligands of the activated tyrosinase from *A. oryzae*. Furthermore, it was found in the study that the His332 residue is also an essential site of the tyrosinase from *A. oryzae*. We also confirmed that the His63Asn, Cys82Ala and His93Asn mutants contain one copper ion that is fully detectable by EPR (Figure 37 and Table 25). We confirmed that the double mutant His63Asn/His332Asn contains almost no copper ions (Table 23). We deduced that the nitrogen donors in the His63Asn and Cys82Ala mutant should have a square-tetrahedral geometry, and those in the mutant His93Asn should have a distorted tetrahedral geometry. Atomic absorption spectrophotometric results on the double mutant His63Asn/His332Asn showed no copper atom.

The imidazole-bridge dimetallic centre in copper-zinc superoxide dismutase (EC 1.15.1.1) was a novel structural feature that had not previously been encountered in co-ordination chemistry [151]. The Cu(II) ion is co-ordinated by four histidine side chains, His44, His46, His118 and His61, and there is evidence for a fifth axial water ligand.

This is the first paper to determine the essential seven histidine residues, His63, His84, His93, His290, His294, His332 and His333, and the single cysteine residue, Cys82, for tyrosinase from *A. oryzae*. It is concluded that one pair of copper ions, Cu(A), is liganded by three histidine residues, His63, His84 and His93, and a single cysteine residue, Cys82, whereas the other, Cu(B), is liganded by four histidine residues, His290, His294, His332 and His333.

8.3 Homo-Tetrameric Protyrosinase is Converted to Active Dimers with an Essential Intersubunit Disulfide Bond at Acidic Ph

The quaternary structure of tyrosinase differs depending on the species. The tyrosinase can be found in either latent or active form, and the activating conditions differ depending on the species. Tyrosinase from the mushroom *Agaricus bisporus* is a heterotetramer that is compound of two subunits of 43 kDa (H) and two subunits of 13 kDa (L), with a native molecular mass of 111 kDa, and contains four copper atoms [152, 153]. The isolated subunits do not possess the enzymatic activity. Activation of the mushroom pro-tyrosinase can be effected by protease treatment [154] or by SDS [155]. Mushroom has an isozyme of

tyrosinase which is a monomer of 43 kDa, and also possesses catecholase and cresolase activity [152].

In the case of the filamentous fungus *Neurospora crassa*, tyrosinase is thought to be a 46 kDa monomer with full activity that is formed upon proteolytic processing of a 75 kDa precursor [140]. *Streptomyces* tyrosinase is a monomer of 31 kDa with enzymatic activity [141, 142]. Tyrosinase from *Homo sapiens* melanoma cell is a monomer of 53 kDa that has enzymatic activity [156. *Xenopus laevis* tyrosinase is activated by anionic detergents such as SDS (157). Protyrosinase from epidermis of the frog *Rana esculenta ridibunda* can be activated *in vitro* by several proteinases (trypsin, alpha-chymotrypsin, Pronase) and by light (158). Furthermore, the protyrosinase and tyrosinase have different quaternary structures: it was appeared that the dimeric structure of the protyrosinase was converted to a tetramer after the activation by trypsin.

Aspergillus oryzae protyrosinase (pro-TY) is a homotetramer composed of 60 kDa subunits containing 2 mol of copper per mol of subunit [139]. The proenzyme is inactive at neutral pH, and is activated under conditions of acidic pH [138]. The acid activation is quite unique mechanism for activation of a protyrosinase. To investigate the mechanism of acid activation, and the conformational change following the shift of pH and interactions between the subunits were examined (159).

The acid activation of protyrosinase from *A. oryzae* was most potent at pH 3.0, and the activity was increased logarithmically with increasing acid activation time, with a rate constant of 1.5×10^{-3}/s. Anionic detergent (0.01% SDS) slightly activated the protyrosinase. The specific activity of the SDS-activated tyrosinase was 19% compared with that of the acid-activated tyrosinase (acid-TY). The protyrosinase was not activated by the other reagent tested, including, Tween 20 (0.001-0.1%), urea (0.5-2.0 M), NaCl (0.1-2.0 M), acetonitrils (5-20%), ethanol (5-20%), and protease (trypsin and chymotrypsin).

It is thought that polar interactions are disrupted by protonation at acidic pH or by an anionic detergent, SDS. Ionic bonds and/or hydrogen bonds are appeared to be involved in the interaction between the dimers. A non-ionic detergent, Tween 20, did not activate the protyrosinase, indicating that the contribution of hydrophobic interaction in the dimer-dimer interface was minor. The possibility of processing by a contaminated acid protease was ruled out on SDS-PAGE analysis of the acid-activated tyrosinase, because the band did not shift to lower molecular mass (Figure 38). It is suggested that the protyrosinase is not cleaved for activation in acid treatment. Atomic absorption spectroscopy showed that the protyrosinase and acid-activated tyrosinase contained 2.0 and zero mol of copper per mol of subunit, respectively, after the treatment with EDTA. These results indicate that a conformational change causes exposure of the binuclear copper active center.

The relative molecular mass of both protyrosinase and acid-activated tyrosinase was 60 kDa, as shown by SDS-PAGE (Figure 38). This was agreement with the calculated molecular mass, 60,604, of the protyrosinase. The protyrosinase and acid-activated tyrosinase did not migrate in the polyacrylamide gel in the absence of the reducing agent because of thiol-disulfide interchange reactions that occur between the SDS-denatured proteins. The native molecular masses of the protyrosinase and acid-activated tyrosinase were 266 and 165 kDa, respectively, as estimated by gel-filtration chromatography (Figure 39, Table 26) [159]. The protyrosinase was judged to be a tetramer with a calculated molecular mass of 242,416. It is assumed that the quaternary structure of the acid-activated tyrosinase was increased because of partial unfolding caused by acidic pH. The molecular mass of the protyrosinase under

reducing conditions was 68 kDa, indicating that the quaternary structure was monomeric. Our data suggest that the intersubunit polar interaction is disrupted at pH 3.0, and the tetrameric protyrosinase dissociates to dimmers. The binuclear copper of the native center is then exposed.

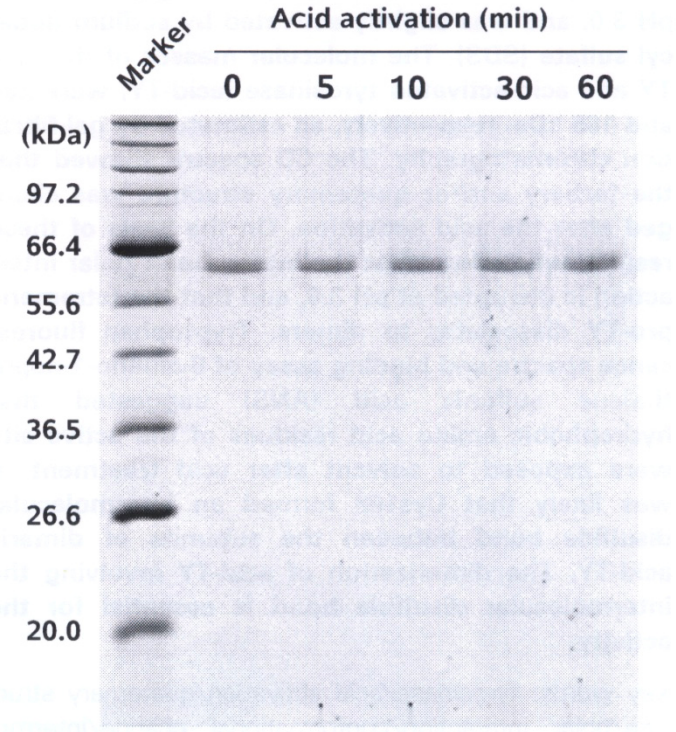

Figure 38. SDS-PAGE analysis of the acid-activated tyrosinase (acid-TY) showing the time course of acid activation at pH 3.0.

The CD spectra in the far-UV region revealed that the pro-tyrosinase and acid-activated tyrosinase had similar secondary structures (Figure 40). On the other hands, the CD signal of acid-activated tyrosinase in the range of 280-290 nm, indicating that the tertiary and/or quaternary structure of the protyrosinase was changed by acid-treatment. On the basis of these results, we deduce that the intersubunit polar interaction is disrupted at pH 3.0, and that the tetrameric protyrosinase dissociates to dimmers.

To detect possible conformational changes caused by acid activation, tryptophan fluorescence spectra were measures. When excited 295 nm, the emission spectrum of the protyrosinase exhibited as average emission wavelength of 339 nm. By comparison, in the spectrum of the acid-activated tyrosinase, the emission intensity was decreased by 62%, and there was a red shift of the average emission wavelength to 346 nm (Figure 41). These results indicate that tryptophan residues are brought into a polar environment by acid activation.

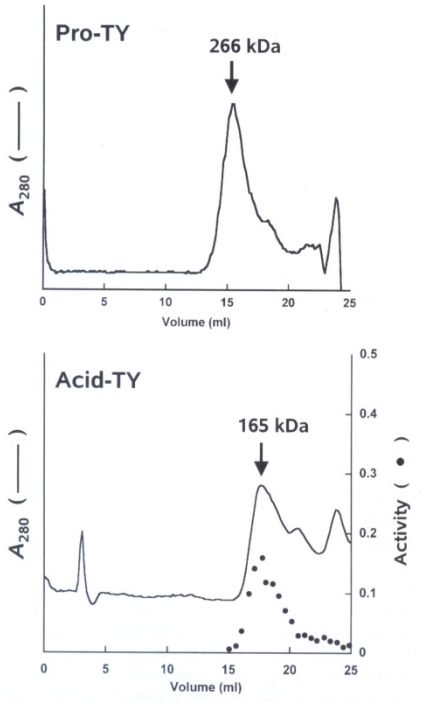

Figure 39. Estimation of molecular mass of the protyrosinase (pro-TY) and acid-activated tyrosinase (acid-TY) by gel filtration chromatography.

Table 26. Specific activity and molecular mass under various conditions of protyrosinase and acid-activated tyrosinase from *A. oryzae*

Condition	Molecular mass (kDa)	Quaternary structure	Specific activity	
			(katal/kg)	(%)
Protyrosinase	266	Tetramer	ND	—
Acid-activated tyrosinase	165	Dimer	1.2	100
Reduced	68[a]	Monomer	—	—
Oligo-C108A	380	Oligomer	0.016	1.3
Mono-C108A	68	Monomer	ND	—

ND, not detected.
aGelfiltration chromatography under reducing conditions was performed in the presence of 2% β-mercaptoethanol at pH 7.0.
(Tatara, Y., et al., Pigment Cell Melanoma Res., 21, 89-96 (2008))

8-Anilino-1-naphathalene sulfonic acid (ANS) is a sensitive hydrophobic patch probe [160]. The protyrosinase did not bind ANS, whereas the acid-activated tyrosinase did bind ANS by an increase of the fluorescence intensity (Figure 42). These results reveal that the

acid activation exposes hydrophobic surface to the solvent. The dissociation of the tetrameric protyrosinase is followed by the exposure of the binuclear copper active center and hydrophobic amino acids.

The protyrosinase from *A. oryzae* has eight cysteine residues [139]. Cys-82 is proposed to be involved in the ligation of CuA in the active center [145] or is covalently linked via a thioether bridge to His84 by analogy to *Neurospora crassa* [144] and the crystal structure of sweet potato catechol oxidase [161]. At least one cysteine contains a free thiol group or forms an intermolecular disulfide bond in the protyrosinase from *A. oryzae*. The quaternary structure of protyrosinase under reducing conditions was monomeric (Table 26). This suggested the possibility that an intermolecular disulfide bond can be formed between the subunits.

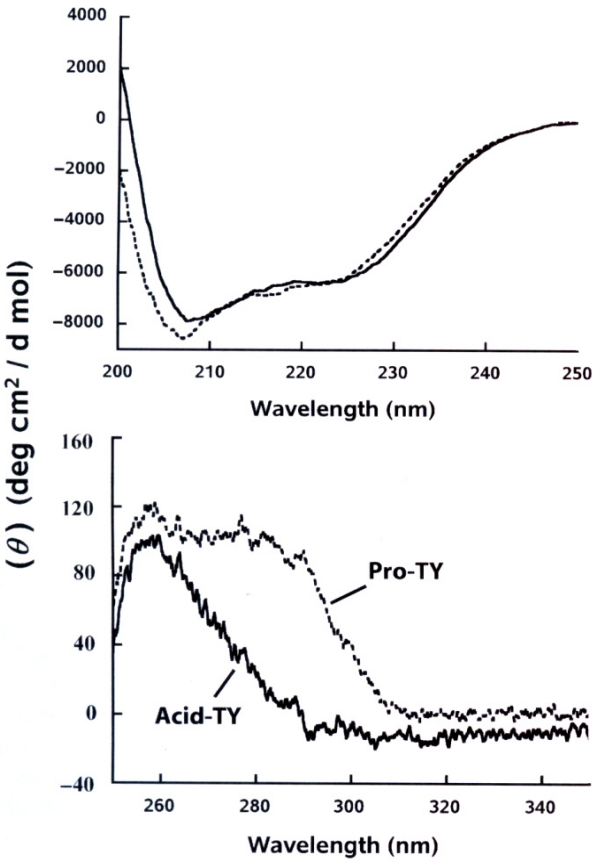

Figure 40. Comparison of CD spectra of the pro-tyrosinase (pro-TY) and acid activated-tyrosinase (acid-TY).

To detect the cysteine residues involved in the intermolecular disulfide bond, free thiol groups were labeled with a fluorogenic reagent, 4-fluoro-7-sulfamoylbenzofurazan (ABD-F) [162] in the presence of a stepwise addition of reducing agent. It was likely that Cys108 found an intermolecular disulfide bond between the subunits of dimeric acid-TY (Figure 43). The dimerization of acid-activated tyrosinase involving the intermolecular disulfide bond is essential for the activity [159].

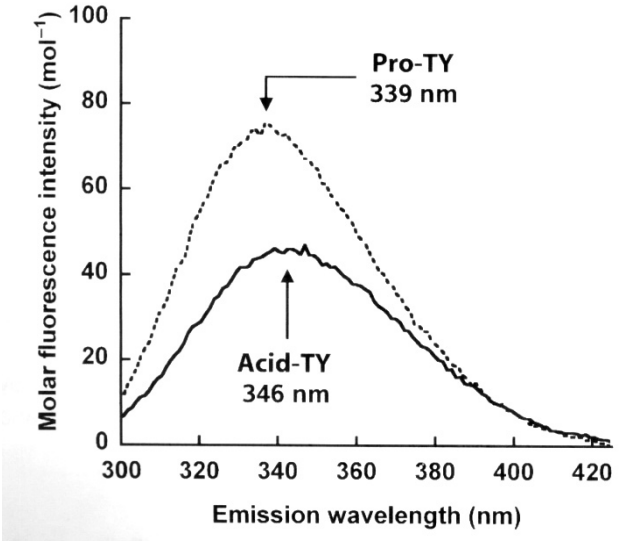

Figure 41. Tryptophan fluorescence spectra of the protyrosinase (pro-TY) (---) and acid- activated tyrosinase (acid-TY) (—).

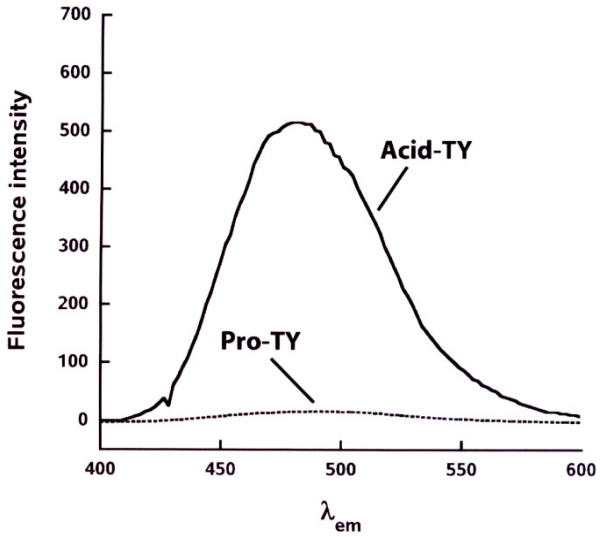

Figure 42. 8-Anilino-1-naphthalene sulfonic acid (ANS) binding assay of the protyrosinase (pro-TY, --) and acid-activated tyrosinase (acid TY, —).

The purified C108A migrated as a 60 kDa band on SDS-PAGE gel. The C108A mutant was eluted with gel-filtration chromatography to investigate the quaternary structure. Two types of molecular mass were appeared as a result of the chromatography (Table 26). One was 68 kDa and the other was 380 kDa. The former was suggested to be a monomer (mono-C108A) and the latter was an oligomer (oligo-C108A). The mono-C108A was enzymatically inactive, whereas the oligo-C108A exhibited the activity of 1.3% relative to that of the wild type of enzyme. It is thought that the lack of the intersubunit disulfide bond causes a failure to form an oligomeric structure of mono-C108A. Disulfide bonds formed by the other cysteines

(Cys174, Cys182, Cys242, Cys234, Cys483, and Cys486) or some interaction may lead to the formation of the oligomeric structure of oligo-C108A. It was suggested that the oligomeric structure is essential for the activity. Cys108 contributes to the oligomerization of the enzyme and hence is important for the activity of the dimeric acid-activated tyrosinase.

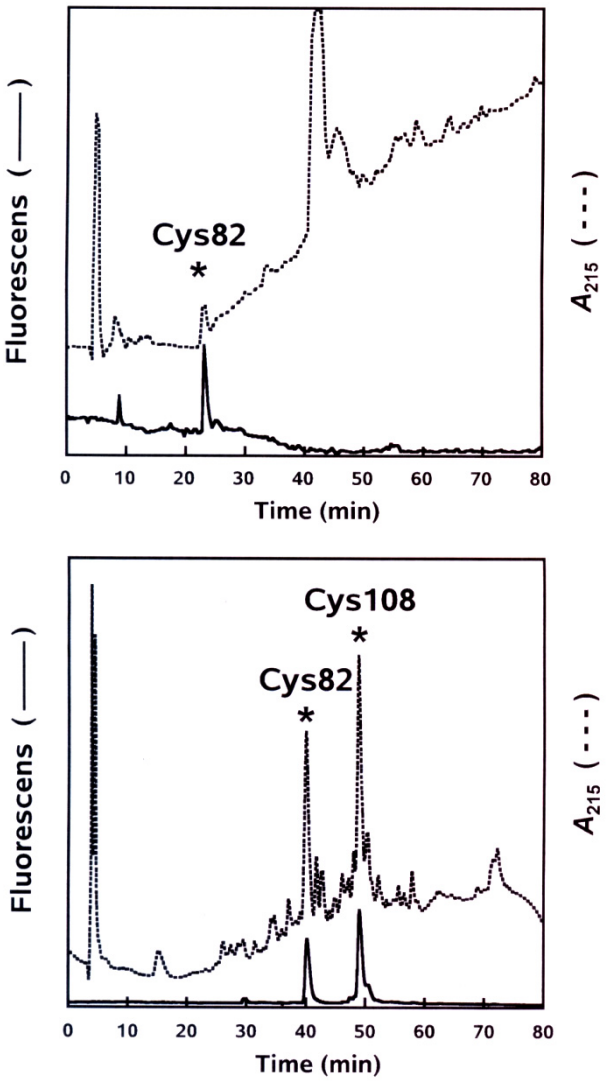

Figure 43. Reverse-phase HPLC of trypsin-degraded protyrosinase (pro-TY) in the absebce (0 mM DTT, upper panel)) and presence (1 mM DTT, lower panel) of reducing agent**.**

It is considered that *A. oryzae* tyrosinase forms the inactive tetrameric conformation to regulate the activity. *A. oryzae* produces many kinds of secondary metabolites, organic acid, kojic acid, and citrate, etc. [163]. When a cell is injured, protyrosinase is activated by extracellular acidic environment to produce melanin, which defends the interior of the cell against the acidic environment. It is considered that the acid activation is an instantaneous response to an acid stress. The acid activation is a quite unique mechanism, in which the

tetrameric proenzyme is activated by dissociation to dimmers resulting from the acid-shift of pH.

The acid-activated tyrosinase remains in the dimeric form via an intersubunit disulfide bond, which is probably formed between the Cys108 residues. The dimerization of the acid-activated tyrosinase is essential for the activity of tyrosinase from *A. oryzae*.

In this connection, we have cloned a novel tyrosinase-encoding gene (*melB*) specifically expressed in solid-state culture (Koji making) of *A. oryzae* [164]. Molecular cloning showed that the gene carried out six exons interrupted by five introns and had an open reading frame encoding 616 amino acid residues. The sequence homology between MelB tyrosinase and MelO tyrosinase was unexpectedly low (24%). These tyrosinases have low similarity with each others, however, the sequences of copper binding domains were highly conserved in these tyrosinases. A novel copper ligand motif has been conserved for *A. oryzae* MelB tyrosinase, i.e., the ligands are His67, His94, His103, and Cys92 for CuA, and His308, His312, His351, and His352 for Cu(B). The active center of MelB tyrosinase was assumed to correspond to Cu(II) ligands in the homologous tyrosinase MelO [His63, His84, His93, and Cys82 for Cu(A), and His290, His294, His332,and His333 for Cu(B)] [145]. When the *melB* gene was expressed under the control of the *melB* promoter in solid-state culture, tyrosinase activity was markedly enhanced and the culture mass was brown with the melanization by MelB tyrosinase. These results indicated that the *melB* gene encodes a novel tyrosinase associated with melanization in solid-culture of *A. oryzae* [164].

9. HYPER PRODUCTION SYSTEM OF *ASPERGILLUS ORYZAE* GLUCOAMYLASE IN SUBMERGED CULTURE UNDER TYROSINASE-ENCODING GENE (*MELO*) PROMOTER CONTROL

9.1. Glucoamylase from *A. Oryzae*

Glucoamylase (α-1,4-glucan glucanohydrolase, EC 3.2.1.3) derived from filamentous fungus *A. oryzae* strains is used in manufacture the Japanese alcoholic beverages 'Sake' (rice wine) and 'Shochu' (distilled rice wine), and soy sauce. *A. oryzae* produces large quantities of a glucoamylase in solid-state culture (Koji) [165], but the productivity in submerged culture is much lower [166]. This is because the *A. oryzae* glucoamylase encoding gene, *glaB*, is highly expressed in solid-state culture but repressed in submerged culture [167].

In solid-state culture (Koji-making) during Sake brewing, *A. oryzae* strains that produce abundant glucoamylase also produce a lot of tyrosinase, which catalyzes both the *o*-hydroxylation of phenols and the oxidation of diphenols to quinones followed by spontaneously polymerization of the quinones to melanins［138]resulting in the production of an unfavorable black sake cake called '*Kurokasu*' whose color is dependent on melanin. This led to the hypothesis that *A. oryzae glaB* and the tyrosinase-encoding gene (*melO*) are subject to the same reguration in solid-state culture [139].

To test this hypothesis, expression of the *glaB* and *melO* genes was compared in a β-glucuronidase (GUS) reporter assay. Regulation of *melO*, however, was completely different from that of *glaB*. The *melO* promoter was repressed in solid-state culture, but more highly expressed in submerged culture than were *A. oryzae amyB* [168], *glaA* [169], and modified

agdA [170], promoter frequently used in *A. oryzae* heterologous gene expressin system. This finding encouraged us to the *melO* gene promoter to establish a novel expression system in *A. oryzae*. [171].

9.2. Hyper Production System of Glucoamylase Under *Melo* Gene Promoter Control

UV-mediated mutagenesis generated a high glucoamylase-prodducing mutant (OSI 1117) of *A. oryzae* exhibiting strong melanization in a solid-state culture. The mutant produced 1.8-fold more glucoamylase and 1.3-fold more tyrosinase than the parent strain and showed higher melanization, indicating that the improvement of glucoamylase production in solid-state culture through UV-mediated mutagenesis simultaneously leads to higher tyrosinase production and melanization.

Expression of the glucoamylase-encoding gene (*glaB*), which is specifically expressed in solid-state culture, and the tyosinase-encoding gene (*melO*), was analyzed using an *E. coli* β-glucuronidase (GUS) reporter-assay to investigate this phenomenon. Although no common regulation was found for *melO* and *glaB* expression, the former was greatly enhanced in submerged culture. Intrestingly, the *melO* gene promoter was about four times stronger for β-glucuronidase production than the powerful promoter *amyB*, *glaA*, and modified *agdA*, previously isolated for industrial heterologous gene expression in *A. oryzae*.

These findings indicated that the *melO* gene promoter would be suitable for hyper-production of heterologous protein in *Aspergillus*. Thus *glaB*-type glucoamylase as the target protein was produced in a submerged culture of *A. oryzae* under the control of the *melO* gene promoter. Figure 44 shows the purities of both culture broths analyzed by SDS-PAGE after 10 days of culture [171]. Many impurities are present in the culture broth of dextran-yeast extract-peptone (DPY) medium (Figure 44, Left), whereas only glucoamylase (*glaB*-type) is present in the standard cultural broth (Figure 44, Right). The maximum yield was 0.8 g/l broth, and the total extracellular protein purity was 99%.

Although, the *melO* expression system was a powerful tool for protein production in submerged culture, it took a long time to obtain high target protein productivity. Because of maked expression of products after the stationary growth phase, repeated batch culture was done for the efficient use of mycelia after the stationary growth phase. The experiment shows that repeated batch culture increased glucoamylase production, the maximum being 3.3 g/l broth on the 12 th day after culture was begun. Productivity for the 21 days from the beginning of repeated batch culture was more than 2 g/l broth, and the product purity was 99% as total extracellular protein throughout the culture period.

The importance of this work is in the establishment of a both high-level and high-purity protein overproduction system in *A. oryzae* by use of the *melO* gene promoter [171].

APPENDIX: ENZYMES REFERRED TO IN CHAPTERS 1-9

The enzymes referred to in the chapters of this review are listed in alphabetical order generally under their recommended names as in *ENZYME NOMENCLATURE*

(Recommendation (1992) of Nomenclature Committee of the International Union of Biochemistry and Molecular Biology), except in a few cases where trivial names are more frequently used.

EC number

Aorsin 3.4.21.−

Activation of trypsinogen by selectively cleavage of Lys^{6}-↓-Ile bond at pH 4. Specific requirement for dibasic residues at P2 and P1; Boc-Gln-Arg-Arg-↓-MCA.

Aspergillopepsin I 3.4.23.18

Hydrolyses proteins with broad specificity. Generally favours hydrophobic residues in P_1 and P_1', but accept Lys in P_1, which leads to activation of trypsinogen. Does not clot milk.

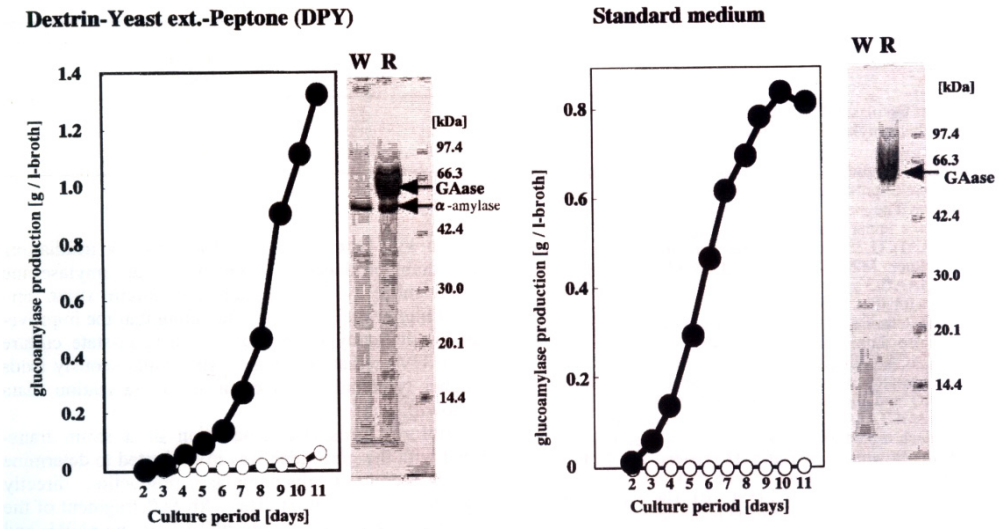

Figure 44. glaB-type glucoamylase production under melO promoter control in submerged culture of A. oryzae.

Carboxypeptidase C 3.4.16.5

Other name: *Aspergillus acid carboxypeptidase*

Release of a C-terminal amino acid with broad specificity at pH 3-5. Prefer hydrophobic residues in the P_1 position.

Catechol oxidase 1.10.3.1

Other name: Tyrosinase

Reaction: 2 Catechol + O_2 = 2 1,2-benzoquinone + 2 H_2O

Deuterolysin 3.4.24.39

Other name: *Aspergillus sojae* neutral proteinase II; Microbial neutral proteinase II

Preferential cleavage of bonds with hydrophobic residues in P_1'; also Asn^{3}-↓-Gln and Gly^{8}-↓-Ser bonds in insulin B chain. For calf thymus histone H4, high activity towards

peptides next to a pair of basic residues at pH 7.0; Lys-Arg^{17}-↓-His, Arg-His^{18}-↓-Arg, Arg-Arg^{36}-↓-Leu.

Enteropeptidase 3.4.21.9
Other name: Enterokinase
Activation of trypsinogen by selectively cleavage of Lys^{6}-↓-Ile bond.

Glucan 1,4-α-glucosidase 3.2.1.3
Other name: Glucoamylase
Hydrolysis of terminal 1,4-linked α-D-glucose residues successively from non-reducing ends of the chains with release of β-D-glucose.

Mannosyl-oligosaccharide 1,2-α-mannosidase 3.2.1.1.113
Other name: 1,2-α-D-mannosidase
Systematic name: 1,2-α-mannosyl-oligosaccharide-α-D-mannohydrolase
Hydrolysis of the terminal 1,2-linkaged α-D-mannose residues in the oligo-mannose oligosaccharide $Man_9(GlcNAc)_2$.

Monophenol monooxygenase 1.14.18.1
Other name: Tyrosinase
Reaction: L-Tyrosine + L-DOPA + O_2 = L-DOPA + dopaquinone + H_2O

Penicillolysin 3.4.24.−
The rate of clupeine hydrolysis is 60-fold greater than that for casein hydrolysis at pH 7.0. High affinity towards the Pro-↓-X, Arg-↓-Arg, and hydrophobic residue (P_1)-↓-X.

Pepsin A 3.4.23.1
Preferential cleavage: hydrophobic, preferably aromatic residues in P_1 and P_1' positions. Clevages Phe^{1}-Val, Gln^{4}-His, Glu1^{3}-Ala, Ala^{14}-Leu, Leu^{15}-Tyr, Tyr^{16}-Leu, Gly^{23}-Phe, Phe^{24}-Phe, and Phe^{25}-Tyr bonds in the B chain of insulin.

ACKNOWLEDGMENTS

I greatfully dedicate this review to my co-workers. The review is compiled in commemoration of our long enzymology research works published in the original articles, and I hope our results will contribute in helping others in attaining greater heights.

I am grateful to thank all of the members of Laboratory of Enzymology, Noda Institute for Scientific Research, Noda, Chiba, Japan, from 1957 to 1958; Laboratory of Enzymology, Kikkoman Coop., Noda, Chiba, Japan, from 1958 to 1969; Laboratory of Microbial Chemistry, Department of Agricultural Chemistry, Faculty of Agriculture, Tokyo University of Agriculture and Technology, Fuchu, Tokyo, Japan, from 1969 to 1987; Laboratory of Molecular Enzymology, Departments of Agricultural Chemistry and Applied Biological Chemistry, Graduate School of Agricultural Science, Tohoku University, Sendai, Japan, from 1987 to 1997; Laboratory of Molecular Enzymology, Faculty of Engineering, Soka

University, Hachioji, Tokyo, Japan, from 1997 to 2006, for their kind collaborations in these works as well as their technical assistances of these works.

REFERENCES

[1] Ichishima, E. (1986). The enzymatic challenge with *Aspergillus* in Japan. *Nippon Jōzōkyōkai Shi* (*J. Brew. Soc. Jpn.*)(*In Japanese*), *81*, 756-763, 844-853.

[2] chishima, E. (2007) *Koji (Japanese Malt made by Aspergillus fungus)* (*In Japanese*). Chiyoda-ku, Kudan-kita, Tokyo: Hosei University Press.

[3] Sakaguchi, K. (2007). *Nihon no Sake (Japanese Rice Wine)* (*In Japanese*). Chiyoda-ku, Jinbochyo, Tokyo: Iwanami-Shoten.

[4] Fukushima, D. (1985). Fermented vegetable protein and related foods of Japan and China. *Food Rev. Int*., *1*, 149-209.

[5] Takamine, J. (1914). Enzymes of *Aspergillus oryzae* and the application of its amyloclastic enzyme to the fermentation industry. *Ind. Eng. Chem*., *6*, 821-828.

[6] Sakaguchi, K., Iizuka, H., and Yamazaki, S. (1951). A study on blask *Aspergilli*, *Nippon Nogeikagakku Kaishi* (in Japanese, *J. Agric. Chem. Soc. Jpn.*), *24*, 138-142.

[7] Ichishima, E. (1970). Purification and mode of assay for acid proteinase of *Aspergillus saitoi*. In: Perlmann, G. E., and Lorand, L. (Eds.), *Methods in Enzymology: Proteolytic Enzymes. Vol. XIX*, (pp.397-406). New York: Academic Press.

[8] Ichishima, E. (2004). Aspergillopepsin I. In: Barrett, A.J., Rawlings, N.D., and Woessner, J.F. (Eds.), *Handbook of Proteolytic Enzymes: Vol. 1*, (Second edition, pp.92-99). Theobald's Road, London: Elsevier Academic Press.

[9] Machida, M. *et al*. (2005). Genome sequencing and analysis of *Aspergillus oryzae*. *Nature, 438*, 1157-1161.

[10] Tang, J. (2004). Pepsin A. In Barrett, A.J., Rawlings, N.D., and Woessner, J.F. (Eds.), *Handbook of Proteolytic Enzymes: Vol. 1*, (Second edition, pp.19-28). Theobald's Road, London: Elsevier Academic Press.

[11] Kay, J. (1985). Aspartic proteinases and their inhibitors. *Biochem. Soc. Trans*., *13*, 1027-1029.

[12] Schechter, I., and Berger, A. (1967). On the size of the active site in proteases. I. Papain. *Biochem. Biophys. Res. Commun*., *27*, 157-162.

[13] Tang, J., James, M. N. G., Hsu, I. N., Jenkins, J. A., and Blundell, T. L. (1978). Structural evidence for gene duplication in the evolution of the acid proteases. *Nature*, *271*, 618-621.

[14] James, M. N. G., and Sielecki, A. (1983). Structure and refinement of penicillopepsin at 1.8 Å resolution. *J. Mol. Biol*., *163*, 299-361.

[15] Suzuki, F., Murakami, K., and Nakamura, Y. (2004). Renin. In Barrett, AJ, Rawlings, ND, and Woessner, JF. (Eds.), *Handbook of Proteolytic Enzymes: Vol. 1*, (Second edition, pp. 54-61). Theobald's Road, London: Elsevier Academic Press.

[16] Foltmann, B. (2004). Chymosin. In: Barret, AJ, Rawlings, ND, and Woessner, JF. (Eds.), *HANDBOOK of Proteolytic Enzymes: Vol. 1*, (Second edition, pp. 29-32). Theobald's Road, London: Elsevier Academic Press.

[17] Ballou, C. E. (1990). Isolation, characterization, and properties of *Saccharomyces cerevisiae mann* mutants with nonconditional protein glycosylation defects. In Goeddel, DV, editor. *Methods in Enzymology, Vol. 185*, Academic Press, San Diego, Calif., pp.440-470.

[18] Tanaka, N., Takeuchi, M., and Ichishima, E. (1977). Purification of an acid proteinase from *Aspergillus saitoi* and characterization of peptide bond specificity. *Biochim. Biophys. Acta*, *485*, 406-416.

[19] Majima, E., Oda, K., Murao, S., and Ichishima, E. (1988). Comparative study on the specificity of several fungal aspartic and acidic proteinases towards the tetradecapeptide of a rennin substrate. *Agric. Biol. Chem*., *52*, 787-793.

[20] Gabeloteau, C., and Desnuelle, P. (1960). On the activation of beef trypsinogen by a crystallized protease of *Aspergillus saitoi. Biochim. Biophys. Acta*, *42*, 230-237

[21] Abita, J. P., Delaage, M., Lazdunski, M., and Savrda, J. (1969). The mechanism of activation of trypsinogen. The role of the four *N*-terminal aspartyl residues. *Eurp.J. Biochem*., *8*, 314-324.

[22] Hofmann, T. (2004). Penicillopepsin. In Barrett, A.J., Rawlings, N.D., and Woessner, J.F. (Eds.), *Handbook of Proteolytic Enzymes: Vol. 1*, (Second edition, pp.99-104). Theobald's Road, London: Elsevier Academic Press.

[23] Sadler, J. E. (2004). Enteropeptidase. In: Barrett, A.J., Rawlings, N.D., and Woessner, J.F. (Eds.), *Handbook of Proteolytic Enzymes: Vol. 2*. (Second Ed. pp.1513-1517). Theobald's Road, London: Elsevier Academic Press.

[24] Morihara, K., and Oka, T. (1973). Comparative specificity of microbial acid proteinases for synthetic peptides. 3. Relationship with their trypsinogen activating ability. *Arch. Biochem. Biophys*., *157*, 561-572.

[25] James, M. N. G., Sielecki, A. R. , Salituro, F., Rich, D. H., and Hofmann, T. (1982). Conformational flexibility in the active site site of aspartyl proteinases revealed by a pepstatin fragment binding to penicillopepsin. *Proc. Nat. Acad. Aci. USA*, **79**, 6137-6141.

[26] James, M. N. G., Sielecki, A.R., and Hofmann, T. (1985). X-ray diffraction studies of penicillopepsin and its complex: the hydrophobic Mechanism. In Kostka, V. (Ed.), *Aspartic Proteinases and Their Inhibitors*. (pp.163-177). Berlin, Walter de Gruyter.

[27] Blundell, T. L., Cooper, J., Foundling, S. I., Jones, D. M., Atrash, B., and Szelk, M. (1987). On the rational design of renin inhibitors: X-ray studies of aspartic proteinase complexed with trasition-state analogues. *Biochemistry*, *26*, 5585-5590.

[28] Suguna, K., Bott, R. R., Padlan, E. A., Subramanian, E., Sheriff, S., Cohen, G. H., and Davies, D. R. (1987). Structure and refinement at 1.8 Å resolution of the aspartic proteinase from *Rhizopus chinensis. J. Mol. Biol*., *196*, 877-900.

[29] Shintani, T., and Ichishima, E. (1994). Primary structure of aspergillopepsin I deduced from nucleotide sequence of the gene and aspartic acid-76 is an essential active site of the enzyme for trypsinogen activation. *Biochim. Biophys. Acta*, *1204*, 257-264.

[30] Shintani, T., Kobayashi, M., and Ichishima, E. (1996). Characterization of the S_1 subsite specificity of aspergillopepsin I by site-directed mutagenesis. *J. Biochem. (Tokyo)*, *120*, 974-981.

[31] Lowther, W. T., Majer, P., and Dunn, B. M. (1995). Engineering the substrate specificity of rhizopuspepsin: the role of Asp 77 of fungal aspartic proteinase in

facilitating the cleavage of oligopeptide substrates with lysine in P_1. *Protein Sci*., *4*, 689-702.

[32] Beppu, T., Park, Y.-N., Aikawa, J., Nishiyama, M., and Horinouchi, S. (1995). Tyrosine 75 on the flap contributes to enhance catalytic efficiency of a fungal aspartic proteinase, *Mucor pusillus* pepsin. In: *Aspartic Proteinase: Structure, Function, Biology, and Biomedical Implications*. Takahashi, T. (Ed.), (pp. 559-563). New York: Plenum Press.

[33] Dhanaraj, V., Dealwis, C. W., Frazao, C., Badasso, M., Sibanda, B. L, Tickle, I. J., Cooper, J. B., Driessen, H. P., Newman, M., Aguilar, C. Wood, S. P., Blundell, T. L., Hobart, P. M., Geophegan, K. F., Ammirati, M. J., Danley, D. E., O'Connor, B. A., and Hoover, D. J. (1992). X-ray analyses of peptide-inhibitor complexes define the structural basis of specificity for human and mouse renins. *Nature*, *357*, 466-472.

[34] Fujinaga, M., Chernaia, M. M., Tarasova N. I., Mosimann, S. C., and James, M. N. G. (1995). Crystal structure of human pepsin and its complex with pepstatin. *Protein Sci.*, *4*, 960-972

[35] Shintani, T., Nomura, K., and Ichishima, E. (1997). Engineering of porcine pepsin: Alteration of S_1 substrate specificity of pepsin to those of fungal aspartic proteinase by site-directed mutagenesis. *J. Biol. Chem*., **272**, 18855-18861.

[36] Lin, X., Wong, R. N. S., and Tang, J. (1989). Synthesis, purification, and active site mutagenesis of recombinant porcine pepsinogen, *J. Biol. Chem*., *264*, 4482-4489.

[37] Tang, J., Sepulveda, P., Marcinszyn, J., Jr. Chen, K. C. S., Huang, W.-Y., Liu, D., and Lanier, J. P. (1973). Amino acid sequence of porcine pepsin. *Proc. Natl. Acad. Sci. USA*, *70*, 3437-3439.

[38] Tsukagoshi, N., Ando, Y., Tomita, Y., Uchida, R., Takemura, T.,Sasaki, T., Yamagata, H., Udaka, S., Ichihara, Y., and Takahashi, K. (1988). Nucleotide sequence and expression in *Escherichia coli* of cDNA of swine pepsinogen: involvement of the amino-terminal porsine of the activation peptide segment in restoration of the functional protein. *Gene*, *65*, 285-292.

[39] Green, B. N., Jones, A. T., and Roberts, N. B. (1996). Electrospray mass spectrometric evidence for the occurrence of two major variants in native pig pepsin A. *Biochem.J*., *313*, 241-244.

[40] Kageyama, T., and Takahashi, K. (1983). Occurrence of two different pathways in the activation of porcine pepsinogen to pepsin. *J. Biochem. (Tokyo)*, *93*, 743-754.

[41] Pohl, J., and Dunn, B. M. (1988). Secondary enzyme-substrate interactions: kinetic evidence for ionic interactions between substrate side chains and the pepsin active site. *Biochemistry*, *27*, 4827-4834.

[42] Takahashi, K. (1995). Proteinase A from *Aspergillus niger*. In Barrett, A. J. (Ed)**.** *Methods in ENZYMOLOGT, Vol. 248. Proteolytic Enzymes: Aspartic and Metallo Peptidases*, (pp. 146-155.). New York; Academic Press.

[43] Murao, S., Oda, K., and Matsushita, Y. (1972). New acid protease from *Scytalidium lignicolum., Agric. Biol. Chem*., *36*, 1647-1650.

[44] Oda, K., Takahashi, T., Tokuda, Y., Shibano, Y., and Takahashi, S. (1994). Cloning, nucleotide sequence, and expression of an isovalery pepstatin-insensitive carboxyl proteinase gene from *Pseudomonas* sp. 101., *J. Biol. Chem*., *269*, 26518-26524.

[45] Oda, K., Nakajima, T., Terashita, T., Suzuki, K., and Murao, S. (1987). Purification and properties of an S-PI (pepstatin Ac)-insensitive carboxyl proteinase from *Xanthomonas* sp. Bacterium. *Agric. Biol. Chem*., *51*, 3073-3080.

[46] Oda, K., Ito, M., Uchida, K., Shibano, Y., Fukuhara, K., and Takahashi, S. (1996). Cloning and expression of an isovaleryl pepstatin-insensitive carboxyl proteinase gene from *Xanthomonas* sp. T-22., *J. Biochem. (Tokyo)*, *120*, 564-572.

[47] Sleat, D. E., Donnelly, R. J., Lackland, H., Liu, C. –G., Sohar, I., Pullarkat, R. K., and Lobel, P. (1997). Association of mutations in a lysosomal protein with classical lateinfantile ceroid lipofuscinosis. *Science*, *277*, 1802-1805.

[48] Wisniewski, K. E., Kaczmarski, A., Kida, E., Connell, F., Kaczmaeski, W., Michaelewski, M. P., Moroziewicz, D. N., and Zhong, N. (1999). Reevaluation of neuronal ceroid lipofuscinoses: atypical juvenile onset may be the result of CLN2 mutations., *Mol. Genet. Metab*., *66*, 248-252.

[49] Junaid, M. A., Wu, G., and Pullarkat, R. K. (2000). Purification and characterization of bovine brain lysosomal pepstatin-insensitive proteinase, the gene product deficient in the human late-infantile neuronal ceroid lipofuscinosis. *J. Neurochem.*, *74*, 287-294.

[50] Rawlings, N. D., and Barrett, A. J. (1999). Tripeptidyl-peptidase I is apparently the CLN2 protein absent in classical late-infantile neuronal ceroid lipofuscinosis. *Biochim. Biophys. Acta*, *1429*, 496-500.

[51] Ezaki, J., Takeda-Ezaki, M., Oda, K., and Kominami, E. (2000). Characterization of endopeptidase activity of tripeptidyl peptidase-I/CLN2 protein which is deficient in classical late infatile neuronal ceroid lipofuscinosis. *Biochem. Biophys. Res.Commun*., *268*, 904-908.

[52] Lin, L., Sohar, I., Lackland, H., and Lobel, P. (2001). The human CLN2 protein/tripeptidyl-peptidase I is a serine protease that autoactivates at acidic pH., *J. Biol. Chem*., *276*, 2249-2255.

[53] Wlodawer, A., Li, M., Dauter, Z., Gustchina, A., Uchida, K., Oyama, H., Dunn, B. M., and Oda, K. (2001). Carboxyl proteinase from *Pseudomonas* defines a novel family of subtilisin-like enzymes. *Natl. Struct. Biol*., *8*, 442-446.

[54] Rawlings, N. D., O'Brien, E. A., and Barrett, A. J. (2002). MEROPS: the protease database. *Nucleic Acids Res*., *30*, 343-346.

[55] Lee, B. R., Furukawa, M., Yamashita, K., Kanasugi, Y., Kawabata, C., Hirano, K., Ando, K., and Ichishima, E. (2003). Aorsin, a novel serine proteinase with trypsin-like specificity at acidic pH. *Biochem. J*., *371*, 541-548.

[56] Oda, K., Fukuda, Y., Murao, S., Uchida, K., and Kainosho, M. (1989). A novel proteinase inhibitor, tyrostatin, inhibiting some pepstatin-insensitive carboxyl proteinases. *Agric. Biol. Chem*., *53*, 405-415.

[57] Oyama, H., Abe, S., Ushiyama, S., Takahashi, S., and Oda, K. (1999). Identification of catalytic residues of pepstatin-insensitive carboxyl proteinases from prokaryotes by site-directed mutagenesis. *J. Biol. Chem*., *274*, 27815-27822.

[58] (58) Sekine, H. (1973). Neutral proteinases II of *Aspergilus sojae*: an enzyme specifically active on protamine and histone. *Agric. Biol. Chem*., *37*, 1765-1767.

[59] Tatsumi, H. (2004). Deuterolysin. In Barrett, A. J., Rawlings, N. D., and Woessner, J. F. (Eds.), *Handbook of Proteolytic Enzymes: Vol. 1*, (Second edition, pp. 786-788). Theobald's Road, London: Elsevier Academic Press.

[60] Tatsumi, H., Murakami, S., Tsuji, R. E., Ishida, Y., Murakami, K., Masaki, A., Kawabe, H., Arimura, H., Nakano, E., and Motai, H. (1991). Cloning and expression in yeast of a cDNA clone encoding *Aspergillus oryzae* neutral protease II, a unique metalloprotease. *Mol. Gen. Genet*., *228*, 97-103.

[61] Tatsumi, H., Ikegaya, K., Murakami, S., Kawabe, H., Nakano, E., and Motai, H. (1994). Elucidation of the thermal stability of the neutral proteinase II from *Aspergillus oryzae. Biochim. Biophys. Acta*, *1208*, 179-185.

[62] Hooper, N.M. (1994). Families of zinc metalloproteases. *FEBS Lett*., *354*, 1-6.

[63] Rawlings, N.D., and Barrett, A. J. (1995). *Evorutionary families of metallopeptidases.* In: Barrett, A. J. (Ed.), *Methods in Enzymology, Vol. 248,* (pp. 183-228). San Diego: Academic Press.

[64] Fushimi, N., Ee, C. E., Nakajima, T.,and Ichishima, E. (1999). Aspzincin, a family of metalloendopeptidase with a new zinc-binding motif. *J. Biol. Chem*., *274*, 24195-24201.

[65] McAuley, K. E., Jia-Xing, Y., Dodson, E. J., Lehmbeck, J., Ostergaard, P. R., and Wilson, K. S. (2001). A quick solution: *ab initio* structure determination of a 19 kDa metalloproteinase using ACORN. *Acta Crystallogr. D.*, *57*, 1571-1578.

[66] Hori, To, Kumasaka, T., Yamamoto, M., Nonaka, N., Tanaka, N., Hashimoto, Y., Ueki, T, and Takoi, K. (2001). Structure of a new 'aspzincin' metalloendopeptidase from *Grifola frondosa*: implications for the catalytic mechanism and substrate specificity based on several different crystal forms. *Acta Crystallogr. D*., *57*, 361-368.

[67] Doi, Y., Lee, B. R., Ikeguchi, M., Ohoba, Y., Ikoma, T., Terao-Kubota, S., Yamauchi, S., Takahashi, K., and Ichishima, E. (2003). Substrate specificities of deuterolysin from *Aspergillus oryzae* and electron paramagnetic resonance measurement of cobalt-substituted deuterolysin. *Biosci. Biotechnol. Biochem*., *67*, 264-270.

[68] (68) Ichishima, E., Yamaguchi, M., Yano, H., Yamagata, Y., and Hirano, K. (1991). Specificity of a new metalloproteinase from *Penicillium citrinum. Agric. Biol. Chem*., *55*, 2191-2193.

[69] Yamaguchi, M., Hanzawa, S., Hirano, K., Yamagata, Y., and Ichishima, E. (1993). Specificity and molecular properties of penicillolysin, a new metalloproteinase from *Penicirium citrinum. Phytochemistry*, *33*, 1371-1321.

[70] Matsumoto, K., Yamaguchi, M., and Ichishima, E. (1994). Molecular cloning and nucleotide sequence of the complementary DNA for penicillolysin gene, *plnC*, an 18 kDa metalloendopeptidase gene from *Penicillium citrinum. Biochim. Biophys. Acta*, *1218*, 469-472.

[71] Ichishima, E. (2004). Penicillolysin. In Barrett, A.J., Rawlings, N.D., and Woessner, J.F. (Eds.), *HANDBOOK of Proteolytic Enzymes: Vol. 1*, (Second edition, pp.784-786). Theobald's Road, London: Elsevier Academic Press.

[72] Doi, Y., Akiyama, H., Yamada, Y., Ee, C. E., Lee, B. R., Ikeguchi, M., and Ichishima, E. (2004). Thermal stabilization of penicillolysin, a thermolabile 19 kDa Zn^{2+}-protease, obtained by site-directed mutagenesis. *Protein Eng. Des. Select*., *17*, 261-266.

[73] Price, N. C. and Stevens, L. (1999). *Fundamentals of Enzymology: Enzyme turnover* (Third edition, pp.370-399). Great Clarendon, Oxford: Oxford University Press.

[74] Matthews, B. W., Nicolson, H., and Becktel, W. J. (1987). Enhanced protein thermostability from site-directed mutagenesis that decrease the entropy of unfolding. *Proc. Natl. Acad. Sci. USA*, *84*, 6663-6666.

[75] Suzuki, Y. (1989). A general principle of increasing protein thermostability. *Proc. Jpn. Acad*., **65**, 146-148.

[76] Suzuki, Y., Oishi, K., Nakano, H., and Nagayama, T. (1987). A strong correlation between the increase in number of praline residues and the rise in thermostability of five *Bacillus* oligo 1,6-glucosidases. *Appl. Microbiol. Biotechnol*., *26*, 546-551.

[77] Auld, D. S. (2004). Carboxypeptidase A. In Barrett, A.J., Rawlings, N.D., and Woessner, J.F. (Eds.), *Handbook of Proteolytic Enzymes: Vol. 1*, (Second edition, pp. 813-821). Theobald's Road, London: Elsevier Academic Press.

[78] Aviles, F. X., and Vendrell, J. (2004). Carboxypeptidase B. In Barrett, A.J., Rawlings, N.D., and Woessner, J.F. (Eds.), *Handbook of Proteolytic Enzymes: Vol. 1*, (Second edition, pp. 831-833). London, Elsevier Academic Press.

[79] Ichishima, E. (1972). Purification and characterization of a new type of acid aroxypeptidase from *Aspergillus. Biochim. Biophys. Acta*, *258*, 274-288.

[80] Ichishima, E., and Arai, T. (1973). Specificity and mode of action of acid carboxypeptidase from *Aspergillus saitoi. Biochim. Biophys. Acta*, *293*, 444-450.

[81] Chiba, Y., Yamagata, Y., Nakajima, T., and Ichishima, E. (1992). A new high-mannose type-*N*-linked oligosaccharide from *Aspergillus* carboxypeptidase. *Biosci.Biotechnol. Biochem*., *56*, 1371-1372.

[82] Chiba, Y., Yamagata, Y., Iijima, S., Nakajima, T., and Ichishima, E. (1993). The carbohydrate moiety of the acid carboxypeptidase from *Aspergillus saitoi*. *Curr.Microbil*., *27*, 281-288.

[83] Takaki, A., Yoshitake, S., Ishiguro, M., and Funatsu, M. (1972). Anticoagulant peptide obtained from fibrinogen degradation products by plasmin. II. Sequence determination of the peptide. *Proc. Japan Acad*., *48*, 525-538.

[84] Chiba, Y., Nieda, Y., Nakajima, T., and Ichishima, E. (1991) Unique enzymatic properties of alpha-amylase-III from suspension-cell cultured rice cells. *Agric. Biol. Chem*., *55*, 901-902.

[85] Yanagida, N., Uozumi, T., and Beppu, T. (1986). Specific excretion of *Serratia marcescens* protease through the outer membrane of *Escherichia coli*. *J. Bacteriol*., *166*, 937-944.

[86] Takeuchi, M., and Ichishima, E. (1989). Action of serine carboxypeptidases from *Aspergillus saitoi* on carboxyterminal amidated peptides. *Agric. Biol. Chem*., *53*, 2301-2306.

[87] Takeuchi, M., Takagi, Y., Ebisui, R., Toyama, T., and Ichishima, E. (1989). Mode of action of fluorogenic substrates of acid carboxypeptidases from *Aspergillus. Agric. Biol. Chem*., *53*, 1177-1178.

[88] Chiba, Y., Midorikawa, T., and Ichishima, E. (1995). Cloning and expression of the carboxypeptidase gene from *Aspergillus saitoi* and determination of the catalytic residues by site-directed mutagenesis. *Biochem. J.*, *308*, 405-409.

[89] Mortensen, U. H., Olesen, K., and, Breddam, K. (2004). Serine carboxypeptidsase C including carboxypeptidase Y. In Barrett, A.J., Rawlings, N.D., Woessner, J.F. (Eds.), *HANDBOOK of Proteolytic Enzymes: Vol. 2*, (Second edition, pp. 1919-1923). Theobald's Road, London: Elsevier Academic Press.

[90] Arai, S., Yamashita, M., Kato, H., and Fujimaki, M. (1970). Applying proteolytic enzymes on soybean. Part V. A nondialyzable bitter peptide in peptic hydrolyzate of

soybean protein and its bitterness in relation to the chemical structure. *Agric. Biol. Chem*., *34*, 729-738.

[91] Umetsu, H., Matsuoka, H., and Ichishima, E. (1983). Debittering mechanism of bitter peptides from milk casein by wheat arboxypeptidase. *J. Agric. Food Chem*., *31*, 50-53.

[92] Hernandez, L. M., and Ballou, L., Alvarado, E., Gillece-Castro, B. L., Burlingame, A. L., and Ballou, C. E. (1989). A new *Saccharomyces cerevisiae mnn* mutant N-linked ologisaccharide structure. *J. Biol. Chem*., *264*, 11849-11856.

[93] Cohen, R. E., Zhnag, W., and Ballou, C. E. (1982). Effects of mannoproteins in *Saccharomyces cerevisiae* core oligosaccharide structure. *J. Biol. Chem*., *257*, 5730-5737.

[94] Ichishima, E., Arai, M., Shigematsu, Y., Kumagai, H., and Sumida-Tanaka, R. (1981). Purification of an acidic α-D-mannosidase from *Aspergillus saitoi* and specific cleavage of 1,2-α-D-mannosidic linkage in yeast mannan. *Biochim. Biophys. Acta*, *658*, 45-53.

[95] Yamashita, K., Ichishima, E., Arai, M., and Kobata, A. (1980). An α-mannosidase purified from *Aspergillus saitoi* is specific for α1,2 linkages. *Biochem. Biophys. Res.Commun*., *96*, 1335-1342.

[96] Trimble, R. B., and Atkinson, P. H. (1986). Structure of yeast external invertase Man_{8-14}GlcNAc processing intermediates by 500-megahertz ^{1}H NMR spectroscopy. *J. Biol. Chem*., *261*, 9815-9824.

[97] Ito, S., Yamashita, K., Spiro, R. G., and Kobata, A. (1977). Structure of carbohydrate moiety of a unit A glycopeptide of calf thyroglobulin. *J. Biochem*., *81*, 1621-1631 (1977).

[98] Öckerman, P. A. (1967). A generalized storage disdorder resembling Hurler's syndrome. *Lancet II*, 239-241.

[99] Öckerman, P. A., Autio, S., and Norder, N. E. (1973) Diagnosis of mannosidosis. *Lancet 1*, 207-208.

[100] Champion, M. J. and Shows, T. B. (1977) Mannosidosis: Assignment of the lysosomal α-mannosidase B gene to chromosome 19 in man. *Proc. Natl. Acad. Sci. USA, 74*, 2968-2972.

[101] Moremen, K.W., Trimble, R. B., and Herscovics, A. (1994). Glycosidases of the asparagines-linked oligosaccharide processing pathway. *Glycobiology*, *4*, 113-125.

[102] Schneikert, J., and Herscovics, A. (1995). Two naturally occurring mouse α-mannosidase IB cDNA clones differ in three point mutations. Mutation of Phe592 to Ser592 is sufficient to abolish enzyme activity. *J. Biol. Chem*., *270*, 17736-17740.

[103] NC-IUBMN, In: Webb, E. C. Editor. *Enzyme Nomenclature 1992*. ed. San Diego, California: Academic Press, Inc. (1992).

[104] Yoshida, T., Inoue, T., and Ichishima, E. (1993). 1,2-α-D-mannosidase from *Penicillium citrinum*: molecular and enzymatic properties of two isoenzymes. *Biochem. J*., *290*, 349-354.

[105] Yoshida, T., Maeda, K., Kobayashi, M., and Ichishima, E. (1994). Chemical modification of *Penicillium* 1,2-α-D-mannosidase by water-soluble carbodi-imide: identification of a catalytic important aspartic acid residue. *Biochem. J*., *303*, 97-103.

[106] Ichishima, E., Ito, Y., and Takeuchi, M. (1985). 1,2-α-D-mannosidase from a wood-rotting Basidiomycete, *Pycnoporus sanguineus. Phytochemistry*, *24*, 2835-2837.

[107] Inoue, T., Yoshida, T., and Ichishima, E. (1995). Molecular cloning and nucleotide sequence of the 1,2-α-D-mannosidase gene, *msdS*, from *Aspergillus saitoi* and expression of the gene in yeast cells. *Biochim. Biophys. Acta*, *1253*, 141-145.

[108] Yoshida, T., and Ichishima, E. (1995). Molecular cloning and nucleotide sequence of the genomic DNA for 1,2-α-D-mannosidase gene, *msdC* from *Penicillium citrinum.Biochim. Biophys. Acta*, *1263*, 159-162.

[109] Jelinek-Kelly, S., and Herscovics, A. (1988). Glycoprotein biosynthesis in *Saccharomyces cervisiae*. Purification of the α-mannosidase which removes one specific mannose residue from $Man_9GlcNAc$. *J. Biol. Chem*., *263*, 14757-14763.

[110] Lipari, F., and Herscovics, A. (1966). Role of the cysteine residues in the 1,2-α-D-mannosidase involved in N-glycan biosynthesis in *Saccharomyces cerevisiae. J. Biol. Chem*., *271*, 27615-27622.

[111] Herscovics, A.,Schneikert, J., Athanassiadis, A., and Moremen, K. W. (1994). Isolation of a mouse golgi mannosidase cDNA, a member of a gene fairy conserved from yeast to mammals. *J. Biol. Chem*., *269*, 9864-9871.

[112] (Ichishima, E., Taya, N., Ikeguchi, M., Chiba, Y., Nakamura, M., Kawabata, C., Inoue, T., Takahashi, K., Minetoki, T., Ozeki, K., Kumagai, C., Gomi, K., Yoshida, T., and Nakajima, T. (1994). Molecular and enzymatic properties of recombinant 1,2-α-mannosidase from *Aspergillus saitoi* overexpressed in *Aspergillus oryzae* cells. *Biochem. J*., *339*, 589-597.

[113] Fujita, A., Yoshida, T., and Ichishima, E. (1997). Five crucial carboxyl residues of 1,2-α-D-mannosidase from *Aspergillus saitoi* (*A. phoenicis*), a food microorganism, are identical by site-directed mutagenesis. *Biochem. Biophys. Res. Commun*., *238*, 779-783.

[114] Tatara, Y., Lee, B. R., Yoshida, T., Takahashi, K., and Ichishima, E. (2003). Identification of catalytic residues of Ca^{2+}-independent 1,2-α-D-mannosidase from *A. saitoi* by site-directed mutagenesis. *J. Biol. Chem.*, *278*, 25289-25294.

[115] Lobsanov, Y. D., Vallee, F., Imberty, A., Yoshida, T., Yip, P., Herscovics, A., and Howell, P. L. (2001). Structure of *Penicillium citrinum* α1,2-mannosidase reveals the basic differences in specificity of the endoplasmic reticulum and Golgi class Ienzymes. *J. Biol. Chem*., *277*, 5620-5630.

[116] Miyake, H., Otsuka, C., Nichimura, S., and Nitta, Y. 1 (2002). Catalytic mechanism of β-amylase from *Bacillus cereus* var. *mycoides*: Chemical rescue of hydrolytic activity for a catalytic site mutant (Gku367→Ala) by azide. *J. Biochem*. (*Tokyo*), *131*, 587-591.

[117] Koivula, A., Ruohonen, L., Wohlfahrt, G., Reinkainen, T., Teeri, T. T., Piens, K., Claeyssens, M., Weber, M., Vasella, A., Becker, D., Sinnott, M. L., Zou, J. Y., Kleywegt, G. J., Szardenings, M., Ståhberg, J., and Jones, T. A. (2002). The active site of cellobiohydrolase Ce16A from *Trichoderma reesei*: The roles of aspartic acids D221 and D175. *J. Am. Chem. Soc*., *124*, 10015-10024.

[118] Koivula, A., Reinikainen, T., Ruohonen, L., Valkeajarvi, A., Claeyssens, M.,Teleman, O., Kleywegt, G. T., Szardenings, M., Rouvinen, J., Jones, T. A., and Teeri, T. T. (1996). The active site of *Trichoderma reesei* cellobiohydrolase II: the role of tyrosine 169. *Protein Eng*., *9*, 691-699.

[119] Zou, J., Kleywegt, G. J., Stahlberg, J., Dringuez, H., Nerinckx, W., Claeyssens, M., Koivula, A., Teeri, T. T., and Jones, T. A. (1999). Crystallographic evidence for substrate ring distortion and protein conformational changes during catalysis in cellobiohydrolase Cel6A from *Trichoderma reesei*. *Structure* (*Lond*.), *7*, 1035-1045.

[120] Hasegawa, K., Kubota, M., and Matsuura, Y. (1999). Role of catalytic residues in α-amylases as evidenced by the structures of the product-complexed mutants of a maltotetraose-forming amylase. *Protein Eng*., *12*, 819-824.

[121] Gonzalez, D. S., Karaveg, K., Vandersall-Nairn, A.S., Lal., A., and Moremen. K. W. (1999). Identification, expressetion, and characterization of a cDNA encoding human endoplasmic reticulum mannosidase I, the enzyme that catalyzes the first mannose trimming step in mammalian Asn-linked oligosaccharide biosynthesis.*J. Biol. Chem*., *274*, 21375-21386.

[122] Schutzbach, J. S., and Forsee, W. T. (1990). Calcium ion activation of rabbit liverα1,2-mannosidase. *J. Biol. Chem*., *265*, 2546-2549.

[123] Oku, H., Hase, S., and Ikenaka, T. (1991). Purification and characterization of neutral α-mannosidase that is activated by Co^{2+} from Japanese quail oviduct. *J. Biochem*. (*Tokyo*), *110*, 29-34.

[124] Yamashiro, K., Itoh, H., Yamagishi, M., Natsuka, S., Mega, T., and Hase, S. (1997).Purification and characterization of neutral α-mannosidase from hen oviduct: Studies on the activation mechanism of Co^{2+}. *J. Biochem.* (*Tokyo*), *122*, 1174-1181.

[125] Lipari, F., and Herscovics, A. (1994). Production, purification and characterization of recombinant yeast processing α1,2-mannosidase. *Glycobiology*, *4*, 697-702.

[126] Jelinek,-Kelly, S., and Herscovics, A. (1988). Glycoprotein biosynthesis in *Saccharomyces cerevisiae*. *J. Biol. Chem*., *263*, 14757-14763.

[127] Lubas, W. A., and Spiro, R. G. (1988). Evaluation of the role of rat liver golgi endo-α-D-mannosidase in processing N-linked oligosaccharides. *J. Biol. Chem*., *263*, 3990-3998.

[128] Lipari, F., and Herscovics, A. (1999). Calcium binding to the class I alpha-1,2-mannosidase from *Saccharomyces cerevisiae* occurs outside the EF hand motif. *Biochemistry*, *38*, 1111-1118.

[129] Tatara, Y., Yoshida, T., and Ichishima, E. (2005). A single free cysteine residue and disulfide bond contribute to the thermostability of *Aspergillus saitoi* 1,2-α-D-mannosidase. *Biosci. Biotechnol. Biochem*., *69*, 2101-2108.

[130] Dobson, C. M. (2003). Protein folding and misfolding. *Nature*, *426*, 884-890.

[131] Sitia, R., and Braakman, I. (2003). Quality control in the endoplasmic reticulum protein factory. *Nature*, *426*, 891-894.

[132] Goldberg, A. L. (2003). Protein degradation and protection against misfolded or damaged proteins. *Nature*, *426*, 859-899.

[133] Lehman, M. A. (2001). Oligosaccharide-based information in endoplasmic reticulumn quality control and other biological system. *J. Biol. Chem*., *276*, 8623-8626.

[134] Kyte, J., and Doolittle, R. F. (1982). A simple method for displaying the hydropathic character of a protein. *J. Mol. Biol*., *157*, 105-132.

[135] Chiba, Y., Suzuki, M., Yoshida, S., Yoshida, A., Ikenaga, H., Takeuchi, M., Jigami, Y., and Ichishima, E. (1998). Production of human compatible high mannose-type ($Man_5GlcNAc_2$) sugar chains in *Saccharomyces cerevisiae*. *J. Biol. Chem*., *273*, 26298-26304.

[136] Garcia-Borron, J. C., and Solano, F. (2002). Molecular anatomy of tyrosinase and its related proteins: beyond the histidine-bound metal catalytic center. *Pigment Cell. Res*., *15*, 162-173

[137] Adman, E. T. (1991). Copper protein structures. *Adv. Protein Chem*., *42*, 145-197.

[138] Ichishima, E., Maeba, H., Amikura, T.,and Sakata, H. (1984). Multiple forms of protyrosinase from *Aspergilus oryzae* and their mode of activation at pH 3.0. *Biochim. Biophys. Acta*, *786*, 25-31.

[139] Fujita, Y., Uraga, Y., and Ichisima, E. (1995). Molecular cloning and nucleotide sequence of the protyrosinase gene, *melO*, from *Aspergillus oryzae* and expression of the gene in yeast cells. *Biochim. Biophys. Acta*, *1261*, 151-154.

[140] Kuper, U., Niedermann, D. M., Travaglini, G. and Lerch, K. (1989). Isolation and characterization of the tyrosinase gene from *Neurospora crassa*. *J. Biol. Chem*., *264*, 17250-17258.

[141] Huber, M., Hintermann, G., and Lerch, K. (1985). Primary structure of tyrosinase from *Streptomyces glaucescence*. *Biochemistry*, *24*, 6038-6044.

[142] Huber, M. and Lerch, K. (1988). Identification of two histidines as copper ligands in *Streptomyces glaucescens* tyrosinase. *Biochemistry*, *27*, 5610-5615.

[143] Known, B. S., Haq, A. K., Pomerantz, S. H., and Halaban, R. (1987). Isolation and sequence of cDNA for human tyrosinase that maps at the mouse-c-albino locus. *Proc. Natl. Acad. Sci. USA.*, *84*, 7473-7477.

[144] Lerch, K. (1982). Primary structure of tyrosinase from *Neurospora crassa*. II. Complete amino acid sequence and chemical structure of a tripeptide containing an unusual thioether. *J. Biol. Chem*., *257*, 6414-6419.

[145] Nakamura, M., Nakajima, T., Ohba, Y., Yamauchi, S., Lee, B. R., and Ichishima, E. (2000). Identification of copper ligands in *Aspergillus oryzae* tyrosinase by site-directed mutagenesis. *Biochem. J*., *350*, 537-545.

[146] Gaykema, W. P. J., Hol., W. G. J., Vereiken, J. M., Soeter, N. M., Bak, H. J., and Beintem, J. J. (1984). 3.2 Å structure of the copper-containing protein *Panulirus interruptus* hemocyanin. *Nature*, *309*, 23-29.

[147] Sakaguchi, U., and Addison, A. W. (1979). Spectroscopic and redox studies of some copper (II) complexes with biomimetic donor atoms: implications for protein copper centres. *J. Chem. Soc. Dalton Trans*., 600-608.

[148] Spritz, R. A., Ho, L., Furanuma, M. and Hearing, Jr. V. J. (1997). Mutational analysis of copper binding by human tyrosinase. *J. Invest. Dermatol*., *109*, 207-212.

[149] Lerch, K.. (1983). *Neurospora* tyrosinase: structural, spectroscopic and catalytic properties. *Mol. Cell. Biochem*., *52*, 125-138.

[150] Katz, E., Thompson, J. C., and Hopwood, A. D. (1983). Cloning and expression of the tyrosinase gene from *Streptomyces antibiotics* in *Streptomyces lividans. J. Gen. Microbiol*., *129*, 2703-2714.

[151] Lippard, S. J., and Berg, J. M. (1994). Electron paramagnetic resonance (EPR) spectroscopy. In *Principles of Bioinorganic Chemistry*, (pp. 84-88). University Science Books, California.

[152] van Gelder, C. W., Flurkey, W. H., and Wichers, H. J. (1997). Sequence and structural features of plant and fungal tyrosinases. *Phytochemistry*, *45*, 1309-1323.

[153]) Seo, S. Y., Sharma, V. K., and Sharma, N. (2003). Mushroom tyrosinase: recent prospects. *J. Agric. Food Chem*., *51*, 2837-2853.

[154] Espín, J. C., van Leeuwen, J., and Wichers, H. J. (1999). Kinetic study of the activation process of a latent mushroom (*Agaricus bisporus*) tyrosinase by serine protease. *J. Agric. Food Chem*., *47*, 3509-3517.

[155] Espín, J. C., and Wichers, H. J. (1999). Activation of a latent mushroom (*Agaricus bisporus*) tyrosinase isoform by sodium dodecyl sulfate (SDS). Kinetics properties of the SDS-activated isoform. *J. Agric. Food Chem*., *47*, 3518-3525.

[156] Wittbjer, A., Odh, G., Rosengren, A. M., Rosengren, E., and Rorsman, H. (1989). Isolation of soluble tyrosinase from human melanoma cells. *Acta Derm. Venereol*. *69*, 125-131.

[157] Wittenberg, C., and Triplett, E. L. (1985). A detergent-activated tyrosinase from *Xenopus laevis*. I. Purification and partial characterization. *J. Biol. Chem*., *260*, 12535-12541.

[158] Penafiel, R., Galindo, J. D., Pedreno, E., and Lozano, J. A. (1982). The process for the activation of frog epidermis pro-tyrosinase. *Biochem. J*., *205*, 397-404.

[159] Tatara, Y., Namba, T., Yamagata, Y., Yoshida, T., Uchida, T., and Ichishima, E. (2008). Acid activation of protyrosinase from *Aspergillus oryzae*: homo-tetrameric protyrosinase is converted to active dimmers with an essential intersubunit disulfide bond at acidic pH. *Pigment Cell Melanoma Res*., *21*, 89-96.

[160] Slavik, J. (1982). Anilinonaphthalene sulfonate as a probe of membrane composition and function. *Biochim. Biophys. Acta*, *694*, 1-25.

[161] Klabunde, T., Eicken, C., Sacchettini, J. C., and Krebs, B. (1998). Crystal structure of a plant catechol oxidase containing a dicopper center. *Natl. Struct. Biol*., *5*, 1084-1090.

[162] Imai, K., and Toyo'oka, T. (1987). Fluorometric assay of thiols with fluorobenzoxadiazoles. In Jakoby, W. (Ed.). *Methods in Enzymology: Sulfur And Sulfur Amino Acids. Vol. 143*, (pp.67-75). New York: Academic Press.

[163] Blumental, C. Z. (2004). Production of toxic metabolites in *Aspergillus niger*, *Aspergillus oryzae*, and *Trichoderma reesei*: justification of mycotoxin testing in food grade enzyme preparations derived from the three fungi. *Regul. Toxicol. Pharmacol*., *39*, 214-228.

[164] Obata, H., Ishida, H., Hata, Y., Kawato, A., Abe, Y., Akao, T., and Ichishima, E. (2004) Cloning of a novel tyrosinase-encoding gene (*melB*) from *Aspergillus oryzae* and its overexpression in solid-state culture (rice-koji). *J. Biosci. Bioeng*., 97, 400-405.

[165] Narahara, H., Koyama, Y., Yoshida, T., Pichangkura, S., Ueda, R., and Taguchi, H. (1982). Growth and enzyme production in a solid-state culture of *Aspergillus oryzae. J. Ferment. Technol*., *60*, 311-319.

[166] Hata, Y., Ishida, H., Kojima, Y., Ichikawa, E., Kawato, A., Suginami, K., and Imayassu, S. (1997). Comparison of two glucoamylases produced by *Aspergillus oryzae* in solid-state culture (koji) and in submerged culture. *J. Ferment. Bioeng*., *84*, 532-537.

[167] Hata, Y., Ishida, H., Ichikawa, E., Kawato, A., Suginami, K., and Imayasu, S. (1998). Nucleotide sequence of an alternative glucoamylase-encoding gene (*glaB*) expressed in solid-state culture of *Aspergillus oryzae. Gene*, *207*, 127-132.

[168] Tada, S., Iimura, Y., Gomi, K., Takahashi, K., Hara, S., and Yoshizawa, K. (1989). Cloning and nucleotide sequence of the genomic Taka-amylase A gene of *Aspergillus oryzae*. *Agric. Biol. Chem*., *53*, 593-399.

[169] Hata, Y., Tsuchiya, K., Kitamoto, K., Gomi,K., Kumagai, C., Tamura, G., and Hara, S. (1991). Nucleotide sequence and expression of the glucoamylase-encoding gene (*glaA*) from *Aspergillus oryzae. Gene*, *108*, 145-150.

[170] Minetoki, T., Kumagai, C., Gomi, K., Kitamoto, K., and Takahashi, K. (1998). Improvement of promoter activity by the introduction of multiple copies of the

conserved region III sequence, involved in the efficient expression of *Aspergillus oryzae* amylase-encoding gene. *Appl. Microbiol. Biotechnol*., *50*, 459-467.

[171] Ishida, H., Matsumura, K., Hata, Y., Kawado, A., Siginami, K., Abe, Y., Imayasu, S., and Ichishima, E. (2001). Establishment of hyper-protein pruduction system in submerged *Aspergillus oryzae* culture under tyrosinase-encoding gene (*melO*) promoter control. *Appl. Microbiol. Biotechnol*., *57*, 131-137.

In: Biochemistry and Histocytochemistry… ISBN: 978-1-60876-283-5
Editors: S. Fuchs, M. Auer, pp. 273-297 © 2010 Nova Science Publishers, Inc.

Chapter 11

EXTRACELLULAR PROTEASES OF ENTOMOPATHOGENIC FUNGI

Lóránt Hatvani, László Kredics, Sándor Kocsubé, László Manczinger, Csaba Vágvölgyi, Zsuzsanna Antal
Department of Microbiology, Faculty of Science and Informatics, University of Szeged, Közép fasor 52., H-6726 Szeged, Hungary

ABSTRACT

During the infection of entomopathogenic fungi, extracellular hydrolytic enzymes are important for the degradation of the insect cuticle, facilitating penetration and providing nutrients for further growth. A common feature between different insect pathogenic fungi is the involvement of extracellular proteolytic enzymes in these processes.

Regarding proteases, the most extensively studied entomopathogenic fungal genera are *Metarhizium* and *Beauveria*. The majority of the protease enzymes described from these genera belong to the family of serine proteases, however, the expression of metalloproteases and aminopeptidases under biocontrol-related conditions was also demonstrated. Detailed knowledge on protease genes and enzymes involved in fungal biological control will assist further strain improvement enabling the overexpression of genes encoding effective proteases.

The aim of this chapter is to summarize the information available about the extracellular proteases of entomopathogenic fungi, focusing on *Metarhizium* and *Beauveria* species. A large number of protease enzymes have been purified, cloned and characterized from these beneficial organisms. These results will be reviewed and data about the regulation of proteases as well as their role during the biocontrol process will be discussed.

INTRODUCTION

It has been known for a long time that entomopathogenic fungi in nature cause a regular and tremendous mortality of several arthropods, including various pests in many parts of the

world, thus constituting an extremely important natural control factor (Steinhaus, 1949). Since entomopathogenic fungi are considered as natural mortality agents and environmentally safe, there is a world-wide interest in the utilization and manipulation of them for the biological control of insects and other arthropod pests. More than 750 species of insect pathogenic fungi spanning 85 genera are known so far (Hegedus and Khachatourians, 1995). Many common and important entomopathogenic fungi belong to the Hypocreales order of Ascomycota, e.g. the anamorphic phases *Beauveria*, *Metarhizium* and the sexual state *Cordyceps*; while others, e.g. *Entomophthora* and *Zoophthora* belong to the Entomophthorales order of Zygomycota. Entomopathogenic fungi attack a wide range of insects and mites, but individual fungal species and strains are more specific. While some species such as **Beauveria bassiana** appear to be generalists, others have narrow host ranges (Samson *et al.*, 1988). Entomopathogenic fungi show a great potential for controlling insects as they are able to infect through the insect cuticle and do not require to be ingested. The first step of the infection is the adhesion of fungal conidia to the host cuticle (Boucias and Pendland, 1991). Then the conidia germinate on the body surface and hyphae penetrate into the body of the insect through its cuticle by secreting hydrolytic enzymes. Death occurs 4-10 days after infection and is caused by tissue destruction and occasionally by toxins produced by the fungus. After death, the fungus frequently emerges from the insect cadaver producing conidia that can spread the infection. The most widely used entomopathogens are *M. anisopliae* and *B. bassiana*.

M. anisopliae grows naturally in soils throughout the world. Its teleomorph has not yet been discovered, although *Cordyceps taii* was shown to be the teleomorph of *M. taii*, so it seems likely that the sexual form of *M. anisopliae* will also turn out to be a *Cordyceps* species. The disease caused by the fungus is called green muscardine disease because of the green color of its spores. The fungus kills the insect within a few days. The lethal effect is very likely aided by the production of insecticidal cyclic peptides called destruxins. The cuticle of the cadaver often becomes red. The fungus has a very broad host range and as a biological insecticide it is being used to control a number of pests such as corn rootworm, white grubs (scarabs), grasshoppers, termites, thrips, etc. The fungus does not appear to infect humans or other animals, therefore it is considered safe as an insecticide. Other insect pathogenic species of the genus include *Metarhizium flavoviride*.

B. bassiana (teleomorph: *Cordyceps* (Rehner and Buckley, 2005)) occurs naturally on some plants and in soils world wide. The insect disease caused by the fungus is called white muscardine disease, because infected insect larvae eventually turn white or gray. *B. bassiana* is a dimorphic fungus: in the soil it grows as a filamentous form and produces conidia, while in the insect hemolymph it may develop through an obligatory parasitic, yeast-like hyphal body phase and multiply by budding. At the time of the insect's death, fungal cells in the hemolymph switch back to the filamentous form and colonize the remaining tissues. When conditions are favorable, the fungus grows through the softer parts of the insect body, producing the characteristic "white bloom" appearance. *B. bassiana* is a species complex, in which different isolates were earlier suspected to have a restricted host range, however, it is recently being realized that this fungus is rather a generalist with no strict host specificity (Wraight *et al.*, 2003). The extremely broad host range involves about 700 species from almost all taxonomic orders of Insecta (Li, 1988; Inglis *et al.*, 2001), including important pests as whiteflies, aphids, grasshoppers, termites, Colorado potato beetle, Mexican bean beetle, Japanese beetle, boll weevil, cereal leaf beetle, bark beetles, lygus bugs, chinch bug,

fire ants, European corn borer and codling moth. Unfortunately, natural enemies like lady beetles are also susceptible, and *B. bassiana* has even been found to infect the lungs of wild rodents and the nasal passages of humans. A possible application method that may avoid harming beneficial insects is the use of fungus-contaminated insect baits that are attractive to pest species only. Several products containing **B. bassiana** are already commercially available as microbial insecticides. In addition to infecting insects, **B. bassiana** can colonize corn plants, having the capability of living in the vascular tissue of certain corn cultivars as an endophyte, persisting throughout the season and providing significant suppression of corn borers (Wagner and Lewis, 2000). Besides *B. bassiana, B. brongniartii* is the other main insect pathogenic species of the genus.

EXTRACELLULAR PROTEASE ENZYMES AND THEIR IMPORTANCE FOR ENTOMOPATHOGENIC FUNGI

Proteases can be subdivided into two major groups: exopeptidases cleaving the peptide bond proximal to the amino or carboxy terminal of the substrate, and endopeptidases cleaving distant from the termini (Rao *et al.*, 1998). According to the functional group at the active site, proteases are further classified into four groups: serine proteases, aspartyl proteases, cysteine proteases and metalloproteases. Based on the pH optimal for their functioning, proteolytic enzymes can be characterised as alkaline, neutral or acidic proteases.

During the infection of entomopathogenic fungi, extracellular hydrolytic enzymes are important for the degradation of the insect cuticle, facilitating penetration and providing nutrients for further growth. Like most fungal pathogens, *Metarhizium* and *Beauveria* use a combination of enzymes and mechanical force to penetrate the host cuticle and access the nutrient-rich hemolymph. Studies on the induction of extracellular cuticle-degrading enzymes revealed that proteases and esterases are produced first, while chitinase and lipase activities appear substantially later than enzymes of the proteolytic complex (St. Leger *et al.*, 1986). The structure of insect cuticle, where cuticle proteins surround chitin fibrils (Blackwell and Weih, 1980) suggests the importance of proteases during penetration.

PURIFICATION AND CHARACTERIZATION OF PROTEASES FROM ENTOMOPATHOGENIC FUNGI

Several extracellular proteases have been purified and characterized from entomopathogenic fungi. Molecular weights, isoelectric points and specific inhibitors of some of these enzymes are summarized in Table 1. The majority of them belong to the family of serine proteases.

St Leger *et al.* (1987b) characterized two subtilisin-like proteases (chymoelastases) and three trypsin-like proteases from *M. anisopliae*. A subtilisin-like protease (Pr1; pI=10.3, Mw=25 kDa) and a trypsin-like protease (Pr2; pI=4.42, Mw=28.5 kDa) were purified to homogeneity. Inhibition studies have revealed that both enzymes possess essential Ser and His residues in the active site. Pr1 exhibited higher activity to locust cuticle than Pr2 and it showed activity to elastin as well.

Table 1. Properties of extracellular proteases purified from entomopathogenic fungi

Organism	Name of protease	Type of protease	Molecular weight (kDa)	Isoelectric point	Inhibitors	Reference
M. anisopliae	Pr1 isoforms	subtilisin-like serine	28.5-30.2	9.0-10.2	tetra-butyl-oxycarbonyl-Gly-Leu-Phe-chloromethyl ketone	St. Leger *et al.* (1994a)
	Pr2 isoforms	trypsin-like serine	27-30	4.4-5.2	PMSF	St. Leger *et al.* (1994a, 1996a)
	Pr4	trypsin-like cysteine	26.7	4.6	iodoacetic acid, *N*-ethylmaleimide, pCMB, DTNB, DEPC, TLCK, protein inhibitors from soya bean and chicken ovoinhibitor	Cole *et al.* (1993)
	M. anisopliae thermolysin	thermolysin-like metallo	43	7.3	1,10-phenanthroline, phosphoramidon	St. Leger *et al.* (1994a)
	M. anisopliae carboxipeptidase	carboxypeptidase	30	9.97	DIFP, 1,10-phenan-throline, potato carboxypeptidase inhibitor	St. Leger *et al.* (1994b)
	MAP-21	trypsin-like serine	27	7.6	PMSF, TLCK, leupeptin, antipain	Pei *et al.* (2000)
B. bassiana	Pr1	subtilisin-like serine	35	10	PMSF	Bidochka & Khachatourians (1987)
	BBP	chymotrypsin-like serine	34.5	7.5	PMSF, chymostatin	Urtz & Rice (2000)
	bassiasin I	serine	32	9.5	PMSF, DIFP	Ko *et al.* (1997)

Table 1. (Continued)

Organism	Name of protease	Type of protease	Molecular weight (kDa)	Isoelectric point	Inhibitors	Reference
B. brongniartii	Ca^{2+}-dependent protease	alkaline	27	8.0	E-64	Erlacher *et al.* (2006)

DEPC: diethyl pyrocarbonate; DIFP: diisopropyl fluorophosphate; DTNB: 5,5'-dithiobisnitrobenzoic acid; pCMB: p-chloromercuribenzoate; PMSF: phenyl-methylsulfonyl fluoride; TLCK: N-tosyl-L-lysine chloromethylketone.

It occurred to have a broad primary specificity toward amino acids with hydrophobic side groups in synthetic ester and amide substrates. Pr2 exhibited rapid hydrolytic activity to casein and substrates containing Arg or Lys, while little or no activity was shown to cuticle, elastin, or substrates for chymotrypsin and elastase. The relation between Pr2 and trypsin was confirmed by the use of specific inhibitors.

A comparative study has also been performed on proteases of the entomopathogenic fungi *M. anisopliae*, *B. bassiana*, *V. lecanii*, *Nomuraea rileyi* and *Aschersonia aleyrodis* (St. Leger *et al.*, 1987a). Nine examined isolates were able to produce basic chymoelastases (pI>7.0) possessing extended binding sites, containing at least four or five subsites, with preference for hydrophobic residues at the primary binding site. Most isolates were found to produce additional acidic enzymes showing similar specificities to ester and amide substrates, but they did not have any activity against elastin. Both acidic and basic enzymes hydrolyzed high protein azure or locust cuticle, and inhibition studies revealed the involvement of essential Ser and His residues in their function. Although the catalytic properties of the enzymes were shown to be similar, antibodies generated against a *Metarhizium* chymoelastase cross-reacted only with enzymes of 2 out of 4 *Metarhizium* isolates, while no cross-reaction was observed with the proteases of other species. Two *Metarhizium* isolates were found to produce a third class of proteases, which hydrolyzed *N*-benzoyl-AA-AA-Arg-*p*NA substrates (AA: various amino acids). Peptidases with similar catalytic activity were produced also by other isolates but they were specific for *N*-benzoyl-Phe-Val-Arg-*p*NA and exhibited less sensitivity to trypsin inhibitors (St. Leger *et al.*, 1987a).

St. Leger *et al.* (1994a) separated and characterized proteases of *M. anisopliae* that are produced during growth on cockroach cuticle. Based on their substrate specificity and inhibition patterns they were identified as Pr1 subtilisin-like proteases (four isoforms), Pr2 trypsin-like serine proteases (two major and two minor isoforms) and a thermolysin-like metalloprotease. The four Pr1 components with isoelectric points of 10.2 (Mw=30.2 kDa), 9.8 (Mw=28.5 kDa), 9.3 (Mw=29.5 kDa), and 9.0 (Mw=31.5 kDa) could be separated by preparative isoelectric focusing. All isoforms were shown to hydrolyze a range of solubilized cuticle proteins favoring those with high molecular weight. The metalloprotease was active against the Pr1 substrate *N*-succinyl-Ala-Ala-Pro-Phe-7-amino-4-coumarin trifluoromethyl, however, it was found to be different from the Pr1 isoforms in exhibiting sensitivity to 1,10-phenanthroline and phosphoramidon. The two major isoforms of Pr2 with pI of 4.4 and 4.9, and molecular masses of 30 and 27 kDa, respectively, were also isolated (St. Leger *et al.*, 1996b). Both Pr2 isoforms were found to cleave primarily at the carboxyl sides of positively charged amino acids favoring Arg, while the Pr2 isoform with pI=4.4 also showed significant activity against Lys, but it exhibited low activity against insoluble proteins in *Manduca sexta* cuticle as compared to the subtilisin-like protease (Pr1) of the fungus. However, it was shown to degrade most solubilized cuticle proteins, favoring basic ones with high molecular weight.

Pei *et al.* (2000) purified MAP-21, a further cuticle-degrading serine protease from *M. anisopliae*. Fungal cultures were induced by minimal medium supplemented with *Cicada* exuviae, colloidal chitin, shrimp cuticle, maggot cuticle, horsefly cuticle and silkworm *Chrysalis* cuticle. The recognition site of the protease occurred to be Arg. Studies with different protease inhibitors have revealed that MAP-21 is a trypsin-like protease.

The purification and partial characterization of a novel trypsin-like cysteine protease, Pr4 from *M. anisopliae* was reported by Cole *et al.* (1993). The enzyme, with an isoelectric point of 4.6 and a molecular mass of 26.7 kDa, exhibited trypsin-like specificity, but according to

the results of inhibition and activation studies, it is suggested to belong to the cysteine protease family, and as such it is the first fungal protease which has been found of this type.

A carboxypeptidase produced by *M. anisopliae* during growth on cockroach cuticle was also purified (St. Leger *et al.*, 1994b). Diisopropyl fluorophosphate (DIFP) could inhibit the carboxypeptidase, which suggests the contribution of a Ser residue to the catalytic activity. However, the enzyme was shown to be different from most serine carboxypeptidases as it was inhibited by the metal chelator 1,10-phenanthroline. Furthermore, it had a lower molecular weight, basic isoelectric point and a neutral pH optimum (pH 6.8). These properties are similar to those of some metalloproteases but this enzyme cannot be inhibited by Cd^{2+}; and neither Zn^{2+} nor Co^{2+} is able to restore the decrease in activity caused by phenanthroline. The *N*-terminal sequence (22 residues) of the enzyme showed no similarity to other protein sequences, furthermore, the *M. anisopliae* enzyme could be effectively inhibited by potato carboxypeptidase inhibitor, which is not characteristic for the fungal carboxypeptidases described so far. The enzyme possesses primary specificity toward a wide range of amino acids with hydrophobic side groups in a series of *N*-blocked dipeptides, but it can hydrolyze substrates containing Phe the most rapidly.

Qazi and Khachatourians (2007) reported proteases with gelatinase activity released by hydrated conidia of *M. anisopliae*: inhibition and activation studies revealed the presence of various spore-associated metalloprotease isozymes.

The biochemical features of the subtilisin-like serine protease Pr1 was also investigated in *B. bassiana* (Bidochka and Khachatourians, 1987). The enzyme had an optimum activity at pH 8.5 and 37°C and was rapidly inactivated at 50°C. The activity of *B. bassiana* Pr1 was that of an endopeptidase which hydrolyzed elastin, casein and gelatin but was much less active on bovine serum albumin (BSA) and collagen. No trypsin-like activity was detected. Dithiothreitol, a protective agent of sulfhydryl groups had some stabilizing effect on Pr1 against heat denaturation conditions. However, since iodoacetamide did not inhibit protease activity, the sulfhydryl groups can not be located in the active site. *B. bassiana* Pr1 differs from *M. anisopliae* Pr1 in having a lower pI and in preferring Ala over bulky hydrophobic groups at the P2 and P3 positions in the substrate (St. Leger *et al.*, 1987b).

An extracellular chymotrypsin-like serine protease designated as BBP (*B. bassiana* protease) was purified from a *B. bassiana* isolate by Urtz and Rice (2000). The protease was stable at 25 ºC and had an alkaline pH optimum (7.5-9.5). BBP showed a lower pI than Pr1 and was 0.5 kDa smaller. The two proteases also exhibited differences in substrate specificity with Prl being most active against *N*-succinyl-Ala-Ala-Pro-Phe-*p*NA, and BBP being most active against MeO-succinyl-Ala-Ala-Pro-Met-*p*NA. Chrzanowska *et al*. (2001) purified two chymotrypsin-like serine proteinases from the supernatant of *B. bassiana* culture grown in the presence of ground larvae of *Apis mellifera* (Proteinase I) or porcine blood plasma (Proteinase II). The purified enzymes had a molecular weight of about 32 kDa and were capable of hydrolyzing casein, hide powder azure and azocoll. Both proteinases hydrolyzed *N*-succinyl-Ala-Ala-Pro-Phe-*p*NA. Another extracellular serine protease called bassiasin I was purified from the culture filtrate of *B. bassiana* by Ko *et al.* (1997). The enzyme could be characterized with a pH optimum of 10.5 and was stable over pH 5.0-11.0.

An alkaline Ca^{2+}-dependent protease was purified from *B. brongniartii*, the other main insect pathogenic *Beauveria* species, by Erlacher *et al.* (2006). The enzyme hydrolyzed the chromogenic substrates *N*-succinyl-Ala-Ala-Pro-Phe-*p*NA and *N*-succinyl-Ala-Ala-Pro-Leu-*p*NA. Both of these substrates are specific for serine proteases which is in contrast to the fact

that the enzyme was slightly inhibited by the cysteine protease inhibitor E-64. The enzyme showed little effects against various other protease inhibitors. Metal ions (especially Ca^{2+} and Mg^{2+}) and organic solvents (e.g. isopropanol, ethanol, methanol, dimethyl sulfoxide) were found to enhance the stability of the protease. The enzyme preferentially hydrolyzed wool cuticle scales and was therefore suggested to have potential for the antishrinking pre-treatment of wool fabrics.

CLONING OF EXTRACELLULAR PROTEASE ENCODING GENES FROM ENTOMOPATHOGENIC FUNGI

Since the beginning of the 1990s, several genes encoding extracellular protease enzymes have been cloned from mycoinsecticides. Currently, the expressed sequence tags (ESTs, mRNA populations transcribed under specific conditions and cloned as cDNAs), are proving very useful for large-scale identification of active fungal proteases (Screen and St. Leger, 2000; Bagga *et al.*, 2004). Table 2 provides an overview about a series of extracellular protease encoding genes known from mycoinsecticides with biocontrol potential.

St. Leger *et al.* (1992) reported the isolation and characterization of a cDNA clone of the protease Pr1 of *Metarhizium anisopliae*. Pr1 was found to be synthesized as a large precursor (40.3 kDa) containing a signal peptide, a propeptide, and the mature protein was predicted to have a molecular weight of 28.6 kDa. The primary structure of Pr1 showed high similarity to members of the subtilisin subclass of serine endopeptidases. The Ser, His and Asp components of the active site in subtilisins were found to be preserved in Pr1. Additional positively charged residues on the surface of the Pr1 molecule are supposed to facilitate electrostatic binding to cuticle proteins, which is necessary for activity. In a recent study, Liu *et al.* (2007) performed the structural modeling of Pr1 in comparison with proteinase K and two cuticle-degrading proteases from nematophagous fungi: Ver112 of *Lecanicillium psalliotae* and VCP1 of *Pochonia chlamydospora*. The predicted models of the three cuticle-degrading proteases presented an essentially identical backbone topology and similar geometric properties.

Reverse transcription differential display PCR was used by Joshi *et al.* (1997) to identify genes expressed specifically in *M. anisopliae* during contact with host cuticle. By the use of a homology-based subtilisin-like protease primer, a yet unsuspected, differentially expressed subtilisin-like protease gene (*pr1B*) was identified. The gene of the unique subtilisin was cloned and the deduced amino acid sequence exhibited 54% similarity to Pr1A. The molecular mass of the putative mature protein is approximately 28.7 kDa with an isoelectric point of 8.05. In spite of the sequence similarities, Pr1B contains several substitutions in the highly conserved regions, including the active sites of subtilisins. These changes were supposed to result in differences in the catalytic activity of the enzyme.

Bidochka and Melzer (2000) investigated three isoforms of subtilisin-like proteases (Pr1A, Pr1B, and Pr1C) in certain strains of *M. anisopliae* by restriction fragment length polymorphism (RFLP) analysis. No RFLP variation was detected among *pr1* genes derived from isolates belonging to the same genetically related group. Between isolates from different geographical locations, the greatest variation in RFLP patterns was found in the case of *pr1A*, while as for *pr1B* and *pr1C*, variation was almost exclusively detected at an *Eco*RI site.

Table 2. Characteristics of extracellular protease encoding genes from entomopathogenic fungi

Organism	Type of protease	Gene	Length of ORF (bp)	Length of deduced amino acid sequence	Length of putative signal peptide	Predicted properties of the protein			Reference
						Length	Calculated Mw (kDa)	Calculated pI	
M. anisopliae	subtilisin-like serine	*pr1A-G* *pr1 I-K*	1128-1347	332-533 aa	14-22 aa	NR	26.3-57.0	5.20-8.53	Joshi *et al.* (1997), Bagga *et al.* (2004), Zhang *et al.* (2008b)
	chymotrypsin-like serine	*chy1*	1121	374 aa	19 aa	188 aa	18.5	8.29	Screen & St. Leger (2000)
B. bassiana	subtilisin-like serine	*pr1*	1080	360 aa	18 aa	261 aa	26.8	NR	Joshi *et al.* (1995)
	serine	*bsn1*	1137	379 aa	18 aa	206 aa	28.2	NR	Kim *et al.* (1999)
	tripeptidyl peptidase	*BbTPP*	1731	577 aa	19 aa	558 aa	61.0	NR	Tartar & Boucias (2004)
B. brongniartii	subtilisin-like serine	*pr1*	1140	380 aa	18 aa	250 aa	39.1*	8.0*	Sheng *et al.* (2006)

NR: not reported, *: calculated from the entire length of the protein.

The greatest difference in RFLP patterns at all *pr1* genes was observed in the case of *M. anisopliae* var. *majus* strain 473 and a *M. flavoviride* isolate when compared with other *M. anisopliae* strains. The *pr1* genes were concluded to represent a gene family of subtilisin-like proteases and *pr1A* was supposed to encode for the ancestral enzyme which was subsequently duplicated and rearranged within the genome.

Further, more detailed characterization of the diversity of *M. anisopliae* subtilisins was performed by Bagga *et al.* (2004). Expressed sequence tag (EST) analyses revealed that strain 2575 of *M. anisopliae* sf. *anisopliae*, an isolate possessing multiple hosts, expressed 11 different subtilisins during growth on insect cuticle. Ten of their orthologs were amplified by PCR from strain 820 with multiple hosts and seven from the locust pathogenic strain 324 of *M. anisopliae* sf. *acridum*. *M. anisopliae* subtilisins were grouped into four clusters according to analyses based on sequence similarities and exon-intron structure: a class I ("bacterial") subtilisin (Pr1C), and three clusters of protease K-like class II subtilisins: extracellular subfamily 1 (Pr1A, Pr1B, Pr1G, Pr1I and Pr1K), extracellular subfamily 2 (Pr1D, Pr1E, Pr1F and Pr1J) and an intracellular subtilisin (Pr1H). The evolution of subtilisins has yielded a range of isoforms in *M. anisopliae*, which is supposed to be related to the pathogenicity of the fungus. Pr1A was reported to be the predominant protein produced during the degradation of insect cuticles (St. Leger *et al.*, 1989) and EST analyses revealed the tenfold abundance of Pr1A in comparison with the second most highly expressed subtilisin (Pr1J). This suggests that the other Pr1 subtilisins play a minor role in cuticle degradation. Distinct subtilisins might play different roles in pathogenesis, enhance adaptability and host range, or have different functions in survival in various ecological habitats outside the host.

Recently, a *pr1A* gene was identified and cloned from the locust specific *M. anisopliae* strain CQMa102 by Zhang *et al.* (2008b). According to the results of enzyme assays and the analysis of the predicted amino acid sequence, Pr1A belongs to the subtilisin-like serine protease family, showing significant homology (85–99%) with *M. anisopliae* subtilisin-like serine proteases, and it was found to be the most closely related to the subtilisin Pr1A from *M. anisopliae* var. *acridum* strain FI-985 (over 95% identity). The 1.319 bp cDNA sequence contained a single, 1.170 bp open reading frame extending from the postulated initiator methionine at position 1 to the stop codon, TAA, at position 1171. The cDNA encoded a putative 390 amino acid polypeptide, with a predicted conserved catalytic triad of serine proteases: Asp148 (D), His179 (H), and Ser334 (S). Analysis of the *N*-terminal region of the primary translation product suggested the presence of a signal peptide. The calculated molecular mass of 40.693 Da is in accordance with the estimated 41.000 Da for the primary translation product of Pr1A. The calculated molecular mass of the mature protease (26.297 Da) is in agreement with that of the native protein from CQMa102. Verifying its protease activity, the CQMa102 Pr1A protein was successfully expressed in *Pichia pastoris*. Cuticle degrading activity assays have revealed that the Pr1A gene cloned from *M. anisopliae* strain CQMa102 possesses cuticle-degrading function, suggesting that it might be a potential tool for the development of engineered biopesticides.

The gene of the Pr2 trypsin-like serine protease protein of *M. anisopliae* was also isolated (Smithson *et al.*, 1995). Sequence analysis and RT-PCR have revealed that the gene contains two introns with the length of 94 and 40 bp. The deduced protein consists of 254 amino acids, possesses a putative signal sequence suggesting its transport into the endoplasmic reticulum and it is supposed to undergo a second proteolytic processing step at its *N*-terminus resulting

in the mature enzyme, which exhibits high level of homology with other serine proteases of the trypsin subclass.

Screen and St. Leger (2000) reported the cloning of a chymotrypsin gene, *chy1* from *M. anisopliae*. The protein was identified by expressed sequence tag (EST) analysis and sequence comparisons revealed the closest relationship to *Streptomyces griseus* protease C (55% identity, not including the unique *C*-terminal region of SGPC). Therefore *chy1* was suggested to have arisen by lateral gene transfer from an actinomycete bacterium.

The investigation of the cDNA of *B. bassiana* Pr1 has revealed that the protein is synthesized as a large precursor (M_w=37460 Da) containing a signal peptide, a propeptide and the mature protein (Joshi *et al.*, 1995). The predicted amino acid sequence shows 53.6% identity with *M. anisopliae* Pr1. Both *B. bassiana* and *M. anisopliae* Pr1 sequences contain a hydrophobic *N*-terminal sequence of 18 amino acids resembling signal sequences for excreted proteins. The format includes a charged residue (Arg in *B. bassiana* and His in *M. anisopliae*), a core of eight hydrophobic residues and a helix breaking residue (Pro) four residues before the signal peptide cleavage site (Ala-Pro-Ala in *M. anisopliae* Pr1 and Ala-Pro-Val in *B. bassiana* Pr1). The sequences of *B. bassiana* and *M. anisopliae* Pr1 mature proteases show extensive regions of conserved amino acids with intervening divergent sequences. The highest similarities were found in regions previously identified in subtilisin as the active site and internal helices (Joshi *et al.*, 1995).

The genomic DNA encoding Pr1 in the other main insect pathogenic *Beauveria* species, *B. brongniartii* contains three introns that are 64, 57-, and 61-bp long (Sheng *et al.*, 2006). The deduced amino-acid sequence of the protein shows similarity to that of Pr1 from *M. anisopliae* (67%), and Pr1 from *B. bassiana* (76%). The calculated molecular mass of the Pr1 precursor is 39121 Da and its pI is 8.0. The protein has three active sites characteristic of subtilisin-like serine proteases.

The comparison of the cDNA and genomic sequences revealed that the coding regions of bassiasin I are interrupted by 3 introns which are 69, 62 and 68 bp long (Kim *et al.*, 1999). The calculated molecular mass of the bassiasin I precursor was 38863 Da, while that of the mature protein proved to be 28222 Da. The protein sequence of the bassiasin I precursor showed high homology to members of the subtilisin family of serine proteases. The mature bassiasin I protein shows 78.2% and 73.2% identity to *B. bassiana* Pr1 (Joshi *et al.*, 1995) and *M. anisopliae* Pr1 (St. Leger *et al.*, 1992) respectively. When compared to *B. bassiana* Pr1, the signal peptide and the prosequence were found to be highly homologous (99%), but the *C*-terminal sequences proved to be very different.

In the study of the transcriptome of *B. bassiana* cells grown in infected *M. sexta* larvae in yeast-like hyphal body phase, two protease genes were detected by Tartar and Boucias (2004). One of these proteases was shown to be upregulated during infection and was identified as a tripeptidyl peptidase (TPP). The protein sequence is similar to a sequence identified as a tripeptidyl peptidase A from *Aspergillus oryzae* and exhibits similarity to serine proteases. Molecular weight estimation indicated that the enzyme is ca. 63 kDa when the signal peptide is included, and ca. 61 kDa when the signal peptide is removed.

REGULATION OF PROTEASES PRODUCED BY ENTOMOPATHOGENIC FUNGI

The specific induction of *M. anisopliae* Pr1 was examined by Paterson *et al.* (1994a). The enzyme occurred to be induced specifically by insect cuticle but not by any other soluble or insoluble proteinaceous substrates. The production of Pr1 was not increased significantly following the addition of elastin or collagen to derepressed mycelium starved for carbon and nitrogen, and soluble proteins (BSA and gelatin) rapidly and entirely repressed the enzyme. Carbohydrate polymers like cellulose and xylan resulted in derepressed basal levels of Pr1, while approximately 10-fold increase in the enzyme production was observed following the addition of locust cuticle as compared to that of derepressed mycelium. Expressing enzyme activity per dry mycelial weight revealed that Pr1 production in cultures grown on cuticle increased approximately five- and ninefold after 12 and 24 h, respectively, in comparison with elastin-grown cultures. This finding suggests that the enhanced Pr1 production was induced by a component of the insect cuticle.

The inducibility of Pr1 by proteinaceous compounds released enzymatically from insect cuticle was also studied in *M. anisopliae* (Paterson *et al.*, 1994b). In the case of *Schistocerca gregaria* cuticle treated with KOH in order to remove proteins, no induction of Pr1 production was observed, while cuticle treated with chloroform or ether to remove lipids was able to induce enzyme production. Digestion of cuticle with Pr1 or the trypsin-like protease Pr2 of *M. anisopliae* resulted in peptides mainly in the range of 150-2000 Da. The addition of these peptides at 3 μg Ala equivalents ml^{-1} led to the induction of Pr1 production to a level (75%) similar to that observed in the case of untreated insect cuticle. The ability of various amino acids and peptides abundant in insect cuticular protein (Ala, Gly, Ala-Ala, Ala-Ala-Ala, Ala-Pro and Pro-Ala) to induce Pr1 was tested but none of them was found to increase enzyme production in the levels observed with cuticle, or peptides enzymatically released from the cuticle.

Screen *et al.* (1997) examined the promoter region of *pr1*. Sequencing revealed the presence of putative CreA- and AreA-binding sites. A GST-CreA fusion protein from *A. nidulans* was found to be able to bind to two of the three putative CreA sites confirming their potential role in carbon-catabolite repression. Using a PCR-based method, the *M. anisopliae crr1* (carbon response regulator 1) gene was identified. It was found to encode a protein with significant homology to the CreA proteins of *A. nidulans*, *A. niger*, *T. reesei* and *T. harzianum*. The *crr1* gene was shown to complement the *creA*204 mutation of *A. nidulans*, in that CRR1 protein is able to substitute for *A. nidulans* CreA in the repression of alcohol dehydrogenase I. This confirms that *crr1* encodes a carbon-response regulator protein which is at least partially a functional homologue of the *A. nidulans* CreA. These findings support that the expression of *pr1* in *M. anisopliae* is controlled by carbon-catabolite repression.

The purification and characterization of BmSI-7 and BmSI-6, two subtilisin inhibitors from *Boophilus microplus* (BmSI) was reported by Sasaki *et al*. (2008). The inhibitors were found to exhibit significant inhibition on the activity of purified Pr1 proteases from *M. anisopliae*.

The regulation of the trypsin-like protease Pr2 of *M. anisopliae* was examined by Paterson *et al.* (1993). Three insoluble protein sources, insect cuticle, elastin and collagen, as well as two soluble proteins, gelatine and especially bovine serum albumin (BSA) were found

to induce the enzyme, while cellulose and xylan showed no stimulatory effect. Basal levels of Pr2 were detected after 8 h of carbon and nitrogen starvation but only after 16 h among nitrogen or carbon starvation conditions. A strong repression by nitrogen was observed in the presence of a protein source, while carbon had little effect. Sulphur was shown to have no effect on Pr2 production.

St. Leger *et al.* (1998) examined the influence of ambient pH on the production and activity of various extracellular enzymes in *M. anisopliae*, including subtilisin-like proteases (Pr1A and Pr1B), trypsin-like proteases (Pr2), metalloproteases, aspartyl proteases and aminopeptidase. The maximum enzyme activities were shown to occur at culture pH close to the pH optimum of the certain enzymes irrespective of whether the medium contained an inductive cuticle substrate. Accordingly, the highest levels of aspartyl protease, metalloproteases, aminopeptidase, Pr2 and Pr1 isoforms were observed at culture pHs ranging between 3 and 4, between 6 and 8, at pH 7, between pH 6 and 8, and at pH 8, respectively. Northern analysis confirmed that the pH of the medium played a key role in the regulation of gene expression: expression of both subtilisin genes and of Pr2 was turned off among acidic conditions. The pH of infected cuticle was found to range from about 6.3 to 7.7 during fungal penetration. In accordance with pH regulation of enzyme production, serine and metalloproteases were produced *in situ* during infection, but no production of aspartyl proteases was detected, suggesting that this type of protease does not play a role in the degradation of cuticle components. *M. anisopliae* was shown to be able to grow over a wide pH range (pH 2.5 to 10.5) (Hallsworth and Magan, 1996). However, cytosolic pH was found to be stable between pH 5 and 8, indicating an efficient regulation of cytosolic pH and adaptation to survive in various environments. In order to facilitate nutritional versatility over a wide range of growth conditions, *M. anisopliae* was found to produce various types of proteases only at the pH values where they function effectively. In addition, a concerted action of pH and induction by cuticle on enzyme production was also shown. Pr1 production was found to be derepressed when the ambient pH was alkaline, even in the absence of cuticle. However, the presence of cuticle increased Pr1 production threefold at pH 8. The concerted action of induction by host cuticle and pH may represent a mechanism whereby environmental signals induce the production of certain virulence factors. The ability of *M. anisopliae* of altering ambient pH was also reported and the influence of changes in pH on the production of proteases was investigated (St. Leger *et al.*, 1999). The wild-type strain of *M. anisopliae* underwent mutagenesis with ethyl methanesulphonate, resulting in oxalic acid hyper- (Acid+) and hypoproducer (Acid-) mutants. Wild-type and Acid+ strains grew almost as well at pH 8 as at pH 6, while Acid- mutants showed reduced growth at pH 8, indicating that acid production is required for the ability to grow at higher pH values. Degradation of proteins was tested by measuring clearing zones in pH indicator medium containing skimmed milk. Acid- mutants exhibited a level of protein degradation similar to that of the wild-type strain, while, in spite of growth, a decrease in protease production was observed along with acidification of the medium in Acid+ mutants. However, in buffered liquid culture containing insect cuticle they exhibited levels of protease activity very similar to that of the wild-type strain, demonstrating that the regulation of protease production was not altered in the mutants. A significant increase in pH was observed in the case of wild-type and Acid- mutants, which was found to be the consequence of ammonia production. This resulted in the production of subtilisin proteases, whose activities occur only at basic pH. In accordance with this, protease production by Acid+ mutants of *M. anisopliae* was significantly inhibited by the acidification

of the medium. These findings suggest that alkalinization by ammonia production is an adaptive strategy via facilitating the utilization of proteinaceous nutrients.

Shah *et al.* (2005) studied the production of virulent conidia by *M. anisopliae* in different media, such as susceptible insect hosts, 1% yeast extract, 2% peptone, osmotic stress medium and CN 10:1 medium. Among pathogenicity-related factors, virulent conidia typically exhibited high levels of spore bound Pr1 protein. Using real time PCR, virulent conidia from insects were shown to contain significantly higher levels of *pr1A* transcripts than inocula from artificial media. Among the artificial media studied, yeast extract medium occurred to yield in the most virulent conidia, however, the levels of *pr1A* transcripts were significantly lower than those in insect-derived conidia. Since virulent conidia were produced in all types of media examined, even among starvation conditions where growth and sporulation was weak, it has been concluded that the inoculum is virulent regardless to the original growing medium or insect host. Starvation conditions were thus supposed to result in the derepression of *pr1*, therefore the production of this virulence-related protease is enhanced.

Small and Bidochka (2005) isolated genes expressed during mature conidial production under nutrient-deprived conditions in *M. anisopliae* by suppression subtractive hybridization, and their expression was confirmed by reverse-transcription polymerase chain reaction (RT-PCR) analysis as well. One of the seven conidiation-associated genes was found to encode for the extracellular subtilisin-like protease Pr1. RT-PCR analysis revealed that Pr1 is up-regulated in infected *Galleria mellonella* larvae also at the final stages of the infection, when mycelia emerge and produce conidia on the surface of the dead host.

Fang and Bidochka (2006) applied RT-PCR to determine the relative expression level of *pr1* during the pathogenesis of *M. anisopliae*. No expression of *pr1* was observed when the fungus was grown in YPD (0.2 % yeast extract, 1 % peptone, 2 % dextrose) broth or on YPD agar and in the early stages of infection, but its transcripts were detected in insect cadavers as fungal mycelia emerged. *pr1* was expressed during conidiogenesis and late stages of pathogenesis, supporting the findings of Small and Bidochka (2005). The failure to detect *pr1* expression in the early phases of infection might be a consequence of the low fungal biomass available from these stages.

The effects of different carbon sources, including the cuticle of *B. microplus* on the production of hydrolytic enzymes by *M. anisopliae* was examined by Krieger de Moraes *et al.* (2003). Glucose or *N*-acetylglucosamine (GlcNac) were used as carbon sources, and complex substrates containing chitin, tick cuticle, the combination of tick cuticle or chitin supplemented with different GlcNac concentrations, as well as tick cuticle or chitin plus glucose were also tested. Proteases were produced in all media tested but the levels of activities varied. High subtilisin activities were observed in cultures supplemented with tick cuticle or chitin plus 1.0% GlcNAc, and lower levels were detected in cultures grown on glucose, 1.0% GlcNAc or tick cuticle plus 0.2% GlcNAc. The highest level of trypsin activity was found in medium with chitin added at 0.8%.

Mohanty *et al.* (2008) studied the efficacy of the virulent *M. anisopliae* strain 892 - isolated from *Pyrausta nubilalis* - against mosquito larvae. LC_{50} values of *M. anisopliae* 892 for *Culex quinquefasciatus, Anopheles stephensi* and *Aedes aegypti* were examined. *M. anisopliae* 892 was found to cause approximately 50% mortality of *C. quinquefasciatus* 4 days post inoculation. The production of subtilisin-like (Pr1) and trypsin-like protease (Pr2) was measured in the presence of certain inducers. Significant differences in the production of Pr1 and Pr2 were found following the addition of inducers i.e. cuticles of the three

mosquitoes. The cuticles of *C. quinquefasciatus* were found to result in the highest Pr1 activity in *M. anisopliae* 892 among derepression circumstances, as compared to the other two mosquito cuticles. The larvae of *C. quinquefasciatus* proved to be more susceptible to the spores of *M. anisopliae* 892 than those of *A. stephensi* and *A. aegypti*. The scale of induction of Pr1 in *M. anisopliae* 892 showed positive correlation, while Pr2 induction was found not to correlate with the mortality of mosquito larvae. Decreased Pr1 and Pr2 were observed when de-proteinated cuticles were added as inducers. Since mosquito vector control is an integral part of controlling malaria (WHO 1993), the above findings may contribute to these efforts.

The activicity of *M. anisopliae* carboxypeptidase described by St. Leger *et al.* (1994b) complements that of the subtilisin-like protease (Pr1). Both enzymes have been found to occur during carbon and nitrogen deprivation, suggesting that this exopeptidase exhibits a synergistic function with Pr1 in degrading peptides in order to supply amino acids during starvation and pathogenicity.

Tiago *et al.* (2002) examined the production of Pr1 and Pr2 of a wild-type strain of *M. flavoviride* being developed as a biocontrol agent against the grasshopper *Schistocerca pallens*. Both enzymes were produced in high amounts in a minimal medium supplemented with the cuticle of *S. pallens.* No Pr1 activity was observed in a minimal medium containing nitrate as a sole nitrogen source, whereas Pr2 was produced in higher amounts on defined growth substrate than on cuticle-supplemented medium. The production of Pr1 only in cuticle-containing medium indicates the need of specific components of the host cuticle as inductive agents, similarly to that observed for *M. anisopliae* by Paterson *et al.* (1994b).

Da Silva Pinto *et al.* (2002) investigated the production of Pr1 and Pr2 in several isolates of *M. flavoviride*. The fungi were grown in a mineral medium (MM) containing nitrate, and in MM supplemented with cuticle from *Rhammatocerus schistocercoides* or with casein. Pr1 activity was detected in all media tested but activities were found to be different as a consequence of the growth substrate, being about 2 to 8 times higher in MM+casein and about 4 to 20 times higher in MM+cuticle than in MM, and variability in activities was also observed among certain isolates. Pr2 was produced by all isolates but at lower levels than Pr1 and with less variability between the isolates. The natural variability detected in the production of proteases, particularly Pr1, suggests that the production of Pr1 on insect cuticle is a useful characteristic for the analysis of intraspecific variability of *M. flavoviride* isolates.

Bidochka and Khachatourians (1988a) reported that *B. bassiana* synthesizes and secretes a Pr1-like extracellular serine protease into its growth medium when an exogenous protein, gelatin serves as nitrogen and carbon source. The enzyme had maximum activity at pH 8.5 and was found to be unstable at pH levels below 5. In gelatin-containing cultures at pH 7.0, the synthesis of the protease was repressed in the presence of ammonium and glucose, glycerol, trehalose, or mannitol but not in the presence of maltose. The synthesis of B. *bassiana* Pr1 was found to be regulated by products of chitin degradation: the synthesis was repressed in gelatin medium containing GlcNAc at levels of >1.07 μmol per mg of fungal dry weight (Bidochka and Khachatourians, 1988b). At lower concentrations, protease synthesis was initiated. Free amino acids generated from the hydrolysis of gelatin did not repress protease synthesis. Similarly to *M. anisopliae*, the addition of insect cuticule caused usually a high level of subtilisin activity also in the case of *B. bassiana*. The addition of Ala, the major amino acid found in the cuticle of insects (Hackman and Goldberg, 1987) at an amount of 0.5% to the culture medium repressed subtilisin secretion in *B. bassiana* (Campos *et al.*, 2005).

The comparative analysis of gene expression patterns of a *B. bassiana* isolate grown on cuticular extracts of various insects from diverse orders as well as synthetic medium revealed that in general, the gene expression profile on cuticular extracts of insects was pretty similar (Pathan *et al.*, 2007). This shed light on the putative generalist nature of *B. bassiana* with its ability to penetrate many different insect cuticles possibly due to a rather stereotype gene expression program. Two proteases, subtilisin-like serine protease Pr1 and protease-1 (PRT-1) were identified among the differentially expressed genes. Pr1 was differentially expressed after growth of the fungus on different insect cuticles. Moreover, protease PRT1 was found to be upregulated on the cuticle of the aphid *Aphis craccivora*.

The secretion of subtilisin-like (Pr1) and trypsin-like (Pr2) proteases by *B. bassiana* during the growth either in nitrate-medium or in grasshopper-cuticle-containing medium supplemented with different amino acids were examined by Donatti *et al.* (2008). The production of Pr1 and Pr2 was enhanced by the presence of cuticle, but the production of these proteases did not seem to be coordinately expressed, since both of them were detected after 24 h of growth. The amino acid methionine is either absent or occurs at low levels in grasshopper cuticle, and it seems to play a regulatory role in Pr1 secretion, as both induction and repression seem to be dependent on the concentration of this amino acid in the culture medium. The remaining amino acids tested did not induce the protease to the levels seen with cuticle.

The production of *B. bassiana* Pr1 and Pr2 proteases were examined in media both under buffered and unbuffered conditions (Dias *et al*. 2008). In unbuffered medium supplemented with cuticle, Pr1 and Pr2 activities were detected mainly at a pH of 5.5 or higher. In buffered cultures, both protease types were produced - albeit at lower levels - by carbon and nitrogen derepression alone, indicating a substantial basal level of Pr1 and Pr2. At alkaline pH in the presence of cuticle, the production of these proteases seemed to be induced, suggesting that the culture pH influences their expression.

The production of Pr1 and Pr2 enzymes by conidia of *B. bassiana* during the initial stages of germination on aphid exuviae with or without supplementation of additional carbon and/or nitrogen compounds was investigated by Qazi and Khachatourians (2008). In 0.25 hour upon incubation of conidia, activities of Pr1 and Pr2 were observed in the culture. Addition of exogenous carbon source during the initial stages of germination resulted in higher activities of both enzymes. Conversely at 0.25 h, addition of nitrogen sources repressed the synthesis of Pr2, but not that of Pr1. This repression effects were observed only in the case of exponentially growing mycelia, indicating that the carbon/nitrogen repression occurs only when it is necessary for the *B. bassiana* infective structures to establish a nutritional relationship with the host structures.

THE ROLE OF PROTEASES DURING THE ACTION OF ENTOMOPATHOGENIC FUNGI

In *M. anisopliae,* subtilisin is reported to be intricately related to a strain's ability to penetrate, colonize and macerate insect host tissues (St. Leger *et al.*, 1996a; Bagga *et al.*, 2004). Subtilisins were found to be expressed after growth of *M. anisopliae* on different

insect cuticles but not on artificial medium (Freimoser *et al.*, 2005). A diverse regulation of subtilisins may thus be an essential part of the infection process of different insect hosts.

Pr1 of *M. anisopliae* is an important virulence determinant protease which was found to be induced by insect cuticle, derepressed under starvation condition and repressed in the presence of excess nutrients (Butt et al. 1998). St. Leger *et al*. (1988a) used either IgG antibodies against Pr1 or turkey egg white inhibitor, a potent specific inhibitor of Pr1 in order to reveal the potential relationship between Pr1 and the virulence of *M. anisopliae* towards *M. sexta*. The application of the inhibitor to *M. sexta* during infection resulted in a significantly delayed mortality. The inhibitor also caused a reduced melanization of cuticle, which phenomenon is known to be an early host response to fungal infection and invasion of the hemolymph, furthermore, the host's growth rate remained on a normal level. A delayed penetration through the cuticle was observed according to the incorporation of the antibodies or the inhibitor, however, spore viability, growth and formation of appressoria on the cuticle surface were not altered. These findings suggest that the inhibition of Pr1 reduces the scale of infection via decreasing the ability of the fungus to penetrate through the insect cuticle. The dependence of the accumulation of protein degradation products from cuticle - including ammonia - on active Pr1 was revealed by *in vitro* studies, which confirmed the major role of Pr1 in solubilizing cuticle proteins, thus making them available as nutrients for the fungus. Pr1 is concluded to act as a virulence factor by catalizing the localized destruction of cuticle proteins, which allows the rapid invasion of the susceptible host.

To improve the efficacy of mycoinsecticide agents, the gene encoding Pr1 was overexpressed in *M. anisopliae* which greatly enhanced the strain's virulence and reduced the time to kill (St. Leger *et al.*, 1996b). A range of recombinants were constructed expressing *pr1* under the transcriptional control of the constitutive glyceraldehyde 3-phosphate dehydrogenase (*gpd*) promoter from *A. nidulans*. Four strains showing wild-type levels of growth and conidiation, as well as producing large elastin clearing zones were tested for the constitutive production of Pr1 in comparison with the parental strain. Copy numbers of *prl* cDNA varied from three to six in the transformants. All strains were shown to produce Pr1 while cultivated in a medium containing cockroach cuticle, but only the transformants produced Prl during growth on GlcNAc, which was reported to repress the synthesis of Prl in the wild-type strain (St. Leger *et al.*, 1988b), indicating the expression of the heterologous promoter and synthesis and secretion of Prl. Bioassays carried out with the recombinant strains against the larvae of *M. sexta* led to a 25% reduction in time of death and reduced food consumption by 40% as compared to infections by the wild-type fungus. In larvae infected by the transformant strains, partial hydrolysis of the hemolymph proteins was observed. Western blot analysis revealed the presence of Pr1 in the hemolymph, which indicated that Pr1 was produced even after penetration through the cuticle. This finding was confirmed by the precipitation of hemolymph samples with Prl-specific antibody, since in the transgenic strains a 50-fold higher amount of Pr1 was detected then in the wild-type parent. Insects infected with the transformants were rapidly melanized, suggesting the increased function of the prophenoloxidase system of the host. The combined toxic effects of Prl and the reaction products of phenoloxidase enabled the transformant strains to express a more efficient entomopathogenic activity. The resulting insect cadavers were poor substrates for fungal sporulation, which suggests a reduced environmental persistence of the genetically engineered fungus, providing a tool for biological containment. Such genetically improved strains with increased activity might be potential candidates for biocontrol of insect pests.

The effect of *pr1* gene deficiencies on the entomopathogenic activity of *M. anisopliae* was investigated by Wang *et al.* (2002). A wild-type isolate, as well as three spontaneous *pr1A*- and *pr1B*-deficient mutants of the fungus were involved in the study. The lack of *pr1A* and *pr1B* genes in the mutants was revealed by nested PCR and radiolabelling, while they could be detected in the wild-type strain. The mutants shared the same phenotype, and molecular characterization of the isolates carried out by RAPD-PCR and sequencing of partial 28S rDNA demonstrated that they were identical genetically as well, but they exhibited morphological differences from the wild-type. Enzyme assays performed in order to determine Pr1, Pr2, elastase and non-specific protease activities revealed that Pr1 and elastase production of the mutants was significantly lower than that observed in the wild-type parent, while their Pr2 and non-specific protease activities occurred to be similar. Bioassays demonstrated that similarly to the wild-type strain, the mutants caused approximately 100% mortality on the larvae of *G. mellonella*, whereas they exhibited significantly reduced lethal activity on *Tenebrio molitor*. These findings suggest that a stable mutant strain lacking the most important *pr1* genes is still able to infect its hosts, furthermore, it is not uncommon for *M. anisopliae* to loose its virulence genes during maintenance on artificial medium.

Hu and St. Leger (2002) performed experiments with transformant derivatives of a *M. anisopliae* strain in order to test their survival among field conditions. The wild-type and the recombinant strain *gpd*-Pr1-4 (containing four copies of the *pr1A* subtilisin gene under control of the constitutive *gpd* promoter from *A. nidulans*) were transformed with a variant of *Aequorea victoria* green fluorescent protein (*gfp*) gene alone or with additional *pr1* gene under the control of the *gpd* promoter of *Cryphonectria parasitica*, resulting in derivatives GMa and GPMa, respectively. The study proved the applicability of *gfp* for monitoring biocontrol strains in field populations over time. Little dissemination of transgenic strains was observed and no evidence of transmission by nontarget insects was found. Recombinant fungi occurred to be genetically stable over 1 year under field conditions, and the application of the transgenic strains was shown not to harm the culturable indigenous fungal microflora. However, GPMa showed reduced persistence in soil as compared to GMa.

It was demonstrated with gold-labelled rabbit antiserum that Prl is produced by *M. anisopliae* during penetration of *M. sexta*, the enzyme was secreted by appressoria on the cuticle surface and found to be ultrastructurally located in the host cuticle during the early stages of penetration (Goettel *et al.* 1989). Isoforms of *M. anisopliae* Pr2 were also monitored by immunocytochemical investigation using gold-labelled rabbit antisera during penetration through the *M. sexta* cuticle (St. Leger *et al.*, 1996a). Both isoforms were found to be associated with appressoria, but they were also detected in the extracellular sheath around hyphae, on the cuticle surface, as well as in the penetrant hyphae within the cuticle, suggesting that they are necessary in the early stages of infection. The presence of the Pr2 isoforms in infection structures suggests their role in degrading extracellular proteins in synergysm with Pr1. Hydrophilic Arg-Y or Lys-Y units, the targets of Pr2 isoforms are expected to be located on the periphery of globular proteins, while in the case of Pr1 that possesses specificity for hydrophobic residues, potential substrates may be found in the interior parts of proteins. Trypsin activity is supposed to complement Pr1 via making proteins accessible for further hydrolysis, facilitating penetration and providing peptides to be utilized as nutrients. Thus Pr1 and Pr2 isoforms may represent a part of a cascade of pathogen reactions during the penetration of host cuticles.

The incubation of spores in water represents a nutritional starvation, which may occur during the field application of entomopathogenic fungi, when conidiospores are sprayed in water or as invert emulsion in oil. In aqueous supernatants, spore-associated metalloprotease isoenzymes were found to be released during the pre-germination period or swelling phase of *M. anisopliae*, and their activity was detectable up to 4 days (Qazi and Khachatourians, 2007). By releasing these metalloproteases, hydrated conidia are supposed to act as a backup system to complement Pr1.

Extracellular proteases appear to be important virulence factors also in the case of *B. bassiana* (Bidochka and Kkachatourians 1994). Subtilisin-like serine protease Pr1 of *B. bassiana* has been characterized with high activity against insect cuticule (Bidochka and Khachatourians, 1987; St. Leger *et al.*, 1987a). Proficient and deficient strains of *B. bassiana* for production of extracellular protease in liquid culture and their virulence toward *Melanoplus sanguinipes* were studied by Bidochka and Khachatourians (1990). The investigation revealed that the protease-deficient mutant strain which produced less than 10% of protease when compared to the protease-proficient strain had the highest LT_{50} (11.34 days), while the protease-proficient strain showed the lowest LT_{50} (5.71–6.80 days) against the migratory grasshopper, indicating that Pr1 facilitates the penetration through the host cuticule. Gupta *et al*. (1992) showed that proteases produced by five different strains of *B. bassiana* are maximally expressed when the fungus is grown on wax moth (*G. mellonella*) cuticle. A subsequent study revealed that a high level of Pr1-like proteases produced by *B. bassiana* appears to be related to the early onset of mortality in *G. mellonella* larvae (Gupta et al. 1994). Shimizu *et al.* (1993) demonstrated with the aid of enzyme-linked immunosorbent assay that *B. bassiana* produced a substantial amount of extracellular protease in the haemolymph of infected silkworms (*Bombyx mori*).

Pr1 was used by Zhang *et al.* (2008a) as an additive of sprays of *B. bassiana* used against adults of the aphid *Myzus persicae*. The LC_{50} value decreased with increasing Pr1 concentrations, and on days 5-7 after spraying, the LC_{50} values were reduced 1.5-2.5-fold at the concentrations of 20-100 μg ml^{-1} of Pr1. However, sprays of Pr1 aqueous solution alone had no significant effect on aphid mortality. These results confirm that the Pr1 protease enhanced fungal virulence due to acceleration of conidial germination and cuticle penetration.

In order to improve the insecticidal efficacy of *B. bassiana*, it was genetically engineered via two-step transformations with the gene *aaIT* encoding an insect-specific scorpion neurotoxin, and the extracellular subtilisin-like serine protease gene Pr1A of *M. anisopliae* (Lu et al. 2008). The bioassay of transformants against the larvae of a pine caterpillar (*Dendrolimus punctatus*) and a wax moth (*G. mellonella*) revealed that the pathogenicity of the genetically engineered strains was substantially increased: the LC_{50} spore concentration was 15-fold less for the single transformants carrying the scorpion neurotoxin gene and 8-fold less for the double transformants carrying both genes. The lack of synergism in the case of binary transformants was explained with the degradation of the scorpion neurotoxin by the Pr1A protease. The results suggested that the virulence improvement in binary transformants is mainly attributable to the secretion of Pr1A. This study also emphasized the necessity to evaluate protein interactions when performing genetical modifications with multiple genes including proteases.

CONCLUSION

A common feature between different entomopathogenic fungi is the involvement of extracellular hydrolases including proteolytic enzymes in the biocontrol process. Identification of pathogenicity-related proteases from different entomopathogenic fungi helps us to gain information on host preference, substrate selection and pathogenicity-related domains at the protein level. Such information will be important for improving the efficacy of mycoinsecticides. Several extracellular proteases have been purified and characterized from *Metarhizium* and *Beauveria* species, and for some of them, the complete sequences of the encoding genes are already available. The majority of the described enzymes belong to the family of serine proteases, however, the expression of other types like metalloproteases and aminopeptidases under biocontrol-related conditions was also demonstrated. Detailed knowledge on protease genes and enzymes involved in fungal biocontrol will assist further strain improvement enabling the overexpression of genes encoding effective proteases.

Nowadays, more and more fungal species are subjected to genome sequencing and analysis, and genomic approaches like ESTs proved very useful for the large-scale identification of fungal genes. Therefore it can be expected in the near future, that the amount of data on extracellular proteases will further increase, thus providing more insight into the role of host protein degradation by entomopathogenic fungi during the biocontrol process.

ACKNOWLEDGMENTS

LK is a grantee of the János Bolyai Research Scholarship (Hungarian Academy of Sciences).

REFERENCES

Bagga, S., Hu, G., Screen, S. E., and St. Leger, R. J. (2004). Reconstructing the diversification of subtilisins in the pathogenic fungus *Metarhizium anisopliae*. *Gene, 324*, 159-169.

Bidochka, M. J., and Khachatourians, G. G. (1987). Purification and properties of an extracellular protease produced by the entomopathogenic fungus *Beauveria bassiana*. *Applied and Environmental Microbiology, 53,* 1679-1684.

Bidochka, M. J., and Khachatourians, G. G. (1988a). Regulation of extracellular protease in the entomopathogenic fungus *Beauveria bassiana*. *Experimental Mycology, 12,* 161-168.

Bidochka, M. J., and Kachatourians, G. G. (1988b). *N*-acetyl-D-glucosamine-mediated regulation of extracellular protease in the entomopathogenic fungus *Beauveria bassiana. Applied and Environmental Microbiology, 54,* 2699-2704.

Bidochka, M. J., and Khachatourians, G. G. (1990). Identification of *Beauveria bassiana* extracellular protease as a virulence factor in pathogenicity toward the migratory grasshopper, *Melanoplus sanguinipes*. *Journal of Invertebrate Pathology, 56,* 362-370.

Bidochka, M. J., and Khachatourians, G. G. (1994). Protein hydrolysis in grasshopper cuticles by entomopathogenic fungal extracellular proteases. *Journal of Invertebrate Pathology, 63,* 7-13.

Bidochka, M. J., and Melzer, M. J. (2000). Genetic polymorphisms in three subtilisin-like protease isoforms (Pr1A, Pr1B, and Pr1C) from *Metarhizium* strains. *Canadian Journal of Microbiology, 46,* 1138-1144.

Blackwell, J., and Weih, M. A. (1980). Structure of chitin-protein complexes: ovipositor of the Ichneumon fly *Megarhyssa*. *Journal of Molecular Biology, 137,* 49-60.

Boucias, D. G., and Pendland, J. C. (1991). The fungal cell wall and its involvement in the pathogenic process in insect hosts. In: J. P. Latge, and D. G. Boucias (Eds.), *Fungal Cell Wall and Immune Response*, (vol. H 53, pp. 303-316). Berlin: Springer-Verlag.

Butt, T. M., Segers, R. J., Leal, S. C. M., and Kerry, B. R. (1998). Variation in the subtilisins of fungal pathogens of insects and nematodes. In: B. P. Couteaudier, and J. Clarkson (Eds.), *Molecular variability of fungal pathogens,* (pp. 149-169). Wallingford: CAB International.

Chrzanowska, J., Banas, J., and Kolaczkowska, M. (2001). Purification and characterization of *Beauveria bassiana* proteinases. *Acta Biotechnologica, 21,* 73-81.

Campos, R. A., Arruda, W., Boldo, J. T., Vanusa da Silva, M., Monteiro de Barros, N., Lucio de Azevedo, J., Schrank, A., and Vainstein, M. H. (2005). *Boophilus microplus* infection by *Beauveria amorpha* and *Beauveria bassiana*: SEM analysis and regulation of subtilisin-like proteases and chitinases. *Current Microbiology, 50,* 257-261.

Cole, S. C. J., Charnley, A. K., and Cooper, R. M. (1993). Purification and partial characterization of a novel trypsin-like cysteine protease from *Metarhizium anisopliae*. *FEMS Microbiology Letters 113,* 189-196.

Da Silva Pinto, F. G., Pelegrinelli Fungaro, M. H., Maldonado Ferreira, J., Valadares-Inglis, M. C., and Furlaneto, M. C. (2002). Genetic variation in the cuticle-degrading protease activity of the entomopathogen *Metarhizium flavoviride*. *Genetics and Molecular Biology, 25,* 231-234.

Dias, B. A., Neves, P. M. O. J., Furlaneto-Maia, L., and Furlaneto, M. C. (2008). Cuticle-degrading proteases produced by the entomopathogenic fungus *Beauveria bassiana* in the presence of coffee berry borer cuticle. *Brazilian Journal of Microbiology, 39,* 301-306.

Donatti, A. C., Furlaneto-Maia, L., Fungaro, M. H. P., and Furlaneto, M. C. (2008). Production and regulation of cuticle-degrading proteases from *Beauveria bassiana* in the presence of *Rhammatocerus schistocercoides* cuticle. *Current Microbiology, 56,* 256-260.

Erlacher, A., Sousa, F., Schroeder, M., Jus, S., Kokol, V., Cavaco-Paulo, A., and Guebitz, G. M. (2006). A new cuticle scale hydrolysing protease from *Beauveria brongniartii*. *Biotechnology Letters, 28,* 703-710.

Fang, W., and Bidochka, M. J. (2006). Expression of genes involved in germination, conidiogenesis and pathogenesis in *Metarhizium anisopliae* using quantitative real-time RT-PCR. *Mycological Research, 110,* 1165-1171.

Freimoser, F. M., Hu, G., and St. Leger, R. J. (2005). Variation in gene expression patterns as the insect pathogen *Metarhizium anisopliae* adapts to different host cuticle or nutrient deprivation *in vitro*. *Microbiology, 151,* 361-371.

Goettel, M. S., St. Leger, R. J., Rizzo, N. W., Staples, R. C., and Roberts, D. W. (1989). Ultrastructural localization of a cuticle degrading protease produced by the

entomopathogenic fungus, *Metarhizium anisopliae* during penetration of host cuticle. *Journal of General Microbiology, 135,* 2223-2239.

Gupta, S. C., Leathers, T. D., El-Sayed, G. N., and Ignoffo, C. M. (1992). Insect cuticle-degrading enzymes from the entomogenous fungus *Beauveria bassiana*. *Experimental Mycology, 16,* 132-137.

Gupta, S. C., Leathers, T. D., El-Sayed, G. N., and Ignoffo, C. M. (1994). Relationships among enzyme activities and virulence parameters in *Beauveria bassiana* infections of *Galleria mellonella* and *Trichoplusia ni*. *Journal of Invertebrate Pathology, 64,* 13-17.

Hackman, R. H., and Goldberg, M. (1987). Comparative study of some expanding arthropod cuticles: the relation between composition, structure and function. *Journal of Insect Physiology, 33,* 39-50.

Hallsworth, J. E., and Magan, N. (1996). Culture age, temperature, and pH affect the polyol and trehalose contents of fungal propagules. *Applied and Environmental Microbiology, 62,* 2435-2442.

Hegedus, D. D., and Khachatourians, G. G. (1995). The impact of biotechnology on hyphomycetous fungal insect biocontrol agents. *Biotechnology Advances, 13,* 455-490.

Hu, G., and St. Leger, R. J. (2002). Field studies using a recombinant mycoinsecticide (*Metarhizium anisopliae*) reveal that it is rhizosphere competent. *Applied and Environmental Microbiology, 68,* 6383-6387.

Inglis, G. D., Goettel, M. S., Butt, T. M., and Strasser, H. (2001). Use of hyphomycetous fungi for managing insect pests. In: T. M. Butt, C. Jackson and N. Magan (Eds.), *Fungi as Biocontrol Agents* (pp. 23-69.). Wallingford: CAB International.

Joshi, L., St. Leger, R. J., and Bidochka, M. J. (1995). Cloning of a cuticle-degrading protease from the entomopathogenic fungus, *Beauveria bassiana*. *FEMS Microbiology Letters, 125,* 211-218.

Joshi, L., St. Leger, R. J., and Roberts, D. W. (1997). Isolation of a cDNA encoding a novel subtilisin-like protease (Pr1B) from the entomopathogenic fungus, *Metarhizium anisopliae* using differential display-RT-PCR. *Gene, 197,* 1-8.

Kim, H. K., Hoe, H. S., Suh, D. S., Kang, S. C., Hwang, C., and Kwon, S. T. (1999). Gene structure and expression of the gene from *Beauveria bassiana* encoding bassiasin I, an insect cuticle-degrading serine protease. *Biotechnology Letters, 21,* 777-783.

Ko, H. J., Kim, H. K., Kim, B. G., Kang, S. C., and Kwon, S. T. (1997). Purification and characterization of protease from entomopathogenic fungus *Beauveria bassiana*. *Agricultural Chemistry and Biotechnology, 40,* 388-394.

Krieger de Moraes, C., Schrank, A., and Vainstein, M. H. (2003). Regulation of extracellular chitinases and proteases in the entomopathogen and acaricide *Metarhizium anisopliae. Current Microbiology, 46,* 205-210.

Li, Z. Z. (1988). A list of insect hosts of *Beauveria bassiana.* In: Y. W. Li, Z. Z. Li, Z. Q. Liang, J. W. Wu, Z. K. Wu, and Q. F. Xi (Eds.), *Study and application of entomogenous fungi in China* (pp. 241-255). Beijing: Academic Periodical Press.

Liu, S.-Q., Meng, Z.-H., Yang, J.-K., Fu, Y.-X., Zhang, K.-Q. (2007). Characterizing structural features of cuticle-degrading proteases from fungi by molecular modeling. *BMC Structural Biology*, 7, 33. DOI 10.1186/1472-6807-7-33.

Lu, D., Pava-Ripoll, M., Li, Z., and Wang, C. (2008). Insecticidal evaluation of *Beauveria bassiana* engineered to express a scorpion neurotoxin and a cuticle degrading protease. *Applied Microbiology and Biotechnology*, *81,* 515-522.

Mohanty, S. S., Raghavendra, K., and Dash, A. P. (2008). Induction of chymoelastase (Pr1) of *Metarhizium anisopliae* and its role in causing mortality to mosquito larvae. *World Journal of Microbiology and Biotechnology, 24,* 2283-2288.

Paterson, I. C., Charnley, A. K., Cooper, R. M., and Clarkson J. M. (1993). Regulation of production of a trypsin-like protease by the insect pathogenic fungus *Metarhizium anisopliae*. *FEMS Microbiology Letters, 109,* 323-328.

Paterson, I. C., Charnley, A. K., Cooper, R. M., and Clarkson, J. M. (1994a). Specific induction of a cuticle-degrading protease of the insect pathogenic fungus *Metarhizium anisopliae*. *Microbiology (UK), 140,* 185-189.

Paterson, I. C., Charnley, A. K., Cooper, R. M., and Clarkson, J. M. (1994b). Partial characterization of specific inducers of a cuticle-degrading protease from the insect pathogenic fungus *Metarhizium anisopliae*. *Microbiology (UK), 140,* 3153-3159.

Pathan, A. A. K., Devi, K. U., Vogel, H., and Reineke, A. (2007). Analysis of differential gene expression in the generalist entomopathogenic fungus *Beauveria bassiana* (Bals.) Vuillemin grown on different insect cuticular extracts and synthetic medium through cDNA-AFLPs. *Fungal Genetics and Biology, 44,* 1231-1241.

Pei, Y., Ji, Z., Yang, X., Lu, X., and Xia, Y. (2000). Purification and characterization of cuticle-degrading protease from entomopathogenic fungus, *Metarhizium anisopliae*. *Wei Sheng Wu Xue Bao, 40,* 306-311.

Qazi, S. S., and Khachatourians, G. G. (2007). Hydrated conidia of *Metarhizium anisopliae* release a family of metalloproteases. *Journal of Invertebrate Pathology, 95,* 48-59.

Qazi, S. S., and Khachatourians, G. G. (2008). Addition of exogenous carbon and nitrogen sources to aphid exuviae modulates synthesis of proteases and chitinase by germinating conidia of *Beauveria bassiana*. *Archives of Microbiology, 189,* 589-96.

Rao, M. B., Tanksale, A. M., Ghatge, M. S., and Deshpande, V. V. (1998). Molecular and biotechnological aspects of microbial proteases. *Microbiology and Molecular Biology Reviews, 62,* 597-635.

Rehner, S. A., and Buckley, E. (2005). A *Beauveria* phylogeny inferred from nuclear ITS and EF1-a sequences: evidence for cryptic diversification and links to *Cordyceps* teleomorphs. *Mycologia, 97,* 84-98.

Samson, R. A., Evans, H. C., and Latgé, J. P. (1988). *Atlas of Entomopathogenic Fungi*. The Netherlands: Springer-Verlag.

Sasaki, S. D., de Lima, C. A., Lovato, D. V., Juliano, M. A., Torquato, R. J. S., and Tanaka, A. S. (2008). BmSI-7, a novel subtilisin inhibitor from *Boophilus microplus*, with activity toward Pr1 proteases from the fungus *Metarhizium anisopliae*. *Experimental Parasitology, 118,* 214-220.

Screen, S., Bailey, A., Charnley, K., Cooper, R., and Clarkson, J. (1997). Carbon regulation of the cuticle-degrading enzyme PR1 from *Metarhizium anisopliae* may involve a trans-acting DNA-binding protein CRR1, a functional equivalent of the *Aspergillus nidulans* CREA protein. *Current Genetics, 31,* 511-518.

Screen, S. E., and St. Leger, R. J. (2000). Cloning, expression, and substrate specificity of a fungal chymotrypsin. *Journal of Biological Chemistry, 275,* 6689-6694.

Shah, F. A., Wang, C. S., and Butt, T. M. (2005). Nutrition influences growth and virulence of the insect-pathogenic fungus *Metarhizium anisopliae. FEMS Microbiology Letters, 251,* 259-266.

Sheng, J., An, K., Deng, C., Li, W., Bao, X., and Qiu, D. (2006). Cloning a cuticle-degrading serine protease gene with biologic control function from *Beauveria brongniartii* and its expression in *Escherichia coli*. *Current Microbiology, 53,* 124-128.

Shimizu, S., Tsuchitani, Y., and Matsumoto, T. (1993). Production of an extracellular protease by *Beauveria bassiana* in the haemolymph of the silkworm, *Bombyx mori, Letters in Applied Microbiology, 16,* 291-294.

Small, C. L., and Bidochka, M. J. (2005). Up-regulation of Prl, a subtilisin-like protease, during conidiation in the insect pathogen *Metarhizium anisopliae*. *Mycological Research, 109,* 307-313.

Smithson, S. L., Paterson, I. C., Bailey, A. M., Screen, S. E., Hunt, B. A., Cobb, B. D., Cooper, R. M., Charnley, A. K., and Clarkson, J. M. (1995). Cloning and characterisation of a gene encoding a cuticle-degrading protease from the insect pathogenic fungus *Metarhizium anisopliae. Gene, 166,* 161-165.

Steinhaus, E. A. (1949). *Principles of Insect Pathology*. New York: McGraw Hill Book Co.

St. Leger, R. J., Bidochka, M. J., and Roberts, D. W. (1994a). Isoforms of the cuticle-degrading Pr1 proteinase and production of a metalloproteinase by *Metarhizium anisopliae*. *Archives of Biochemistry and Biophysics, 313,* 1-7.

St. Leger, R. J., Bidochka, M. J., and Roberts, D. W. (1994b). Characterization of a novel carboxypeptidase produced by the entomopathogenic fungus *Metarhizium anisopliae*. *Archives of Biochemistry and Biophysics, 314,* 392-398.

St. Leger, R. J., Butt, T. M., Staples, R. C., and Roberts, D. W. (1989). Synthesis of proteins including a cuticle-degrading protease during differentiation of the entomopathogenic fungus *Metarhizium anisopliae. Experimental Mycology, 13,* 253-262.

St. Leger, R. J., Charnley, A. K., and Cooper, R. M. (1986). Cuticle-degrading enzymes of entomopathogenic fungi: synthesis in culture on cuticle. *Journal of Invertebrate Pathology, 48,* 85-95.

St. Leger, R. J., Charnley, A. K., and Cooper, R. M. (1987a). Characterization of cuticle-degrading proteases produced by the entomopathogen *Metarhizium anisopliae*. *Archives of Biochemistry and Biophysics, 253,* 221-232.

St. Leger, R. J., Cooper, R. M., and Charnley, A. K. (1987b). Distribution of chymoelastases and trypsin-like enzymes in five species of entomopathogenic deuteromycetes. *Archives of Biochemistry and Biophysics, 258,* 123-131.

St. Leger, R. J., Durrands, P. K., Charnley, A. K., and Cooper, R. M. (1988a). Role of extracellular chymoelastase in the virulence of *Metarhizium anisopliae* for *Manduca sexta*. *Journal of Invertebrate Pathology, 52,* 285-293.

St. Leger, R. J., Durrands, P. K., Cooper, R. M., and Charnley A. K. (1988b). Regulation of production of proteolytic enzymes by the entomopathogenic fungus *Metarhizium anisopliae. Archives of Microbiology, 150,* 413-416.

St. Leger, R. J., Frank, D. C., Roberts, D. W., and Staples, R. C. (1992). Molecular cloning and regulatory analysis of the cuticle-degrading-protease structural gene from the entomopathogenic fungus, *Metarhizium anisopliae*. *European Journal of Biochemistry, 204,* 991-1001.

St. Leger, R. J., Joshi, L., Bidochka, M. J., Rizzo, N. W., and Roberts, D. W. (1996a). Biochemical characterization and ultrastructural localization of two extracellular trypsins produced by *Metarhizium anisopliae* in infected insect cuticles. *Applied and Environmental Microbiology, 62,* 1257-1264.

St. Leger, R. J., Joshi, L., Bidochka, M. J., and Roberts D. W. (1996b). Construction of an improved mycoinsecticide overexpressing a toxic protease. *Proceedings of the National Academy of Sciences of the USA, 93,* 6349-6354.

St. Leger, R. J., Joshi, L., and Roberts, D. (1998). Ambient pH is a major determinant in the expression of cuticle-degrading enzymes and hydrophobin by *Metarhizium anisopliae. Applied and Environmental Microbiology, 64,* 709-713.

St. Leger, R. J., Nelson, J. O., and Screen, S. E. (1999). The entomopathogenic fungus *Metarhizium anisopliae* alters ambient pH, allowing extracellular protease production and activity. *Microbiology (UK), 145,* 2691-2699.

Tartar, A., and Boucias, D. G. (2004). A pilot-scale expressed sequence tag analysis of *Beauveria bassiana* gene expression reveals a tripeptidyl peptidase that is differentially expressed *in vivo*. *Mycopathologia, 158,* 201-209.

Tiago, P. V., Fungaro, M. H. P., and Furlaneto, M. C. (2002). Cuticle-degrading proteases from the entomopathogen *Metarhizium flavoviride* and their distribution in secreted and intracellular fractions. *Letters in Applied Microbiology, 34,* 91-94.

Urtz, B. E., and Rice, W. C. (2000). Purification and characterization of a novel extracellular protease from *Beauveria bassiana*. *Mycological Research, 104,* 180-186.

Wagner, B. L., and Lewis, L. C. (2000). Colonization of corn, *Zea mays*, by the entomopathogenic fungus *Beauveria bassiana*. *Applied and Environmental Microbiology, 66,* 3468-3473.

Wang, C., Typas, M. A., and Butt, T. M. (2002). Detection and characterisation of pr1 virulent gene deficiencies in the insect pathogenic fungus *Metarhizium anisopliae*. *FEMS Microbiology Letters, 213,* 251-255.

World Health Organization (1993) *Implementation of the global malaria control strategy*. WHO Technical Report Series, No. 839. WHO Press.

Wraight, S. P., Ramos, M., Williams, J. E., Avery, S., Jaronski, S., and Vandenberg, J. (2003). Comparative virulence and host specificity of *Beauveria bassiana* isolates assayed against lepidopteran pests of vegetable crops. *Proceedings of the Annual Meeting of the Society for Invertebrate Pathology*, pp. 36.

Zhang, Y. J., Feng, M. G., Fan, Y. H., Luo, Z. B., Yang, X. Y., Wu, D., and Pei, Y. (2008a). A cuticle-degrading protease (CDEP-1) of *Beauveria bassiana* enhances virulence. *Biocontrol Science and Technology, 18,* 551-563.

Zhang, W., Yueqing, C., and Yuxian, X. (2008b). Cloning of the subtilisin Pr1A gene from a strain of locust specific fungus, *Metarhizium anisopliae*, and functional expression of the protein in *Pichia pastoris*. *World Journal of Microbiology and Biotechnology, 24,* 2481-2488.

In: Biochemistry and Histocytochemistry… ISBN: 978-1-60876-283-5
Editors: S. Fuchs, M. Auer, pp. 299-322 © 2010 Nova Science Publishers, Inc.

Chapter 12

GLYCOSIDE HYDROLASES FROM HYPERTHERMOPHILES: STRUCTURE, FUNCTION AND EXPLOITATION IN OLIGOSACCHARIDE SYNTHESIS

Beatrice Cobucci-Ponzano*, Mosè Rossi and Marco Moracci
Institute of Protein Biochemistry – CNR, Via P. Castellino 111, 80131 Naples, Italy

ABSTRACT

Hyperthermophilic microorganisms thrives at temperatures higher than 80°C and proteins and enzymes extracted from these sources are optimally stable and active in the presence of temperatures close to the boiling point of water and of other denaturants, i.e. chaotropic agents, pH, organic solvents, detergents, etc. Therefore, hyperstable enzymes are considered attractive alternatives in biocatalysis and in chemo-enzymatic synthesis. In addition, the molecular bases of the extreme stability to heat and to the ability to work optimally at high temperatures are not completely understood and intrigued biochemists, enzymologists, and biophysics in the last twenty years. In particular, hyperstable glycosidases, enzymes catalysing the hydrolysis of *O*- and *N*-glycosidic bonds, have been studied in detail as they are simple model systems promoting single-substrate reactions, and, more importantly, can be exploited for the enzymatic synthesis of oligosaccharides. The importance of these molecules increased enormously in recent years for their potential application in biomedicine. Hyperstable glycosidases, working in transglycosylation mode, can be excellent alternatives to the classical chemical methods helping in the control of regio- and stereoselectivity as conventional enzymes, but also resisting to the organics used in chemical synthesis. We will review here recent advances in the isolation and characterization of glycosidases from hyperthermophilic microorganisms and the methods used for their application in oligosaccharide synthesis.

* To whom the correspondence should be addressed: Tel. +39-081-6132564; Fax +39-081-6132277; (E-mail b.cobucciponzano@ibp.cnr.it).

INTRODUCTION

Carbohydrates serve as structural components and energy source of the cell and are involved in a variety of molecular recognition processes in intercellular communication [Varki 1993; Sears and Wong 1996]. The knowledge that these biomolecules have a key informative role in biology is becoming more obvious every day confirming their potential as therapeutic agents [Zopf and Roth 1996]. For these reasons, great interest arose in carbohydrate-based compounds and the development of techniques for the analysis and synthesis of oligosaccharides. However, despite the advances achieved with both regio- and stereoselectivity [Toshima and Tatsuta 1993], the synthesis of complex carbohydrates for large-scale production still cannot be easily performed by the classical chemical procedures, which require long protection–deprotection steps and give low final yields. Thus, the enzyme-catalyzed synthesis of oligosaccharides represents an interesting alternative to the classical chemical methods, allowing the control of both the regioselectivity and the stereochemistry of bond formation.

The enzymatic approach involves mainly two class of enzymes: glycosyl transferases and glycoside hydrolases. Glycosyl transferases have been used for oligosaccharide synthesis [Gijsen et al. 1996], but their low availability and the high cost of their substrates have limited their exploitation. Glycoside hydrolases, a widespread group of enzymes that hydrolyse glycosidic bonds, allow the use of relatively inexpensive substrates, representing an alternative choice. They play multiple roles in the cell such as the degradation of poly- and oligosaccharides to be utilized as energy sources, the hydrolysis of the cell-wall polysaccharides for the plant cell division, and the turnover of glycoconjugates involved in several biological functions. Thousands of genes encoding for glycoside hydrolases are known and they have been classified in more than 100 families and 14 clans on the basis of their sequence similarity (http://www.cazy.org) [Cantarel et al. 2008]. These enzymes follow two distinct mechanisms, which are termed *inverting* or *retaining*, depending on whether the enzymatic cleavage of the glycosidic bond liberates a sugar hemiacetal with the opposite or the same anomeric configuration compared with the glycosidic substrate, respectively. *Inverting* enzymes use a direct displacement mechanism in which the two carboxylic acid residues in the active site are positioned so that one acts as a general acid and the other provides general base catalytic assistance to the attack of water. The catalytic mechanism of *retaining* enzymes (Figure 1) proceeds via a two-step double-displacement mechanism involving the formation of a covalent glycosyl intermediate. The two carboxylic residues in the active site play different roles in this case, one acting as the nucleophile and the other as a general acid or base catalyst of the reaction. In the first step, termed glycosylation, the concerted action of the nucleophile and of the general acid residues leads to glycosidic oxygen protonation and the departure of the aglycon group with the formation of a glycosyl–ester intermediate. In the second step (deglycosylation), a water molecule partially deprotonated by the conjugate base of the catalytic acid attacks the anomeric carbon and cleaves the glycosyl–ester intermediate, leading to the overall retention of the anomeric configuration of the substrate. When acceptors other than water intercept the reactive glycosyl–enzyme intermediate, *retaining* enzymes work in transglycosylation mode. This property makes the *retaining* glycoside hydrolases interesting tools for the synthesis of carbohydrates.

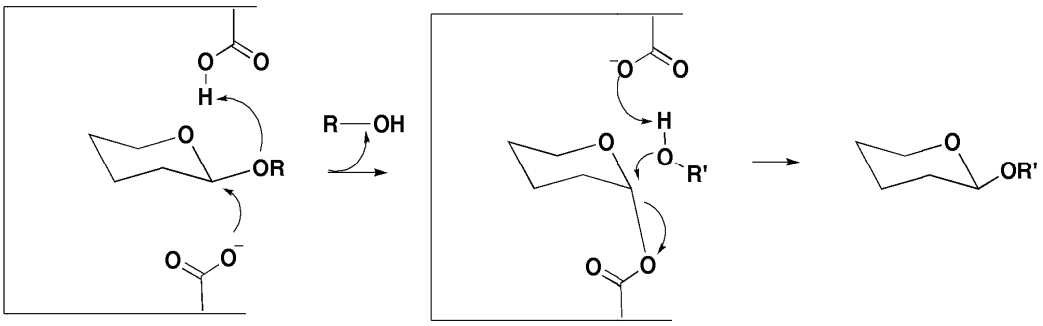

Figure 1. Reaction mechanism of retaining b-glycosidases. R: aglycon group. R' = H, hydrolysis. R' = alcohol, transglycosylation.

Despite the differences, the two mechanisms show significant similarities: both classes of enzymes employ a pair of carboxylic acids at the active site and both mechanisms operate via transition states with substantial oxocarbenium ion character. However, strong evidence indicates that a covalent intermediate is formed in retainers [Sinnot 1990; McCarter and Withers 1994].

The identification of key active-site residues in glycoside hydrolase is crucial to understand the catalytic mechanism [McCarter and Withers 1994; Zechel and Withers 2000], to allow the classification of this class of enzymes [Henrissat and Bairoch 1993; Henrissat and Davies 1997], and to produce glycoside hydrolases with novel characteristics [Perugino et al. 2004]. These residues can be identified by many techniques [McCarter and Withers 1994; White and Rose 1997; Ly and Withers 1999]. Successful approaches for the identification of the nucleophile residues include specific labeling with mechanism-based inhibitors such as activated 2-deoxy-2-fluoro-glycosides, in combination with mass spectrometry, amino acid sequence alignment, and crystal structure inspection [Zechel and Withers 2000]. Among others, the use of mechanism-based inhibitors is nowadays the most powerful method for the direct identification in retainers of the carboxyl group acting as the nucleophile of the reaction, even in the absence of the amino acid sequence of the enzyme [Withers and Aebersold 1995]. By contrast, no reliable chemical methods for the identification of the acid/base catalyst are currently available. Site-directed mutagenesis followed by kinetic analysis of the mutants remains, however, the approach most used for the definition of the role played by the active site carboxylic groups. Aspartic/glutamic acid residues identified by sequence analysis and conserved in the family of interest are mutated. Mutations of the catalytic residues with non-nucleophilic amino acids lead to the strong reduction or even abolition of the enzymatic activity [Ly and Withers 1999]. However, these mutants can be reactivated in the presence of external nucleophiles such as sodium azide. Reactivated mutants in the acid/base catalyst produce glycosyl-azide with the same anomeric configuration of the substrate (Figure 2A) By contrast, the isolation of glycosyl-azide products with an anomeric configuration opposite to that of the substrate allows the identification of the catalytic nucleophile of the reaction (Figure 2B) [Ly and Withers 1999]. The classification of glycoside hydrolases into families and superfamilies on the basis of their amino acid sequence and three-dimensional (3-D) structure are commonly used to identify the active site residues and the reaction mechanism of any newly identified glycosyl hydrolase.

A)

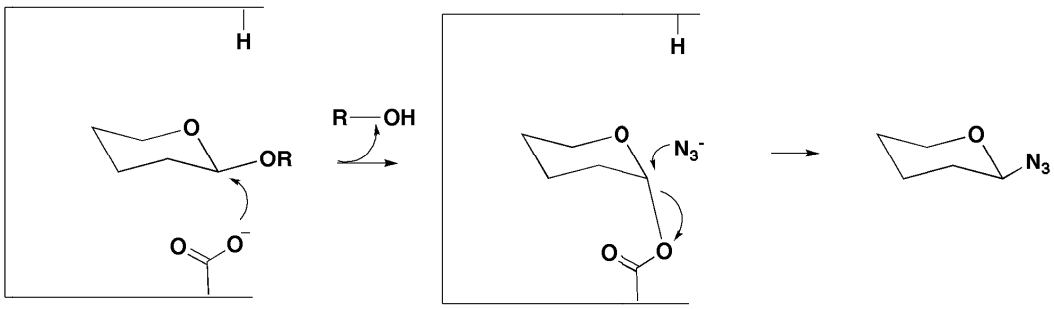

B)

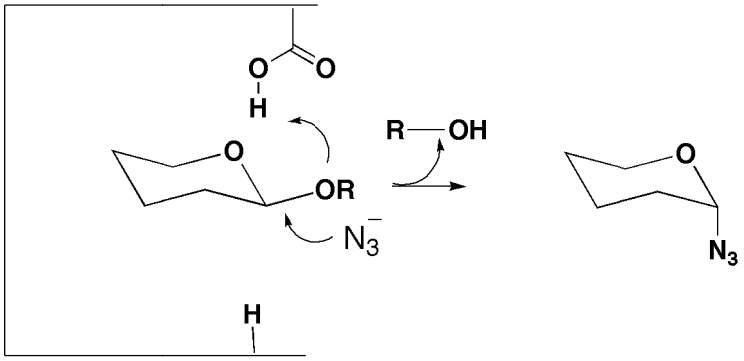

Figure 2. Azide rescue of an acid/base catalyst (A) and a nucleophile (B) mutant of a retaining b-glycosidase. R: aglycon group.

Glycosidases are exploited in synthetic reactions by two main approaches, reverse hydrolysis (equilibrium-controlled synthesis) or transglycosylation (kinetically controlled process), in which the glycosyl–enzyme intermediate is transferred to an acceptor other than water. The former method offers modest yields of oligosaccharide products [Withers 2001], whereas kinetically controlled synthesis, which requires a *retaining* glycosidase, provides better yields (10 to 40%), but is not generally economical for large-scale synthesis. In fact, since the product of the reaction is a new substrate for the enzyme it can be hydrolyzed to reduce the final yields of the reaction. Thus, in order to maintain high yields, the reaction conditions have to be strictly controlled. To avoid these problems, a new class of engineered glycosidase has been produced to promote the synthesis of sugars with almost quantitative yields; these novel enzymatic activities have been termed *glycosynthases* (reviewed in Perugino et al. 2004; Perugino et al. 2005, and Hancock et al. 2006). These enzymes, developed for the first time in 1998 in the laboratory of Stephen Withers, are *retaining* glycoside hydrolases mutated in the catalytic nucleophile, that synthesise complex oligosaccharides in high yields [Mackenzie *et al.* 1998]. Because of the essential nature of this residue, when it is mutated with a non-nucleophilic amino acid (typically Ala, Gly, or Ser) the mutant is almost completely inactive. Nevertheless, the rest of the active site is intact and the small cavity created on mutation can accommodate a small anion (i.e. sodium formate). Under these conditions and in the presence of a substrate with good leaving group

ability, which assists the glycosylation step of the reaction, the activity of the mutant can be restored (Figure 3A). The methodology described can be usefully applied to the synthesis of carbohydrates. In fact, these modified glycoside hydrolases, lacking their catalytic nucleophile, can act only on activated substrates by synthesizing new glycosidic bonds but cannot hydrolyze the products formed. These compounds, in fact, show groups with poor leaving ability, which are resistant to the attack of the external nucleophiles and which accumulate in the reaction. In the literature, several β-glycoside hydrolases modified in glycosynthases are reported, demonstrating that this methodology could be of general applicability for β-glycoside hydrolases, involving both *exo*- and *endo*-enzymes from diverse sources and with different functions and specificities [Perugino et al. 2004].

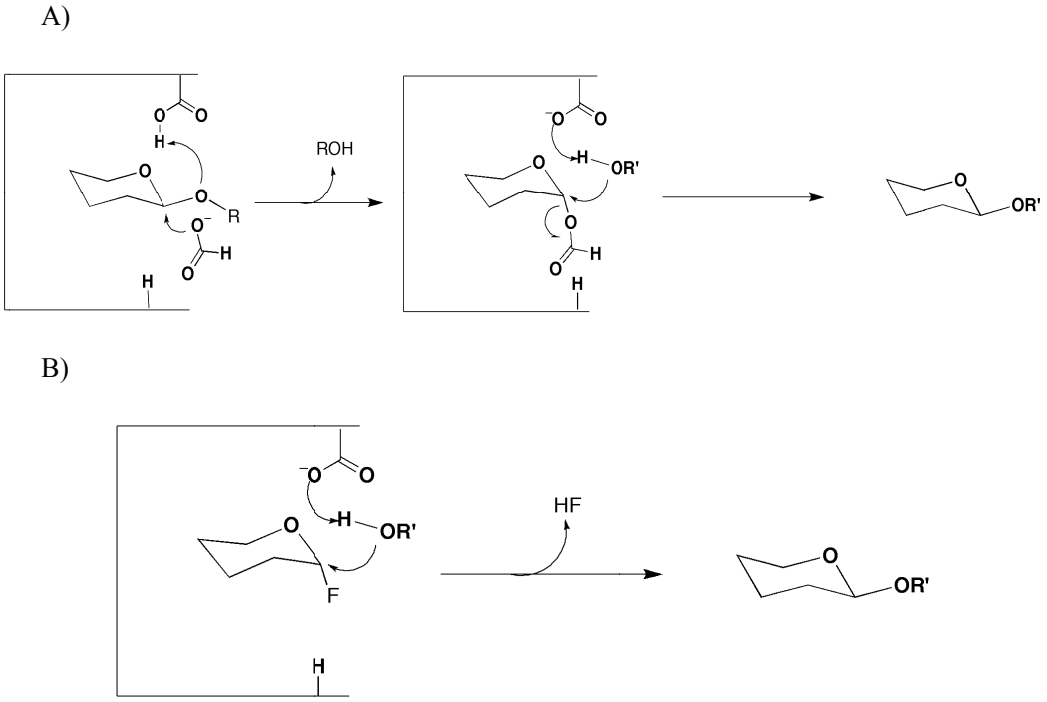

Figure 3. Reaction mechanism of *retaining* (A) and *inverting* (B) β-glycosynthases. R': alcohol.

GLYCOSIDE HYDROLASES FORM HYPERTHERMOPHILES

Among the glycoside hydrolases available, the enzymes from hyperthermophilic microorganisms are of particular interest for both basic and applied research. In fact, the function of the glycoconjugates identified in hyperthermophiles and of the enzymes involved in their synthesis and degradation is still largely unknown [Lower and Kennelly 2002]. On the other hand, the harsh conditions of growing of these organisms (temperatures > 80°C) have hindered *in vivo* microbiological and genetic studies; therefore, the isolation of the genes encoding for hyperthermophilic glycoside hydrolases and the detailed enzymological characterization is the only approach to define their role *in vivo*. In addition, the rise of interest in thermophilic enzymes, or thermozymes, as potential biotechnological tools is

historically based on their intrinsic resistance to the harsh conditions used in several bioprocesses, such as high temperatures, high concentrations of substrate, and organic solvents. However, the interest in thermozymes is also motivated by their biodiversity, which has revealed novel enzymatic activities [Hough and Danson 1999]; in particular, thermophilic glycoside hydrolases show peculiar enzymological properties, such as unique substrate specificities or reduced substrate/product inhibition [Trincone et al. 1991], and allow the synthesis of new products that are not produced by their mesophilic counterparts [Fischer et al. 1996].

Sulfolobus solfataricus is an extremely thermoacidophilic archaeon which thrives in hot springs at 80-87 °C and pH 2.0-3.0. The genome of this microorganism has been completely sequenced [She et al. 2001] and revealed genes encoding for 22 putative glycosyl hydrolases and 33 putative glycosyl transferases. Remarkably, 36% of the glycosyl hydrolases maps in a region of the genome of about 70 kb, and are likely to be involved in the degradation of sugars for energy metabolism. However, the lack, so far, of molecular genetic tools for these microorganisms has hampered the experimental testing of the *in vivo* function of these genes. In the framework of the exploitation of glycosyl hydrolases from hyperthermophiles for the synthesis of useful oligosaccharides, the sequence of the *S. solfataricus* genome has provided access to a number of novel glycoside hydrolases.

In this chapter the study of three glycosyl hydrolases from this archaeon, focussing on their use in the synthesis of oligosaccharides, will be described.

THE β-D-GLYCOSIDASE

The β-glycosidase from *S. solfataricus* (Ssβ-gly), classified in Family 1 of glycosyl hydrolases (GH1), has been extensively studied and an increasing amount of structural and biochemical data on this enzyme is available in several reviews [Moracci et al., 1994, Moracci et al., 2001]. The enzyme is a homotetramer (240 kDa) with 56-kDa subunits; it is thermostable (half life 48 hr at 85 °C), resistant to detergents and organic solvents and shows maximal activity above 95 °C [Pouwels et al. 2000]. Recombinant Ssβ-gly has been crystallised and the 3D-structure has been solved at 2. Å [Gloster et al. 2004]. The enzyme follows a *retaining* reaction mechanism (Figure 1) with the Glu206 and Glu387 residues acting as the acid/base catalyst and the nucleophile of the reaction, respectively [Moracci et al. 1996].

Interesting properties of Ssβ-gly include wide substrate specificity, the ability to hydrolyse oligosaccharides from their non-reducing end, and to perform oligosaccharide synthesis by transglycosylation reactions with yields ranging between 10-40% [Cobucci-Ponzano et al. 2003]. The wide substrate specificity of Ssβ-gly in the reaction of hydrolysis was confirmed also in the synthesis by using, in transglycosylation reactions, alkyl- and aryl-alcohols acceptors and different aryl-glycosides as donors [Cobucci-Ponzano et al. 2003]. The study of the stereo- and regioselectivity of the enzyme revealed that the primary hydroxyl groups were always favoured if compared to the secondary hydroxyl groups, although the overall regioselectivity of the reaction depended on the complexity of the molecule. The yield of the reaction depended upon chain length and OH position but a marked improvement can be obtained increasing the molar excess of alcohol. In this respect, the increased stability of

Ssβ-gly to organic solvents allowed the use of reaction mixtures in which the alcohol and/or organic cosolvent concentrations were up to 95-97%.

The glycosynthase derived from Ssβ-gly (Ssβ-glyE387G), the first hyperthermophilic enzyme of this class, promoted the oligosaccharide synthesis from activated aryl-β-glycosides in the presence of sodium formate as external nucleophile by following the mechanism described in Figure 3A [Moracci et al. 1998; Trincone et al. 2000]. In fact, Ssβ-glyE387G is almost completely inactive, but it can host a donor with the same anomeric configuration of the wild type enzyme (β-anomer). In the first step of the reaction, the external nucleophile finds room in the active site of the enzyme and attacks the anomeric centre of the substrate. In the same time, the acid/base catalyst promotes the departure of the aglycon group of the substrate whereas sodium formate and the glyconic group form a metastable intermediate. At this stage, it is essential that the aglycon group of the activate substrate has good chemical leaving ability. In fact, the mutation greatly slows the first step of the reaction and the enzyme, even in the presence of the formate ion, cannot hydrolyze stable substrates. In the second step, the attack of the intermediate by an acceptor molecule, together with the action as general base of the carboxylate, completes the reaction allowing the formation of the product. The oligosaccharides produced by the enzyme accumulate in the reaction mixture for the reasons stated above, in fact, they are not activated donors and can not be hydrolysed by the glycosynthase. These enzymes were named *retaining* glycosynthases [Perugino et al. 2004].

In addition to this mechanism it has been demonstrated that *Ss*β-glyE387G, in the presence of a substrate with an anomeric configuration opposite to that of the natural substrate, typically, α-glycosyl-fluoride (α-F-Glc) for β-glycosynthases, the enzyme catalyses the synthesis of oligosaccharides by transferring the α-F-Glc donor to sugar acceptors (Figure 3B). The oligosaccharide products, containing bonds in the β-anomeric configuration, cannot be hydrolysed by the mutant and accumulate in the reaction [Mackenzie et al. 1998; Malet et al. 1998]. On the basis of the anomeric configuration of the donor and the acceptor, the enzymes following the mechanism shown in Figure 3A were named *inverting* glycosynthases [Perugino et al. 2004].

Remarkably, Ssβ-glyE387G was able to follow both mechanisms shown in Figure 3. In the presence of 2M sodium formate as external nucleophile and activated β-glycoside donors, such as 2,4-dinitrophenyl- or 2-nitrophenyl-β-Glc and 2-nitrophenyl-β-Fuc, Ssβ-glyE387G followed the reaction mechanism shown in Figure 3B producing branched oligoglucosides (85% total efficiency, with 50% disaccharides, 40% trisaccharides and 10% tetrasaccharides using 2-Np-β-Glc) [Trincone *et al.* 2000]. In addition, in the presence of α-F-Glc substrate, Ssβ-glyE387G synthesised 2-NP-β-D-laminaribioside in 90% yields by following the mechanism in Figure 3B [Trincone *et al.* 2000].

After the first hyperthermophilic glycosynthase, three more enzymes of this class were produced by engineering the β-glycosidases from *Thermosphaera aggregans*, *Pyrococcus furiosus,* and *Pyrococcus horikoshii* [Perugino et al. 2003; Perugino et al. 2006]. Interestingly, we reported that the synthetic activity of these *retaining* glycosynthases could be greatly enhanced at acidic conditions [Perugino et al. 2003]. In fact, the reaction mechanism of *retaining* glycosynthases involves a glycosylation step in which the general acid/base catalyst and the formate ion co-operate (Figure 3A). The removal of the catalytic nucleophile in *retaining* glycosidases causes a downward shift in the pK_a of the acid/base

catalyst [McIntosh et al. 1996]. Consequently, this group, which is ionised at neutral pH, could perform the first step of the reaction less efficiently. To maintain the acid/base group in the protonated catalytically efficient form, glycosynthetic reactions were performed in sodium formate buffer pH 3.0-6.0. At these conditions, the Ssβ-glyE387G enzyme, and the glycosynthases from *T. aggregans* and *P. furiosus*, showed improved efficiency in the synthetic reaction and enhanced synthetic repertoire [Perugino et al. 2003].

The branching functionalisation is a unique characteristic of the glycosynthases from *S. solfataricus* and *T. aggregans* and it has never been reported for other enzymes of this kind. *T. aggregans* and *S. solfataricus* glycosynthases differ in their regioselectivity: the former synthesises the glucose disaccharides β-1,3: β-1,4: β-1,6 as 59:28:12 ratios whereas the composition of the regioisomers synthesised by the enzyme from *S. solfataricus* was 80:2:18 [Perugino et al. 2003]. The compounds produced can be of applied interest in the pharmaceutical and food fields [Kiho et al. 1992] and can also be used as new substrates and/or inhibitors for glycosidases.

The ability of the hyperthermophilic glycosynthases to promote the synthesis of oligosaccharides is a clear example of how the unique characteristics of stability to high temperatures and acidic pH of the glycosidases from hyperthermophilic archaea allows the development of a novel strategy for the chemo-enzymatic synthesis of oligosaccharides.

THE α-D-XYLOSIDASE

Among the putative glycosyl hydrolases present in *S. solfataricus*, an α-D-xylosidase (XylS), was identified. The gene, which is actively transcribed in the archaeon, was cloned and expressed in *E. coli*, producing an enzyme that, in native conditions, is a monomer of about 85 kDa [Moracci et al. 2000]. XylS displays maximal activity at 90°C and high stability to heat (half life of 38 h at 90°C) and reveals clear selectivity for xylose-containing substrates such as 4-nitrophenyl-α-D-xyloside (4-Np-α-Xyl) and the disaccharide isoprimeverose (α-D-xylopyranosyl-(1,6)-D-glucopyranose), which is the disaccharidic unit of the hemicellulose xyloglucan, and 4-Np-β–isoprimeveroside which are hydrolysed from the non-reducing end showing that the enzyme is an exo-glycosidase (Table 1) [Moracci et al., 2000]. In contrast, the activity on maltose and different maltooligosaccharides is lower, and completely absent on isomaltose, trehalose, and sucrose. It is worth noting that the extreme specificity of the exo-xylosidase activity of XylS has been exploited to characterize complex oligosaccharides. In fact, XylS, coupled to a β-glucosidase, was used to determine unequivocally the structure of a xyloglucan oligosaccharide synthesized by a novel α-xylosyltransferase from *Arabidopsis* [Faik et al 2002].

Xyloglucan, the principal hemicellulose component in the primary cell wall and one of the most abundant storage polysaccharides in seeds, is widely distributed in plants. Xyloglucans are involved in complex biological roles. For instance, some xyloglucan oligosaccharides can promote the elongation of stem segments [Lorences and Fry 1994] and therefore play a role in the regulation of plant growth. In plant seeds, the hydrolysis of xyloglucan occurs after germination, during the mobilization of this storage polysaccharide. This polymer is composed of a β–(1,4)-glucan backbone, with α-(1,6)-D-xylose groups linked to about 75% of the glucosyl residues.

Table 1. Kinetic constants of XylS

Substrates	k_{cat} (s^{-1})	K_M (mM)	k_{cat}/K_M ($s^{-1}mM^{-1}$)
4-NP-α-xylopyranoside	4.69 ± 0.27	17.0 ± 2.1	0.28
4-NP-β-isoprimeveroside	16.0 ± 1.6	1.72 ± 0.46	9.30
4-NP-α-glucopyranoside	0.05 ± 0.00	2.05 ± 0.44	0.02
Isoprimeverose	31.0 ± 1.5	28.9 ± 3.5	1.07
Maltose	1.51 ± 0.07	17.0 ± 3.2	0.09
Maltotriose	0.92 ± 0.04	3.45 ± 0.97	0.27

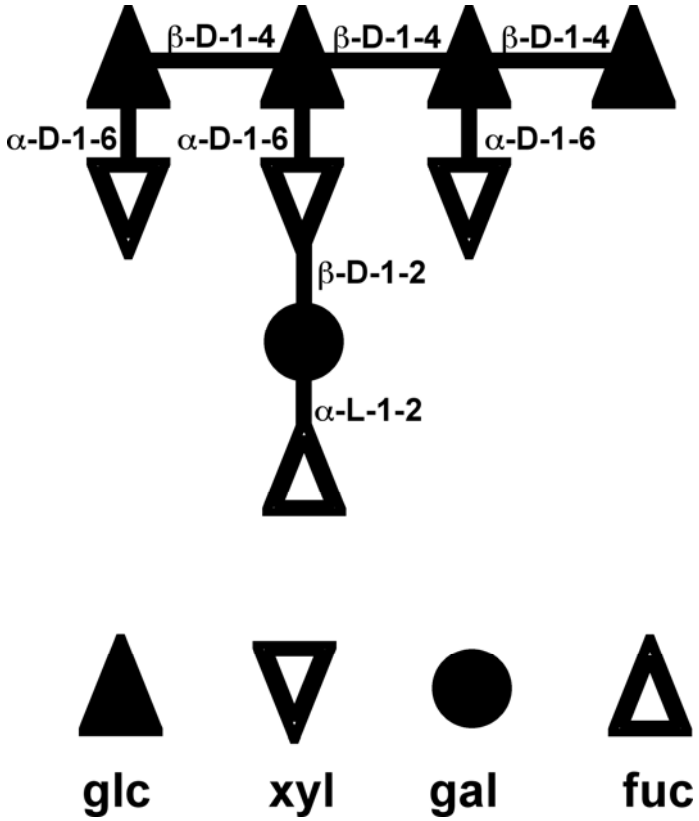

Figure 4. Schematic structure of a xyloglucan oligosaccharide.

Thus, the disaccharide isoprimeverose represents the building block of xyloglucan. Additional ramifications of β-D-galactosyl-(1,2)-α-xylosyl and α-L-fucosyl-(1,2)-β-D-galactosyl-(1,2)-α-xylosyl chains are α-(1,6)-linked at a lesser extent to the main backbone (Figure 4) [Crombie, et al 1998]. XylS is active on xyloglucan oligosaccharides from which it produces xylose, suggesting that the enzyme recognizes isoprimeverose units at the non-reducing end of xyloglucan fragments and promotes the release of xylose residues from these compounds [Moracci et al 2000].

In the xyloglucan polymer, xylose groups are α-1,6-linked to most of the glucose units forming the β-(1,4)-glucan backbone of this polysaccharide and the incubation of XylS and *Ss*β-gly enzymes determined the complete hydrolysis of the oligosaccharides. In fact, XylS and *Ss*β-gly are both *exo*-acting enzymes, thus, they could attack alternatively the non-reducing ends of the xyloglucan oligosaccharides. The identification of *xylS* gene and the substrate specificity of its gene product strongly suggest the involvement of this enzyme in the degradation of di- and oligosaccharides containing α-1,6-linked xylose, which are the building blocks of xyloglucan. Moreover, the cooperation of XylS and *Ss*β-gly in the degradation of xyloglucan oligosaccharides *in vitro*, and the vicinity of the encoding genes on the *S. solfataricus* chromosome could suggest that the two enzymatic systems are functionally related also *in vivo*. The solfataric fields, in which *S. solfataricus* grows under aerobic conditions, are rich in plant debris containing hemicellulosic material. XylS *in vivo* could recognize isoprimeverose units at the non-reducing end of xyloglucan fragments and promote the release of the xylose that can be used as an energy source. However, the complex structure of xyloglucan would require the combined action of several enzymatic activities and protein transporters for its efficient hydrolysis and assimilation.

The importance of xyloglucan oligosaccharides in several biological events determined the need of purified xyloglucan oligosaccharides and isoprimeverose for enzymological and metabolic studies [Lorences and Fry 1994; Chaillou et al. 1998]. Relatively little is known about the mechanism of xyloglucan degradation and the enzymatic systems involved in the metabolism of xyloglucan oligosaccharides and isoprimeverose. These compounds can be prepared by several steps of hydrolysis of the natural polymer xyloglucan by different glycoside hydrolases [Kato and Matsuda. 1980]. This approach is limited by the huge number of different enzymatic activities required and by the production of mixtures of oligosaccharides difficult to purify. These drawbacks can be overcome by synthesizing isoprimeverose and specific xyloglucan oligosaccharides by using the enzymes involved in the degradation of xyloglucan in transglycosylating mode. Interestingly, XylS is able to transfer xylose in a transxylosylation reaction. In fact, the enzyme, which follows the retaining reaction mechanism as do the other members of GH31, forms 4-nitrophenyl-β-isoprimeveroside (11% average yields) by transxylosylation with 4-Np-α-Xyl and 4-nitrophenyl-β-D-glucoside (4-Np-β-Glc) as donor and acceptor, respectively (Table 2) [Moracci et al. 2000]. Different regioisomers, in which xylose is transferred to different glucose positions, possibly the OH in C3 and C4, were observed in trace amounts. Free isoprimeverose was obtained, with 10-12% average yields, by using glucose and α-xylosyl fluoride as acceptor and donor, respectively [Moracci et al 2001, Trincone et al., 2001]. With the same α-xylosyl fluoride donor, and 4-Np-β–cellobioside as acceptor, XylS synthesises the trisaccharidic unit of xyloglucan XG (15% average yields) in which xylose is attached on the C6 of the external glucose of the acceptor (Table 2). These findings demonstrate that the typical exo-acting hydrolysis of this enzyme is also operative in synthetic mode [Trincone et al., 2001; Cobucci-Ponzano et al, 2003a]. For these reasons, XylS could be used for the synthesis of the building blocks of xyloglucan oligosaccharides, which, acting as growth regulators of plant cells, may find application in agro-food technology.

Table 2. Oligosaccharide synthesis by the α-xylosidase from *S. solfataricus*

Donor	Acceptor	Products
4-NP-α-Xyl	4-NP-β-Glc	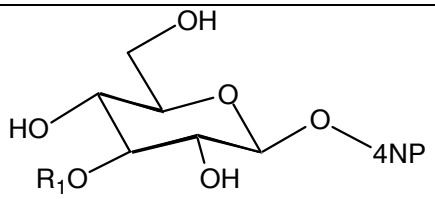 R_1=α-Xyl
α-xylosyl-F	Glucose	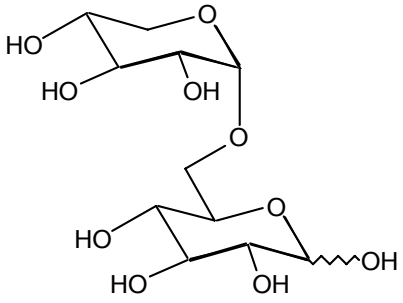
α-xylosyl-F	4-NP-β-cellobioside	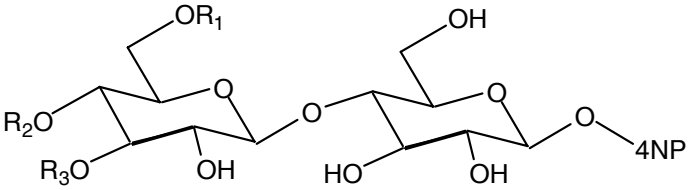 1. R_1=α-Xyl; R_2=R_3=H 2. R_1=R_2; R_3=α-Xyl 3. R_1=H; R_2=α-Xyl; R_3=H

THE α-L-FUCOSIDASE

The interest in α-L-fucosidase and fucosyl-transferase activities is due to the central role of fucosylated oligosaccharides in a variety of biological events [Staudacher et al., 1999]. α-L-Fucosidases (3.2.1.51) are *exo*-glycosidases capable of cleaving α-linked L-fucose residues from glycoconjugates, in which the most common linkages are α-(1,2) to galactose and α-(1,3), α-(1,4), and α-(1,6) to *N*-acetylglucosamine residues. These compounds are involved in a variety of biological events as growth regulators and as the glucidic part of receptors in signal transduction, cell-cell interactions, and antigenic response [Vanhooren and Vandamme 1999]. The central role of fucose derivatives in biological processes explains the interest in α-L-fucosidase and fucosyl-transferase activities.

Family 29 of glycoside hydrolases classification (GH29) groups α-L-fucosidases from plants, vertebrates, and pathogenic microbes of plants and humans [Henrissat 1991]. The first archaeal α-L-fucosidase was identified in *S. solfataricus* (reviewed in Cobucci-Ponzano et al 2008). The analysis of the genome of *S. solfataricus* [She et al. 2001] revealed the presence of

the gene fucA1, consisting of two ORFs, SSO11867 and SSO3060, encoding for polypeptides of 81 and 426 amino acid that are homologous to the *N*- and the *C*-terminal parts, respectively, of full-length bacterial and eukaryal GH29 fucosidases [Cantarel et al. 2008]. The two ORFs, actively co-transcribed *in vivo*, are separated by a -1 frameshift in a 40 bases overlap and lead to a truncated product. This suggested that the gene is expressed *in vivo* by a mechanism of *recoding*, consisiting of a localized deviation from the standard trnslational rules, called programmed -1 frameshifting [Cobucci-Ponzano et al 2003b; Cobucci-Ponzano et al 2006]. In fact, a detailed analysis of the DNA sequence of the region of overlap between the two ORFs revealed the presence of a stretch of six adenines followed by a thymine (Figure 5A) that resembles one of the heptamers involved in programmed -1 frameshifting. This is a mechanism of regulation of the expression of a minority of genes already reported in Eucarya and Bacteria, but not in Archaea, in which the modification of the translational frame takes place in a programmed way [Farabaugh 1996]. Typically, the sites cis-regulating these events consist of a 'slippery' heptameric sequence of the general form X-XXY-YYZ (codons are in the zero frame and X, Y and Z can be identical or different nucleotides) and a downstream mRNA secondary structure that promotes the pausing of the ribosome facilitating the frameshifting at the slippery sequence [Farabaugh 1996]. A similar organisation was found in the region of overlap between the ORFs SSO11867 and SSO3060, which shows the slippery sequence A-AAA-AAT immediately followed by a stem-loop (Figure 5A). In the mechanism of programmed -1 frameshifting proposed for Eukarya and Bacteria, two tRNAs, hybridised to the XXY and YYZ codons of the X-XXY-YYZ sequence, are proposed to slip simultaneously backwards on the mRNA to the -1 frame, hybridising to XXX and YYY codons. The AAT triplet, coding for Asn78 in SSO11867, corresponds to the YYZ codon, and is the last one decoded in the zero frame [Farabaugh 1996]; after this triplet, the ribosome would shift onto the TTC codon of the Phe10 (SSO3060 numbering) continuing the translation in the -1 frame (Figure 5A). To restore a single frame between the two ORFs, a T in the region following the slippery heptamer and the conservative mutation AAA →/AAG (encoding for Lys77 in SSO11867), to increase the translational fidelity by disrupting the heptameric sequence, were inserted (Figure 5B). These mutations were designed on the basis of the programmed -1 frameshifting mechanism. The single ORF obtained was used to express the enzyme in *E coli.* The native recombinant enzyme, named Ssα-fuc, showed high specificity for the 4-NP-α-L-fucoside (4-NP-α-L-Fuc) substrate at 65°C (K_M and k_{cat} values of 0.028/± 0.004 mM and 2879/± 11 s^{-1}, respectively; k_{cat}/K_M 10,250 $s^{-1}mM^{-1}$). Moreover, Ssα-fuc is thermoactive and thermostable, as expected for an enzyme from a hyperthermophilic microorganism. The optimal temperature of the enzyme is 95°C and it displayed high stability at 75°C, showing even 40% activation after 30 min of incubation and maintaining 60% residual activity after 2 h at 80°C [Cobucci-Ponzano et al 2003b]. Small angle X-ray scattering experiments revealed that *Ss*α-fuc is a nonamer of 57 kDa molecular mass subunits, showing an unusual oligomeric assembly resulting from the association of nine subunits, endowed with 3-fold molecular symmetry [Rosano et al. 2004].

It is worth noting that the mutation inserted to obtain the recombinant Ssα-fuc was designed on the basis of the programmed -1 frameshifting mechanism [Farabaugh 1996] therefore, the functionality of the full-length enzyme gave support to the hypothesis that a translational *recoding* event, known so far only in Eukarya and Bacteria [Baranov et al. 2002] could be used to regulate the expression of this gene in *S. solfataricus* [Cobucci-Ponzano et al. 2005a].

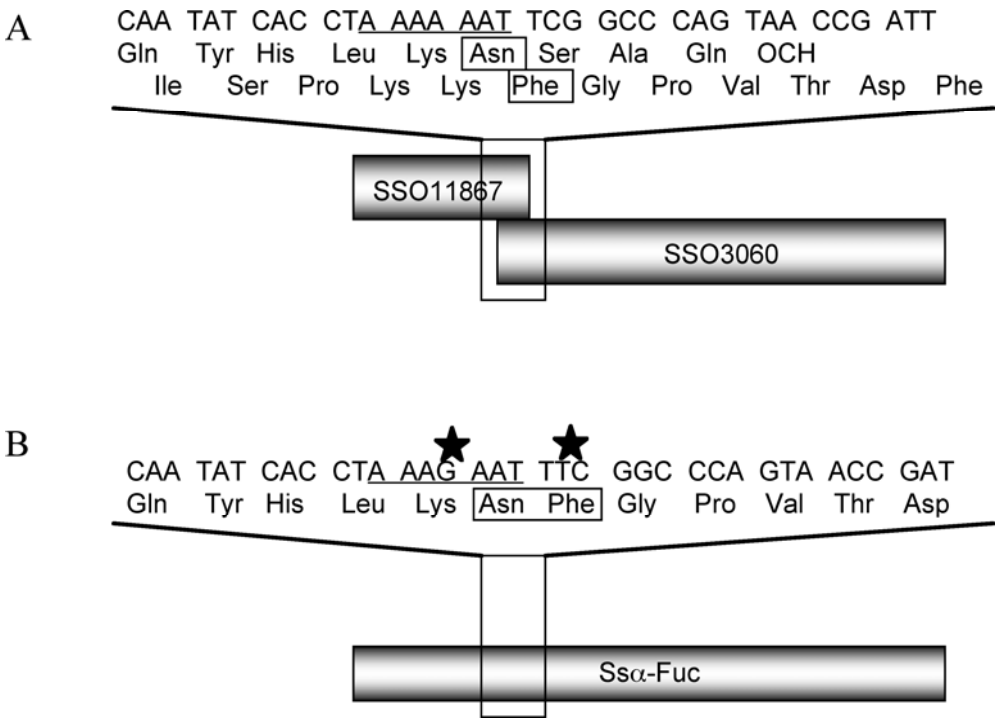

Figure 5. The a-L-fucosidase wild type gene organization (A) and preparation of the full-lenght mutant Ssa-fuc (B). The adjacent ORFs SSO11867 and SSO3060 and the sequence of overlap are shown. The slippery sequence is underlined. The mutated bases are indicated with a star.

More recently, the study of the expression of the wild-type split gene fucA1 and of its site-directed mutants in the slippery sequence demonstrated that fucA1 is expressed by programmed -1 frameshifting in both *E. coli* and *S. solfataricus*. This was the first experimental demonstration that this kind of recoding is present in the Archaea domain of life and, thus, universally conserved [Cobucci-Ponzano et al 2006].

*Ss*α-Fuc is capable of functioning in transglycosylation mode as reported for several mesophilic α-fucosidases [Murata et al 1999; Farkas et al 2000]. The synthetic ability of the thermophilic enzyme was demonstrated by using, in transfucosylation reactions, 4-NP-α-L-Fuc and 4-nitrophenyl-α-D-glucoside (4-NP-α-D-Glc) as donor and acceptor, respectively. The fucosylated products, with 14% total yield with respect to 4-NP-α-L-Fuc, were disaccharides of the acceptor in which the α-L-fucose moiety is attached at positions 2 and 3 of Glc (α-L-Fuc*p*-(1,2)-α-D-Glc-*O*-4-NP and α-L-Fuc*p*-(1,3)-α-D-Glc-*O*-4-NP, respectively) [Cobucci-Ponzano et al. 2003b]. In addition, the α-anomeric configuration of the interglycosidic linkages in the products demonstrated, for the first time by following transglycosylation reaction, that GH29 α-fucosidases follow a *retaining* reaction mechanism [Cobucci-Ponzano 2003b]. The hydrolytic activity of *Ss*α-fuc on the disaccharide α-L-Fuc-(1,3)-α-L-Fuc-*O*-4-NP revealed that the enzyme is an *exo*-glycosyl hydrolase that attacks substrates from their non-reducing end [Cobucci-Ponzano et al 2003b].

The nucleophile of GH29 α-L-fucosidases was identified, for the first time, by reactivation with sodium azide of a site-directed mutant of *Ss*α-fuc and by analyzing the anomeric configuration of the fucosyl-azide product [Cobucci-Ponzano et al. 2003c]. The

residue Asp242, invariant in all members of the family, was changed into glycine by site-directed mutagenesis to completely remove the side chain of the aspartic acid. The Ssα-fucD242G mutant showed a k_{cat} of 0.24 s^{-1}, on 4-NP-α–L-Fuc, which is 1.0 x 10^{-3} times that of the wild-type activity (245 s^{-1}). In the presence of 2M sodium azide the mutant revealed a k_{cat} value of 11 s^{-1}, indicating a 46-fold activation by azide (Table 3) [Cobucci-Ponzano et al 2003b]. This activation falls in the range of chemically rescued activities of β-glycoside hydrolases [Wang et al 1994; Viladot et al 1998]. The reactivation experiment with sodium azide indicated that the D242G mutation affected a residue involved in catalysis in *Ss*α-fuc [Cobucci-Ponzano et al. 2003c]. As mentioned in the Introduction, one of the methods used to identify the acid/base or the nucleophile of the glycosidases is to characterise the stereochemistry of the products of mutants reactivated by azide [Ly and Withers 1999]. The isolation of glycosyl-azide products with an anomeric configuration opposite to that of the substrate would allow the identification of the catalytic nucleophile of the reaction. In this case, in fact, the azide acts as nucleophile of the reaction leading to a stable product. The fucosyl-azide product obtained by the Ssα-fucD242G mutant was found in the inverted (β-L) anomeric configuration compared with the substrate. This finding allowed, for the first time, the unambiguous assignment of Asp242 and its homologous residues as the nucleophilic catalytic residues of GH29 α-L-fucosidases [Cobucci-Ponzano et al 2003c].

The azide rescue method has been used so far only for *retaining* β-D-glycosidases, whereas it has never been used for *retaining* α-(D/L)-glycosidases, and it is generally based on substrates that are very reactive (showing leaving groups with p*K*a < 5) to facilitate the first step of the reaction [Shallom et al. 2002]. Therefore, it is worth noting that Ssα-fucD242G was efficiently reactivated on 4-NP-α-L-Fuc, which shows leaving group with p*K*a = 7.18. By comparison, β-glycosidases from GH1 and GH52, mutated in the nucleophile, could not be reactivated by azide on 4-NP-glycosides, but require substrates with excellent leaving groups for an efficient chemical rescue of their activity [Moracci et al 1998; Shallom et al 2002]. The identification, for the first time, of the nucleophile of a α-L-glycosidase by following this approach showed that it could be of general applicability for *retaining* enzymes.

Table 3. Steady-state kinetic constants of wild type and mutants a-fucosidases

	k_{cat} (s^{-1})	K_M (mM)	k_{cat}/K_M (s^{-1} mM^{-1})
Wild type	287±11	0.028±0.004	10,250
D242G			
+ sodium azide	9.66±0.28	0.19±0.02	51.55
+ sodium formate	5.91±0.20	1.03±0.11	5.76
H46G	419±99	17.0±5.7	25
H123G[a]	ND[b]	ND[b]	5.96
E58G[a]	ND[b]	ND[b]	2.63
E292G	1.860±0.093	0.056±0.013	33

[a]No saturation observed on up to 25 mM 4NP-Fuc; the specificity constants were calculated from the Lineweaver-Burk plots.

[b]Not Determined.

By following a different approach, the corresponding residue of the α-L-fucosidase from the hyperthermophilic bacterium *Thermotoga maritima* (Tmα-fuc) was identified [Tarling et al. 2003]. In addition, the same authors obtained the crystal structure of complexes of Tmα-fuc with α-L-fucose and with a mechanism-based inhibitor. This study allowed the identification of Glu266 as the general acid/base catalyst of the enzyme through the inspection of the 3D-structure and the detailed kinetic characterization of active-site mutants [Sulzenbacher et al. 2004]. Remarkably, although the residues Glu266 and Glu66, with the latter being involved in the substrate binding, were both essential for activity, they were not conserved in GH29 and could be identified only through inspection of the 3D structure.

To identify other amino acids involved in the mechanism of reaction as acid/base catalyst or have different funcion in Ssα-fuc, several residues that, from sequence alignments of GH29 and from the 3D-structure of Tmα-fuc, were predicted to be involved in catalysis, were modified by site-directed mutagenesis. The kinetic characterization of the mutants Ssα-fucH46G and Ssα-fucH123G in Ssα-fuc revealed that these residues are involved in substrate binding [Cobucci-Ponzano et al. 2005b] as predicted by the crystal structure of Tmα-fuc complexed to α-L-fucose [Sulzenbacher et al. 2004]. Thus, the reduced affinity for the substrate of Ssα-fucH46G and Ssα-fucH123G mutants (Table 3) and the absence of reactivation by external ions clearly support the hypothesis that these residues interact with the hydroxyl groups bound to C4 and C2 of the substrate. In contrast, as mentioned above, the acid/base catalyst of Tmα-fuc, Glu266, and another residue, Glu66, which is also located in the active site of the enzyme, are conserved to a lesser extent in GH29. However, a pairwise alignment of Ssα-fuc and Tmα-fuc showed that these residues corresponded to Ssα-fuc Glu58 and Glu292. To determine whether Glu58 or Glu292 was the acid/base catalyst, the classical approach was followed in which the glutamic acids are replaced by glycine and the obtained mutants are kinetically characterized. The mutation of the residues Glu58 and Glu292 almost inactivates the enzymes [Cobucci-Ponzano et al 2005b]. The first diagnostic tool to test if the general acid/base has been removed by mutation is the analysis of the steady state kinetic constants; in fact, it has been pointed out that, if the acid/base of a retaining glycosidase is removed, this affects both steps of the reaction, but the effect depends on the substrate used [Ly et al 1999]. In the case of poor substrates, showing groups with worse leaving ability (aglycons with p*K*a > 8), the first step of the reaction (glycosylation) requires the participation of the general acid/base catalyst. Instead, for good substrates (aglycons with p*K*a < 8), the glycosylation step needs less assistance and the second step of the reaction (deglycosylation) is dependent on the assistance of the acid/base catalyst that functions as a general base at this stage [MacLeod et al 1996; Vallmitjana et al 2001; Li at al 2002]. The 4-NP-α-L-Fuc substrate has a p*K*a value of the leaving group 4-nitrophenol of 7.18 suggesting that the limiting step in the hydrolysis is at the borderline between glycosylation and deglycosylation and, thus, hampering to establish in advance which is the limiting step of the reaction of Ssα-fuc with the 4NP-Fuc substrate. The kinetic characterization of the Ssα-fucE58G and Ssα-fucE292G mutants gave unexpected results. In fact, the lack of saturation on the 4-NP-α-L-Fuc substrate of Ssα-fucE58G mirrors that of the acid/base mutant in *T. maritima* enzyme (Tmα-fucE266A) [Sulzenbacher et al 2004]. Instead, Ssα-fucE292G showed the classical behavior of a mutated acid/base catalyst with a 150-fold reduction of k_{cat} and a K_M almost unchanged (Table 3) [Cobucci-Ponzano et al. 2005b]. In fact, the leaving

ability of 4-NP-α-L-Fuc could be good enough to complete the glycosylation step; therefore, when the acid/base catalyst is removed, the k_{cat} value, assessing the deglycosylation step, is significantly reduced. The reduction in the catalytic rate results in accumulation of the fucosyl-enzyme intermediate and consequently determines a decrease of the K_M value [Ly et al 1999]. Presumably, the K_M did not decrease in Ssα-fucE292G because the K_M of the wild-type is already very low. It is worth noting that the removal of the residue acting as the acid/base catalyst in Tmα-fuc produced a mutant that could not be saturated with 4-NP-α-L-Fuc [Sulzenbacher et. al 2004]. This behavior has never been reported in retaining glycosidases and may suggest that the catalytic machinery of α-L-fucosidase may differ from those known so far. A second diagnostic tool for the assessment of the acid/base catalyst is the pH dependence. Typically, glycosidases have a bell-shaped pH dependence, and when the acid/base is removed, the basic limb is severely affected [Ly et al 1999]. Wild-type Ssα-fuc has a peculiar pH dependence showing a reproducible increase of activity at pH 8.6 (Figure 6). This behavior suggests that more than two ionizable groups are involved in catalysis [Debeche et al 2002]. The pH profile resulted in a large change in the case of the Ssα-fucE58G mutant, producing a typical bell-shaped curve with a pH optimum at 4.6 sharper than that of the wild-type (3.0-5.0) (Figure 6), suggesting that the removal of Glu58 unmasked the ionization of a group responsible for the basic limb (p*K*a 5.3) and possibly increased the p*K*a of the nucleophile of the reaction mainly determining the acidic limb [Cobucci-Ponzano et al. 2005b].

The most definite tool to determine the acid/base catalyst is the chemical rescue of the activity of the mutants by nucleophilic anions. Replacing the acid/base catalyst with the small non-ionizable glycine residue generally reduces dramatically the activity of the mutant. In addition, the presence of the glycine results in sufficient space in the active site so that a small nucleophile can be accommodated in this cavity after the formation of the glycosyl-enzyme intermediate. In these cases, rate enhancement and the isolation of a glycosyl-azide product with the same anomeric configuration of the substrate are expected [Ly et al 1999]. Activity rate enhancements by means of external nucleophiles is the most effective method to unequivocally identify the acid/base catalyst. Remarkably, Ssα-fucE58G was activated by more than 70-fold in the presence of sodium azide, formate, acetate, and chloride (Table 4). However, no α-fucosyl-azide product could be identified. In striking contrast, the activity of Ssα-fucE292G could not be rescued by any of the nucleophiles used. From these results, the role of the acid/base catalyst of Ssα-fuc was assigned to Glu58 and suggested that in Ssα-fuc a catalytic triad, namely, Glu58, Glu292, and Asp242, is involved in catalysis [Cobucci-Ponzano et al. 2005b].

Fucose derivatives play a central role in biological processes including the regulation of plant growth [de La Torre et al. 2002] and several physiological and pathological events in mammals [Listinsky et al. 1998; Mori et al. 1998; Noda et al. 1998]. Therefore, the efficient synthesis of fucosylated oligosaccharides has potential applications in biomedicine [Vanhooren and Vandamme 1999]. Although the preparation of a glycosynthase from a specific glycosidase is, in principle, a simple strategy, this has not led to a large variety of different enzymes and the glycosynthases available so far are limited to glycoside families GH1, 2, 5, 7, 8, 10, 16, 17, 26 and 31 out of the more than 100 glycosidase families described.

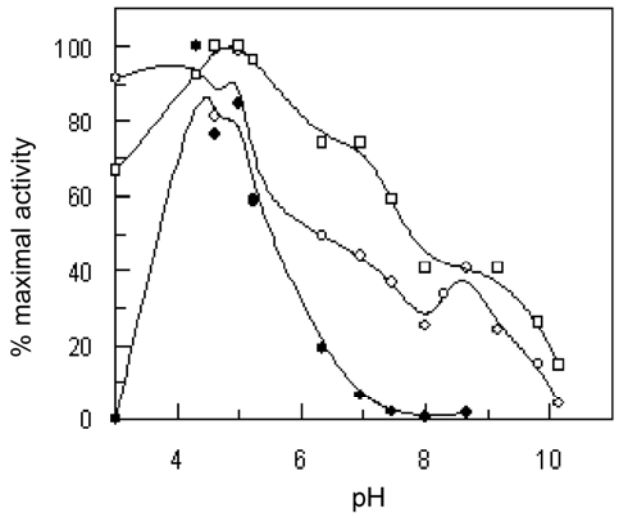

Figure 6. Dependence on pH of Ssa-Fuc and mutants The wild-type is reported as ❍, and E58G and E292G are reported as ● and ❑, respectively.

Table 4. Steady-state kinetic constants of wild type and E58G in different buffers

	k_{cat} (s^{-1})	K_M (mM)	k_{cat}/K_M ($s^{-1}M^{-1}$)	Reaction conditions	pH
wt	287±11	0.028±0.004	10,250	Sodium phosphate	6.3
	430±49	0.26±0.09	1,624	Sodium citrate	5.0
E58G	ND[a]	ND[a]	2.63	Sodium phosphate	6.3
	143±8	1.6±0.3	89	Sodium citrate	4.6
	586±43	0.62±0.18	950	Sodium acetate	4.6
	846±46	1.07±0.18	790	Sodium formate	4.6
	679±32	2.96±0.43	229	Sodium phosphate + NaN_3	6.3

[a]Not Determined; no saturation was observed with up to 25 mM 4NP-Fuc. The specificity constant was calculated from the Lineweaver-Burk plots.

In fact, there are reports of several enzymes which are recalcitrant to becoming glycosynthases: for instance, only one α-glycosynthase is known so far [Okuyama et al. 2002], and enzymes from families 29, 35 and 39 modified to this end, did not yield glycosynthases (Cobucci-Ponzano et al. 2003c; Perugino et al. 2005). Attempts to produce a fucosynthase from Ssα-fuc were not successful. The mutant Ssα-fucD242G in the presence of sodium formate acting as external nucleophile and the substrate 4-NP-α-L-Fuc produced a 16-fold reactivation, but no fucosylated oligosaccharide could be observed [Cobucci-Ponzano et al. 2003b]. The absence of synthetic products could be due to the nature of the ion used to the acidic pH exploited or to the insufficient leaving ability of the aglycon group in 4-nitrophenol to perform glycosynthesis. The analysis of the activity of the Ssα−fucD242G mutant under a variety of conditions, including sodium formate or sodium acetate buffers at different pHs, sodium formate, sodium acetate or sodium chloride as different nucleophiles in

sodium phosphate buffer, in the presence of glycoside acceptors, and at different concentrations of 4-NP-α-L-Fuc substrate donor showed that, under most of the reactivation conditions tested, the hydrolytic activity of Ssα−fucD242G was increased [Cobucci-Ponzano et al. 2008]. In particular, sodium formate was by far the best nucleophile tested while higher concentrations of 4-NP-α-L-Fuc did not improve the activity. Moreover, addition of either α- or β-D-gluco, or -galactosides to the reaction mixture did not increase the activity; instead, it hampered the chemically rescued activity, suggesting that they were poor acceptors and probably compete with 4-NP-α-L-Fuc in the donor site [Cobucci-Ponzano et al. 2008]. However, the analysis of the reaction mixture did not reveal any product of synthesis, confirming that the mutant did not work as a glycosynthase. Hyperthermophilic β-glycosynthases efficiently produced oligosaccharides when using 2-nitrophenyl-β-D-glycoside substrates, in which 2-nitrophenol, although having a pKa similar to that of 4-nitrophenol (pKa 7.22 and 7.18, respectively), can form a chelate ring by hydrogen bonding, thereby increasing the leaving ability upon protonation [Perugino et al. 2003]. However, since no α-L-fucosides containing aglycons with a leaving ability better than 4-nitrophenol are commercially available, the substrate 2-chloro-4-nitrophenyl α-L-fucopyranoside (2-Cl-4-NP-α-L-Fuc), was synthesized [Cobucci-Ponzano et al. 2008]. The aglycon 2-chloro-4-nitrophenol has a pKa of 5.45 [Tehan et al. 2002], which is noticeably lower than that of 4-nitrophenol (7.18); this difference making the 2-chloro-4-nitrophenol a much better leaving group. The steady-state kinetic constants of the mutant Ssα−fucD242G on 4-NP- and 2Cl-4-NP-α-L-Fuc in the presence of 2M sodium azide were compared with those of the wild type Ssα−fuc without external ions (Table 5).

The specificity constant k_{cat}/K_M of the mutant on 2-Cl-4-NP-α-L-Fuc was more than 7-fold higher than that found on 4-NP-α-L-Fuc [Cobucci-Ponzano et al. 2008]. This activation reflected mainly the increment in k_{cat}, while the K_M values remained almost unaltered, indicating that the affinity of Ssα-fucD242G was the same for 4-NP- and 2-Cl-4-NP-α-L-Fuc. Interestingly, the wild type on the latter substrate produced kinetic constants similar to those obtained with 4-NP-α-L-Fuc (Table 5), indicating that the different leaving abilities of the aglycons in the two substrates did not change the reaction rates [Cobucci-Ponzano et al, 2008]. In contrast, the presence of the activated leaving group greatly enhanced the activity of the mutant showing that the D242G mutation affects the first step of the reaction.

Table 5. Steady-state kinetic constants of wild type and D242G mutant Ssafuc

	k_{cat} (sec^{-1})	K_M (mM)	k_{cat}/K_M (sec^{-1} mM^{-1})
D242G+ 2M NaN_3			
4Np-Fuc	9.66±0.28	0.19±0.02	51.55
2-Cl-4-NP-α-L-Fuc	55.3±2.7	0.14±0.02	384.29
wild type			
4Np-Fuc	287±11	0.028±0.004	10,250
2-Cl-4-NP-α-L-Fuc	157±9	0.013±0.004	11,602

However, also the impaired catalytic activity of the α-L-fucosidase nucleophile mutant was significantly improved in the presence of external ions and of a synthetic aryl-α-L-fucoside substrate, the enzyme did not synthesize products and, hence, was not a glycosynthase, suggesting that a successful glycosynthetic reaction is the result of a delicate balance between the most suitable characteristics of the mutant enzyme, the substrate, and external nucleophiles [Cobucci-Ponzano et al, 2008]. The work on this enzyme is currently in progress to define the reaction conditions to obtain an α-L-fucosintase.

CONCLUSION

Traditionally, the enzymes from thermophilic sources find most of their applications in biotransformations performed under harsh conditions. However, these applications, especially in the field of carbohydrate modifications, are of real interest in only a limited number of cases. The exploration of the biodiversity of glycosidases from hyperthermophiles can widen their applicative perspective. We have shown in this chapter that glycosidases from hyperthermophiles can be useful tools for the synthesis of target oligosaccharides not only because of their intrinsic stability to heat, high molar excess of organics and nucleophilic compounds, and acid conditions, but also because of their intrinsic catalytic properties, such as efficiency in performing transglycosylation reactions, and their regio-, and stereospecificity. Our studies indicate that the expression of functional genes obtained from genomic data will give access to a vast repertoire of these enzymes. These studies confirmed the importance of the biodiversity of hyperthermophilic enzymes for the isolation of new

enzymatic activities and for increasing the development of oligosaccharides to be used for both applied and basic research.

REFERENCES

Baranov, P.V., Gurvich, O.L., Fayet, O., Prere, M.F., Miller, W.A., Gesteland, R.F., Atkins, J.F. and Giddings, M.C. (2001). RECODE: a database of frameshifting, bypassing and codon redefinition utilized for gene expression. *Nucleic Acids Res, 29*, 264–267.

Cantarel, B.L., Coutinho, P.M., Rancurel, C., Bernard, T., Lombard, V., and Henrissat, B. (2008) The Carbohydrate-Active EnZymes database (CAZy): an expert resource for Glycogenomics. *Nucleic Acids Res*. doi:10.1093/nar/gkn663

Chaillou, S., Lokman, B.C., Leer, R.J,. Posthuma, C., Postma, P.W. and Pouwels, P.H. (1998). Cloning, sequence analysis, and characterization of the genes involved in isoprimeverose metabolism in *Lactobacillus pentosus*, *J Bacteriol, 180*, 2312–2320

Cobucci-Ponzano, B., Perugino, G., Trincone, A., Mazzone, M., Di Lauro, B., Giordano, A., Rossi, M. and Moracci, M. (2003a). Applications in biocatalysis of glycosyl hydrolases from the hyperthermophilic archaeon *Sulfolobus solfataricus*. *Biocat. Biotrans*, *21*, 215-221

Cobucci-Ponzano, B., Trincone, A., Giordano, A., Rossi, M. and Moracci, M., (2003b). Identification of an archaeal alpha-L-fucosidase encoded by an interrupted gene.

Production of a functional enzyme by mutations mimicking programmed -1 frameshifting, *J Biol Chem, 278*, 14622–14631.

Cobucci-Ponzano, B., Trincone, A., Giordano, A., Rossi, M. and Moracci, M. (2003c). Identification of the catalytic nucleophile of the family 29 alpha-L-fucosidase from *Sulfolobus solfataricus* via chemical rescue of an inactive mutant. *Biochemistry, 42*, 9525-9531.

Cobucci-Ponzano, B., Rossi, M. and Moracci, M. (2005a) Recoding in archaea. *Mol Microbiol. 55*, 339-348.

Cobucci-Ponzano, B., Mazzone, M., Rossi, M. and Moracci, M. (2005b) Probing the catalytically essential residues of the alpha-L-fucosidase from the hyperthermophilic archaeon *Sulfolobus solfataricus*. *Biochemistry*, *44,* 6331-6342.

Cobucci-Ponzano, B., Conte, F., Benelli, D., Londei, P., Flagiello, A., Monti, M., Pucci, P., Rossi, M. and Moracci, M. (2006). The gene of an archaeal alpha-L-fucosidase is expressed by translational frameshifting. *Nucleic Acids Res, 34*, 4258-4268.

Cobucci-Ponzano, B., Conte, F., Mazzone, M., Bedini, E., Corsaro, M. M., Rossi, M. and Moracci, M. (2008). Design of new reaction conditions for characterization of a mutant thermophilic **α**-l-fucosidase. *Biocatalysis and Biotransformation*, *26*, 18-24.

Crombie, H.J., Chengappa, S., Hellyer, A. and Reid, J.S.G. (1998). A xyloglucan oligosaccharide-active, transglycosylating beta-D-glucosidase from the cotyledons of nasturtium (*Tropaeolum majus* L) seedlings — purification, properties and characterization of a cDNA clone. *Plant J.,* 15, 27–38.

Debeche, T., Bliard, C., Debeire, P. and O'Donohue, M. J. (2002). Probing the catalytically essential residues of the α-L-arabinofuranosidase from *Thermobacillus xylanilyticus*. *Protein Eng. 1*, 21-28.

de La Torre, F., Sampedro, J., Zarra, I. and Revilla, G. (2002). AtFXG1, an Arabidopsis gene encoding alpha-L-fucosidase active against fucosylated xyloglucan oligosaccharides. *Plant Physiol. 128*, 247–255

Faik, A., Price, N.J., Raikhel, N.V. and Keegstra, K. (2002). An Arabidopsis gene encoding an α-xylosyltransferase involved in xyloglucan biosynthesis. *Proc. Natl. Acad. Sci. USA,* 99, 7797–7802.

Farabaugh, P.J. (1996) Programmed translational frameshifting. *Annu. Rev. Genet.*, *30*, 507-528.

Farkas, E., Thiem, J. and Ajisaka, K., (2000). Enzymatic synthesis of fucose-containing disaccharides employing the partially purified alpha-L-fucosidase from *Penicillium multicolor. Carbohydr. Res., 328*, 293–299.

Fischer, L., Bromann, R., Kengen, S.W.M., de Vos, W.M. and Wagner, F. (1996) Catalytical potency of b-glucosidase from the extremophile *Pyrococcus furiosus* in glucoconjugate synthesis. *Biotechnology 14*, 88–91.

Gijsen, H.J.M., Qiao, L., Fitz, W. and Wong, C.H. (1996) Recent advances in the chemoenzymatic synthesis of carbohydrates and carbohydrate mimetics. *Chem Rev, 96*, 443–473.

Gloster, T.M., Roberts, S., Ducros, V.M., Perugino, G., Rossi, M., Hoos, R., Moracci, M., Vasella, A. and Davies, G.J. (2004) Structural studies of the beta-glycosidase from *Sulfolobus solfataricus* in complex with covalently and noncovalently bound inhibitors. *Biochemistry*, *43*, 6101-6109.

Hancock, S.M., Vaughan, M.D. and Withers, S.G. (2006) Engineering of glycosidases and glycosyltransferases. *Curr Opin Chem Biol. 10*, 509-519.

Henrissat, B. and Bairoch, A. (1993) New families in the classification of glycosyl hydrolases based on amino acid sequence similarities, *Biochem. J. 293*, 781-788.

Henrissat, B. and Davies, G. (1997) Structural and sequence-based classification of glycoside hydrolases, *Curr. Opin. Struct. Biol. 7*, 637-644.

Henrissat, B. (1991) A classification of glycosyl hydrolases based on amino acid sequence similarities, *Biochem. J.,* 280, 309–316.

Hough, D.W. and Danson, M.J. Extremozymes. (1999) *Curr Opin Chem Biol*, *3*, 39-46.

Kato, Y. and Matsuda, K. (1980) Structure of oligosaccharides obtained by controlled degradation of mung bean xyloglucan with acid and *Aspergillus oryzae* enzyme preparation. *Agric Biol Chem 44* , 1751–1758

Kiho, T., Katsuragawa, M., Nagai, K., Ugai, S. and Haga, M. (1992) Structure and antitumor activity of a branched (1-3)-β-D-glucan from the alkaline extract of *Amanita muscaria. Carbohydr. Res. 224*, 237-243.

Li, Y. K., Chir, J., Tanaka, S. and Chen, F. Y. (2002). Identification of the general acid/base catalyst of a family 3 *β*-glucosidase from *Fla*V*obacterium meningosepticum*, *Biochemistry 41*, 2751-2759.

Listinsky, J.J., Siegal, G.P. and Listinsky, C.M. (1998). Alpha-L-fucose: a potentially critical molecule in pathologic processes including neoplasia. *Am J Clin Pathol, 110,* 425–440.

Lorences, E.P. and Fry, S.C. (1994). Sequencing of xyloglucan oligosaccharides by partial Driselase digestion: the preparation and quantitative and qualitative analysis of two new tetrasaccharides. *Carbohydr Res. 263*, 285-293.

Lower, B.H. and Kennelly, P.J. (2002) The membrane-associated protein-serine/threonine kinase from Sulfolobus solfataricus is a glycoprotein. *J Bacteriol*, *184,* 2614-2619.

Ly, H. D. and and Withers, S. G. (1999) Mutagenesis of glycosidases. *Annu. Re*V. *Biochem. 68*, 487-522.

Malet, C., and Planas, A. (1998) From beta-glucanase to beta-glucansynthase: glycosyl transfer to alpha-glycosyl fluorides catalyzed by a mutant endoglucanase lacking its catalytic nucleophile. *FEBS Lett. 440*, 208-212.

Moracci, M., Capalbo, L., Ciaramella, M., and Rossi, M. (1996) Identification of two glutamic acid residues essential for catalysis in the β-glycosidase from the thermoacidophilic archaeon *Sulfolobus solfataricus*. *Protein Eng. 12*, 1191-1195.

Moracci, M., Ciaramella, M. and Rossi, M. (2001) β-Glycosidase from *Sulfolobus solfataricus. Methods Enzymol. 330*, 201-215.

McCarter, J.D. and Withers, S.G. (1994) Mechanisms of enzymatic glycoside hydrolysis. *Curr Opin Struct Biol, 4*, 885–892.

Mackenzie, L.F., Wang, Q., Warren, R.A.J., and Withers, S.G. (1998) Glycosynthases: mutant glycosidases for oligosaccharide synthesis. *J. Am. Chem. Soc. 120*, 5883-5884.

MacLeod, A. M., Tull, D., Rupitz, K., Warren, R. A. and Withers, S. G. (1996) Mechanistic consequences of mutation of active site carboxylates in a retaining *β*-1,4-glycanase from *Cellulomonas fimi*, *Biochemistry 35*, 13165-13172.

McIntosh, L.P., Hand, G., Johnson, P.E., Joshi, M.D., Korner, M., Plesniak, L.A., Ziser, L., Wakarchuk, W.W. and Withers, S.G. (1996) The pKa of the general acid/base carboxyl

group of a glycosidase cycles during catalysis: a 13C-NMR study of *Bacillus circulans* xylanase. *Biochemistry 35*, 9958-9966.

Moracci, M., Ciaramella, M., Nucci, R., Pearl, L.H., Sanderson, I., Trincone, A. and Rossi, M. (1994) Thermostable β-glycosidase from *Sulfolobus solfataricus*. *Biocatalysis, 11*, 89-103.

Moracci, M., Trincone, A., Perugino, G., Ciaramella, M. and Rossi, M. (1998) Restoration of the activity of active-site mutants of the hyperthermophilic beta-glycosidase from *Sulfolobus solfataricus*: dependence of the mechanism on the action of external nucleophiles. *Biochemistry, 37*-17262 17270.

Moracci, M., Cobucci-Ponzano, B., Trincone, A., Fusco, S., De Rosa, M., van der Oost, J., Sensen, C.W., Charlebois, R.L. and Rossi M (2000) Identification and molecular characterization of the first a-xylosidase from an archaeon. *J Biol Chem 275*, 22082–22089

Moracci, M., Trincone, A., Cobucci-Ponzano, B., Perugino, G., Ciaramella, M., and Rossi, M. (2001) Enzymatic synthesis of oligosaccharides by two glycosyl hydrolases of *Sulfolobus solfataricus*. *Extremophiles*. 5:145-152.

Mori, E., Hedrick, J.L., Wardrip, N.J., Mori, T. and Takasaki, S. (1998) Occurrence of reducing terminal N-acetylglucosamine 3-sulfate and fucosylated outer chains in acidic N-glycans of porcine zona pellucida glycoproteins. *Glycoconj J, 15*, 447–456.

Noda, K., Miyoshi, E., Uozumi, N., Gao, C.X., Suzuki, K., Hayashi, N., Hori, M. and Taniguchi, N. (1998) High expression of alpha-1-6 fucosyltransferase during rat hepatocarcinogenesis. *Int J Cancer, 75*, 444–450.

Murata, T., Morimoto, S., Zeng, X., Watanabe, S. and Usui, T. (1999) Enzymatic synthesis of alpha-L-fucosyl-N-acetyllactosamines and 3'-O-alpha-L-fucosyllactose utilizing alpha-L-fucosidases. *Carbohydr Res, 320*, 192-199.

Okuyama, H. Mori, K. Watanabe, A. and Kimura, S. Chiba. (2002). α–glucosidase mutant catalyzes 'α-glycosynthase'-type reaction. *Biosci Biotechnol Biochem*, *66,* 928-933.

Perugino, G., Trincone, A., Giordan,o A., van der Oost, J., Kaper, T., Rossi, M., and Moracci, M., (2003) Activity of hyperthermophilic glycosynthases is significantly enhanced at acidic pH. *Biochemistry*, *42*, 8484-8493.

Perugino, G., Trincone, A., Rossi, M., and Moracci, M., (2004) Oligosaccharide synthesis by glycosynthases. *Trends Biotechnol*, *1*, 31-37.

Perugino, G., Cobucci-Ponzano, B., Rossi, M., and Moracci, M, (2005) Recent advances in the oligosaccharide synthesis promoted by catalytically engineered glycosidases. *Ad. Synth. Catal.*, *347*, 941-950.

Perugino, G., Falcicchio, P., Corsaro, M.M., Matsui, I., Parrilli, M., Rossi, M., and Moracci, M., (2006) Preparation of a glycosynthase from the β-glycosidase of the hyperthermophilic Archaeon *Pyrococcus horikoshii*. *Biocat, Biotrans., 24*, 23-29

Pouwels, J., Moracci, M., Cobucci-Ponzano, B., Perugino, G., van der Oost, J., Kaper, T., Lebbink, J.H., de Vos, W.M., Ciaramella, M., and Rossi, M. (2000) Activity and stability of hyperthermophilic enzymes: a comparative study on two archaeal β-glycosidases. *Extremophiles, 3*, 157-164.

Sears, P. and Wong, C.H. (1996) Intervention of carbohydrate recognition by proteins and nucleic acids, *Proc. Natl. Acad. Sci. USA, 93*, 12086–12093.

Shallom, D., Belakhov, V., Solomon, D., Shoham, G., Baasov, T., and Shoham, Y. (2002) Detailed kinetic analysis and identification of the nucleophile in alpha-L-arabinofuranosidase from Geobacillus stearothermophilus T-6, a family 51 glycoside hydrolase. *J. Biol. Chem. 277*, 43667-43673.

She, Q., Singh, R. K., Confalonieri, F., Zivanovic, Y., Allard, G., Awayez, M. J., Chan-Weiher, C. C., Clausen, I. G., Curtis, B. A., De Moors, A., Erauso, G., Fletcher, C., Gordon, P. M., Heikamp-de Jong, I., Jeffries, A. C., Kozera, C. J., Medina, N., Peng, X., Thi-Ngoc, H. P., Redder, P., Schenk, M. E., Theriault, C., Tolstrup, N., Charlebois, R. L., Doolittle, W. F., Duguet, M., Gaasterland, T., Garrett, R. A., Ragan, M. A., Sensen, C. W. and Van der Oost, J. (2001) The complete genome of the crenarchaeon Sulfolobus solfataricus P2. *Proc. Natl. Acad. Sci. U. S. A., 98,* 7835–7840

Sinnot, M.L. (1990) Catalytic mechanisms of enzymic glycosyl transfer. *Chem Rev, 90,* 1171–1202

Staudacher, E., Altmann, F., Wilson, I.B. and März, L. (1999) Fucose in N-glycans: from plant to man.*Biochim Biophys Acta. 147,* :216-236.

Sulzenbacher, G., Bignon, C., Nishimura, T., Tarling, C. A., Withers, S. G., Henrissat, B. and Bourne, Y. (2004) Crystal structure of *Thermotoga maritima* α-L-fucosidase. Insights into the catalytic mechanism and the molecular basis for fucosidosis, *J. Biol. Chem. 279*, 13119-13128.

Tarling, C. A., He, S., Sulzenbacher, G., Bignon, C., Bourne, Y., Henrissat, B. and Withers, S. G. (2003) Identification of the catalytic nucleophile of the family 29 α-L-fucosidase from *Thermotoga maritima* through trapping of a covalent glycosylenzyme intermediate and mutagenesis, *J. Biol. Chem. 278*, 47394-47399.

Tehan, B.G., Lloyd, E.J., Wong, M.G., Pitt, W.R., Montana, J.G., Manallack, D.T. and Gancia, E. (2002). Estimation of pKa using semiempirical molecular orbital methods. part 1: application to phenols and carboxylic acids. *Quant Struct-Act Relat, 21,* 457-472.

Toshima, K., Tatsuta, K. (1993) Recent progress in *O*-glycosylation methods and its application to natural products synthesis. *Chem Rev* , *93*, 1503–1531

Trincone, A., Nicolaus, B., Lama, L. and Gambacorta, A. (1991) Stereochemical studies of enzymatic transglycosylation using *Sulfolobus solfataricus*. *J Chem Soc Perkin Trans, 1*, 2841–2844

Trincone, A., Cobucci-Ponzano, B., Di Lauro, B., Rossi, M., Mitsuishi, Y. and Moracci, M. (2001) Enzymatic synthesis and hydrolysis of xylogluco-oligosaccharides using the first archaeal alpha-xylosidase from *Sulfolobus solfataricus*. *Extremophiles*, *5,* 277-282.

Trincone, A., Perugino, G., Rossi, M., and Moracci, M. (2000) A novel thermophilic glycosynthase that effects branching glycosylation. *Bioorg. Med. Chem. Lett*., *10*, 365-368.

Vallmitjana, M., Ferrer-Navarro, M., Planell, R., Abel, M., Ausin, C., Querol, E., Planas, A. and Perez-Pons, J. A. (2001) Mechanism of the family 1 *β*-glucosidase from *Streptomyces* sp: Catalytic residues and kinetic studies, *Biochemistry 40*, 5975-5982.

Vanhooren, P.T. and Vandamme, E.J. (1999) L-Fucose: occurrence, physiological role, chemical, enzymatic and microbial synthesis. *J. Chem. Technol. Biotechnol., 74*, 479–497.

Varki, A. (1993) Biological roles of oligosaccharides: all of the theories are correct, *Glycobiology, 2*, 97–130.

Viladot, J.L., de Ramon, E., Durany, O. and Planas, A. (1998) Probing the mechanism of Bacillus 1,3-1,4-beta-D-glucan 4-glucanohydrolases by chemical rescue of inactive mutants at catalytically essential residues. *Biochemistry*, *37*, 11332-11342

Wang, Q., Graham, R.W., Trimbur, D., Warren, R.A.J. and Withers, S.G. (1994). Changing enzymatic reaction mechanisms by mutagenesis: conversion of a retaining glucosidase to an inverting enzyme. *J Am Chem Soc, 116,* 11594 11595.

White, A. and Rose, D.R. (1997) Mechanism of catalysis by retaining β-glycosyl hydrolases. *Curr Opin Struct Biol, 7*, 645–651

Withers, S.G. and Aebersold, R. (1995) Approaches to labeling and identification of active site residues in glycosidases. *Protein Sci.* , *4*, 361-372

Withers, S.G. (2001) Mechanisms of glycosyl transferases and hydrolases. *Carb. Polymers., 44*, 325–337.

Zechel, D.L. and Withers, S.G. (2000) Glycosidase mechanisms: anatomy of a finely tuned catalyst. *Acc Chem Res, 33*, 11–18

Zopf, D. and Roth, S. (1996) Oligosaccharide anti-infective agents. *Lancet*, *347*, 1017–1021.

In: Biochemistry and Histocytochemistry… ISBN: 978-1-60876-283-5
Editors: S. Fuchs, M. Auer, pp. 323-334 © 2010 Nova Science Publishers, Inc.

Chapter 13

STUDIES ON THE THERMAL STABILITY OF THE THERAPEUTIC ENZYME L-ASPARAGINASE FROM ERWINIA CAROTOVORA

Katerina Lappa, Georgia A. Kotzia and Nikolaos E. Labrou*
Laboratory of Enzyme Technology, Department of Agricultural Biotechnology, Agricultural University of Athens, Iera Odos 75, 11855-Athens, Greece

ABSTRACT

L-Asparaginase (E.C.3.5.1.1, L-ASNase) catalyzes the hydrolysis of L-Asn, producing L-Asp and ammonia. This enzyme is an anti-neoplastic agent; it is used extensively in the chemotherapy of acute lymphoblastic leukemia (ALL). L-asparaginase from *Erwinia carotovora* (*Eca*L-ASNase) was cloned and expressed in *E. coli*. The enzyme was purified to homogeneity by a two-step procedure comprising cation-exchange chromatography and affinity chromatography on immobilized L-asparagine. The purified enzyme was subjected to thermal inactivation studies. Thermodynamic parameters (E_a, $\Delta H^{\neq}$ and $\Delta S^{\neq}$) for the thermal inactivation process of the enzyme were determined. It was concluded that the low thermal stability of the enzyme is of entropic origin and is most likely due to structural determinants that cause a higher degree of local disorders at specific locations.

Keywords: *L-asparaginase; hydrolase; enzyme engineering; leukaemia; thermal stability*.

* Corresponding author.Laboratory of Enzyme Technology, Department of Agricultural Biotechnology, Agricultural University of Athens, Iera Odos 75, 11855 – Athens, Greece. Email: Lambrou@aua.gr. Fax: +30-210-5294308.

ABBREVIATIONS USED

ALL, acute lymphoblastic leukaemia;
L-ASNase,
L-asparaginase;
*Eca*L-ASNase,
L-asparaginase from *Erwinia carotovora*;
PAGE, polyacryamide gel electrophoresis;
SDS, sodium dodecyl sulfate.

1. INTRODUCTION

L-asparaginase (L-asparagine amino hydrolase, L-ASNase, E.C.3.5.1.1) catalyzes the hydrolysis of L-asparagine to L-aspartic acid and ammonia. L-ASNase has been a clinically acceptable anti tumor agent for the effective treatment of acute lymphoblastic leukemia (ALL) and lymphosarcoma (Graham, 2003). L-Asn is an essential amino acid for the growth of tumor cells, whereas the growth of normal cells is not dependent on its requirement as it can be synthesized in amounts sufficient for their metabolic needs with their own enzyme L-asparagine synthetase (Duval et al., 2002). The action of L-ASNase deprives tumor cells of an important growth factor and they fail to survive (Lee et al., 1989). However, L-ASNase therapy is often accompanied by serious side effects. In addition to hypersensitivity reactions, long-term treatment may lead to liver damage, acute pancreatitis, and other disturbances. It is thought that many of these effects are caused by its high glutaminase activity (Howard and Carpenter, 1972). Glutamine is the major transport form of amino nitrogen in the blood and also an amino group donor for many biosynthetic reactions. A prolonged decline of plasma glutamine levels, therefore, impairs a variety of biochemical functions, especially those of the liver. In view of these facts, enzymes best suited for ALL treatment would be those with a high activity, a low *Km*, and a strong preference for asparagine over glutamine (Hawkins et al., 2004). The enzyme isolated and recently characterized from *Erwinia carotovora* (*Eca*L-ASNase) attracts attention since it is pharmacologically active and is as effective as the enzyme from *E. coli* in the treatment of ALL. In addition, *Eca*L-ASNase exhibits very low glutaminase activity compared to *E. coli* and *E. chrisanthemii* enzymes (Krasotkina et al., 2004; Kotzia and Labrou, 2005).

Bacterial-type L-asparaginases can be further classified into two subtypes: type I and type II (Kozak et al., 2002). Two types of L-ASNases, found in *E. coli*, have been designated AsnI and AsnII in *E. coli* K-12. Type I was found to be expressed constitutively, whereas type II is induced by anaerobiosis. Only the type II L-asparaginases show anti-tumor activity. All bacterial type II L-asparaginases are active as homotetramers containing approximately 330 amino acids per monomer and four identical non-cooperative active sites (Palm et al., 1996; Aung et al., 2000). Two active sites are formed at the dimerization interface between the A and C subunits (as well as between B and D), the so-called intimate dimer, and two such intimate dimers form a tetramer with 222 symmetry. Each L-ASNase subunit consists of two easily identifiable α/β domains, a larger N-terminal and a smaller C-terminal domain, connected by a loop consisting of about twenty residues (Aghaiypour et al., 2001a,b).

In an effort to determine the structural stability and the physicochemical properties of the recombinant L-ASNase from *Erwinia carotovora*, purification and heat inactivation studies were carried.

2. MATERIALS AND METHODS

2.1. Materials

L-Asn and L-Gln were obtained from Serva (Heidelberg, Germany). Nessler's reagent was obtained from Fluka (Taufkirchen, Germany). 1,4-Butanediol diglycidyl ether and all other reagents and chromatographic materials were of analytical grade and obtained from Sigma-Aldrich (USA).

2.2. Methods

2.2.1. Cloning, Expression and Purification

Cloning and expression of *Eca*L-ASNase in *E. coli* BL21pLysS cells were carried out as described in Kotzia and Labrou (2005).

2.2.2. Enzyme Purification

The purification of the *Eca*L-ASNase was carried out essentially according to the published procedure (Kotzia and Labrou, 2005; Kotzia et al., 2007). Briefly, enzyme purification was accomplished at 4 °C by a two-step procedure, comprising of a purification step using a CM-Sepharose CL6B, followed by affinity chromatography on immobilized L-Asparagine-Sepharose CL 6B column.

2.2.2.1. Synthesis of L-Asparagine-Sepharose CL 6B Affinity Adsorbent

L-asparagine-Sepharose CL 6B affinity adsorbent was synthesized as described in Kotzia and Labrou (2005) using 1,4-butanediol diglycidyl ether as a coupling agent. Briefly, to washed cross-linked agarose gel (Sepharose CL6B, 5g) was added 5 mL of 0.6 M, sodium hydroxide solution. The suspension was tumbled for 4 h at room temperature prior to adding 5 mL of 1,4-butanediol diglycidyl ether, and 10 mg of solid sodium borohydrite ($NaBH_4$). The reaction was left to proceed with slow agitation at 25 °C overnight. Suction filtration was used to recover and wash (ddH_2O, 100 mL) the activated gel. To the washed activated gel was added a solution of L-Asn (0.6 g dissolved in 10 mL of 0.5 M sodium carbonate buffer, pH 10). The coupling reaction was allowed to proceed at room temperature for 64 h with slow agitation. After completion of the reaction, the gel was recovered by suction filtration, washed with ddH_2O and stored in 20% ethanol at 4 ºC.

2.2.2.2. Chromatographic Procedure

Crude enzyme extract (20 mM potassium phosphate buffer, pH 5.5, 1.8 mL, 17.9 units) was applied to a column of CM-Sepharose CL 6B which was previously equilibrated with 20 mM potassium phosphate buffer, pH 5.5. Non-adsorbed protein was washed off with 20 mL

equilibration buffer. Bound *Eca*L-ASNase was eluted with 20 mM potassium phosphate buffer, pH 7.5 (12 mL). Collected fractions were assayed for *Eca*L-ASNase activity and protein (Bradford method). To the eluted *Eca*L-ASNase activity from the previous column was added ddH_20 to reduce the ionic strength of the solution and directly applied on L-Asn-Sepharose CL 6B affinity column which was previously equilibrated with 5 mM potassium phosphate buffer, pH 7.5. Non-adsorbed protein was washed off with 10 mL of equilibration buffer followed by 3 mL of the same buffer containing L-Asn (10 mM). Bound Collected fractions (2 mL) were assayed for *Eca*L-ASNase activity and protein (Bradford method).

2.2.3. Assay of Enzyme Activity

Enzyme assays were performed at 37°C at a Hitachi U-2000 double beam uv-vis spectrophotometer carrying a thermostated cell holder (10 mm pathlength). Activities were measured by determining the rate of ammonia formation, by coupling with glutamate dehydrogenase (GDH), according to (Balcao et al., 2001; Kotzia and Labrou, 2005). Alternatively, the rate of ammonia formation was measured at 37 ºC using the Nessler's reagent (Wriston, 1973). One unit of Asparaginase activity is defined as the amount of enzyme that liberates 1 μmol of ammonia from Asn per minute at 37°C.

*2.2.4. Thermal Inactivation Studies of Eca*L-Asnase

Thermal inactivation of *Eca*L-ASNase was monitored by activity measurements. Samples of the enzyme, in potassium phosphate buffer (10mM, pH 7), were incubated at a range of temperatures from 35 ºC to 50 ºC. The rates of inactivation were followed by periodically removing samples for assay of enzymatic activity. Observed rates of inactivation (k_{in}) were deduced from plots of log (% remaining activity) *versus* time. To obtain the thermodynamic parameters from these inactivation rates, two analyses were carried out according to Stein and Staros (1996). An empirical activation energy, E_a, for the inactivation process can be obtained from an Arrhenius plot according to the equation:

$$\ln(k_{in}) = -\frac{E_a}{RT} + C \tag{1}$$

where k_{in} is the inactivation rate, R is the gas constant, T is the absolute temperature and C is a constant. From transition-state theory, the activation Gibbs free energy change from the initial state to the transition state for the inactivation process, $\Delta G^{\neq}$, is:

$$\Delta G^{\neq} = -RT\ln\left(\frac{hk_{in}}{k_b T}\right) \tag{2}$$

where h is Planck's constant and k_b is Boltzmann's constant. The activation enthalpy, $\Delta H^{\neq}$, and the activation entropy, $\Delta S^{\neq}$, for the change from the initial state to the transition state for the inactivation process can be obtained from the equation:

$$\Delta G^{\neq} = \Delta H^{\neq} - T\Delta S^{\neq} \tag{3}$$

Substituting equation (2) into equation (3) and rearranging yields:

$$\ln\left(\frac{hk_{in}}{k_b T}\right) = \frac{\Delta H^{\neq}}{RT} + \frac{\Delta S^{\neq}}{R} \tag{4}$$

Under the assumption that $\Delta H^{\neq}$ and $\Delta S^{\neq}$ are independent of T, their values can be obtained from the slope and intercept, respectively, of a semi-log plot by the use of equation (4) (Eyring equation).

3. RESULTS AND DISCUSSION

3.1. Enzyme Purification

*Eca*L-ASNase was purified in a two-step procedure. As a first step in the purification scheme, a cation-exchange chromatography on CM-Sepharose column was employed as described in Kotzia and Labrou (2005). Non-pre-treated enzyme extract was applied directly to the cation-exchanger column equilibrated at pH 5.5. The theoretical isoelectric point of *Eca*L-ASNase is 8.5, thus at pH 5.5 the enzyme quantitatively adsorbed to the cation-exchanger. As a next step in the purification procedure, affinity chromatography L-asparagine-Sepharose CL 6B was employed. The affinity adsorbent was synthesized as shown in Figure 1A using 1,4-butanediol diglycidyl ether as a coupling agent. The enzyme was absorbed at pH 7.5 and eluted specifically using L-Asn (10 mM) as eluting agent. A typical purification is shown in Table 1. The purity of the final *Eca*L-ASNase preparation was evaluated by SDS-PAGE, which showed the presence of a single polypeptide chain (Figure 1B).

3.2. Kinetic Stability of *Eca*L-Asnase

Kinetic analysis of the thermal inactivation of the *Eca*L-ASNase was carried out at temperatures between 35ºC and 50ºC. A typical example for the course of thermal inactivation is shown in Figure 2.

One approach to interpretation of the data is to assume an unfolding limited first-order kinetic process, which can be analyzed using the Arrhenius equation (Stein and Staros, 1996; Twomey and Doonan, 1997). There are several possible mechanisms of inactivation, including chemical modification and protein unfolding. Analysis of the inactivation rate data using the Arrhenius plot yields an empirical activation energy E_a (or more precisely, the enthalpic contribution to the activation energy), which —for reactions in solution— is essentially equivalent to the activation enthalpy $\Delta H^{\neq}$ (Tinoco et al., 1985; Stein and Staros, 1996). An Arrhenius plot of the inactivation rate data (Figure 3A) yields an E_a value of 68.5

kJ/mol (Table 2). This value is comparable to the previously measured activation energies for unfolding of soluble proteins (Segel, 1975; Stein and Staros, 1996; Twomey and Doonan, 1997).

If one makes the simplifying assumption that the inactivation process occurs through a single transition state, transition state theory can be applied, which yields not only the activation enthalpy ($\Delta H^{\neq}$) but also the activation entropy ($\Delta S^{\neq}$) of the process (Stein and Staros, 1996). An Eyring plot of the rates of inactivation observed in the 35–50°C temperature range (Figure 3B) yields $\Delta H^{\neq}$ and $\Delta S^{\neq}$ values, and the results are listed in Table 2.

A

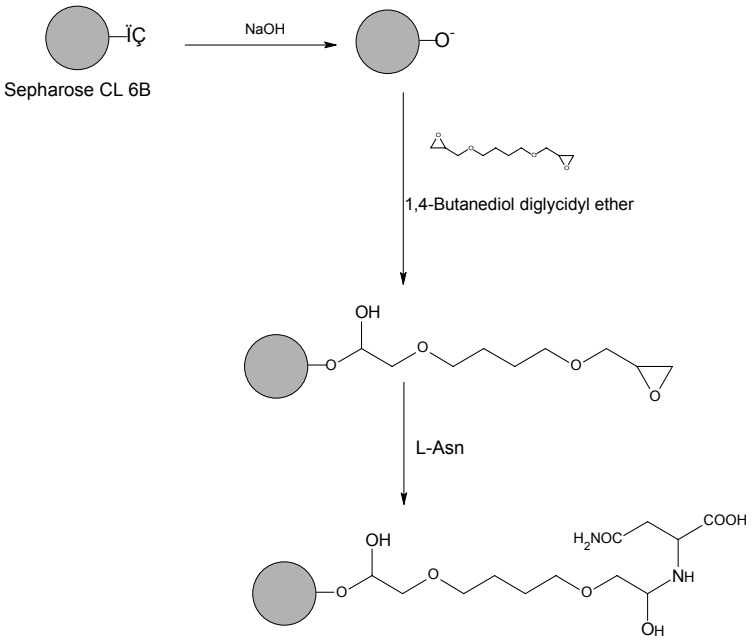

B

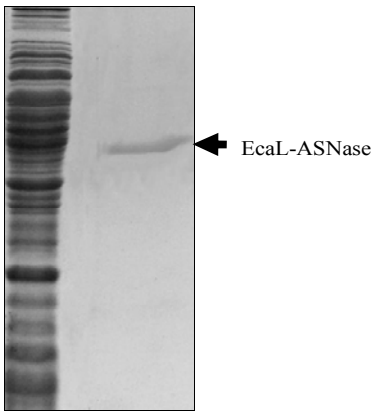

Figure 1. A. The synthetic route that is used for the synthesis of L-Asn-Sepharose CL 6B affinity adsorbent. B: SDS-polyacrylamide gel electrophoresis of *Eca*L-ASNase purification. Lane 1: *E. coli* crude extract after induction with 1 mM IPTG; Lane 2: *EcaL*-ASNase purified according to the two-step procedure using cation-exchange and affinity chromatography.

Table 1. Purification of *Eca*L-ASNase using a two-step procedure employing cation-exchange chromatography on CM-Sepharose and affinity chromatography on immobilized L-Asn. The procedure was carried out at 4ºC

Step	Volume (mL)	Units	Protein (mg)	Specific activity (Units/mg)	Purification (fold)	Yield (%)
Crude extract	1.8	17.94	25.02	0.717	1	100
Cation-exchange chromatography on CM-Sepharose	3	16.19	0.63	25.62	35.74	90.28
Affinity chromatography on immobilized L-Asn-Sepharose CL 6B column	3	4.16	0.023	177.56	247.70	31

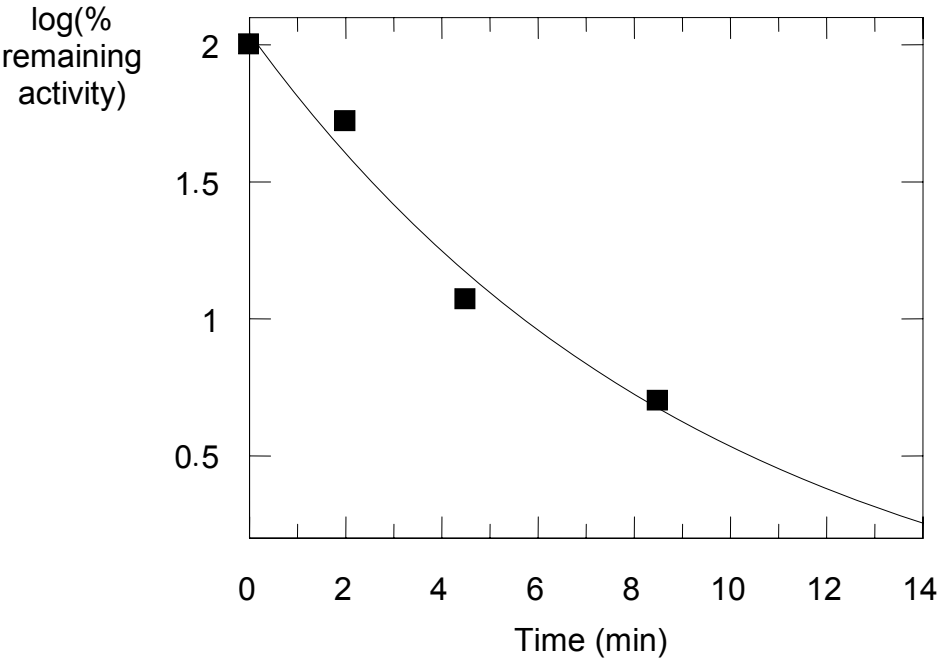

Fgure 2. Time course of the thermal inactivation of *Eca*L-ASNase at 50 ºC. The rate of inactivation was followed by periodically removing samples for assay of enzymatic activity.

A

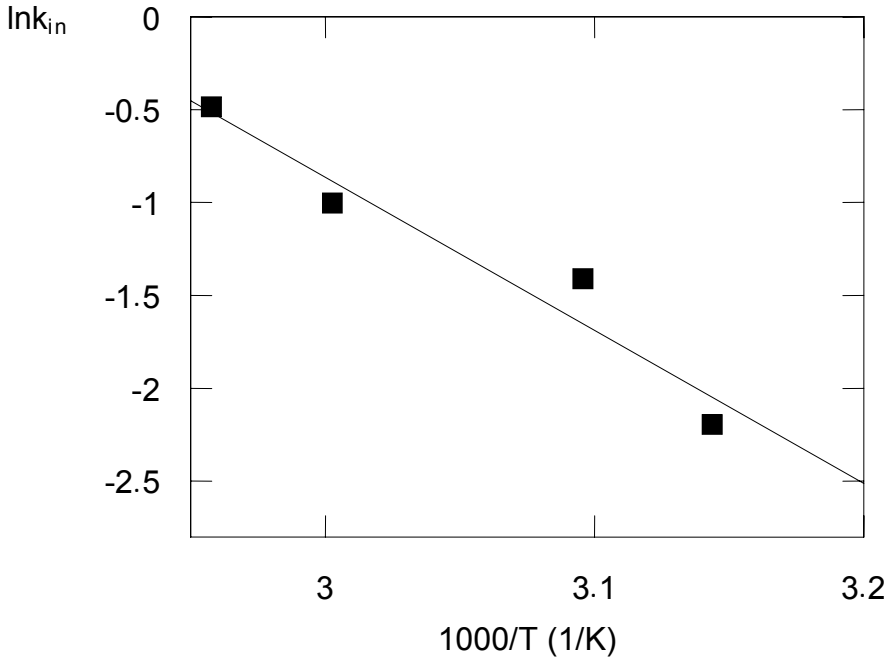

B

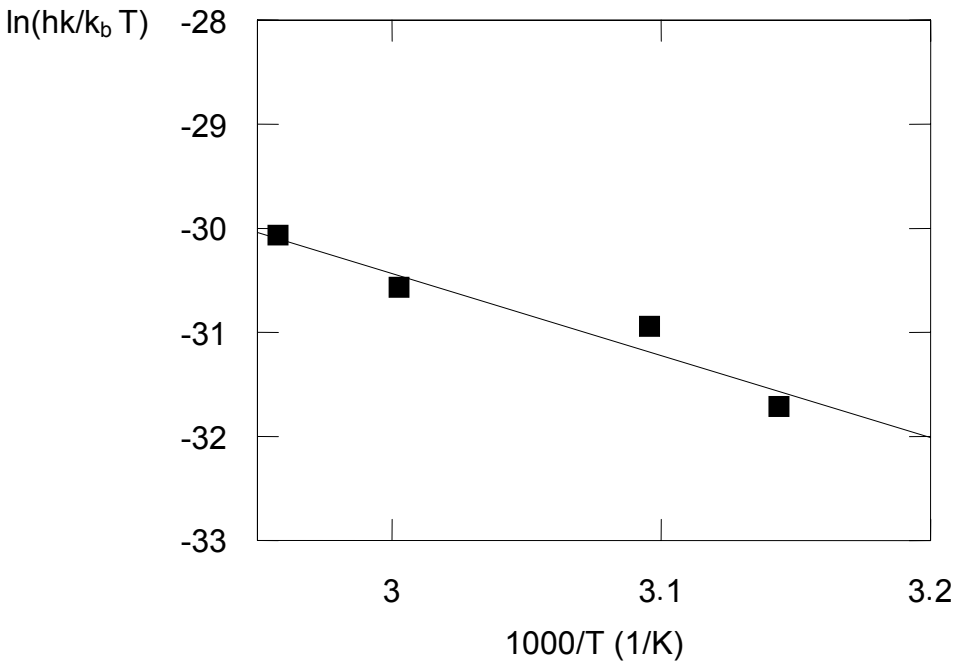

Figure 3. Calculation of thermodynamic parameters for the inactivation of the *Eca*L-ASNase. A: Arrhenius plot. B: Eyring plot.

Table 2. Thermodynamic parameters for the thermal inactivation of *Eca*L-ASNase at 10 mM potassium phosphate buffer pH 7

Enzyme	E_a (kJ/mol)	$\Delta H^{\neq}$ (kJ/mol)	$\Delta S^{\neq}$ (kJ/mol K)
*Eca*L-ASNase	68.5±5.8	65.6±5.6	0.56±0.05

These results emphasize the importance of the positive entropic contribution to the activation step of the inactivation process of the enzyme. The relatively greater increase in entropy from the ground state to the transition state of the inactivation process of the enzyme indicates local disordering of the *Eca*L-ASNase.

The conclusion from the results in Table 2 is that the relative rates of thermal inactivation are dictated largely by the entropic contributions. To gain a deeper insight into the structural basis of thermal stability, *in silico* structural analysis of the *Eca*L-ASNase was carried out. In principle, the entropy of inactivation consists of two parts: the increased configurational entropy due to partial unfolding of the protein in the transition state and the decrease in entropy of the solvent due to exposure of hydrophobic side chains. The latter effect is likely to be small at elevated temperatures (Privalov and Gill, 1988; Freire et al., 1990) and the major contribution must then be the increase in configurational entropy. Thus, the low thermal stability of *Eca*L-ASNase is probably mainly due to greater flexibility or disordering of the transition state with some contribution from a lower degree of exposure of hydrophobic residues. To analyze whether *Eca*L-ASNase is a flexible protein, we analyzed the plots of the crystallographic B-factors along the polypeptide chain of the enzyme structure. This plot can give an indication of the relative flexibility of portions of the protein (Ricci et al., 2003; Yuan et al., 2003; Kotzia and Labrou, 2005). As shown in Figure 4, the structure displays a well-defined flexibility pattern. Several highly mobile regions throughout the entire sequence can be identified, and these are separated by a number of segments with low mobility. This may cause local disordering of the enzyme tetramer (Figure 5) with increased flexibility, which may contribute to the increase in configurational entropy (Papageorgiou et al., 2008).

4. CONCLUSION

In the present report we address questions regarding the structural stability of *Eca*L-ASNase. The results of the present work form the basis for a rational design of new engineered forms of *Eca*L-ASNase with enhanced thermal stability. Enhancement of enzyme's thermostability is of particular importance to the processes of production, storage, and therapeutic use. This would result in more efficient enzyme variants that would be able to exhibit their therapeutic efficacy in a lower dose, thereby minimizing their toxic effects to patients.

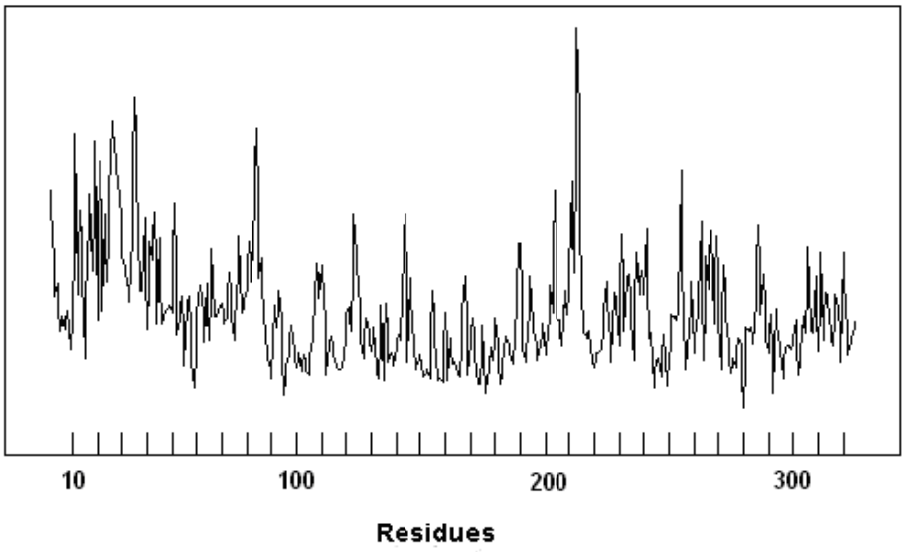

Figure 4. The dynamics of *Eca*L-ASNase. A plot of the crystallographic B-factors along the polypeptide chain obtained from the crystal structure of *E. carotovora* L-asparaginase, (PDB code 1ZCF). The plot was produced by WHAT IF software package (Barrow, 1973; Vriend, 1990). The height at each residue position indicates the average B-factor of all atoms in the residue.

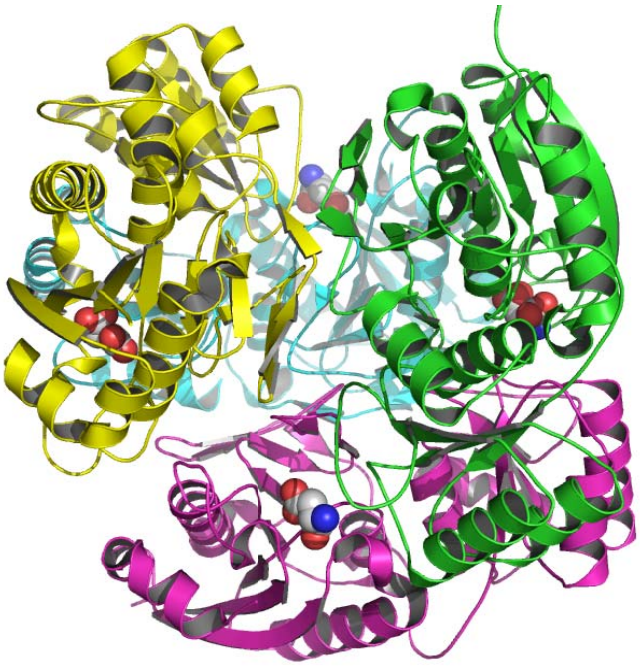

Figure 5. Structural representations of *Eca*L-ASNase. Diagram of the tetrameric enzyme (PDB code 2JK0) with L-Asp bound to the active site. The bound ligand (L-Asp) is shown in a ball representation. The figure was created by PyMOL (DeLano, 2002).

ACKNOWLEDGMENT

This work was financially supported by the Hellenic General Secretariat for Research and Technology: Operational Program for Competitiveness, Joint Research and Technology Program.

REFERENCES

Aghaiypour, K., Wlodawer, A. and Lubkowski, J. (2001a). Do bacterial l-asparaginases utilize a catalytic triad Thr-Tyr-Glu? *Biochim. Biophys. Acta 1550*, 117-128.

Aghaiypour, K., Wlodawer, A. and Lubkowski, J. (2001b). Structural basis for the activity and substrate specificity of *Er. chrysanthemi* L-asparaginase. *Biochemistry 40*, 5655-5664.

Aung, H. P., Bocola, M., Schleper, S. and Rohm, K. H. (2000). Dynamics of a mobile loop at the active site of *Escherichia coli* asparaginase. *Biochim. Biophys. Acta* 1481, 349-359.

Balcao, V. M., Mateo, C., Fernandez-Lafuente, R., Malcata, F. X. and Guisan, J. M. (2001). Structural and functional stabilization of L-asparaginase via multisubunit immobilization onto highly activated supports. *Biotechnol. Prog. 17 (3)*, 537-542.

Barrow, G. M. (1973). *Physical Chemistry*. New York, ST: McGraw-Hill.

Bradford, M. A. (1976). A rapid and sensitive method for the quantitation of microgram quantities of protein utilizing the principle of protein-dye binding. *Anal. Biochem*. *72*, 248-254.

DeLano, W. L. (2002). *The PyMOL Molecular Graphics System*. San Carlos USA, ST: DeLano Scientific.

Duval, M., Suciu, S., Ferster, A., Rialland, X., Nelken, B., Lutz, P., Benoit, Y., Robert, A., Manel, A. M., Vilmer, E., Otten, J. and Philippe, N. (2002). Comparison of *Escherichia coli*–asparaginase with *Erwinia*–asparaginase in the treatment of childhood lymphoid malignancies: results of a randomized European Organization for Research and Treatment of Cancer-Children's Leukemia Group phase 3 trial. *Blood 99*, 2734-2739.

Freire, E., van Osdol, W. W., Mayorga, O. L. and Sanchez-Ruiz, J. M. (1990). Calorimetrically determined dynamics of complex unfolding transitions in proteins. *Annu. Rev. Biophys. Biophys. Chem*. *19*, 159-188.

Graham, M. L. (2003). Pegaspargase: a review of clinical studies. *Adv. Drug Deliv. Rev. 55*, 1293-1302.

Hawkins, D. S., Park, J. R., Thomson, B. G., Felgenhauer, J. L., Holcenberg, J. S., Panosyan, E. H. and Avramis, V. I. (2004). Asparaginase pharmacokinetics after intensive polyethylene glycol-conjugated L-asparaginase therapy for children with relapsed acute lymphoblastic leukemia. *Clin. Cancer Res. 10*, 5335-5341.

Howard, J. B. and Carpenter, F. H. (1972). L-asparaginase from *Erwinia carotovora*. Substrate specificity and enzymatic properties. *J. Biol. Chem. 247*, 1020-1030.

Kotzia, G. A. and Labrou, N. E. (2005). Cloning, expression and characterisation of *Erwinia carotovora* L-asparaginase. *J. Biotechnol. 119*, 309-323.

Kotzia, G. A., Lappa, K. and Labrou, N. E. (2007). Tailoring structure-function properties of L-asparaginase: engineering resistance to trypsin cleavage. *Biochem J. 404(2)*, 337-343.

Kozak, M., Borek, D., Janowski, R. and Jaskolski, M. (2002). Crystallization and preliminary crystallographic studies of five crystal forms of *Escherichia coli* L-asparaginase II (Asp90Glu mutant). *Acta Crystallogr. Sect. D Biol. Crystallogr. 58*, 130-132.

Krasotkina, J., Borisova, A., Gervaziev, Y. and Sokolov, N. (2004). One-step purification and kinetic properties of the recombinant L-asparaginase from *Erwinia carotovora*. *Biotechnol. Appl. Biochem. 39*, 215-221.

Lee, S. M., Wroble, M. H. and Ross, J. T. (1989). L-Asparaginase from *Erwinia carotovora*: an improved recovery and purification process using affinity chromatography. *Appl. Biochem. Biotechnol. 22*, 1-11.

Palm, G. J., Lubkowski, J., Derst, C., Schleper, S., Rohm, K. H. and Wlodawer, A. (1996). A covalently bound catalytic intermediate in *Escherichia coli* asparaginase: crystal structure of a Thr-89-Val mutant. *FEBS Lett. 390 (2)*, 211-216.

Papageorgiou, A. C., Posypanova, G. A., Andersson, C. S., Sokolov, N. N. and Krasotkina, J. (2008). Structural and Functional Insights into *Erwinia carotovora* L-Asparaginase. *FEBS J. 275*, 4306-4316.

Privalov, P. L., and Gill, S. J. (1988). Stability of protein structure and hydrophobic interaction. *Adv. Prot. Chem. 39*, 191-234.

Ricci, G., Caccuri, A. M., Lo Bello, M., Parker, M. W., Nuccetelli, M., Turella, P., Stella, L., Di Iorio, E. E. and Federici, G. (2003). Glutathione transferase P1-1: self-preservation of an anti-cancer enzyme. *Biochem. J. 376(1)*, 71-76.

Segel, I. H. (1975). *Enzyme Kinetics*. New York, ST: John Wiley and Sons.

Stein, R. A. and Staros, J. V. (1996). Thermal inactivation of the protein tyrosine kinase of the epidermal growth factor. *Biochemistry 35*, 9197-9203.

Tinoco, I. Jr., Sauer, K., and Wang, J. C. (1985). *Physical Chemistry: Principles and Applications in Biological Sciences* (2nd ed.). New Jersey, ST: Prentice-Hall, Inc., Englewood Cliffs.

Twomey, C. and Doonan, S. (1997). A comparative study of the thermal inactivation of cytosolic and mitochondrial aspartate aminotransferases. *Biochim. Biophys. Acta 1342*, 37-44.

Vriend, G. (1990). WHAT IF: a molecular modelling and drug design program. *J. Mol. Graph 8*, 52-56, 29.

Wriston, J. C. Jr. and Yellin, T. O. (1973). L-asparaginase: a review. *Adv. Enzymol. Relat. Areas Mol. Biol. 39*, 185-248.

Yuan, Z., Zhao, J. and Wang, Z. X. (2003). Flexibility analysis of enzyme active sites by crystallographic temperature factors. *Protein Eng. 16(2)*, 109-114.

In: Biochemistry and Histocytochemistry… ISBN: 978-1-60876-283-5
Editors: S. Fuchs, M. Auer, pp. 335-336 © 2010 Nova Science Publishers, Inc.

Expert Commentary

A NOVEL METHOD FOR GENERATION OF MONOCLONAL ANTIBODIES

Masahiro Tomita*
Division of Chemistry for Materials, Graduate School of Engineering,
Mie University, 1577 Kurima-Machiya-cho, Tsu, Mie 514-8507, Japan

It was more than 30 years ago that generation of monoclonal antibodies was first reported by Köhler and Milstein [1]. It has subsequently become well published that monoclonals are highly specific for their target antigens, and this has ensured wide use for many purposes. The poly(ethylene glycol)(PEG)-mediated method is still generally employed to yield monoclonal antibodies [2], but with this conventional method difficulties may be encountered because of non-specific fusion, not only between B cell-myeloma cell pairs, but also B cell-B cell and myeloma cell-myeloma cell pairs. More recently, pearl-chain formation [3] and laser radiation [4] methods have been reported to efficiently produce monoclonal antibodies, but they also do not guarantee selective fusion of target B cells with myeloma cells.

To address this problem, we have developed a new technology based on B-cell targeting [5-9]. The approach features three critical steps: antigen-based pre-selection of B cells; formation of B cell and myeloma cell complexes by exploiting the specificity and strength of the interaction between biotin and avidin; and selective fusion of B cell-myeloma cell complexes with electrical pulses. This confers at least a 5-40-fold increase in efficiency over that obtained with the PEG-mediated method [8]. Recently, we have successfully confirmed the efficacy of all three critical steps of B-cell targeting on the basis of immunofluorescence analysis [9].

We propose that this advanced technology has clear advantages over conventional methods for selective generation of novel monoclonal antibodies. It may also allow efficient production of stereo-specific monoclonal antibodies against native structure antigens with application of antigen-expressing myeloma cells.

* Email:tomita@chem.mie-u.ac.jp, Tel: +81-59-231-9428, Fax: +81-59-231-9430.

REFERENCES

[1] Köhler, G. & Milstein, C. (1975). Continuous cultures of fused cells secreting antibody of predefined specificity: *Nature*, *256*, 495-497.

[2] De St. Groth, S.F. & Scheidegger, D. (1980). Production of monoclonal antibodies: strategy and tactics: *J. Immunol. Methods*, *35*, 1-21.

[3] Zimmermann, U. (1982). Electric field-mediated fusion and related electrical phenomena: *Biochim. Biophys. Acta*, *694*, 227-277.

[4] Ohkohchi, N., Itagaki, H., Doi, H., Taguchi, Y., Satomi, S. & Satoh, S. (2000). New technique for producing hybridoma by using laser radiation: *Lasers Surg. Med.*, *27*, 262-268.

[5] Lo, M.M.S., Tsong, T.Y., Conrad, M.K., Strittmatter, S.M., Hester, L.D. & Snyder, S.H. (1984). Monoclonal antibody production by receptor-mediated electrically induced cell fusion: *Nature*, *310*, 792-794.

[6] Tomita, M. & Tsong, T.Y. (1990). Selective production of hybridoma cells: antigenic-based pre-selection of B lymphocytes for electrofusion with myeloma cells: *Biochim. Biophys. Acta*, *1055*, 199-206.

[7] Tsong, T.Y. & Tomita, M. (1993). Selective B lymphocyte-myeloma cell fusion: *Methods Enzymol*., *220*, 238-246.

[8] Tomita, M., Sugi, H., Ozawa, K., Tsong, T.Y. & Yoshimura, T. (2001). Targeting antigen-specific receptors on B lymphocytes to generate high yields of specific monoclonal antibodies directed against biologically active lower antigenic peptides within presenilin 1: *J. Immunol. Methods*, *251*, 31-43.

[9] Tomita, M., Fukuda, T., Ozu, A., Kimura, K., Tsong, T.Y. & Yoshimura, T. (2006). Antigen-based immunofluorescence analysis of B-cell targeting: advanced technology for the generation of novel monoclonal antibodies with high efficiency and selectivity: *Hybridoma (Larchmt)*, *25*, 283-292.

INDEX

A

absorption, 98, 199, 207, 224, 227, 230, 232, 234, 237, 244, 245, 246, 249, 250, 251
absorption coefficient, 207, 227
absorption spectra, 224
absorption spectroscopy, 251
acceleration, 93, 134, 151, 291
acceptor, 197, 234, 302, 305, 308, 311
acceptors, 300, 304, 305, 316
accommodation, 203
acetate, 7, 155, 156, 185, 188, 189, 195, 246, 314, 315
acetic acid, 16, 86
acetone, 87, 93
acetylcholine, 3, 16, 23, 47
acidification, 186, 193, 285
action potential, 47
activation energy, 188, 195, 326, 327
activation enthalpy, 326, 327, 328
activation entropy, 326, 328
active site, 184, 186, 191, 192, 193, 197, 203, 230, 234, 244, 249, 261, 262, 263, 268, 275, 279, 280, 283, 300, 301, 302, 305, 313, 314, 319, 322, 324, 332, 333, 334
acute glomerulonephritis, 75
acute lung injury, 6
acute lymphoblastic leukemia, xii, 323, 324, 333
acute stress, 54, 59
Adams, 150, 180
adaptability, 282
adaptation, 28, 29, 36, 55, 285
adducts, 91
adenocarcinoma, 111
adenosine, 46
adenosine triphosphate, 46
adenylyl cyclase, 5, 50
ADHD, 27, 30, 40
adhesion, 116, 274
adipocyte, 137
adipose, 72
adipose tissue, 72
administration, 6, 14, 37, 55, 56, 57, 58, 71, 73
adrenaline, 22
adrenoceptors, 21, 50, 51, 54, 55, 58, 59, 64
adriamycin, 106
adult, 2
adults, 17, 77, 291
adverse event, 75
Aedes, 286
aetiology, 18
affective disorder, viii, 45
affective states, 44
afferent nerve, 75
agammaglobulinemia, 165, 177
agar, 286
Agaricus bisporus, 250, 270, 271
age, 10, 13, 41, 75, 167, 170, 171, 172, 294
agent, xii, 14, 86, 116, 251, 254, 256, 279, 287, 323, 324, 325, 327
agents, vii, viii, x, xii, 45, 100, 143, 144, 146, 149, 274, 287, 289, 294, 299, 300, 322
aggregates, 107
aggregation, 2, 10
aggression, 10, 12, 39
aggressive behavior, 21, 62
aging, 2, 18, 20, 22
aging population, 2
agonist, 5, 7, 8, 11, 14, 16, 55
aid, ix, 66, 291
air, 86
alanine, 191, 218, 230, 236, 240
albumin, 157, 204
albuminuria, 75
alcohol, 86, 87, 90, 284, 301, 303, 304
alcohols, 88, 304
aldehydes, 91
aldosteronism, 79
algorithm, 216

ALK, 83, 103
alkali, 221, 223
alkaline, x, 89, 93, 94, 104, 118, 145, 146, 186, 193, 212, 222, 275, 277, 279, 285, 288, 319
alkaline phosphatase (ALP), x, 89, 94, 118, 145, 146
ALL, xii, 323, 324
allele, 69, 162
allelic exclusion, 174
ALP, x, 118, 131, 132, 134, 135
alpha, 18, 20, 21, 22, 23, 61, 75, 89, 171, 251, 266, 269, 317, 318, 319, 320, 321
alpha adrenergic receptors, 20
alternative, 26, 87, 99, 100, 109, 146, 148, 151, 271, 300
alternatives, xii, 299
alters, 297
aluminum, 88
alveolar macrophages, 6
Alzheimer's disease, 10, 16, 18, 19, 20, 21, 22, 23, 24
American Psychiatric Association, 40
amide, 87, 111, 185, 187, 189, 191, 205, 215, 249, 278
amine, 93
amines, 2, 15, 16
amino acids, 40, 86, 161, 167, 197, 199, 200, 201, 212, 213, 216, 219, 239, 240, 254, 278, 279, 282, 283, 284, 287, 288, 301, 313, 324
amino groups, 85, 86, 111
aminopeptidase, 186, 285
ammonia, xii, 285, 289, 323, 324, 326
ammonium, 154, 287
amniotic fluid, 157
amygdala, 2, 47, 54, 55, 61, 64
amylase, 215, 233, 234, 266, 268, 269, 271, 272
amyloid, 7, 10, 11, 17, 18, 19, 20, 24
amyloid plaques, 11
amyloid precursor protein, 19
amyotrophic lateral sclerosis, 19
analog, 235
anaplastic lymphoma kinase (ALK), 83
anatomy, 22, 269, 322
angioplasty, 74
angiosarcoma, 103
Angiotensin, 208
Angiotensin II, 71, 74, 75, 78, 79, 80, 208
animal models, 11, 13, 15, 71, 75, 164
animal studies, 38, 74, 76
animals, 11, 12, 38, 59, 133, 274
ANS, 2, 253, 255
antagonism, 63
antagonist, 5, 6, 7, 8, 9, 12, 22, 23, 37, 50, 51, 56, 62
antagonists, 5, 6, 8, 14, 51, 58, 59
anthropometry, 76
anti-apoptotic, 163, 172
antibiotics, 270
anticancer, 149, 151, 334
anticancer drug, 151
anticoagulant, 215
antidepressant, viii, 24, 32, 33, 36, 37, 38, 40, 42, 43, 45, 57, 59, 62, 63
antidepressants, 30, 33, 36, 37, 38, 44, 47, 49, 59, 63
antiferromagnetic, 246
antigen presenting cells, 160
antigenicity, 86, 88, 111
Antigens, 103
antinociception, 61, 64
antipsychotic drugs, 49, 58, 63
antipsychotics, 61
antitumor, 319, 324
ants, 275
anxiety, viii, 45, 54, 55, 56, 58, 59, 60, 61
anxiety disorder, 55, 56
APA, 27
apathy, 10, 13
apoptosis, 20, 137, 162, 163, 164, 171
apoptotic cells, 103
appetite, 72
applied research, 303
apraxia, 10
aqueous solution, 291
arachidonic acid, vii, 1
archaea, 306, 310, 311, 318
arginine, 64, 93, 199, 204, 212
aromatic rings, 85
arrest, 161, 170, 176
Arrhenius equation, 327
ARs, 5, 6, 7, 8
artery, 72, 74
arthritis, 173, 177, 180
arthropod, 274, 294
arthropods, 273
articular cartilage, 122, 125, 127, 128, 137
articulation, 121
asparagines, 202, 203, 204, 226, 267
aspartate, 334
Aspergillus fungi, xii, 182
Aspergillus niger, 263, 271
aspiration, 84
assertiveness, 39
assessment, ix, 29, 30, 31, 34, 81, 103, 104, 105, 106, 108, 109, 110, 112, 113, 114, 116, 314
assessment tools, 31
assignment, 312
assimilation, 308

astrocytes, vii, 1, 7, 8, 9, 11, 14, 18, 19, 20, 21, 22, 23
astroglial, 17
asymptomatic, 66, 76
ATF, 10
atoms, 240, 241, 249, 250, 270, 332
ATP, 46, 47
ATPase, 73, 79
atrophy, 131
attachment, 26, 28, 29
attacks, x, 143, 300, 305, 311
attitudes, 29
attractiveness, 32
Australia, 65, 81, 97
autism, 27, 30
autoantibodies, xi, 159, 161, 162, 164, 165, 166, 176, 178, 180
autoantibody, 146, 161, 164, 174, 176, 178
autoantigens, xi, 159, 175, 178
autocrine, 16
autoimmune, xi, 14, 24, 159, 160, 162, 163, 164, 165, 166, 167, 169, 170, 171, 172, 173, 174, 176, 177, 179, 180
autoimmune disease, xi, 14, 159, 160, 162, 163, 164, 165, 167, 169, 173, 174, 176, 177, 180
autoimmune diseases, xi, 159, 160, 165, 167, 169, 174, 177
autoimmune disorders, 165
autoimmune responses, 160
autoimmunity, xi, 159, 160, 168, 172, 173, 178
autolysis, 84, 114
automation, 97
autonomic nervous system, 2
autoreactive T cells, 164
availability, viii, 29, 45, 99, 108, 163, 300
aversion, 59
awareness, 54
axon, 11, 18
axon terminals, 11, 18
axons, 2, 11, 18
Aβ, 12

B

β2-adrenergic receptor, 15
B cell activating factor, 162
B cell lymphoma, 104
B lymphocytes, 5, 160, 174, 175, 336
babies, 75
BAC, 148
Bacillus, 233, 266, 268, 320, 322
back, 47, 91, 274
bacteria, xi, 143, 181
bacterium, 283, 313
BAFF, 162, 163, 175
baroreceptor, 73, 75
barriers, 87, 93
basal forebrain, 24
basal lamina, 82, 113
base pair, 209, 242
basement membrane, 180
basic research, 317
basket cells, 56
baths, 90
BCIP, 89
Bcl-2, 107, 116
beef, 262
beetles, 274
behavior, 31, 39, 40, 42, 54, 55, 56, 57, 60, 61, 64, 99, 138, 313
behavioral effects, 55, 62
behaviours, viii, 12, 25, 27, 30, 31, 32, 33, 34, 37, 38, 39, 40, 43
Beijing, 81, 294
bell, 314
bell-shaped, 314
benchmark, 101, 109
beneficial effect, 14, 26, 58, 59
benefits, 28, 76, 147, 156
benign, 98, 99
benzodiazepines, 59
benzoquinone, 259
beta-blockers, 18
beverages, 257
bias, 31, 37, 40
binuclear, 251, 252, 254
bioassay, 291
biocatalysis, xii, 299, 317
biocontrol, vii, xii, 273, 280, 287, 289, 290, 292, 294
biodiversity, 304, 317
biogenic amines, 2, 15
biological control, xii, 273, 274
biological processes, 309, 314
biomarker, 149
biomarkers, 149
biomass, 286
biomolecules, 300
biophysics, xii, 299
biopsies, xi, 84, 85, 153, 154, 157
biopsy, ix, 79, 82, 84, 86, 110
biosynthesis, 21, 221, 241, 268, 269, 318
biotechnology, xii, 182, 294
biotin, x, 82, 93, 97, 98, 104, 111, 116, 143, 144, 145, 147, 150, 335
Biotransformation, 318
biotransformations, 317
bipolar, 30, 57, 58, 60, 61, 63, 64

bipolar disorder, 57, 58, 63, 64
bipolar illness, 57
birth, 75, 121, 125, 126, 127
birth weight, 75
blame, 39
blaming, 33
blocks, 5, 62, 88, 99, 147, 308
blood, 5, 6, 14, 23, 66, 67, 68, 70, 71, 72, 73, 74, 75, 77, 78, 84, 135, 164, 279, 324
blood flow, 74
blood group, 84
blood plasma, 279
blood pressure, 66, 67, 68, 70, 71, 73, 74, 75, 77, 78
blood vessels, 135
blot, 87, 93, 145, 217, 226, 228, 237, 241, 243, 244, 289
BMI, 68
body weight, 67, 72
boiling, xii, 299
bolus, 73
bonding, 28, 38, 43, 94, 191, 192, 195, 197, 316
bonds, xii, 39, 94, 183, 187, 189, 194, 195, 200, 204, 207, 209, 251, 255, 259, 260, 299, 300, 303, 305
bone density, 140
bone growth, 139
bone marrow, 5, 18, 161, 162, 166, 175
bone remodeling, 137
bone resorption, 132
borderline, 313
bovine, x, 9, 114, 153, 154, 187, 188, 197, 264, 279, 284
bowel, 104
bradykinesia, 13, 14
brain, vii, 1, 2, 7, 9, 10, 11, 12, 13, 14, 15, 16, 17, 19, 20, 21, 22, 23, 38, 46, 47, 51, 54, 57, 58, 59, 61, 62, 63, 73, 74, 94, 110, 156, 207, 208, 264
brain stem, 2
brainstem, 47, 54
branching, 129, 306, 321
Brazilian, 293
breakdown, 90, 160, 165, 173
breast cancer, 96, 99, 100, 104, 105, 106, 108, 110, 111, 112, 113, 114, 115, 116, 147, 150, 151
breast carcinoma, 83, 88, 111, 113, 114, 148
budding, 274
buffer, 90, 92, 94, 95, 97, 109, 113, 154, 155, 185, 193, 232, 245, 246, 306, 316, 325, 326, 331
building blocks, 308
bupropion, 47, 49, 57, 58

C

Ca^{2+}, 4, 5, 50, 171, 199, 227, 230, 231, 232, 234, 235, 236, 268, 277, 279
cadaver, 274
calcification, 128, 134
calcium, 10, 92, 114, 199, 202, 232
calf, 146, 204, 205, 259, 267
calorimetric enthalpy, 227
calvaria, 134
cAMP, 4, 5, 6, 8, 9, 12, 22, 58
cancer, 83, 100, 104, 107, 110, 111, 112, 114, 115, 116, 148, 149, 150, 151
cancer cells, 83, 147, 149
cancer treatment, 83
candidates, 146, 207, 232, 289
carbazole, 89
carbohydrate, 201, 212, 221, 232, 266, 267, 300, 317, 318, 320
carbohydrates, 300, 303, 318
carbon, 284, 285, 286, 287, 288, 295, 300
carboxyl, 85, 183, 190, 195, 197, 198, 201, 202, 213, 214, 215, 232, 233, 263, 264, 268, 278, 301, 319
carboxyl groups, 233
carboxylates, 197, 319
carboxylic acids, 228, 301, 321
carboxylic groups, 301
carcinogen, 90
carcinoma, 83, 86, 88, 105, 111, 148
cardiac risk, 78
cardiac risk factors, 78
cardiovascular disease, viii, 65, 66, 74
carrier, 83
cartilage, x, 117, 120, 121, 122, 123, 124, 125, 126, 127, 128, 134, 137, 138, 139, 140, 141
cartilaginous, x, 117, 118, 119, 120, 123, 124
casein, 183, 185, 186, 187, 188, 204, 207, 208, 219, 260, 267, 278, 279, 287
catalysis, 185, 202, 218, 249, 268, 312, 313, 314, 319, 320, 322
catalyst, 230, 232, 233, 300, 301, 302, 304, 305, 313, 314, 319, 322
catalytic activity, 244, 249, 250, 278, 279, 280, 317
catalytic properties, 183, 192, 270, 278, 317
catechol, 241, 254, 271
catecholamine, 2, 6, 16, 17, 21, 45, 57, 63, 64
catecholamines, 2, 5, 6, 15, 16, 17, 18, 71, 20, 24
categorization, 30
cation, xii, 218, 235, 236, 323, 327, 328, 329
cavities, 91
CD30, 115
CD5, 170
CD5+, 170
cDNA, 185, 186, 192, 201, 209, 216, 217, 242, 263, 265, 267, 268, 269, 270, 280, 282, 283, 289, 294, 295, 318
CEA, 47, 51, 92, 103, 112

cell culture, 12, 99, 266
cell cycle, 134
cell death, 7, 8, 10, 11, 14, 20, 179
cell differentiation, 129, 132, 139, 141, 160, 165, 166, 170
cell division, 127, 300
cell fate, 125, 170
cell fusion, 336
cell line, 6, 10, 16, 17, 99, 102, 128, 139, 145, 149, 170
cell lines, 17, 99, 102, 128, 145, 149
cell membranes, 113
cell surface, 83, 127, 162, 167, 174
cellulose, 284, 285
cementum, 133
central nervous system, 2, 74
cerebellum, 2, 12
cerebral cortex, 2, 16
cerebrospinal fluid, 79
c-fos, 61
changing environment, 55
channels, 5, 50
chaperones, x, 118
chemical reactions, 92
chemoattractant, 6
chemokines, 7
chemoreceptors, 74
chemotaxis, 5
chemotherapeutic agent, 100
chemotherapy, xii, 110, 115, 323
chicken, 207, 276
chicks, 127
childhood, 333
children, 333
China, 25, 81, 261, 294
chitin, 275, 278, 286, 287, 293
chloride, 90, 314, 315
chloroform, 284
cholinergic, 10, 12, 19, 24
cholinergic neurons, 10
chondrocyte, 118, 119, 123, 127, 136, 140
chondrocytes, 121, 122, 123, 124, 125, 126, 127, 137, 138, 140
chromatin, 164, 165, 178
chromatography, xii, 186, 218, 222, 223, 251, 253, 255, 323, 325, 327, 328, 329, 334
chromatophore, 247
chromosomal abnormalities, 147, 150
chromosome, 83, 267, 308
chronic kidney disease, 77
chronic pain, 54, 56
chronic renal failure, 66
chronic stress, 21
chymotrypsin, 251, 276, 278, 279, 281, 283, 295
circulation, 167, 168
cis, 310
CISH, 93, 113, 114, 147, 148
cis-regulating, 310
citalopram, 33
classes, 301
classical, xii, 2, 3, 165, 198, 264, 299, 300, 313
classification, 27, 43, 301, 309, 319
cleavage, 4, 93, 184, 186, 188, 193, 194, 195, 197, 200, 205, 208, 216, 244, 259, 260, 263, 267, 283, 300, 333
cleavages, 184, 207, 208
clinical depression, 28
clinical symptoms, vii, 1
clinical trial, 14, 104, 111, 146
clinical trials, 104, 111, 146
clone, 96, 148, 265, 280, 318
clonidine, 8, 55
cloning, 168, 257, 265, 268, 270, 283, 296
close relationships, 26
clustering, 114
clusters, 107, 282
CNS, 2, 3, 7, 8, 10, 11, 14, 19, 20, 47, 63
Co, xi, 11, 43, 100, 115, 137, 162, 182, 205, 206, 207, 219, 296
coagulation, 122, 123
cobalt, 90, 206, 207, 265
cockroach, 278, 279, 289
codes, 244
coding, 209, 216, 242, 283, 310
codon, 186, 216, 282, 310, 317
codons, 310
cofactors, 211
cognition, viii, 2, 3, 21, 24, 30, 45, 55, 56, 61, 62
cognitive disorders, 18
cognitive dysfunction, 18
cognitive function, 11, 12, 47, 55, 59
cognitive impairment, 10, 12, 18
cognitive process, 60
cohesion, 30
cohort, 69, 77, 80
coil, 133, 224, 245
collagen, 75, 119, 120, 122, 123, 124, 127, 135, 137, 138, 140, 149, 151, 173, 180, 279, 284
colon, 111, 115
colon cancer, 115
colorectal cancer, 104, 107, 110, 111, 114, 115, 116
communication, 2, 27, 33, 39, 116, 300
community, 28
competence, 41
competition, 161
competitiveness, 175

complement, 7, 30, 284, 290, 291
complement components, 7
complementarity, 161
complementary DNA, 265
complex carbohydrates, 300
complexity, 304
complications, 66, 67
components, xi, 7, 89, 123, 127, 131, 159, 160, 161, 169, 170, 172, 173, 179, 278, 280, 285, 287, 300
composition, 84, 87, 94, 165, 167, 206, 221, 246, 271, 294, 306
compounds, vii, 9, 47, 63, 89, 284, 288, 300, 303, 306, 307, 308, 309, 317
computer software, 36
concentrates, 95
concentration, 10, 14, 23, 55, 56, 71, 85, 90, 95, 97, 102, 155, 189, 199, 225, 230, 232, 235, 244, 247, 288, 291
concordance, 100, 101, 102, 105, 107, 109, 111
condensation, 121, 122, 125
conditioning, 55, 56, 61
conductance, 50
confidence, 39
configuration, 87, 93, 300, 301, 305, 311, 314
conflict, 39
conformational diseases, 178
confrontation, 39
confusion, 212
congestive heart failure, 66, 76
conidiophore, 182
connective tissue, 82
connectivity, 14
consensus, 28, 91, 101, 105, 108, 111, 198, 216
conservation, 195
consolidation, 39, 55
construction, 153, 186, 227
consumption, 163, 289
contamination, 228
continuity, 129
control group, 129, 131, 132, 134, 135
conversion, 186, 322
cooling, 92
copper, 91, 241, 242, 244, 245, 246, 247, 249, 250, 251, 252, 254, 257, 270
copper oxide, 91
corn, 274, 275, 297
correlation, 11, 57, 107, 110, 113, 145, 207, 247, 249, 266
correlation coefficient, 107
correlations, 247
cortex, 11, 20, 47, 56, 61, 62, 63
cortical neurons, 20
corticosterone, 61
corticotropin, 3, 21, 62
cortisol, 38, 64
couples, 138
coupling, 246, 325, 326, 327
covalent, 87, 94, 242, 300, 301, 321
covalent bond, 94
covalent bonding, 94
COX-1, 8, 19
COX-2, 6, 8, 11, 19
creatinine, 67
CREB, 5, 61
crops, 297
crosslinking, 86, 93, 111, 154, 155
cross-linking reaction, 93
cross-sectional, 66
cross-validation, 100
crystal structure, 198, 254, 301, 313, 332, 334
CSF, 5, 11, 12, 24
CSR, 164, 170
C-terminal, 171, 203, 214, 215, 216, 244, 259, 283, 310, 324
culture, 12, 99, 151, 186, 198, 201, 212, 216, 225, 226, 227, 237, 238, 239, 244, 257, 258, 259, 271, 272, 279, 285, 287, 288, 291, 296
cuticle, xii, 273, 274, 275, 278, 279, 280, 282, 284, 285, 286, 287, 288, 289, 290, 291, 293, 294, 295, 296, 297
cycles, 87, 90, 320
cyclic AMP, 79
cyclin D1, 103
cycling, 61, 64, 95
cyclooxygenases, 8
cyst, 157
cysteine, 203, 235, 236, 237, 238, 239, 240, 242, 249, 250, 254, 268, 269, 275, 276, 278, 280, 293
cysteine proteases, 275
cysteine residues, 235, 238, 242, 254, 268
cysts, 157
cytokeratins, 114
cytokine, 6, 7, 19, 22, 23, 163
cytokines, vii, xi, 1, 6, 7, 8, 9, 10, 22, 24, 132, 159, 160
cytology, 155
cytometry, 147
cytoplasm, 103, 107, 124, 125, 126, 127, 129, 131, 132, 133
cytotoxicity, 7, 8

D

daily living, 10
danger, 54
database, 198, 209, 264, 317
de novo, 164

death, 7, 8, 10, 11, 14, 16, 20, 84, 179, 274, 289
decision making, 55
decisions, 100
defects, 127, 139, 163, 165, 176, 262
defense, 7, 141
deficiency, 3, 11, 20, 99, 139, 165, 172, 177
deficit, 27
deficits, 13, 27, 41
definition, 26, 28, 30, 301
deformation, 55
degradation, xii, 84, 88, 200, 240, 266, 269, 273, 275, 282, 285, 287, 289, 291, 292, 300, 303, 304, 308, 319
degrading, 275, 278, 280, 282, 287, 290, 293, 294, 295, 296, 297
dehydration, 85, 86, 91, 154
dehydrogenase, 284, 289, 326
delivery, 101
dementia, 11, 12, 13, 15, 16, 19, 20, 21, 23, 24, 62
demyelinating disease, 14
denaturation, 91, 209, 211, 235, 236, 237, 238, 240, 279
dendritic cell, 166
denervation, 71, 73, 74, 75, 76, 78, 79, 80
density, 11, 21, 69, 102, 132, 140
dentate gyrus (DG), 47
dependent variable, 32
dephosphorylation, 146
deposition, 18, 75, 144, 150
deposits, 10
depressed, 26, 27, 28, 29, 31, 34, 36, 37, 41, 42, 44, 56
depression, viii, 3, 13, 14, 16, 18, 20, 24, 25, 26, 27, 29, 30, 31, 38, 40, 41, 42, 43, 45, 56, 57, 58, 59, 60, 61
depressive disorder, 3, 16, 28, 43, 56, 62, 63
Depressive disorders, 42
depressive symptoms, 26, 28, 57
deprivation, 287, 293
derivatives, 205, 221, 290, 309, 314
desensitization, 58
desipramine, 43, 47, 49, 57, 58
destruction, 244, 274, 289
detection, ix, x, 81, 83, 88, 89, 94, 97, 98, 104, 105, 112, 114, 116, 143, 144, 145, 146, 147, 148, 150, 151, 178
detection techniques, x, 143, 144
detergents, xii, 251, 299, 304
developmental process, 122
deviation, 129, 310
dexamethasone, 16
dextrose, 286
diabetes, viii, 65, 66, 67, 73, 76, 177
diabetes mellitus, viii, 65, 66, 76
diacylglycerol, 4
Diagnostic and Statistical Manual of Mental Disorders, 40
diagnostic criteria, 97
diagnostic markers, 100
dialysis, 67, 193
dibutyryl cAMP, 10
diet, 75
dietary, 78
differential diagnosis, 147
differential scanning, 227
differential scanning calorimetry, 227
differentiation, x, 117, 118, 123, 124, 125, 127, 128, 129, 132, 133, 134, 135, 136, 137, 138, 139, 140, 141, 160, 162, 163, 164, 165, 166, 167, 169, 170, 173, 177, 296
digestion, 89, 90, 91, 94, 97, 109, 184, 209, 225, 319
diluent, 98
dimer, 251, 324
dimeric, 223, 251, 254, 256, 257
dimerization, 254, 257, 324
dipeptides, 213, 279
disabled, 195
discomfort, 29
disease progression, vii, 1, 14, 173
diseases, viii, 7, 65, 66, 160, 165, 177
disorder, 13, 16, 27, 42, 56, 62, 74, 129
displacement, 125, 300
dissociation, 50, 195, 197, 254, 257
distraction, 127, 140
distribution, vii, x, 91, 103, 105, 110, 117, 124, 125, 126, 127, 128, 132, 133, 137, 146, 297
disulfide, 203, 207, 209, 210, 235, 237, 238, 251, 254, 255, 257, 269, 271
disulfide bonds, 207, 209
diversification, 292, 295
diversity, 83, 203, 282
division, 127, 300
DNA, 93, 160, 164, 165, 166, 168, 171, 176, 177, 178, 179, 185, 242, 268, 283, 295, 310
DNase, 90
dogs, 79
donor, 234, 247, 270, 305, 308, 311, 316, 324
donors, 168, 247, 250, 304, 305
dopamine, viii, 2, 3, 13, 14, 18, 19, 20, 21, 22, 23, 40, 45, 53, 61, 63
dopaminergic neurons, 13, 23
dosage, 138
downregulating, 167
down-regulation, 15, 22
drug action, 30, 42
drug design, 334

drugs, viii, 3, 5, 16, 19, 21, 45, 46, 47, 51, 59, 63
drying, 86, 88
DSM, 27, 30
DSM-IV, 27, 30
duplication, 261
duration, ix, 11, 32, 33, 34, 68, 81, 84, 85, 86, 87, 90, 97, 102, 108, 109
dyes, 144, 148
dyskinesia, 14, 16
dysregulated, 170, 171, 172, 173
dysthymia, 41

E

E. coli, xii, 186, 187, 192, 193, 244, 245, 246, 248, 258, 306, 311, 323, 324, 325, 328
EAE, 14
E-cadherin, 82, 110
ecological, 33, 282
EEG, 12
eicosanoids, 7
elastin, 275, 278, 279, 284, 289
elderly, 10
election, 109
electrical pulses, 335
electroencephalogram, 23
electrolyte, 75
electromagnetic fields, 90
electron, vii, x, 89, 90, 153, 156, 157, 206, 241, 246, 265
electron microscopy, vii, x, 89, 153, 157
electron paramagnetic resonance, 206, 265
electronic structure, 246
electrophoresis, 324, 328
electrophysiological study, 61
electrostatic interactions, 87, 197
ELISA, 168
elongation, 306
e-mail, 181
embryology, 118
emission, 57, 252
emotion, 31, 34, 36, 37, 40, 41, 61
emotional, 29, 41, 42, 54, 59, 64
emotional bias, 42
emotional memory, 64
emotional stimuli, 54
emotions, viii, 3, 30, 34, 36, 45, 54, 55
encoding, xii, 165, 167, 168, 177, 201, 209, 257, 258, 265, 269, 271, 272, 273, 280, 281, 283, 289, 291, 292, 294, 296, 300, 303, 304, 308, 310, 318
encouragement, 39
endocrine, 104, 112
endometrial glands, 104
endometrium, 111
endoplasmic reticulum, 221, 236, 239, 241, 268, 269, 282
endothelial cell, 9, 136
endothelial cells, 9, 136
endothelial dysfunction, 73
end-stage renal disease, viii, ix, 65, 66, 68, 75, 76, 77, 79
energy, 56, 57, 58, 72, 90, 91, 92, 94, 188, 195, 207, 300, 304, 308, 326, 327
engagement, 38, 178
enterokinase, 184
enthusiasm, 97
entrapment, 103
entropy, 265, 331
environment, 10, 30, 162, 207, 240, 247, 249, 252, 256
environmental conditions, 55
enzymatic activity, 216, 225, 242, 245, 249, 250, 251, 301, 326, 329
enzyme-linked immunosorbent assay, 92, 291
epidemic, 76
epidermal growth factor, 108, 114, 115, 116, 151, 334
epidermal growth factor receptor, 108, 115, 116, 151
epidermis, 103, 251, 271
epinephrine, 2, 4, 45, 46
epistasis, 176
epithelium, 107
epitope, 98, 114
epitopes, 86, 87, 91, 93, 95, 103, 116
epoxy, 183
EPR, 206, 241, 246, 247, 248, 249, 250, 270
equilibrium, 84, 302
Erlotinib, 104
erosion, 180
Escherichia coli, 186, 242, 263, 266, 296, 333, 334
escitalopram, 52, 57, 59, 61
EST, 282, 283
ester, 199, 278, 300
esterases, 275
estrogen, 85, 86, 95, 101, 102, 105, 106, 110, 111, 112, 114, 115
ethanol, 87, 155, 222, 251, 280, 325
ethylene, 84, 335
ethylene glycol, 84, 335
etiology, xi, 159, 169, 173
eukaryotes, 203
eukaryotic cell, 226, 239
evolution, 89, 177, 261, 282
examinations, 21, 127
excision, 87
excitability, 62
exclusion, 176

excretion, 70, 71, 72, 73, 74, 79, 266
exercise, 101
exons, 242, 257
experimental allergic encephalomyelitis, 16, 24
experimental autoimmune encephalomyelitis, 14, 24
expertise, 109, 147
exploitation, 300, 304
exposure, ix, 54, 56, 73, 81, 85, 87, 88, 93, 94, 240, 251, 254, 331
expressed sequence tag, 280, 283, 297
extinction, 55, 56, 61, 62, 64
extracellular matrix, 123
extraction, 85, 86, 91
exuviae, 278, 288, 295
eye, 13, 27, 32, 33, 34, 38, 84
eye contact, 27, 32, 33, 34, 38

F

facial expression, 34, 41, 43
failure, ix, 39, 43, 74, 82, 239, 255, 286
false positive, ix, 82, 103, 104
family, xii, 28, 29, 30, 45, 50, 127, 138, 146, 168, 177, 183, 184, 198, 202, 203, 207, 219, 236, 264, 265, 273, 275, 279, 282, 283, 292, 295, 301, 312, 318, 319, 321
family members, 28, 29, 236
family relationships, 29, 30
FDA, 104
fear, 54, 55, 56, 61, 62, 64
feedback, 75
fermentation, xi, 181, 261
ferritin, 89
fetal, 122, 123, 137, 138, 139
fibers, 47, 71, 129, 130
fibrils, 275
fibrinogen, 266
fibroblast, 123, 128, 137
fibroblast growth factor, 123, 137
fibroblasts, x, 118, 128, 129, 130, 131, 132, 133, 134, 135, 136, 139, 141, 156
fidelity, 310
filament, 111
filtration, 72, 73, 74, 198, 199, 212, 218, 219, 227, 244, 251, 253, 255, 325
fine needle aspiration, 84
fire, 275
first generation, 134
fish, 219
FISH, 100, 102, 106, 107, 110, 113, 147, 148, 150
FITC, 148
fixation, ix, 81, 83, 84, 85, 86, 87, 89, 91, 92, 93, 98, 99, 101, 102, 103, 108, 109, 111, 112, 113, 114, 115, 116, 133, 146, 156
flatness, 129
flexibility, 55, 56, 63, 211, 262, 331
flow, 72, 74, 104, 147
fluctuations, 24
fluid, xi, 75, 79, 153, 154, 157
fluid balance, 75
fluorescence, 82, 107, 111, 147, 235, 252, 253, 255
fluorescence in situ hybridization, 107, 111, 147
fluoride, 277, 305, 308
fluorides, 319
fluoxetine, 36, 37, 59, 62, 63
fMRI, 37
focal segmental glomerulosclerosis, 73
focusing, xii, 31, 273, 278
folding, 180, 203, 239, 240, 269
food, xi, xii, 181, 182, 212, 219, 268, 271, 289, 306, 308
Food and Drug Administration (FDA), 104, 112
food production, xi, 181
forebrain, 2
forgetting, 61
formaldehyde, 84, 85, 87, 91, 93, 111, 112, 113, 157
fornix, 2
Fox, 56, 178
fractionation, 221, 222
fragility, 154
free energy, 326
free rotation, 237
freezing, 54, 88
frequency distribution, 110
friendship, viii, 25, 27, 29, 39
frog, 251, 271
functional magnetic resonance imaging, 37
fungal infection, 289
fungi, xi, xii, 181, 182, 183, 212, 226, 271, 273, 275, 276, 278, 280, 281, 287, 290, 291, 292, 294, 296
fungus, 182, 203, 225, 251, 257, 261, 274, 278, 282, 286, 288, 289, 290, 291, 292, 293, 294, 295, 296, 297
furniture, 32
fusiform, 37
fusion, 47, 83, 103, 172, 244, 284, 335, 336
fusion proteins, 172

G

G protein, 4
GABA, 47, 51, 53, 54, 56, 57, 63
GABAergic, 22
gait, 17
ganglia, 46
ganglion, 71
gas, 223, 326
gas chromatograph, 223

gastric mucosa, 192
gastrin, 215
gastrointestinal, 83, 104, 111
GDP, 216
gel, 149, 151, 154, 155, 156, 157, 198, 212, 218, 219, 227, 241, 242, 251, 253, 255, 324, 325, 328
gelatin, 154, 156, 204, 279, 284, 287
gels, 228
gene amplification, 111, 147, 148, 151
gene expression, 17, 119, 122, 123, 127, 134, 138, 163, 167, 258, 285, 288, 293, 295, 297, 317
gene promoter, 258
gene targeting, 179
gene therapy, 180
gene transfer, 283
generalized anxiety disorder, 56, 62
generation, vii, 41, 63, 91, 101, 123, 125, 134, 170, 335, 336
genes, xii, 5, 9, 14, 15, 82, 123, 126, 134, 138, 167, 168, 174, 175, 177, 218, 257, 273, 280, 281, 282, 283, 285, 286, 288, 290, 291, 292, 293, 300, 303, 304, 308, 310, 317
genetic abnormalities, 83
genetic alteration, 82
genetic testing, 147
genome, xii, 182, 282, 292, 304, 309, 321
genome sequencing, 292
genomic, 148, 169, 185, 200, 242, 268, 271, 283, 292, 317
geography, 203
germination, 288, 291, 293, 306
GFAP, 103
Gibbs, 326
Gibbs free energy, 326
glass, 155
glial, 9, 15, 22, 103
glial cells, 9, 15, 103
glomerulonephritis, 75, 79
Glucan, 260
glucoamylase, 257, 258, 259, 271
glucose, 12, 89, 234, 260, 286, 287, 306, 308
glucose metabolism, 12
glucose oxidase, 89
glucosidases, 266
glucoside, 308, 311
glutamate, 8, 50, 51, 53, 326
glutamic acid, 186, 202, 204, 213, 301, 313, 319
glutamine, 202, 209, 324
glutaraldehyde, 154, 157
glycans, 226, 320, 321
glycerol, 90, 287
glycine, 94, 200, 213, 214, 236, 240, 312, 313, 314
glycoconjugates, 300, 303, 309
glycol, 18, 84, 86, 333, 335
glycoprotein, 212, 219, 221, 268, 269, 319
glycoproteins, 220, 221, 226, 241, 320
glycoside, 300, 301, 302, 303, 304, 305, 308, 309, 312, 314, 316, 319, 321
glycosides, 301, 304, 305, 312
glycosyl, 234, 300, 301, 302, 304, 305, 306, 311, 312, 314, 317, 319, 320, 321, 322
glycosylated, 218, 223, 224, 240
glycosylation, 201, 216, 239, 262, 300, 303, 305, 313, 321
goal-directed, 64
goal-directed behavior, 64
gold, 87, 89, 100, 115, 290
gold standard, 87, 100, 115
G-protein, 50
grades, 101
grading, 102
grapes, xi, 181
graph, 24, 96
gray matter, 24
green fluorescent protein, 290
grey matter, 14
grids, 155, 156
groups, 4, 8, 29, 39, 47, 85, 87, 91, 108, 111, 133, 136, 184, 203, 214, 215, 233, 235, 254, 275, 278, 279, 301, 303, 304, 306, 308, 309, 312, 313
growth, xii, 8, 75, 78, 83, 108, 111, 112, 114, 115, 116, 120, 123, 127, 137, 138, 139, 140, 151, 225, 258, 273, 275, 278, 279, 282, 285, 286, 287, 288, 289, 295, 306, 308, 309, 314, 324, 334
growth factor, 8, 108, 111, 112, 114, 115, 116, 123, 137, 140, 151, 324, 334
growth factors, 8, 140
growth rate, 289
GST, 284
guidance, 26, 29, 60
guidelines, 62, 100, 101, 108, 114
gyrus, 2

H

habituation, 61
half-life, 199, 210, 211, 236
hallucinations, 10, 13
handling, 78, 155
hands, 252
harm, 290
health, viii, 43, 65
heart, 65, 67, 70, 74, 76, 78
heart failure, 66, 67, 74, 76
heat, xii, 11, 89, 90, 91, 92, 93, 94, 109, 112, 141, 209, 219, 279, 299, 306, 317, 325
heat shock protein, 11, 141

heating, 90, 91, 92, 109, 112, 115, 116
heavy metal, 89, 90, 94
height, 332
helix, 187, 203, 207, 209, 210, 224, 227, 245, 247, 283
helplessness, 33, 38
hemicellulose, 306
hemodialysis, 67, 68
hemoglobin, 93, 187, 188, 193, 204
hemolymph, 274, 275, 289
hepatocarcinogenesis, 320
HER2, 87, 93, 100, 101, 104, 106, 107, 111, 114, 115, 116, 147, 148, 151
heterodimer, 171
heterogeneity, 16, 21, 107, 148
high blood pressure, 72
high resolution, 192
high risk, 75
high temperature, xii, 92, 299, 304, 306
high-level, 170, 258
hippocampus, 11, 16, 20, 22, 23, 47, 54, 55, 56
histidine, 203, 204, 209, 242, 244, 245, 249, 250, 269
histochemical, 150
histology, 114, 118, 120, 155
histone, 204, 205, 259, 264
HIV, 183
HLA, 21
homeostasis, x, 2, 10, 13, 72, 75, 118, 135
homogeneity, xii, 186, 219, 226, 227, 275, 323
homolog, 134
homology, 203, 257, 280, 282, 283, 284
hormonal therapy, 105
hormone, 3, 73, 87, 105, 200
hormones, 45, 46, 82
Horseradish peroxidase, 145
hospital, 84
host, 201, 274, 275, 280, 282, 285, 286, 287, 288, 289, 290, 291, 292, 293, 294, 297, 305
host tissue, 288
hot spring, 304
HPA, 54, 56
HPA axis, 56
HPLC, 17, 221, 222, 223, 230, 235, 241, 244, 256
HRP, 144, 145
HSP, 135, 136
human brain, 2, 49, 63
human immunodeficiency virus, 183
human neutrophils, 17
human subjects, 38, 54
humans, xi, 11, 38, 54, 55, 60, 62, 66, 67, 71, 73, 75, 76, 134, 138, 159, 274, 275, 309
hybrid, 110, 241
hybridization, x, 93, 117, 122, 123, 128, 139, 140, 144, 147, 151, 216, 286
hybridoma, 82, 336
hydrates, 84
hydration, 212
hydrochloric acid, 94
hydrogen, 86, 94, 189, 191, 192, 195, 197, 234, 238, 251, 316
hydrogen bonds, 87, 94, 190, 197, 251
hydrolases, 232, 292, 299, 300, 301, 302, 303, 304, 306, 308, 309, 312, 317, 319, 320, 322
hydrolysates, 207, 219, 221
hydrolysis, xii, 91, 183, 185, 186, 191, 193, 194, 195, 197, 202, 205, 207, 208, 213, 214, 215, 227, 230, 232, 260, 287, 289, 290, 293, 299, 300, 301, 302, 304, 306, 308, 313, 319, 321, 323, 324
hydrolyzed, 187, 188, 193, 194, 195, 197, 204, 205, 213, 278, 279, 302
hydrophobic groups, 279
hydrophobic interactions, 94
hydrophobicity, 240
hydroxide, 325
hydroxyl, 85, 190, 191, 235, 304, 313
hydroxyl groups, 304, 313
hydroxylation, 241, 257
hyperactivity, 27, 57, 77
hyperinsulinemia, 12, 77
hypersensitivity, 324
hypersensitivity reactions, 324
hypertension, viii, ix, 65, 66, 67, 69, 70, 71, 72, 73, 74, 75, 76, 77, 78, 79, 80
hypertrophy, 77, 123
hypoplasia, 134
hypothalamic-pituitary-adrenal axis, 2
hypothalamus, 2, 47, 54, 63, 64
hypothesis, 3, 10, 13, 18, 26, 28, 32, 38, 58, 172, 173, 257, 310, 313

I

ICAM, 9
ice, 92
id, 235
identification, 37, 82, 100, 115, 219, 232, 235, 267, 280, 292, 301, 308, 312, 313, 321, 322
identity, 100, 203, 209, 282, 283
IFN, 6, 7, 9
IgG, 94, 164, 165, 166, 176, 178, 289
IL-1, 6, 7, 8, 9, 10, 11, 12, 15, 20, 22, 180
IL-10, 12
IL-17, 180
IL-2, 160
IL-4, 12, 180
IL-6, 6, 7, 8, 9, 10, 11, 12, 20

images, 129
imaging, 12, 56, 57, 109
imaging systems, 109
immersion, 86, 88, 154
immobilization, 333
immune activation, 14
immune cells, 5, 17, 166
immune disorders, 166
immune function, 2, 5, 6
immune reaction, 160, 164
immune response, 7, 163, 164
immune system, 2, 5, 17, 19, 160, 174, 176
immunity, 5, 164, 177
immunization, 180
immunoassays, 150
immunocytochemistry, 110, 111
immunodeficiency, 177
immunofluorescence, 89, 94, 110, 147, 335, 336
immunoglobulin, xi, 98, 113, 159, 160, 174, 175, 179
immunoglobulins, 94
immunohistochemical, x, 18, 83, 87, 105, 107, 109, 110, 111, 113, 114, 115, 116, 117, 118, 119, 120, 122, 123, 124, 126, 128, 135, 137, 138, 139, 145, 150
immunohistochemistry, vii, ix, x, 81, 82, 86, 87, 97, 99, 110, 111, 112, 114, 115, 116, 117, 118, 129, 133, 143, 150
immunology, 174, 175, 178, 179
immunopathology, 180
immunoreactivity, 92
immunostain, 98, 102
immunosuppressive, vii, 1, 14
impairments, 64
impurities, 258
in situ, x, 102, 117, 122, 123, 128, 139, 140, 144, 147, 151, 285
in situ hybridization, x, 107, 111, 117, 122, 123, 128, 139, 140, 144, 147, 151
in vitro, 2, 7, 12, 14, 21, 23, 134, 135, 149, 151, 157, 170, 172, 186, 241, 251, 289, 293, 308
in vivo, 2, 6, 12, 62, 63, 64, 135, 138, 149, 157, 164, 186, 239, 297, 303, 304, 308, 310
inactivation, xiii, 6, 93, 134, 162, 212, 323, 325, 326, 327, 328, 329, 330, 331, 334
inactive, 206, 207, 213, 218, 230, 233, 251, 255, 256, 302, 305, 318, 322
incidence, viii, 65, 66
inclusion, xi, 10, 39, 159, 160, 162, 171, 174, 175, 186, 193
inclusion bodies, 10, 186
increased access, 91
incubation, 92, 97, 102, 199, 228, 236, 245, 288, 291, 308, 310
incubation time, 97, 102
indication, 105, 203, 331
indices, 95, 113, 135, 238
indigenous, 290
indole, 111, 212
induction, 8, 11, 20, 21, 22, 54, 127, 134, 135, 138, 160, 163, 168, 171, 275, 284, 285, 287, 288, 295, 328
industrial application, xi, 181
industry, xi, 181, 261
infection, xii, 273, 274, 275, 283, 285, 286, 289, 290, 293
infections, 7, 289, 294
inflammation, 7, 8, 17, 19, 20, 75
inflammatory mediators, vii, 1, 7, 9, 12
inflammatory response, 8, 9, 11, 14, 15, 17, 19
inflammatory responses, 8, 14, 17, 19
information processing, 37
inhibition, 5, 10, 12, 15, 16, 42, 51, 53, 54, 55, 57, 58, 59, 60, 61, 63, 127, 134, 164, 191, 199, 212, 232, 278, 279, 284, 289, 304
inhibitor, 8, 10, 14, 15, 36, 40, 44, 52, 57, 186, 189, 192, 199, 217, 235, 263, 264, 276, 279, 280, 289, 295, 313
inhibitors, viii, 3, 6, 45, 47, 49, 63, 144, 190, 192, 199, 212, 261, 262, 275, 276, 278, 280, 284, 301, 306, 318
inhibitory, 11, 23, 49, 50, 59, 134, 135, 178
inhibitory effect, 23, 49, 50, 59
initial state, 326
initiation, 167, 176, 216
injection, 11
injections, 11
injury, iv, viii, ix, 6, 7, 15, 17, 20, 65, 66, 67, 69, 70, 72, 73, 74, 76, 177
innervation, 11, 24, 57, 63
inoculation, 286
inoculum, 286
inorganic, 91, 246
iNOS, 6, 7, 9, 11, 15, 16
inositol, 4, 58
insecticide, 274
insecticides, 275
insects, 274, 275, 286, 287, 288, 290, 293
insertion, 129, 133, 192, 195, 197
insight, 180, 292, 331
inspection, 301, 313
instability, 83, 114, 115
instruction, 32
instruments, 91
insulin, 12, 77, 160, 165, 168, 184, 259, 260

insulin resistance, 77
integration, 26, 28, 29, 37, 150
integrity, 12, 94, 109
interaction, 19, 26, 27, 28, 29, 30, 31, 32, 34, 38, 39, 42, 74, 93, 164, 185, 186, 188, 191, 197, 204, 215, 240, 251, 252, 256, 334, 335
interaction effect, 26
interaction effects, 26
interactions, 21, 33, 38, 39, 51, 53, 61, 74, 87, 94, 197, 211, 251, 263, 291, 309
interdependence, 212
interface, 17, 251, 324
interferon (IFN), 5, 18
interleukin, 6, 17, 19, 21, 23
interleukin-1, 17, 19, 23
interleukin-6, 21
intermolecular, 254
internalization, 170
interneurons, 54
interpersonal events, 26
interval, 26
intervention, 42, 43
interview, 28, 42
intrinsic, 93, 304, 317
intron, 242, 282
introns, 201, 257, 282, 283
invasive, 102, 111
Investigations, 156
ionizable groups, 314
ionization, 215, 314
ionizing radiation, 90
ions, 102, 183, 206, 220, 241, 242, 244, 245, 249, 250, 280, 313, 316, 317
irradiation, 86, 90, 92, 110, 113
ischemic, 74, 84
isoelectric point, 199, 275, 278, 279, 280, 327
isoenzymes, 267, 291
isoforms, 8, 276, 278, 280, 282, 285, 290, 293
isolation, vii, xii, 280, 299, 301, 303, 312, 314, 317
isoleucine, 215, 236, 239, 240
isotope, vii, 69
isozyme, 250
isozymes, 279

J

Japan, viii, xi, xii, 65, 117, 143, 181, 182, 260, 261, 266, 335
Japanese, xi, xii, 77, 181, 182, 257, 261, 269, 274
JNK, 138
job loss, 42
joining, 162
joint ventures, 36
joints, xi, 138, 159, 168
judge, 34, 36
Jung, 174
justification, 271

K

K^+, 5, 50, 79
K-12, 324
kappa, 175, 178, 179
Ki-67, 95, 102
kidney, 70, 71, 73, 74, 75, 76, 77, 78, 97, 176
kidneys, 70, 73, 74, 75
kinase, x, 4, 8, 79, 114, 143, 144, 165, 177, 319, 334
kinase activity, x, 143
kinases, 177
kinetic constants, 312, 313, 315, 316
kinetic parameters, 187, 189, 191, 195, 199
kinetic studies, 321
kinetics, 91, 92
King, 89, 112
knee, 138
knockout, 22, 134
KOH, 284
koji, 271

L

L2, 128, 134
labeling, 94, 106, 107, 157, 301, 322
laboratory studies, 30
Lactobacillus, 317
lambda, 146, 174, 175, 180
lamina, 82, 113
larvae, 274, 279, 283, 286, 289, 290, 291, 295
laser, 223, 335, 336
laser radiation, 335, 336
late-onset, 15
lateral sclerosis, 19
learning, 55, 60, 61, 62, 64
learning task, 64
left ventricular, 66, 76
leisure, 29, 30
lens, 105
leptin, 73, 77, 78, 79
lesioning, 54
lesions, 13, 20, 21, 61
leucine, 214, 219, 236
leukemia, xii, 104, 323, 324, 333
leukemias, 82
leukocyte, 170
levodopa, 16, 45
Lewy bodies, 13, 23
life span, 163

ligament, x, 118, 128, 129, 135, 136, 138, 139, 140, 141
ligand, 112, 126, 164, 176, 180, 189, 202, 203, 247, 248, 249, 250, 257, 332
ligands, 63, 127, 137, 141, 166, 203, 207, 242, 249, 250, 257, 270
limbic system, viii, 2, 45, 54, 63
limitation, 30, 179
limitations, 40, 147
linkage, 67, 69, 86, 219, 222, 249, 267
links, 85, 87, 168, 295
lipase, 275
lipids, 284
lipopolysaccharide, 5, 17, 21, 23, 160
Lithium, 58, 62
liver, 104, 269, 324
liver damage, 324
localization, 82, 89, 94, 97, 103, 107, 108, 109, 123, 125, 129, 137, 138, 146, 168, 293, 296
location, 50, 130, 210
locus, vii, 1, 2, 16, 18, 19, 20, 21, 22, 23, 24, 47, 53, 60, 61, 62, 63, 64, 160, 162, 166, 168, 174, 270
locus coeruleus, vii, 1, 2, 16, 18, 19, 20, 21, 22, 23, 24, 47, 53, 60, 61, 62, 63, 64
London, 25, 43, 112, 261, 262, 264, 265, 266
longitudinal study, 41
losses, 41
low molecular weight, 84
low-power, 105
LPS, 5, 6, 7, 8, 9, 10, 160, 165, 168
LTP, 56
lung, 6, 104, 112
lung cancer, 104, 112
lungs, 275
lupus, xi, 159, 174, 176, 177, 178, 180
lymphocyte, 16, 94, 106, 113, 174, 175, 177, 336
lymphocytes, 5, 16, 20, 21, 160, 164, 174, 175, 336
lymphoid cells, 180
lymphoid organs, 2, 162, 163
lymphoma, 83, 103, 104, 115, 150
lymphomas, 82
lysine, 189, 199, 204, 212, 263, 277
lysosomes, 104
lysozyme, 93

M

mAb, 146, 147
machinery, 6, 160, 314
macrophage, 10, 16, 20, 23
macrophages, 5, 6, 7, 10, 18, 20, 23, 75, 104, 166
magnetic resonance, 12, 37
magnetic resonance imaging, 12, 37
maintenance, ix, 29, 65, 66, 71, 76, 163, 175, 290
major depression, 24, 60, 62, 64
major depressive disorder, 3, 43, 63
major histocompatibility complex, 19
malaria, 287, 297
malignant, 113
malignant mesothelioma, 113
maltose, 287, 306
mammalian cell, 226
mammalian cells, 226
mammals, 141, 268, 314
management, 14, 16, 42, 61, 173
mandible, x, 117, 118, 119, 122, 127, 138, 139
mandibular, x, 117, 118, 119, 120, 121, 122, 123, 124, 125, 127, 128, 137, 138, 139, 140, 141
mania, 27, 30, 57, 59
manic episode, 57, 58
manipulation, 30, 36, 40, 109, 274
mannitol, 223, 287
mantle, 104
mantle cell lymphoma, 104
manufacturer, 109
MAO, 47, 57
MAPK, 5, 10
marrow, 5, 18, 161, 162, 166, 175
Mars, 178
mask, 37, 92, 172
masking, 87, 91, 97, 146
mass spectrometry, 193, 301
mast cell, 5, 18
mast cells, 5, 18
mastectomy, 86
matrix, 119, 123, 124, 149, 154, 155, 156
matrix protein, 119, 124
maturation, 123, 138, 163, 164, 169, 170, 176, 187, 226
MCA, 185, 198, 199, 200, 202, 205, 206, 216, 259
mean arterial pressure, 71
measurement, ix, 17, 32, 36, 82, 265
measures, ix, 29, 33, 40, 82, 99, 109, 252
mechanical stress, x, 117, 118, 128, 129, 131, 132, 133, 135, 136, 140
media, 8, 286, 287, 288
medial prefrontal cortex, 18, 62, 64
mediation, 57
mediators, vii, 1, 7, 8, 9, 12, 132
medications, viii, 45, 59, 60, 62
medulla, 46, 47
medulla oblongata, 47
melanin, 2, 241, 245, 256, 257
melanoma, 251, 271
melting, 209, 227, 238
melting temperature, 209, 227, 238

memory, 10, 12, 18, 42, 55, 56, 61, 62, 63, 64, 164, 167, 168, 169, 173, 176
memory deficits, 10
memory performance, 55
memory retrieval, 61, 62
men, 41, 67
mental disorder, 26
mentorship, 60
mesenchymal stem cell, 133
mesenchymal stem cells, 133
mesenchyme, 137
mesothelioma, 113
messages, 2, 38
metabolic syndrome, 69, 77, 78
metabolism, 8, 12, 17, 21, 49, 304, 308, 317
metabolite, 16, 18
metabolites, 15, 16, 21, 56, 256, 271
metalloproteinase, 265, 296
metalloproteinases, 203
metastatic, 105, 111, 116
methamphetamines, 47
Methamphetamines, 49
methanol, 86, 280
methionine, 215, 216, 282, 288
methylene, 84, 85, 155
methylphenidate, 14, 17
Mexican, 274
Mg^{2+}, 230, 280
MHC, 9, 24, 160, 171, 175
MHC class II molecules, 24
mice, 6, 11, 12, 15, 19, 20, 22, 119, 122, 123, 124, 127, 128, 129, 134, 138, 139, 140, 141, 161, 162, 163, 164, 170, 171, 172, 173, 176, 179, 180
microaneurysms, 75
microarray, 134
microbes, 309
microdialysis, 59, 62, 63, 64
microflora, 290
microglia, vii, 1, 7, 8, 11, 14, 19, 21, 22, 23
microglial cells, 17, 19, 21
microorganism, xi, 181, 212, 268, 304, 310
microorganisms, vii, xii, 182, 299, 303, 304
microscope, 89, 90, 154, 155, 156
microscopy, vii, x, 89, 114, 153, 157
microtome, 155
microwave, 91, 92, 110, 112, 113, 114, 115, 116, 206
microwaves, 86, 113, 114, 115
midbrain, 13, 14, 18
migration, 162, 199
mild cognitive impairment, 10, 18
milk, 183, 259, 267, 285
milnacipran, 58, 62
mimicking, 318
mineralization, 139
minority, 310
mirror, 31
misfolded, 239, 240, 269
misfolding, 269
misleading, 99
mites, 274
mitochondria, 103
mitochondrial, 334
mitogen, 5
mitogen-activated protein kinase, 5
mixing, 154
mobility, 130, 218, 331
moclobemide, 47, 49
modality, 94
model system, xii, 114, 299
modeling, 234, 240, 280, 294
models, 6, 11, 13, 15, 24, 71, 75, 118, 128, 164, 165, 172, 176, 237, 280
moderators, 43
modulation, 3, 5, 18, 51, 54, 60, 61, 72
mold, xi, 181
mole, 236, 246
molecular mass, 183, 198, 200, 201, 207, 209, 212, 216, 217, 218, 220, 221, 223, 241, 244, 249, 250, 251, 253, 255, 278, 280, 282, 283, 310
molecular oxygen, 241
molecular pathology, 151
molecular structure, 144, 225
molecular weight, 84, 110, 278, 279, 280
molecules, vii, xii, 1, 12, 24, 46, 47, 83, 85, 86, 89, 90, 92, 94, 127, 203, 232, 247, 299
monkeys, 21, 63
monoamine, 3, 16, 20, 46, 47, 49, 62
monoamine oxidase, 3, 16, 62
monoamine oxidase inhibitors, 3
monoclonal antibodies, vii, 83, 111, 115, 146, 335, 336
monoclonal antibody, 75, 104
monocytes, 5
monomer, 199, 212, 223, 251, 255, 306, 324
mononuclear cell, 5, 14, 21
mononuclear cells, 5, 14, 21
monosaccharide, 222
monotherapy, 111
Montana, 321
Montenegro, 42
mood, viii, 37, 38, 41, 45, 58, 59
mood disorder, viii, 45, 58, 59
mood states, 37, 38
morbidity, 42
morphine, 61

morphogenesis, 119, 123, 125, 127, 132, 134
morphology, 82, 90, 94, 109, 110
mortality, 66, 67, 273, 286, 289, 290, 291, 295
mosquito vector, 287
mosquitoes, 287
motivation, 28, 29, 36, 41, 58
motives, 40
mouse, x, xi, 5, 6, 13, 15, 19, 20, 24, 61, 64, 94, 117, 118, 120, 122, 123, 125, 129, 133, 134, 137, 138, 139, 141, 146, 147, 149, 159, 163, 165, 167, 169, 172, 173, 174, 175, 226, 263, 267, 268, 270
mouse model, xi, 13, 15, 24, 159, 165, 169, 172
movement, 13, 31, 33, 91, 93, 128, 129, 131, 135, 137, 138, 139, 140, 141
movement disorders, 13
MPTP, 20, 22
mRNA, 8, 9, 11, 23, 120, 124, 125, 126, 167, 172, 280, 310
mucosa, 84, 192
multi-infarct dementia, 20
multiple sclerosis, 14, 17, 20, 22, 24
multipotent, 137
multivariate, 67
murine model, 178, 180
muscle, 69, 74
muscles, 127
music, 41
mutagenesis, 185, 186, 191, 192, 197, 201, 203, 218, 227, 240, 242, 245, 249, 258, 262, 263, 264, 265, 266, 268, 270, 285, 301, 312, 313, 321, 322
mutant proteins, 209
mutation, 145, 179, 186, 188, 193, 195, 204, 210, 211, 284, 302, 305, 310, 312, 313, 316, 319
mutations, 164, 165, 187, 188, 191, 193, 195, 210, 211, 218, 228, 235, 236, 264, 267, 310, 318
mycelium, 284
myeloma, 335, 336
myoglobin, 104

N

Na^+, 79
N-acety, 227, 286, 292, 309, 320
NaCl, 212, 235, 251
naphthalene, 255
National Academy of Sciences, 176, 297
National Institutes of Health, 105
natural, 87, 93, 164, 179, 274, 275, 287, 305, 308, 321
natural enemies, 275
necrosis, 5, 19, 21, 22, 23, 103, 137
negative influences, 26
negative relation, 28
negative selection, 161
nematodes, 293
neoplasia, 319
neoplasias, 110
neoplasm, 100
neoplasms, ix, 81, 82, 110
neoplastic cells, 138
nephrectomy, 74
nephritis, 164, 176
nephron, 70
nerve, vii, viii, ix, 17, 20, 47, 51, 57, 65, 66, 67, 69, 70, 71, 73, 74, 75, 76, 77, 78, 79, 80
nerve cells, 20
nerve fibers, 71
nerves, 71, 78, 79
nervous system, 23, 72
Nessler's reagent, 325, 326
nested PCR, 290
Netherlands, 45, 159, 295
network, 5, 26, 28, 40, 54, 191, 196, 197
neural crest, 137
neural mechanisms, 78
neurodegeneration, vii, 1, 16
neurodegenerative disease, 2, 7, 8, 10, 15, 198
neurodegenerative diseases, 2, 7, 8, 15
neurodegenerative disorders, 7, 15
neurodegenerative processes, vii, 1
neuroendocrine, 47, 59, 74
neurofibrillary tangles, 10
neuroinflammation, vii, viii, 1, 2, 14, 15
neuron death, 16
neuronal cells, 69
neuronal ceroid lipofuscinoses, 264
neuronal loss, 10, 11, 13
neurons, vii, 1, 2, 8, 9, 10, 11, 12, 13, 14, 16, 19, 20, 22, 23, 24, 45, 47, 50, 51, 52, 53, 54, 56, 57, 58, 59, 61, 62, 63, 64
neuropathology, 12, 56
neuropeptide, 215
neuropeptides, 20, 75
neuroprotection, 17
neuropsychopharmacology, 41
neuroscience, 60
neurotensin, 207
neurotoxic effect, 12, 18
neurotoxicity, 20
neurotransmission, 21, 58
neurotransmitter, vii, viii, 1, 2, 3, 13, 21, 30, 45, 69
neurotransmitters, vii, 1, 13, 21, 45, 75
neurotrophic factors, 3, 12
neutrophil, 6
neutrophils, 5, 17
next generation, x, 143
nickel, 90

nitrate, 9, 287, 288
nitric oxide (NO), 7, 16, 17, 20, 22, 64, 73, 79
nitric oxide synthase, 17, 20, 22, 79
nitrogen, 189, 191, 203, 247, 249, 250, 284, 285, 287, 288, 295, 324
nitrogen compounds, 288
N-methyl-D-aspartic acid, 8
NMR, 219, 220, 221, 267, 320
NO synthase, 7
nociception, 54, 55, 56
nodules, 128
noise, 89, 109
non-clinical, 30
non-clinical population, 30
non-small cell lung cancer (NSCLC), 104
non-steroidal anti-inflammatory drugs, 19
non-thermal, 93
nonverbal, 32, 37
noradrenaline, vii, viii, 16, 17, 18, 20, 22, 23, 25, 36, 37, 38, 40, 41, 43, 60, 61, 62, 63, 64, 79
noradrenergic systems, 22
norepinephrine, vii, viii, ix, 1, 2, 12, 16, 17, 18, 21, 23, 24, 41, 42, 44, 45, 47, 48, 49, 52, 53, 60, 61, 62, 63, 65, 66, 67, 68, 69, 70, 71, 74, 75, 76, 77, 78, 79
normal, viii, 2, 4, 15, 17, 22, 31, 65, 67, 68, 74, 78, 79, 82, 86, 107, 111, 122, 124, 163, 167, 171, 172, 175, 179, 233, 240, 247, 289, 324
normal aging, 2
normal conditions, 172
normal development, 124
NOS, 17
NSCLC, 105, 145
NSE, 94
N-terminal, 205, 235, 262, 279, 282, 283, 324
nuclear, 9, 12, 87, 95, 96, 102, 103, 108, 109, 113, 165, 178, 204, 295
nuclei, vii, 1, 47, 74, 125, 126, 131, 133
nucleic acid, 320
nucleophiles, 230, 301, 303, 314, 315, 317, 320
nucleosome, 170
nucleotide sequence, 199, 209, 216, 242, 262, 263, 265, 268, 270, 271
nucleotides, 201, 310
nucleus, 4, 24, 47, 54, 61, 62, 103, 125, 127, 129, 130, 133, 206
nursing, 12, 15, 22
nursing home, 12, 15, 22
nurturance, 26
nutrient, 275, 286, 293
nutrients, xii, 273, 275, 286, 289, 290

O

obese, 70, 72, 73, 78, 79
obesity, viii, ix, 65, 66, 67, 69, 70, 72, 73, 76, 77, 78, 79
observations, ix, 56, 65, 66, 69, 73, 93, 139
OCT, 155
octapeptide, 208
oestrogen, 110, 113
oil, 291
olanzapine, 59, 63
olfactory, 55, 64
oligomer, 255
oligomerization, 256
oligomers, 84
oligopeptide, 263
oligosaccharide, vii, xii, 219, 220, 222, 223, 224, 226, 260, 266, 267, 269, 299, 300, 302, 304, 305, 306, 307, 315, 318, 319, 320
oligosaccharides, xii, 219, 221, 222, 226, 240, 241, 269, 299, 300, 302, 304, 305, 306, 307, 308, 309, 314, 316, 317, 318, 319, 320, 321
oncogene, 114
Oncology, 108, 116, 150
operator, 97
optical, 102
optical density, 102
optimal performance, 60
optimization, 88, 97, 100, 109
oral, 6, 138
orbitofrontal cortex, 61
organ, 6, 76, 78, 79, 139, 141
organelle, 103, 109
organelles, 82
organic compounds, 103
organic solvent, xii, 280, 299, 304, 305
organic solvents, xii, 280, 299, 304, 305
organism, 5
orientation, 10, 197, 204, 216, 217
osmium, 156
ossification, 118, 119, 121, 122, 123, 124, 127, 138, 140, 141
osteoblasts, x, 118, 119, 124, 127, 128, 130, 131, 132, 133, 134, 135, 136
osteocalcin, 119, 139, 140
osteoclasts, 128, 129, 132, 135
osteocytes, 134
osteonectin, 140
osteopontin, 122, 139, 140
overproduction, 258
oviduct, 269
oxalic acid, 285
oxidation, 46, 47, 110, 241, 249, 257

oxidative stress, 10, 14, 23
oxide, 79
oxides, 91
oxygen, vii, 1, 7, 189, 203, 241, 249, 300
oxygenation, 241, 244
oxytocin, 62

P

p38, 10
p53, 102, 107, 112, 116
pain, 51, 54, 56, 64
pancreatitis, 324
panic attack, 56
panic disorder, 56
Papain, 261
paraffin-embedded, ix, 82, 89, 94, 95, 108, 110, 113, 114, 115, 144, 147, 149, 150, 157
parameter, 188, 195
paraventricular nucleus, 62
parenchymal, 73
Parkinson, 17, 23, 24, 57, 113
Parkinson's disease (PD), vii, 1, 13, 15, 17, 23, 24
Parkinsonian symptoms, 23
paroxetine, 34, 37
particles, 89, 153, 157
passive, 27, 39
pathogenesis, xi, 2, 3, 7, 12, 14, 15, 19, 67, 70, 71, 73, 74, 76, 159, 163, 166, 177, 282, 286, 293
pathogens, 7, 164, 275, 293
pathologist, 109
pathology, vii, 1, 7, 11, 13, 16, 19, 20, 24, 56, 59, 108, 114, 144, 151, 160, 165, 166, 169, 170, 172, 173
pathophysiology, viii, 18, 20, 45
pathways, 7, 47, 49, 55, 56, 91, 263
PCR, 186, 192, 280, 282, 284, 286, 290, 293, 294
peer, 108
peer group, 108
pepsin, 90, 183, 184, 185, 187, 190, 191, 192, 193, 194, 195, 196, 197, 198, 225, 263
peptidase, 198, 264, 281, 283, 297
peptide bonds, 200
perception, 31, 34, 41, 42, 51, 107
periodic, 13
periodicity, 51
periodontium, 128, 129, 130, 131, 133, 134
peripheral blood, 5, 21
peripheral blood mononuclear cell, 5, 21
permit, 164
personality, 41, 42
personality disorder, 41
pests, 273, 274, 289, 294, 297
PET, 12, 57
PFC, 47, 51, 54, 55, 56, 58, 59
pH values, 94, 114, 195, 199, 285
phagocytic, 6, 18
phagocytosis, 5, 7, 12, 20
pharmacokinetics, 333
pharmacological treatment, ix, 66
pharmacology, 50
phenol, 111
phenotype, 83, 171, 172, 173, 290
phenylalanine, 189, 213, 214, 216, 219, 236, 237, 239, 242
phenytoin, 23
phorbol, 7
phosphate, 46, 89, 154, 155, 246, 289, 315, 316, 325, 326, 331
phospholipase C, 4, 50
phosphoprotein, 170
phosphorylation, 5, 79, 144, 145, 146, 170, 171
photographs, 34
photon, 90
phylogeny, 295
physical mechanisms, 94
physicochemical properties, 198, 199, 249, 325
physiological, 118, 120, 122, 125, 128, 140, 153, 314, 321
physiology, 50
pI, 199, 207, 227, 275, 278, 279, 281, 283
Pichia pastoris, 282, 297
pig, 16, 263
pilot study, 146
pituitary, 104
PKC, 7, 58
placebo, 22, 34, 37, 38, 39, 42, 112
placenta, 157
plants, 274, 306, 309
plaque, 11, 20
plaques, 10, 15, 24
plasma, vii, viii, ix, 56, 61, 65, 66, 67, 68, 69, 70, 71, 72, 76, 77, 79, 163, 169, 170, 172, 173, 279, 324
plasma cells, 163, 169, 170, 172, 173
plasmid, 185, 186, 200, 216, 218, 227
plasminogen, 200
plastic, 115
plasticity, 175
platelet, 140
platforms, 144
play, vii, viii, 1, 6, 7, 9, 28, 38, 40, 45, 59, 66, 70, 75, 94, 108, 125, 128, 134, 160, 169, 187, 191, 197, 282, 285, 288, 300, 306, 314
PLC, 4, 50
pleasure, 39
PMSF, 199, 276, 277
PNMT, 46

point mutation, 164, 218, 267
polyacrylamide, 251, 328
polyethylene, 86, 333
polymer, x, 97, 98, 143, 144, 145, 212, 306, 308
polymerase, 286
polymerase chain reaction, 286
polymer-based, x, 143, 144
polymerization, 2, 155, 257
polymers, 89, 284
polymorphism, 69, 76, 280
polymorphisms, vii, ix, 65, 66, 67, 77, 78, 293
polymorphonuclear cells, 6
polyp, 98
polypeptide, 216, 222, 237, 282, 327, 331, 332
polypeptides, 87, 310
polysaccharide, 306, 308
polysaccharides, 300, 306
pons, 2, 47
poor, viii, ix, 25, 27, 28, 39, 81, 88, 89, 106, 109, 115, 149, 203, 289, 303, 313, 316
population, 2, 13, 15, 30, 43, 67, 69, 70, 76, 77, 101, 167, 168
positive correlation, 12, 287
positive relation, 38
positive relationship, 38
positron, 57
positron emission tomography, 57
postmortem, 15, 21, 23
postsynaptic, 50
posttraumatic stress, 56, 62
posttraumatic stress disorder, 56, 62
potassium, 50, 73, 325, 326, 331
potato, 254, 274, 276, 279
powder, 198, 279
power, 33, 93, 105, 133
praline, 266
precipitation, 91, 222, 289
precursor cells, 133, 134
prediction, 105, 216
predictive marker, 100
preference, 184, 195, 196, 197, 214, 278, 292, 324
prefrontal cortex (PFC), 11, 18, 20, 47, 62, 63, 64
preschoolers, 40
presenilin 1, 336
press, 77, 112
pressure, ix, 26, 66, 67, 68, 70, 71, 72, 73, 74, 75, 77, 78, 81, 90, 105, 116, 128, 129, 130, 131, 132, 133, 135, 163
presynaptic, 21, 47, 50
prevention, ix, 66, 151
probability, 55, 101
probe, 148, 187, 253, 271
productivity, 257, 258
progenitor cells, 127
progenitors, 137
progesterone, 101, 105, 113, 115
prognosis, 76, 105, 114, 151
prognostic factors, 87, 114
prognostic marker, ix, 81, 83, 106
program, 107, 288, 334
progressive supranuclear palsy, 22
proinflammatory, xi, 7, 10, 23, 24, 159, 160
prokaryotes, 203, 264
proliferation, 75, 83, 95, 97, 113, 121, 122, 125, 134, 140, 160, 167, 169, 174
promoter, 5, 9, 17, 169, 186, 192, 193, 216, 257, 258, 259, 271, 272, 284, 289, 290
promoter region, 169, 284
propionic acid, 212
propranolol, 5, 6, 8, 9, 22, 37, 41
prostaglandin, 8
prostaglandins, 7
prostate, 114, 157
protease inhibitors, 278, 280
proteases, vii, xii, 207, 261, 273, 275, 276, 278, 279, 280, 282, 283, 284, 285, 287, 288, 291, 292, 293, 294, 295, 296, 297
protection, 14, 23, 269, 300
protective role, 28, 41
protein denaturation, 91
protein folding, 239, 240
protein hydrolysates, 219
protein kinase C (PKC), 4
protein kinases, 5
protein sequence, 205, 279, 283
protein structure, 86, 91, 269, 334
protein synthesis, 10
proteinase, 90, 183, 184, 186, 187, 191, 192, 195, 198, 201, 203, 204, 212, 215, 218, 219, 259, 261, 262, 263, 264, 265, 280, 296
Proteinases, 262
proteinuria, 66, 73, 79
proteolysis, 219
proteolytic enzyme, xi, xii, 90, 181, 266, 273, 275, 292, 296
protocol, 101, 108, 116
protocols, x, 33, 88, 90, 108, 116, 153, 155, 156
PRT, 288
Pseudomonas, 234, 263, 264
psychiatric disorder, viii, 25, 30, 31
psychiatric disorders, viii, 25, 30, 31
psychiatric illness, 27
psychoactive drug, 31
psychological health, 29
psychological stress, 29
psychological well-being, 26

psychopharmacological, 30, 37, 40
psychosocial functioning, 28
psychotropic drug, viii, 25
psychotropic drugs, viii, 25
PTSD, 56
pulp, 135, 136, 139
punitive, 33
purification, 226, 244, 263, 269, 278, 284, 318, 325, 327, 328, 334
pyramidal cells, 50

Q

quail, 269
quality assurance, 95, 107
quality control, 99, 239, 269
quality of life, 15
questionnaire, 29, 33
questionnaires, vii, viii, 25, 26, 28, 30, 40, 42
quinones, 241, 257

R

radiation, 90, 335, 336
rain, 9
random, 102, 160, 224, 245
range, viii, ix, x, 2, 65, 67, 72, 81, 82, 85, 89, 90, 94, 95, 99, 113, 133, 153, 155, 156, 183, 186, 203, 214, 215, 230, 237, 252, 274, 278, 279, 282, 284, 285, 289, 312, 326, 328
RAPD, 290
raphe, 47
rapid eye movement sleep, 13
rat, 9, 14, 17, 18, 20, 21, 22, 23, 47, 58, 61, 62, 63, 64, 79, 80, 133, 137, 138, 139, 140, 269, 320
rating scale, 30, 42
ratings, 31, 36
rats, 14, 16, 23, 24, 38, 54, 61, 62, 63, 64, 71, 73, 78, 79
reaction mechanism, 301, 304, 305, 308, 311, 322
reaction rate, 92, 228, 316
reaction time, 36, 37
reactive oxygen, vii, 1, 7
reactive oxygen species (ROS), vii, 1, 7
reactive sites, 90
reactivity, 94, 103, 111, 112, 144, 162, 247
reading, 60, 167, 168, 209, 216, 242, 257, 282
reagent, 89, 95, 98, 146, 147, 251, 254
reagents, ix, 81, 83, 86, 87, 88, 90, 94, 97, 99, 103, 105, 325
real time, 286
reality, 100
receptor-positive, 106
receptors, xi, 3, 4, 5, 8, 11, 17, 20, 21, 22, 23, 50, 51, 54, 55, 58, 59, 60, 61, 63, 75, 87, 104, 105, 113, 127, 137, 140, 159, 175, 177, 178, 179, 309, 336
reciprocal interactions, 51
recognition, 10, 36, 37, 40, 64, 82, 89, 99, 163, 164, 184, 187, 191, 195, 197, 278, 300, 320
recombination, 160, 162, 164, 167, 170, 174
reconstruction, 157
recovery, 23, 36, 334
red shift, 252
redox, 270
reflexes, 13
refractory, 71, 75, 76, 80, 110, 111, 115
regional, 78
regioselectivity, 300, 304, 306
regression, 67
regular, 273
regulation, vii, viii, xii, 1, 15, 16, 17, 19, 21, 22, 23, 45, 47, 56, 64, 71, 74, 75, 79, 83, 119, 125, 137, 140, 169, 173, 176, 258, 273, 284, 285, 289, 292, 293, 295, 296, 306, 310, 314
regulators, 177, 308, 309
reinforcement, 29
rejection, viii, 25, 27, 32, 34, 39, 41
relapse, viii, 45
relationship, viii, ix, 23, 25, 26, 27, 28, 29, 38, 39, 43, 61, 65, 72, 74, 153, 192, 211, 283, 288, 289
relationships, vii, viii, ix, 25, 26, 28, 29, 30, 38, 39, 42, 44, 65, 66, 67, 71, 74, 76
relatives, 27
relaxation, 246
relevance, 13, 93, 102
reliability, 105, 107, 115, 116, 133, 149, 154
remodeling, 129, 133
renal, vii, viii, ix, 65, 66, 67, 68, 69, 70, 71, 72, 73, 74, 75, 76, 77, 78, 79, 80, 104, 110
renal disease, viii, ix, 65, 66, 68, 70, 73, 74, 75, 76, 77, 79
renal dysfunction, 73
renal failure, 73, 79
renal function, vii, viii, ix, 65, 66, 67, 69
renal medulla, 73
renin, 70, 71, 72, 73, 74, 75, 183, 185, 191, 262
renin-angiotensin system, 70, 71, 72, 74, 75
repair, 83, 156
repression, 284, 285, 288
Reserpine, 49
resin, 157
resistance, 29, 71, 77, 78, 156, 203, 225, 304, 333
resolution, viii, 25, 28, 192, 206, 261, 262
resources, 29
responsiveness, 147
restriction fragment length polymorphis, 280

retaliation, 33
retention, 74, 78, 241, 300
reticulum, 221, 236, 239, 241, 268, 269, 282
reverse transcriptase, 192
Reynolds, 10, 16, 19, 21
RFLP, 280, 282
rheumatic, 177
rheumatic diseases, 177
rheumatoid arthritis, xi, 159, 174, 177, 179
rheumatoid factor, 165, 166, 178, 179
rhizosphere, 294
rhythm, 23
ribosome, 310
rice, xi, 181, 215, 257, 266, 271
rigidity, 13, 14
risk, 29, 74, 75, 76, 77, 90
risk factors, 78
risks, viii, 65
risperidone, 51, 59, 61
RNA, 103, 178, 192
rodent, 17
rodents, 18, 55, 275
room temperature, 88, 91, 93, 155, 325
ROS, 140
rubber, 133

S

Saccharomyces cerevisiae, 235, 241, 242, 262, 267, 268, 269
sadness, 33, 34, 41
safety, 75, 80, 116
saline, 86, 154
salt, 71, 79
salts, 230
sample, 84, 99, 100, 108, 154, 155
sampling, 69, 87
SAS, 29
SASS, 29, 30, 36, 40
satisfaction, 30
saturation, 312, 313, 315
scattering, 310
Schiff, 91, 178
Schiff base, 91
schizophrenia, 18, 27, 31, 58
sclerosis, 14
scores, 26, 36, 99, 100, 104, 105, 106, 109
scripts, 32
SDS, 185, 186, 187, 193, 198, 199, 212, 218, 219, 223, 226, 227, 228, 241, 244, 245, 250, 251, 252, 255, 258, 271, 324, 327, 328
search, 7, 32, 37, 201, 203
Second World, xi, 181
Second World War, xi, 181
secrete, xii, 164, 171, 182
secretion, 6, 20, 73, 240, 287, 288, 289, 291
security, 28
seed, xi, 181
seedlings, 318
seeds, 306
selecting, 30
selective serotonin reuptake inhibitor, 52, 63
selectivity, 18, 57, 306, 336
Self, 29, 36, 41, 159, 160
self-antigens, 160, 162, 164, 165
self-confidence, 39
self-definition, 26, 30
self-esteem, 29, 39
self-expression, 39
self-report, 30, 36, 40
SEM, 293
senile, 16, 19, 20, 24
senile dementia, 16, 19, 20, 24
sensing, 165
sensitivity, 12, 54, 73, 82, 83, 88, 89, 95, 97, 101, 105, 109, 144, 278
sequelae, 12, 15
sequencing, 167, 193, 216, 235, 261, 290, 292
series, 37, 99, 213, 241, 279, 280
serine, xii, 198, 202, 215, 216, 218, 221, 236, 240, 264, 266, 270, 273, 275, 276, 278, 279, 280, 281, 282, 283, 285, 287, 288, 291, 292, 294, 296, 319
serology, 165
serotonin, viii, 2, 3, 15, 21, 38, 41, 42, 45, 46, 49, 52, 53, 61, 62, 63, 64
Serotonin, 53, 63
serum, x, 6, 99, 146, 153, 154, 161, 170, 171, 172, 217, 244, 279, 284
serum albumin, x, 153, 154, 279, 284
services, iv
severity, 6, 11, 21, 57, 66, 71
sex, 41
sham-operated, 75
shape, 129, 130, 131, 133, 160, 162
SHM, 164
shock, 11, 141, 244, 245, 247
shocks, 59
short period, 73, 125
Short-term, 43
shrimp, 278
side effects, 324
signal peptide, 227, 280, 281, 282, 283
signal transduction, 18, 50, 58, 79, 309
signaling, x, 5, 10, 12, 19, 62, 117, 123, 125, 127, 128, 137, 139, 141, 161, 163, 164, 165, 166, 167, 169, 170, 171, 175, 179
signaling pathway, 127, 163

signaling pathways, 163
signals, 4, 61, 74, 87, 120, 124, 127, 137, 147, 148, 150, 160, 169, 171, 219, 237, 285
signs, 10, 12, 13, 21, 168
silkworm, 278, 296
silver, 89, 148
similarity, 216, 257, 279, 280, 283, 300
simulation, 206
sites, vii, x, 87, 90, 128, 143, 144, 145, 183, 184, 201, 205, 216, 234, 247, 249, 278, 284, 310, 324
Sjögren's syndrome, 165
skeletal muscle, 104
skeleton, 127
skills, viii, 25, 26, 27, 29, 41
skin, 84, 99
SLE, xi, 159, 164, 165, 166, 167, 168, 173
sleep, 10, 13, 14
sleep disorders, 13, 14
sleep disturbance, 10, 13
SNS, 2
social activities, 27, 36
social adjustment, 28, 29
social behavior, 30, 33, 40, 42, 44
social behaviour, viii, 25, 27, 28, 30, 31, 32, 34, 36, 38, 39, 40, 43
social exchange, 30
social hierarchy, 39
social integration, 26, 28, 29, 37
social network, 26, 28, 40, 41
social relations, 26, 28, 39, 42, 44
social relationships, 26, 28, 39, 42, 44
social situations, 38
social skills, viii, 25, 26, 27, 29
social support, viii, 25, 26, 27, 28, 29, 30, 40, 41, 43, 44
sodium, 50, 71, 73, 74, 75, 78, 79, 188, 189, 195, 232, 246, 271, 301, 302, 305, 306, 311, 312, 314, 315, 324, 325
sodium dodecyl sulfate (SDS), 271
sodium hydroxide, 325
soft tissue tumors, 82, 104, 147
software, 153, 332
soil, 274, 290
soils, 274
solid tumors, 146, 147
solid-state, 257, 258, 271
solvent, 254, 331
solvents, xii, 280, 299, 304, 305
somatostatin, 104
somnolence, 13
soy, xi, 181, 257
soybean, 219, 266
soybeans, xi, 181
spatial, 55, 63
spatial memory, 55
species, vii, xi, xii, 1, 7, 8, 18, 91, 94, 98, 181, 206, 250, 273, 274, 278, 279, 283, 292, 296
spectrophotometry, 232, 234, 245, 249
spectroscopy, 206, 246, 267, 270
spectrum, 91, 193, 206, 207, 209, 219, 220, 252
speech, 10, 32, 33, 34
spin, 246
spinal cord, 2, 14, 24, 47, 54, 56, 156
spindle, 121, 129, 130, 131, 133
spleen, 179
sporadic, 16
spore, 279, 286, 289, 291
Sprague-Dawley rats, 75
sprouting, 11
SRD, 66
SSB, 165
stability, xii, xiii, 203, 209, 211, 219, 225, 232, 234, 238, 265, 280, 299, 304, 306, 310, 317, 320, 323, 325, 331
stabilization, 91, 188, 191, 195, 197, 211, 265, 333
stabilize, 236, 240
stabilizers, 58, 59
stages, 10, 14, 85, 133, 161, 169, 286, 288, 290
standardization, 83, 87, 101, 102, 108, 109, 110, 111, 116, 150
standards, 99, 100, 101, 109
starch, xi, 181
starvation, 285, 286, 287, 289, 291
statistical analysis, 100
steady state, 313
stem cells, 134
stereospecificity, 317
stereotype, 288
steric, 87, 93, 94, 191, 240
stimulus, 10, 74, 132, 138, 164
stock, 154
storage, 17, 21, 46, 47, 49, 84, 90, 99, 116, 267, 306, 331
strain, xii, 176, 200, 201, 206, 211, 212, 258, 273, 282, 285, 286, 287, 289, 290, 291, 292, 297
strain improvement, xii, 273, 292
strains, 163, 257, 274, 280, 282, 285, 289, 290, 291, 293
strategies, 60, 64, 144, 173
strength, 36, 170, 326, 335
streptavidin, 145
Streptomyces, 242, 251, 270, 283, 321
stress, x, 10, 14, 21, 23, 26, 27, 28, 29, 30, 41, 43, 54, 55, 56, 59, 61, 63, 117, 118, 128, 129, 131, 132, 133, 135, 136, 140, 256, 286
stress-related, 55

stretching, 130
striatum, 13, 20
stroke, 34
stromal, 83, 104, 111
strong interaction, 195
structural gene, 201, 296
students, 26
subcortical nuclei, 24
subjective, 31, 37, 96, 99, 107
subjectivity, 107, 108
Substance P, 208
substances, vii, 1, 7
substantia nigra, 13, 21, 24
substantia nigra pars compacta, 13
substitutes, 87
substitution, 98, 188, 191, 192, 193, 197, 219, 249
substrates, 42, 184, 187, 189, 190, 191, 192, 194, 195, 197, 198, 199, 200, 204, 205, 206, 212, 213, 214, 216, 263, 266, 278, 279, 284, 286, 289, 290, 300, 303, 305, 306, 311, 312, 313, 316
subtilisin, 264, 275, 276, 278, 279, 280, 281, 282, 283, 284, 285, 286, 287, 288, 290, 291, 293, 294, 295, 296, 297
sucrose, 155, 306
sugar, xi, 181, 219, 220, 221, 222, 227, 230, 234, 240, 241, 269, 300, 305
sugars, xi, 181, 223, 302, 304
suicide, 57
sulfate, 271, 320, 324
sulfur, 240
sulphate, 90
sulphur, 247, 250
superiority, 147
supernatant, 216, 279
superoxide, 7, 16, 250
superoxide dismutase, 250
supply, 99, 287
suppression, 6, 24, 51, 54, 275, 286
surface tension, 97
surgical, 75, 114, 156, 157
surgical pathology, 114
survival, viii, 14, 34, 65, 74, 76, 105, 161, 163, 165, 282, 290
survival rate, 74
survival value, 34
surviving, 19
susceptibility, 177
suspensions, 155
swelling, 291
symmetry, 310, 324
sympathetic denervation, 80
sympathetic nervous system, 2, 19, 67, 70, 71, 72, 74, 76, 77, 78, 79
symptom, viii, 25, 28
symptomatic treatment, 15
symptoms, vii, 1, 3, 13, 14, 15, 16, 23, 26, 27, 28, 38, 41, 44, 57
synapse, 46
synaptic clefts, 69
synaptic vesicles, 46, 47
synchronous, 17
syndrome, 24, 69, 178, 180, 267
synergistic, 97, 287
synthesis, vii, xii, 6, 8, 10, 17, 21, 73, 287, 288, 289, 295, 296, 299, 300, 302, 303, 304, 305, 306, 308, 309, 314, 316, 317, 318, 319, 320, 321, 328
systemic lupus erythematosus, xi, 159, 166, 174, 176, 177, 178, 180

T

T cell, 160, 161, 164, 169, 176
T cells, 160, 164, 169, 176
T lymphocyte, 160
T lymphocytes, 160
T regulatory cells, 176
tactics, 336
targets, 7, 36, 56, 75, 87, 93, 146, 169, 290
taste, 54, 219
tau, 10
technical assistance, 261
teeth, 133
telencephalon, 47
temperature, 85, 86, 88, 90, 91, 92, 95, 98, 102, 110, 114, 116, 148, 155, 199, 203, 209, 211, 224, 232, 237, 294, 306, 310, 325, 326, 328, 334
tension, x, 26, 97, 118, 128, 129, 130, 131, 132, 133, 135, 140
terminals, 13, 51
termites, 274
test procedure, ix, 81
TGF, 75
thalamus, 2, 12, 23
therapeutic agents, vii, x, 143, 149, 300
therapeutics, 18
therapy, 14, 38, 59, 83, 104, 105, 112, 146, 147, 160, 173, 174, 180, 324, 333
thermal denaturation, 235, 236, 238
thermal energy, 92
thermal stability, xiii, 202, 209, 211, 232, 265, 323, 331
thermodynamic parameters, 326, 330
thermostability, 236, 238, 240, 265, 266, 269, 331
thesaurus, 31
thioredoxin, 244, 245
Thomson, 333
threat, 162

threonine, 185, 202, 221, 236, 240, 319
threshold, 54, 101
thresholds, ix, 82
thymine, 310
thymus, 204, 205, 259
thyroglobulin, 267
TLR, 161, 164, 166, 169
TLR9, 166, 178
TNF, 5, 6, 7, 8, 9, 12, 15, 20, 75
TNF-alpha, 75
TNF-α, 12, 15
tolerance, xi, 159, 160, 161, 162, 163, 164, 165, 166, 167, 168, 170, 171, 172, 173, 174, 175, 176, 177, 179, 199
Toll-like, 178
tonsils, 167
topology, 280
toxic, vii, 1, 90, 239, 271, 289, 297, 331
toxic effect, 289, 331
toxicity, 18, 22, 87, 157
toxins, 274
trabecular bone, 121
training, 32
trans, 295
transactions, 27, 30, 44
transcriptase, 192
transcription, x, 5, 9, 10, 21, 117, 119, 123, 128, 129, 132, 134, 136, 138, 140, 280, 286
transcription factor, x, 5, 10, 117, 123, 128, 129, 132, 134, 136, 138, 140
transcription factors, 129, 132, 134, 138
transcripts, 286
transduction, 19
transfer, 4, 221, 283, 308, 319, 321
transformation, xii, 46, 182
transformations, 291
transgenic mice, 12, 19, 162, 173
transgenic mouse, xi, 159, 175
transition, 137, 162, 188, 191, 195, 197, 233, 236, 238, 249, 301, 326, 328, 331
transitions, 333
translation, 282, 310
translocation, 83, 103, 147, 148
transmission, viii, 37, 38, 45, 54, 55, 56, 57, 58, 59, 61, 157, 290
transmission electron microscopy, 157
transport, 46, 73, 282, 324
trastuzumab, 111, 116, 146, 147, 150
trastuzumab therapy, 147
treatment-resistant, 60, 63
tremor, 13
trial, 14, 33, 43, 75, 114, 115, 333
trichloroacetic acid, 244
tricyclic antidepressant, 3, 47
tricyclic antidepressants, 47
trifluoroacetate, 223
triggers, 66
tripeptide, 270
Trp, 214, 215
trypsin, 90, 184, 185, 193, 194, 197, 199, 200, 201, 235, 251, 256, 264, 275, 276, 278, 279, 282, 284, 285, 286, 288, 293, 295, 296, 333
tryptophan, 30, 42, 215, 252
Tryptophan, 237, 255
TSA, 144
tumor, 5, 19, 21, 22, 23, 82, 85, 86, 98, 99, 101, 102, 104, 105, 106, 108, 112, 113, 116, 137, 324
tumor cells, 98, 99, 101, 104, 105, 106, 108, 324
tumor necrosis factor, 5, 19, 22, 23, 137
tumors, 82, 83, 99, 100, 103, 104, 105, 106, 111, 146, 147
tumours, 113, 116
turnover, 216, 265, 300
two-state model, 237
type 1 collagen, 119, 120, 122, 123, 124
type 1 diabetes, 177
tyramine, 112
tyrosine, 3, 11, 46, 93, 114, 165, 177, 178, 213, 214, 236, 237, 239, 243, 244, 260, 263, 268, 334
tyrosine hydroxylase, 3, 11, 46

U

ultrasound, 93
ultrastructure, 153, 156
uncertainty, 60
unfolded, 211, 232, 237, 240
uniform, 85, 102, 125, 126, 127
university students, 26
unmasking, 85, 110, 111
urea, 94, 186, 193, 225, 251
uric acid, 77
urinary, 70
urine, 57, 73
UV, 209, 227, 232, 237, 252, 258

V

validation, 41, 43, 100, 101, 102, 109, 146, 149, 151
validity, 29, 32, 33, 36, 83
valine, 214, 216, 236, 240
values, 27, 83, 94, 102, 104, 105, 107, 114, 188, 195, 197, 199, 200, 202, 205, 206, 207, 213, 219, 224, 227, 228, 229, 232, 234, 235, 237, 238, 241, 245, 246, 247, 249, 285, 286, 291, 310, 316, 327, 328
van der Waals, 192, 195, 238, 239, 240
variability, 287, 293

variables, ix, 32, 81, 82, 83, 84, 88, 91, 94, 95, 98, 99, 101, 102, 108, 109, 112
variation, ix, 32, 81, 83, 90, 94, 102, 112, 129, 280, 293
vascular dementia, 11
vasculature, 71, 127
vasoactive intestinal peptide, 20
vasoconstriction, 71
vasodilation, 72, 79
vector, 216, 217, 227, 241, 287
VEGF, 107, 116
vein, 26, 103
velocity, 213
venlafaxine, 15, 24, 47, 49
ventricle, 2
versatility, 285
vertebrates, 192, 309
vesicles, 46, 47
vessels, 102, 135
victims, 57
virulence, 285, 286, 289, 290, 291, 292, 294, 295, 296, 297
virus, 183
visible, 82, 84, 124
visualization, 89, 103, 144, 145, 148
visuospatial, 10
vitamin C, 46
voice, 32
Volunteers, 37, 38, 39

W

water, xii, 71, 84, 87, 90, 203, 234, 250, 267, 291, 299, 300, 302
water-soluble, 267
wavelengths, 237
weight gain, 77, 78
weight loss, 38, 72, 78
Weinberg, 17, 19
wellbeing, 26, 42
western blot, 134, 146
wheat, xi, 181, 216, 219, 267
white blood cells, 5
white matter, 15
WHO, 76, 287, 297
wild type, 228, 229, 230, 231, 232, 234, 235, 237, 243, 255, 305, 311, 312, 315, 316
wine, xi, 181, 257
women, 41, 76, 111
wood, 267
wool, 280
workers, 260
working memory, 55, 62, 63
World Health Organization, viii, 65, 297

X

xenograft, 149
xenografts, 146
X-linked, 165, 177
X-ray diffraction, 262
xylene, 87
Xyloglucan, 306

Y

yeast, xi, 181, 185, 216, 217, 218, 219, 220, 226, 227, 241, 242, 258, 265, 267, 268, 269, 270, 274, 283, 286
yield, 166, 222, 244, 258, 286, 304, 311, 315, 335
young adults, 77

Z

Zea mays, 297
zinc, 138, 202, 203, 204, 206, 207, 250, 265

(Celada et al., 2004; El Mansari and Blier 2005; Marek et al., 2005; Szabo and Blier 2002a), Moinfar F, Stamatakos MD, et al.